



This work is protected by copyright and other intellectual property rights and duplication or sale of all or part is not permitted, except that material may be duplicated by you for research, private study, criticism/review or educational purposes. Electronic or print copies are for your own personal, non-commercial use and shall not be passed to any other individual. No quotation may be published without proper acknowledgement. For any other use, or to quote extensively from the work, permission must be obtained from the copyright holder/s.

Synthesis and biological evaluation of three novel antimalarial series

A thesis submitted to Keele University for the degree
of Doctor of Philosophy

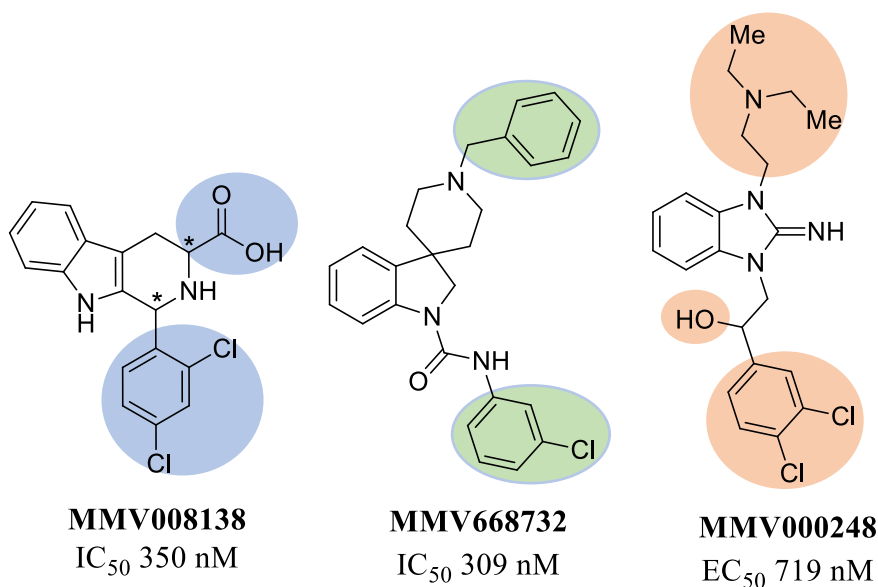
June 2018

Lucy Victoria Tunstall

Keele University

Abstract

This research explored the optimisation of three novel antimalarial series based on the MMV compound leads shown below. ⁽¹⁾

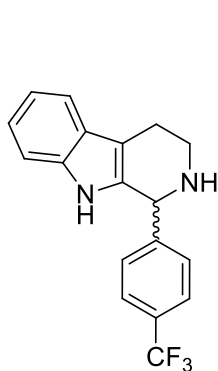


Extensive research began to optimise these potent hits through exploration of multiple functional group substitutions on two or more sites of the core structure (shown above).

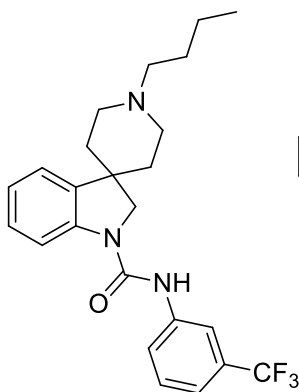
The highest activity tetrahydro- β -carboline analogue discovered during this research was **LVT30** (IC₅₀=1 μ M) which possesses an absent C³ interaction and a *p*-trifluoromethyl R² substitution. Meanwhile, of the spirocyclic subset of derivatives, a high nanomolar activity compound was generated **LVT86** (IC₅₀=960 nM), possessing a butyl R¹ chain and a *m*-trifluoromethyl R² group and future work will include optimisation of this analogues pharmacokinetic properties.

The most fruitful subseries of this project was a catalogue of 2-iminobenzimidazole compounds. In an attempt to optimise activity and increase potency, exploration involved variation of all three R positions and as a result, generated the most potent derivative over all three series. Compound **LVTa95** possesses an inhibitory concentration of 33.4 nM and

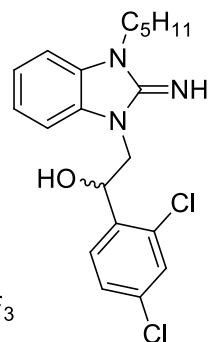
exhibits: a pentane R^1 group, 2,4-dichloro R^2 substitution and a hydroxy R^3 group. As this compound existed as enantiomers, they were subsequently separated, and it was found both stereoisomers had similar activity.



LVT30
1 μ M



LVT86
960 nM



LVTa95
33.4 nM

Acknowledgements

I would first like to thank my thesis supervisors, Dr Tess Phillips and Dr Mike Edwards, of which the door to both mentors was always open whenever I needed advice or help. In particular, I would like to thank Mike for his diligent proof reading ability and persistent positive mental attitude during my time at Keele.

Furthermore, I would like to thank Charnwood Molecular for funding my research and Professor Steve Allin for being a valuable sponsor. I will be forever grateful to him for giving me the opportunity to work at his company during my PhD, which enhanced my chemistry knowledge and practical capabilities. Also, thank you to Tony Mete at Medsyndesign for his expert consultancy during project meetings.

I would like to highlight the immense support given to me from the biology team testing the compounds I synthesised. In particular, thank you to Dr Paul Horrocks for his superior expertise in the malaria field and allowing me to undergo training in his laboratory. Furthermore, thank you to my assay experts Farhana and Viji for putting up with endless phone calls and messages to discuss biological data. My thesis would not have been possible without their hard work and support.

I would like to thank Keele University for being my home for the past 6 years and, the Keele Synthesis and Medicinal Chemistry research group. I have had the pleasure of working alongside a group of highly experienced and mostly entertaining chemists. In addition, thank you to the technical staff within the chemistry department for coming to my rescue in times of crisis.

Most importantly I would like to say a huge thank you to my close friends and loving family. To my Mum, Amy, Savannah and Grandad – without you I would not be where I am today. Thank you for always believing in me and giving me constant encouragement. I love you all very much.

List of Contents	Page Number
Abstract	i
Acknowledgements	iii
Contents	iv
List of Figures	viii
List of Tables	x
Abbreviations and definitions	xi

Chapter 1: Malaria: An Introduction

1:1 The malaria parasite	1
1:1:1 <i>Plasmodium</i> pathogenesis	1
1:1:2 Clinical features	3
1:1:3 IPP synthesis	4
1:2 Overview of malaria progress	8
1:2:1 Prevention, treatment and elimination	8
1:2:2 Medicine for Malaria Venture reports (2014–2016)	12
1:3 Antimalarial Chemotherapies	17
1:3:1 Quinine and Chloroquine	17
1:3:1:1 Historical Malaria Chemotherapy	17
1:3:1:2 Derivatives	19
1:3:1:3 Synthesis	22
1:3:2 Artemisinin	25
1:3:2:1 Antimalarial history	25
1:3:2:2 Derivatives and ACTs	28
1:3:2:3 Synthesis	30
1:3:3 Upcoming clinical candidates	32
1:3:3:1 NITD609	32
1:3:3:2 DDD498	34
1:3:3:3 MMV390048	36

Chapter 2: Tetrahydro-β-carbolines	Page Number
2:1 Indole alkaloids	39
2:2 MMV008138	42
2:2:1 Initial leads	42
2:2:2 Background work	48
2:3 The Pictet-Spengler reaction	53
2:3:1 Background	53
2:3:2 Reaction scope	57
2:3:3 Thermodynamic control: <i>trans</i> selectivity	61
2:3:4 Kinetic control: <i>cis</i> selectivity	63
2:3:5 Lewis acid catalysis	66
2:4 Biological results and discussion	68
2:4:1 Tryptamine derivatives	68
2:4:2 Tryptophan methyl ester derivatives	72
2:4:2:1 Tryptophan methyl ester biological data	75
2:4:2:2 Methyl ester NITD609 derivative	77
2:4:3 Tryptophan benzyl ester derivatives	78
2:4:3:1 Tryptophan substituted benzyl ester derivatives	81
2:4:3:2 Tryptophan benzyl ester biological data	83
2:4:3:3 IPP reversal experiment results	86
2:4:4 Tryptophan benzyl amide derivatives	88
2:4:4:1 Tryptophan benzyl amide biological data	90
2:4:4:2 Methyl amide derivatives	92
2:5 Enantiomeric resolution of tryptamine derivative	94
2:6 Future work	97
2:7 Summary	103
 Chapter 3: Spiroindolines	
3:1 Spirocycles in drug discovery	104

	Page Number
3:2 Spirocyclic synthetic strategies	106
3:2:1 Asymmetric catalysis	106
3:2:2 Convergent metal-free approach	109
3:3 Spirocyclic antimalarials	112
3:3:1 NITD609	112
3:3:2 Mechanism of action	118
3:3:3 NITD609 in 2017	120
3:4 MMV spiroindoline lead	121
3:4:1 Discovery	121
3:4:2 Early analogue proposals	123
3:4:3 Synthetic strategy	125
3:4:4 Preliminary biological results and discussion	127
3:5 Project proposals	131
3:5:1 Synthetic strategy	134
3:5:2 Biological results and discussion	138
3:6 Next generation compounds	143
3:6:1 Biological results and discussion	145
3:7 Future work	147
3:8 Summary	149
 Chapter 4: 2-Iminobenzimidazoles	
4:1 Benzimidazole background	152
4:1:1 Biological significance	152
4:1:2 2-Aminobenzimidazole synthesis	154
4:1:3 Conventional benzimidazole pharmaceuticals	155
4:1:4 Antimalarial activity	160
4:2 Bioactive 2-iminobenzimidazoles	162
4:2:1 2-Iminobenzimidazole antimalarials	163

List of Figures

Figure 1	<i>Plasmodium</i> lifecycle
Figure 2	FOS-DOXP structural comparison and FOS docking within DOXP reductase
Figure 3	Global malaria cases in 2013
Figure 4	Estimated <i>P.falciparum</i> infectious cases amongst children aged 2–10 years
Figure 5	Countries remaining endemic for malaria in 2016
Figure 6	Sweet woodworm
Figure 7	Artemisinin and free radical formation
Figure 8	Migration of ACT resistance
Figure 9	Future multistage antimalarial
Figure 10	Investigation of the SAR
Figure 11	Lead compound MMV121
Figure 12	Synthetic route to DDD498
Figure 13	HTS hits
Figure 14	Route to MMV390048
Figure 15	mc72a and compound optimisation strategy
Figure 16	Compounds targeting the apicoplast
Figure 17	CTP to CDP-ME conversion <i>via</i> IspD
Figure 18	Docking of the (1 <i>R</i> , 3 <i>S</i>) stereoisomer of MMV008138 within IspD
Figure 19	Early analogues (R=H/Me)
Figure 20	Latest analogue proposals
Figure 21	Further compound proposals
Figure 22	Steric and electronic transition state interactions
Figure 23	Surprising Pictet-Spengler product
Figure 24	Tryptamine analogue and MMV008138
Figure 25	Tryptamine and tryptophan methyl ester comparison
Figure 26	α -methyl tryptamine analogues
Figure 27	NITD609 structure comparison
Figure 28	Substituted benzyl ester derivatives
Figure 29	IPP fold-change results
Figure 30	Methyl amide derivative
Figure 31	Sites for further optimisation
Figure 32	Tryptamine proposals
Figure 33	α -methyl tryptamine proposals
Figure 34	Future analogues and NITD609
Figure 35	Benzyl ester analogue proposals
Figure 36	Benzyl amide proposals
Figure 37	Tetrahydro- β -carboline summary
Figure 38	Two ring spiro formula
Figure 39	Ketimine reaction scope
Figure 40	3-Vinylindole variation
Figure 41	Substrate scope
Figure 42	Original hit
Figure 43	Optimum analogue 9x
Figure 44	Summary of findings
Figure 45	Spiroindoline hit with point of variation and simplified sister compound
Figure 46	Retrosynthesis
Figure 47	Initial spiroindoline exploration
Figure 48	Analogue comparison
Figure 49	Linker comparison of AKE1 and AKE6
Figure 50	Spiroindoline template
Figure 51	Benzyl exploration
Figure 52	Benzoyl analogues
Figure 53	Drug-like moieties
Figure 54	Non-aromatic/aryl functional groups
Figure 55	Urea and carbamate comparison
Figure 56	Morpholine moiety exploration
Figure 57	Aliphatic compound comparison
Figure 58	Next generation proposals

Figure 59	Piperidine analogue and branched alkyl derivatives
Figure 60	Benzyl substitution exploration
Figure 61	Potential analogue
Figure 62	Candidate suggestion
Figure 63	Isomerisation of benzimidazole
Figure 64	Analogue under exploration
Figure 65	Benzimidazole dimer
Figure 66	Active scaffold
Figure 67	Novel core investigated and guanidine
Figure 68	Hit compound and key features
Figure 69	2-Iminobenzimidazole leads
Figure 70	Compound A (bis TFA salt) and MMV000444
Figure 71	SAR exploration
Figure 72	Potent leads
Figure 73	Predicted moieties important for SAR
Figure 74	Alternate 2-iminobenzimidazole leads
Figure 75	2-Iminobenzimidazole analogue proposals
Figure 76	nOe experiment
Figure 77	nOe spectrum
Figure 78	Initial biological screening
Figure 79	Hit analogues and key features
Figure 80	Representation of analogue growth rates at 3 different drug concentrations
Figure 81	Poor activity compounds
Figure 82	Screening data
Figure 83	Analogue separation
Figure 84	Activated Noyori's catalyst and starting materials
Figure 85	Potential derivatives
Figure 86	EWG phenyl substitution analogues
Figure 87	Future candidates
Figure 88	LVTa95 improved pharmacokinetic properties
Figure 89	Alternative compounds
Figure 90	Further pharmacokinetic improvements
Figure 91	Potent antimalarial leads
Figure 92	Hit 2-iminobenzimidazole derivatives

List of Tables

Table 1	Parasite lifecycle definitions
Table 2	Comparison of Lipinski's rule
Table 3	Attributes desired to target parasite elimination
Table 4	Summary of <i>P.falciparum</i> drug attributes
Table 5	Summary of malaria cases over 3 years
Table 6	Individual diastereoisomer activity results
Table 7	Initial data July 2013
Table 8	2013 results
Table 9	Synthetic route d.r. comparison
Table 10	Yield comparisons
Table 11	Methyl ester derivatives
Table 12	NITD609mimic results
Table 13	Method comparison
Table 14	Substituted benzyl ester
Table 15	Benzyl ester inhibitory concentration data
Table 16	Inhibitory concentration results
Table 17	Method comparison
Table 18	Benzyl amide and benzyl ester comparison
Table 19	Methyl amide biological data
Table 20	First generation spiroindoline results
Table 21	Spiroindoline product yields
Table 22	Isolated yields from <i>N</i> -alkylation
Table 23	Second generation alkylation product yields
Table 24	Biological data for spiroindoline subseries
Table 25	Further analogue data
Table 26	Biological data collected for final set of derivatives
Table 27	Inhibitory concentration assay results
Table 28	Enantiomeric ratios
Table 29	LVTa95 pharmacokinetic parameter comparison

Abbreviations

Abbreviation	Expansion
ADP	Adenosine 5'-diphosphate
ATP	Adenosine triphosphate
ART	Artemether
ACT	Artemisinin combination therapy
cAMP	Cyclic adenosine monophosphate
AIBN	Azobisisobutyronitrile
PhH	Benzene
Bn	Benzyl
<i>n</i> -Butyl	Butyl
Boc	<i>Tert</i> -butyloxycarbonyl
CSA	(±)-camphor-10-sulfonic acid
CDI	Carbonyldiimidazole
Cbz	Carboxybenzyl
mCPBA	<i>m</i> -Chloroperoxybenzoic acid
CTP	Cytidine triphosphate
CY	Cytochrome
DHEA	Dehydroepiandrosterone
DNA	Deoxyribose nucleic acid
DOXP	1-deoxy-D-xylulose-5-phosphate
d.r	Diastereomeric ratio
DBDMH	1,3-Dibromo-5,5-dimethylhydantoin
DMA	Dimethylacetamide
DMAP	4-dimethylaminopyridine
DMF	Dimethylformamide
DMSO	Dimethylsulfoxide
CDP-ME	4-diphosphocytidyl-2-C-methyl-D-erythritol
Et ₂ O	Diethyl ether
ee	Enantiomeric excess
EWG	Electron withdrawing group
EDG	Electron donating group
e.r.	Enantiomeric ratio
ESI	Electrospray ionisation
EtOH	Ethanol
EtO	Ethoxide
Et	Ethyl
EtOAc	Ethyl acetate
h.	Hour(s)
FOS	Fosmidomycin
HFIP	hexafluoroisopropanol
IR	Infrared
MDR	Multi drug resistant
HRMS	High resolution mass spectrometry
HCl	Hydrochloric acid
HBD	Hydrogen bond donors
HBA	Hydrogen bond acceptors
HCN	Hydrogen cyanide
IPP	Isopentenyl pyrophosphate
LC-MS	Liquid chromatography-mass spectrometry
MS	Mass spectrometry
MMV	Medicine for malaria venture
mRNA	Messenger ribonucleic acid
MeOH	Methanol

OMe	Methoxy
Me	Methyl
MEP	2-C-methyl-D-erythritol 4-phosphate
NMP	N-Methyl-2-pyrrolidone
MW	microwave
Mr	Molecular weight
NMR	Nuclear magnetic resonance
nOe	nuclear Overhauser effect
MB	Open access malaria box
ppm	Parts per million
Pet.ether	Petroleum ether
<i>P.falciparum</i>	<i>Plasmodium falciparum</i>
<i>P.knowlesi</i>	<i>Plasmodium knowlesi</i>
<i>P.malariae</i>	<i>Plasmodium malariae</i>
<i>P.ovale</i>	<i>Plasmodium ovale</i>
<i>P.vivax</i>	<i>Plasmodium vivax</i>
PSA	Polar surface area
ROS	Reactive oxygen species
rt.	Room temperature
RO(3/5)	Rule of (3/5)
tRNA	Transfer ribonucleic acid
SAR	Structure-activity relationship
<i>p</i> -TSA	<i>p</i> -toluenesulfonic acid
TFA	Trifluoroacetic acid
PhMe	Toluene
Trp	Tryptophan
TLC	Thin layer chromatography
TBAB	Tetrabutylammonium bromide
TBAI	Tetrabutylammonium iodide
THF	Tetrahydrofuran
WHO	World health organisation
Tr	Trityl
TEA	Trimethylamine
TMOF	Trimethyl <i>ortho</i> formate
<i>t</i> -BuOH	<i>Tert</i> -butanol
TMSOTf	Trimethylsilyl trifluoromethanesulfonate
Ts	Tosyl

Definitions

logP	A measurement of lipophilicity. Octanol-water partition coefficient of a molecule between water and a lipophilic solvent (usually octanol).
clogP	Predictive calculation of logP based on the molecular fragments which make up the molecule, also known as fragmentary logP.
IC ₅₀	The quantity of substance required to inhibit a specific biological or biochemical response at half its maximal inhibitory concentration (IC ₅₀).
EC ₅₀	The effective concentration (EC ₅₀) required to stimulate a biological or biochemical response to half the maxima.
Drug-like	Qualitative description of how 'druglike' a compound is in respect to its pharmacokinetic parameters such as, molecular weight, potency, bioavailability and logP.
Ames test	A method employed during drug discovery which uses bacteria to test whether a given substance can cause DNA mutations in the target organism.
hERG	A gene that codes for a potassium ion channel protein which contributes to electrical stimulation of the heart i.e. the heartbeat. It is used during drug discovery to determine the amount of substance required to interfere with this protein and therefore cause heart problems.
Different malaria strains:	
NF54	Wild-type malaria
KI	Wild-type chloroquine resistant malaria
Dd2	Cultured chloroquine resistant malaria
3D7	Cultured chloroquine sensitive malaria

Chapter 1: Malaria: An Introduction

1:1 The malaria parasite

1:1:1 *Plasmodium* pathogenesis

Malaria is a parasite transmitted by the genus, *Anopheles*, of which there are five common species that can infect humans: *Plasmodium falciparum*, *Plasmodium vivax*, *Plasmodium ovale*, *Plasmodium knowlesi* and *Plasmodium malariae*.⁽²⁾ There are approximately 3,500 species across the world, of these, around 40 are capable of transmitting malaria to humans. The female *Anopheles* act as a vector for the parasite, and subsequently transmit the parasite to humans, upon taking human blood (see Figure 1).

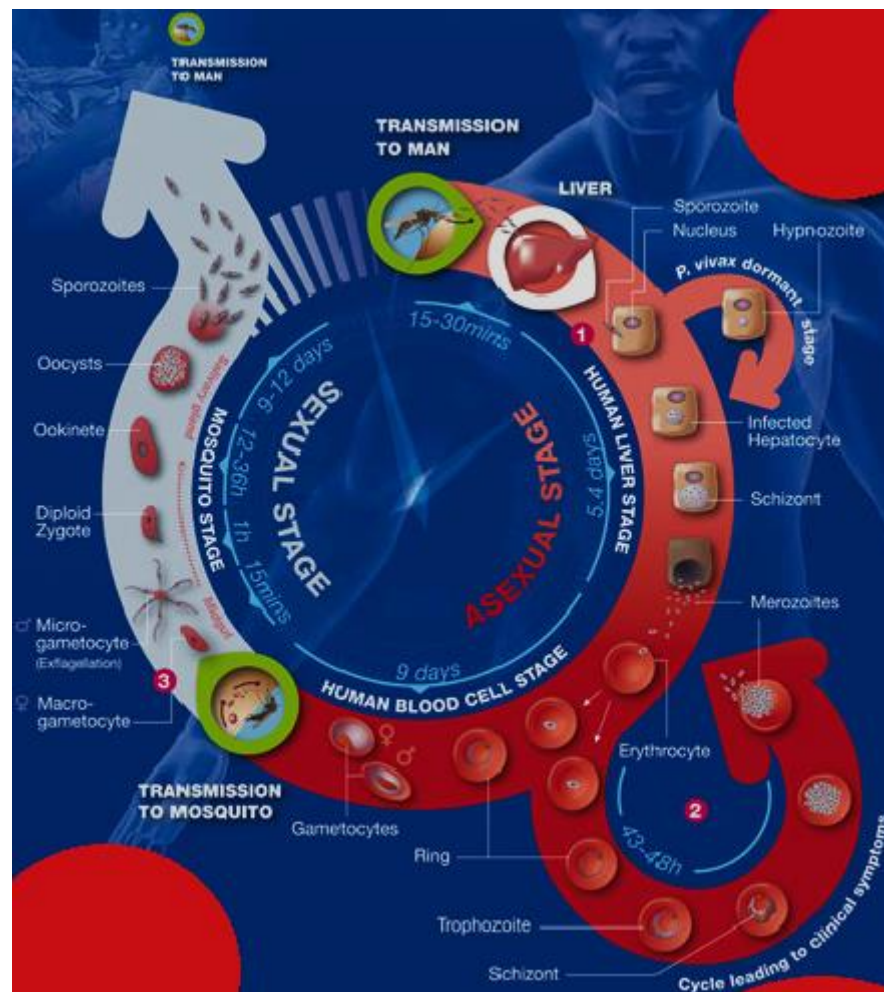


Figure 1: Plasmodium lifecycle⁽¹⁾

Approximately 30 minutes post infection the asexual parasite form travels to the liver, where a dormancy stage is reached which can cause reinfection months or even years later. During the next 48 hours, active merozoites circulate within host red blood cells and transform into schizonts, which give rise to the clinical features of a malaria infection. The schizont form (see Table 1 for definitions) multiplies producing more merozoites, until the red blood cell finally bursts and releases more parasite into the bloodstream, thus proliferates the life cycle. Whilst in the red blood cells, gametocytes form 10 days later, which is known as ‘the sexual stage’ of the lifecycle. Upon the female taking a second blood meal from the host, the parasite is transported inside the mosquito vector and results in ‘the mosquito stage’. The parasite situates itself in the midgut of the insect and over a period of two weeks reproduces sexually to create schizonts, which travel to the salivary glands of the insect where the life cycle restarts and waits for blood feeding to commence (see Table 1 for definitions).

Parasite Stage	Definition
Schizont	Seen in both blood and liver stages of the parasite, this is a development stage which contains many merozoites.
Merozoite	Formed by asexual development. Schizonts contain many merozoites and once the schizont is mature within the RBCs – both the cell and schizonts erupt, releasing the merozoites ready to infect further RBCs
Trophozoite	Another development form during the blood stage of the malaria parasite. Once the merozoites have invaded RBCs, they develop into trophozoites. This stage known as ‘rings’ develop into schizonts
Gametocyte	Sexual stage of the parasite, typically crescent shaped. Microgametocyte (male) and macrogametocytes (female) are within RBCs in circulation. If ingested by <i>Anopheles</i> , they undergo sexual reproduction, which restarts the parasite life cycle.

Table 1: Parasite lifecycle definitions

1:1:2 Clinical features

Once infection occurs the patient symptoms are categorised as, ‘uncomplicated’ or ‘complicated’ malaria – the latter being more severe. An ‘incubation period’ occurs 7–30 days post infection, which results in most patients being asymptomatic. *P. falciparum* infected patients display symptoms sooner, due to the severity of this species. The most critical cases are caused by ‘cerebral malaria’, which is due to infected erythrocytes adhering to the vascular endothelium of venular blood vessel walls within the brain and as a result, higher mortality rates are seen for *P. falciparum* infections. On the other hand, due to the delayed onset of symptoms, in some cases, malaria can be misdiagnosed or missed altogether – often mistaken for common cold or infection. Therefore, visual blood tests under microscopy are required to make a formal diagnosis.

Uncomplicated malaria patients experience common symptoms such as; fever, chills, sweats, headache, nausea and general body ache. However, if uncomplicated symptoms are left untreated they can progress and manifest themselves as: high temperature, enlarged spleen, mild jaundice, enlarged liver and increased heart rate. In addition, if a patient has organ, blood or metabolism abnormalities, complicated malaria symptoms arise which include: cerebral malaria, severe anaemia (destruction of red blood cells), inflammation of the lungs, blood clotting problems, kidney failure, low blood pressure, hyperparasitemia, acidity in the blood and tissues and hypoglycaemia. ⁽²⁾

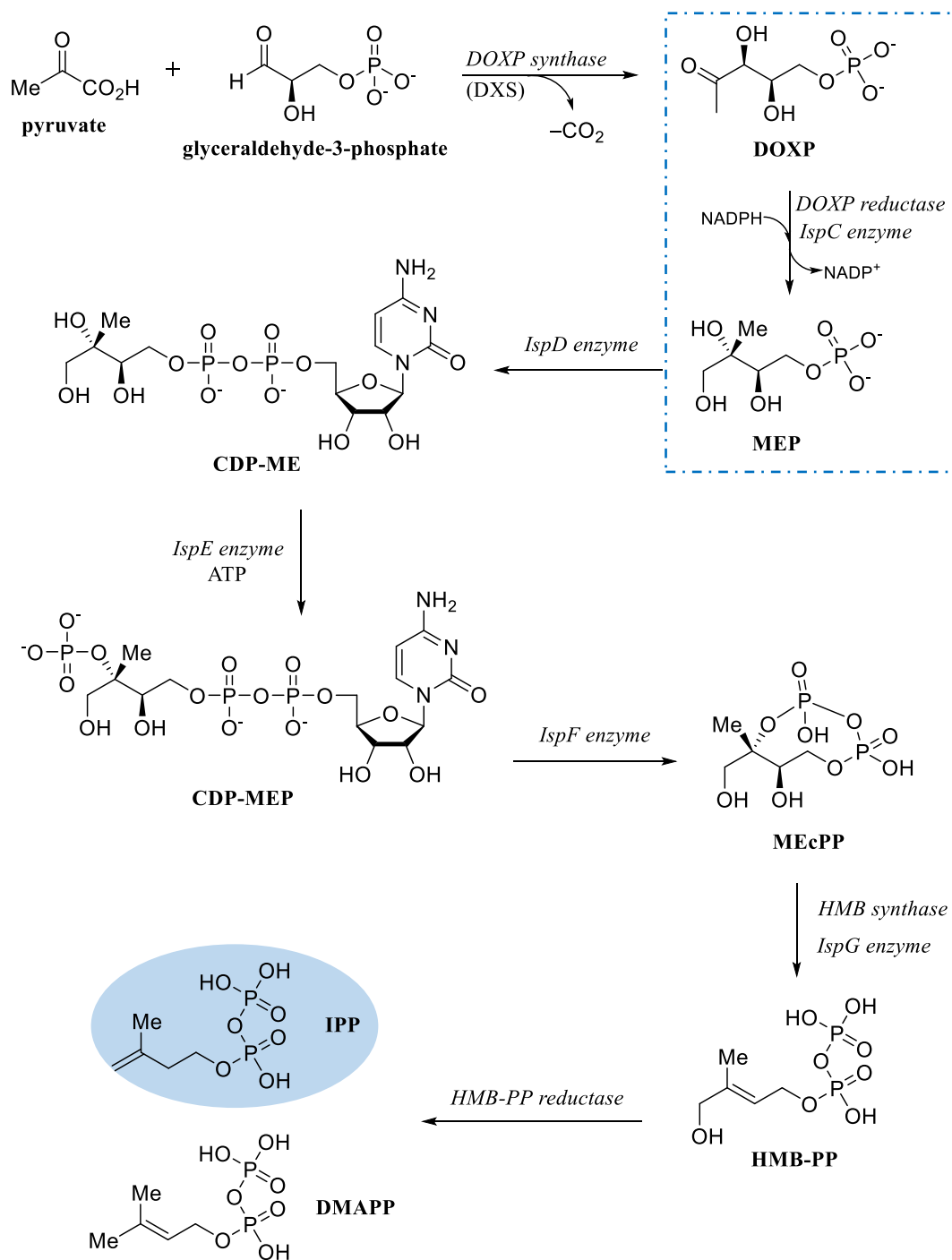
The most vulnerable group to infection are children under 5 years and pregnant women, who consequently suffer from complications due to their compromised immune systems. The widespread problem of gestational malaria results in: low birth weight, severe anaemia and haemorrhage at childbirth, which leads to increased infant fatalities. ⁽³⁾ Furthermore, pregnant women are most at risk from *P. falciparum* infections, which also leads to

premature labour and stillbirth. Congenital malaria also occurs in 5% of cases but clears spontaneously in 62% of cases. ⁽³⁾

1:1:3 IPP synthesis

The mevalonate pathway is an essential metabolic process that takes place in eukaryote cells, within an organelle known as the apicoplast. ⁽⁴⁾ The apicoplast possesses its own genome and expresses a small number of genes, it is a nonphotosynthetic plastid and has functions such as: fatty acid synthesis, isoprenoid, and haem synthesis, which are vital for parasite survival. ⁽⁵⁾

The primary function of this pathway is to biosynthesise key building blocks: isopentenyl pyrophosphate (IPP) and dimethylallyl pyrophosphate (DMAPP). These two crucial precursors are used to generate isoprenoids, which are central to the synthesis of compounds that play key roles within development and sustaining life for example: cholesterol, fatty acids, coenzymes, steroidal hormones, and haem. However, malaria uses an alternate pathway absent in humans known as the non-mevalonate pathway, which generates the vital precursors IPP and DMAPP *via* 1-deoxy-D-xylulose 5-phosphate (DOXP) (see Scheme 1).



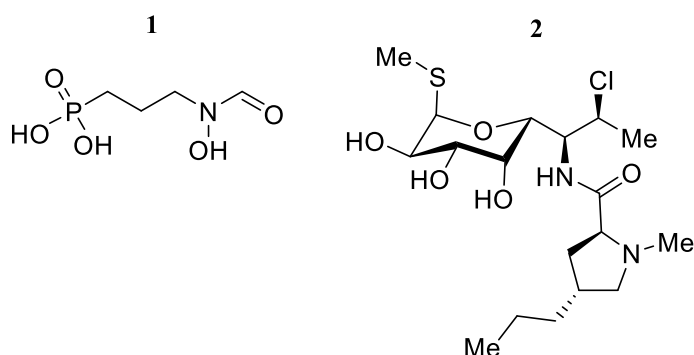
Scheme 1: Non-mevalonate pathway

During the second step of the pathway DOXP reductase also known as IspC, is the enzyme which converts DOXP into a methylerythrose intermediate (MEP). DOXP reductase is a homodimer with three constituent domains: a *N*-terminal cofactor binding domain, a central domain consisting of the many active site residues, a flexible segment acting as a gate for the catalytic centre and a C-terminal alpha helical domain. ⁽⁶⁾ The mechanism starts with the

cofactor binding first followed by the substrate DOXP. Two mechanisms have been suggested for initial isomerisation that converts DOXP to a methylerythrose intermediate, an α -ketol rearrangement or a retro aldol/aldol reaction. The intermediate is then reduced by the hydride source NADPH.

During research carried out on IPP inhibitors that target the non-mevalonate pathway it has been shown by supplementing apicoplast absent parasites with IPP, it can reverse the effects of apicoplast removal. IPP reversal assays can therefore be used to screen drugs thought to target this pathway by firstly dosing the parasite with the test drug and then supplementing the parasite with IPP and measuring subsequent parasitic growth.

DOXP reductase has been targeted for *P. falciparum* chemotherapies and a more recent study testing the antibiotic fosmidomycin (FOS, **1**). FOS resulted in growth inhibition of *P. falciparum* and has cured malaria infected mice. ⁽⁷⁾



FOS contains a hydroxamate moiety and has been found to inhibit the enzyme through coordination of the metal ion Mn^{2+} to mimic the DOXP substrate (see Figure 2). ⁽⁶⁾ Furthermore, the phosphate group provides a tether to the enzyme at the catalytic centre, which subsequently targets metabolism within the apicoplast. However, due to high parasite reoccurrence levels, FOS has been trialled as a combination therapy with another antibiotic clindamycin (**2**), which is a slow acting antibiotic. As this pathway is absent in humans it is

an ideal target for anti-malarials as none of the enzymes used for human IPP and DMAPP production would be affected.

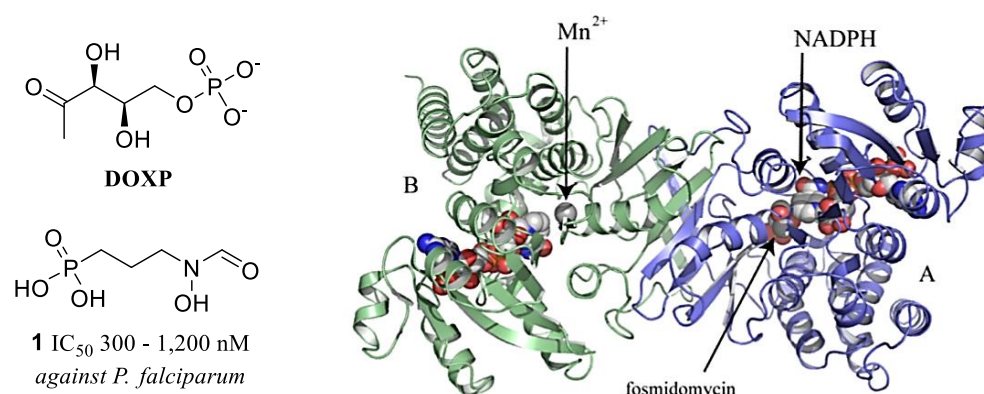


Figure 2: FOS-DOXP structural comparison and FOS docking within DOXP reductase ⁽⁷⁾

Genetic analysis has shown this reductoisomerase is required for intraerythrocytic development of the *P. falciparum* parasite. Therefore, to exploit this pathway for a potential chemotherapy the drug candidate would need to reach the enzyme target by passing into the parasite and then crossing the apicoplast membrane, thus keeping Lipinski's rules in mind when designing such chemotherapy. ⁽⁶⁾ For example, Table 2 shows the comparison in the Lipinski values for both FOS and DOXP. Both compounds adhere to all four parameters but most importantly, the logP values show they are highly polar molecules. This high polarity will allow them to cross the cell membrane within the apicoplast thus, any potential candidate would need to have similar polarity to access the same target within the apicoplast.

Lipinski parameter	FOS	DOXP
HBA (<10)	6	6
HBD (<5)	3	4
logP (<5)	- 0.32	- 1.09
Molecular weight/gmol ⁻¹ (<500)	138.10	198.11

Table 2: Comparison of Lipinski's rule

1:2 Overview of malaria progress

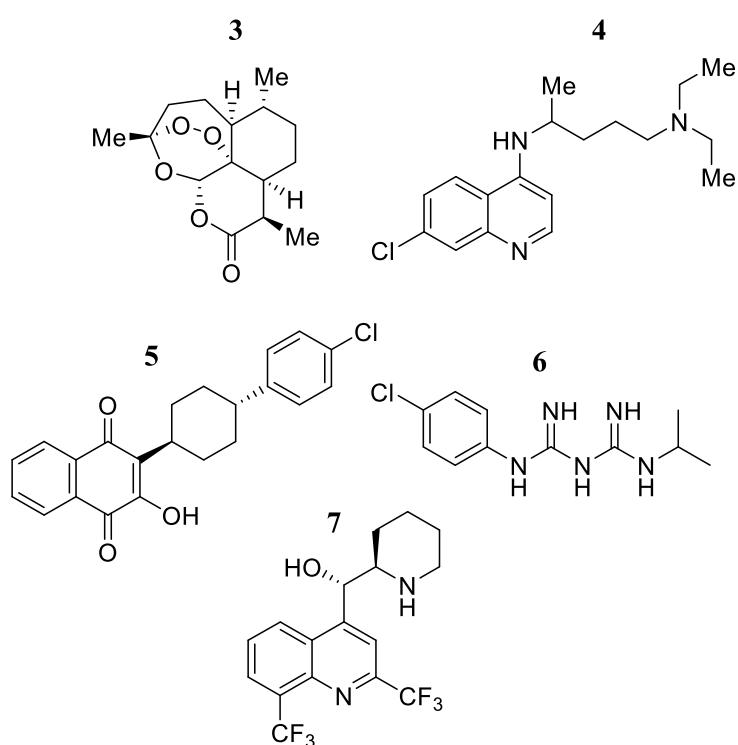
1:2:1 Prevention, treatment and elimination

Despite an increase in malaria intervention over the past two decades, malaria still causes the most fatalities and is the most prevalent parasitic disease facing humans to date. The disease is transmitted across poverty afflicted countries inhabited by an estimated 3 billion people and is still considered to be endemic in 91 of those 108 countries at the beginning of 2016. ⁽⁸⁾ However, it is estimated that 663 million clinical cases of malaria were averted between 2000 and 2015. Many of the improvements were from: bed nets 68%, artemisinin combination therapies (ACT) 22% and indoor residual sprays 10%. ⁽⁹⁾

However, complacency should not prevail and action is being taken to generate a healthy bank of new antimalarials and insecticides. This project is driven by product development partnerships coordinated by the Medicine for Malaria Venture (MMV), who update their portfolio every three months and the Innovation Vector Control Consortium. The long-term goal is vaccine development, which would ultimately reduce parasite transmission and progress endemic countries to malaria eradication.

Alongside annual MMV reports, an 'Open Access Malaria Box' (MB) has been compiled for malaria with the hope of provoking interest in malaria drug research. ⁽¹⁰⁾ Through use of a high throughput screening (HTS) programme they have highlighted over 400 diverse new compound leads with promising activity against malaria. The compounds compiled have confirmed activities against the asexual intraerythrocytic stages of *P. falciparum* and have low cytotoxicities, but the mechanisms of action are still unknown for the majority. From this, the lead compounds can be exploited as a foundation for research groups, to help the development of new drugs with novel mechanisms of action against this deadly disease.

Furthermore, the target candidate profiles for treatment and prophylaxis have a stringent set of biological traits to filter through new clinical candidates. The candidates are compared to current gold standards for each type of chemotherapy and are as follows: fast parasite clearance Artemisinin **3**; long duration 4-aminoquinolines **4**; relapse prevention and chemo prophylaxis atovaquone **5**/proguanil **6**/mefloquine **7**.⁽¹¹⁾ This new framework provides open access information to create a new strategy for malaria drug development and sustained investment into these programmes is essential to assist the long-term goal of malaria eradication.



In line with the World Health Organisation (WHO) recommendations, Table 3 highlights the target product profiles of drug clinical candidates for both treatment and prophylaxis chemotherapies. The most important feature of a new clinical candidate is to target the parasite *via* an alternative mechanism of action to current drugs, which will help combat the biggest issue in current chemotherapies, parasitic resistance.

Treatment	Prevention
<ul style="list-style-type: none"> - Single exposure - Radical cure of all five species infecting humans - Clinical transmission blocking - Affordable 	<ul style="list-style-type: none"> - Single exposure/affordable - Suitable for mass administration at infrequent intervals (one per month) - Chemo-protection against all five species infecting humans
<ul style="list-style-type: none"> - Fast parasitic clearance - Long duration/post treatment - All lifecycle stages - High barrier to resistance 	<ul style="list-style-type: none"> - Different mechanism of action

Table 3: Attributes desired to target parasite elimination ⁽¹¹⁾

A specific report was published by MMV for *P. falciparum*, as this severe strain results in 90% of fatalities and highlighted desirable attributes for potential chemotherapies targeting this species (see Table 4).

Desired feature	Resolution
Combination therapies	Decrease the resistance opportunities
Maximum of 3-day dosing	Once/twice daily helps keep costs low and patient compliance
Development of fixed combination doses	Avoids misuse compared to monotherapies
New mechanism of action	To tackle resistant strains
Effective as a paediatric and adult chemotherapy	Infants and children under 5 years have highest mortality rates

Table 4: Summary of *P. falciparum* drug attributes ⁽¹²⁾

The majority of current chemotherapies target the early blood stage of the malaria lifecycle, due to the symptomatic display from the patient. However, parasite targets fall into several categories to target both host and vector stages such as; blood stage, growth/replication

within infected erythrocytes, sexual stage, liver stage and insect stage. ⁽¹⁾ An ideal drug candidate would possess activity against several stages of the parasite life cycle.

1:2:2 Medicine for Malaria Venture reports (2014–2016)

In 2013, 198 million cases of malaria occurred globally of which, 82% arose in African WHO regions, 12% in South East Asia WHO regions and 5% in East Mediterranean WHO regions (see Table 5). Of those cases, 584 000 deaths resulted, with 90% of mortalities occurring in the WHO African regions and 78% of those occurred in children aged 5 and under.

Year	N° of cases/million	WHO region percentage of cases/%		
		African	South East Asian	East Mediterranean
2013	198	82	12	5
2015	214	88	10	2
2016	212	90	7	2

Table 5: Summary of malaria cases over 3 years

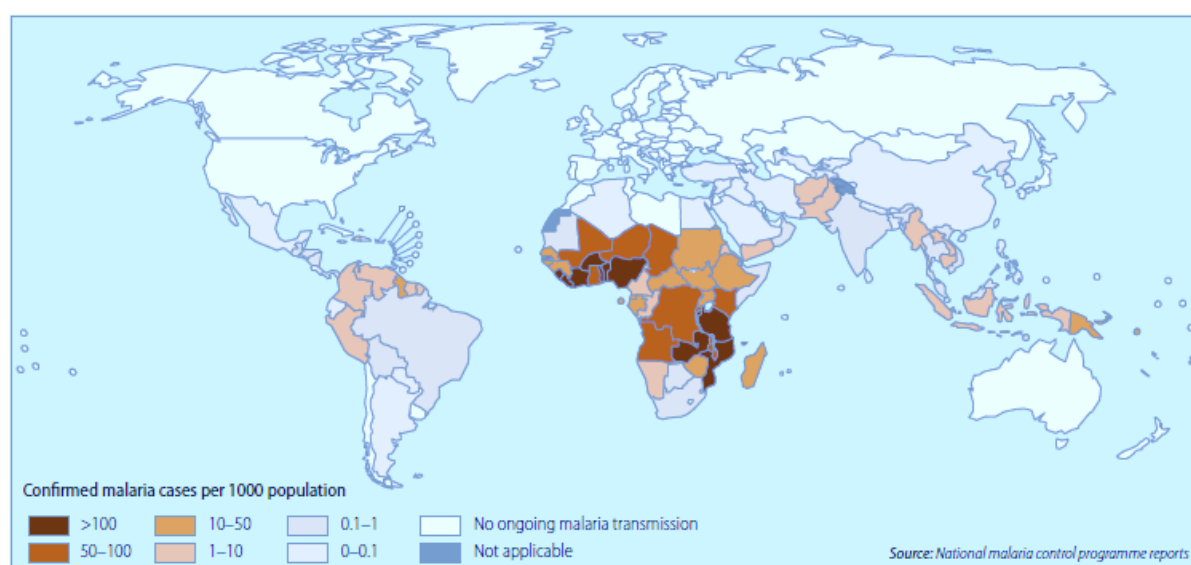


Figure 3: Global malaria cases in 2013 ⁽¹³⁾

Furthermore, 128 million people were infected with *P. falciparum* in sub-Saharan Africa at any one time, with 37 million infectious cases in Nigeria and 14 million infectious cases in Democratic Republic of the Congo (see Figure 3). ⁽¹³⁾

Funding for control and elimination totalled US\$ 2.7 billion in 2013 and the report details future plans to decrease malaria cases. Substantial funding was proposed for preventative

strategies including: increased distribution of insecticide-treated nets (ITNs) for pregnant women and children 5 and under specifically, long lasting insecticidal nets (LLIN), indoor residual sprays and wider distribution of diagnostic tests. Also, treatment strategies prioritise the expansion of access to artemisinin combination therapies (ACTs). Shortfalls in access to prevention/diagnostic testing and post-infection chemotherapies were due to low levels of education and poverty, with a high proportion of malaria sufferers not seeking care or receiving treatment that was available. ⁽¹³⁾

In 2015, there were 214 million cases of malaria infection and considering population growth, this results in a decrease of cases by 37% from the year 2000. Furthermore, of these 214 million cases: 88% of cases occurred in the WHO African regions, 10% in South East Asia WHO regions and 2% in East Mediterranean WHO regions (see Table 5). The country persistent with highest mortality was the African WHO region, of which 438 000 deaths occurred. The mortality rate for children under 5 decreased from 723 000 in 2000 to 306 000 in 2015, but despite these improvements malaria remains a prevalent killer of children – particularly in sub-Saharan Africa, taking the life of a child every 2 minutes (see Figure 4).

(14)

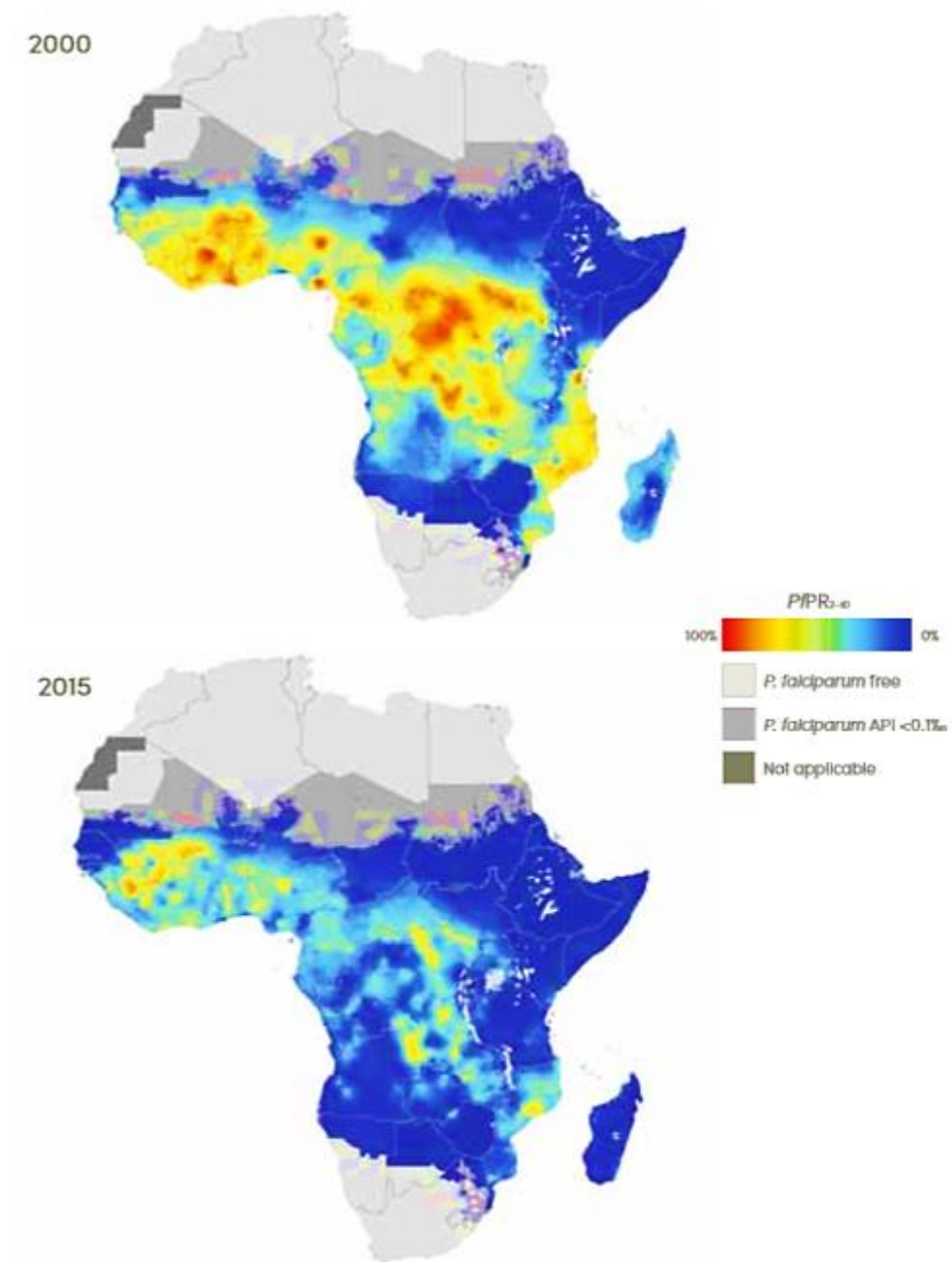


Figure 4: Estimated *P. falciparum* infectious cases amongst children aged 2–10 years ⁽¹⁴⁾

Proposed strategies still consist of those set in the 2014 report, but despite progress there is a slow decline of cases in high-burden countries and access to essential prevention services and post-infection chemotherapies are still primary issues.

Highlighted in the 2016 report is an urgent movement to relieve the malaria burden and the WHO have strategized an accelerated programme titled ‘Action and Investment to defeat malaria 2016–2030’. ⁽⁸⁾ The programme details the importance of open access to interventions for malaria prevention, diagnosis and treatment, and this will allow advanced progress in the elimination of the malaria burden.

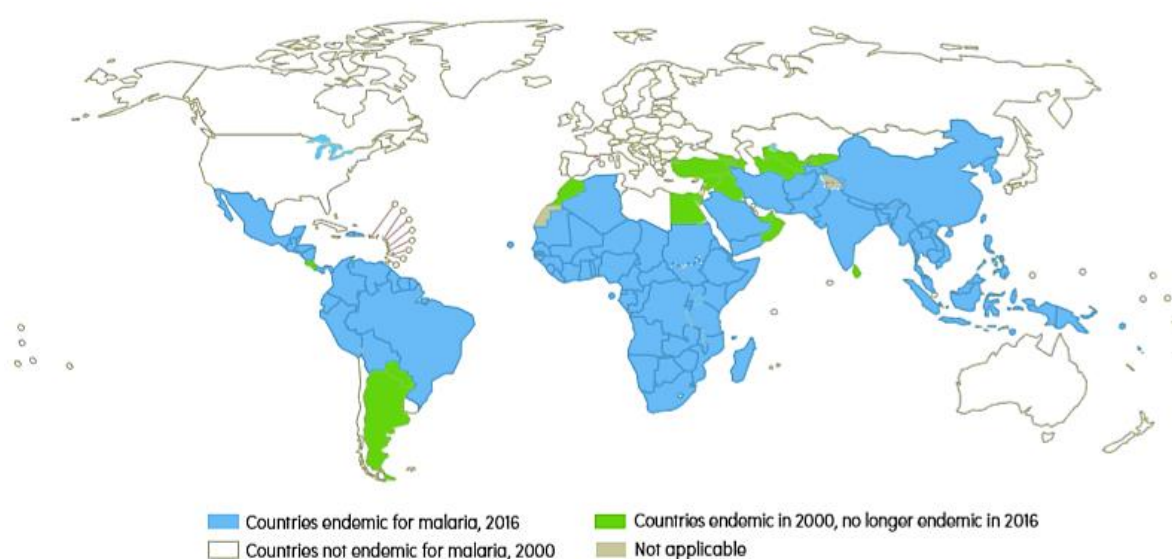


Figure 5: Countries remaining endemic for malaria in 2016 ⁽¹⁰⁾

Figure 5 displays the countries which remain endemic for malaria in 2016 and the projections for 2030 aim to: reduce malaria cases and malaria mortalities by $\geq 90\%$, eliminate malaria from at least 35 of the infected countries and, prevent re-establishment of malaria in all countries that are malaria free. ⁽⁸⁾

To summarise, over the past three years each report has highlighted the overall improvement in malaria prevention and treatment since the year 2000, reducing deaths by 50%. However, in more recent years the milestones are not as advanced and indicate a need for new chemotherapies with novel mechanisms of action to target the growing issue of resistance. Meanwhile, a continued effort to widen the access to ITNs, other prevention strategies and

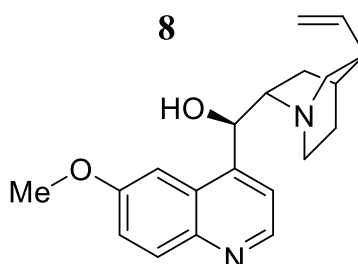
diagnostic testing for poverty-stricken countries is necessary upkeep. Furthermore, the information gathered from individual research groups needs to be shared on an open network, to increase the awareness of new parasite targets, to subsequently generate novel antimalarials.

1:3 Antimalarial chemotherapies

1:3:1 Quinine and Chloroquine

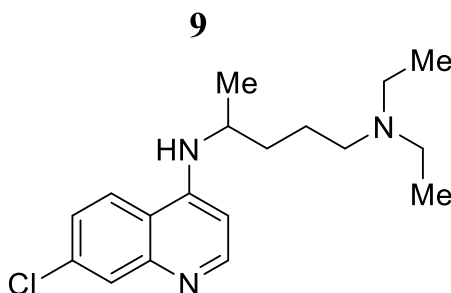
1:3:1:1 Historical Malaria Chemotherapy

In 1820 two French chemists, Pierre Joseph Pelletier and Joseph Caventou isolated quinine **8** from the South American native cinchona tree bark. The use of its medicinal tree bark has been dated back to the 17th century and became a treatment of reference for intermittent fever throughout the world. ⁽¹⁵⁾ Furthermore, since the 1940's this antipyretic drug has been used as an antimalarial treatment and despite the widespread discovery of quinine resistant parasite, it remains an important and effective treatment for severe malaria cases. Quinine is an alkaloid which consists of an aromatic quinoline ring system connected to a tertiary amine *via* a hydroxymethine moiety.



The antimalarial mechanism of action is still unknown however, it is documented to act on the blood schizont stage and interferes with the parasites ability to digest haemoglobin, which results in a toxic accumulation of haem, causing parasite death. ⁽¹⁵⁾ Additionally, it has shown gametocidal activity in *P. vivax* and *P. malariae*, but not in *P. falciparum*. Quinine is a weak base, and therefore concentrates itself in the acidic pH food vacuole of *P. falciparum* and has a rapid onset of action, reaching peak concentration 1–3 hours after dosing. Furthermore, quinine readily crosses the placental barrier and has also been ascertained in cerebral fluid, which is an important feature for severe cerebral malaria treatment. ⁽¹⁵⁾

Meanwhile, a more efficacious and less toxic antimalarial is a derivative of **8**, chloroquine **9**, which was developed by German scientists in 1934.



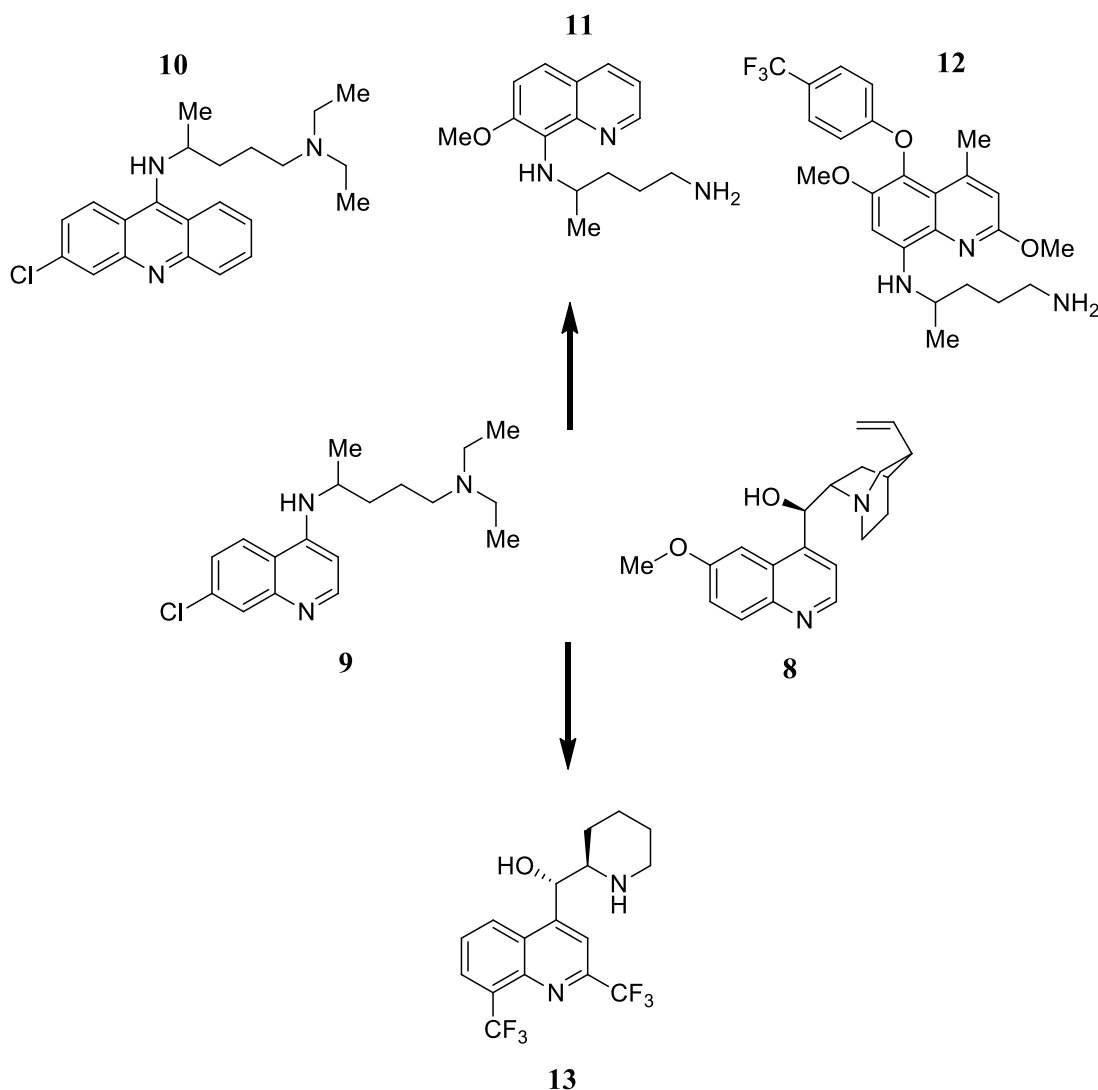
From 1947 the use of chloroquine was extensive, and it was subsequently listed as a World Health Organisation essential medicine for antimalarial eradication.⁽¹⁵⁾ As a result, over the next 50 years chloroquine resistant *P. falciparum* was discovered: in 1957 in four separate locations along the Thai-Cambodian border; in 1960 in Venezuela and parts of Columbia; in the mid 1970's in Papua New Guinea and; in 1978 in Kenya and Tanzania, spreading to Sudan, Uganda, Zambia and Malawi in 1983.^(15,16) This led to the resurgence of quinine use in cases where the infected patient did not respond to chloroquine. To date, chloroquine is used as the 'gold standard' in biological assay testing as the positive control.

1:3:1:2 Derivatives

Since the discovery of quinine **8** and subsequently chloroquine **9**, the natural product scaffold has been retained to synthesise a variety of synthetic antimalarial derivatives. To obtain quinine, an extraction process of the natural tree bark was necessary, but this was lengthy and consequently did not fulfil demand. This propelled the optimisation of the quinine structure shown below are a variety of derivatives that have been synthesised since the 1920's.

Prior to the discovery of compound **9**, quinacrine **10** was developed by Bayer and approved in 1930 to treat malaria, and even though it provided no stronger efficacy or physiochemical advantages over compound **8**, the compound could be synthetically generated to meet demand. ⁽¹⁷⁾ Not only does quinacrine have antimalarial potency, but it also displays anticancer potential. The compound has been shown to act on breast and colon cancer by interfering with the S phase of the cell cycle (DNA replication stage), resulting in cancer cell death. ⁽¹⁷⁾

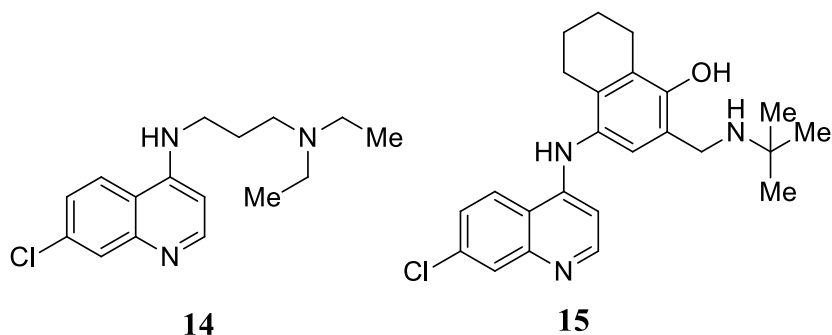
On the other hand, in 2014 primaquine **11** was shown to inhibit pyridoxal kinase (allows conversion of ATP to ADP through phosphorus transfer), which effects interaction of the parasite mitochondria, resulting in the energy supply of the cell being cut off, causing parasite death. ⁽¹⁷⁾ This derivative is primarily useful in the hepatic stages of *P. vivax* and *P. ovale* infections, as it prevents a relapse infection occurring. To date, it is the only marketed antimalarial with the key feature of hypnozoite activity, however tafenoquine **12** is now in phase III clinical trials for *P. vivax* hypnozoite treatment. ⁽¹⁶⁾



Due to high antimalarial demand, in the 1980's mefloquine **13** was used to treat infected patients before phase III clinical trials had been completed and has questionable side effects concerning the nervous system and gastro intestines, which now appear on the packaging as a warning. ⁽¹⁶⁾ Marketed at Lariam, compound **13** can cause serious neuropsychiatric side effects that can persist after treatment withdrawal. The type of neurological symptoms which can occur include: dizziness, tinnitus and loss of balance. Also, psychiatric symptoms experienced by some patients include: suicidal thoughts, depression, anxiety and vivid dreams therefore, mefloquine is not recommended in the use of patients who have a history of psychiatric problems. Lariam is more effective than both quinine and chloroquine and like quinine, results in the accumulation of toxic haem. This analogue also interacts with

phosphatidylinositol, which blocks the membrane transport system through inhibition of this particular group of lipids from regulating intracellular signalling.⁽¹⁷⁾

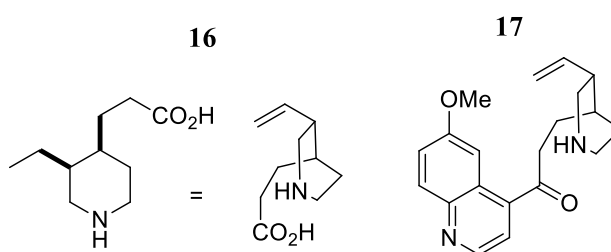
Further structural derivatives arose in the early 1990's from investigating shortening of the alkyl chain (AQ13, **14**) and the addition of an aromatic component (naphthoquine, **15**), with the former being active against chloroquine resistant malaria.



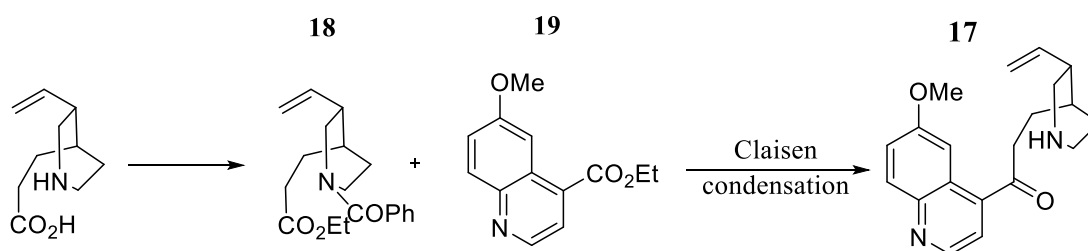
The partner compound **15** can be found within a fixed-dose Artemisinin combination therapy and is recommended as a single-dose treatment for malaria and is marketed in Papua New Guinea among other tropical countries.⁽¹⁸⁾

1:3:1:3 Synthesis

Since publication of the ‘total synthesis of quinine’ in 1945 by Woodward and Doering, consistent discussion has been carried out as to whether the collaboration synthesised the chiral 4-aminoquinoline. The total synthesis of quinine attributed to the Nobel Prize given to R. B. Woodward in 1965, for his outstanding achievements in organic synthesis. Both himself and Doering state ‘they had succeeded, where generations of great scientists had failed’. However, a review of the quinine synthetic journey concluded what they actually obtained was *d,l*-homomeroquinene **16** and isolated *d*-quinotoxine **17**.⁽¹⁹⁾

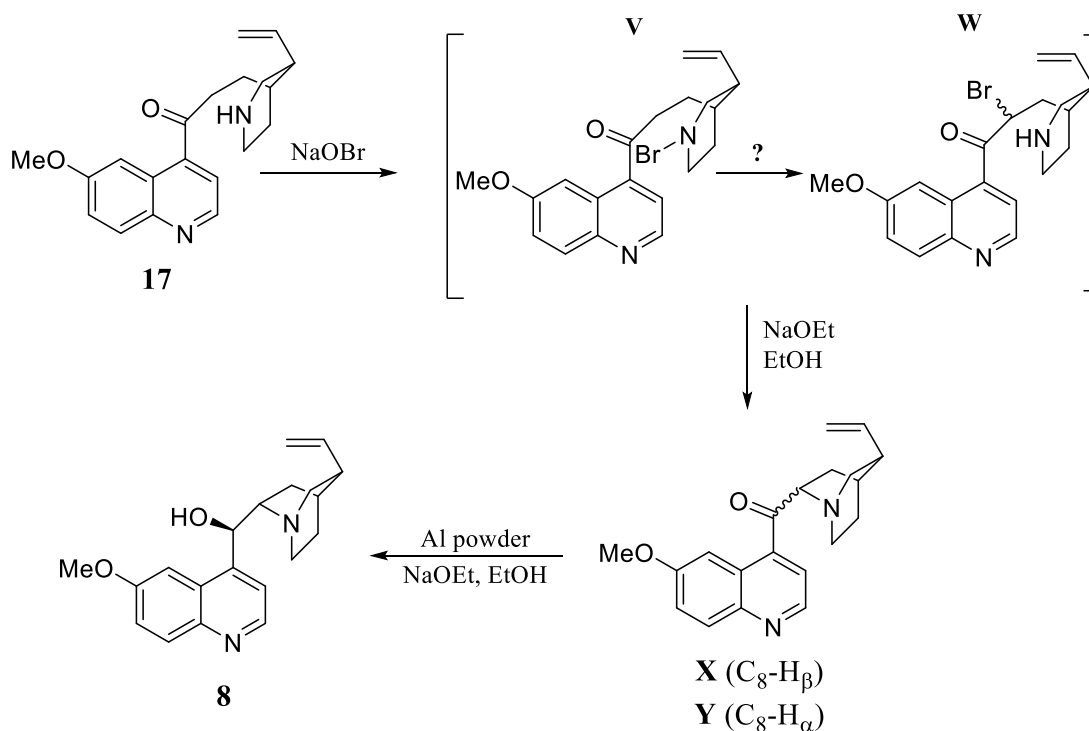


Also, previous research conducted in 1943 by Proštenik and Prelog obtained non-racemic homomeroquinene from degradation of the natural product cinchonine. They performed a Claisen condensation reaction and generated a β-keto ester protected intermediate **18**. This was then combined with 4-quinoline carboxylate **19** in another condensation reaction to give **17** (see Scheme 2). Their contribution is highlighted in the review and they state the synthesis of quinine should be referred to as the Woodward-Doering/Proštenik-Prelog/Rabe-Kindler total synthesis of quinine.



Scheme 2: Proštenik-Prelog synthesis

In 1918 fellow chemists Rabe and Kindler performed a 3-step conversion of **17** into **8** and were ‘the first’ to synthesise this illusive compound. They based their confirmation on the physical properties of quinine i.e. melting point and optical rotation measurements (see Scheme 3).⁽¹⁹⁾



Scheme 3: Rabe and Kindler conversion of *d*-quintoxine **17** into quinine **8**⁽²⁰⁾

The first step involves bromination of *d*-quintoxine with sodium hypobromate to generate proposed intermediate **V** but, intermediate **W** was also highlighted. Rabe and Kindler proposed that based on their primary observations intermediate **V** did not react with methyl iodide therefore, it was unlikely **W** had been formed. The next step in the synthesis takes **V** and reacts it with sodium ethoxide in ethanol to generate quinonone **X** and its less soluble epimer quinidinone **Y**. Treatment with sodium ethoxide in ethanol has two effects: to cause cyclisation to **X** and **Y** and, to establish an equilibrating mixture of these two ketones. They did not fully understand in 1918 that both **X** and **Y** are formed and interconverted under basic conditions. This observed interconversion is critical for the next step which involves reduction with aluminium powder alongside sodium ethoxide in ethanol. It is unknown if

Rabe and Kindler used a pure source of compound **Y** or a mixture of **X** and **Y** but, it is not important as the presence of sodium ethoxide and ethanol ensure conversion between **X** and **Y**. Issues surrounding this procedure outlined by Rabe and Kindler arose due to no experimental detail being published in the original paper and could therefore not be replicated. When Doering was questioned about the replicability of Rabe's work he said, 'it is almost never possible to reproduce published details. They assume an indefinable amount of experience and cannot be written for the first time cook who has never mastered the elementary techniques.'

It wasn't until 2001 when Stork *et al* published the first stereoselective synthesis of quinine, generating 22% of the desired product over 15 steps.⁽²¹⁾ Due to the multistep synthetic route used to generate quinine, it would not be viable to scale up to bulk production and would not produce high enough overall yield to be worthwhile. To date, the most effective way to obtain quinine for antimalarial purposes is through extraction from its natural source, cinchona tree bark.

1:3:2 Artemisinin

1:3:2:1 Antimalarial history

A common herb used by Chinese herbalists for thousands of years, Artemisinin was first isolated in the early 1970's by Chinese scientists from the *Artemisia annua* plant, also known as sweet woodworm (see Figure 6). The promising compound was found to be efficacious as an antimalarial and possessed comparable activity to quinine and chloroquine. Artemisinin quickly became a first-line of defence malaria treatment, particularly in South-East Asia.



Figure 6: Sweet woodworm

Artemisinin **20** is a fast acting antimalarial and useful in the treatment of severe cases of malaria, but it is also eliminated rapidly following administration to the patient. Even though the mechanism of action is unproven, reports have highlighted that the endoperoxide moiety present is necessary for antimalarial activity.⁽²²⁾ It is noted this moiety is a source of a reactive oxygen species (ROS), which generate free radicals. ROS can consist of radical and non-radical oxygen containing species for example, a hydroxyl radical or hydrogen peroxide. They are produced endogenously within mitochondria but can also arise from exogenous sources such as, xenobiotic compounds. Furthermore, high levels of ROS within the body

can result in oxidative stress which leads to ROS-mediated damage of: nucleic acids, proteins, lipids and has been implicated in neurodegeneration, diabetes and aging. ⁽²³⁾

The parasite is rich in haem-iron and this subsequently activates artemisinin, through catalytic activation (see Figure 7). This results in the artemisinin derived free radicals damaging intracellular components within the parasite (it is hypothesised *via* alkylation). There are multiple proposals of action involving the artemisinin-derived free radicals for example, artemisinin forms covalent bonds with haem and prevents the digestion of haemoglobin and protein alkylation. ⁽²²⁾ Not only do these endoperoxides have activity against erythrocytic stages of the parasite, particularly the ring stage, but also against gametocytes which helps prevention of transmission.

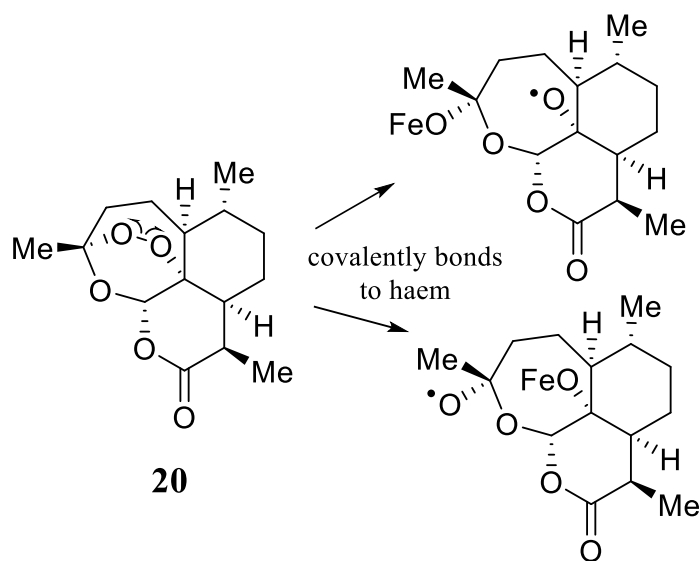


Figure 7: Artemisinin and free radical formation

Since the eruption of its use against malaria, cases of artemisinin resistant malaria have been commonly reported since 2009. To tackle the primary issue of resistance artemisinin-combination therapies (ACTs) replaced first-line of defence drug treatments in 79 countries.

⁽⁹⁾ This decision has played a key role in the overall motion of malaria eradication. Resistance initially grew along the Cambodia-Thailand border, which has resulted in higher rates of failure to ACTs. It has been reported in some parts, that the malaria strain observed is

resistant to four different ACTs (see Figure 8). ⁽⁸⁾ Decreased parasite clearance rates have been seen in patients and more recently, resistance is wide spread across South-East Asia. ⁽²⁴⁾ The role of ACTs is to provide a paired mechanism of action approach, which helps to reduce the cases of resistance. The artemisinin component reduces the biomass of the parasite and combined with a relatively slow acting drug, can reduce parasite burden and proves an effective chemotherapy.

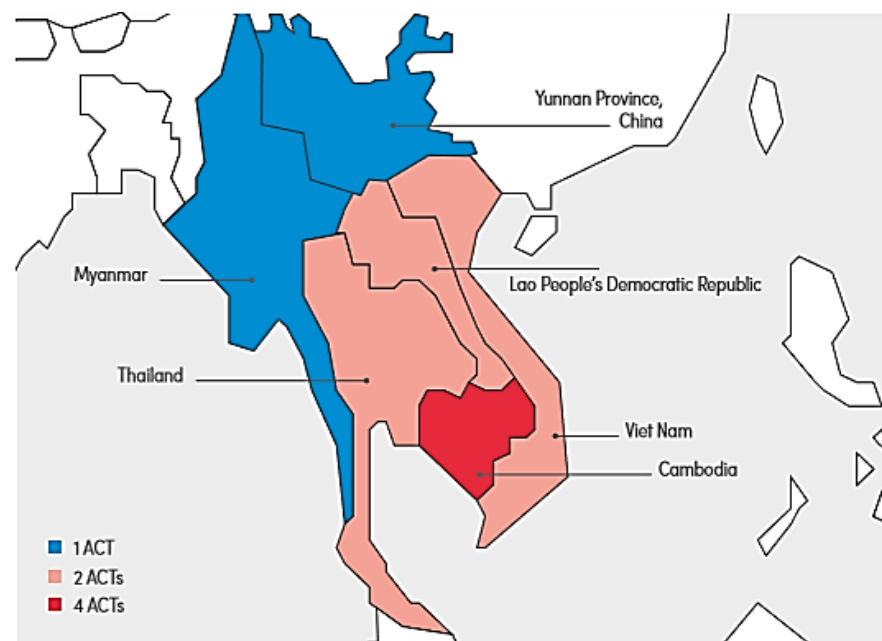
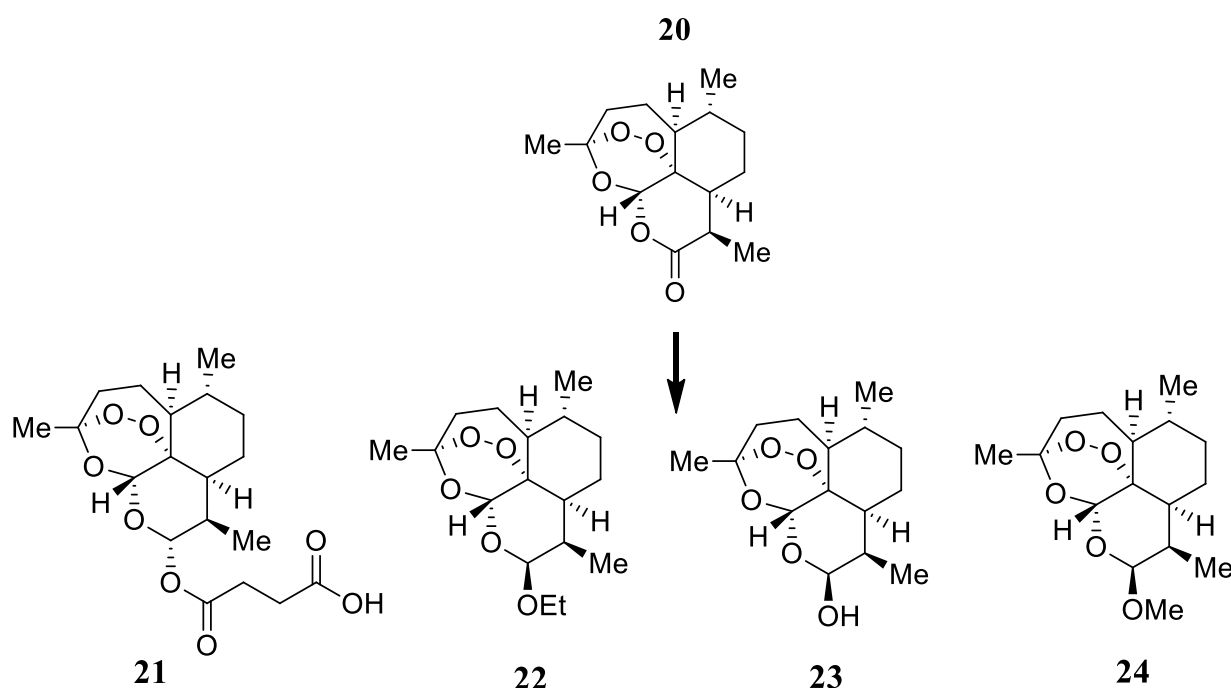


Figure 8: Migration of ACT resistance ⁽⁹⁾

1:3:2:2 Derivatives and ACTs

The endoperoxide class of antimalarials are the most widely used compounds as both monotherapies and combination therapies in chloroquine resistant malaria. The primary derivatives are; artesunate **21**, arteether **22** dihydroartemisinin **23** and artemether (ART, **24**), with the latter semisynthetic compound being significantly more effective than the other derivatives. The derivative **24** has demonstrated haemoglobin consumption within the parasites digestive vacuole, which generates ROS *via* oxidative stress and ultimately causes death of the parasite. Furthermore, ART has been found to inhibit the calcium ion transport protein PfaTP6, resulting in calcium ion homeostasis disruption within *P. falciparum*.⁽¹⁷⁾



Derivative **21** is the most frequently prescribed derivative and intravenous artesunate is most popular for cerebral malaria, as the free carboxylate moiety enhances water solubility.⁽¹⁶⁾ In combination with a drug partner possessing a longer half-life, several therapies exist which combine these endoperoxides with alkaloid derivatives such as: Coartem (artemether-lumefantrine **25**), artesunate-amodiaquine **26**, artesunate-mefloquine **27** and artesunate-sulfadoxine-pyrimethamine, in the hope of reducing resistance cases.

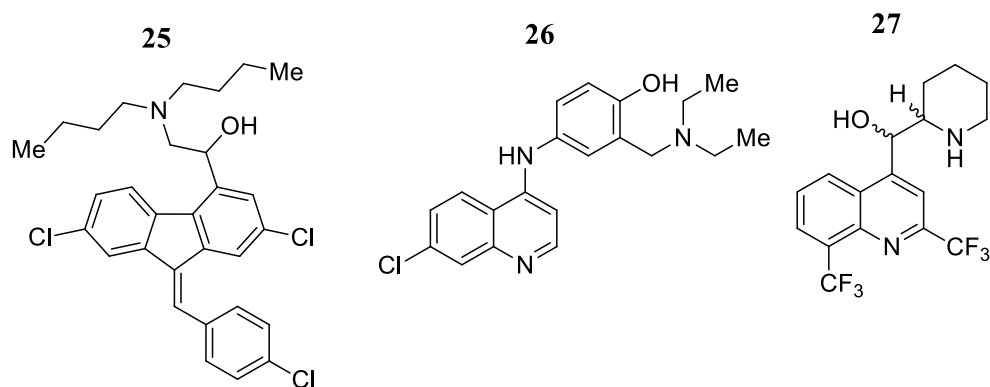


Figure 9 displays a future hybrid antimalarial, which has been designed to combine fast acting artemisinin and chloroquine derivative, primaquine. This futuristic compound has been found to target both blood and liver stage parasitaemia and is currently under investigation in early *in vivo* studies.⁽¹⁶⁾

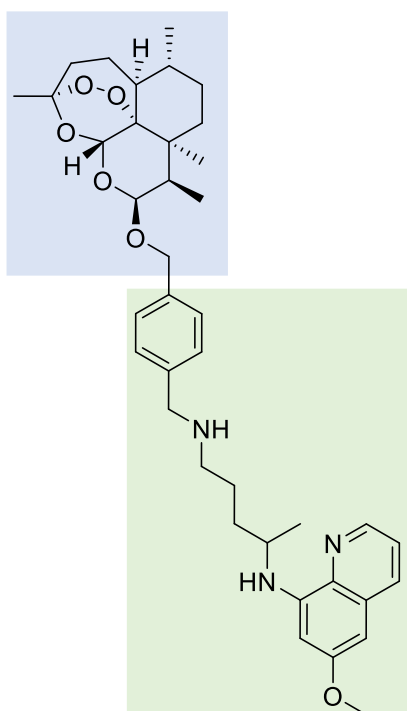
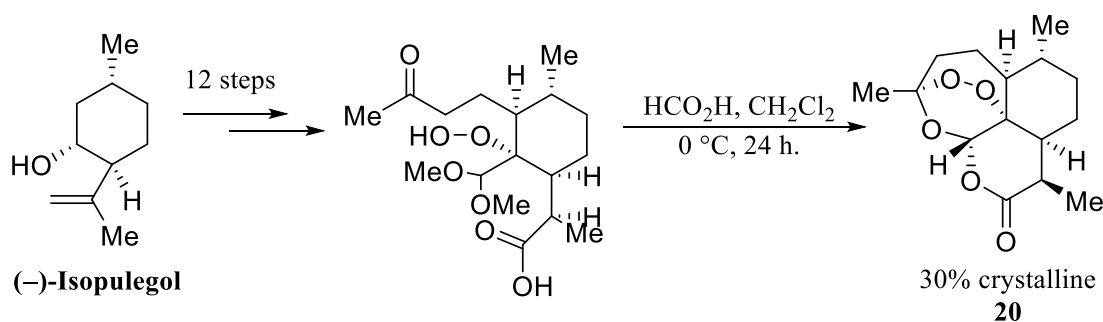


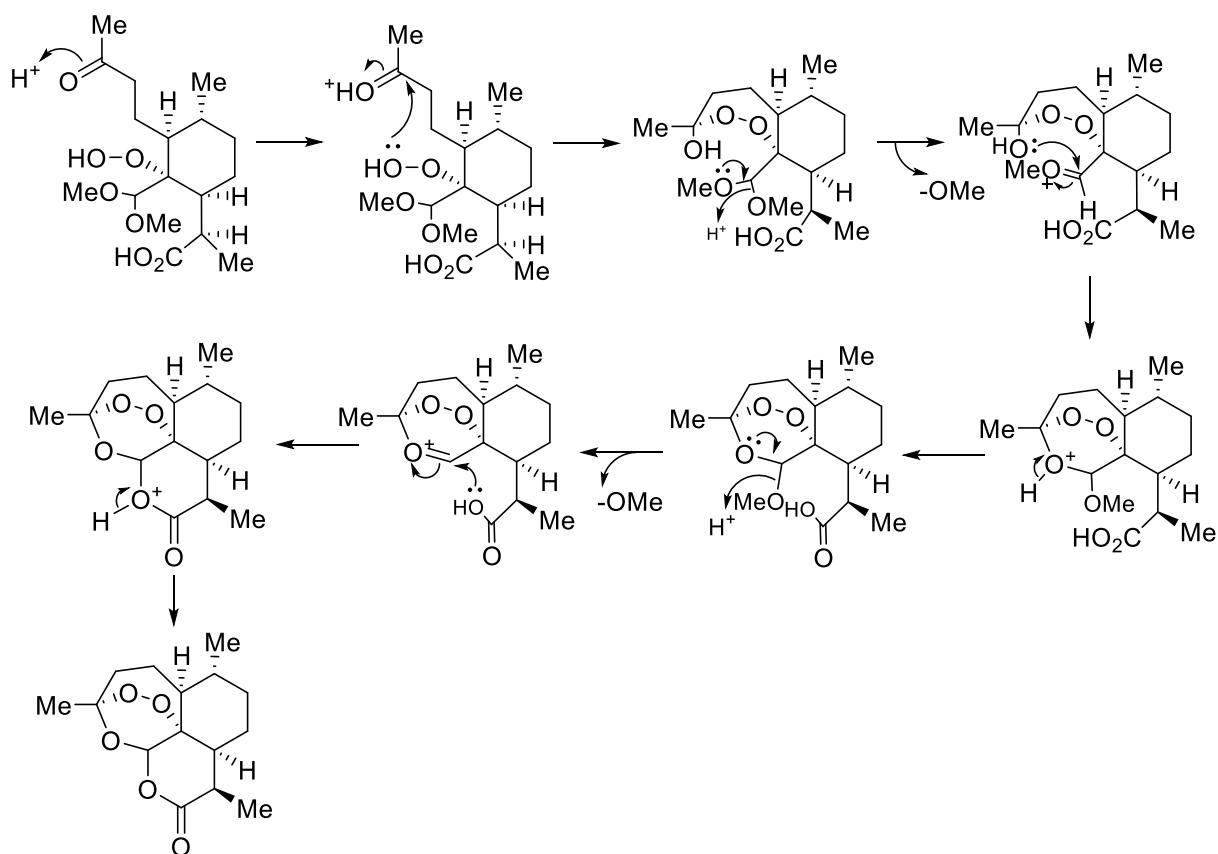
Figure 9: Future multistage antimalarial

1:3:2:3 Synthesis

Like quinine, the only viable means of sourcing artemisinin is through extraction of the active component from its natural plant source, which leads to high extraction costs to meet desired demand. In 1983 Schmid and Hofheinz synthesised artemisinin from (–)-Isopulegol and over a 13-step synthesis they generated the natural product in a 5% yield (see Scheme 4).⁽²⁵⁾



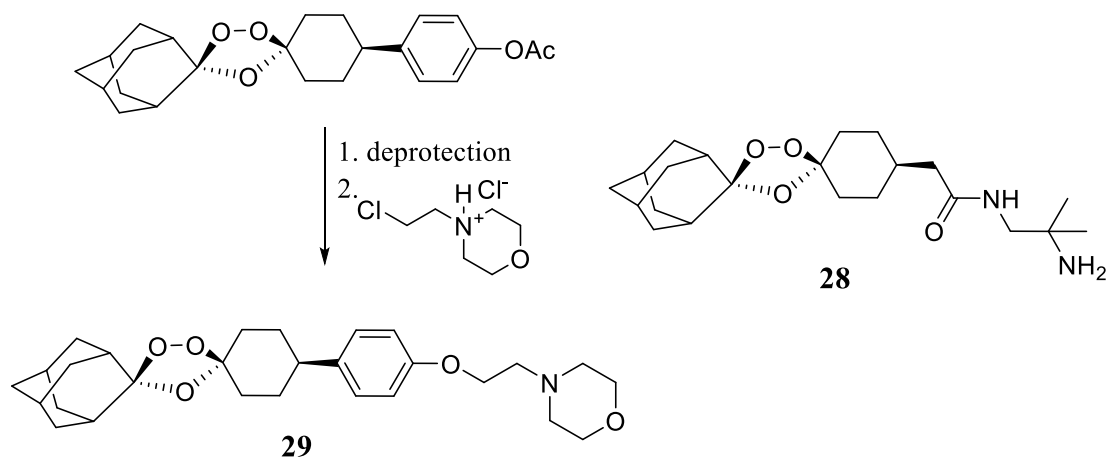
Scheme 4: Artemisinin synthesis



Scheme 5: Peroxide formation

Scheme 5 shows one possible mechanistic pathway to generate Artemisinin. Step 2 highlights the key peroxide bond formation followed by an S_N1 reaction eliminating methanol. Step 6 shows a second S_N1 reaction that generates the final carbonyl electrophile which is attacked in step 7 to create a new 6 membered ring seen in step 8.

Significant efforts have been made to investigate synthetic and semi-synthetic artemisinin analogues. For example, OZ277 **28** was the first synthetic ozonide to be evaluated clinically and is now in phase III clinical trials as a combination therapy with piperazine phosphate.⁽²⁶⁾ However, it displays reduced plasma exposure as well as a short half-life *in vivo*. From this, an optimisation compound OZ439 **29** was generated and shows improved pharmacokinetic properties as well as proving to be a very successful clinical candidate (IC₅₀ of 3.4 nM against *P. falciparum*, see Scheme 6).



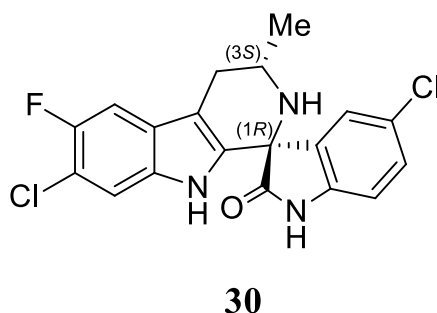
Scheme 6: Synthetic route to **29**

Furthermore, enzymes present in *A. annua*, which take part in the bioproduction of the artemisinin precursor, artemisinic acid, have been cloned into bacteria. This biological approach alongside a fermentation process has allowed partial biosynthetic artemisinin to be synthesised.⁽¹⁶⁾ Despite these advances in synthetic progress, the sheer demand for a successful chemotherapy requires the drug to be cheap and easily prepared.

1:3:3 Upcoming clinical candidates

1:3:3:1 NITD609

The most promising candidate in 20 years, NITD609 (also known as Cipargamin, **30**), possess a novel mechanism of action and within the last year has completed a phase IIa clinical trial study. This highly potent compound has an IC₅₀ of 1 nM against *P. falciparum* and has shown rapid suppression of protein synthesis in the parasite, in fact, it has demonstrated protein synthesis blocking within 1 hour of exposure. ^(27,28) Not only have extensive studies highlighted NITD609 to possess high potency against symptomatic asexual stages of the parasite but also, shown to be as efficacious against early and late stage gametocyte development. ⁽²⁹⁾ Therefore, the hit compound inhibits several stages of the parasite lifecycle and prevents transmission of the parasite through prevention of fertilisation within the mosquito midgut.



Yeung *et al* investigated the structure-activity relationship of this spiro-tetrahydro- β -carboline and highlighted the important features which are important for antimalarial activity. ⁽³⁰⁾ Firstly, the 1*R*, 3*S* configuration is essential for activity, as they tested several derivatives with a 1*S*, 3*R* stereocentre and for the majority resulted in a complete loss of activity. Meanwhile, the chlorophenyl moiety contributed a balance between potency, favourable pharmacokinetics and synthetic accessibility. Also, analogues with varying central carbon ring sizes were tested for example, they increased the ring size to 7 and 8

carbon rings, this small change resulted in compound inactivity. Finally, the single methyl group enhances potency 5-fold, whereas alternate *n*-propyl and *gem*-dimethyl bulky groups decreased antimalarial potency (see Figure 10).⁽³⁰⁾

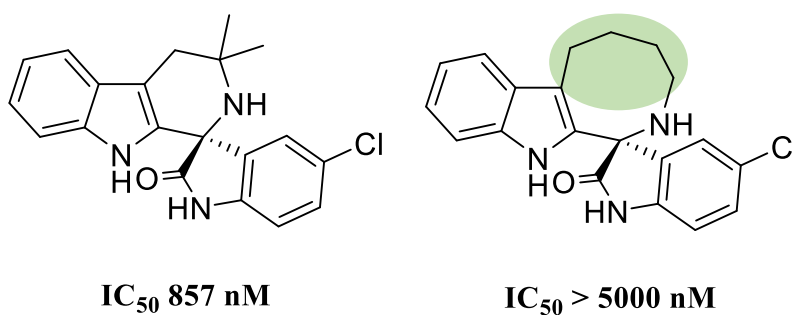


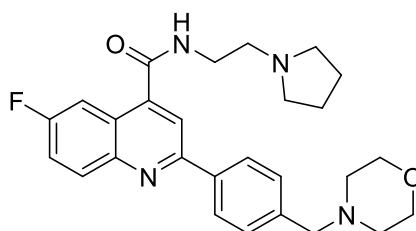
Figure 10: Investigation of the SAR

Further details and discussion on the structural and biological evaluation of NITD609 can be found in Chapter 3.

1:3:3:2 DDD498

In a collaboration with the University of Dundee Drug Discovery unit, a highly potent quinoline multistage chemotherapy was uncovered, DDD498 (also known as, MMV121).

⁽³¹⁾ This potent antimalarial shown in Figure 11 has shown activity against: resistant parasite strains, possess a long half-life and inhibits gametocyte formation, as well as liver stage and blood stage parasites. This unique multi-stage compound was discovered *via* a screening of over 4700 antimalarial active compounds.



P.falciparum activity

Blood stage **IC₅₀ 1 nM**

Blood Stage gametocytes **IC₅₀ 1.8 nM**

Mosquito Stage **IC₅₀ 5 nM**

Figure 11: Lead compound DDD498

However, the initial hit required further medicinal chemistry optimisation as it was too lipophilic and metabolically unstable. Firstly, swapping bromine for fluorine reduced ClogP and subsequently replacing pyridine with an alkyl chain and tertiary amine increased solubility and metabolic stability. Finally, the addition of a morpholine group dramatically: increased *in vivo* potency, further reduced logP, increased metabolic stability and increased solubility (see Figure 12). ⁽³²⁾

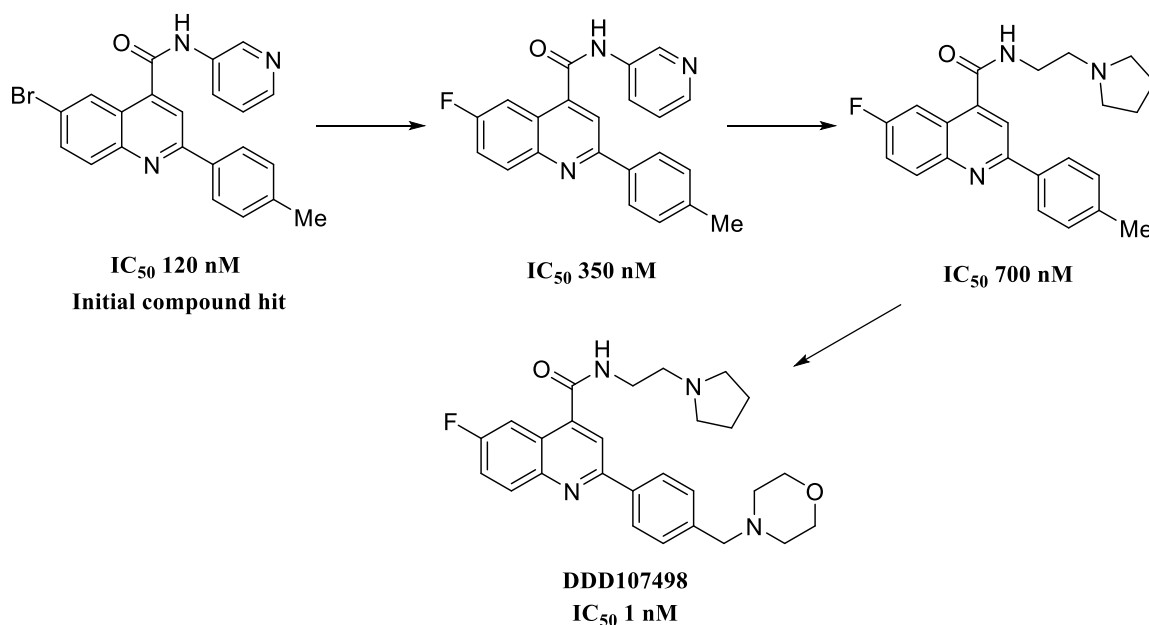


Figure 12: Synthetic route to DDD498

Although not fully understood, the mechanism of action is thought to target translation elongation factor 2, which coordinates tRNA and mRNA moving through the ribosome (disrupts protein synthesis). This theory is supported by the compounds ability to target multiple stages of the parasite life cycle.⁽³²⁾ Hit compound DDD498 has now been approved by Merck for progress as a clinical candidate and the compound is predicted to undergo human studies in 2017, after toxicology and pharmacokinetic *in vitro* and *in vivo* studies have been performed to establish safe dosage quantities.

1:3:3:3 MMV390048

In 2014 a highly potent compound entered phase I clinical trials, with the hope of MMV390048 becoming a single dose cure for malaria. The first African-led team at the University of Cape Town Drug Discovery and Development Centre (H3D) synthesised and screened over 350 compounds. ⁽³³⁾ Of the library generated, 8 aminopyridine hits were highlighted with varying aryl group at positions 3 and 5 of the aminopyridine core and displayed >80% parasite inhibition at the screening dose 1.82 μ M (see Figure 13). ⁽³⁴⁾

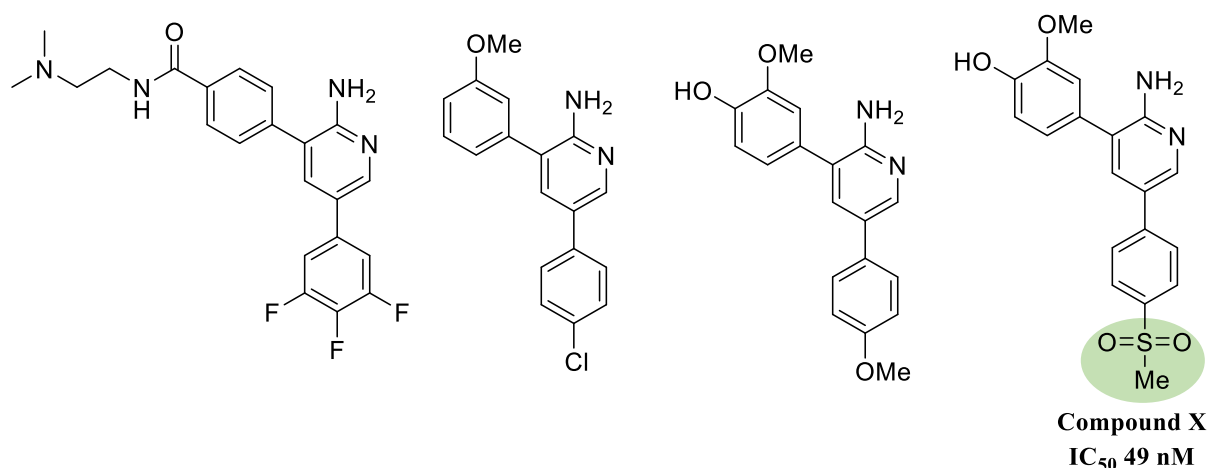


Figure 13: HTS hits

Compounds possessing a methylsulfonyl phenyl substitution at position 5 of the aminopyridine core displayed the best potencies. Therefore, optimisation studies took place using the original hit, compound X which possesses an IC₅₀ of 49 nM. ⁽³⁴⁾

The first stage of optimisation removed the ‘metabolic hot spot’ present on compound X which resulted in the addition of a methoxypyridyl moiety seen in compound Y. Not only did this change increase metabolic stability but also, when tested *in vivo* cured mice with a 50 mg/kg dose after 4-day treatment. Further optimisation replaced the methoxy group with a trifluoromethyl group which increased potency (DDD498, see Figure 14). The MMV compound cured mice of *P. berghei* following a single dose of either 30 or 100 mg/kg which

is significant as chloroquine, mefloquine and artemisinin do not achieve a single dose oral dose cure in the same *P. berghei in vivo* model. From the study DDD498 showed the best activity alongside: good metabolic stability, low potential for CYP450 inhibition, negative Ames test and moderate hERG activity. ⁽³⁴⁾

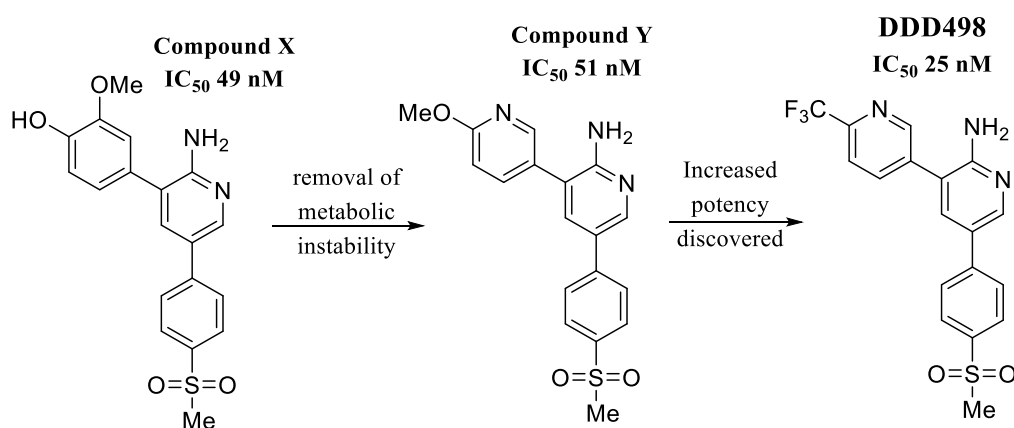
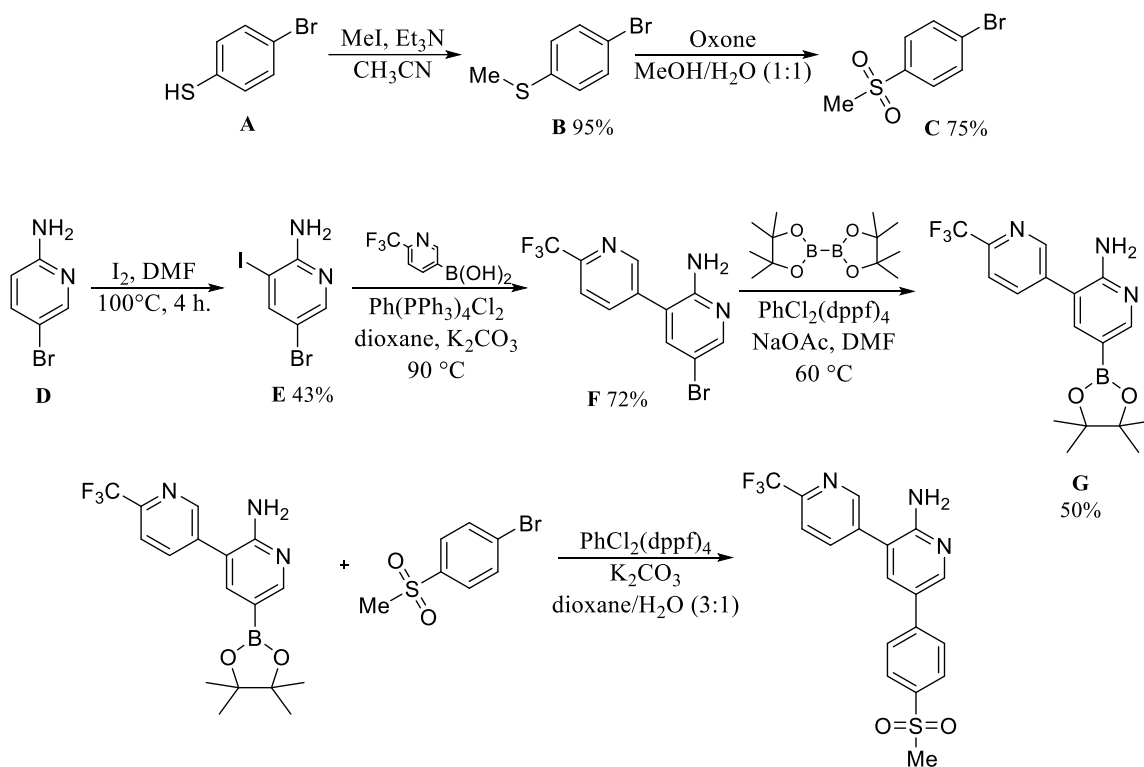


Figure 14: Route to MMV390048

The compound showed promising activity *in vitro* against *Plasmodium falciparum* KI, NF54, 3D7 and Dd2 strains. The mechanism of action is shown to competitively inhibit the binding of a single protein, P14 kinase, which plays a role in phosphorylation of proteins within the cell and in turn affects cell signalling and inhibits the parasites ability to function. Also, it has shown activity against several stages of the parasite lifecycle as well as resistant strains, therefore **DDD498** plays a promising role in the future of malaria control, transmission and eradication.

Firstly, to synthesise this lead compound 4-bromobenzenethiol underwent methylation using triethylamine and methyl iodide. The research group also tested the reaction with potassium carbonate and DIPEA as the base however, both resulted in side products (not included) and low yield of the desired product (35%).



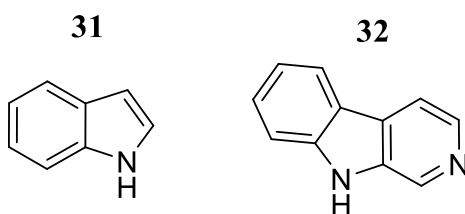
Scheme 7: Synthetic route to **DDD498**

Then, intermediate **B** underwent sulfur oxidation and the resultant sulfone was collected in 75% yield. The oxidised product **C** was kept to undergo Suzuki cross-coupling later on in the synthesis. Next, a boronate ester intermediate was generated over a three-step synthesis and started with iodination of 5-bromopyridin-2-amine **D**. Then, a Suzuki-Miyaura coupling took place with (6-(trifluoromethyl)pyridin-3-yl)boronic acid and intermediate **E**. A catalytic borylation takes place with intermediate **F** and bis(pinacolato)diboron to generate the desired boronate ester in 50% yield. The two intermediates **C** and **G** were combined through Suzuki coupling and the hit **32** was collected in 90% yield.⁽³⁵⁾

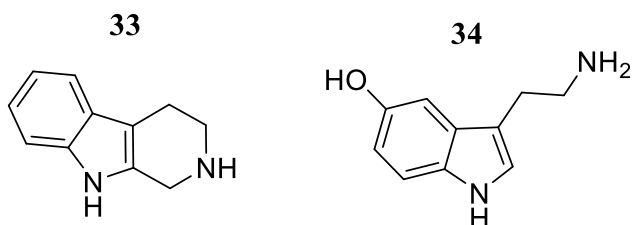
Chapter 2: Tetrahydro- β -carbolines

2:1 Indole alkaloids

An indole core moiety can be found at the structural centre of a variety of biologically active compounds and the majority are found within their natural plant source, for example indole **31** and β -carboline **32**. The diversity surrounding these structures has given rise to compounds possessing activity against numerous biological processes. These compounds have been utilised for decades within the pharmaceutical industry as: antiparasitics, antimicrobials, anticonvulsants, antivirals, and antipsychotics.

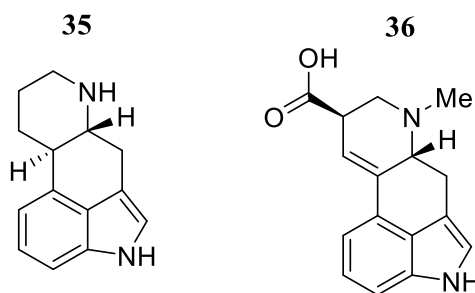


For example, the planar β -carboline structure consists of an aromatic pyridine ring fused to the indole moiety and compounds containing this core have been shown to: intercalate DNA, interact with serotonin/benzodiazepine receptors, and inhibit topoisomerases and monoamine oxidases. ⁽³⁶⁾ Also, on reduction of the pyridine ring a tetrahydro- β -carboline moiety is revealed and an example such as, tryptoline has shown to act as a reuptake inhibitor of serotonin (note the structural similarities between tryptoline, **33** and serotonin, **34**). ⁽³⁷⁾

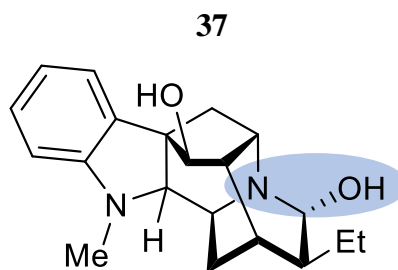


A type of fungi called Ergot produces a wide variety of these alkaloidal compounds. For example, the biological activity of ergoline **35** has been exploited in the treatment of

migraines *via* vasoconstriction and, it has also been investigated in the treatment for Parkinson's disease. Due to the interest in their biological activity to target disease, several derivatives of ergoline have been synthesised. The most common ergoline derivative is lysergic acid, more commonly known as LSD **36** and is an illegal psychedelic compound which has been used recreationally for decades. ⁽³⁸⁾

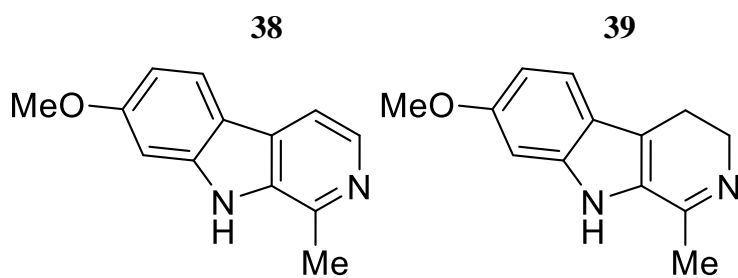


During the 1930's, an alkaloid known as ajmaline **37** was discovered in East Asia and is obtained through extraction of the flowering shrub, snakeroot. This biologically active compound has been utilised in the pharmaceutical industry for its antiarrhythmic properties and works by blocking the sodium channels within a patient who is experiencing an abnormal heart rhythm. It has been suggested that the hemiaminal moiety present in ajmaline is responsible for its activity towards cardiovascular abnormalities. ⁽³⁹⁾



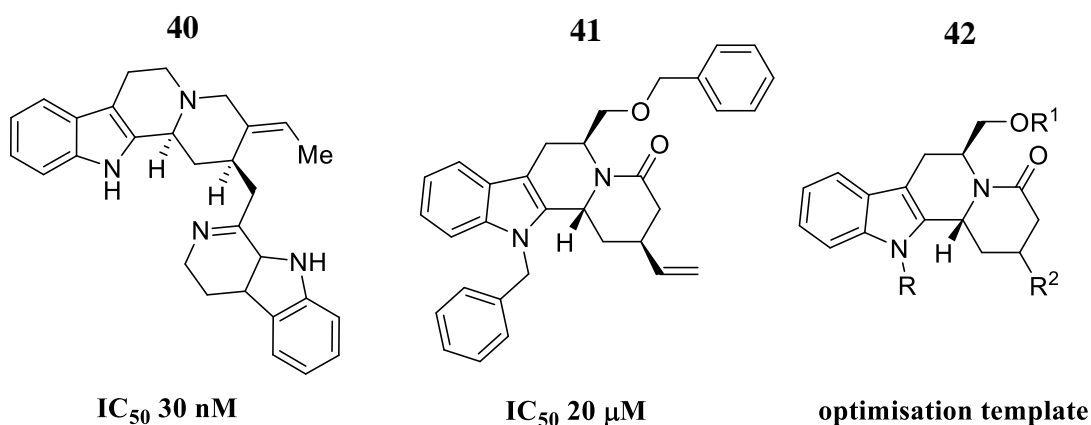
More recently, alkaloids found within the seeds of *Peganum harmala* known as harmala alkaloids, have been tested for their fungicidal activity. Their normal biological function is to reversibly inhibit monoamine oxidases, which has resulted in these compounds being used

to treat depression. ⁽³⁶⁾ They have also been investigated for their antifungal activity and alkaloids such as harmine **38** and harmaline **39** exhibit good activity against 14 different varieties of fungus. ⁽⁴⁰⁾



2:2:1 Initial leads

In 2012 two groups of researchers at Keele university were working on indole alkaloids. The Bailey group were attempting a complete synthesis of ajmaline and the Allin group were investigating the alkaloid scaffold of indoloisoquinolines, which was prompted by historical compounds with structural similarity to the natural product dihydrousambarensine **40**.⁽⁴¹⁾ The potential lead **41** was further optimised by investigating three points of variation on template **42**: indole *N*-substituent (*R*), hydroxymethyl-*O*-substituent (*R*¹) and alkenic substitution around the lactam ring (*R*²).⁽⁴²⁾



Recognising the intermediates made in the route to ajmaline showed structural resemblance to the indoloisoquinolines, the compounds were tested for their antimalarial activity. Of the compounds made, the most active were several tetrahydro-β-carboline compounds which had been synthesised during an investigation of the Pictet-Spengler reaction used to form the tetrahydro-β-carboline ring.^(41,43) Consequently, the discovery of compound **mc72a** was made and displayed an IC₅₀ of 1.3 μM, thus stimulating an interest in a potential new series of antimalarial compounds yet to be investigated.⁽⁴⁴⁾ Two key features of this novel

compound are an allyl ester moiety and electron withdrawing nitro group present on the C¹ aromatic ring. Therefore, a strategy to try and optimise this structure developed with two points of variation: ester linkages (R¹) and C¹ aromatic ring substituents (R²) (see Figure 15). Our initial testing indicated the L *trans* derivative (1*R*, 3*S*) was more active than the L *cis* (1*R*, 3*R*) however, we recognised that a fuller exploration of the stereochemistry of the two chiral positions using both L and D tryptophan would be of interest.

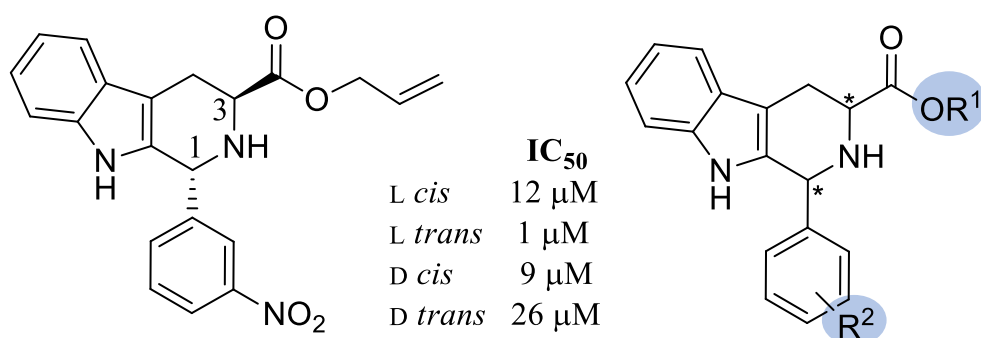
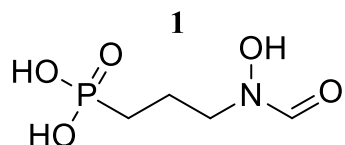


Figure 15: mc72a (left) and compound optimisation strategy (right)

As mentioned earlier, the Open Access Malaria Box (MB) was published in 2013 and over 5,000 compounds were sourced from: GlaxoSmithKline (GSK), Novartis and St. Jude Children's Research Hospital (St Jude). The compound library endured a rigorous filtering process to generate highly potent antimalarial compounds that could be further optimised by external research groups, to generate a catalogue of novel antimalarial compounds. The bank of compounds includes 200 'drug-like' and 200 'probe-like' hits that have: inhibitory concentrations ranging from 30 nM to 4 μM against blood-stage resistant *P. falciparum* strains; have passed cytotoxic tests against HEK-293 cell lines and hand-picked by a group of experienced medicinal chemists considering Lipinski's rules and; already possess structural similarities to aminoquinolines and endoperoxide antimalarials. ⁽⁴⁵⁾

To gather more information regarding the mechanism of action of these 400 compounds, in 2014 Bowman *et al*, highlighted a key compound during the investigation of the previously discussed apicoplast organelle. The loss of the apicoplast can be supplemented *in vitro* with

200 μ M of IPP within experimental growth medium. Therefore, phenotypic screening can be utilised to narrow down the mechanism of action for compounds within the MB by measuring the growth recoveries before and after supplementation. Fosmidomycin (FOS, **1**) is utilised as a control for this experiment because more is known about its mechanism of action towards the apicoplast. ⁽⁴³⁾



A compound which was brought to light by these studies is MMV008138. Phenotypic screening carried out by Bowman showed this compound to have an antiapicoplast mechanism of action. Not only has the compound shown in Figure 16 been identified to target the apicoplast but has also shown to have a different target within the apicoplast. FOS targets DOXP reductase within the non-mevalonate pathway and MMV008138 has shown to act in a similar way by having a direct effect on the metabolism of the apicoplast. Current drugs which target this pathway such as, doxycycline and clindamycin still result in the parasite producing daughter merozoites, however it is the daughter cells which fail to replicate.

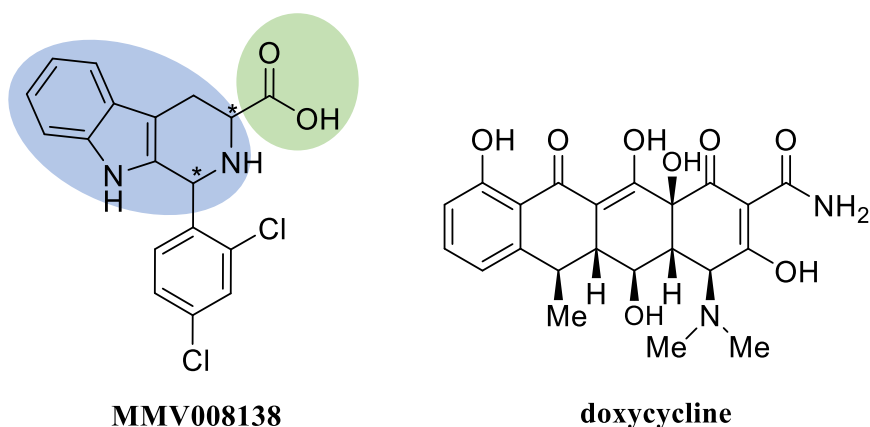
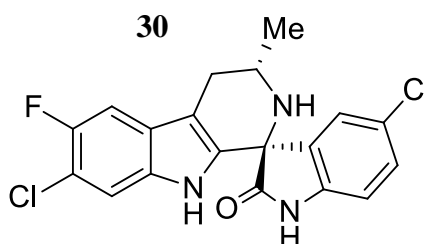


Figure 16: Compounds targeting the apicoplast

Therefore, both FOS and MMV008138 have a direct effect on the metabolism of the apicoplast and no daughter merozoites can be produced, leading to cell death and eventually parasitic death.⁽⁴⁶⁾

The IPP recovery data for MMV008138 demonstrated that greater than 85% recovery of growth inhibition occurs in the presence of 200 μ M IPP after a 72 hour incubation period with the compound. Furthermore, the inhibitory concentration was found to be 350 nM although, no data was yet available about the stereochemical compositions of the compound supplied. They state the important structural features are the pipecolic acid moiety and tetrahydro- β -carboline core seen in compound **30**. In addition, the group propose the (1*R*, 3*R*) stereoisomer best simulates the structural form of the previously discussed antimalarial hit NITD609, which targets the plasma membrane sodium efflux pump.⁽⁴⁶⁾



The similarity of structure between MMV008138 and our own lead molecule **mc72a** affirmed our interest in the tetrahydro- β -carbolines as potential antimalarial compounds and further analogues were designed to investigate the chemical space around the two compounds.

Whilst our investigation was underway a number of other research groups have focused on the investigation into the biological target responsible for the mechanism of action. In 2014 Herrera *et al* were the first group to discover the importance of the 1*R*, 3*S* configuration as it was discovered to be significantly more potent than the other diastereoisomers (see Table 6). As a result, they created (1*R*, 3*S*) MMV008138-resistant *P. falciparum* strains and each strain contained an important mutation correlating to the IspD enzyme, which takes part in

the non-mevalonate pathway generating IPP therefore, they propose MMV008138 targets the IspD enzyme.⁽⁴⁷⁾

Stereoisomer	IC ₅₀ /μM
1 <i>S</i> , 3 <i>S</i>	>25
1 <i>R</i> , 3 <i>S</i>	0.0071
1 <i>R</i> , 3 <i>R</i>	0.17
1 <i>S</i> , 3 <i>R</i>	2.5

Table 6: Individual diastereoisomer activity results

Furthermore, an additional research group in America demonstrated (1*R*, 3*S*)-MMV008138 to competitively inhibit the substrate CTP, which normally reacts with MEP *via* the IspD enzyme to generate a CDP-ME substrate (see Figure 17). They carried out a specific IspD inhibitory concentration assay and (1*R*, 3*S*)-MMV008138 was found to have an IC₅₀ of 47 nM against wild type *Pf*IspD. Also, they include a docking proposal of (1*R*, 3*S*)-MMV008138 within the active site of IspD and believe this will generate future structure-based drug design efforts (see Figure 18).⁽⁴⁸⁾ Figure 18 highlights the important amino acids present within the active site of IspD and includes hydrogen bond interactions with arginine, lysine and threonine.

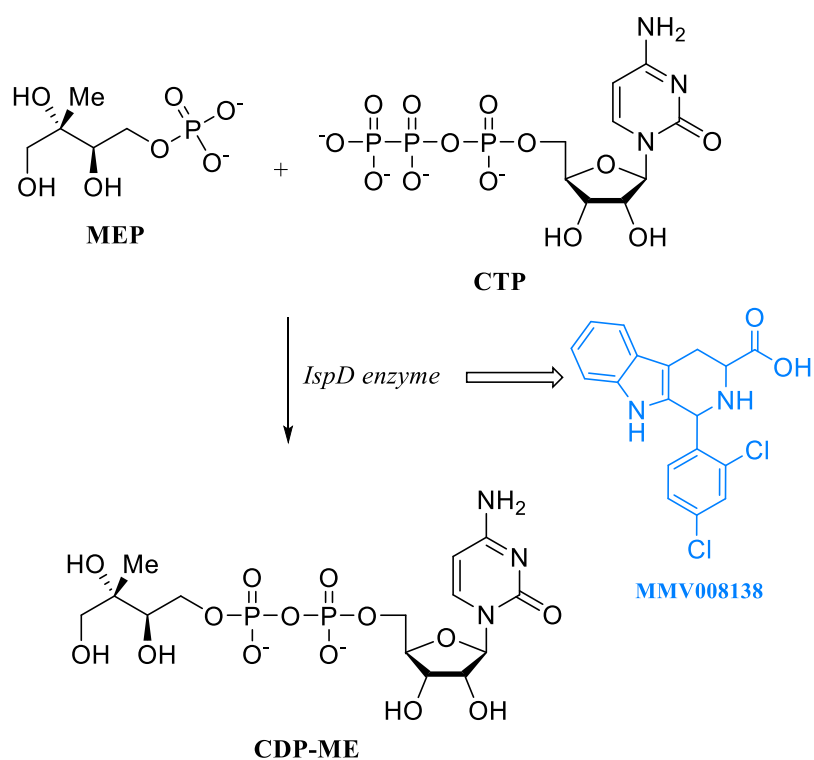


Figure 17: CTP to CDP-ME conversion *via IspD*

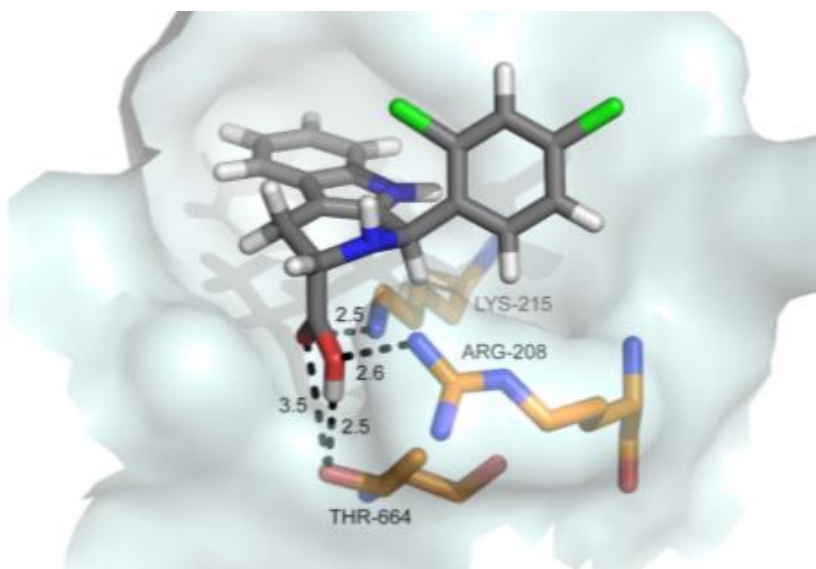
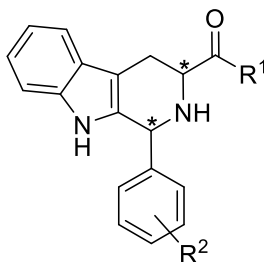


Figure 18: Docking of the (1*R*, 3*S*) stereoisomer of MMV008138 within IspD ⁽⁴⁶⁾

2:2:2 Background work

The first round of analogues focused on the chemical space between our lead molecules and the MMV hit to explore what functional group contributed to activity. Table 7 displays the primary data collected from initial analogues synthesised and from these, compounds which possessed an inhibitory concentration of less than 20 μM were taken forward for further optimisation.



Stereochemistry	R ¹	R ²	IC ₅₀ /μM
L <i>cis</i>		H	19
L <i>cis</i>			17
L <i>cis</i>		3-OMe	36
L <i>trans</i>			20
L <i>cis</i>		4-OMe	39
L <i>trans</i>			34
L <i>cis</i>		3-Cl	27
L <i>trans</i>			32
L <i>cis</i>		4-Cl	22
L <i>trans</i>			18
L <i>cis</i>		4-NO ₂	25
L <i>trans</i>			21
L <i>cis</i>		3-NO ₂	12
L <i>trans</i>			1

Table 7: Initial data July 2013

A benzyl ester link was proposed as this would highlight a need, if any, for hydrophobic interactions or π stacking within the unknown target. Also, exchanging the oxygen hydrogen bond acceptor for benzyl amide derivatives would test whether a hydrogen bond donor or acceptor made any significant difference to inhibitory concentration. Furthermore, a benzyl moiety would allow further optimisation for substitution around this phenyl ring to

investigate whether adding for example, an electron withdrawing group, would have any effect on potency.

Firstly, to bridge the gap with MMV data and the research group data both carboxylic acid and methyl ester derivatives of four analogues were generated during a summer research project in 2013. The methyl ester was chosen over the allyl ester moiety for ease of synthesis and Figure 19 displays the proposed primary structures to explore the MMV008138 structure activity relationship (SAR). Early SAR investigated the acid moiety alongside a new methyl ester group to see the effects a small hydrophobic interaction has on biological activity and whether the acidic proton donor was required for potency.

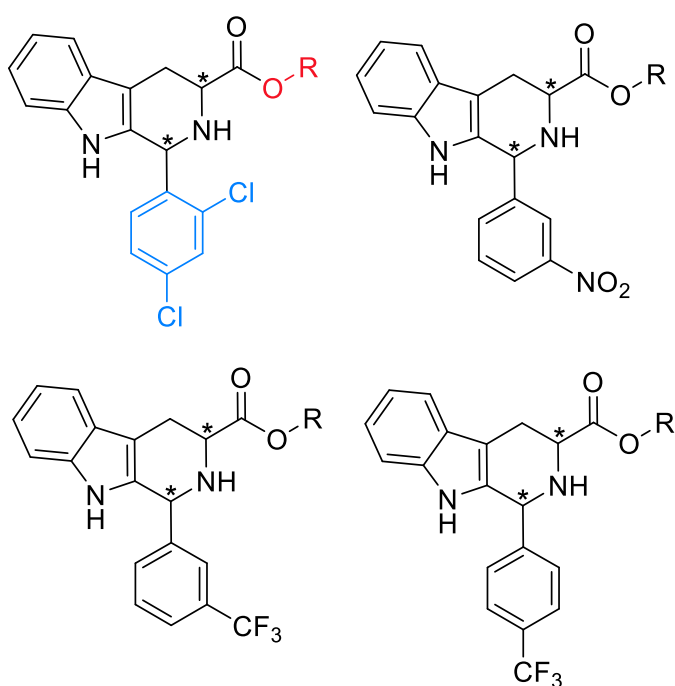
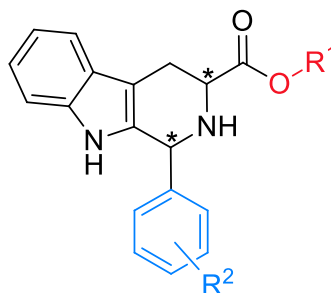


Figure 19: Early analogues (R=H/Me)

The MMV C¹ phenyl 2,4-dichloro substitution was synthesised and used as a standard comparison for alternative substitution patterns. A *m*-nitro moiety was retained, as this was a feature of **mc72a** - the lowest IC₅₀ compound generated previously by the research group. Therefore, by combining a *m*-nitro group with both acid and methyl ester moieties it gave the research group further information regarding which moieties were necessary for potent

activity and began to explore the importance of functional group position on the C¹ phenyl ring.



R ¹	R ²	IC ₅₀ /μM			
		<i>L cis</i>	<i>L trans</i>	<i>D cis</i>	<i>D trans</i>
Me	2,4-Cl ₂	26.5	11.3	23.0	25.8
H (MMV008138)		12.0	0.36	1.31	8.16
Me	<i>m</i> -NO ₂	64.8	17.7	8.30	45.5
H		> 50	> 50	> 50	> 50
Me	3-CF ₃	31.2	25.7	5.10	23.3
Me	4-CF ₃	23.5	25.4	10.6	23.8

Table 8: 2013 results

Table 8 displays a comparison of the four diastereoisomers for both MMV008138 and the methyl ester derivative. The data shows the superior antimalarial activity of the *L trans* form of MMV008138 (360 nM). From this data, it was thought the ester linkage provided vast potential scope for further substrate analogues therefore, it was concluded at the time to keep the methyl ester link, even though the acid MMV008138 displayed higher potency.

Also, Table 8 highlights a preference for the *m*-NO₂ and methyl ester combination therefore, gives further evidence to retain ester functionality. In contrast to the MMV008138 data, the methyl ester *m*-nitro derivatives have the lowest IC₅₀ for the *D cis* configuration (**BB6-A**), therefore both *L* and *D* tryptophan should be explored in future analogues.

Further exploration proposed to see what effect increasing electrophilicity on the C¹ phenyl ring had on biological activity and naturally a trifluoromethyl moiety was explored in both

meta and *para* positions to see what effect each substitution pattern has on biological activity. However, the summer project student struggled to isolate the acid analogues and the compounds that were generated displayed poor activity.

In correlation with the *m*-nitro derivative, both the *meta* and *para* trifluoromethyl analogues displayed favoured activity for the D *cis* configuration (**BB10-A**) and resulted in the lowest inhibitory concentration 5.10 μ M (see Table 8). Although, the 2,4-dichloro derivatives retain superior activity as neither trifluoromethyl analogue possessed lower activity than MMV008138. Both L *trans* and D *cis* configurations have shown to be of importance for activity and they both possess the phenyl group in the 1*R* position. Therefore, predicted low IC₅₀ analogues would correlate with previous discussion involving the antimalarial NITD609, which requires a stereochemistry of 1*R*,3*R* (D *cis*) for biological activity.

A primary focus for the beginning of this PhD project was to generate the derivatives outlined in Figure 20 to investigate alternate ester linkages and compared their activity to the allyl ester lead compound **mc72a**. As our previous results had demonstrated a methyl ester group was inferior to the allyl ester, but the allyl group does not possess good medicinal chemistry properties for example, it is a target for oxidation during metabolism. So, the focus was shifted onto benzyl ester and amide analogues which showed promising initial data. Due to previous evidence suggesting an electron withdrawing group is highly favourable, pyridine groups were proposed to strengthen the evidence for this (see Figure 20).

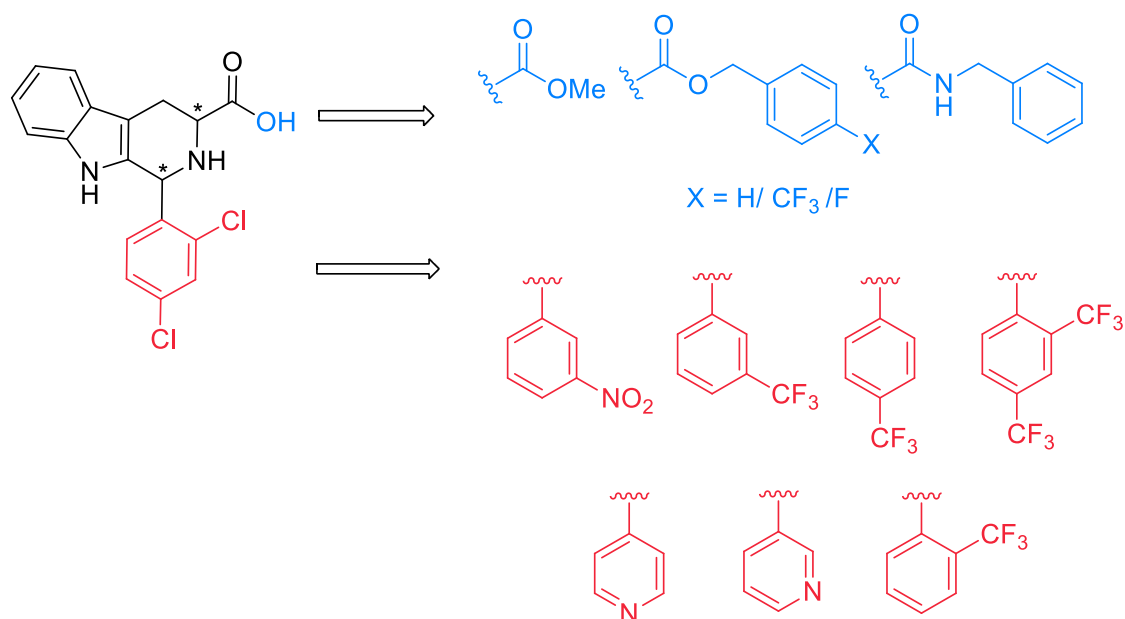


Figure 20: Latest analogue proposals

Figure 21 highlights two compounds derived from tryptamine and α -methyl tryptamine. The purpose of these analogues is to explore the 3D space where the carboxylic acid group is present on the MMV analogue.

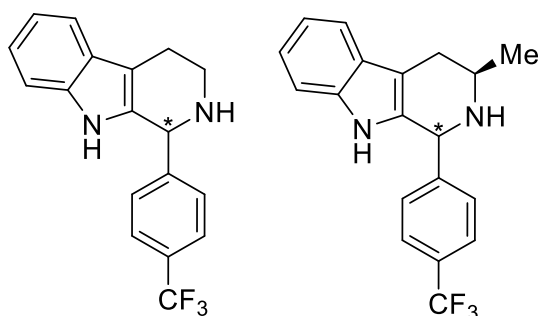


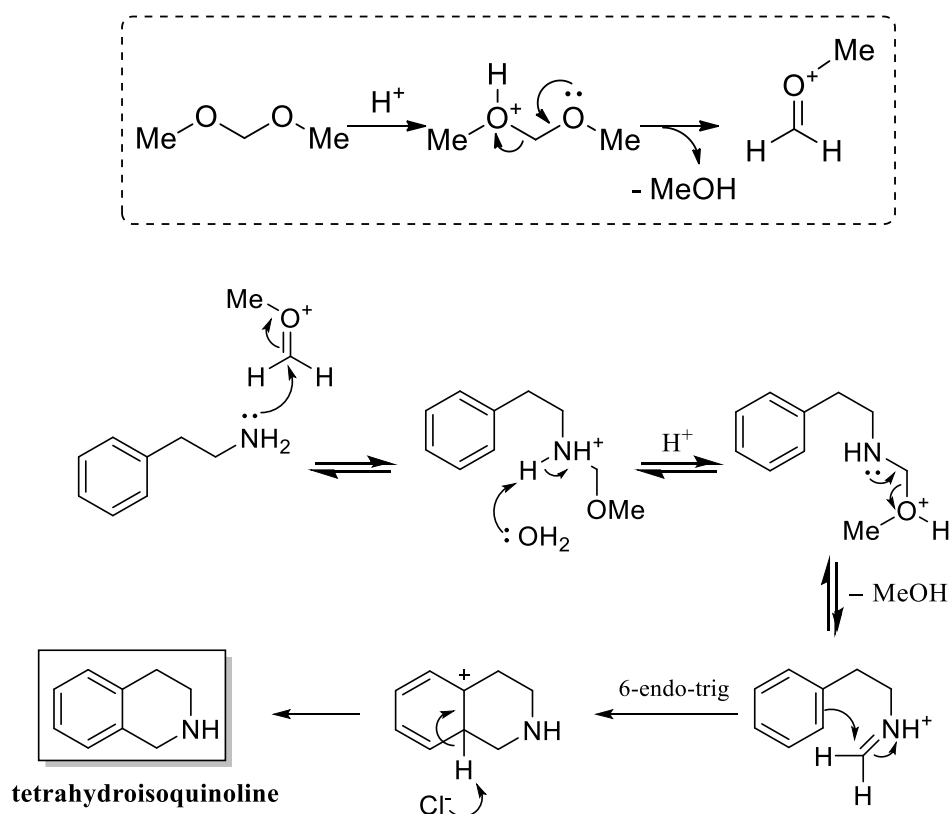
Figure 21: Further compound proposals

To summarise, at the early stage of this PhD project it was forecast that by combining either a benzyl ester or benzyl amide moiety with a *m*-nitro or *p*-chloro substituted C¹ ring it would lead to a more active compound in comparison to the allyl ester derivative which possessed an unsubstituted C¹ ring and poor activity.

2:3 The Pictet-Spengler reaction

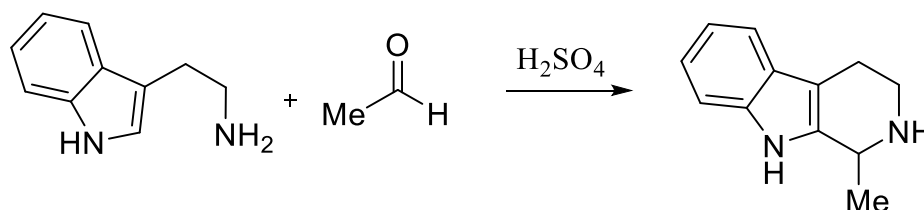
2:3:1 Background

The Pictet-Spengler (PS) reaction is an essential step in accessing the scaffold of pharmaceutically active isoquinolines and indole alkaloids such as MMV008138. In 1911 Pictet and Spengler came across their eponymous condensation reaction by reacting β -phenylethylamine and formaldehyde dimethylacetal under acidic reaction conditions (see Scheme 8).⁽⁴⁹⁾ The one step cyclisation quickly became a standard synthesis for the preparation of tetrahydroisoquinolines (THIQs). The reaction is thought to occur naturally within plants to biologically synthesise important alkaloidal compounds *via* condensation of β -arylethylamines and a variety of carbonyl compounds.



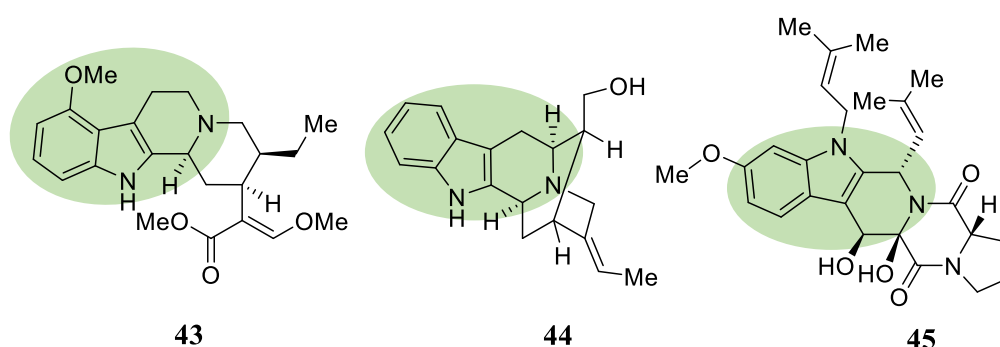
Scheme 8: Mechanism of original tetrahydroisoquinoline formation

Furthermore, in 1928 Tatsui came across the use of the PS reaction for the formation of indole scaffolds, during the preparation of 1-methyl-1,2,3,4-tetrahydro- β -carboline (THBC) under traditional acid catalysed, aprotic conditions (see Scheme 9).⁽⁵⁰⁾

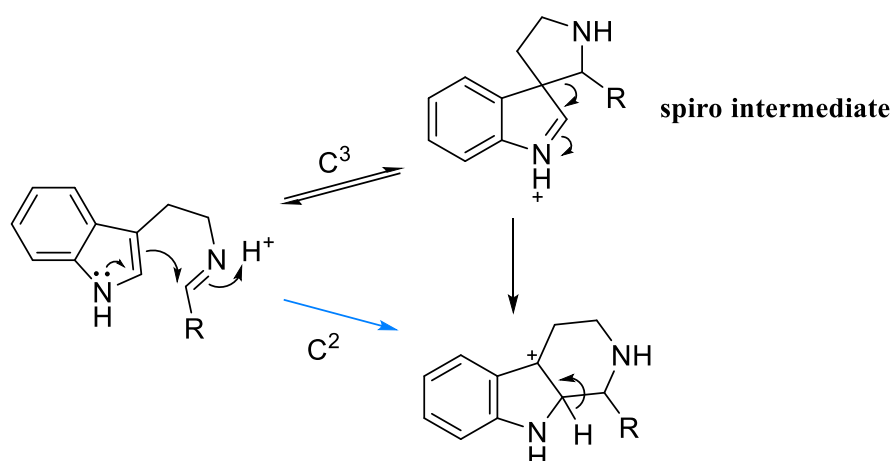


Scheme 9: Straight forward indole formation

Not only does the PS reaction allow for the formation of structurally simple alkaloids, but it can also be utilised in the construction of more complex alkaloids that have been well documented for their uses in traditional medicine. Complex examples include: (–)-Mitragynine **43**, a strong analgesic and opium substitute used in native medicines; Koumidine **44**, a natural indole alkaloid tested for its use treating neuralgia and obtained from the poisonous *Gelsemium* plant and Fumitremergin B **45**, a mycotoxic compound used by many fungi to destroy crops.⁽⁵¹⁻⁵³⁾



Firstly, the condensation reaction begins with the formation of an iminium ion followed by nucleophilic attack but, the iminium ion can add directly at position C² or at C³ to form a spiro intermediate (Scheme 10). The spiro route (C³) uses the delocalisation of the nitrogen lone pair and avoids disruption of the benzene aromaticity.⁽⁵⁴⁾



Scheme 10: Pictet-Spengler intermediates

Consequently, analysis of the transition state took place to examine interactions between the indole moiety and aldehyde substituent, prior to cyclisation. Figure 22 highlights the steric and electronic consequences for both *cis* and *trans* isomers during the imine transitions state.

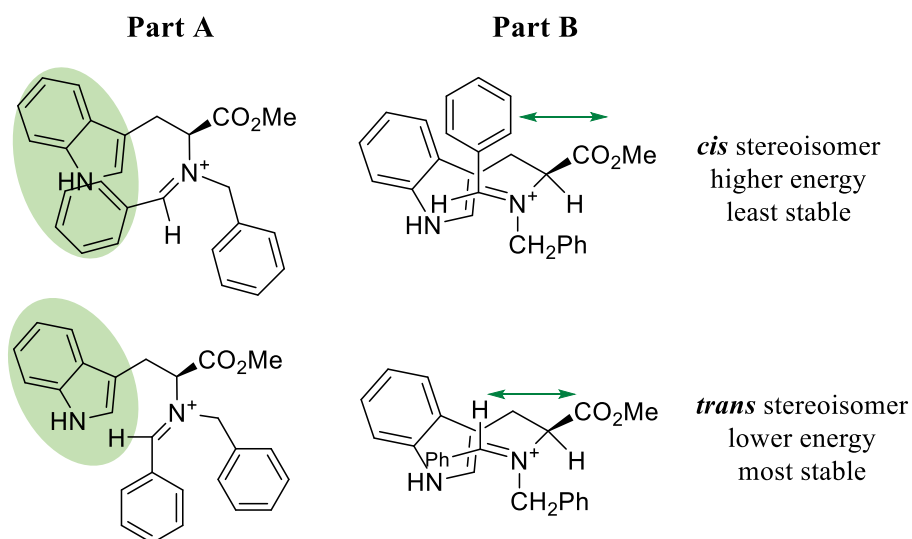


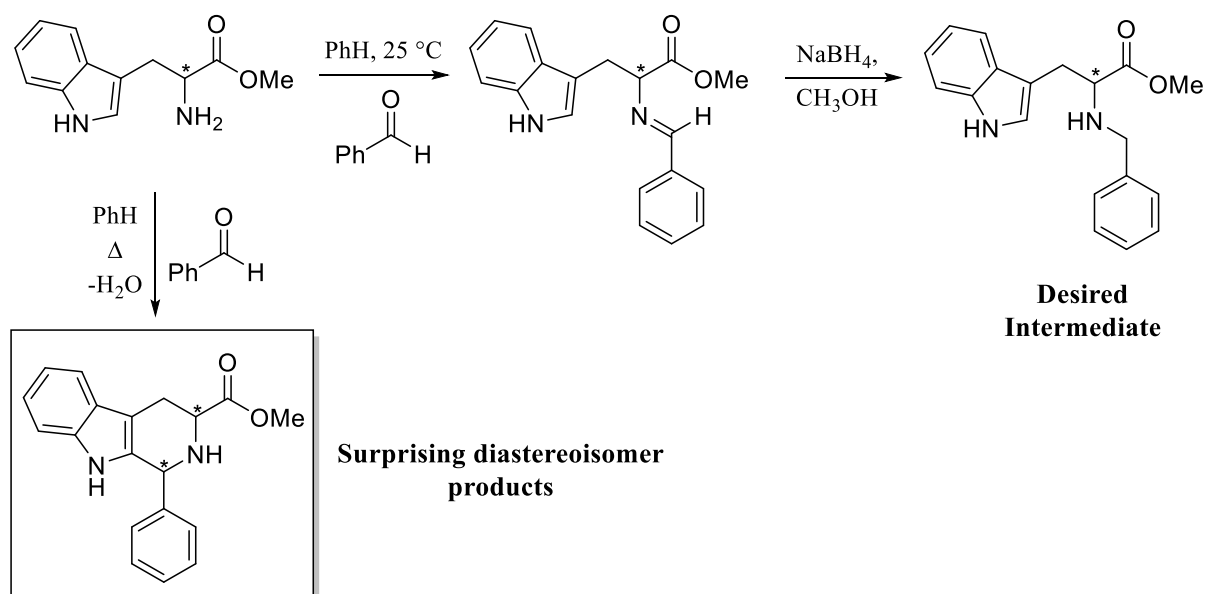
Figure 22: Steric and electronic transition state interactions

Part **A** displays the transition state interactions between the indole and would be C¹ phenyl group, which are more repulsive for the *cis* isomer (top) due to the two bulky rings whereas, the *trans* isomer only has a hydrogen-indole interaction (bottom). Furthermore, as the imine begins to approach sp³ hybridisation, disfavoured electronic interactions between the

aldehyde substituent and methyl ester moiety occur for the *cis* isomer, in comparison to the *trans* isomer which possess a single hydrogen atom interacting with the ester group shown in part **B**. Cook states in a review of this particular observation; *trans* selectivity is thermodynamically controlled, as a consequence of combined stereoelectronic and conformational interaction influences i.e. *trans* is more stable. ⁽⁵⁵⁾

2:3:2 Reaction scope

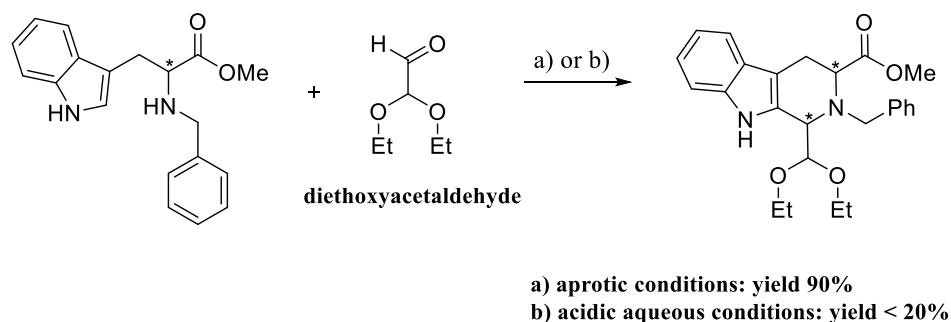
Research carried out by Yoneda in 1965 discovered the PS reaction can be carried out in nonacidic conditions, as opposed to the classical acidic conditions in an aqueous medium. These findings from non-conventional synthesis led to exploration of reaction scope and understanding the factors which underlie stereochemical control of this condensation reaction. Initial research carried out to generate a desired benzyl amine intermediate led to the start of a surprising investigation into aprotic PS conditions (see Scheme 11).^(56,57)



Scheme 11: Non-acidic Pictet-Spengler conditions

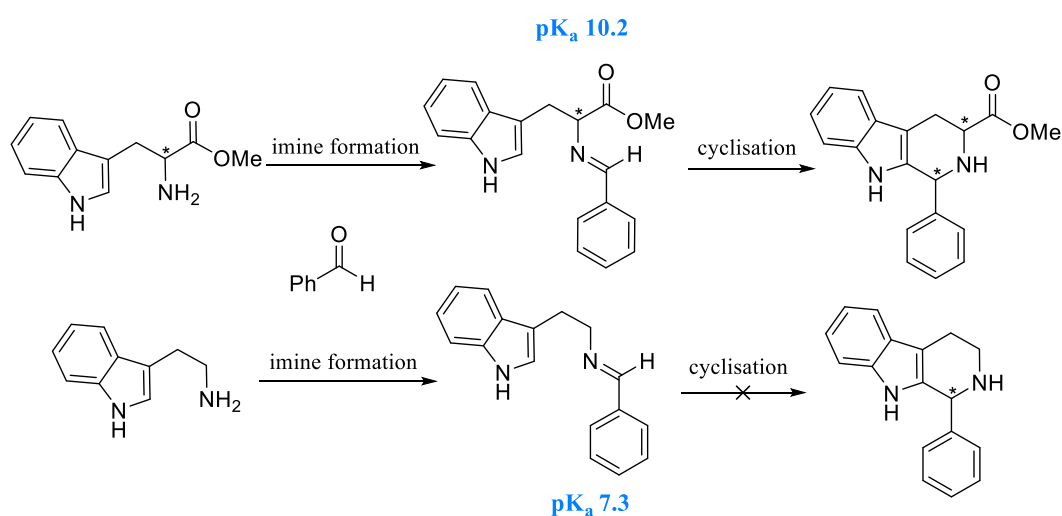
In 1979 Cook *et al* heated the reactants in benzene at reflux with Dean-Stark apparatus fitted to remove the water formed as the reaction proceeds, and to the groups surprise, they saw two diastereoisomer products as opposed to the imine they previously made when stirred at 25 °C in benzene. As a result, the investigation revealed this unusual method could be utilised with the condensation of acid-labile aldehydes and produce better yields for general aldehydes in this aprotic reaction. For example, the reaction of an *N*-benzyl protected tryptophan methyl ester with diethoxyacetaldehyde produced superior yields in aprotic

conditions (see Scheme 12). They extended the library of aldehydes with different functionalities to include: acetals, esters, amides and acetonitriles. ^(56,58)



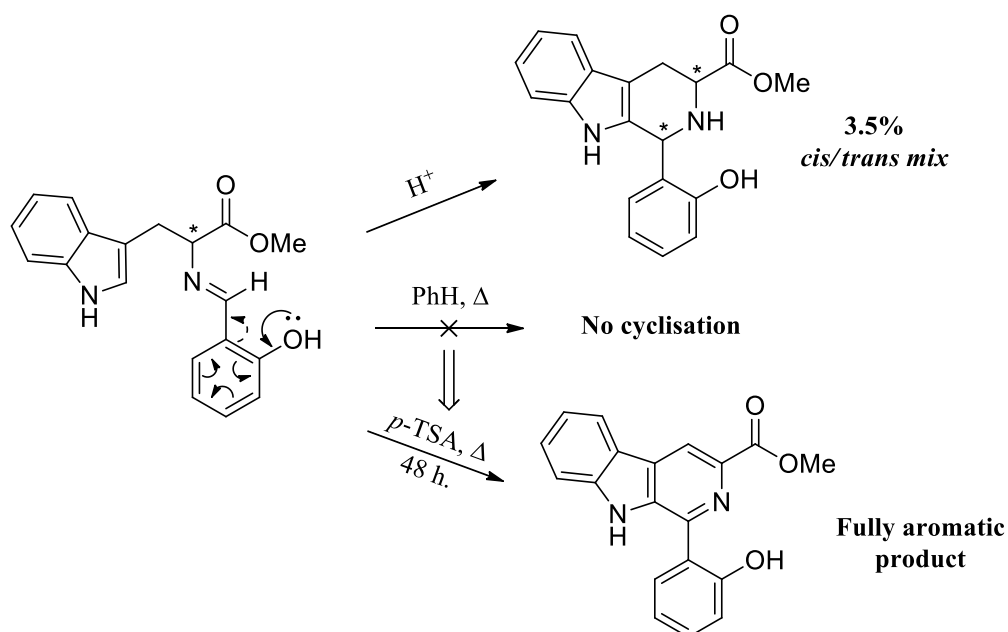
Scheme 12: Acid-labile aldehydes

Cook and co-workers investigated the aprotic approach to study the electrophilic nature of the imine intermediate double bond. Previous protonation of the nitrogen atom in protic conditions complicated the analysis of the imine and it is this property which is the driving force of the cyclisation. The investigation began by comparing tryptophan methyl ester and tryptamine intermediates, which resulted in only the Schiff base being formed for the latter, compared to a yield of 90% for the methyl ester cyclised product. Analysis of the pK_a for the iminium showed the tryptophan methyl ester intermediate being more electrophilic, when compared with the tryptamine iminium which fails to cyclise (see Scheme 13). ⁽⁵⁸⁾



Scheme 13: Imine study under aprotic conditions

To solidify findings, mesomeric effects were studied by reacting an aldehyde possessing an electron donating group with tryptophan methyl ester. Under traditional acidic conditions the reaction overall yield was 3.5% of a *cis/trans* diastereoisomer mix, however under aprotic conditions only imine was detected. In fact, the imine was so unreactive the intermediate was reacted with *p*-toluenesulfonic acid and heated at reflux for 2 days and resulted in the fully aromatic product under these harsh conditions (see Scheme 14).⁽⁵⁶⁾

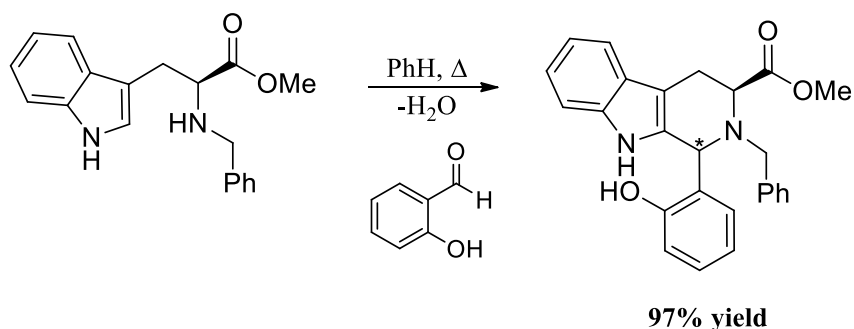


Scheme 14: Effects of electron donating groups on imine reactivity

Also, Scheme 14 shows how the phenolic oxygen electron donation leaves the imine double bond less electrophilic in comparison to the tryptophan methyl ester substrate which results in un-cyclised imine. On the other hand, if acetylation of the phenolic oxygen takes place, this new functionality retards the electron donation from the oxygen and allows cyclisation to occur and results in a yield of 40% cyclised *cis/trans* mix of diastereoisomers.

Alternatively, if the indole substrate is *N* β -benzylated, the resultant imine intermediate readily undergoes cyclisation. This approach is useful for unreactive intermediates and can simply be removed later through traditional catalytic hydrogenation. Cook *et al*, found the

temporary benzylation increased the speed of cyclisation and improved overall yield of the reaction. For example, Scheme 15 shows the previously reluctant salicylaldehyde undergoing cyclisation and with this approach now results in a yield of 97% product. However, it is detailed some aldehydes can distil through Dean-Stark apparatus, which contributes to poor yield and is therefore essential to ensure the boiling point of the chosen aldehyde is higher than that of the solvent. ⁽⁵⁵⁾

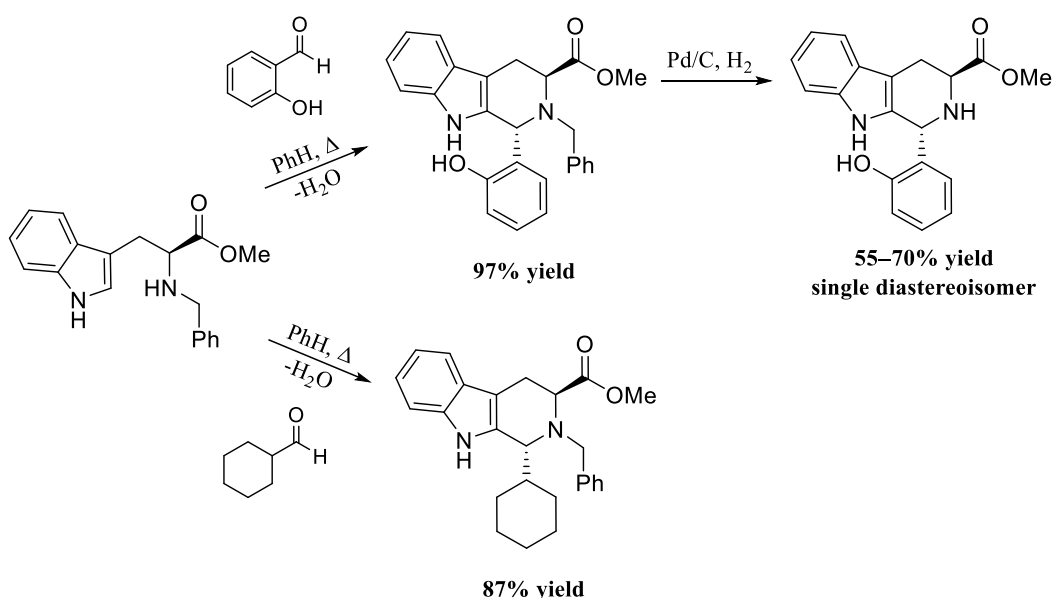


Scheme 15: *N*_β-benzylation to increase imine reactivity

Proposed analogues for this project involve electron withdrawing groups substituted on the C¹ phenyl ring therefore, the activity of the imine intermediate formed should not create any problems as there is no electron donation into the phenyl ring. Also, traditional protic conditions have been selected to generate this set of tetrahydro-β-carbolines to eliminate any unforeseen problems during imine formation as well as ease of synthesis.

2:3:3 Thermodynamic control: *trans* selectivity

During the condensation of salicylaldehyde with *N*_β-benzylated tryptophan methyl ester, it was noted that only a single diastereoisomer was obtained (see Scheme 16). Cook proposed this observation was due to the phenolic hydrogen causing hydrogen bonding interactions, which favoured *trans* selectivity. However, on repeating the Pictet-Spengler reaction with cyclohexanecarboxaldehyde under aprotic conditions, a *trans* cyclised product was obtained in 87% yield thus, ruling out hydrogen bonding as a cause for stereocontrol. A further reaction was carried out with unprotected tryptophan methyl ester, which resulted in a mixture of *cis/trans* cyclised products. ⁽⁵⁶⁾



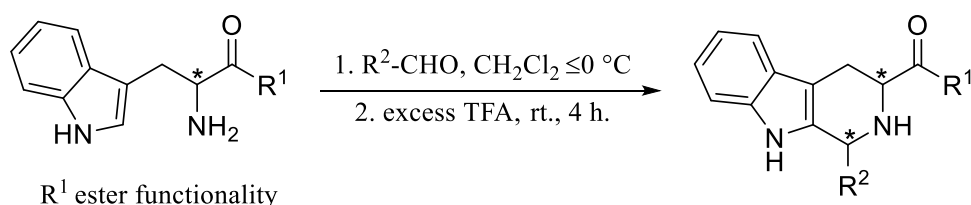
Scheme 16: Primary investigations into *trans* selectivity

Also, if a percentage of the *N*-benzyl *cis* diastereoisomer is formed it can be converted to the more thermodynamically favoured *trans* diastereoisomer *via* epimerisation under acidic conditions. If this method was employed to generate derivatives for this project, a terminal *N*-benzyl deprotection step would have to be carried out to achieve the tetrahydro- β -carboline core we desire. However, this project requires both *cis* and *trans* diastereoisomers for biological testing. As a result, a *trans* selective approach would only become of use if a

synthesised novel *trans* compound proves highly active and larger quantities of the compound is required.

2:3:4 Kinetic control: *cis* selectivity

Bailey *et al*, comprised a set of reaction conditions which involves preformation of the imine intermediate before adding an excess of acid at low temperature to form the final cyclised product (see Scheme 17).



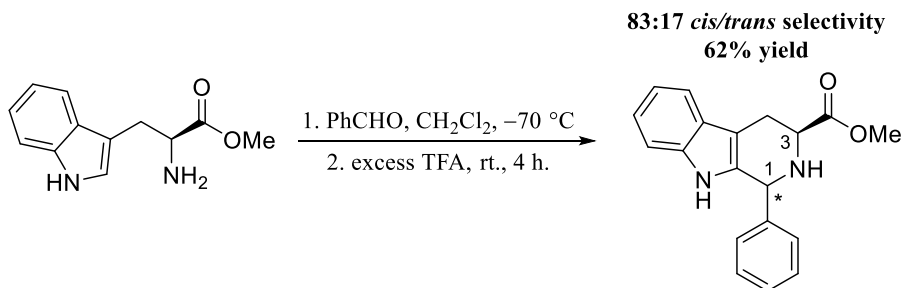
Scheme 17: General Bailey Pictet-Spengler conditions

A disadvantage of thermodynamic conditions is the possibility of product racemisation, which would be unfortunate for the synthesis of natural products containing multiple chiral centres. Furthermore, most natural products possess a 1,3-substituted *cis* relationship, such as the previously mentioned natural product, Koumidine, so a *cis* relationship is highly desired.

Investigations into kinetic control followed the observations of Cook *et al*, looking into the conformations of imine transition states of N_β-benzyl tryptophan methyl esters previously discussed in chapter 2:3:1. Bailey states 1,3-disubstituted tryptophan methyl ester would prefer to be equatorial, reducing 1,3-diaxial interactions, and therefore results in *cis* selectivity in the absence of N_β-benzylation. To support this, Pictet-Spengler reactions were carried out at low temperatures to demonstrate this hypothesis of *cis* selectivity to be the case. Additionally, they report the high temperature conditions do not reduce the kinetic selectivity, but more so the fact that the reaction conditions proposed by Cook are reversible.

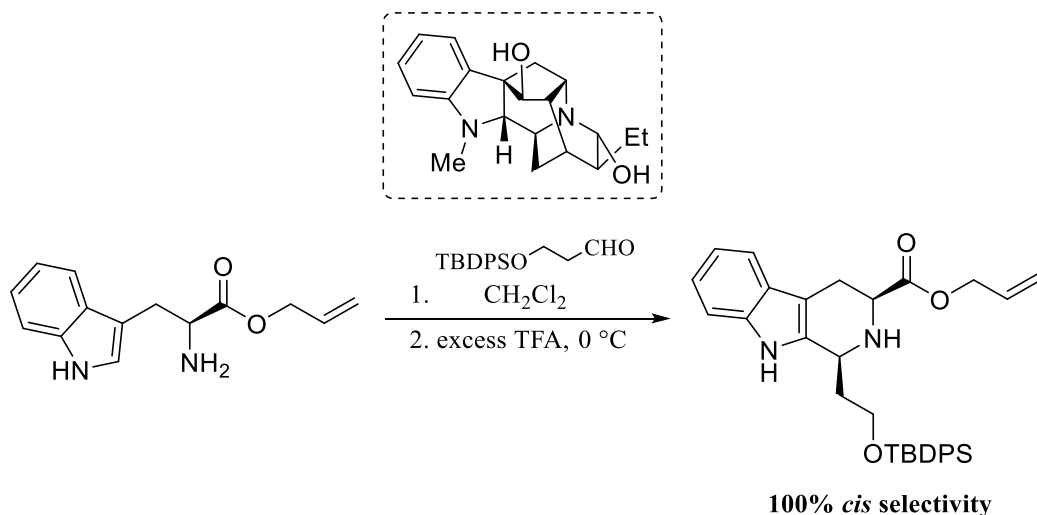
This statement is supported by experimental evidence, through subjecting pure *cis* cyclised product to Cook conditions and the observed outcome resulted in 1:2 *cis/trans* selectivity (see Scheme 18). From the tryptophan methyl ester derivatives generated, Bailey *et al* found

a general 4:1 *cis/trans* selectivity for a reaction carried out at room temperature and all products obtained retain their optical integrity, therefore no racemisation took place utilising these conditions.⁽⁵⁹⁾



Scheme 18: *Cis* selectivity in tryptophan methyl esters

Later, Bailey reported further scope for the *cis* selective Pictet-Spengler reaction conditions, whilst conducting research into the total synthesis of ajmaline. The group discovered a certain combination of ester and aldehyde which, under kinetic conditions, produced virtually 100% *cis* cyclised tetrahydro- β -carboline (see Scheme 19).



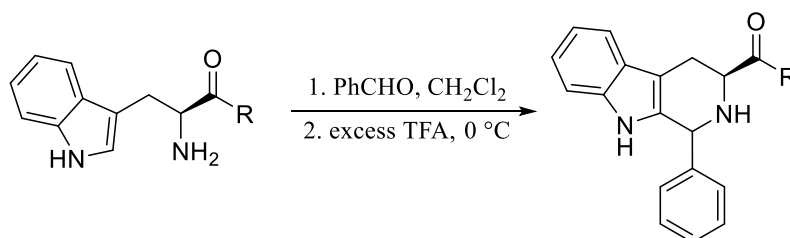
Scheme 19: Ajmaline (above) and surprising *cis* selectivity (below)

Bailey summarised over 10 years after his initial research was conducted that only allyl esters display 100% *cis* selectivity, as replacing allyl with a propyl ester generated 4:1 *cis/trans* selectivity. Also, only aryl aldehydes produced >95 *cis* selectivity, as alkyl aldehydes such as butanal produced 78:22 *cis/trans* selectivity.⁽⁴³⁾ Furthermore, this method

uses milder reaction conditions which tolerate aryl aldehyde substrates with a variety of electron donating/withdrawing groups in *ortho*, *meta* or *para* positions. For example, *p*-methoxybenzaldehyde generates >95:5 *cis/trans*, and identically 4-chlorobenzaldehyde generates >95:5 *cis/trans*.⁽⁴³⁾

Moreover, in 2009 Bailey *et al* identified good selectivity in tryptophan substrates which possessed a C³ carbonyl π bond alongside an aldehyde substrate with an appropriate π moiety, to achieve high *cis* selectivity. The tryptophan allyl ester substrate repeatedly produced the highest *cis* selectivity when compared to other substrates tested (Scheme 20).

(41)



R	Yield/%	<i>cis/trans</i> selectivity
-OBn	74	4.7:1
-OMe	74	4.6:1
-i-Pr	>95	7.3:1
-OAllyl	57	>20:1

Scheme 20: Variety of substrate scope

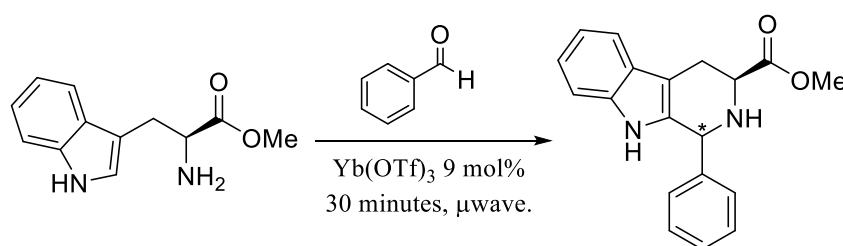
Compared to Cook's *trans* selective synthesis the Bailey method offers the generation of both diastereoisomers (general 4:1 selectivity at room temperature), which this project desires. Furthermore, if a novel compound with a *cis* relationship is found to be highly active then this synthetic strategy could be tailored i.e. reaction temperature decrease to generate more of the desired *cis* compound under these kinetic conditions.

2:3:5 Lewis acid catalysis

In the last 15 years various Pictet-Spengler catalysts have been investigated to improve: reaction times, yields and broaden substrate scope. Lewis acids have been probed alongside microwave irradiation, to shorten reaction times further. Ganesan *et al* investigated multiple Lewis acids and categorised into poor, moderate and high activity PS catalysts. Examples include: AgOTf – poor activity, Cu(OTf)₂ – moderate activity and Sc(OTf)₃ – high activity.

⁽⁶⁰⁾ The Lewis acids possessing the less nucleophilic triflate counterparts were superior compared to metal chlorides such as TiCl₄, for which a competing imine hydrolysis reaction was found to take place. ⁽⁶⁰⁾

Yb(OTf)₃ gave the best yields when reacted with the intermediate imine and it was shown to only require 5 mol% of catalyst and 30 minutes in a microwave reactor to achieve high imine conversion, with both aromatic and aliphatic imines. In comparison, a one-pot synthesis could also be applied by generating the imine *in situ* with excess aldehyde, which resulted in higher yields and cleaner product mixtures. For example, Scheme 21 shows the reaction of L-tryptophan methyl ester with benzaldehyde, generating a crude product of 1:1.6 *cis/trans* selectivity with an overall 85% yield. ⁽⁶⁰⁾



Scheme 21: Lewis acid one-pot microwave reaction

The reaction can also be carried out in a conventional oil bath heated to 120 °C for 50 minutes, which was found to give comparable yields to using microwave irradiation.

The Lewis acid approach can also be applied to both electron donating and electron withdrawing aldehydes, the former previously discussed for causing frequent problems for Pictet-Spengler cyclisation due to the low reactivity of imine intermediate. However, with this method aldehydes such as 3,4,5-(trimethoxy)phenyl aldehyde, can be reacted with L-tryptophan methyl ester to give 1:1.4 *cis/trans* selectivity and 93% yield. Furthermore, tryptamine can be reacted with the same electron donating aldehyde, and combined with the poor tryptamine imine, surprisingly still produces 89% yield (as a mixture of enantiomers, see Figure 23). ⁽⁶⁰⁾

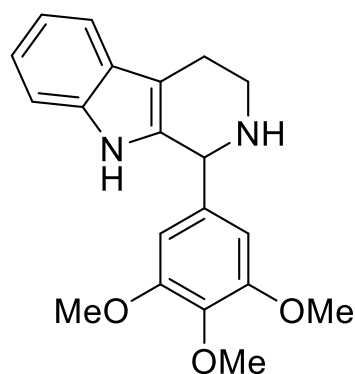


Figure 23: Surprising Pictet-Spengler product

For this medicinal chemistry project, a Lewis acid approach would generate more even quantities of both *cis* and *trans* diastereoisomers. Therefore given: the shorter reaction times, increased product yield and more even *cis/trans* formation, this method would greatly benefit analogue generation.

2:4 Biological results and discussion

2:4:1 Tryptamine derivatives

During the investigation, the key interaction was removed to see the effects this had on biological activity. Figure 24 displays the analogue generated and possess a *p*-trifluoromethyl group chosen to retain the important electron withdrawing functionality.

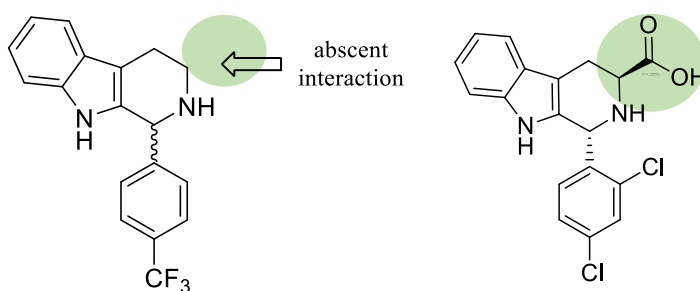
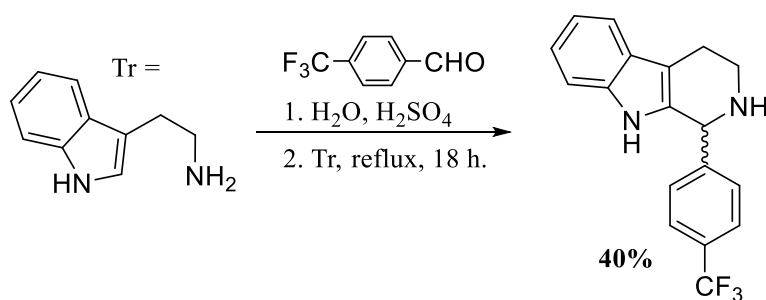


Figure 24: Tryptamine analogue (left) and MMV008138 (right)

This derivative was synthesised *via* traditional aqueous, acid catalysed conditions, discovered by Tatsui. Firstly, *p*-trifluoromethyl benzaldehyde was pre-stirred in water containing 5 drops of sulfuric acid for 30 minutes. Then, tryptamine was added into the solution and stirred overnight at reflux. Some viscous insoluble solid forms within the reaction mixture and is thought to contribute to low overall yield. However, the product was purified using column chromatography and easily separated from its constituents, to yield a white solid.



Scheme 22: Tryptamine analogue synthesis

Biological results showed this tryptamine analogue to have an IC_{50} of 1 μM , which is the lowest inhibitory concentration discovered for this tetrahydro- β -carboline series. Furthermore, in direct comparison to the methyl ester analogue possessing the same phenyl substituent the tryptamine analogue has superior activity (see Figure 25). In 2012 research carried out by Gellis and co-workers highlighted a similar compound possessing an electron donating group which possessed lower activity than the tryptamine compound synthesised in this project. ⁽⁶¹⁾ Early assumptions highlighted the carbonyl link as essential for antimalarial activity particularly for MMV008138, in combination with orientation.

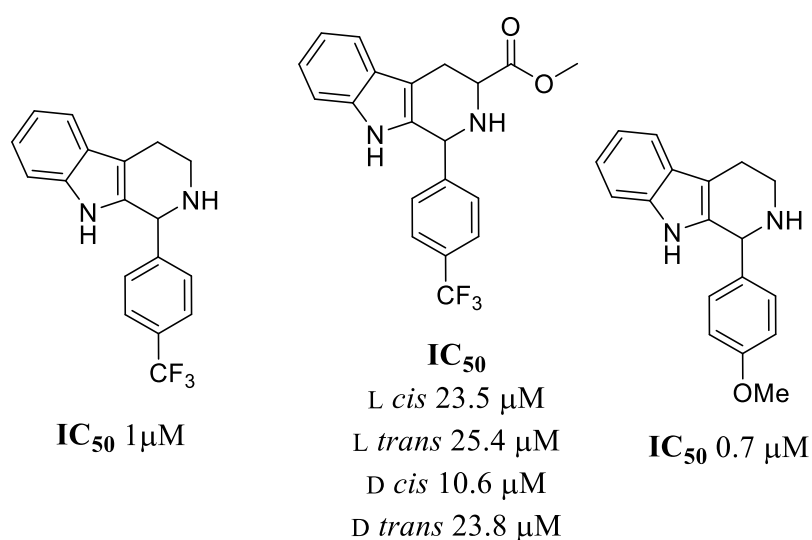
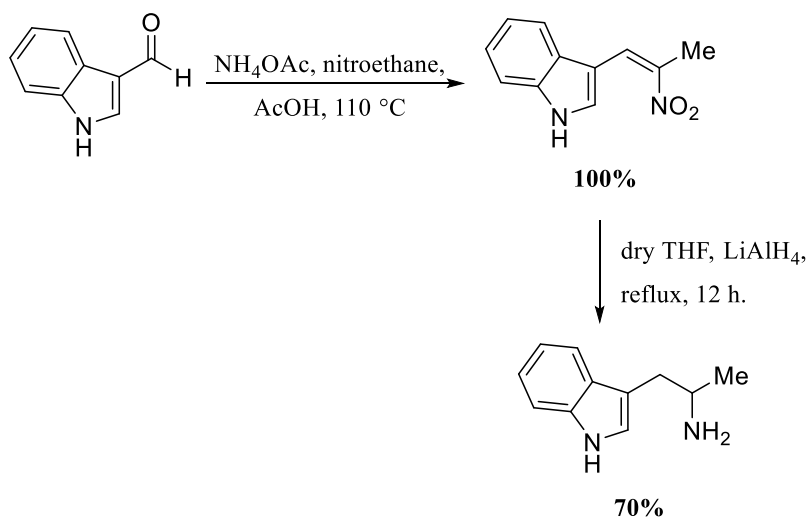


Figure 25: Tryptamine and tryptophan methyl ester comparison

However, these two compounds indicate the primary predictions may be inaccurate but, it is still unknown if this result is due to general toxicity of the compound, as opposed to a targeted mechanism of action. Therefore, more biological tests need to be carried out before making any deductions. More tryptamine derivatives should be synthesised to probe this interesting find.

Following these findings two α -methyl tryptamine derivatives were synthesised to explore the interaction of a short hydrophobic R^1 alkyl substitution. Hence, Scheme 23 shows the

route taken to first synthesise the desired α -methyl tryptamine starting material, *via* a nitroalkene intermediate.



Scheme 23: Preparation of α -methyl tryptamine

Tatsui Pictet-Spengler conditions were then used to generate the desired cyclised product, as previously shown in the case of tryptamine and the diastereomeric pairs were separated *via* column chromatography. Biological data gathered, gave inhibitory concentrations as follows; 4.5 μM for **LVT33-1** and 1.4 μM for **LVT33-2** (see Figure 26).

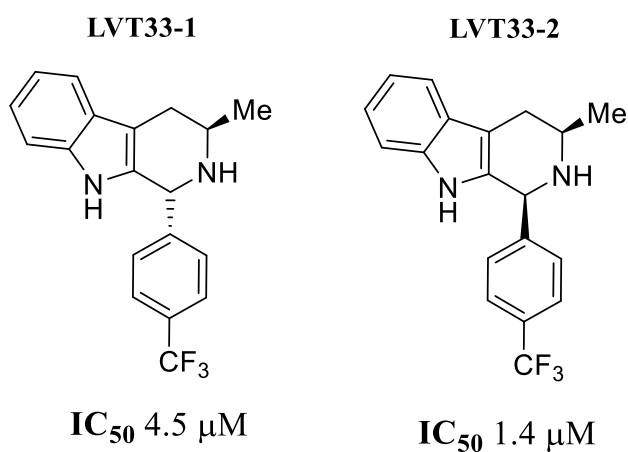


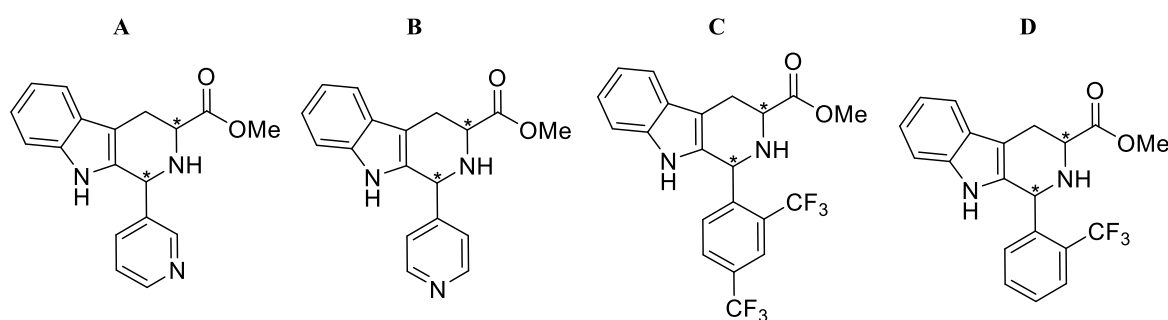
Figure 26: α -methyl tryptamine analogues

Consequently, these analogues indicate that the carboxylic acid interaction is not vital for activity but, more derivatives with a short methyl interaction should be generated to

strengthen this observation. Also, the *p*-trifluoromethyl C¹ phenyl substitution seems to be important as low activity compounds are observed and should therefore be retained in future derivatives.

2:4:2 Tryptophan methyl ester derivatives

This set of synthetic targets retained the methyl ester and looked at varying the nature of the electron withdrawing aromatic substituent at C¹. For example, compounds **A** and **B** have a nitrogen atom within the phenyl ring and therefore, offer alternative electronic interactions. Compound **C** explores the effects of two strong electron withdrawing groups in a 2,4-substitution pattern to mimic the original MMV compound. Finally, compound **D** possesses an *ortho* EWG group thus, offering a complete look at the effects an EWG has at all positions on the phenyl ring.

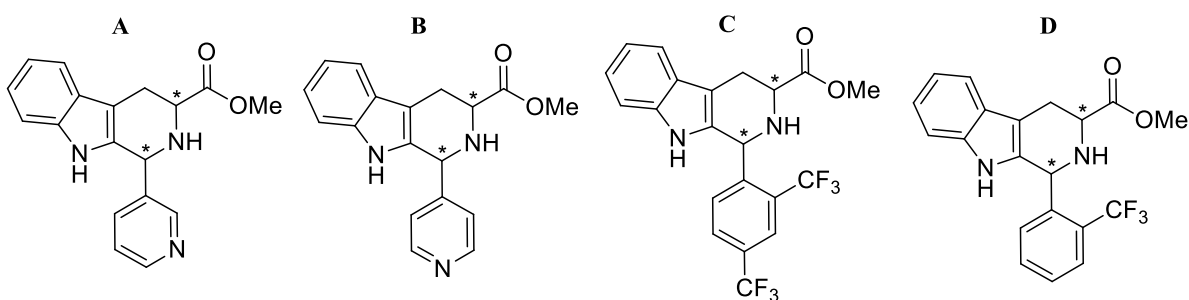


Structure	Stereochemistry	Bailey d.r. <i>cis:trans</i>	Yb(OTf) ₃ d.r. <i>cis:trans</i>
A	L <i>trans</i>	1.7:1	1.2:1
	L <i>cis</i>		
	D <i>trans</i>	2:1	1.3:1
	D <i>cis</i>		
B	L <i>trans</i>	2.2:1	1.2:1
	L <i>cis</i>		
	D <i>trans</i>	1.6:1	1.2:1
	D <i>cis</i>		
C	L <i>trans</i>	2.3:1	1.1:1
	L <i>cis</i>		
	D <i>trans</i>	1.6:1	1.1:1
	D <i>cis</i>		
D	L <i>trans</i>	3:1	1.3:1
	L <i>cis</i>		
	D <i>trans</i>	1.6:1	1.2:1
	D <i>cis</i>		

Table 9: Synthetic route d.r. comparison

This subset of analogues were generated by both the Bailey method (TFA, rt, 4 h) and the Lewis acid microwave conditions (Yb(OTf)₃, 100 °C, 0.5 h). Table 9 highlights the comparison of diastereomeric ratio observed for both methods.

The Bailey method shows a range of 1.6–3:1 d.r. on the other hand, the Pictet-Spengler reaction carried out *via* Lewis acid catalysis displays lower selectivity with a d.r. range of 1.1–1.3:1 selectivity. The Lewis acid method overall gives better yielding products and the crude reaction mixture does not contain any unreacted imine, which makes separation of the diastereoisomers simpler (see Table 10).



Structure	Stereochemistry	Bailey Yield/%	Yb(OTf) ₃ Yield/%
A	L <i>trans</i>	31	31
	L <i>cis</i>	29	32
	D <i>trans</i>	8	31
	D <i>cis</i>	15	29
B	L <i>trans</i>	17	40
	L <i>cis</i>	35	35
	D <i>trans</i>	16	33
	D <i>cis</i>	18	29
C	L <i>trans</i>	8	40
	L <i>cis</i>	42	37
	D <i>trans</i>	19	36
	D <i>cis</i>	21	37
D	L <i>trans</i>	10	38
	L <i>cis</i>	18	37
	D <i>trans</i>	6	37
	D <i>cis</i>	4	31

Table 10: Yield comparisons

For example, the entries highlighted in Table 10 show very poor yield for the *trans* diastereoisomer generated by the Bailey method. This can be explained by the favoured generation of the *cis* diastereoisomer in combination with tricky purification i.e. unreactive imine with similar retention factors and solubility issues.

The overall lowest yield is seen for the D *cis* diastereoisomer of compound D and an explanation for this comes from the compound itself being very insoluble. As a result, only a small amount of the diastereoisomer mix could be dissolved and subsequently purified to obtain each diastereoisomer for biological testing.

Additionally, the Bailey method involves preformation of the imine before acid catalysed cyclisation, so requires an 18 hour stir before allowing 4 hours for cyclisation. It was observed that this method leads to unreacted imine within the crude mixture after monitoring the reaction by TLC over 4 hours which contributes to lower yields, as seen in Table 10. This issue can be overcome by adding more than 2 equivalents of TFA, but leaving the reaction longer was not found to increase cyclised product. Higher quantities of TFA could also risk racemisation of the chiral centre. The imine intermediates have similar retention factors to the desired cyclised product, it makes purification more complex and results in isolated yields not being consistent. In comparison, the Lewis acid methodology only requires a reaction time of 30 minute in a one-pot microwave irradiation reaction, which can be purified straight away after an aqueous work up. Overall, the Pictet-Spengler reaction carried out utilising Yb(OTf)₃ should be employed for future analogue generation due to both, cleaner and faster reactions.

2:4:2:1 Tryptophan methyl ester biological data

Following synthesis of the proposed methyl ester derivatives, the inhibitory concentrations were obtained for *Plasmodium falciparum* and are displayed in Table 11.

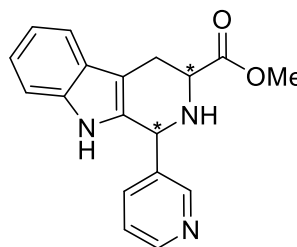
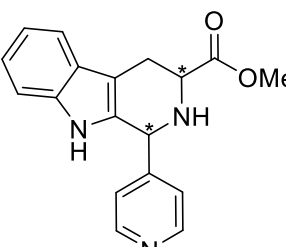
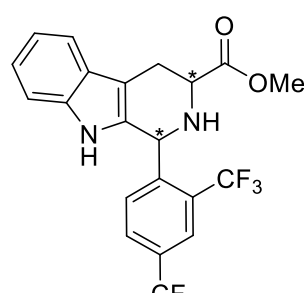
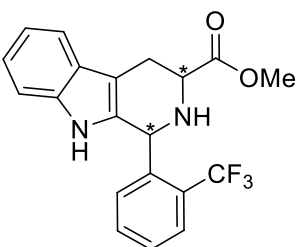
<div style="display: flex; justify-content: space-around; align-items: flex-end;"> <div style="text-align: center;"> A  </div> <div style="text-align: center;"> B  </div> <div style="text-align: center;"> C  </div> <div style="text-align: center;"> D  </div> </div>			
Structure	Stereochemistry	IC ₅₀ /μM <i>Dd2 strain</i>	
A	L <i>trans</i>	24.5	
	L <i>cis</i>	30.0	
	D <i>trans</i>	> 50	
	D <i>cis</i>	25.6	
B	L <i>trans</i>	16.7	
	L <i>cis</i>	>50	
	D <i>trans</i>	31.0	
	D <i>cis</i>	39.5	
C	L <i>trans</i>	5.40	
	L <i>cis</i>	8.90	
D	L <i>trans</i>	10.5	
	L <i>cis</i>	22.3	
	D <i>trans</i>	5.20	
	D <i>cis</i>	3.30	

Table 11: Methyl ester derivatives

The pyridine moiety did not produce compounds with high activity in either, D or L conformation nor, 3-pyridinyl or 4-pyridinyl positions about the phenyl ring. The lowest inhibitory concentration achieved, as highlighted in Table 11 is 16.7 μM. The alternate electronic properties offered by the addition of a nitrogen atom within the aromatic ring does not warrant further investigation.

On the other hand, attempts to optimise the structure activity relationship of MMV008138 resulted in the replacement of the original 2,4-dichloro moiety with a more electron withdrawing functional group i.e. trifluoromethyl group. Further to this, a 2,4-disubstitution relationship was retained as it is thought to be of importance for antimalarial activity, even though a previously discussed methyl ester analogue possessed a 3-trifluoromethyl substitution and has an IC_{50} of 4.9 μM . Overall, the L diastereoisomers of compound **C** possess good activity for example; the L *trans* conformation has lower activity (IC_{50} of 5.4 μM) compared to L *cis* (IC_{50} 8.9 μM), which supports previous evidence suggesting a 1*R*, 3*S* relationship is required for better activity.

Furthermore, *o*-trifluoromethyl substitution was investigated (compound **D**) to ensure all substitution positions on the phenyl ring had been explored thus, allowing a full set of biological data to be gathered. Surprisingly, the D *cis* diastereoisomer of compound **D** (IC_{50} 3.3 μM) has even better activity than the L *trans* diastereoisomer of compound **C**, therefore this observation provides insight that functional group position may not be as crucial as first thought and it is more the conformation of the diastereoisomer, in combination with the functional group present.

2:4:2:2 Methyl ester NITD609 derivative

As previously highlighted, recent clinical candidate NITD609 possesses a spiro core and a *trans* configured chlorine-amide relationship. Therefore, attempts to mimic this active structure was explored through synthesis of a 2,5-disubstituted compound, which includes a chlorine and acetamide moiety. The structural comparison can be seen in Figure 27 however, biological results indicate only good activity for example; the *L trans* diastereoisomer has an IC_{50} of 5 μ M, which is not significant, but nevertheless reinforces the significance of a (1*R*, 3*S*) conformation (see Table 12).

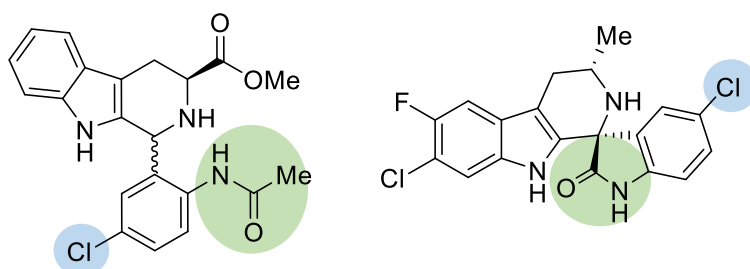
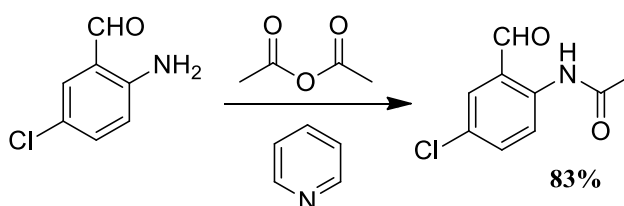


Figure 27: NITD609 structure comparison

Stereochemistry	Bailey d.r. <i>cis:trans</i>	Yb(OTf) ₃ d.r. <i>cis:trans</i>	Bailey Yield/%	Yb(OTf) ₃ Yield/%	IC_{50}/μ M
<i>L trans</i>	1.7:1	1.1:1	20	22	5.00
<i>L cis</i>			11	24	8.80

Table 12: NITD609 mimic results

The protected aldehyde was first prepared before carrying out the Pictet-Spengler cyclisation. The starting material 2-amino-5-chlorobenzaldehyde was stirred in acetic anhydride and pyridine at room temperature overnight and once purified, leaves a yellow solid in good yield (see Scheme 24).

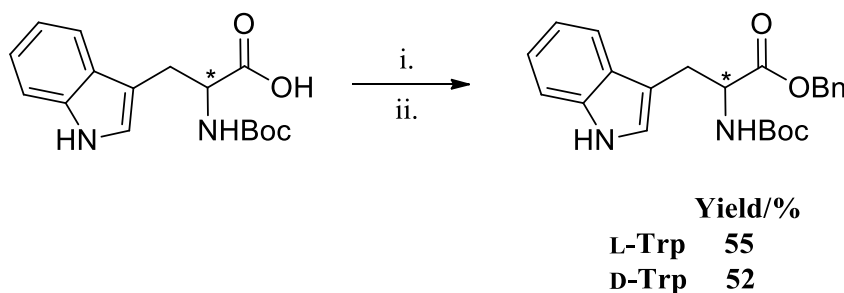


Scheme 24: Aldehyde synthesis

2:4:3 Tryptophan benzyl ester derivatives

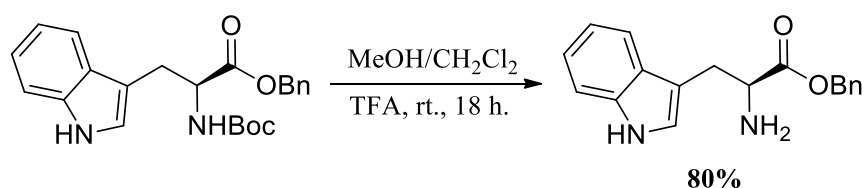
To explore the importance of carboxylate functionality, a series of benzyl ester derivatives were synthesised. As previously highlighted the lead benzyl ester analogue possessed an unsubstituted C¹ phenyl ring and the tested L *cis* diastereoisomer had an IC₅₀ of 19 μ M. Therefore, the purpose of this series was to attempt to improve the activity observed and to probe the effects a large hydrophobic interaction has on biological activity in comparison to previous methyl ester derivatives and the original MMV acid proton donor. A benzyl group offers π -stacking interactions as well as, the potential for further substitution on a second ring structure within the molecule. Therefore, this sub-set has the potential for a wide range of potential candidates.

To access the desired benzylated tryptophan starting material a benzylation was carried out with the relevant Boc-protected tryptophan i.e. D or L-Trp, obtaining moderate yield, without epimerisation at the α -centre (see Scheme 25).



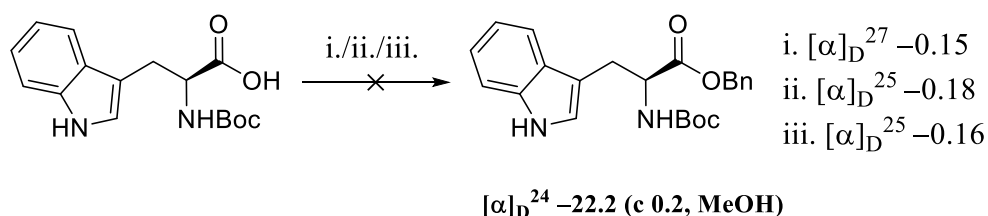
Scheme 25: Tryptophan benzyl ester formation i. MeOH, H₂O, Cs₂CO₃, ii. DMF, BnBr, rt.

Once benzylated, a required deprotection step takes place to remove *N*-Boc protection using trifluoroacetic acid in methanol/dichloromethane and produces a yellow oil in good yield that solidifies on standing (see Scheme 26). The reaction is followed easily by TLC due to the unprotected product being considerably more polar than the starting material, thus allowing simple purification by column chromatography.



Scheme 26: *N*-Boc deprotection

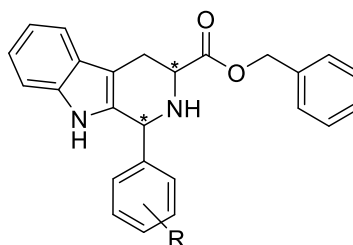
Alongside this methodology, more direct synthetic approaches were carried out to achieve the desired starting material whilst avoiding racemisation of the resultant product. However, all alternate attempts resulted in a racemic mixture, which was confirmed through optical rotation measurements (see Scheme 27).



Scheme 27: Alternate strategies

i. K_2CO_3 , CH_3CN , $BnBr$, Δ ; ii. $NaHCO_3$, CH_3CN , $BnBr$, Δ ; iii. Cs_2CO_3 , CH_3CN , $BnBr$, rt

The traditional Bailey method was initially employed to synthesis all benzyl ester derivatives, but the Lewis acid approach was subsequently carried out to allow comparison of diastereomeric ratios and yields - to see if the latter produces consistent results for alternate functional groups present during the cyclisation step.



R	Stereochemistry	Bailey d.r. <i>cis:trans</i>	Bailey Yield/%	Yb(OTf)₃ d.r. <i>cis:trans</i>	Yb(OTf)₃ Yield/%
<i>m</i> -NO ₂	<i>L trans</i>	3:1	25	1.2:1	36
	<i>L cis</i>		29		40

<i>p</i> -CF ₃	L <i>trans</i>	3:1	29	1.1:1	36
	L <i>cis</i>		32		41
<i>m</i> -CF ₃	L <i>trans</i>	3.3:1	23	1.2:1	36
	L <i>cis</i>		26		35
	D <i>trans</i>	3:1	24	1.1:1	24
	D <i>cis</i>		26		27
2,4-Cl ₂	L <i>trans</i>	3:1	15	1.1:1	32
	L <i>cis</i>		20		30
	D <i>trans</i>	3.1:1	13	1.1:1	31
	D <i>cis</i>		12		35

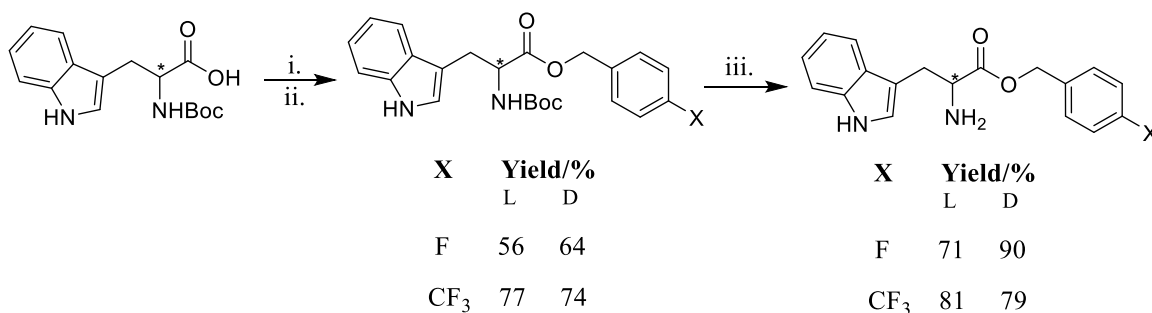
Table 13: Method comparison

A comparison for diastereomeric ratios can be seen in Table 13 and, as previously seen in all methyl ester derivatives, the Lewis acid method provides moderately equal quantities of both *cis* and *trans* cyclised product (average selectivity 1.1:1 *cis/trans*). Furthermore, yields are higher for the Lewis acid approach, when compared to the Bailey method. For example, the Lewis acid approach for 2,4-dichloro substituted analogues produced nearly twice the amount of product compared to the Bailey method (highlighted in Table 13). Also, purification was more straightforward compared to methyl ester derivatives, as the margin of separation on thin layer chromatography is larger.

2:4:3:1 Tryptophan substituted benzyl ester derivatives

In addition, successive analogues were synthesised to explore the contribution of an electron withdrawing group located on the benzyl ester ring for example, *para* trifluoromethyl and a *para* fluoro group. The substitution allows comparison of activity with the original MMV compound, by retaining a 2,4-dichloro moiety, and seeing the effects this change has on biological activity. A small fluorine group provides a strong electronegative interaction with hydrogen bond acceptor capabilities therefore, if this type of interaction is favourable then the inhibitory concentration should decrease. Also, a trifluoromethyl group was tested to see the effects a significantly more electronegative moiety had on biological activity.

To access this follow-on set of benzyl derivatives, the relevant substituted benzyl bromide was interchanged in the synthesis of the tryptophan ester to synthesise the desired starting material, which was then taken through to *N*-Boc deprotection and then Pictet-Spengler cyclisation (Scheme 28).

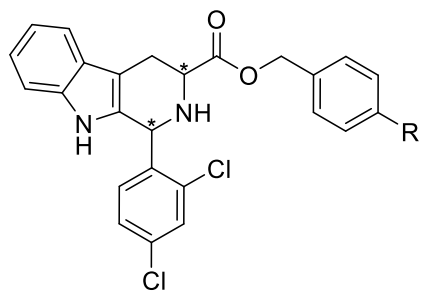


Scheme 28: Substituted benzyl ester synthesis

i. MeOH, H₂O, Cs₂CO₃, ii. DMF, X-PhCH₂Br, rt., iii. MeOH/CH₂Cl₂, TFA, rt., 18 h.

The comparable diastereomeric ratios are highlighted in Table 14 as well as yields, for the traditional Bailey method and Lewis acid method. On average the selectivity is ~3:1 for the Bailey method, and 1.1:1 for the Lewis acid method, therefore consistent with previous subsets. Also, product yields for both methods are similar with two exceptions highlighted

in Table 14, although unforeseen purification issues are the likely to be the cause of this discrepancy.

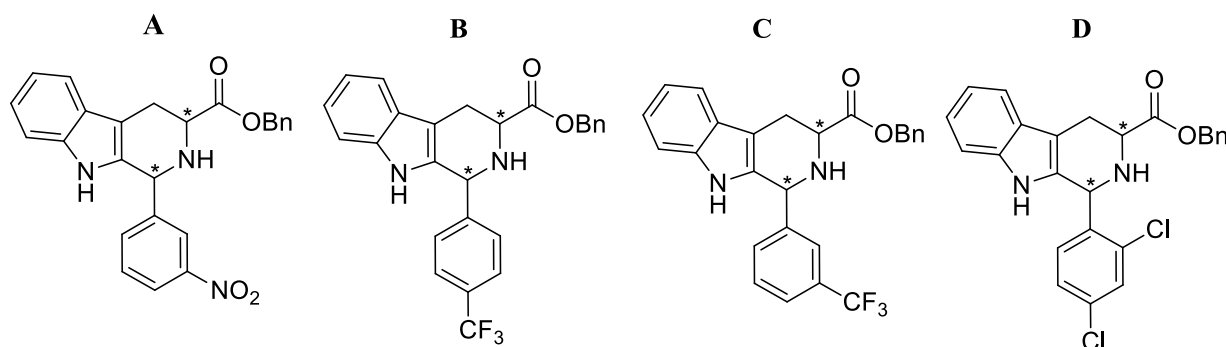


R	Stereochemistry	Bailey d.r. <i>cis:trans</i>	Bailey Yield/%	Yb(OTf)₃ d.r. <i>cis:trans</i>	Yb(OTf)₃ Yield/%
F	L <i>cis</i>	3:1	27	1.1:1	24
	L <i>trans</i>		36		30
	D <i>trans</i>	3.1:1	18	1.1:1	33
	D <i>cis</i>		32		36
CF ₃	D <i>trans</i>	3:1	27	1.2:1	24
	D <i>cis</i>		36		25
	L <i>trans</i>	3:1	28	1.3:1	27
	L <i>cis</i>		14		29

Table 14: Substituted benzyl esters

2:4:3:2 Tryptophan benzyl ester biological data

Table 15 displays the inhibitory concentrations obtained for the synthesised benzyl ester derivatives and those which possess an IC₅₀ of less than 6 µM have been highlighted.



Structure	Stereochemistry	IC ₅₀ /µM <i>Dd2 strain</i>
A	<i>L trans</i>	15.2
	<i>L cis</i>	13.7
B	<i>L trans</i>	3.6
	<i>L cis</i>	13.7
C	<i>L trans</i>	5.3
	<i>L cis</i>	3.1
D	<i>L trans</i>	2.3
	<i>L cis</i>	4.4
	<i>D trans</i>	5.4
	<i>D cis</i>	3.2

Table 15: Benzyl ester inhibitory concentration data

Both diastereoisomers of compound **A** possess activity ten times lower than the primary lead compound **mc72a** of which, the only difference is the ester linker, i.e. benzyl versus allyl ester. Therefore, as no improvement in activity was observed and the disfavoured medicinal chemistry properties of a nitro group, it was decided not to pursue nitro functionality any further.

Meanwhile, a benzyl ester derivative displaying good activity is the *L trans* diastereoisomer of compound **B** (IC₅₀ 3.6 µM) and the *L cis* conformation shows poor activity (**LVT15-2**

IC₅₀ 13.7 μ M) thus supporting the favoured 1*R* position of the phenyl ring. Furthermore, compound **C** L *trans* (5.3 μ M) and L *cis* (3.1 μ M) have moderate inhibitory concentrations. On the contrary to conformation trend the L *cis* compound displays lower activity, therefore the activity prediction cannot always follow through to observation. Overall, compounds which have a benzyl ester link in combination with a trifluoromethyl group show moderate activity and should be considered when making future compounds.

To compare a benzyl ester link to the original carboxylic acid moiety present for MMV008138, the 2,4-dichloro moiety was retained so a comparison could be made on inhibitory concentration. All four diastereoisomers of compound **D** in particular, the L *trans* and D *cis* conformations display marginally better activity than their partners, therefore complying with the prediction that the C¹ phenyl group is required to be in the 1*R* configuration for good activity. Although, the lowest activity of 2.3 μ M (L *trans*) is still not superior to both, (1*R*, 3*S*)-MMV008138 and **mc72a**. The activity is not dissimilar from the trifluoromethyl benzyl ester derivatives, nevertheless, there is potential for further functionalisation on the benzyl ester ring, so more derivatives were synthesised to explore this novelty in the compound.

A subset of substituted benzyl ester derivatives were synthesised however, biological data was only obtained for the L *trans* and D *cis* stereoisomers. Interestingly, the D *cis* diastereoisomer of compound **F** (6.57 μ M) is preferred over L *trans* diastereoisomer (48.1 μ M). Whereas, the L *trans* conformation (4.35 μ M) of compound **E** displayed higher activity compared to the D *cis* (32.3 μ M) diastereoisomer (see Figure 28). This could suggest for a (1*R*, 3*S*) configuration a larger electronegative interaction is favoured for this specific orientation, whereas a (1*R*, 3*R*) configuration desires a small electronegative interaction which provides the possibility of a hydrogen bond interaction.

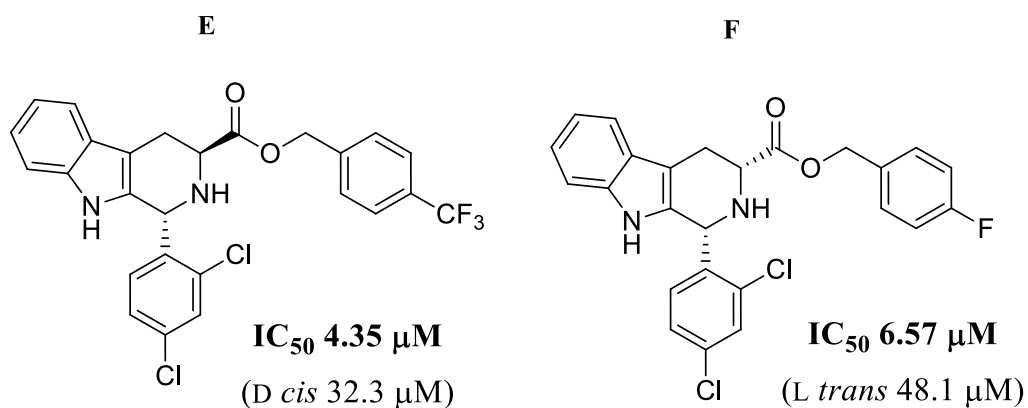
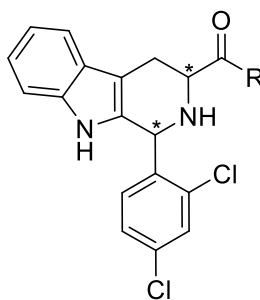


Figure 28: Substituted benzyl ester derivatives

As only two electron withdrawing moieties have been tested and produced unpredictable results in biological activity, further derivatives with alternate functionality such as, electron donating should be generated to probe these findings further before any conclusions can be made.

2:4:3:3 IPP reversal experiment results

To investigate the mechanism of action for this set of benzyl derivatives another biological experiment was conducted by the biology department known as an IPP reversal assay. The derivatives chosen to undergo this investigation represent a range of inhibitory activity observed across the compound screening as well as, reflecting the favoured *L trans* and *D cis* conformations. Table 16 shows the inhibitory concentrations for the nine compounds chosen and it is to be proven whether a low inhibitory concentration correlates to an increase in fold-change during the IPP assay. A large fold-change indicates the derivative is targeting the IspD enzyme and those that do not possess a fold-change are likely to act on an unknown target yet to be deciphered.



Reference	Stereochemistry	R	IC ₅₀ / μ M
942	<i>L trans</i>		48.1
962	<i>D cis</i>		6.57
971	<i>L trans</i>		4.35
952	<i>D cis</i>		32.3
1281	<i>L trans</i>	-OH	0.34
1282	<i>L cis</i>		16.9
1291	<i>D trans</i>		8.08

Table 16: Inhibitory concentration results

The assay was carried out on the trophozoite parasites due to the expression of a luciferase reporter protein at this stage which allows the experimenter to monitor parasite viability following exposure to an IC₅₀ dose. Alongside dosing the parasite with an IC₅₀ amount, one group is subject to IPP supplementation and the other group is not. Therefore, between the

two data groups the fold-change in parasite viability is calculated (i.e. luciferase counts) and Figure 29 displays the outcome of this experiment.

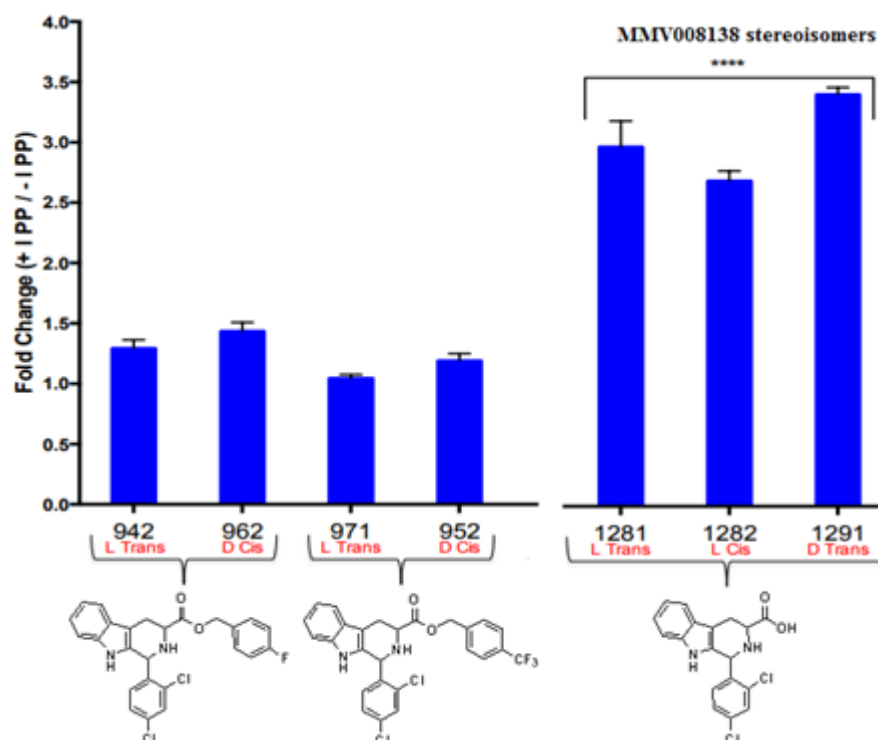
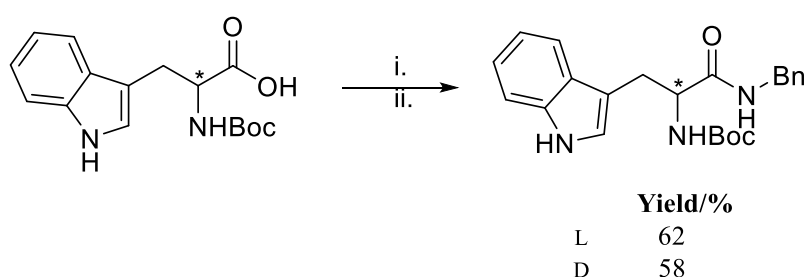


Figure 29: IPP fold-change results

As a result of the IPP reversal assay it is clear that supplementing the benzyl ester derivatives has minimal or no effect in reversing the initial inhibitory effect of the derivatives. On the other hand, IPP supplementation of the original MMV008138 stereoisomers shows the opposite and a significant fold-change is seen for these three compounds (Figure 29, far right). Also, each compound was dosed with an individual IC_{50} amount and since the IPP reversal effect is observed to be similar for these three acid compounds it suggests they all target the IspD enzyme regardless of their individual potencies. Further statistical analysis was carried out and it was concluded that there is no likely correlation between the inhibitory concentration potency and the ability to reverse the inhibition by IPP supplementation. However, to strengthen these findings the IPP reversal assay would need to be carried out on numerous derivatives. ⁽⁶²⁾

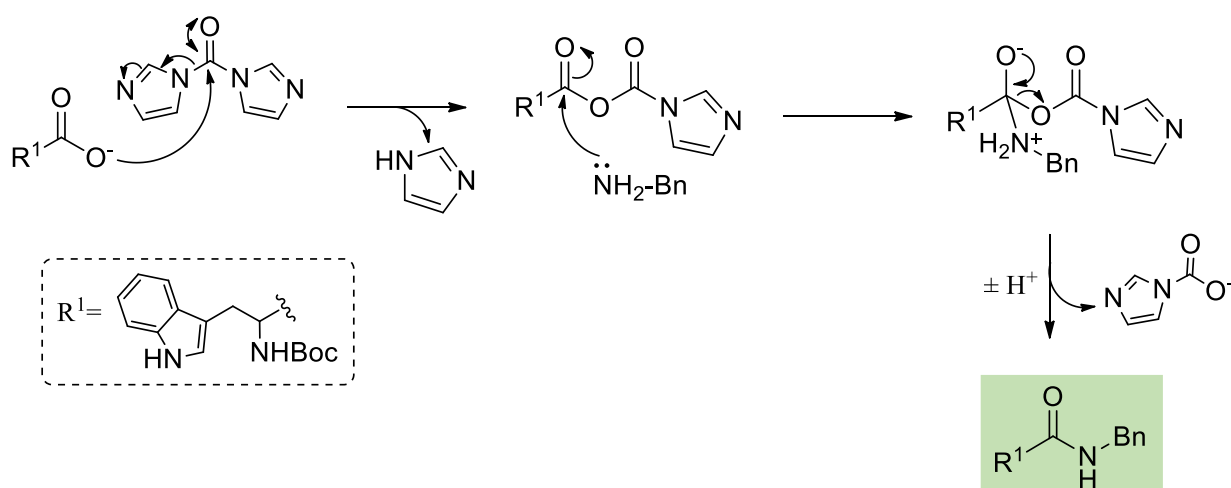
2:4:4 Tryptophan benzyl amide derivatives

Initial testing for the original benzyl amide lead possessed an unsubstituted C¹ phenyl ring and had an IC₅₀ of 17 μ M. As a result, the benzyl amide link was explored to see if activity could be improved and to probe the effects a proton donor next to the carbonyl carbon has on biological activity. Scheme 29 shows the first step in this synthetic strategy towards this small subset of analogues, which involves a primary amide coupling reaction.



Scheme 29: Amide coupling i. 1,4-dioxane, CDI, 45 °C, 3h., ii. 0 °C, BnNH₂, 18 h.

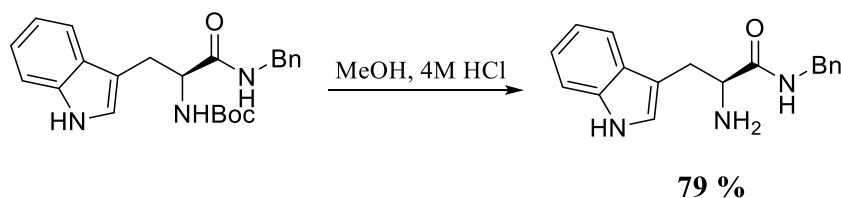
CDI was used to generate the benzyl amide link desired *via* the mixed anhydride for which the mechanism is shown in Scheme 30.



Scheme 30: CDI coupling mechanism

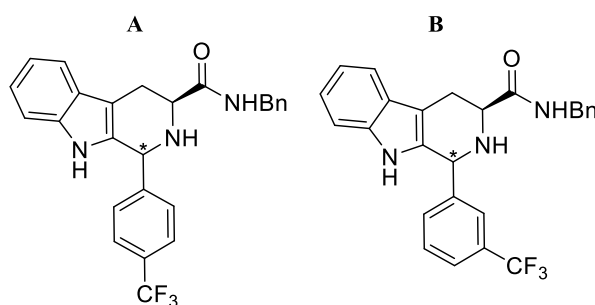
A simple *N*-Boc deprotection step was then carried out using methanol and 4M HCl under standard atmospheric conditions (see Scheme 31). The reaction time for this step was trialed

at 6 hours however, high amounts of starting material resided therefore, the reaction was left for 18 hours and the final product collected in good yield.



Scheme 31: Benzyl amide *N*-Boc deprotection

Table 17 displays a method comparison of diastereomeric ratios and yield for both, the Bailey method and Lewis acid approach. As previously seen the Bailey method produces much higher selectivity 2.5–3:1, whereas the Lewis acid method generates almost equal quantities of cyclised product. Also, purification of this subset of diastereoisomers proved less straightforward and a combination of this and high *cis* selectivity seen for the Bailey method resulted in particularly low yields for **A** and **B**.

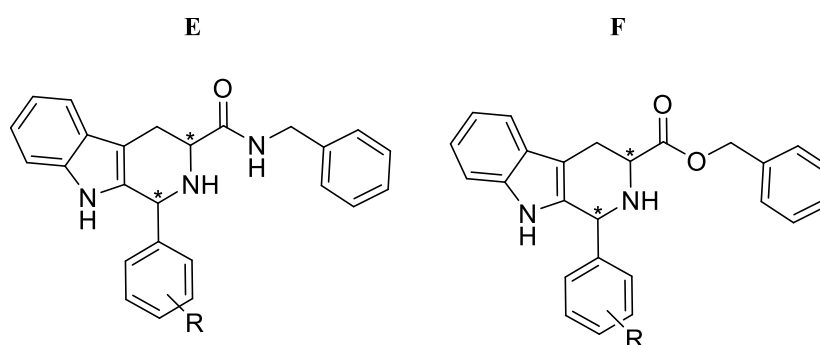


Structure	Stereochemistry	Bailey d.r. <i>cis:trans</i>	Bailey Yield/%	Yb(OTf) ₃ d.r. <i>cis:trans</i>	Yb(OTf) ₃ Yield/%
A	<i>L trans</i>	2.5:1	9	1.1:1	21
	<i>L cis</i>		53		21
B	<i>L trans</i>	3:1	8	1.1:1	24
	<i>L cis</i>		15		23

Table 17: Method comparison

2:4:4:1 Tryptophan benzyl amide biological data

Highlighted in Table 18 are the biological results obtained for this subset of benzyl amide analogues. The data obtained shows both the *L trans* for a *p*-CF₃ group and the *L cis* diastereoisomer for a *m*-CF₃ group is favoured. For example, the *L trans* diastereoisomer for compound **F** has the lowest inhibitory concentration (IC₅₀ of 3.6 µM), whereas the *L cis* diastereoisomer of compound **E** has the lower IC₅₀ of 2.3 µM compared to the *L trans* diastereoisomer (13.4 µM). To gather further insight into this observed pattern more benzyl amide derivatives would need to be synthesised to investigate.



R	Stereochemistry	IC ₅₀ /µM E	IC ₅₀ /µM F
<i>p</i> -CF ₃	<i>L trans</i>	3.5	3.6
	<i>L cis</i>	18.3	13.7
<i>m</i> -CF ₃	<i>L trans</i>	13.4	5.3
	<i>L cis</i>	2.3	3.1

Table 18: Benzyl amide and benzyl ester comparison

The inhibitory concentrations collected for the analogues possessing a benzyl amide link can now be compared to those obtained for compounds with a benzyl ester link. This will allow a primary comparison if any, between a proton donor and acceptor. Table 18 shows the comparison of the values obtained thus far and certain deductions can be extracted. There is no preference in stereochemistry overall and the differences in activity are negligible. Furthermore, no improvement in biological activity has been observed over the original

MMV hit. Although, novel compounds showing better activity than the original benzyl amide lead (17 μ M) and benzyl ester lead (19 μ M) have been discovered.

2:4:4:2 Methyl amide derivatives

The investigation of a small hydrophobic interaction is important, as a comparison with previously synthesised methyl ester analogues can then be made. The most active methyl ester derivative possessed a phenyl *m*-CF₃ substitution and an IC₅₀ of 5.10 μ M. The comparison will allow conclusions to be made regarding the importance of a proton donor in place of the proton acceptor next to the carbonyl group at C³ (see Figure 30). Also, it gives insight into what environment the compound is interacting with, i.e. a tight hydrophobic pocket displacing fewer interacting water molecules, compared to a benzyl group which interacts with a bigger surface area and offers π -stacking, as well as large hydrophobic interactions. Furthermore, R substitutions retained electron withdrawing properties and consisted of varying halogen patterns.

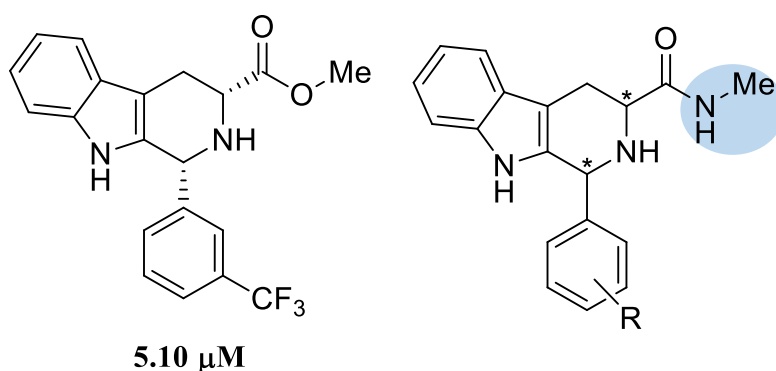


Figure 30: Methyl amide derivative

Initial screening was carried out on the 7 derivatives synthesised as part of another PhD project and the results highlighted an overall loss of potency. However, two of the more active compounds were taken and tested for their inhibitory concentration. Table 19 shows the biological activity of both methyl amide derivatives tested for their inhibitory concentration. Both methyl amide compounds tested display a large decrease in activity from the original MMV hit as well as, a loss of potency compared to the best methyl ester analogue (5.10 μ M).

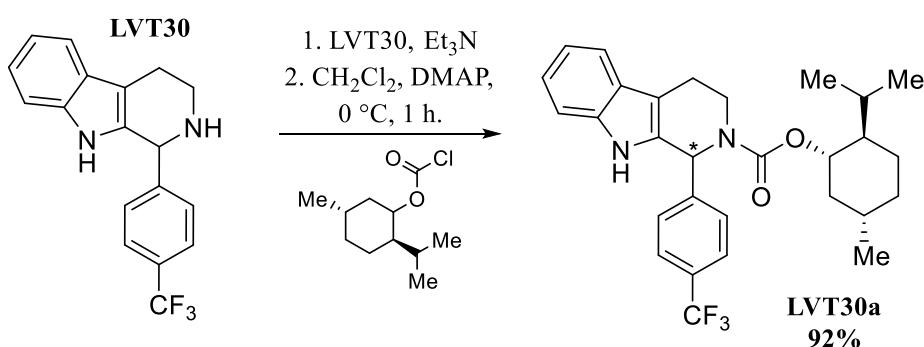
R	IC₅₀/ μM
<i>p</i> -CF ₃	> 100
<i>m</i> -CF ₃	> 100
2,4-Cl ₂	8.79
<i>p</i> -F	> 100
<i>p</i> -Cl	172
<i>m</i> -Cl	> 100
2,4-CF ₃	> 100

Table 19: Methyl amide biological data

Unfortunately, only one diastereoisomer was isolated from the reaction mixture so, *cis* and *trans* stereochemistry could not be assigned as both carbon NMR spectra are required to do this. As a result, a methyl amide moiety in place of a methyl ester group has provided no benefit for antimalarial activity. However, only seven analogues have been screened therefore no definite conclusions can be drawn.

2:5 Enantiomeric resolution of tryptamine derivative

Meanwhile, as **LVT30** provided the best activity tetrahydro- β -carboline thus far, it was proposed the enantiomeric mixture should be separated into (*R*) and (*S*) configurations and tested separately for inhibitory concentration. A chiral moiety was incorporated *via* amide coupling as shown in Scheme 32, which generates diastereoisomers. Subsequently, separating the diastereoisomers and the temporary chiral group removed, to allow testing of (*R*)-**LVT30** and (*S*)-**LVT30**.

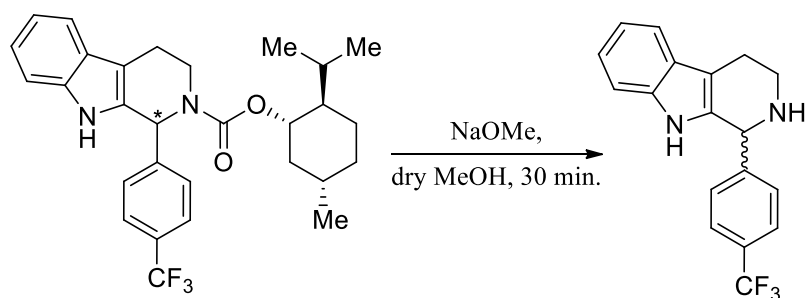


Scheme 32: Generation of **LVT30** diastereoisomers

An alternative chiral Mosher's acid chloride was also coupled to **LVT30** to generate the diastereoisomers but more material was produced for the menthyl compound and was therefore used for enantiomer resolution. Firstly, thin layer chromatography was employed to attempt diastereoisomer separation with different mobile phases on SiO₂ but no separation was observed. As a result, other methods of separation had to be considered. Eventually, HPLC separation was carried out to obtain the separated enantiomers with the hope of then cleaving the amide bond created from menthyl chloroformate.

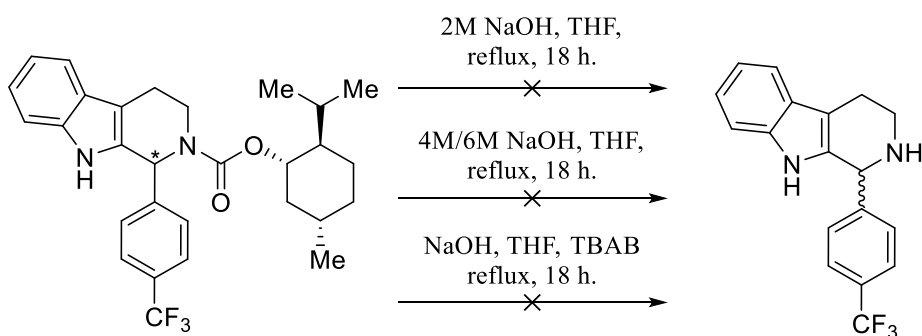
The only literature preparation found for cleavage of this particular menthyl amide bond is outlined in Scheme 33. Compound **LVT30a** and sodium methoxide were subjected to anhydrous conditions inside a round bottom flask and flushed with nitrogen. Then, dry methanol was added *via* syringe and the resultant solution left at room temperature to stir for

30 minutes.⁽⁶³⁾ After 30 minutes, a TLC was taken of the reaction mixture and showed only starting material therefore the reaction was left overnight. Unfortunately, only starting material was shown on TLC after 18 hours so this method was abandoned.



Scheme 33: Sodium methoxide amide cleavage

Due to very limited methodologies focusing on menthyl amide hydrolysis, a straightforward sodium hydroxide hydrolysis was investigated. Consequently, a 2M NaOH solution was stirred in a round bottom flask, along with an equal volume of tetrahydrofuran (THF) and **LVT30a** was added (see Scheme 34). The mixture was stirred at reflux for 18 hours and thin layer chromatography revealed solitary starting material.

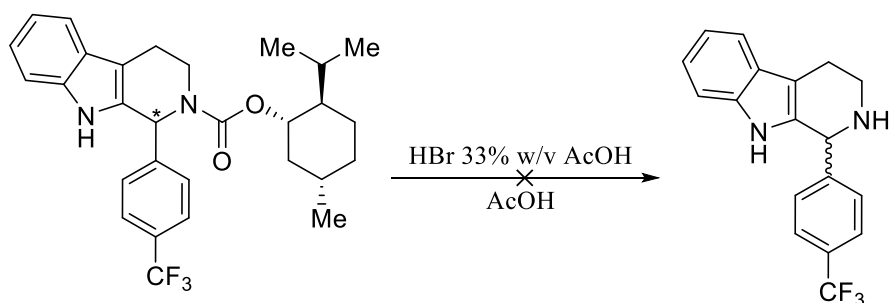


Scheme 34: Sodium hydroxide hydrolysis

Therefore, higher concentrations of 4M and 6M NaOH were also tested, to see if a higher concentration was required to perform the hydrolysis. Unfortunately, neither concentration of NaOH successfully hydrolysed the menthyl amide group. To understand if reaction phase was the issue, tetrabutylammonium bromide (TBAB, 1.2 eq.) was added as a carrier, to aid

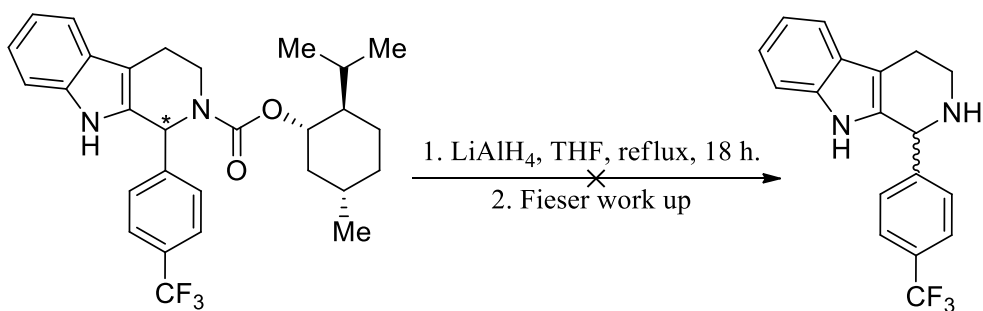
transfer of starting material between the aqueous and organic phase however, this methodology was ineffective.

Scheme 35 displays an alternate method using hydrogen bromide. A TLC could not be taken on reaction completion as the reaction mixture was too acidic and the product would be protonated so is unlikely to move on TLC. Therefore, toluene (4 mL) and water (4 mL) were subsequently added and left to stir for 5 minutes. The organics were extracted and TLC sadly revealed simply starting material.



Scheme 35: Hydrogen bromide method

The final method employed lithium aluminium hydride to attempt cleavage of this stubborn menthyl amide bond (see Scheme 36). Unfortunately, this hopeful methodology was not successful and the aim to hydrolyse this menthyl amide was retired until future investigations take over.



Scheme 36: Lithium aluminium hydride method

2:6 Future work

The central tetrahydro- β -carboline moiety offers great potential for additional optimisation, as only two sites of functionality have been investigated thus far and no improvement in activity has been found compared to the MMV hit.

Figure 31 highlights prospective sites surrounding this core, which are yet to be explored for antimalarial potential, or still have potential for further optimisation.

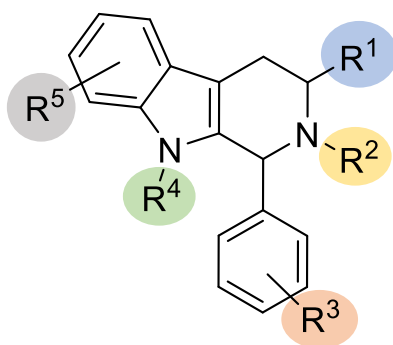


Figure 31: Sites for further optimisation

Even though the R¹ group has been the focus of this series of analogues, there are still suggestions of alternate functionality to be researched. For example, a small interaction is required at the R¹ position for this IPP mechanism of action; an *isopropyl* ester could explore a small branch interaction. Furthermore, it would be interesting to observe a primary amine linked to the carbonyl carbon, to permit a comparison with the original MMV008138 carboxylic acid. Finally, a carboxylic acid alternative such as, a tetrazole functional group could provide insight into the size of moiety required at the R¹ position, while retaining an acidic environment.

However, priority should be given to further tryptamine and α -methyl tryptamine derivatives as these proved the most active. Developing the α -methyl subset further could include: α -ethyl, α -*isopropyl*, α -acetyl and a digeminal methyl group – to observe what functionality gives the lowest inhibitory concentration. Figure 32 displays potential future structures,

which should be synthesised to allow conclusions to be drawn regarding an absent C³ carbonyl group interaction.

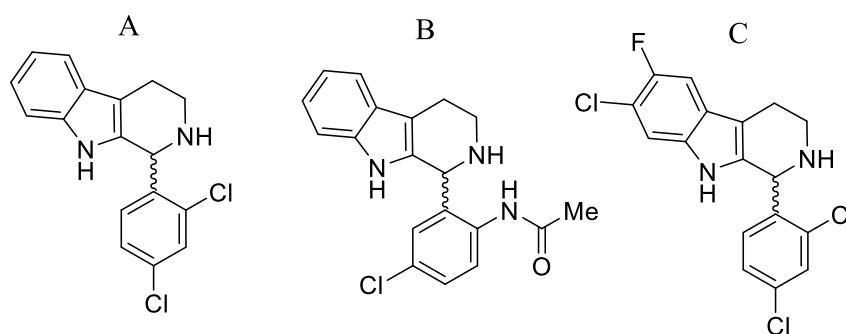


Figure 32: Tryptamine proposals

Compound A retains a 2,4-dichloro moiety, which will allow direct comparison to MMV008138 and therefore provide a stronger insight as to whether the carboxylic acid moiety is required for activity targeting IPP inhibition. On the other hand, compound B and C explore the structure activity relationship further, as both compounds simulate NITD609 functionality therefore, allowing comparisons to be made to another superior antimalarial hit.

By generating more α -methyl tryptamine derivatives alongside varying functionalities at R³ it would give way to further insight into the important features required for high activity and probe this solitary short hydrophobic interaction over the original carboxylic acid moiety (see Figure 33).

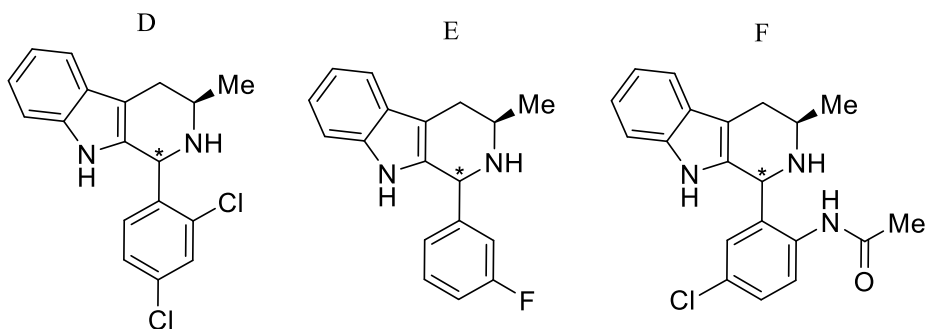


Figure 33: α -methyl tryptamine proposals

A 2,4-dichloro moiety (D) would allow direct comparison to **MMV008138**, as well as observing activity with a new fluorine analogue (E) that offers a small electronic interaction, with the potential for hydrogen bond accepting. The proposed compound F mimics NITD609 thus allows direct comparison and offers potential for further optimisation on the central indole moiety.

Future compounds in the methyl ester subset should not include pyridine substitutes as they do not show good activity. Also, this set of compounds has indicated the position of the electron withdrawing group is not necessarily as important as first thought. The key feature is the moiety attached to the carbonyl carbon, which, in combination with an electron withdrawing group – gives good compound activity. However, in this subset no arrangement synthesised so far has come close to the superior activity of (1*R*, 1*S*)-**MMV008138**. Figure 34 displays future compound suggestions which includes a 2,4-difluoro moiety, and an analogue which retains the features of previously discussed compound simulating NITD609 with the addition of further R⁵ substitutions.

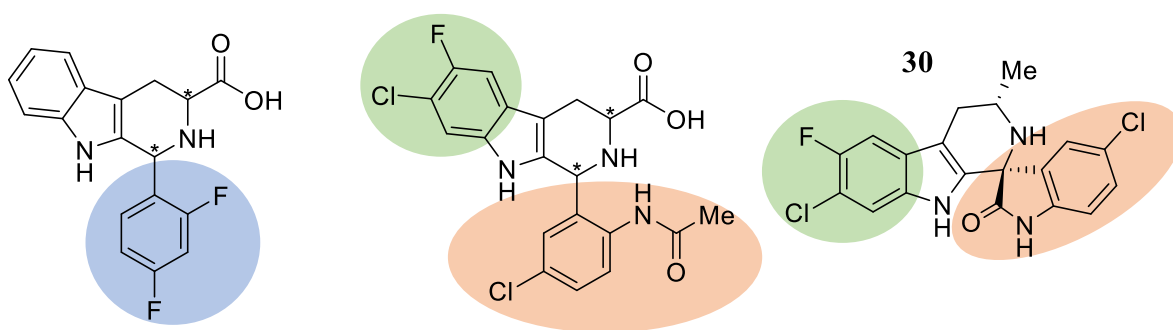


Figure 34: Future analogues and NITD609

A 2,4-difluoro substitution offers two, small, highly electronic interactions, as well as the ability to offer hydrogen bond interactions – which is yet to be investigated. Simulating NITD609 offers an interesting comparison, therefore by synthesising a (1*R*, 3*S*) version of a tetrahydro- β -carboline alternative, comparisons of the biological activities can be made.

Alternatively, biological data obtained from the benzyl ester series has provided insight into what features should not be retained for future analogues for example, the nitro group. Also, inhibitory concentrations obtained for trifluoromethyl derivatives were comparable to compounds possessing a 2,4-dichloro moiety, therefore negligible differences would inspire future analogues to retain a 2,4-dichloro substitution as this provides lower molecular weight. However, substituted benzyl ester derivatives provide a wider scope for future generation of compounds, as shown in Figure 35.

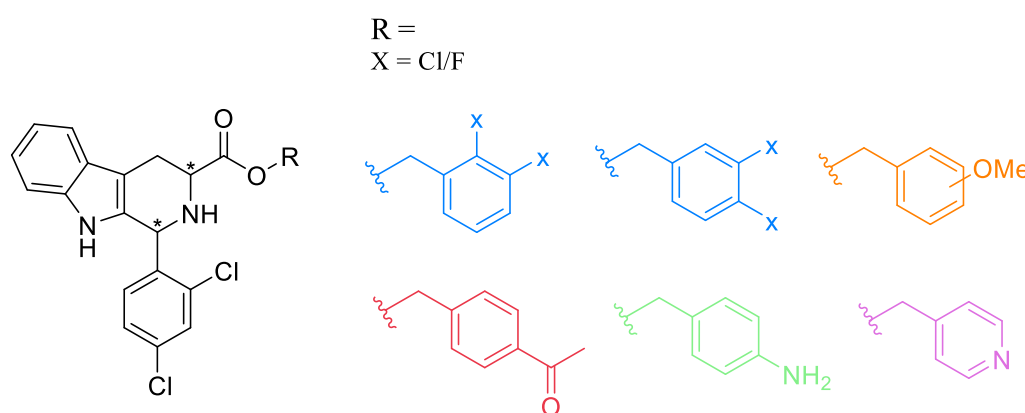


Figure 35: Benzyl ester analogue proposals

Through retention of a 2,4-dichloro moiety alongside novel benzyl ester substitutions it will allow the investigation into the effects of: importance of substitute position, an electron withdrawing group and hydrogen bond acceptor/donor. Also, as previously discussed for methyl ester compounds, further substitution on the tetrahydro- β -carboline ring system should be investigated.

Furthermore, at this stage of optimisation all four diastereoisomers still need to be generated as there is no guarantee both, D *cis* and L *trans* conformations possess the best activity. The subsequent wider set of derivatives will give insight into what moieties are important for low activity and positional significance, with the projection of generating compounds with significantly lower inhibitory concentrations.

The same statement can be applied to the benzyl amide derivatives, as shown in Figure 36 to explore the contribution of the benzyl amide link. Future analogue suggestions include further benzyl amide substitution to investigate interactions surrounding the novel phenyl ring.

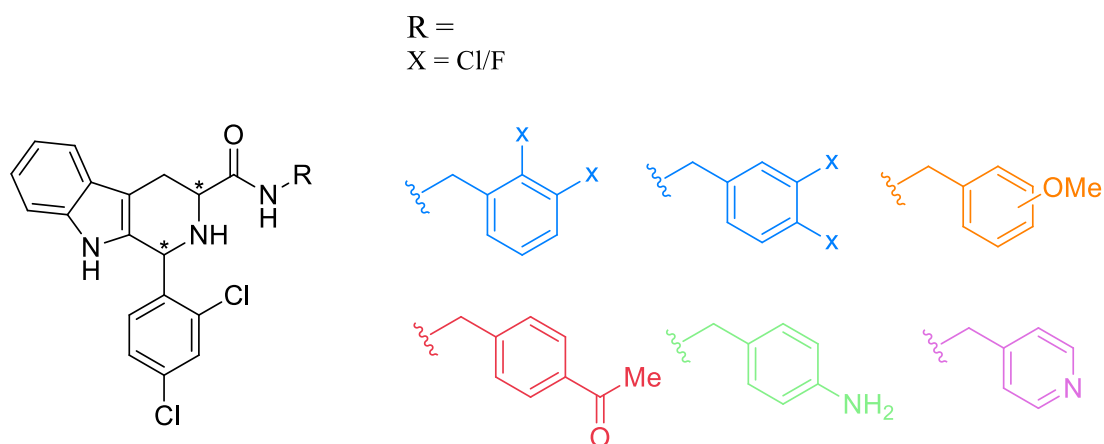
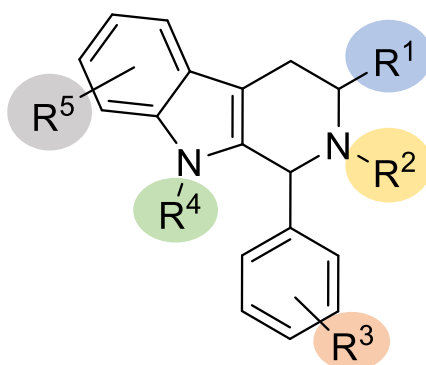


Figure 36: Benzyl amide proposals

At this stage there is no discrepancy between benzyl ester and benzyl amide analogues and neither subset produced a compound with better activity than the original MMV hit or our lead **mc72a**. Overall it can be concluded that future analogues possessing either benzyl link would not display superior antimalarial activity compared to the original hit. Both benzyl links have comparative stability in drug compounds and can be cleaved either by esterase or peptidase enzymes, so one does not offer advantages over the other.



On the other hand, changes to R^4 offers limited potential for multiple variation however, should not be overlooked as there is great difference between a hydrogen bond interaction and a methyl/ethyl hydrophobic interaction. Meanwhile, R^2 substitution provides a wider scope of functionality through *N*-substitution for example inserting an; acetyl group, alkyl chain or an amide/ester link, thus derivatives of this nature should be generated to see the effects they have on biological activity.

Finally, R^5 has yet to be explored, as seen in compound NITD609 a chlorine and fluorine moiety are situated in similar positions and are required for potent activity. Therefore, as previously discussed in detail, it would be essential to explore activity of different functionalities on the indole core, to see if positive effects are observed in biological activity.

2:7 Summary

Over 50 novel compounds have been generated to investigate the optimisation of (1*R*, 3*S*)-MMV008138, of which, each subset highlighted essential insight into which structural features are required for good activity. Figure 37 shows the relatively flat structure-activity relationship and summarises all analogue features generated which all resulted in overall decreased in activity compared to the original MMV008138 hit.

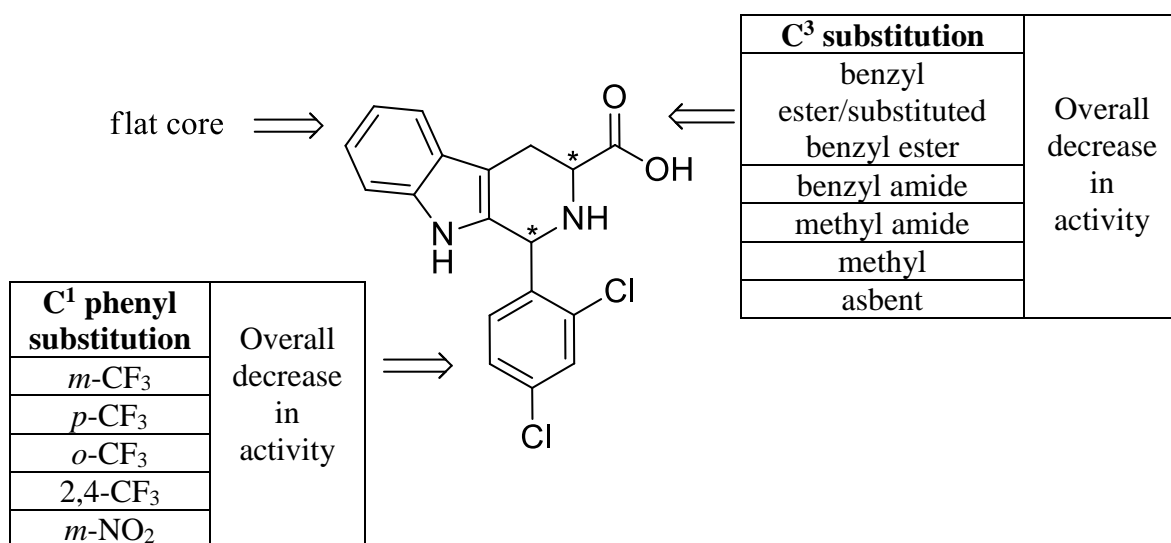


Figure 37: Tetrahydro- β -carboline summary

Meanwhile, biological assay data has provided evidence that the mechanism of action is different for the analogues generated during this project, in comparison to MMV008138 as they are not reversed by IPP supplementation. To conclude, although this smaller project still has potential to generate further derivatives, it seems unlikely that any new derivative generated by this project are likely to offer a compound with superior inhibitory concentration over (1*R*, 3*S*)-MMV008138.

Chapter 3: Spiroindolines

3:1 Spirocycles in drug discovery

Natural and synthetic compounds containing two rings fused by a solitary shared atom are known as spirocyclic and are abundant in natural products. Figure 38 displays the general spiro format and some examples.

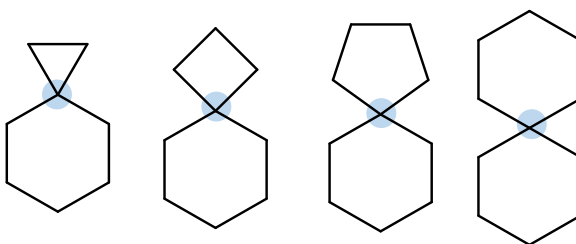
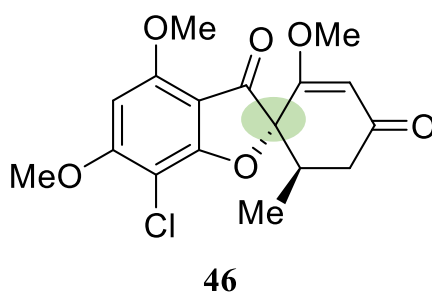


Figure 38: Two ring spiro formula

For example, Griseofulvin **46** was discovered in 1939 within *Penicillium* mould and is now present on the World Health Organisation (WHO) list of essential medicines. It is an oral antifungal treatment for nail and skin infections after primary antifungal cream failure and does not work as a topical formula. Griseofulvin binds to tubulin and on disrupting microtubule function, results in mitosis inhibition.⁽⁶⁴⁾



Over the past two decades this spirocyclic feature has risen in popularity for its 3-dimensionality to generate novel drug candidates. The most common ring systems are five or six membered rings, which provide molecular complexity in a drug molecule and may offer greater benefit over flat ring systems.⁽⁶⁵⁾ However, these types of structures have been

labelled as difficult to synthesise due to the presence of a stereogenic quaternary carbon fusing the two rings. As a result, recent progress has produced new synthetic routes to generate these spiro building blocks which have allowed incorporation of this desired scaffold into synthetic bioactive molecules.⁽⁶⁵⁾

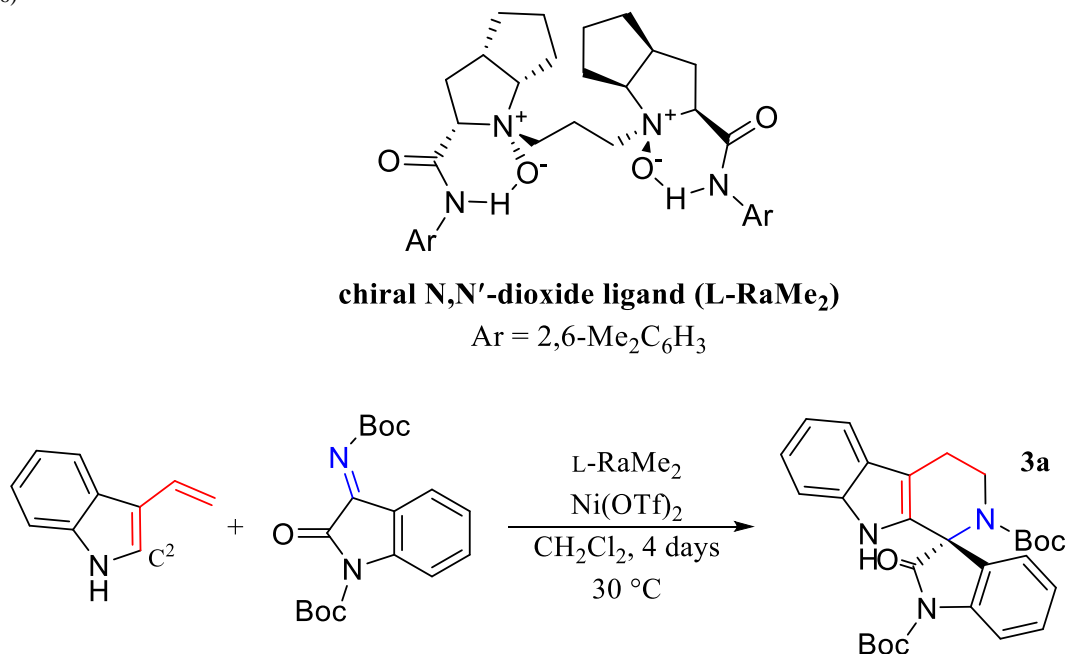
Although, introducing spirocyclic fusion tends to impose rigidity if this feature is incorporated within the core of the molecule but if present within the periphery of a compound this conformational impact is reduced. It has been suggested that compounds with too many flat rings have disfavoured physical properties and are less likely to become developed drugs. Therefore, adding a peripheral spirocyclic moiety allows modulation of physical properties such as: water solubility, logP and metabolic stability. Additionally, opposed to flat aromatic systems, a spiro group introduces structural novelty – which allows access to novel patent space.⁽⁶⁵⁾ Consequently, spiro compounds have become a popular area of development within the pharmaceutical industry to exploit bioactive molecules.

3:2 Spirocyclic synthetic strategies

3:2:1 Asymmetric catalysis

As previously discussed the antimalarial candidate NITD609 requires a 1*R*, 3*S* configuration to generate the highest potency form (0.9 nM). This specificity results in expensive separation techniques on a chiral column to obtain the desired form. Therefore, Feng *et al* suggested using asymmetric catalysis to generate optically active spirocyclic oxindoles to combat some of the issues surrounding this type of synthesis such as: diastereo and enantioselectivity, the spirocyclic fused core and the tertiary carbon centre (see Scheme 37).

(66)



Scheme 37: Enantioselective Nickel(II)-mediated asymmetric synthesis with chiral ligand

They state by reacting 3-vinylindoles with ketimines in a aza-Diels-Alder cycloaddition it can generate a high regio, diastereo and enantioselective synthesis. Two Boc groups are used with the notion that the catalyst would activate the aza-dienophile (ketimine) by binding to the two carbonyl groups in a bidentate form. The C² of the indole bonds to the electron poor carbon-nitrogen double bond however, after 48 hours only 13% of the product **3a** had been generated in 68:32 e.r.. Therefore, the reaction conditions were optimised and as a result the

reaction was carried out at $-10\text{ }^{\circ}\text{C}$ using an alternate L-RaPr₃ catalyst constituent, which produced 78% of **3a** with 97.5:2.5 e.r.⁽⁶⁶⁾ Since the reaction conditions were optimised, the research group turned their attention to reaction substrate scope.

Firstly, ketimine variation was explored and it was found to tolerate electron donating groups such as a nitro group as well as electron withdrawing groups such as halogens which are important in the case of NITD609 (**30**, see Figure 39).

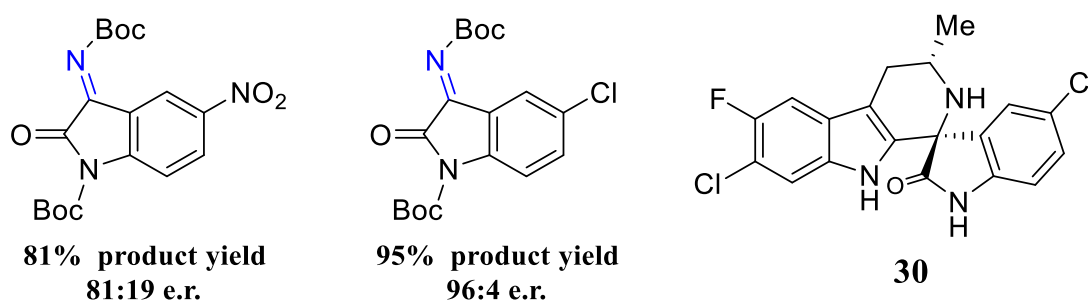


Figure 39: Ketimine reaction scope

During the investigation into substituted 3-vinylindole starting materials, they decreased the reaction temperature to $-30\text{ }^{\circ}\text{C}$ to give good enantioselectivity. The primary derivatives explored both single and double halogen group substitutions at position 5/6 but, in the case of NITD609, a 5,6-dihalo substitution is required and was achieved in similar compound (*S*)-**3v** (see Figure 40). Furthermore, an *E/Z* mixture of 3-propen-yl-indole gave intermediate **4y** in 63% yield, 99:1 d.r. and an e.r. of 99.5:0.5 (see Figure 40). They found the *E*-configuration of the vinylindole only participated under the optimised reaction conditions, which produced high diastereoselectivity.⁽⁶⁶⁾

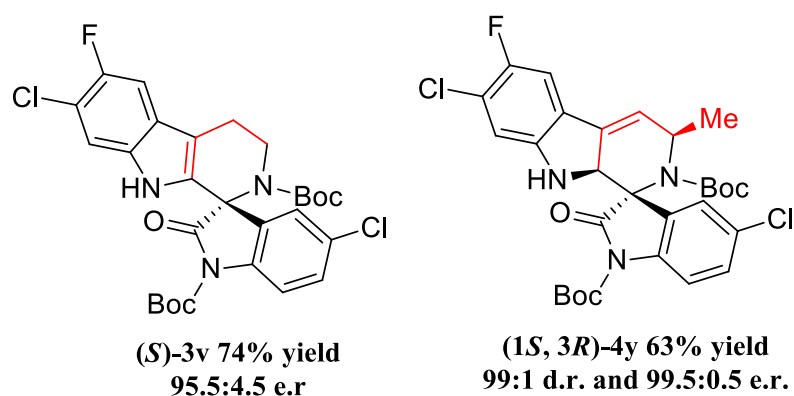
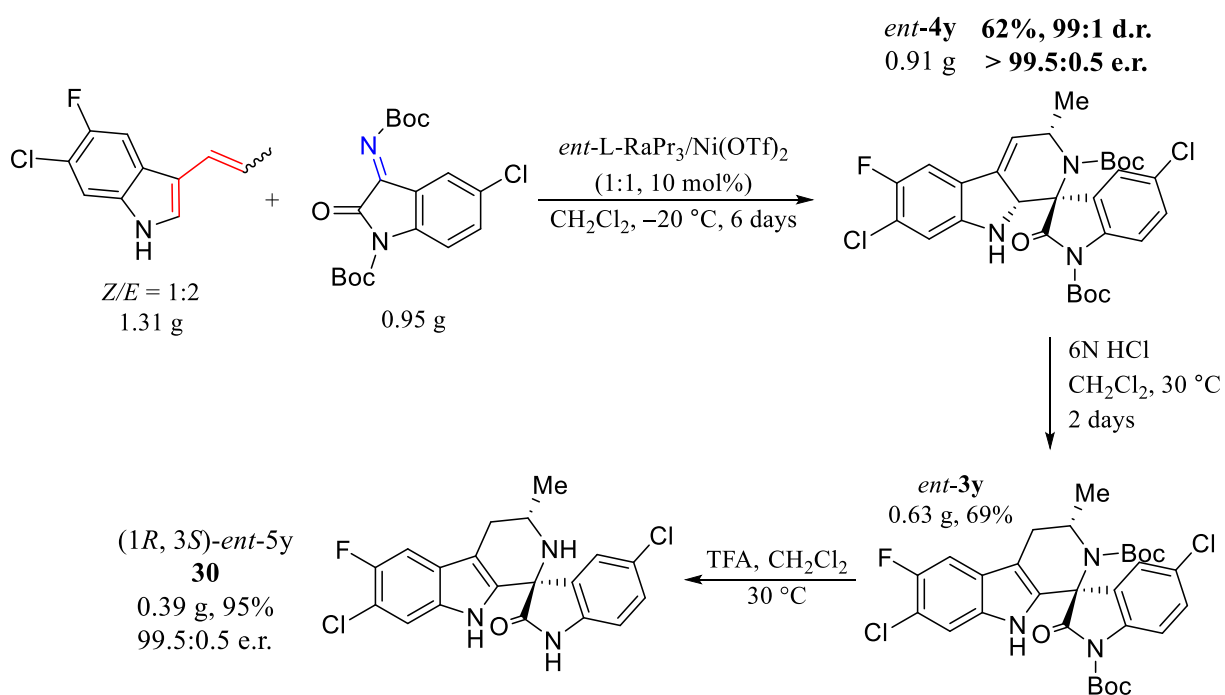


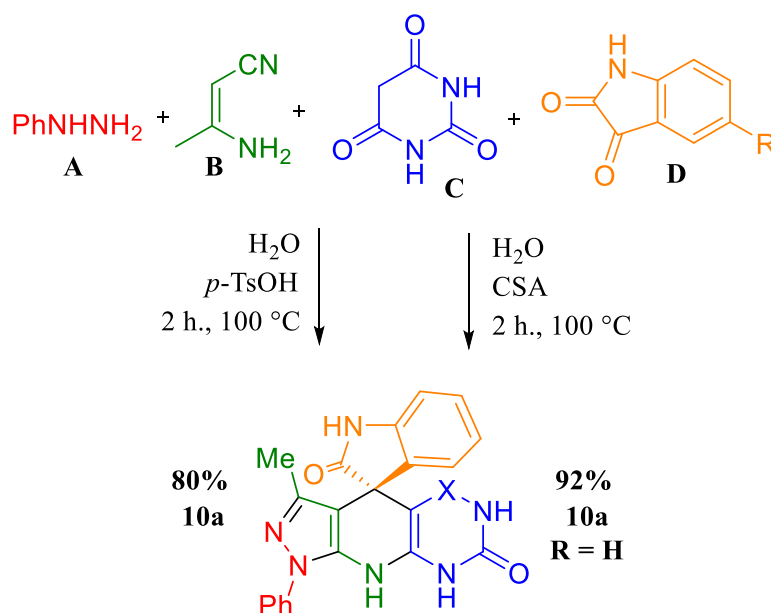
Figure 40: 3-Vinylindole variation

To incorporate both variation points detailed above, they generated NITD609 on a one gram scale through a 3-step, efficient, straightforward asymmetric catalytic synthesis with high selectivity (see Scheme 38).⁽⁶⁶⁾



3:2:2 Convergent metal-free approach

Balamurugan *et al* proposed a racemic one pot, four component, domino reaction involving: phenylhydrazine **A**, 3-amino-crotononitrile **B**, cyclic 1,3-diketones **C** and substituted isatins **D** in an aqueous medium to generate a spirocyclic centre (see Scheme 49). The original route carried out involved 1 equivalence of *p*-toluenesulfonic acid (*p*-TsOH) under reflux for 10 hours however, this afforded 80% yield of compound **10a** (see Scheme 39). During reaction condition optimisation they utilised 0.5 equivalents of (±)-camphor-10-sulfonicacid (CSA) which produced **10a** in 92% yield in 2 hours. Therefore, they concluded using CSA in a water medium produced the best reaction conditions for generating the spirocyclic product in high yields. ⁽⁶⁷⁾



Scheme 39: One-pot, four component syntheses (X=C=O, R=H, Cl, NO₂) ⁽⁸⁰⁾

As optimal conditions were achieved they explored substrate scope and found this synthesis can tolerate a range of starting materials. For example, the spiro heterocycle can include two conjoined aromatic rings and the cyclic 1,3-diketone can possess a sulfur component as well as an alternate dimethyl substituent (see Figure 41).

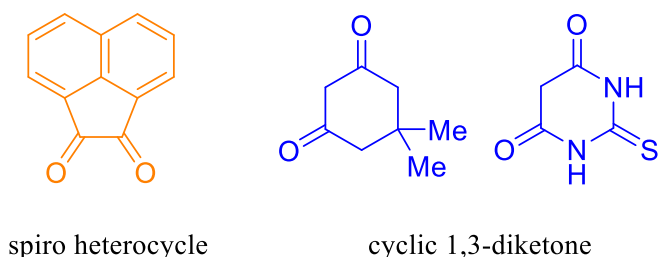
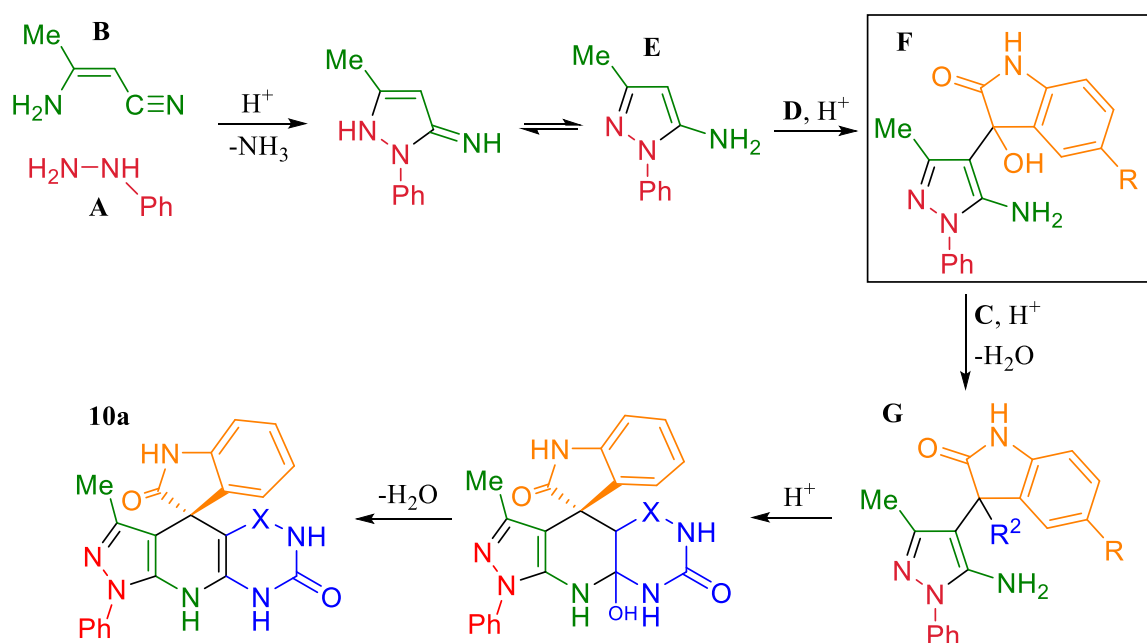


Figure 41: Substrate scope

A proposed mechanism for this reaction involves a phenylpyrazole intermediate **E** which is thought to be responsible for activating the domino sequence of reactions. This intermediate is created from the acid-catalysed reaction of phenylhydrazine and 3-aminocrotononitrile and generates **E** in 98% yield. Then, **E** goes on to react with isatin **D** which generates a second intermediate compound **F** and has been isolated as the sole product in some of the optimisation reactions. Subsequently, **F** undergoes a reaction with the cyclic 1,3-diketone under acidic conditions. Finally **G** carries out annulation then, a dehydration step occurs to produce **10a** (see Scheme 40).



Scheme 40: Proposed reaction mechanism (X=C=O and R=H)

Overall, Balamurugan *et al* state to have created a convergent, short reaction time, excellent yielding, easy operation, broad scope and an environmentally friendly synthetic route to incorporate a spirocyclic moiety.

3:3 Spirocyclic antimalarials

3:3:1 NITD609

In 2010 Yeung *et al* reported novel compound **47** to display potent antimalarial activity and was highlighted during high-throughput screening. Compound **47** possesses an inhibitory concentration of 90 nM against wild type malaria (NF54) and 80 nM against a chloroquine-resistant strain (KI) (see Figure 42). After further biological probing, **47** was found to be active against *P. berghei* in mouse models and a single 100 mg/kg dose resulted in a 96% reduction in parasitic activity.⁽⁶⁸⁾ Therefore, optimisation of this promising compound was undertaken to increase potency and *in vivo* activity.

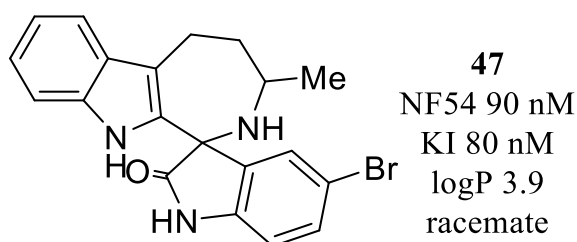
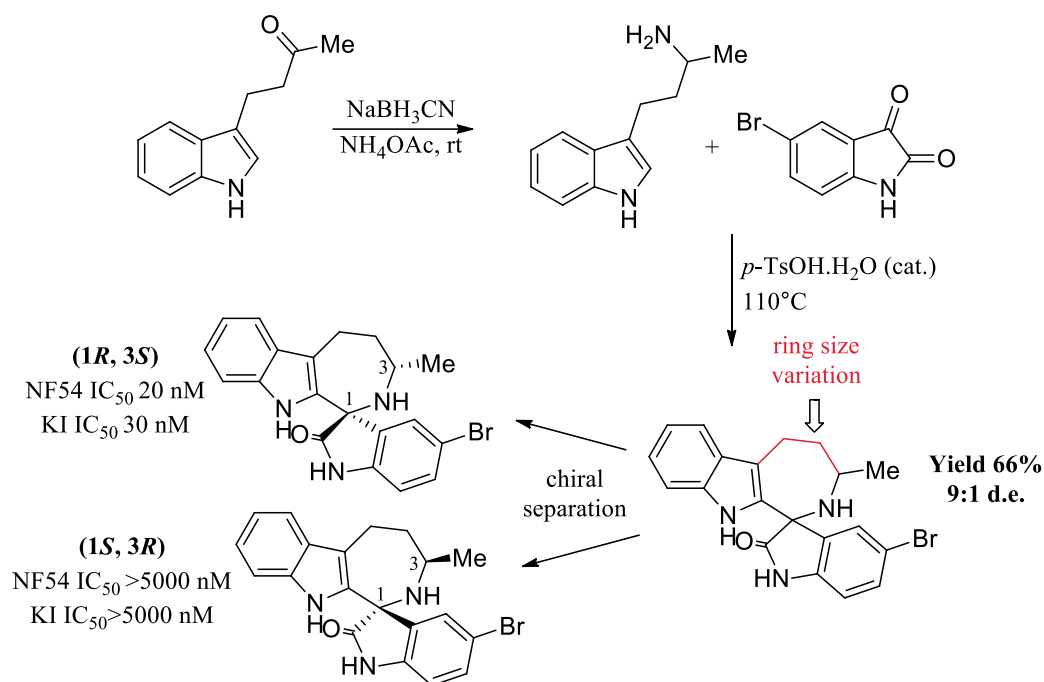


Figure 42: Original hit

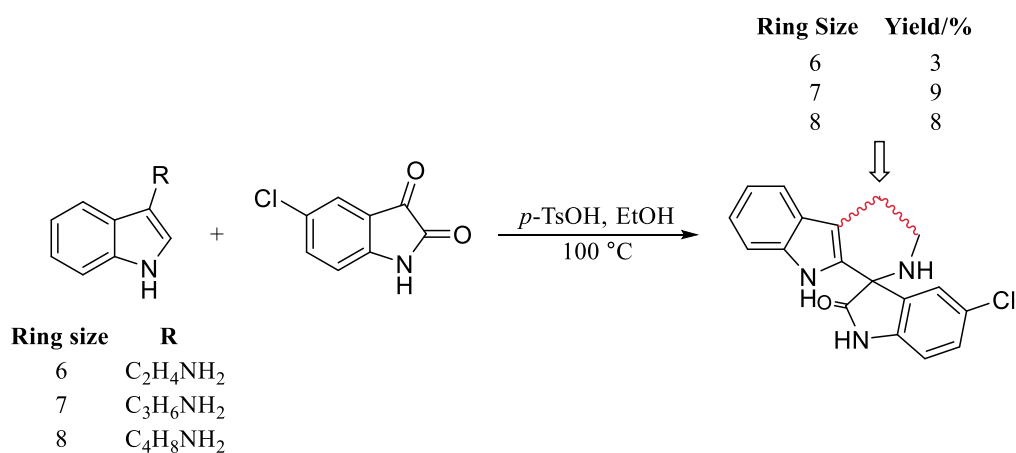
Firstly, the research group intended to synthesise this novel compound as it existed as a racemic mixture. Therefore, Scheme 41 displays the synthetic route to generate **47**. The novel compound can exist as (1*S*, 3*S*) and (1*R*, 3*R*) or (1*R*, 3*S*) and (1*S*, 3*R*) stereoisomers and, the favoured pair were found to be (1*R*, 3*S*) and (1*S*, 3*R*) in ~9:1 diastereomeric excess after chiral separation and confirmatory X-ray structure determination.⁽⁶⁸⁾

The individual diastereoisomers were tested *in vivo* and were found to possess significantly different potencies. For example, the most potent stereoisomer (1*R*, 3*S*) was found to be over 250 times more potent than its sister (1*S*, 3*R*) stereoisomer (see Scheme 41).



Scheme 41: Hit synthesis and diastereoisomer activity comparison

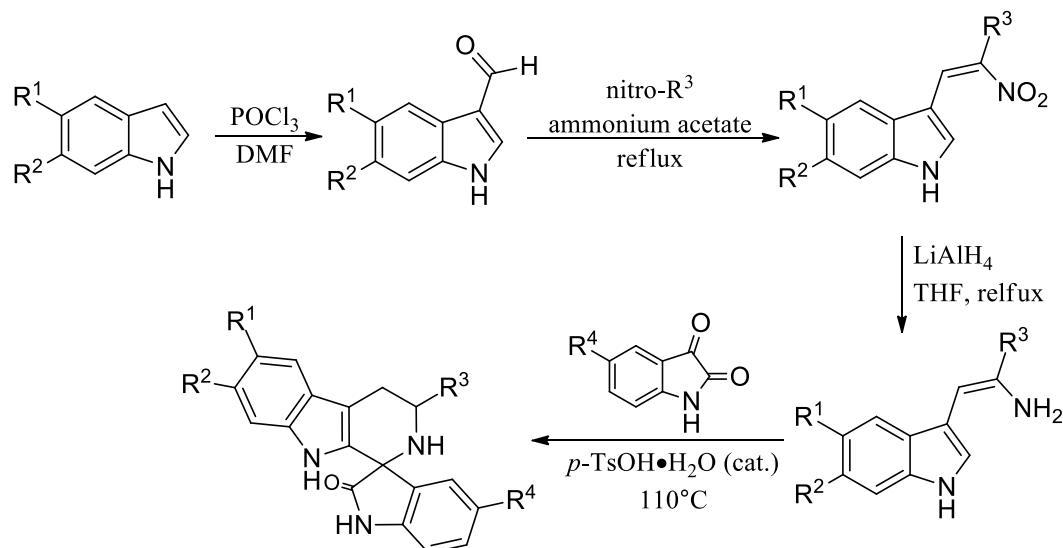
To explore the effect of ring size variation (highlighted above) on activity six, seven and eight membered ring derivatives were generated from 5-chloroisatin *via* the synthetic route shown in Scheme 42.



Scheme 42: Ring size variation

Alternatively, a second synthetic route was employed to generate the majority of analogues during the optimisation stage (see Scheme 43). This strategy employed indole as the starting

reagent and the desired product formed *via* a Vilsmeier-Haack intermediate with a high degree of diastereoselectivity.⁽⁶⁸⁾



Scheme 43: Alternate synthetic route $R^1, R^2, R^4 = \text{F/Cl}$ and $R^3 = \text{H/CH}_3/(\text{CH}_3)_2$

Furthermore, (1*R*, 3*S*) and (1*S*, 3*R*) enantiomers were resolved by chiral chromatography and differentiated by their optical rotation measurements. The minor pair of diastereoisomers were not always isolated from the reaction mixture, except in a few cases. Analogue **9x** demonstrates the vast difference in antimalarial activity of each stereoisomer pair, with the most active (1*R*, 3*S*) stereoisomer possessing an IC_{50} of 9 nM (**9a**) which is superior to the original hit compound (racemate, 20 nM) against NF54. Also, compound **9x** possessed the overall lowest inhibitory concentration (27 nM) during exploration of ring size and C3 substitution (see Figure 43). A digeminal methyl substitution was tested at C3 but resulted in a decrease in potency (857 nM) and an increase of the ring size to 8 carbons resulted in an inhibitory concentration of >5000 nM.⁽⁶⁸⁾ Therefore, the optimum combination taken forward for further optimisation was a 6-membered ring with a single methyl substitution at C³.

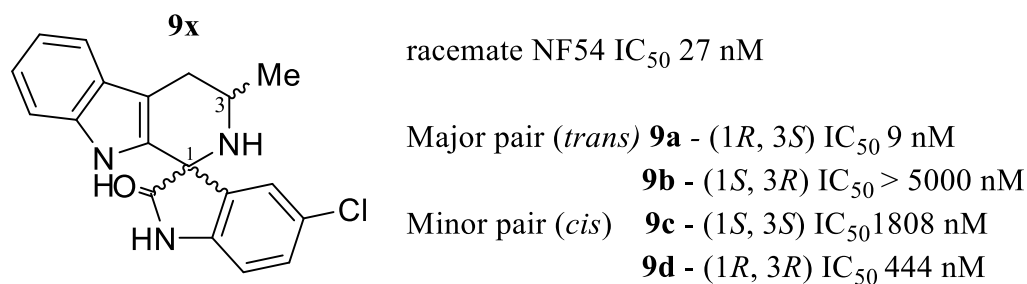
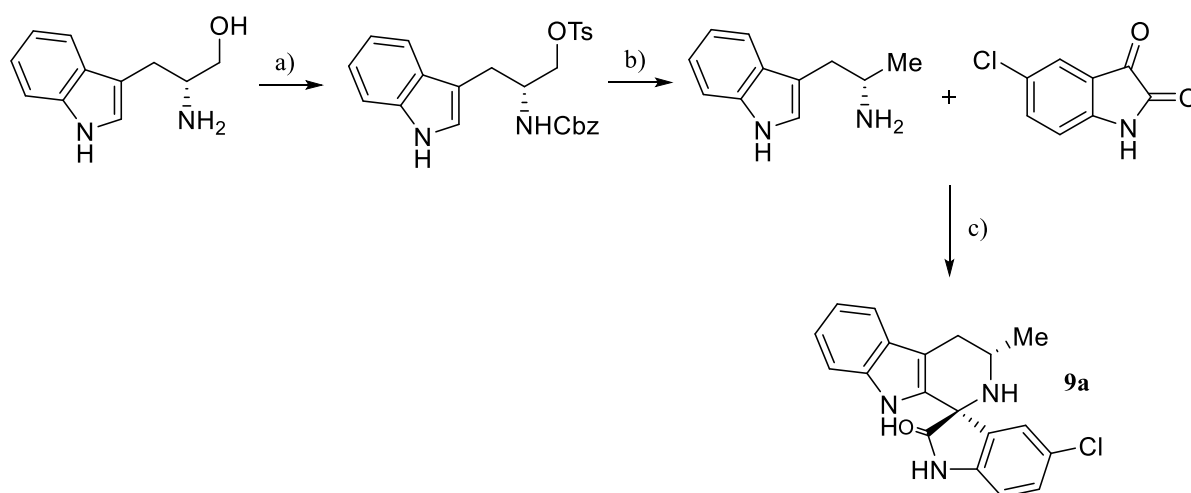


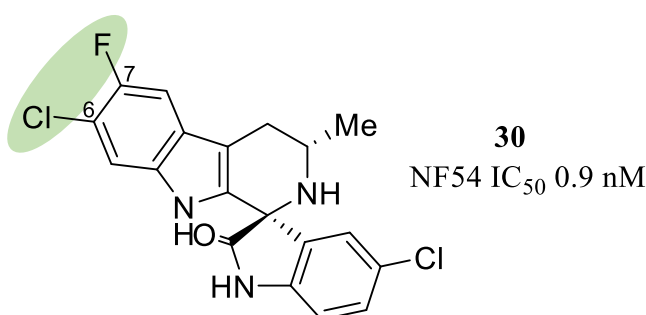
Figure 43: Optimum analogue **9x**

This observed trend in diastereoisomer activity was consistent across all analogues synthesised therefore, the research group concluded that the (1*R*, 3*S*) configuration was an essential feature in *Plasmodium falciparum* activity.⁽⁶⁸⁾ This led to primary testing of the racemic mixtures and if the inhibitory concentration displayed high potency it was assumed on chiral separation, potency would be further improved on isolation of the (1*R*, 1*S*) stereoisomer. To obtain a higher degree of diastereoselectivity, enantiopure 5- α -methyl indoleamines were used to form the desired single pair of stereoisomers instead of relying on expensive chiral separation. For example, the active stereoisomer **9a** was generated from the corresponding *S*- α -methyl indoleamine (see Scheme 44).



Scheme 44: Higher selectivity pathway a) i. CbzCl, Na₂CO₃, rt, ii) TsCl, Et₃N, rt, b) H₂, Pd(OH)₂, rt, c) *p*-TsOH•H₂O (cat.), 110 °C

Further derivatives were synthesised to investigate the structure-activity relationship on the indole aromatic ring. Two highly potent compounds (1*R*, 3*S*)-**17a** (3 nM) and (1*R*, 3*S*)-**18a** (4 nM) were discovered during this exploration and possessed a C6-fluoro moiety and C7-chloro moiety respectively. As a result, the two substitutions were combined and generated **30** (NITD609). The group stated positions C6 and C7 were prone to oxidation during metabolism and resulted in high clearance of the derivatives during testing. Therefore, this dihalogen substitution blocks oxidation at those positions and counteracts the high clearance issue.⁽⁶⁸⁾



Also, the group found the less active (1*S*, 3*R*) configuration to show: greater metabolic stability lower *in vivo* clearance and fewer drug-drug interactions (CYP450 liabilities). Whereas, the most potent form displayed the complete opposite pharmacokinetic properties and was even found to inhibit CYP2C9, an enzyme important for the metabolism of: warfarin, angiotensin II receptor blockers, antidiabetics and non-steroidal anti-inflammatory drugs. Therefore, future work needs to include increasing metabolic stability and reducing CYP2C9 binding. Overall, the derivatives did not show any signs of cytotoxicity across the several human lines tested and low hERG activity was observed, as well as being negative for the Ames test.⁽⁶⁸⁾

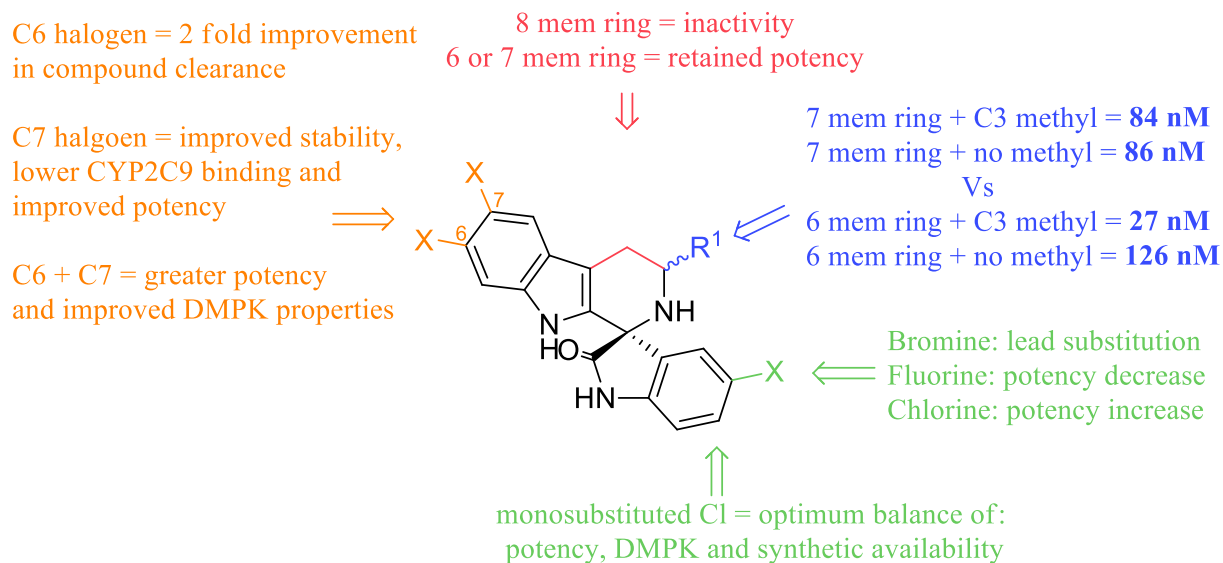
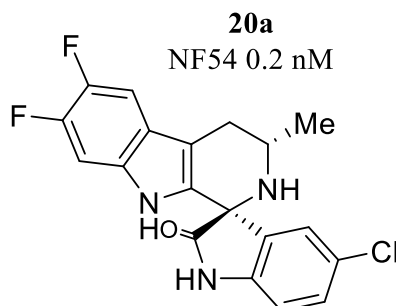


Figure 44: Summary of findings

In conclusion, the research group denoted key features which they found essential for high activity and state should be retained in future optimisation programmes (see Figure 44).

Surprisingly, the research group discovered an even better compound displaying an inhibitory concentration of 0.2 nM and Yeung *et al* predict the data obtained for compound **20a** shows the potential analogue to become a single dose or low dose cure for malaria. Compound **20a** possesses: low hepatic clearance in human and mouse models and low CYP2C9 binding, thus solving the problems seen for **30**.⁽⁶⁸⁾ However, analogue **30** has only been seen to be taken forward into clinical studies, as seen in the current published literature resources and the rest of the series is still undergoing preclinical evaluation.



3:3:2 Mechanism of action

In late 2010 research was carried out by Rottman *et al* looking at spiroindolones as an antimalarial treatment. The screening carried out identified 275 primary hits with submicromolar activity against *P. falciparum*. Of these, the compounds not retaining activity against multidrug resistant parasites and displaying cytotoxic properties against mammalian cells were eliminated. The hits still present were analysed for their pharmacokinetic and physical properties and from these, 17 compounds resulted. They state, spiroindolone compound NITD609 stood out as a basis for further medicinal chemistry optimisation and displayed good drug-like attributes as well as, physiochemical properties consistent with conventional tablet format. ⁽⁶⁹⁾

Initial hypotheses suggested the mechanism of action involved disruption of a P-type cation transporter ATPase4 (PfATP4), which regulates sodium ion homeostasis. Firstly, an *in vitro* experiment was carried out to determine which stage(s) of the parasite was most affected by NITD609. The experiment involved 3 stages of the parasite lifecycle which includes: rings, trophozoites and schizonts. The three forms were treated separately with NITD609 and left for different lengths of time: 1, 6, 12 and 24 hours, before removing the dosed drug and allowing culture continuation for a further 24 hours. They found at high concentrations of the drug ($100 \times \text{IC}_{50}$ value) all stages of the parasite were similarly sensitive. Whereas, at low concentration (1 or $10 \times \text{IC}_{50}$ value) schizonts were the most susceptible form therefore, they concluded the drug target to be present in all 3 stages tested but schizonts are particularly vulnerable. It was also found NITD609 did not inhibit growth as quickly as artemether, as $>90\%$ inhibition was seen at 1.6 nM after 24 hours whereas, artemether inhibits the same amount at 8 nM after 6 hours. ⁽⁶⁹⁾

To investigate further a second experiment was conducted which involved ^{35}S radiolabelled methionine and cysteine, two components important in protein synthesis. An incorporation assay involved uptake of the radiolabelled amino acids within the parasite and the amount of each amino acid was measured at different intervals after dosing with the chosen drug. They revealed NITD609 to block protein synthesis in *P. falciparum* within 1 hour compared to artemisinin and mefloquine which showed < 25% decrease in [^{35}S] met/cys within 1 hour. They state this rapid suppression of protein synthesis suggests a different mode of action to both traditional antimalarial agents. ⁽⁶⁹⁾

To strengthen their hypothesis a resistance experiment was conducted which created a NITD609-resistant strain of parasite. They created the resistant strain by repeated exposure of NITD609 to the parasite at increasing concentrations over a period of 3-4 months. Amongst the resistant strain 27 genetic differences were observed and of these, 7 mapped to a single gene for PfATP4 – strongly suggesting this spiroindoline specifically selects for a mutation of PfATP4. This mutated form was taken and the PfATP4 gene sequenced and showed changes noted as 11 mutations. Therefore, these highlighted mutations were inserted into wild-type or resistant lines of malaria which displayed an increase in inhibitory concentration towards NITD609 whereas, artemisinin and mefloquine showed retained potency. ⁽⁶⁹⁾ Thus, resistance was specific to the spiroindoline however; it is difficult to distinguish the exact process of PfATP4 action as little is known about the molecular function of PfATP4.

Meanwhile, in 2012 Pelt-Koops *et al* explored NITD609 gametocyte activity and concluded the compound to show a dose-dependent effect on all stages of gametocyte development *in vitro*. Not only does the compound show activity against the asexual stage of the parasite but also, demonstrates significant activity for gametocyte reduction at the lowest tested concentration of 5 nM. Furthermore, the compound was found to completely block

transmission of the parasite at 500 nM. They state the potent drug can be used to treat asymptomatic carriers of the parasite who possess a reservoir of mature gametocytes in areas of high parasite transmission. Finally, they predict NITD609 could be part of a novel combination therapy with transmission blocking activity. ⁽⁷⁰⁾

In 2014, Bowman *et al* conducted an antiapicoplast and gametocytocidal screen of the Medicine for Malaria Venture (MMV) box. They refer to (1*R*, 3*S*)-NITD609 and state it targets PfATPase4, a plasma membrane sodium ion efflux pump. ⁽⁷¹⁾

3:3:3 NITD609 in 2017

Currently NITD609 (known as Cipargamin) has completed first phase IIa clinical trials as a short-duration monotherapy and is now being prepared for dose escalation studies in infected patients. This antimalarial is the first validated new molecule target in 20 years and has very rapid onset for killing the parasite with the potential to become a transmission blocking agent.

3:4 MMV spiroindoline lead

3:4:1 Discovery

In 2014 Spangenberg *et al* explored the MMV box and screened the library of compounds for their blood-stage *P. falciparum* activity. During the compound selection process, they applied a strict ‘rule of 5’ filter however; they highlight several compounds which would not have been retrieved under this type of selection. For example, compound **16x** shown in Figure 45 has a molecular mass of $414.54 \text{ g mol}^{-1}$ and a logP of 5.3. Compound **16x** contains an attractive spiro[indoline-3,4-piperidine] fragment with a potency of 990 nM against the 3D7 parasite strain.⁽⁷²⁾ This initial hit displayed 3 points of variation therefore: the original cyano moiety was replaced with a chlorine atom, the allyl group substituted with a benzyl group and finally, the methyl moiety on the indole centre was removed to simplify the structures core (MMV668732, see Figure 45).

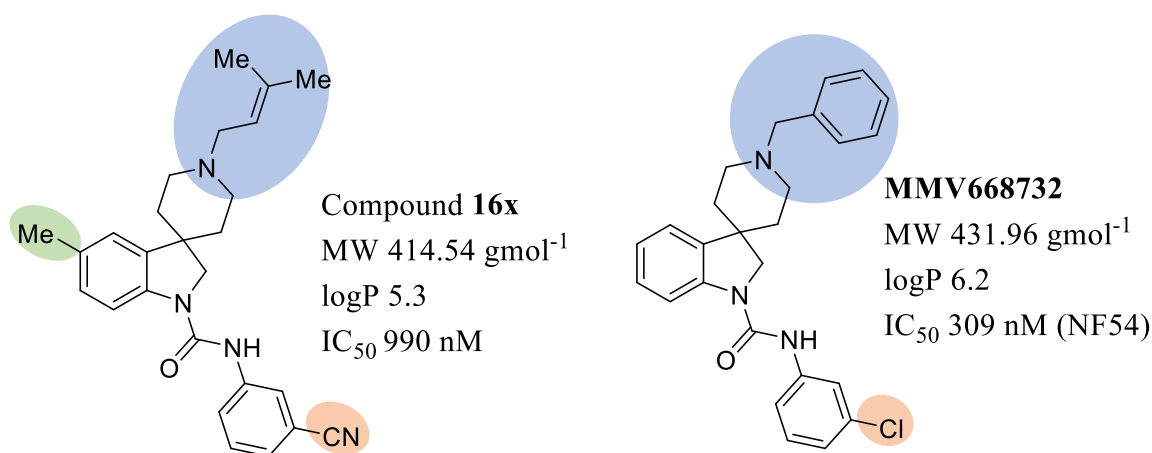


Figure 45: Spiroindoline hit with point of variation (left) and simplified sister compound

The novel derivative MMV668732 possesses a higher molecular weight than the parent hit and an undesirable logP but, the structure is less complex and allows investigation of the structure activity relationship at the two positions highlighted in Figure 45. Furthermore, due to the high level of interest in the potent antimalarial NITD609, a spiroindoline feature in drug molecules has grown in popularity. As a result, in July 2015, MMV668732 provided a

novel starting point for further optimisation and work was undertaken by a Keele undergraduate student to generate potential antimalarial hits.

3:4:2 Early analogue proposals

Initially, three points of variation were explored as shown in Figure 46. The purpose of these primary derivatives was to give insight into the type of functionality which gave rise to an increase/decrease in antimalarial activity. Through retrosynthetic analysis the desired spirocyclic structure can be synthesised from phenylhydrazine and *N*-benzylpiperidine-4-carboxaldehyde.

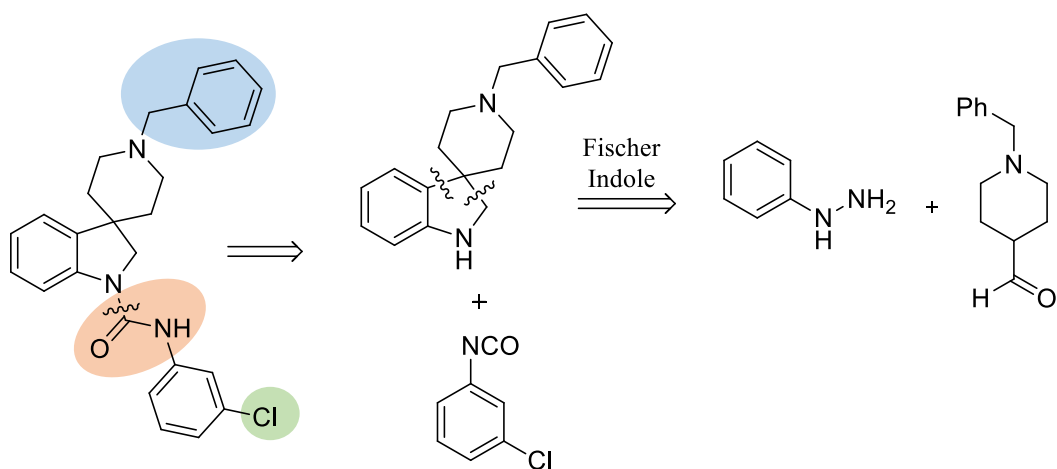


Figure 46: Retrosynthesis

This gave an opportunity to explore: a range of ureas from substituted isocyanate substrates, amide derivatives and ketone derivatives from α -halo ketones (see Figure 47).

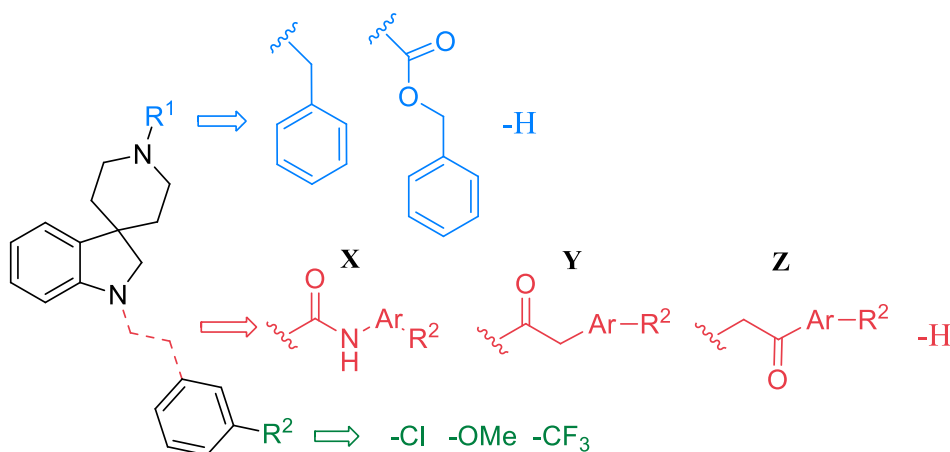


Figure 47: Initial spiroindoline exploration

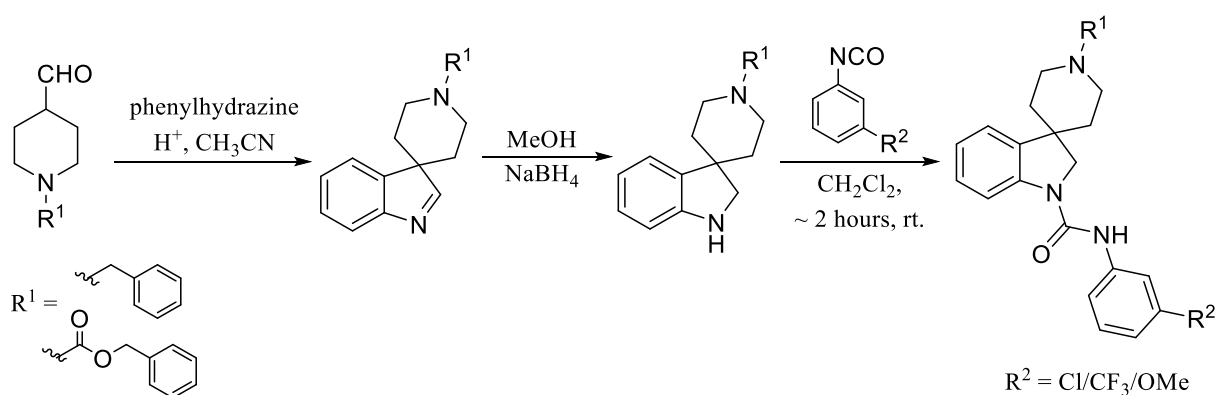
The piperidine starting material was available as *N*-benzyl and *N*-carbamate so both were used and tested. However, the carbamate group offers an additional hydrogen bond acceptor and was found to be easier to synthesise and purify compared to the benzyl protected nitrogen.

Furthermore, the importance of the benzyl group was probed by generating an analogue where it was removed. So, an analogue possessing a free piperidine amine was proposed to remove all previous hydrophobic interactions and see the effects a hydrogen bond donor has on biological activity.

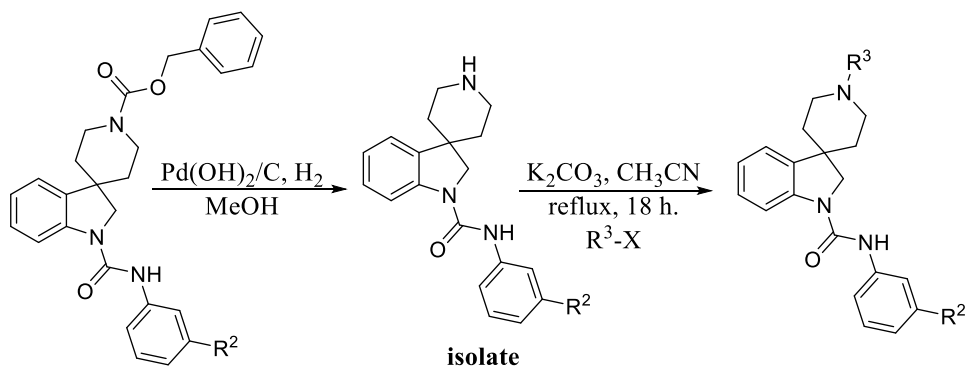
Meanwhile, the urea linker seen in the initial lead was kept and a small range of substituted isocyanates were used to generate ureas **X** with EWG (CF₃) and EDG (OMe) groups. Analogues were also made to look at the contribution of the second nitrogen seen in MMV668732 by replacing the urea link with an amide link **Y**. Also, moving the position of the carbonyl was also tested with an alternate α -amino ketone linker **Z**.

3:4:3 Synthetic strategy

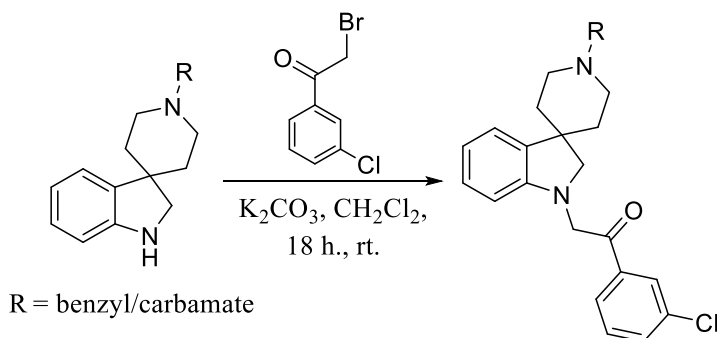
The MMV hit and other *N*-benzyl derivatives were generated by carrying out a Fischer-Indole reaction with *N*-benzylpiperidine-4-carboxaldehyde and phenylhydrazine under acidic conditions, followed by a straightforward sodium borohydride reduction to the indoline (see Scheme 45). To insert the hit compound urea link, the relevant substituted phenyl isocyanate was taken and stirred with the *N*-benzyl starting material in dichloromethane at room temperature overnight.



Furthermore, to generate the analogue possessing a free amine the carbamate protected starting material was first coupled with the urea linker and then, the carbamate was removed using Pearlman's catalyst under a hydrogen atmosphere to reveal the desired derivative (see Scheme 46). A nucleophilic substitution reaction can then be performed using the amine to insert different functional groups (R^2).

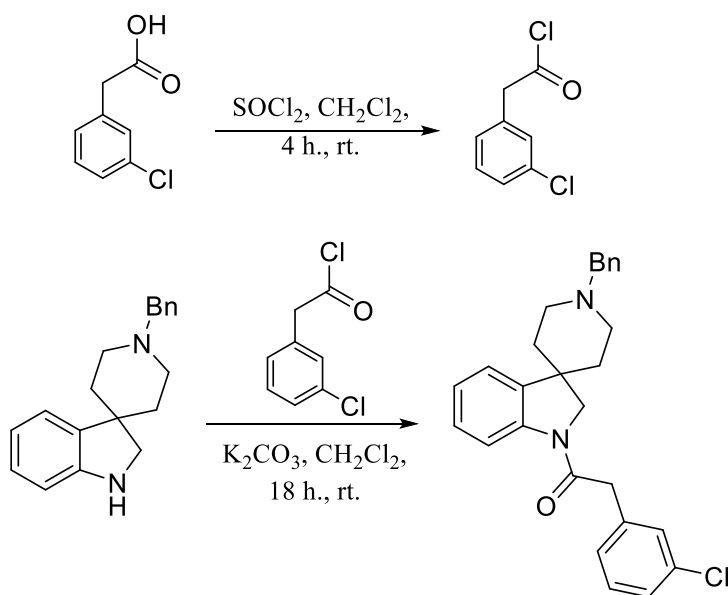


To insert the α -amino ketone linkers, an alternate approach was carried using the relevant 3-chloro-2-bromoacetophenone alongside potassium carbonate in dichloromethane (see Scheme 47).



Scheme 47: Ketone insertion

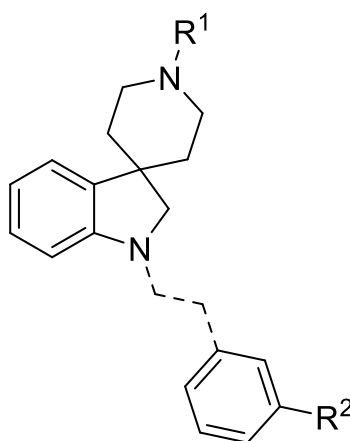
Finally to create the amide link derivative, 2-(3-chlorophenyl)acetyl chloride had to be synthesised which was then coupled to the spirocyclic substrate shown below (see Scheme 48).



Scheme 48: Amide insertion

3:4:4 Preliminary biological results and discussion

During the undergraduate 8-week research project, 8 compounds were generated which included the original hit compound MMV668732. The IC₅₀ values were originally carried out at 48 hours and later at 72 hours. Table 20 displays the biological data obtained for this preliminary set of compounds.



Reference	R ¹	Linker	R ²	IC ₅₀ / μ M 48 hour assay
AKE6 MMV668732	benzyl	urea	Cl	2.45
AKE5	benzyl	-NH	N/A	20.0
AKE9	benzyl	urea	CF ₃	3.27
AKE10	benzyl	urea	OMe	19.2
AKE20	benzyl	N-C=OC-Ar	Cl	15.3
AKE1	carbamate	urea	Cl	7.06
AKE31	carbamate	N-CC=O-Ar	Cl	11.3
SA	carbamate	-NH	N/A	26.6
AKE2	-NH	urea	Cl	3.40

Table 20: First generation spiroindoline results

The biological data shown for the original hit MMV668732 (**AKE6**) shows a dramatic difference in inhibitory concentration when compared to the original data published by Avery *et al*, which found an IC₅₀ of 309 nM whereas for this project an IC₅₀ of 2.45 μ M was obtained. ⁽⁷²⁾ The data discrepancies are thought to lie within the biological testing methodology chosen to run the inhibitory concentration assays.

Firstly, visualisation by Avery *et al* was carried out by detecting specific areas of fluorescence within the parasite alongside non-DNA based components whereas, the biological data obtained during this project used an alternate fluorescence-based detection method known as Malaria SYBR Green I fluorescence (MSF), which uses a DNA intercalating agent and measures total fluorescence intensity output. Furthermore, the Avery assays were run over 72 hours on ring stage chloroquine sensitive parasites on the other hand, to obtain this data 48-hour assays were carried out on trophozoite chloroquine sensitive parasites. ⁽⁷³⁾

Finally, the growth medium contained 0.5% albumax but was absent of human serum during the Avery testing however, the assays ran during this project contained both albumax and human serum within the growth medium. Therefore, the latter carries a risk of plasma-protein binding to the proteins contained within the human serum which subsequently leads to reduced bioavailability of the tested drug and in turn, could lead to the increase in inhibitory concentration observed. ⁽⁷³⁾

From the 48 hour data both **SA** and **AKE5** demonstrate the absence of a linker and substituted phenyl group result in a loss of antimalarial activity, as both inhibitory concentrations significantly increase (IC_{50} 26.6 μ M and 20.0 μ M respectively). Therefore, when designing future analogue generations, it is important to note both interactions provided by the linker and phenyl functionality must be essential for activity. Even though only one electron donating group R^2 substitution was synthesised, it demonstrated a loss of potency (**AKE10** IC_{50} 19.2 μ M) compared to MMV668732 **AKE6** (2.45 μ M) thus, indicating an electron withdrawing group is necessary for good activity. Inserting a more electron withdrawing group such as, a trifluoromethyl group resulted in a good activity compound (**AKE9** 3.27 μ M). As the difference in activity was minimal and keeping in mind

the strong electron withdrawing properties of this moiety it was kept for the next generation of derivatives.

While retaining the original *m*-chlorine moiety two alternate R¹ groups were tested, shown in Figure 48. Both the carbamate functional group and free amine resulted in a loss of potency, although not as significant as the previous analogues discussed. As a result, it could be proposed to keep either the benzyl moiety or free amine for future compound synthesis, however they offer significantly different interactions i.e. a large hydrophobic interaction vs a single hydrogen bond donor. Therefore, as the lowest activity is seen for the benzyl moiety and to simplify analogue comparison this hydrophobic group should be retained and investigated further.

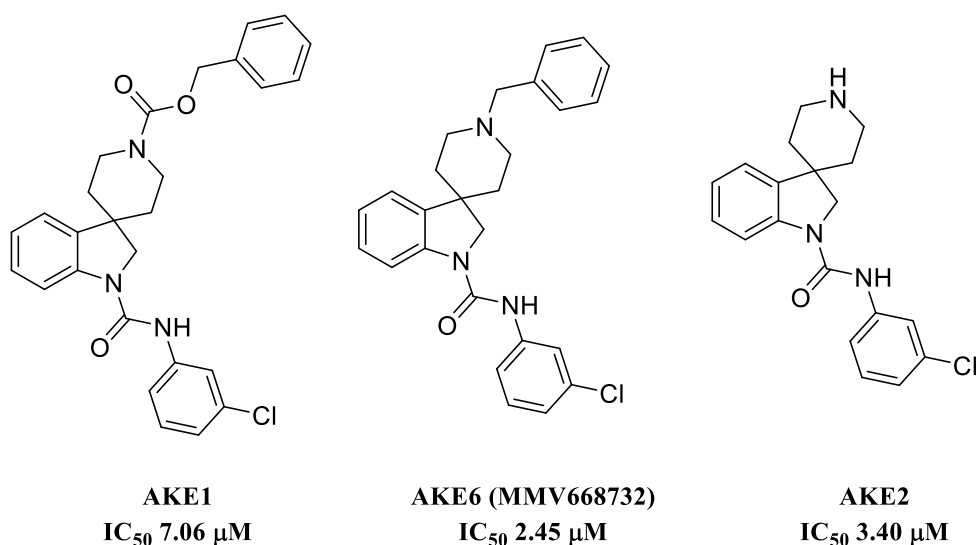


Figure 48: Analogue comparison

On the other hand, two compounds were synthesised possessing a ketone and amide linker instead of the original urea moiety and both resulted in a loss of potency (see Figure 49). The α -amino ketone was the most promising of the two, assuming a direct correlation between these analogues and the ureas **AKE1** and **AKE6**. However, the urea linker remained the best option and thus was retained for future analogue synthesis.

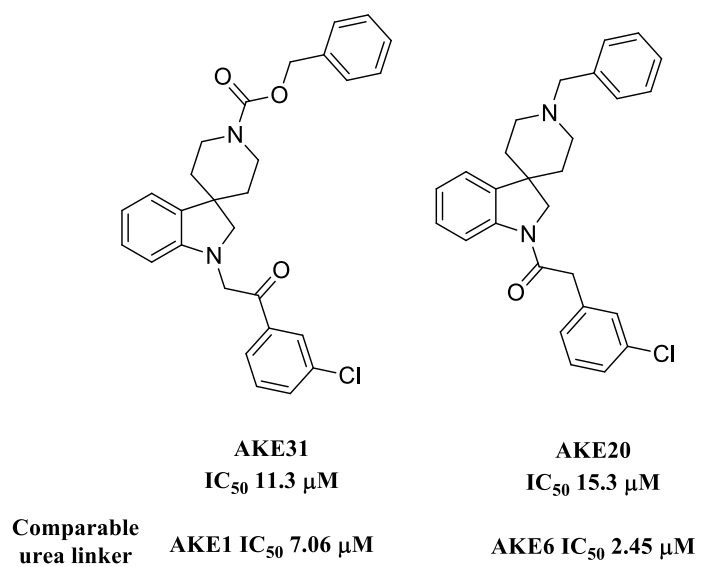


Figure 49: Linker comparison of AKE1 and AKE6

3:5 Project proposals

Due to these preliminary findings, a second generation of analogues were proposed for this project, of which all possessed a *m*-trifluoromethyl phenyl substitution and a urea linker.

The next generation of spiroindoline compounds possessed one variant (R), with the hope of generating a more potent compound than the original MMV668732 hit (see Figure 50). Based on previous knowledge gained from the first generation of analogues, the next area for investigation was the benzyl moiety. Alternate groups to benzyl moiety were tested to explore different functionalities with an attempt to make the compound more drug like. As previously stated, the urea link was kept as a significant loss of activity was observed when removed. Furthermore, a *m*-trifluoromethyl group was initially retained as an electron withdrawing group was necessary for activity and the isocyanate required for this synthesis was readily available in the laboratory.

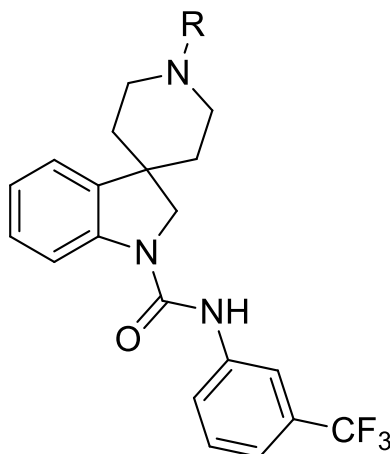


Figure 50: Spiroindoline template (R details below)

Therefore, seven substituted benzyl derivatives were proposed which included: three benzoyl chlorides, two methyl ester groups, morpholine, pyran, piperidine, dimethylamine, a butyl chain and other drug-like moieties.

Firstly, the benzyl moieties were substituted in the *para* position, furthest away from the central structure to try and achieve a positive interaction within the potential target site. Thus, if any of these derivatives displayed fruitful potency, further exploration of substitute position could be carried out. Furthermore, a range of functionalities were investigated which included: electron withdrawing groups such as, halogens, a nitro moiety and electron donating groups such as, a methoxy group, to see the effects these opposing groups have on antimalarial activity (see Figure 51).

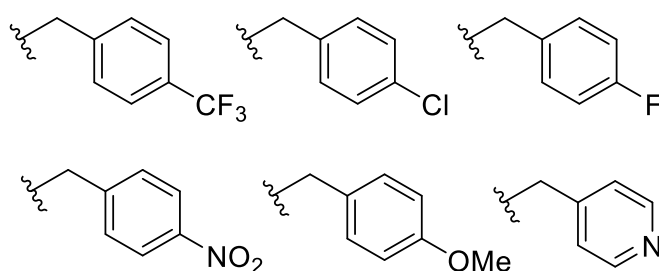


Figure 51: Benzyl exploration

Three benzoyl groups were proposed to observe the effects on activity with the addition of a hydrogen bond acceptor as well as hoping to reduce the high logP value for this series. A further direct comparison can be made between the original MMV compound and a simple benzoyl group, allowing conclusions to be made about this additional interaction (see Figure 52).

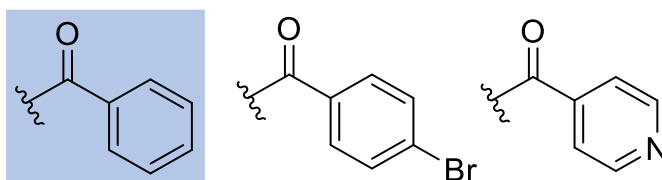


Figure 52: Benzoyl analogues

To address the issue of high logP further functional groups possessing more drug-like qualities were proposed to combat this, with the hope of also increasing activity (see Figure 53). For example, a morpholine group was created as this offers a hydrogen bond acceptor and provides an area of electronegativity which could prove to be beneficial. Also, the

morpholine group was investigated further by removing the nitrogen and oxygen atom, in turn, to see which atom is of importance or to see if both atoms are required for any observed activity.

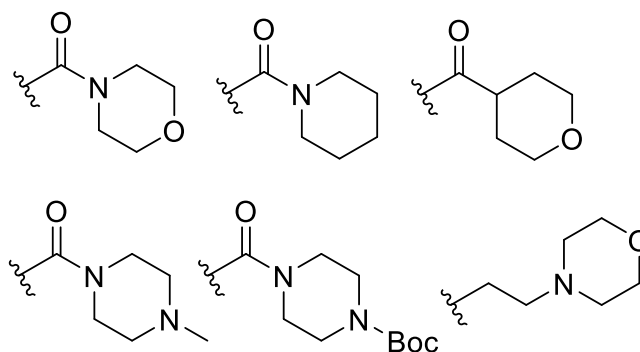


Figure 53: Drug-like moieties

Finally, a moderately hydrophobic butyl group offers significant van der Waal's interactions whereas, a methyl ester moiety and a dimethyl amide group offers alternate interactions with short hydrophobic methyl groups, in combination with a hydrogen bond acceptor (see Figure 54). Overall, a wide range of functionalities were outlined and from this series of biological data, a third generation of compounds were proposed.

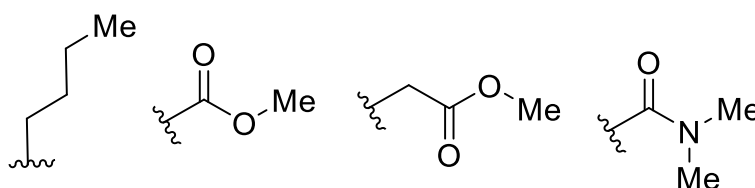
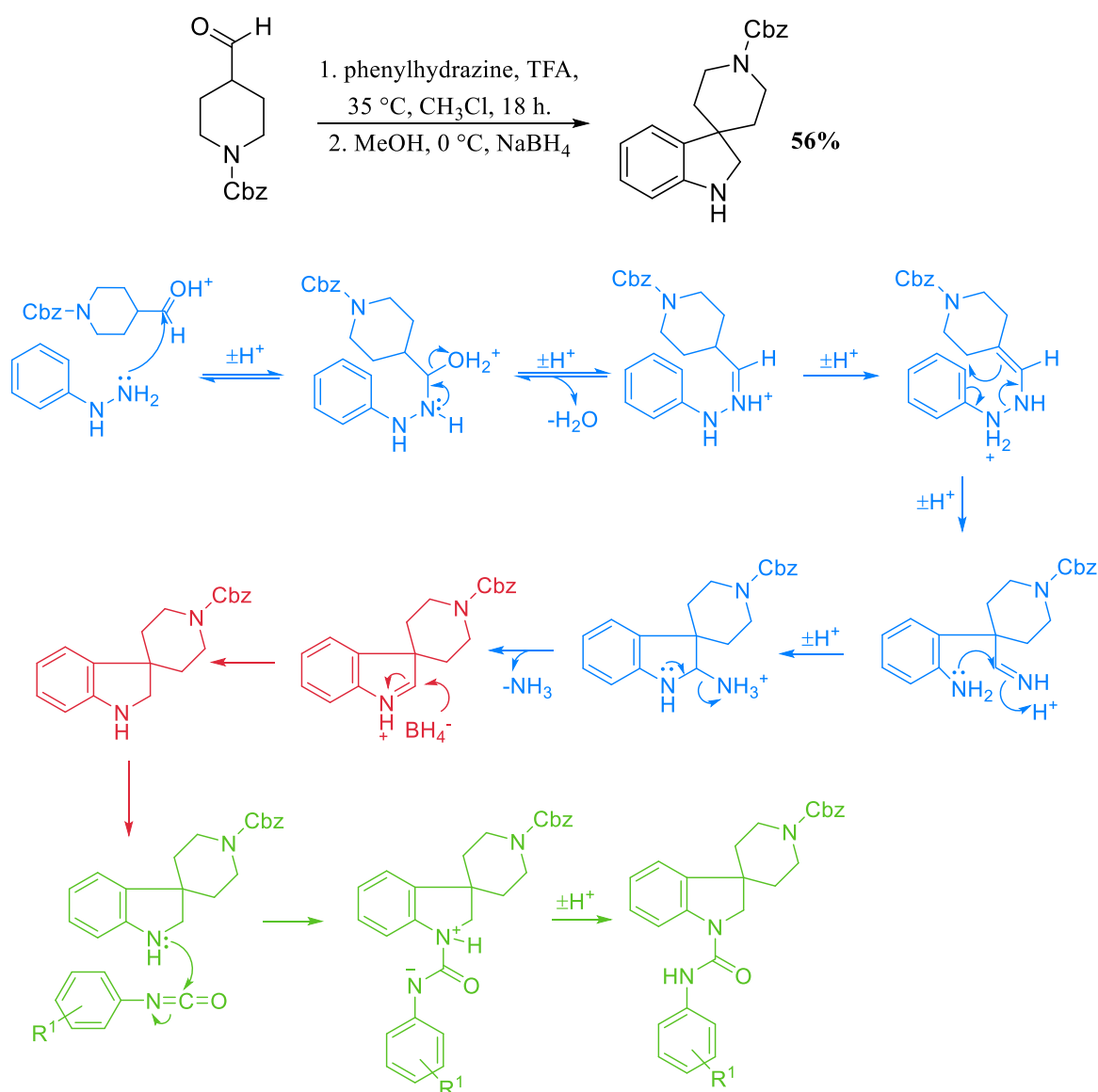


Figure 54: Non-aromatic/aryl functional groups

3:5:1 Synthetic strategy

During this postgraduate research project, the *N*-carbamate starting material was prepared performing a Fischer-Indole reaction using benzyl 4-formyl-1-piperidinecarboxylate, in place of the previously used *N*-benzyl constituent (see Scheme 49). The carbamate starting material was chosen over the *N*-benzyl as it is easily cleaved further on in the synthetic route and is easier to purify.

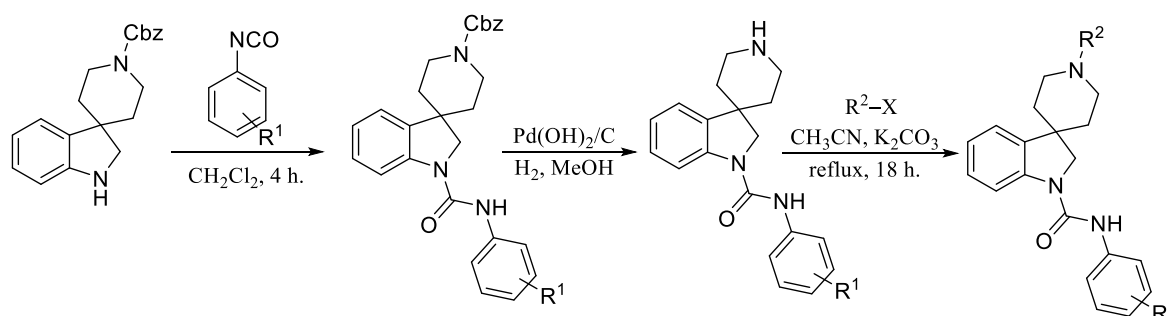


Scheme 49: Fischer-Indole (blue), NaBH₄ reduction (red) and urea formation (green)

A one-pot strategy involved carrying out the Fischer-Indole reaction followed by a sodium borohydride reduction without isolating the imine intermediate. ⁽⁷⁴⁾ However, during the

purification step much of the mass was found to be the unreduced product and therefore, was collected and subject to reduction conditions once more, to obtain the highest possible yield of 56%.

To achieve each novel derivative, the desired substituted phenyl isocyanate was coupled with benzyl 4-formyl-1-piperidinecarboxylate and each product purified using column chromatography, to produce a urea intermediate. The novel derivatives were then generated by stirring the free amine intermediate in acetonitrile along with potassium carbonate and the chosen halogen substituted R^2 substrate (see Scheme 50). The reaction was left to stir at reflux overnight which resulted in each analogue in good yields (see Table 21).



Scheme 50: Synthetic route

Starting materials	R^1	R^2	Yield/%
	3-CF ₃	Cbz	97
	3,4-Cl ₂	Cbz	77
	3-Cl	Cbz	67
	3-F	Cbz	62
	3,4-F ₂	Cbz	55
	3-CF ₃	H	67
	3,4-Cl ₂	H	90
	3-Cl	H	97
	3-F	H	87
	3,4-F ₂	H	85

Table 21: Spiroindoline product yields

Accordingly, the obtained product was coupled with the chosen isocyanate to produce the urea linker in good yields. Next, the carbamate protecting group was removed using $\text{Pd}(\text{OH})_2/\text{C}$ and H_2 to generate the desired free amine in good yield, which could then take part in further $\text{S}_{\text{N}}2$ substitution to create the set of analogues (see Scheme 50 and Table 21).

Finally, the multiple R^2 groups were created by use of the relevant substituted benzyl bromide, phenyl substituted acid chloride, ester/amide acid chloride or alkyl bromide, alongside potassium carbonate as the base in acetonitrile at reflux stirring overnight.

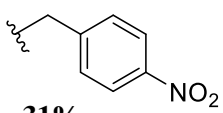
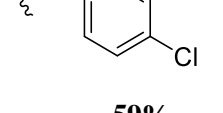
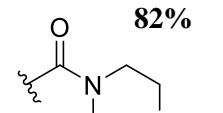
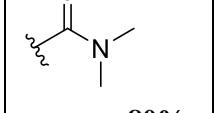
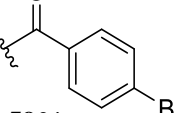
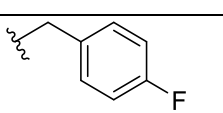
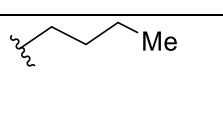
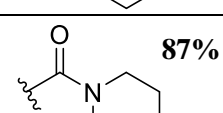
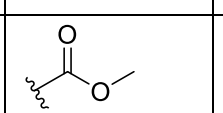
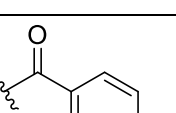
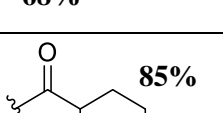
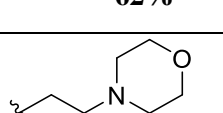
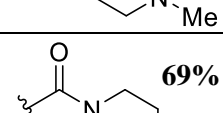
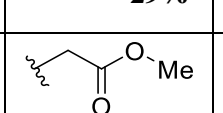
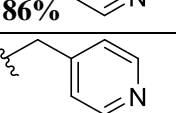
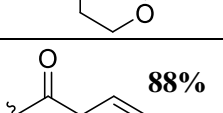
R^2 and isolated yields $\text{R}^1=\text{CF}_3$				
 31%	 59%	 82%	 80%	 59%
 68%	 62%	 87%	 29%	 86%
 85%	 52%	 69%	 35%	 48%
 88%				

Table 22: Isolated yields from *N*-alkylation

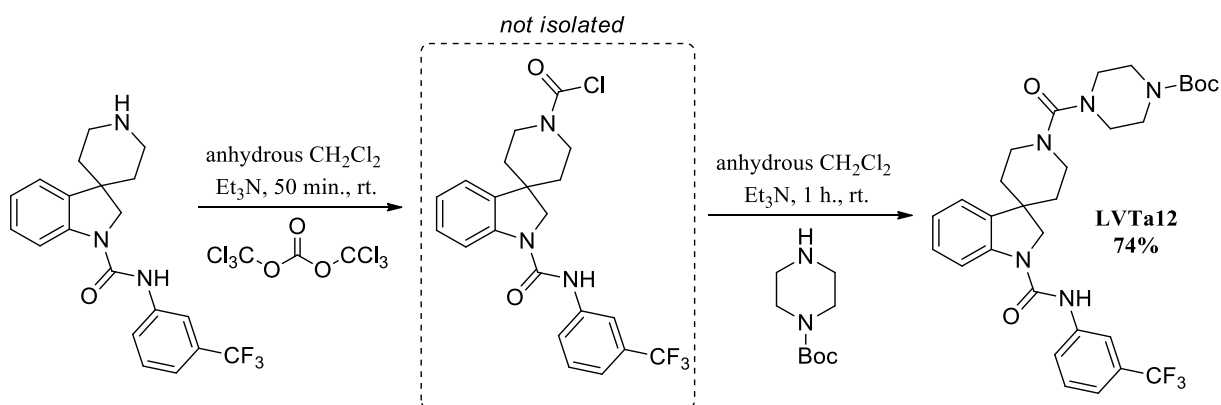
For 3-trifluoromethyl phenyl derivatives most products were produced in yields between 29–88% and this was therefore a useful method of compound generation (see Table 22).

Table 23 shows the isolated yields for 3-chlorophenyl, 3-fluorophenyl and two disubstituted R^1 derivatives and overall the compounds were generated in good yield.

R ¹	R ²	Yield/%
3-Cl	ethyl piperidine	53
3-Cl	C ₅ H ₁₁	70
3-Cl	C ₆ H ₁₃	72
3-F	morpholine	70
3,4-F ₂	morpholine	66
3,4-Cl ₂	morpholine	74

Table 23: Second generation alkylation product yields

In one case the imidoyl chloride was not available so a telescoped reaction was carried out using triphosgene to create the acid chloride of the spiro starting material *in situ* which was then reacted with the free amine of the R¹ substituent (see Scheme 51). Therefore, 1-boc-piperazine was available and coupled to the spirocyclic acid chloride generated *in situ* to give **LVTa12** in 74% yield.



Scheme 51: Triphosgene approach

3:5:2 Biological results and discussion

Table 24 displays the inhibitory concentrations obtained for the spiroindoline derivatives generated.

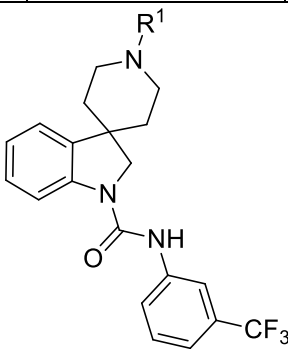
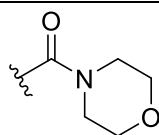
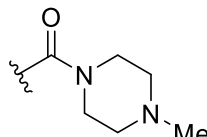
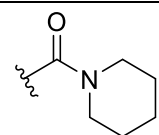
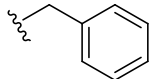
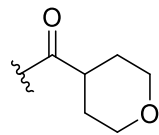
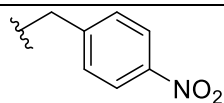
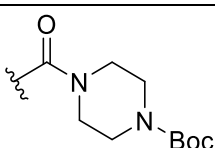
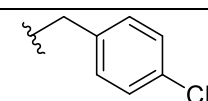
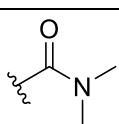
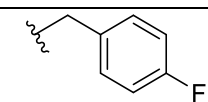
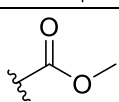
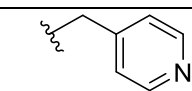
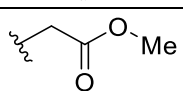
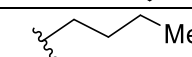
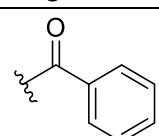
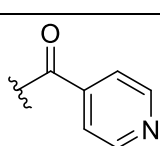
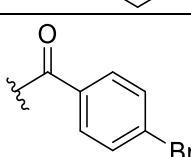
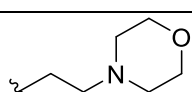
Reference	R ¹	IC ₅₀ /μM	Reference	R ¹	IC ₅₀ /μM
 Template			LVT59		1.77
			LVTa18		2.76
			LVTa1		1.15
AKE6 MMV668732		2.45	LVTa2		2.09
LVT66		5.94	LVTa12		3.74
LVT69		9.07	LVTa4		4.34
LVT70		6.77	LVTa14		6.72
LVT72		5.31	LVT54		16.9
LVT86		0.96	LVTa5		3.85
LVTa3		18.4	LVT71		7.04
LVT81		5.41			

Table 24: Biological data for spiroindoline subseries

Of this primary series, the compounds showing higher potency than the original MMV lead (**AKE6**, 2.45 μM) have been highlighted.

The *para* substituted benzyl analogues all possess moderate activity ranging from 5.31 μM for the 4-pyridyl analogue (**LVT72**) to the poorest activity 9.23 μM for a *p*-trifluoromethyl substitution (**LVT69**). Surprisingly, both the trifluoromethyl and chloro group caused the greatest decrease in activity for an electron withdrawing group and the small electronegative fluorine atom (**LVT70**, 6.77 μM) had the best activity.

Of the benzoyl derivatives, the best activity was observed for the non-substituted benzoyl ring (**LVTa5**, 3.85 μM). However, the addition of a hydrogen bond acceptor did not increase potency beyond the original benzyl hit (**AKE6**, 2.45 μM). Further evidence is seen in the loss of activity with the addition of a carbonyl by comparing the two pyridine derivatives **LVTa3** (18.4 μM) and **LVT72** (5.31 μM). Overall, the benzyl derivative had higher activity than the benzoyl analogue. Further derivatives such as the dimethyl amide **LVTa4** (4.34 μM) and carbamate **LVTa14** (6.72 μM) possessed moderate potency, but no better than the original hit (see Figure 55).

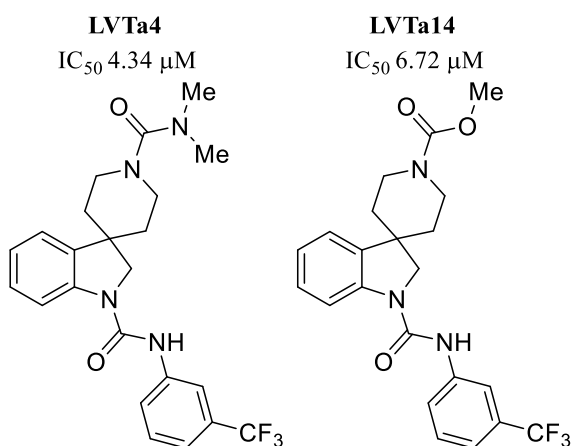


Figure 55: Urea and carbamate comparison

The piperazine **LVTa18** (2.76 μ M) and was preferred over the *N*-Boc protected derivative **LVTa12** (3.74 μ M). Even more promising was **LVT59** (1.77 μ M), which possesses a morpholine group and shows an improved inhibitory concentration compared to the original hit (2.45 μ M). Figure 56 displays the structural and activity comparison between the morpholine analogue and in turn, removal of the nitrogen and oxygen atom. Compound **LVTa1** exhibits a second urea moiety and is absent of the morpholine oxygen atom which provides a hydrogen bond acceptor. Alternatively, the amide **LVTa2** retains the oxygen hydrogen bond acceptor. There are small differences in the biological activities thus making conclusions regarding the preference over each interaction difficult, even though a marginally better activity is seen for **LVTa1** (1.15 μ M).

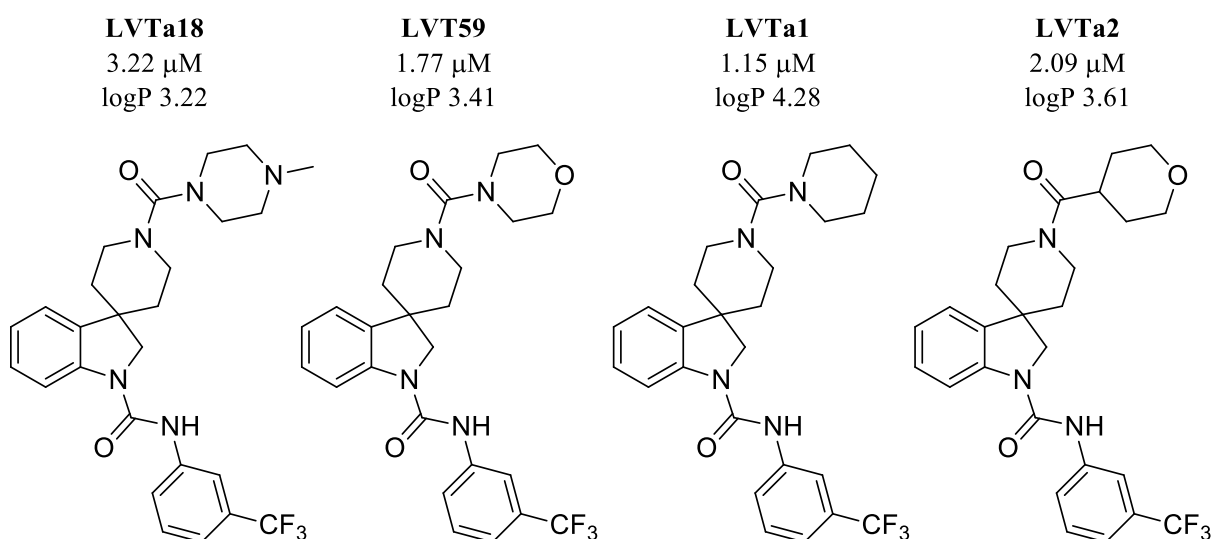


Figure 56: Morpholine moiety exploration

Unexpectedly, the best compound discovered was **LVT86** which possesses a butyl chain and has an inhibitory concentration of 960 nM. The lipophilic chain provides a mid-length hydrophobic interaction and has resulted in the most potent compound of this sub set and, is significantly more active than the original MMV hit lead (see Figure 57). Unfortunately, this moiety contributes to a disfavoured high logP value thus, making this analogue less drug-

like. However, this compound should be taken forward and explored further to probe the structure-activity relationship and attempt to improve the pharmacokinetic properties.

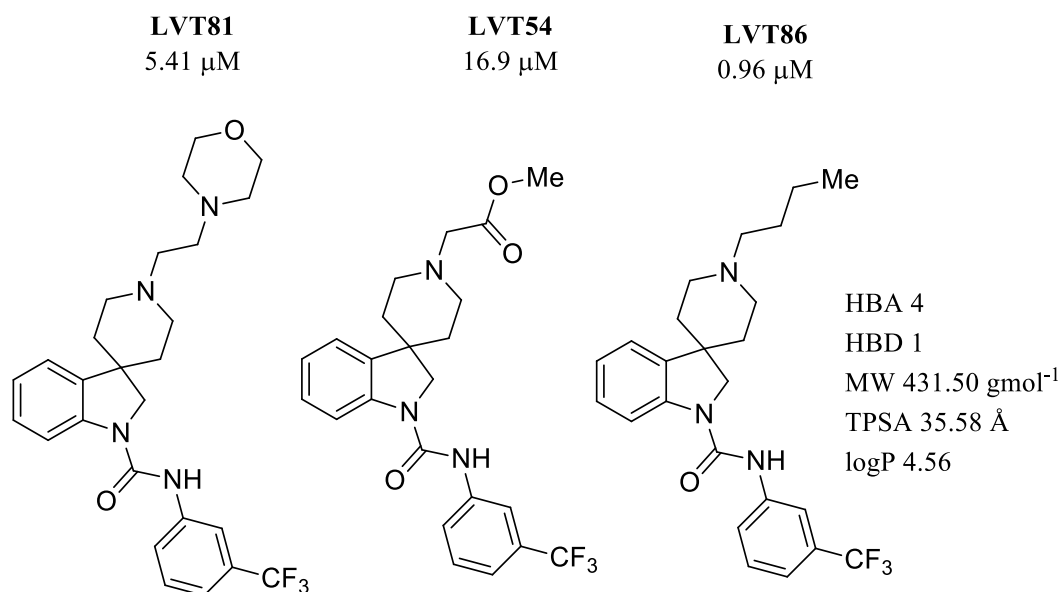
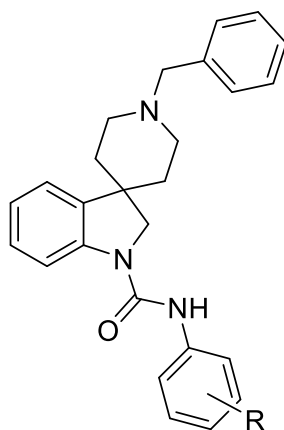


Figure 57: Aliphatic compound comparison

Attempts to include a polar group further along the chain resulted in **LVT81** and **LVT54** which unfortunately led to a significant loss of activity (see Figure 57).

Meanwhile, a small set of analogues were generated by an undergraduate project student in which the original benzyl R^2 group was kept, but the substituents at the R^1 were altered. A 3,4-dichloro R^1 phenyl substituent (**DD3**, 1.63 μM) displayed greater activity than the original hit (**AKE6**, 2.45 μM). On the other hand, a 2,4-dichloro pattern dramatically decreases potency (**DD1**, 18.8 μM) and a 3-bromo moiety causes a marginal decrease (**DD2**, 6.52 μM), see Table 25.



Reference	R	IC ₅₀ / μ M
DD1	2,4-Cl ₂	18.8
DD2	3-Br	6.52
DD3	3,4-Cl ₂	1.63

Table 25: Further analogue data

Taking into consideration the findings discussed, the next generation of spiroindoline derivatives should investigate: the alkyl R² substitution, the morpholine moiety and chloro/fluoro phenyl substitutions.

3:6 Next generation compounds

A third set of analogues were outlined to progress optimisation of the potent novel compound discovered during the latest subset of derivatives, **LVT86** (IC₅₀ 960 nM). To make the analogue more drug-like the highly electron withdrawing *m*-trifluoromethyl group was replaced with a *m*-chloro substitution and *m*-fluoro (both result in a decrease in logP and molecular weight). The favoured 3,4-dichloro pattern found most recently was also investigated although, this resulted in higher logP values. The 3,4-difluoro analogue was also selected as this lowered logP.

Furthermore, the fluorine atom has the potential to act as a hydrogen bond donor as well as providing a small electronegative interaction. Therefore, both *m*-fluoro and 3,4-difluoro patterns were coupled with a morpholine moiety, with the hope of generating a superior analogue (see Figure 58).

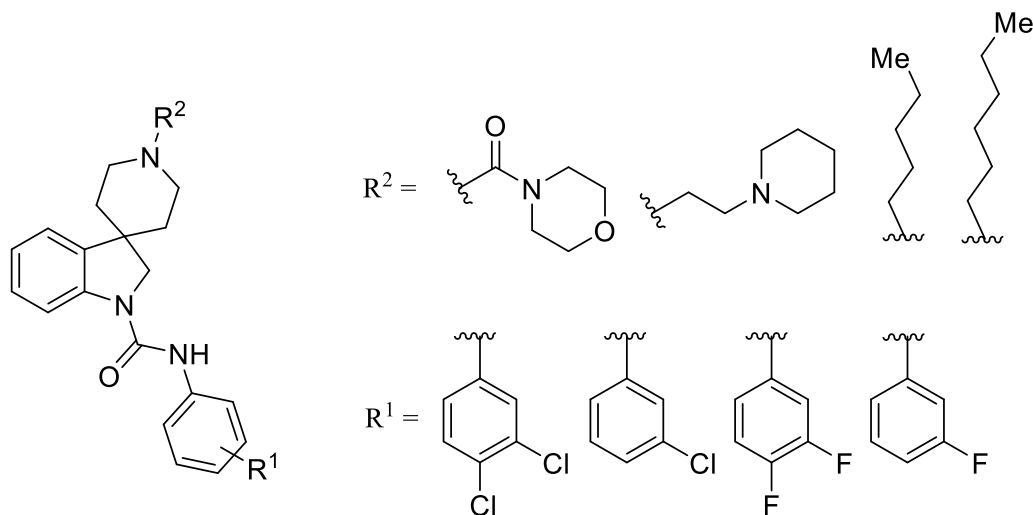


Figure 58: Next generation proposals

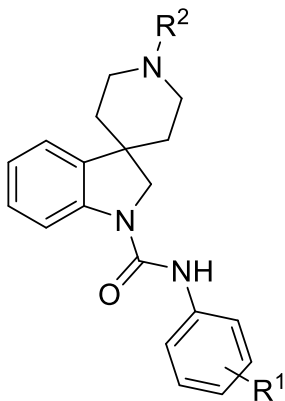
Firstly, a R¹ *m*-chloro substitution was paired with a R² morpholine group, which provided high activity previously and can potentially help optimise the pharmacokinetic properties of the lipophilic spiroindoline. Additionally, the morpholine group was paired with a 3,4-

dichloro phenyl substitution as good activity had been observed for both thus, combining them could result in a highly potent derivative. Alternatively, an ethyl piperidine moiety was proposed to see if a bulkier alkyl group helps to improve biological activity and the nitrogen provides a disruption in a dense area of lipophilicity (see Figure 58).

Meanwhile, a pentane and hexane chain were suggested to observe what happens to activity if the aliphatic chain is extended by one or two carbon atoms and, even though logP would increase it is important to explore what the optimum chain length would be for high activity (Figure 58).

3:6:1 Biological results and discussion

Previous hit **LVT59** (1.77 μ M) possesses a *m*-trifluoromethyl group in place of the chlorine and this resulted in one of the most active analogues in the second subset of derivatives (see Table 26).



Reference	R ¹	R ²	IC ₅₀ / μ M
AKE6	<i>m</i> -Cl	CH ₂ Ph	2.45
LVTa19	H	CH ₂ Ph	5.59
LVT86	<i>m</i> -CF ₃	C ₄ H ₉	0.96
LVTa124	<i>m</i> -Cl	C ₅ H ₁₁	1.54
LVTa125	<i>m</i> -Cl	C ₆ H ₁₃	1.01
LVT59	<i>m</i> -CF ₃		1.77
LVTa128	<i>m</i> -F		6.70
LVTa10	H		10.7
LVTa132	3,4-F ₂		5.75
LVTa135	3,4-Cl ₂		4.03
DD3	3,4-Cl ₂	CH ₂ Ph	1.63
LVTa121	<i>m</i> -Cl		3.56

Table 26: Biological data collected for final set of derivatives

To summaries by replacing the original *m*-CF₃ (**LVT59**) substitution with the alternate substitution patterns displayed in Table 26 a loss of activity is seen in the order of

F>H>F₂>Cl₂. These findings were not predicted as **LVT59** displayed good activity therefore, a combination of a morpholine group with a highly electron withdrawing trifluoromethyl group must have provided the low inhibitory concentration in this case and cannot be substituted with alternate halogen atoms.

Compound **LVTa135** (4.03 μ M) displayed good activity with a 3,4-Cl₂ disubstitution pattern but, a loss in potency is seen compared to the *m*-CF₃ derivative (**LVT59**, 1.77 μ M). However, the 3,4-Cl₂ disubstitution pattern in combination with a benzyl R² group (**DD3**, 1.63 μ M) possessed better activity than both **LVT59** (1.77 μ M) and the MMV compound **AKE6** (2.45 μ M). As a result, including a morpholine moiety within future derivatives may not be as useful as first thought, regardless of the contribution it makes to improving pharmacokinetic properties. Also, replacement of the original *m*-Cl group with a hydrogen atom (**LVTa19**, 5.59 μ M) gave a drop in activity.

Both pentane and hexane substituted analogues displayed better inhibitory concentrations compared to **AKE6**, but unfortunately no significant increase in potency was seen when compared to **LVT86** (960 nM). Although a slight preference is seen for the hexane derivative (**LVTa125**, 1.01 μ M), only a small margin of activity difference can be observed and therefore, no conclusions can be drawn as to which chain length is optimal for best activity.

Attempting to introduce a polar group in the chain can be seen for **LVTa121** (3.56 μ M) and displayed good activity but does not provide any improvement in activity when compared to **AKE6** (2.45 μ M) or the more recent **LVT86** (960 nM) analogue. In conclusion, the alkyl possessing derivatives are proving most activity so, to retain good active and optimal pharmacokinetic properties i.e. lower molecular weight and logP, a shorter butyl chain should be retained in comparison to either the pentane or hexane chain length.

3:7 Future work

To progress this series of antimalarial spiroindolines, further derivatives need to be generated to decipher the best functional group combination for high activity. So far, it has been shown either a *m*-trifluoromethyl or 3,4-dichloro phenyl substitution pattern gives the most active derivatives. These substitutions should be retained with caution due to the higher logP obtained over, for example the single chloro substituent. Also, more derivatives should probe the 3,4-dichloro substitution pattern to see if it is beneficial in other analogues.

Furthermore, a morpholine moiety provided compound **LVT59** (1.77 μ M) possessing good activity however, when this functionality was probed further a loss of potency was observed in later compounds. Therefore, including a morpholine moiety in future analogues will most likely provide no significant increase in antimalarial activity or may even cause a loss of potency as previously shown. Alternatively, derivative **LVTa1** (1.15 μ M) displayed the lowest activity during the morpholine group exploration therefore this second urea formation could be investigated in future derivatives (see Figure 59).

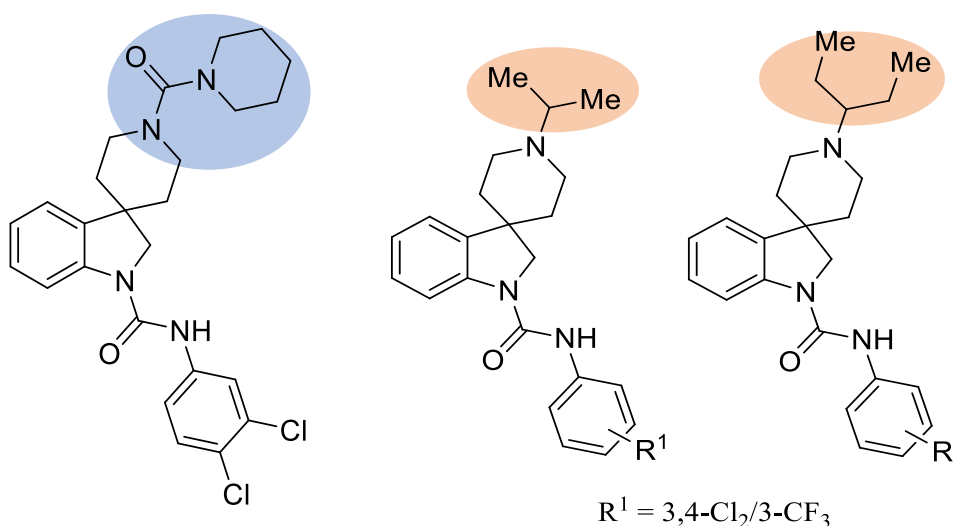


Figure 59: Piperidine analogue and branched alkyl derivatives

Meanwhile during this series of investigations, hydrophobic alkyl chains have provided the highest potency compounds when combined with a phenyl *m*-electron withdrawing group. To probe this interaction further branched alkyl chains should be generated such as, isopropyl thus showing the effects of spreading out the hydrophobic interaction and the impact this has on biological activity (see Figure 59).

In addition, there is a potential benefit in returning to the original benzyl substitution pattern exploration as a single *para* substitution has only thus far been investigated. Therefore, more analogues could explore the significance of substitute position on the benzyl ring i.e. *ortho* and *meta*, to highlight any favoured position for interaction and potentially leading to a more potent compound. For example, moving the nitrogen atom found in **LVTa72** (5.45 μ M) or the fluorine atom seen in **LVT70** (6.77 μ M) could bring to light a more potent compound (see Figure 60).

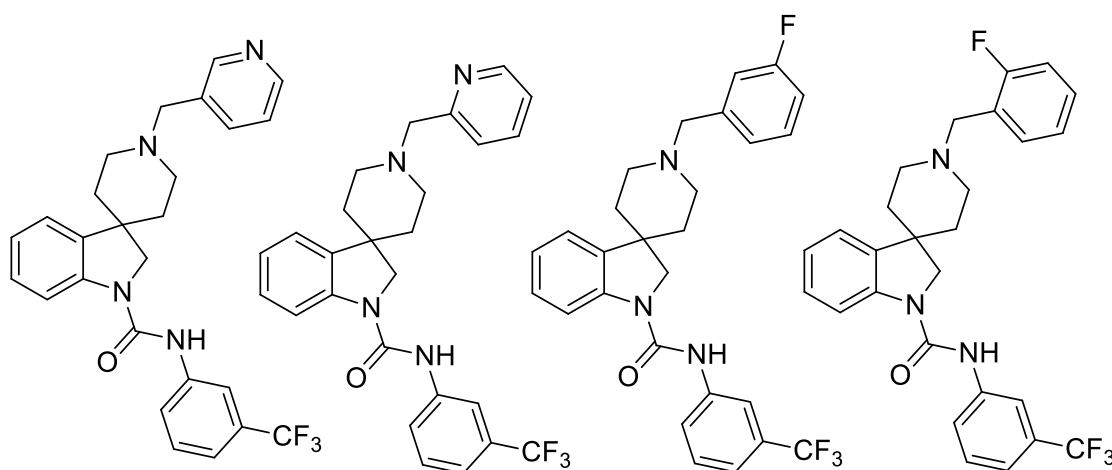


Figure 60: Benzyl substitution exploration

3:8 Summary

In this sub-series, 40 novel spiroindoline analogues have been generated based on the hit compound MMV668732 and tested for their biological activity against *Plasmodium falciparum*.

Bridge substitution	Activity
Carbonyl favoured with urea link + 6 mem saturated ring	Increase
Aliphatic amide	Decrease

Substitution	Activity
Short greasy chain	Increase
Morpholine moiety	Increase
Both EDG and EWG on benzyl ring	Decrease

Substitution	Activity
EDG	Decrease
CF ₃	Small decrease

Investigations of the structure-activity relationship has been extensively explored and highlighted two compounds which warrant further investigation, **LVT86** (960 nM) and **LVTa1** (1.15 μ M). Therefore, to try and improve the logP value of compound **LVT86** as well as preserve the potent activity, a hybrid of **LVT86** and **LVTa1** could be generated whilst retaining a 3,4-dichloro phenyl substitution pattern (see Figure 61). However, more investigation on the dichloro substitution should be carried out first and the *m*-CF₃ group should also be probed for this proposed derivative. Furthermore, longer chain lengths could be created in the hybrid compound as a simple methyl chain is shown but, this would result in an increase in logP.

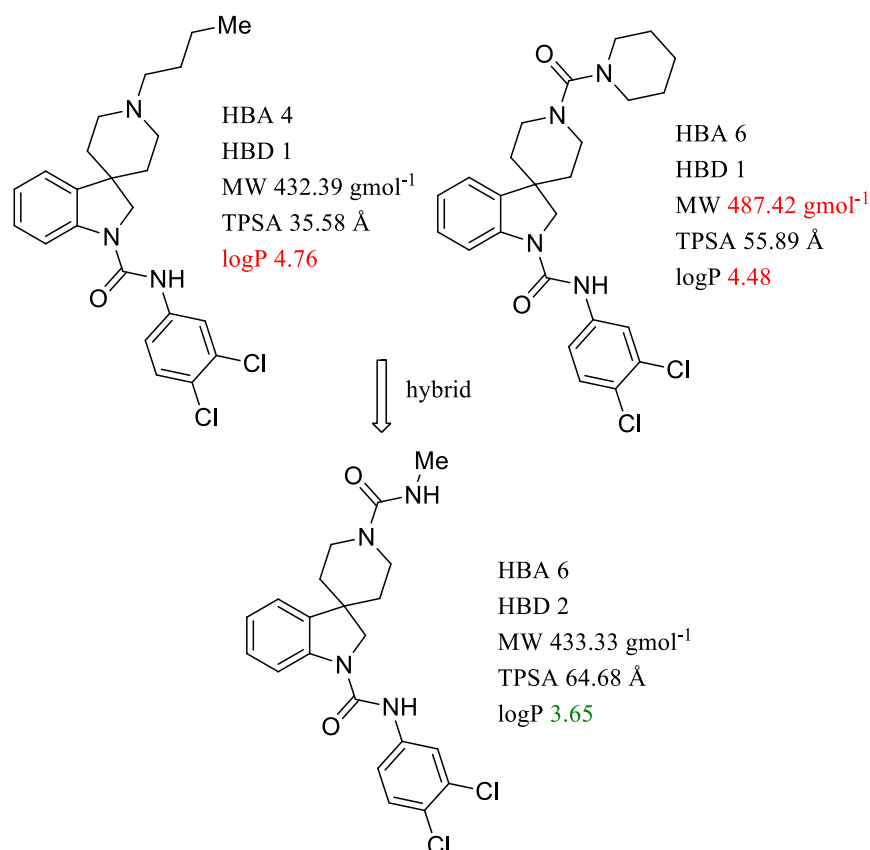


Figure 61: Potential analogue

Finally, additional work researching a central indole substitution could be carried out, to see if any benefit towards activity can be observed. Not only would this new substitution provide an additional interaction but would also help block potential sites of metabolic activity which could cause problems in later biological testing. Figure 62 displays one suggestion for a potential analogue whereby a nitrogen atom has been incorporated into the central structure. This variation would block potential oxidation at that exposed ring position and would contribute to an overall reduction in logP. To achieve this extra point of variation, a substituted hydrazine could be purchased and used to carry out the required Fischer-Indole reaction to generate the desired starting material.

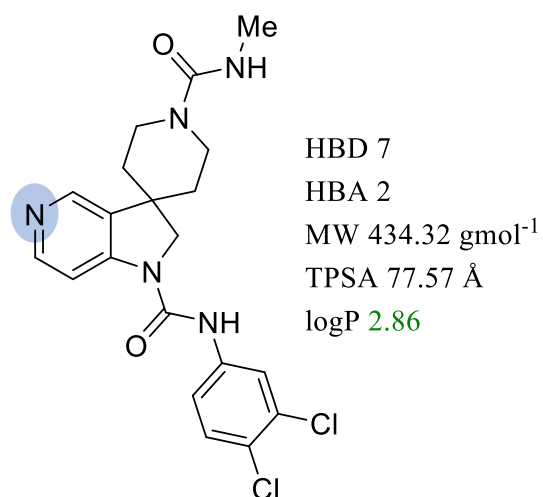


Figure 62: Candidate suggestion

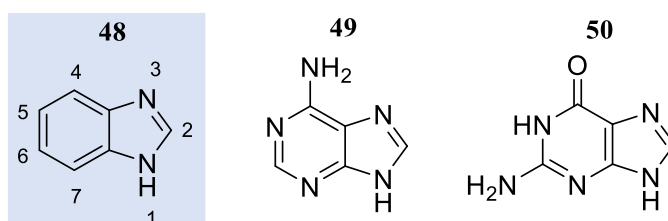
Chapter 4: 2-Iminobenzimidazoles

4:1 Benzimidazole background

4:1:1 Biological significance

The biological activity of benzimidazole **48** was noted in the 1940's, as Woolley speculated benzimidazole to act in a similar way to purines when stimulating a biological response. The research undertaken observed the effects of benzimidazole on yeast and bacteria growth inhibition and furthermore, examining the effects of reversing this inhibition with purines.

⁽⁷⁵⁾ Examples of purines include DNA bases such as adenine **49** and guanine **50**.



This core feature highlighted above is involved in a wide range of bioactive compounds such as: anticonvulsants, analgesics, antihistamines, antihypertensives, antiviral, anticancer, antifungal and more significantly, antiparasitics. ⁽⁷⁶⁾ The benzimidazole structure is readily tautomerised due to the nitrogen lone pair and can therefore cause isomerisation in derived compounds. As a result, two numbering systems can be used, shown in Figure 63.

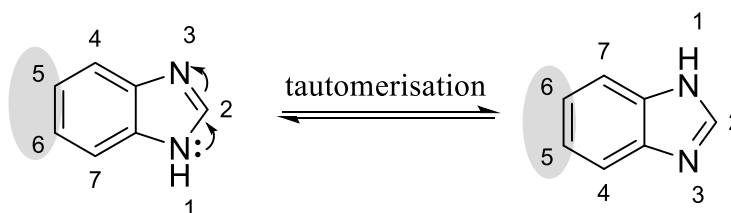
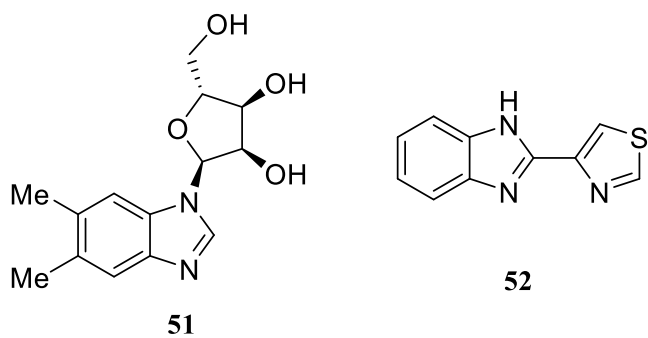


Figure 63: Isomerisation of benzimidazole

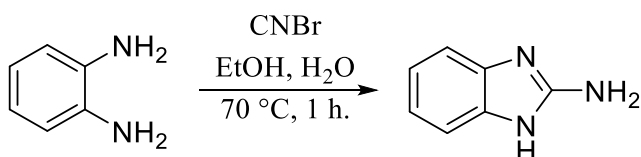
Benzimidazole derivatives rose to popularity within the pharmaceutical industry after compound 5,6-dimethyl-1-(α -D-ribofuranosyl)benzimidazole now known as α -ribazole **51**,

was discovered to be an integral part of vitamin B₁₂ during the 1950's. Consequently in 1962, thiabendazole **52** was the first benzimidazole compound licensed for human pharmaceutical use. Thiabendazole is an effective fungicide and parasiticide drug which is most commonly used to control roundworm and hookworm in: wild animals, livestock and humans. ⁽⁷⁷⁾



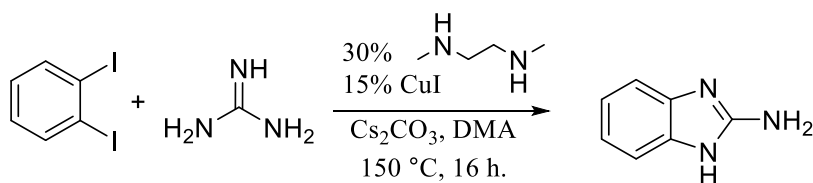
4:1:2 2-Aminobenzimidazole synthesis

The general method for synthesis of 2-aminobenzimidazole has remained the same since the 1940's. Scheme 52 displays the common method used which generates the desired product by reacting 1,2-phenylenediamine with cyanogen bromide in ethanol and water at 70 °C for 1 hour. ⁽⁷⁸⁾



Scheme 52: 2-Iminobenzimidazole synthesis

However, in 2014 Bandyopadhyay and Sathe *et al* generated a 1,2-diiodobenzene intermediate before reacting it with guanidine to create 2-aminobenzimidazole *via* a copper catalysed double amination reaction. Scheme 53 shows the synthesis of 2-aminobenzimidazole from 1,2-diiodobenzene and guanidine in the presence of copper iodide. ⁽⁷⁹⁾

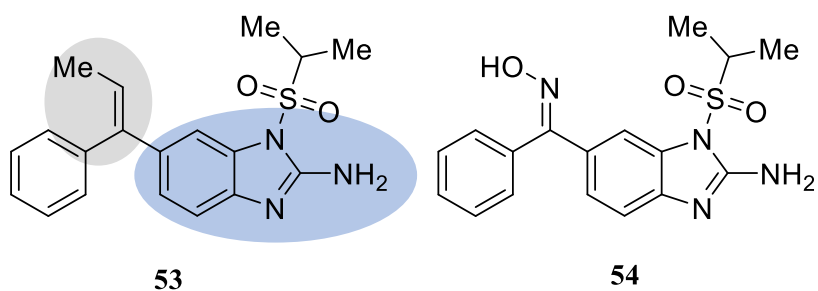


Scheme 53: Alternate 2-aminobenzimidazole synthesis

4:1:3 Conventional benzimidazole pharmaceuticals

Antiviral

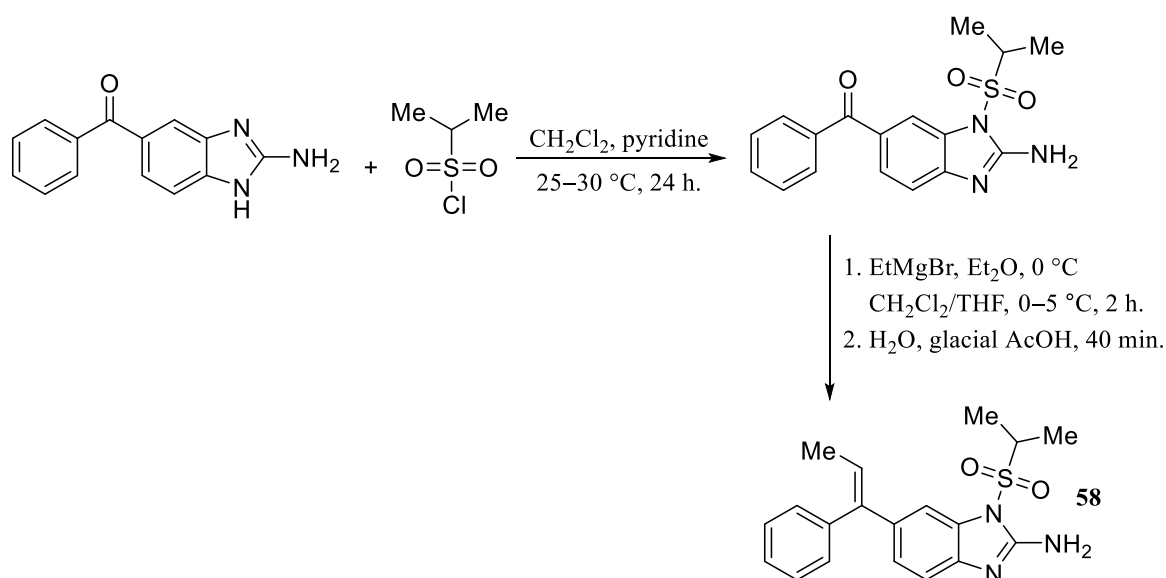
Highlighted below are two common aminobenzimidazole antiviral medications Enviroxime **53** and Enviroxime **54** which were first discovered in the 1980's to use in clinic as a broad-spectrum inhibitor of RNA viruses. For example, both compounds were found to target rhinovirus, responsible for the common cold and, enterovirus, accountable for gastrointestinal tract infections. They possess a central 2-aminobenzimidazole core alongside a propyl sulfonamide and an sp^2 bridge to a phenyl ring.



During biological testing, compound **54** displayed poor oral bioavailability and emetic side effects in humans. On the other hand, compound **53** showed superior oral bioavailability in rats and dogs as well as no emetic side effects – although very poor oral blood levels were found. Therefore, radiolabel studies were carried out and it was found low blood levels of **53** were due to rapid metabolism, by allylic oxidation of the vinyl methyl group (highlighted above). However, both drugs are still used as they exhibit potent broad spectrum anti-rhinovirus and anti-enterovirus activity which is desirable as ‘colds’ are caused by over 100 different virus strains. ⁽⁸⁰⁾

Scheme 54 displays the synthetic route to generate **53** which involves the mixing of 2-amino-5-benzoyl benzimidazole and isopropylsulfonyl chloride. The number of equivalents of starting sulfonyl halide used to generate the desired product 5-benzoyl-*N'*-isopropylsulfonyl-

o-benzimidazole, was found to be of significance. If excess sulfonyl halide was used an unwanted bissulfonyl product was observed, as well as the wrong mono-sulfonyl compound adding to the 2-amino group instead. Therefore, it was found only modest equivalence should be used to ensure the chosen phenylenediamine was fully reacted as desired i.e. 1 equivalents of sulfonyl halide to 1.2 equivalent of phenylenediamine.⁽⁸¹⁾ Also, during this step higher temperatures generated more of the undesired isomeric product, adding to the amino group.

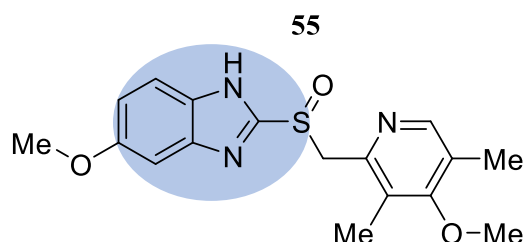


Scheme 54: Enviradine synthesis

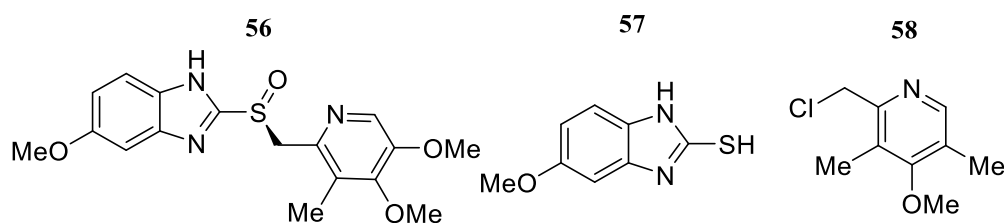
The desired *trans* Grignard product was generated in two steps firstly, 4–6 equivalents of the bromo substituted Grignard reagent was reacted with the sulfonyl starting material. Furthermore, co-solvents were used during this step such as, dichloromethane and tetrahydrofuran as the sulfonyl starting material is not highly soluble in the Grignard solvent diethyl ether. The resultant hydroxy intermediate is not isolated and added directly to dilute aqueous acid to obtain the dehydrated product. The desired product was easily collected by crystallisation from toluene or isopropanol.⁽⁸¹⁾

Proton pump inhibitors

One of the first licensed drugs containing benzimidazole was omeprazole **55** and is on the World Health Organisation's (WHO) list of essential medicines. This drug decreases the amount of acid produced in the stomach by greater than 90% and is prescribed to treat gastroesophageal reflux problems and more severely, peptic ulcers. A covalent disulfide bond is formed between a cysteine residue of the proton pump enzyme in the stomach and the drug itself therefore, irreversibly inhibiting the gastric proton pump within the gastric cells, known as parietal cells. ⁽⁸²⁾

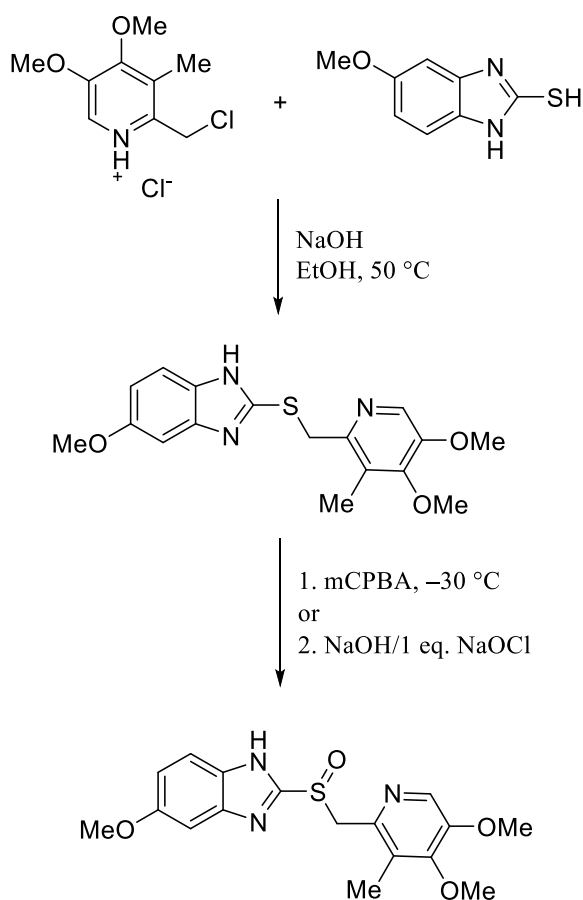


Compound **55** exists as a sulfoxide racemic mixture however, the (*S*)-enantiomer has a better metabolic profile. Both enantiomers are equally active, because the chiral centre is destroyed before the drug binds to the enzyme. Pure (*S*)-sulfoxide (Esomeprazole, **56**) has been synthesised and is marketed as Nexium. ⁽⁸³⁾ Omeprazole can be easily prepared from two commercially available 2-thiobenzimidazole **57** and chloromethylpyridine **58**.



Scheme 55 displays the synthetic route to generate Omeprazole and begins with a nucleophilic substitution reaction between an alkyl chloride and the thiol moiety of a

substituted 2-mercaptobenzimidazole. The resultant sulfide intermediate was then oxidised to generate the desired compound **55**.

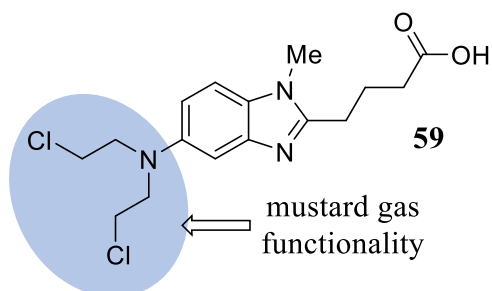


Scheme 55: Omeprazole synthesis ⁽⁸⁴⁾

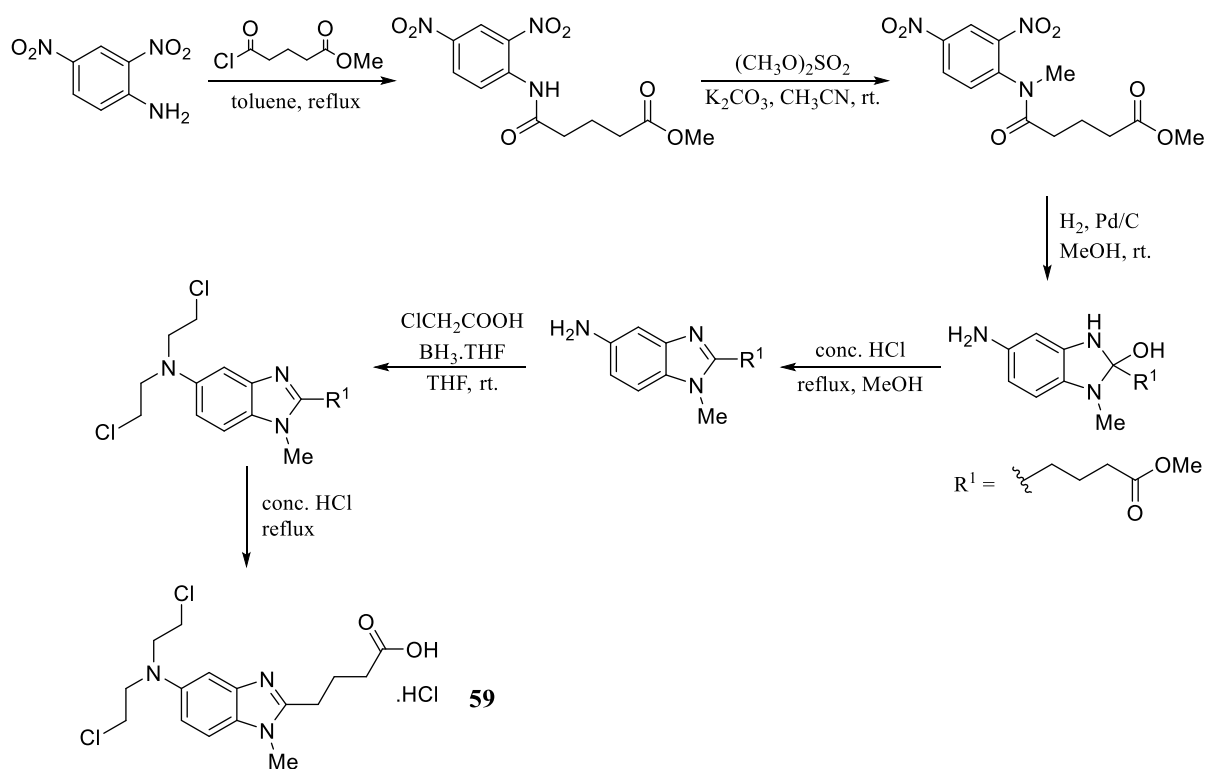
Antitumor

A compound administered as intravenous chemotherapy is Bendamustine **59**, used to treat chronic leukemia and non-Hodgkin's lymphoma. Marketed as Treanda this drug is also on the list of WHO essential medicines and interferes with DNA and RNA operations. Highlighted below is the key functionality responsible for the mechanism of action, causing inter and intra strand cross links between DNA bases. The antitumor agent was originally

developed from mustard gas and has recently been administered alongside the antibody Rituximab, which has shown to improve drug efficacy.



The efficient synthesis of **59** is displayed in Scheme 56 and begins with an amide coupling between, 2,4-dinitroaniline and methyl 4-(chloroformyl)butyrate. ⁽⁸⁵⁾



Scheme 56: Bendamustine synthesis ⁽⁸⁵⁾

4:1:4 Antimalarial activity

In 2011 Camacho *et al*, investigated a novel series of *N*-substituted-2-(5-nitrofuran or nitrothiophene)-3*H*-benzol[*d*]imidazole-5-carbohydrazide compounds for their antiprotozoal activity (Figure 64).

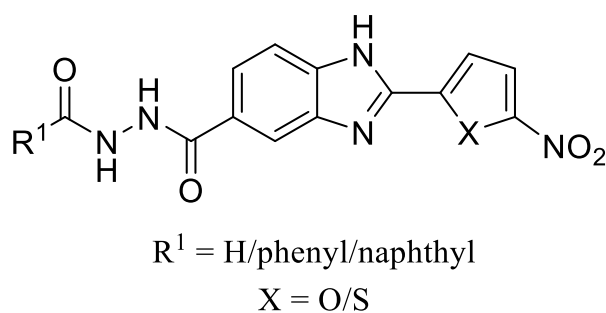


Figure 64: Analogue under exploration

Once the nitrofuran or nitrothiophene moiety had become attached it was found to encourage antimalarial activity *in vivo* for *Plasmodium berghei*. They also reported cytotoxic activity against several cancer cell lines as well as showing evidence for antitubercular activity. ⁽⁸⁶⁾

Gomez *et al* explored the potential of a substituted benzimidazole dimer as an antimicrobial and antiprotozoal agent (Figure 65).

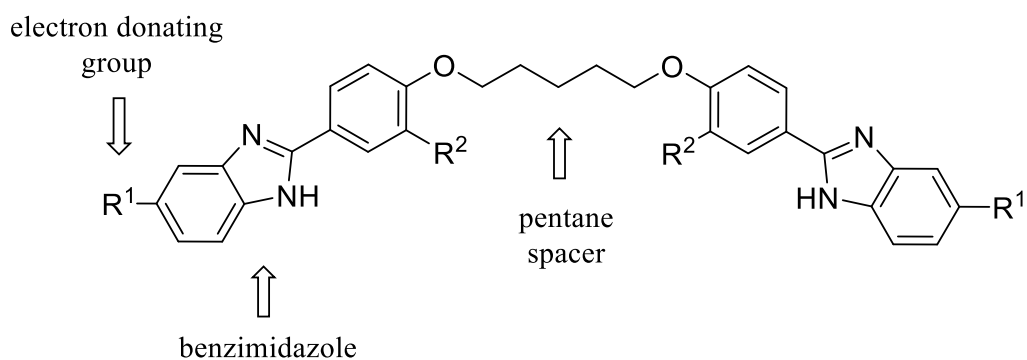


Figure 65: Benzimidazole dimer

The novel compound requires an electron donating group positioned on C5 of both benzimidazole sections (R^1), as well as a pentane spacer for activity against *Trichomonas vaginalis*, *Giardia lamblia*, *Entamoeba histolytica* and *Leishmania mexicana*. However, activity against *P. berghei* was observed when a surprising electron withdrawing group ($R^1=CF_3$) was substituted onto the benzimidazole component and possessed an inhibitory concentration of 6.53 μM .

Furthermore, in 2011 antiplasmodial agents were considered by Saify *et al*, who found the compound shown in Figure 66 to target *P. falciparum* plasmepsin II – one of the essential components of the *P. falciparum* hemoglobin-degradation pathway. ⁽⁸⁷⁾

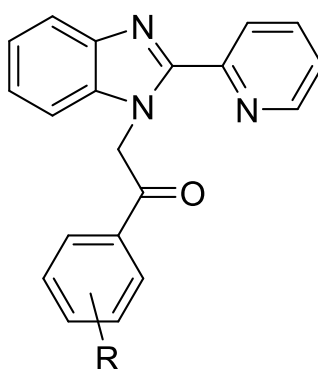
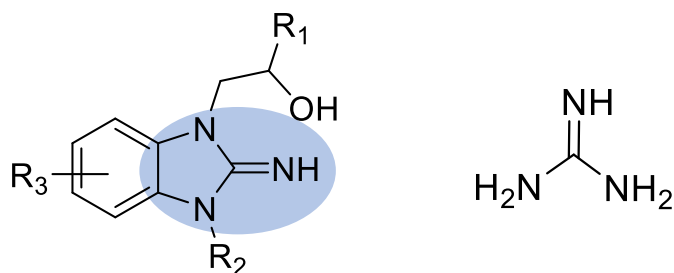


Figure 66: Active scaffold $R=Cl/NO_2$

They discovered the presence of a chloro or nitro moiety substituted on the ketone linked phenyl ring was necessary to enhance *Plasmodium* activity and a further phenyl group substituted as R also resulted in higher activity. ⁽⁸⁸⁾

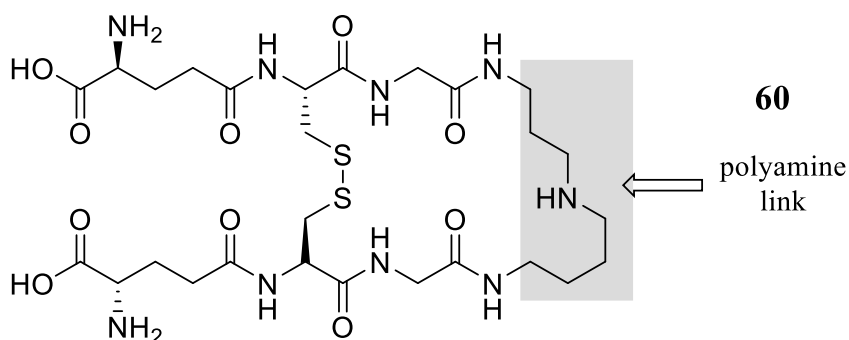
In 2003 a patent application highlighted a group of guanidine compounds as anaesthetics for the treatment of nervous system disorders. These novel compounds possess the general formula, shown in Figure 67, and are defined as effective sodium ion channel blockers in neuronal mammalian cells. ⁽⁸⁹⁾



Their applications include: anaesthetics and/or analgesics – particularly local spinal/epidural, for alleviation of neuropathic pain and, for producing anticonvulsant effects.

(89)

Furthermore, in 2007 Holloway *et al* discovered that compounds with an identical core structure to the patented compound above displayed good antibacterial activity and was found to inhibit Trypanothione reductase. Trypanothione **60** is found in protozoa such as leishmania and trypanosomes and is the alternate form to glutathione (two molecules of glutathione joined by a polyamine linker).⁽⁹⁰⁾



The research group discovered a compound that exhibited one basic side chain in combination with an aromatic ring side chain, which subsequently lead to an antibacterial hit (see Figure 68). Through removal of the latter aromatic chain, a loss of potency was observed as well as, replacing the basic side chain with a hydrophobic group. ⁽⁹⁰⁾

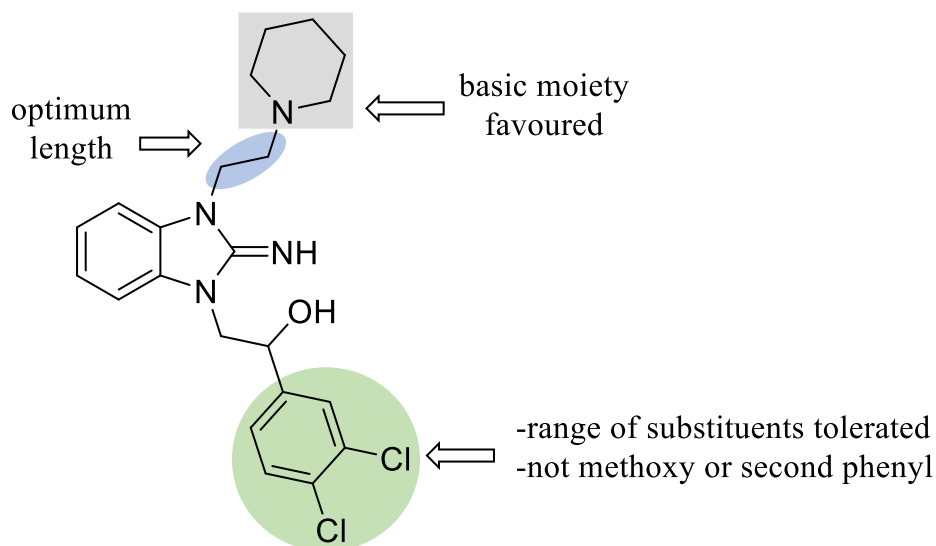
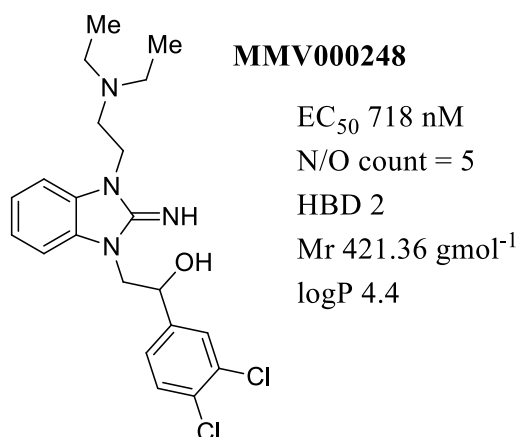


Figure 68: Hit compound and key features

They highlight several features which reduce and enhance potency for example: a piperidine or diethylamine basic moiety produces the best activity, a loss of potency was seen on the addition of a morpholine group, extension of the basic chain from the benzimidazole nitrogen saw a loss of activity, a variety of alcohol substituents were tolerant without significant loss of activity, 4-methoxy substitution on the phenyl ring was distinctively less favoured and, a second 4-phenyl group saw a loss of activity. They conclude their findings to indicate a relatively tolerable binding site with the potential to host a wide range of different structures and state this is consistent with previous studies which show inhibitors of Trypanothione reductase to have multiple binding modes. ⁽⁹⁰⁾

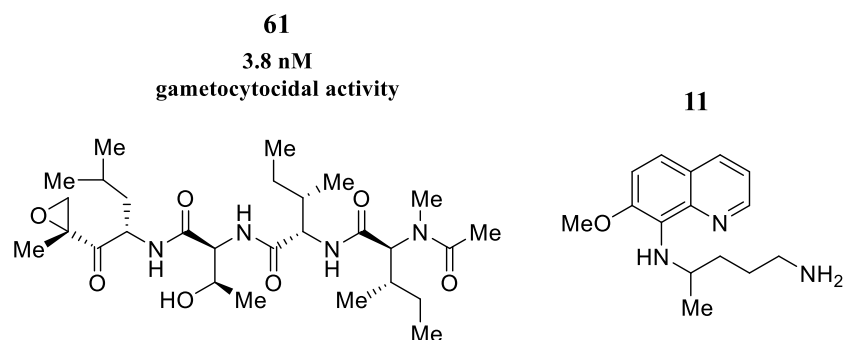
4:2:1 2-Iminobenzimidazole antimalarials

As previously discussed, in June 2013 the Open Access Malaria Box was published to create a bank of drug-like and probe-like antimalarial leads for alternative research groups to optimise and progress. Their aim was to support the malaria eradication agenda, which requires the discovery of new drugs with transmission blocking or liver stage properties. Of the thousands of compounds screened and subsequent optimisation to extract a balance between potency and chemical diversity, a 2-iminobenzimidazole compound **MMV000248** appears within the final 400 leads. In this publication, Spangenberg *et al* highlight important features of **MMV000248** which include: nitrogen + oxygen count=5, number of rotational bonds=0, hydrogen bond donors=2, molecular weight 421.36 gmol⁻¹ and logP=4.4.⁽⁹¹⁾



Furthermore, in 2014 Bowman *et al* investigated antimalarial compounds present within the MMV box for their gametocytocidal activity. To evaluate their activity against alternate stages of the parasite lifecycle 22 compounds were tested for their gametocyte viability at 5 µM and those which displayed >85% inhibition were taken forward. Of the original 22 compounds, 18 were carried forward and of those, 12 displayed an IC₅₀ of <1 µM against the gamete stage, as well as acting on the asexual stage, drug resistant and drug sensitive parasite.⁽⁹²⁾

All compounds tested for their gametocytocidal activity were tested alongside a positive control epoxomicin **61**, which has been previously reported to target the gametocyte stage of the parasite lifecycle.⁽⁹³⁾



Primaquine **11** is currently the only antimalarial drug active against late stage gametocytes and only a small number of potential candidates are currently going through clinical trials this therefore highlighting the need for new leads against this malaria stage.⁽⁹⁴⁾ **MMV000248** showed mid-nanomolar inhibitory concentration in late stage gametocytes (NF54 310 nM) and low nanomolar inhibitory concentrations in the asexual stage of the parasite (NF54 50 nM and Dd2 90 nM).⁽⁹²⁾

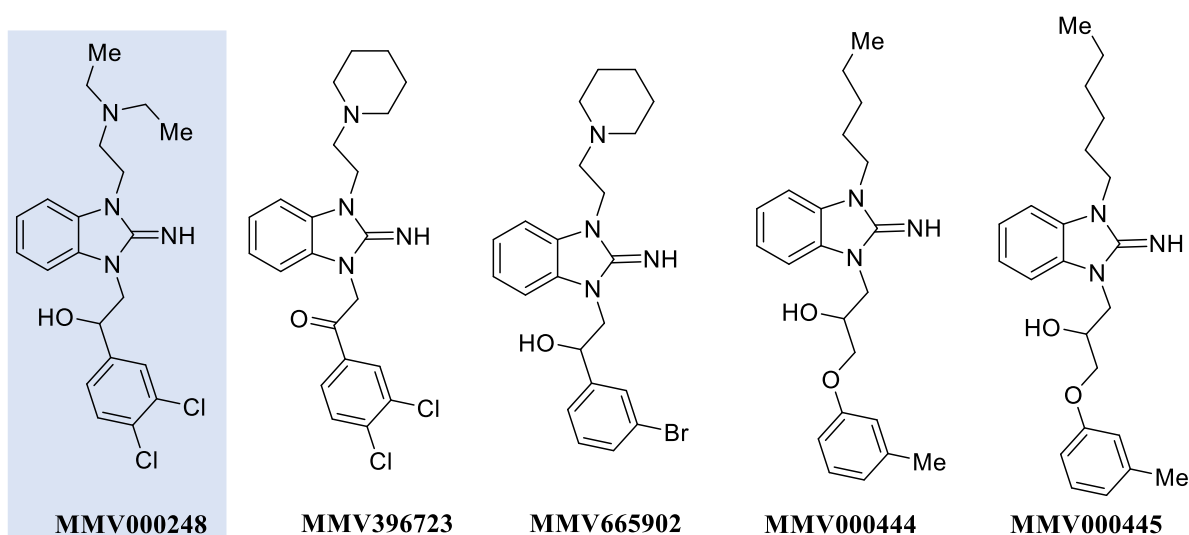


Figure 69: 2-Iminobenzimidazole leads

Two pharmacophores were identified as an outcome of gametocytocidal exploration of which, the benzimidazole imine core was one. Additionally, in 2013 Spangenberg *et al* found four other analogues present within the MMV box possessing the same benzimidazole imine scaffold, but lack confirmatory gametocytocidal activity (see Figure 69).⁽⁹¹⁾ Overall, the gametocyte activity data obtained indicates strict structural requirements for both gametocytocidal and asexual activity within the benzimidazole imine scaffold. From this investigation **MMV000248** has been highlighted with the potential of having multistage activity that could be further optimised to generate a cure and stop malaria transmission.⁽⁹²⁾

4:3 Alternative therapeutics for 2-iminobenzimidazoles

In 2015 a research group Rubin *et al* investigated the inhibition of a gram-negative bacterium, *Acinetobacter baumannii*. This bacterium contributes to multi-drug resistant (MDR) in-hospital infections of which, 63% of *A. baumannii* varieties are MDR. As a result, they screened novel compounds selectively targeting bacterial oxidative phosphorylation (OxPhos), which plays an essential role in bacterial energy production in the form of ATP. Therefore, inhibition of this pathway is known to significantly impair bacteria viability.⁽⁹⁵⁾

The research group conducted a high through put screening programme to filter a library of compounds that possessed activity towards OxPhos inhibition. Structure-activity exploration led to the synthesis of over 100 compounds and uncovered a promising scaffold, shown in Figure 70. They state compound **A** displayed a good spectrum of antibacterial activity against *A. baumannii* and was the most potent amongst the original hits, possessing an inhibitory concentration of 1.9 μM for the inhibition of ATP synthesis.⁽⁹⁵⁾

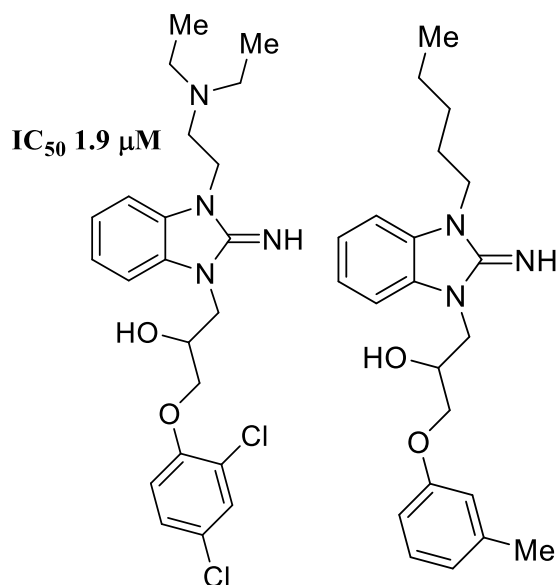


Figure 70: Compound **A** (bis TFA salt, left) and **MMV000444** (right)

Structural similarities can be seen with antimalarial compounds **MMV000444/MMV000445** shown in Figure 70, as identical ether-alcohol moieties are present within the linker between a benzimidazole core and substituted phenyl component.

During the investigation, they probed the SAR by synthesising analogues which removed each component they hypothesised to be responsible for activity. Figure 71 highlights four key derivatives which indicate the constituents required for overall potency. Replacement of the 2-imino group on benzimidazole with a ketone moiety resulted in 6 times decrease in biological activity (IC_{50} 12 μ M). Also, removal of the alcohol and ether present in the linker resulted in over 2 times decrease in potency (5 μ M).⁽⁹⁵⁾

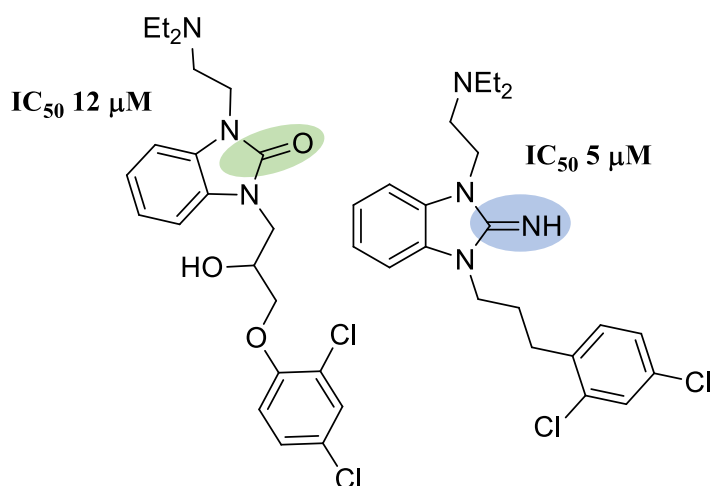


Figure 71: SAR exploration

They discovered two compounds which possessed higher potency than the original hit which are displayed in Figure 72. Firstly, they solely removed the hydrogen bond donor constituent from the phenyl linker, which resulted in 3 times increase in potency (IC_{50} 0.6 μ M). Secondly, they not only removed the alcohol component but also, the tertiary amine linked *via* an ethyl chain and surprisingly, generated a compound with an IC_{50} of 0.9 μ M, so this character may not be necessary for activity (see Figure 72).⁽⁹⁵⁾ Exploration of this mechanism of action and SAR against *A. baumannii* is still ongoing.

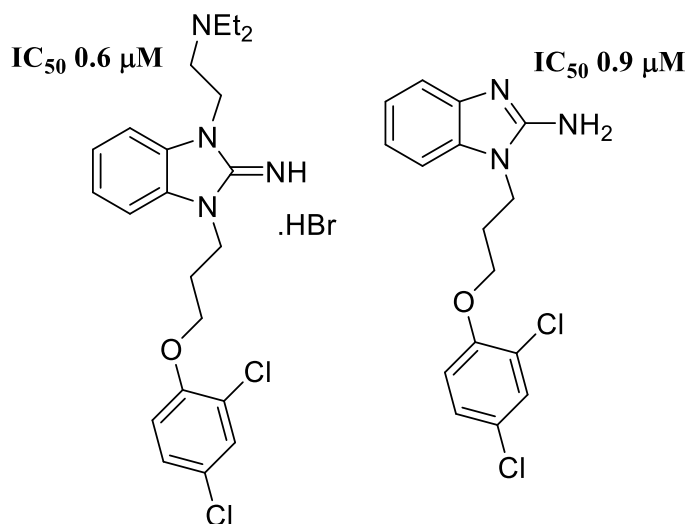
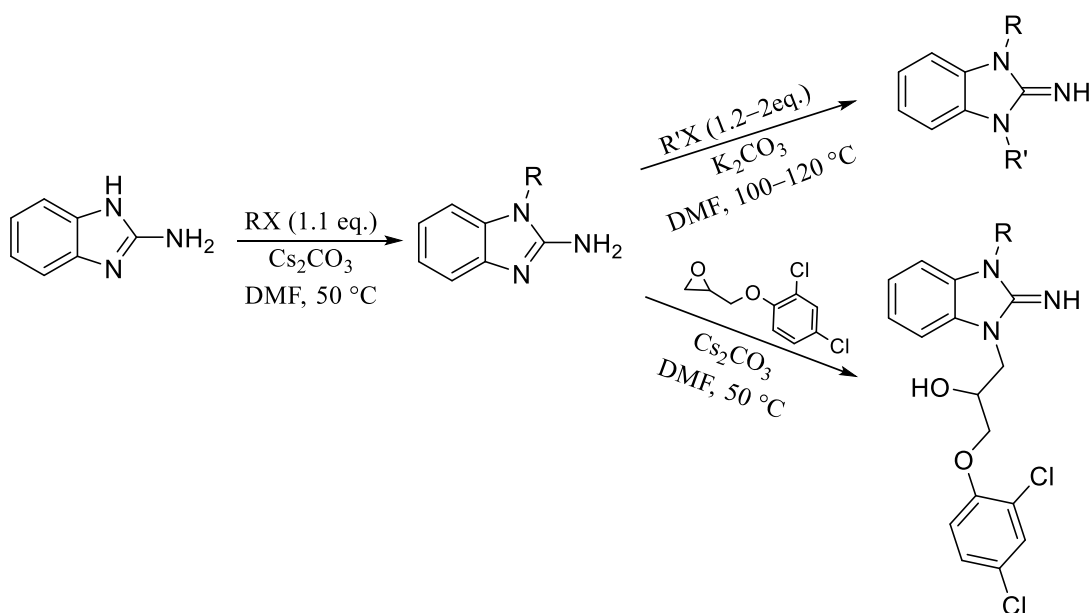


Figure 72: Potent leads

The exploration of this SAR provides key insight into the moieties required for high activity against this bacterium and therefore could be applied to our investigation into analogues targeting malaria.

To access these analogues Rubin *et al* performed two consecutive alkylation reactions which can be adapted to synthesise the antimalarial compounds proposed in this research project (see Scheme 57).



Scheme 57: Synthesis of benzimidazole derivatives

4:4 Postgraduate project

MMV000248 possess the lowest EC_{50} of the five MMV structures and highlights some key features for high activity (see Figure 73). Firstly, three of the five lead compounds have a tertiary amine connected to the benzimidazole core *via* an ethyl linker. Secondly, two of the higher activity derivatives have a chiral alcohol group situated next to a substituted phenyl moiety. Thirdly, three analogues have a halogen substituent on the phenyl ring.

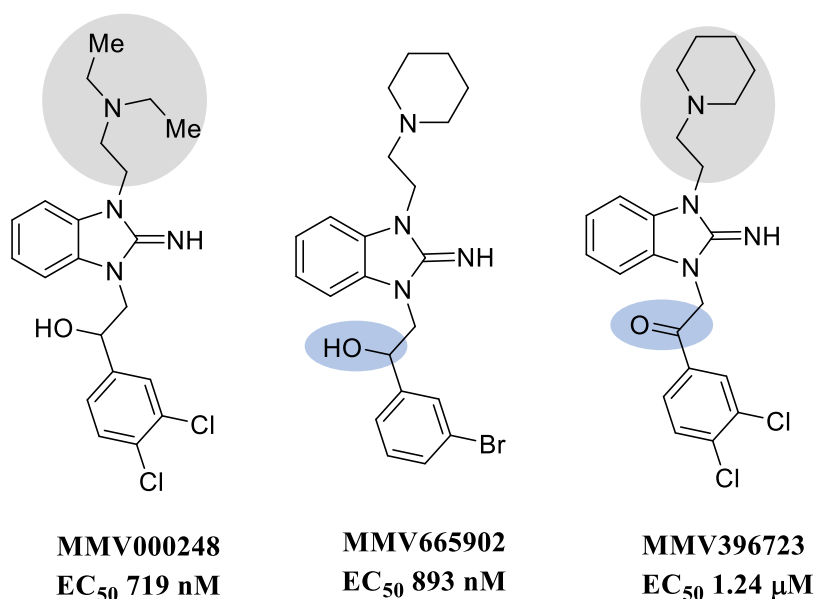


Figure 73: Predicted moieties important for SAR

Compound **MMV396723** retains the 3,4-dichloro moiety seen in **MMV000248** but has an alternate ketone functionality next to the phenyl ring, and this resulted in a significant loss of potency (719 nM to 1.24 μ M). Therefore, we reasoned that the alcohol group is required for high activity.

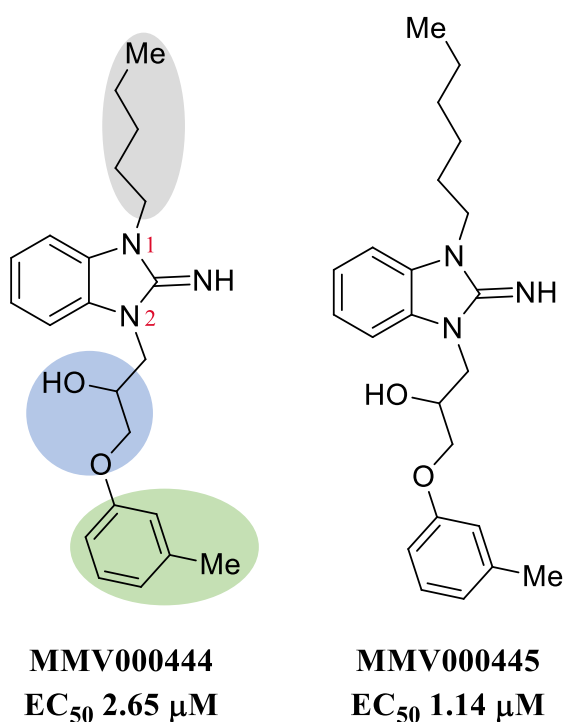


Figure 74: Alternate 2-iminobenzimidazole leads

The last two 2-iminobenzimidazole MMV compounds maintain the position of the alcohol group, with an ether spacer to the substituted phenyl ring (see Figure 74). The top nitrogen is substituted with a straight chain alkyl group (pentyl and hexyl chain). These compounds only possess low micromolar activity however, it is unclear whether this is a result of the changes to the substituents at N¹ or N².

As a result, we proposed to synthesise a small library of analogues with single structural modifications to allow direct comparisons between structure and activity. Our analogues consist of a mixture of the features discussed such as: tertiary amine with ethyl linker; hexane and pentane moieties; phenyl substituents with halogen substituents and also; alternative electron withdrawing groups such as: 3,5-dichloro, 2,4-dichloro, 3-bromo, 3-chloro, 4-trifluormethyl and 3-nitro (see Figure 75).

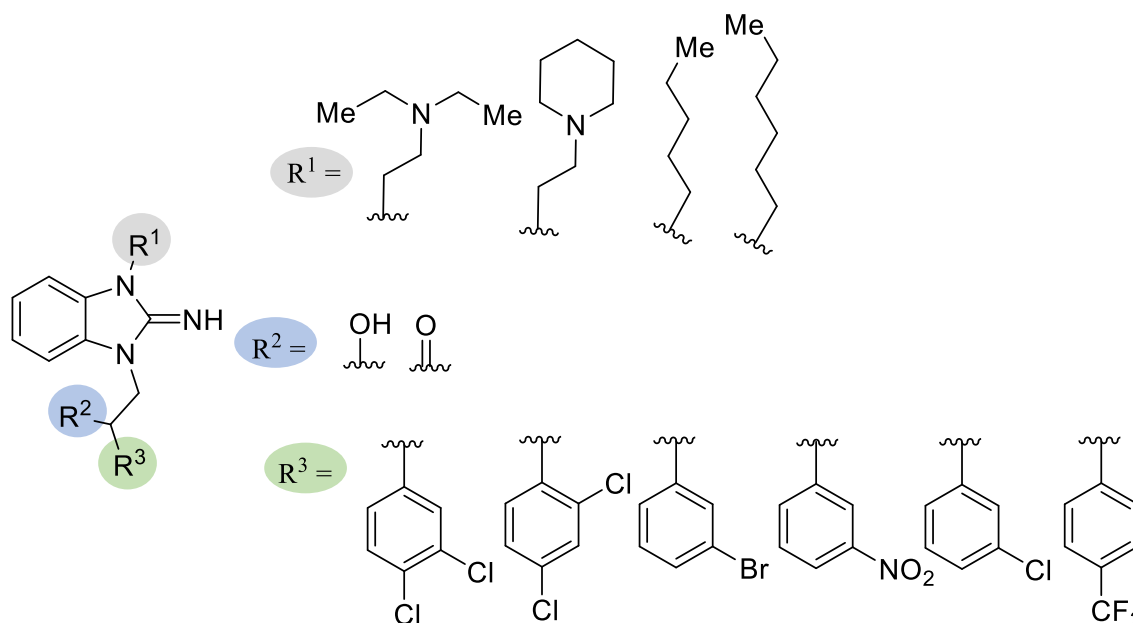


Figure 75: 2-Iminobenzimidazole analogue proposals

As we envisioned these analogues would be synthesised *via* *N*-alkylation with a α -bromo ketone derivative. Our route would generate the keto form, as seen in the MMV and then reduced to the desired alcohol however, both analogues would be retained for testing. The ether-linker analogues are limited to the MMV compounds at this stage but, should be explored in future.

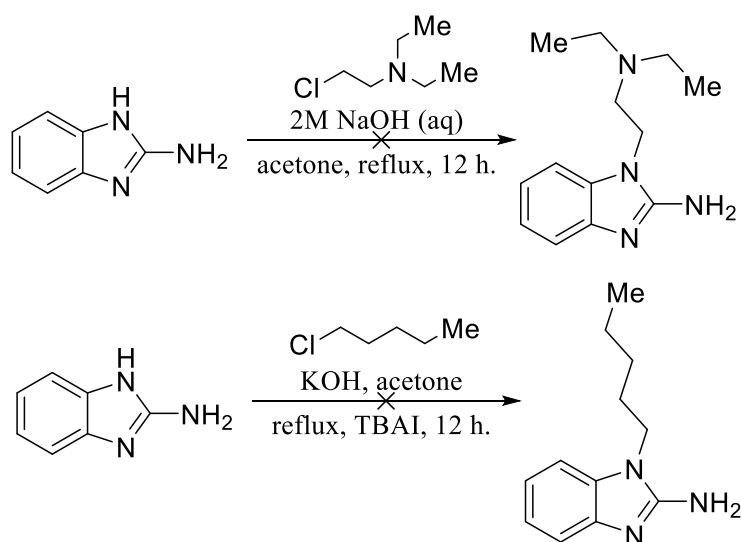
To conclude, all R^1 substituents should be interchanged with each corresponding substituted phenyl R^3 and both ketone and alcohol R^2 should be tested. This will generate a bank of 50 2-iminobenzimidazole derivatives for antimalarial screening to probe this structure-activity relationship.

The proposals also include the synthesis of compounds **MMV000444/445** which will be synthesised from 2-((*m*-tolyl)oxy)methyl)oxirane and the relevant pentane/hexane alkylated 2-iminobenzimidazole.

4:5 Results and Discussion

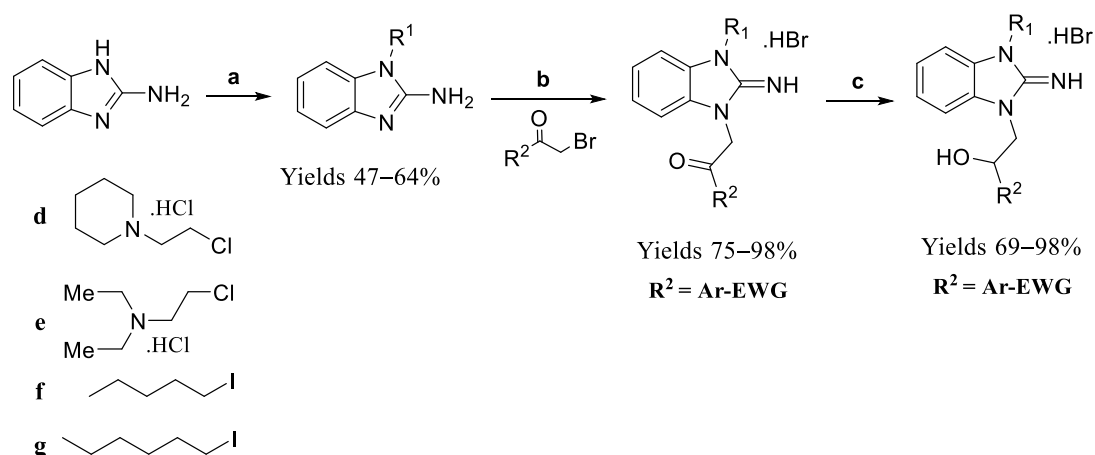
4:5:1 Substitution of 2-iminobenzimidazole

To access these novel benzimidazole derivatives two simple consecutive alkylation reactions can be carried out on 2-iminobenzimidazole, which is readily available. Previous work carried out by an undergraduate student explored alkylation conditions of 2-iminobenzimidazole to generate **MMV000248**. During this project several reaction solvents and bases were tested and from this the conditions used to generate these analogues were developed. For example, alkylation was attempted to form the diethyl ethylamine substrate in a 2M NaOH/acetone solution, however after leaving at reflux overnight no product peak (233 peak) was observed in the LC-MS chromatogram. Also, potassium hydroxide and TBAI were utilised to try and form the pentane compound from chloropentane but, after leaving at reflux overnight, no product peak could be seen in the LC-MS chromatogram (see Scheme 58).



Scheme 58: Unsuccessful alkylation conditions

As a result, the reaction conditions shown in Scheme 59 were deduced and the desired starting materials and products were generated in good yields.



Scheme 59: 2-Iminobenzimidazole derivative synthesis

a) d/e/f/g, KOH, 60 °C, 1h. acetone., b) DMF, 60 °C, 1 h

Firstly, the chosen alkyl halide/ethyl tertiary amine halide was stirred along with 2-iminobenzimidazole and potassium hydroxide in acetone at 60 °C for 1 hour. Once completed, the acetone was removed under reduced pressure and the resulting mixture partitioned between EtOAc and water. The collected organics were washed with brine, dried over magnesium sulfate, filtered and the solvent removed under reduced pressure. For purification, ice-cold acetone was added to generate both tertiary amine precipitates, whereas the pentane substrate requires cold diethyl ether. The required solvent was cooled in an ice bath and added into the relevant reaction flask until a precipitate formed the solid was then filtered off *via* Büchner filtration and subsequently washed through with the ice-cold solvent. The hexane substrate was a brown waxy solid, and therefore proves difficult to filter once ice cold diethyl ether was added. As a result, the best purification method for this hexane intermediate was column chromatography (10% MeOH in CH₂Cl₂) and is easily separated from its constituents and impurities.

The alkyl halide producing the best result was the iodo- substituted alkyl chain, as both chloro- and bromo- starting materials: produced minimal quantities of product or none and

had much longer reaction times which allowed impurities to form, giving an unclear reaction mixture.

As we recognised there are two possible sites for alkylation on 2-iminobenzimidazole as shown in Figure 76, we ran a nuclear Overhauser effect (nOe) NMR experiment to ascertain the actual position of alkylation. To run the experiment a sample of the diethyl ethylamine substrate was made up in D₆-DMSO and the protons highlighted at 4.00 ppm were irradiated and the signal corresponding to the proton at 7.13 ppm was predicted to be enhanced.

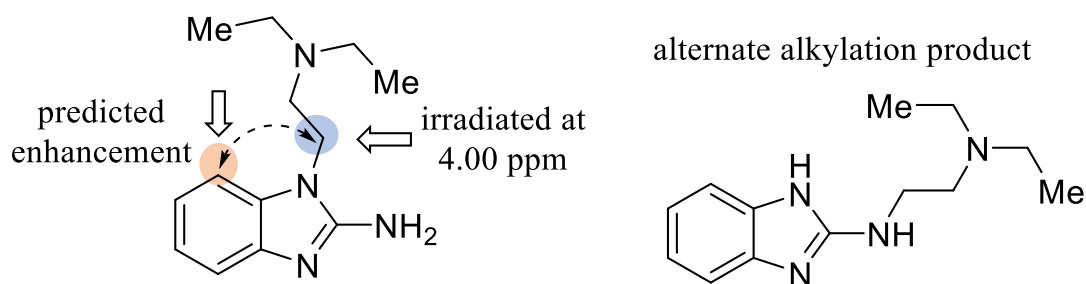


Figure 76: nOe experiment

From the nOe spectra displayed in Figure 77, the peak corresponding to the expected aromatic proton highlighted above is enhanced (red) when the proton at 4.00 ppm is irradiated (blue) and therefore, confirms the structure we desire has been successfully synthesised. If the alternate alkylation product had been generated, no aromatic protons would have been enhanced.

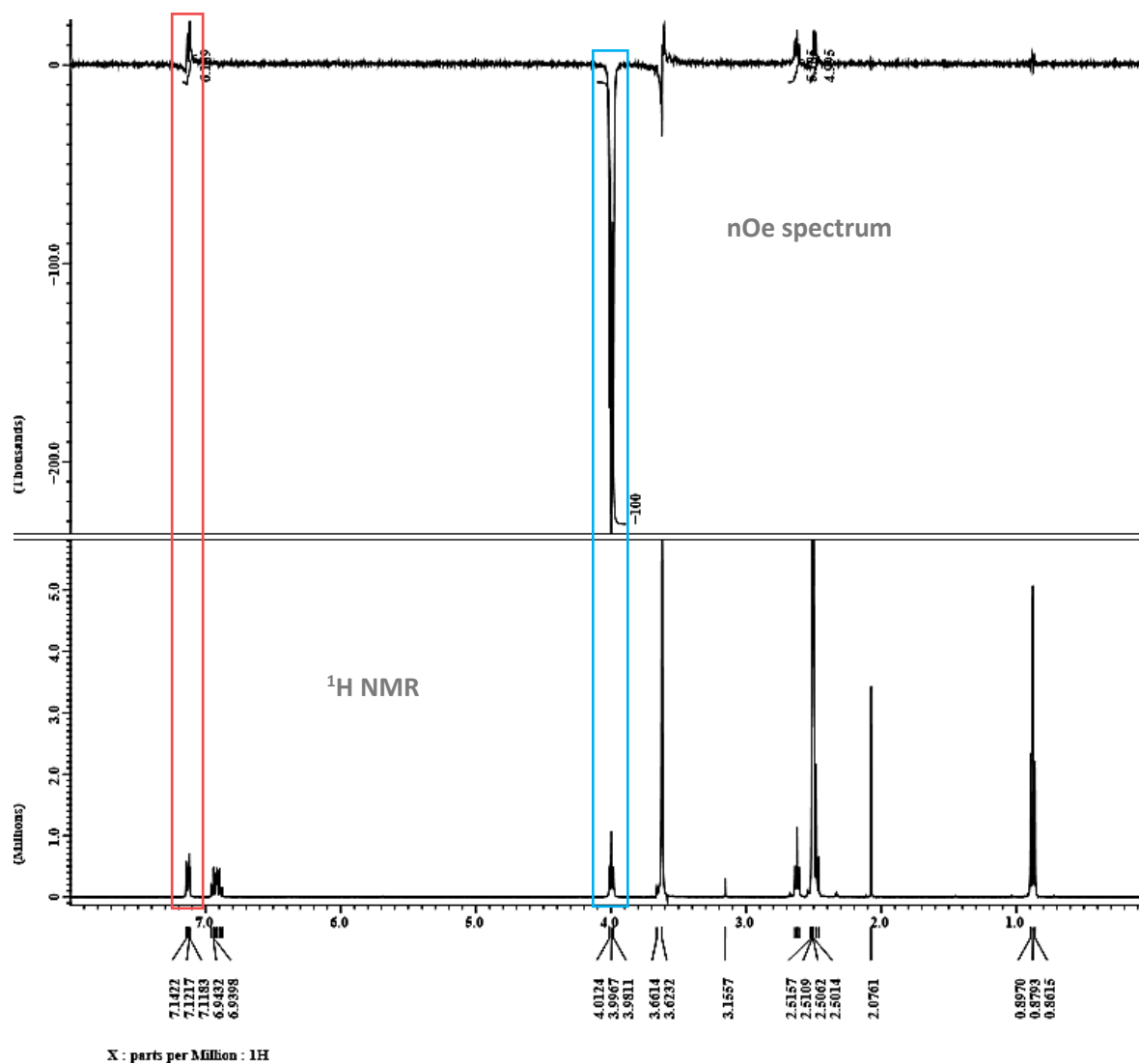
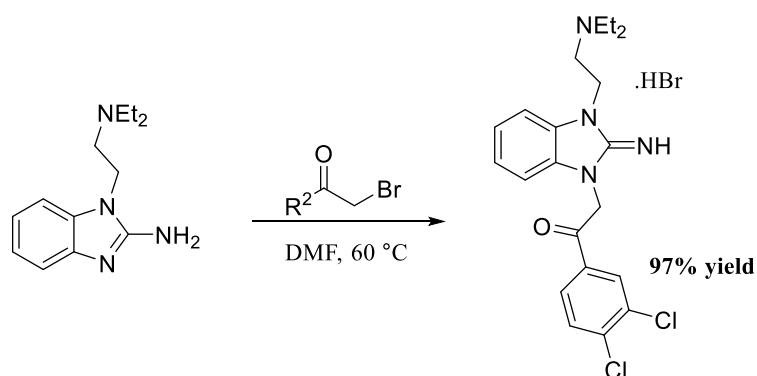


Figure 77: nOe spectrum

The second alkylation was carried out in DMF and stirred for 1 hour at 60 °C and found to be successful (see Scheme 60). These reaction conditions were based on the previously discussed synthetic strategy carried out by Rubin *et al.*

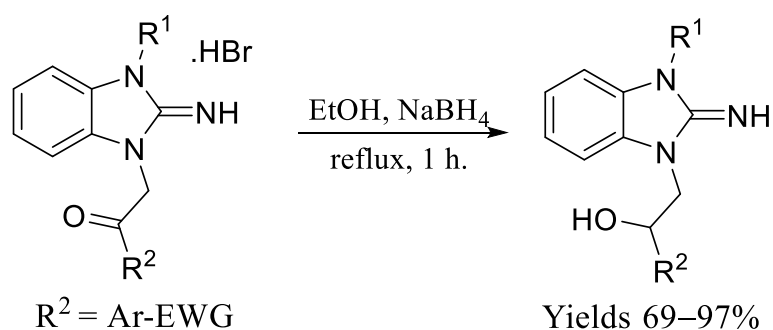


Scheme 60: Alkylation exploration ($R^2=3,4$ -dichlorophenyl)

Subsequently, on removal of DMF a white solid appears amongst red coloured impurities in all cases. The desired product hydrogen bromide salt is insoluble in acetone and so simply filtered *via* Hirsch funnel under suction and washed with acetone (20 mL) to reveal the pure product. Furthermore, the yield range for the ketone analogues was 75–98%, which is very good due to little purification needed and each product was confirmed by LC-MS displaying the calculated product mass.

4:5:2 Ketone reduction

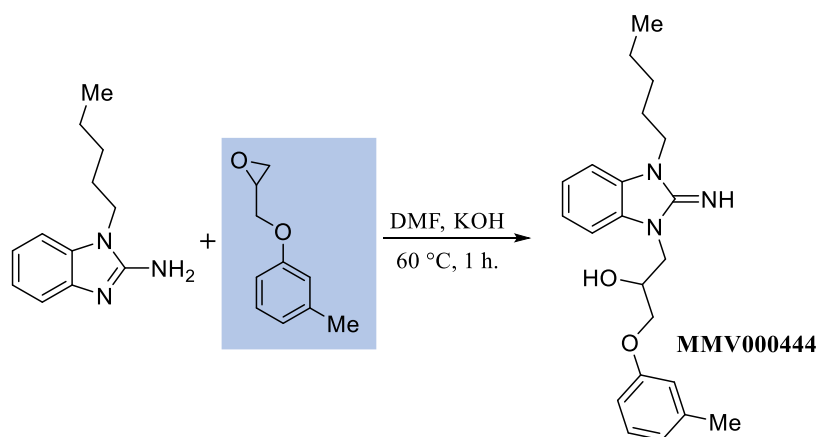
Approximately 100 mg of each ketone hydrobromide salt was taken and subjected to a straightforward NaBH_4 reduction stirring in ethanol at reflux for 1 hour (see Scheme 61). A small sample was taken from the reaction mixture and ran through LC-MS to ensure all the ketone had been reduced. After an aqueous work up the products were isolated in good yield with a range of 69–97%, therefore generated sufficient material for both analytical and biological assay testing.



Scheme 61: Ketone reduction

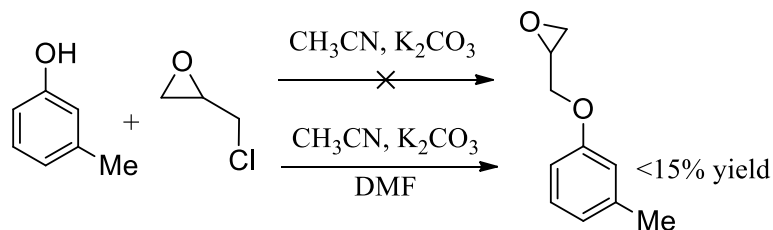
4:5:3 Epoxide synthesis

Formation of compounds **MMV000444** and **MMV000445** require a different synthetic route due to the additional ether group and extra carbon atom in the linker connecting the phenyl ring to the benzimidazole core. We planned to generate these two compounds from the epoxide, as shown in Scheme 62.



Scheme 62: Alkylation with *m*-cresol epoxide

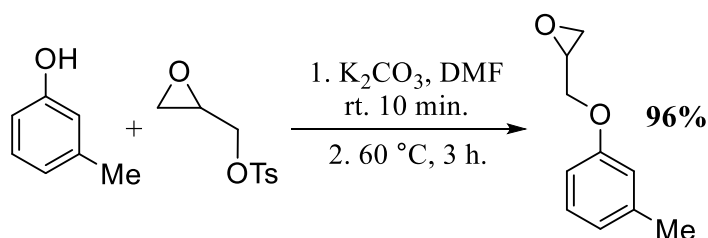
The *m*-cresol epoxide was not commercially available we attempted to synthesise it by following a literature procedure which involves mixing K_2CO_3 and *m*-cresol in acetonitrile for 30 minutes at room temperature. Then, epichlorohydrin was added *via* syringe and the resulting reaction mixture was left to stir at reflux for 18 hours. However, the reaction was monitored by TLC and at this stage only displayed both starting materials. The literature states they experience a problem with a biphasic mixture, so this was thought to be the cause for no product formation. ⁽⁹⁶⁾ As a result, a small volume of DMF was added to increase solubility and retain more base within solution, and the reaction was left to stir at reflux for a further 12 hours (see Scheme 63). This time the reaction TLC indicated a minimal amount of product within the reaction mixture, therefore a more efficient synthesis was required.



Scheme 63: Attempted synthesis of epoxide

In addition, the epichlorohydrin component carries safety concerns due to its link with carcinogenicity, therefore this steered the search for an alternate starting material. Consequently, a colleague proposed using glycidyl tosylate known from his own previous research, which is a stable solid and provides a better tosylate leaving group.

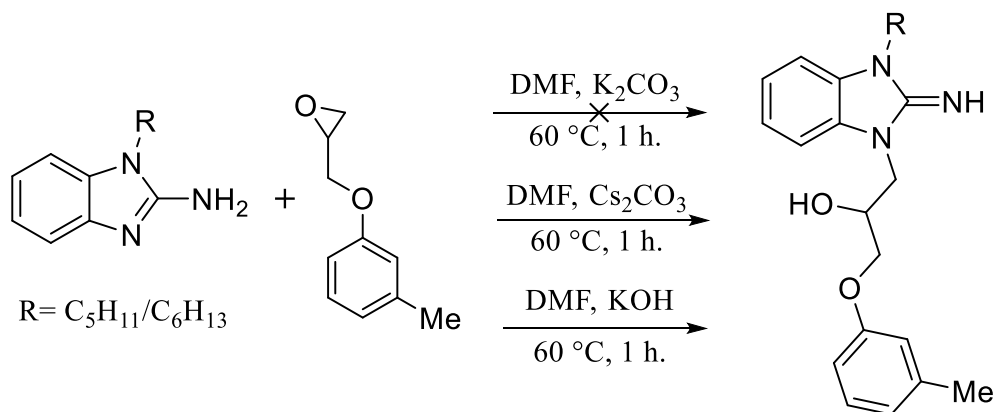
A stirred solution of *m*-cresol in DMF under nitrogen was treated with K_2CO_3 then, (*S*)-glycidyl tosylate was added as a DMF solution *via* needle and syringe then, left to stir at room temperature for 10 minutes. The solution was subsequently heated to 60 °C and left for a further 3 hours to generate the desired starting material.⁽⁹⁷⁾ The product was obtained in excellent yield as a yellow oil and subsequently used in the second alkylation (see Scheme 64).



Scheme 64: Tosylate strategy

To prepare both MMV compounds, K_2CO_3 was used as the base in the alkylation reaction and surprisingly no product could be seen by reaction TLC after 1 hour at 60 °C. Therefore, two equivalents of Cs_2CO_3 was added and after 1 hour, only minimal product could be observed on TLC. As a result, a separate reaction was carried out with KOH as the base, and

after 1 hour a larger amount of product could be seen along with a depletion of starting material, therefore these conditions were used to generate the two MMV analogues (see Scheme 65).



Scheme 65: Epoxide alkylation conditions

4:6 Biological screening

Preliminary screening of this series of benzimidazole derivatives has provided essential insight into the key structural features required for high antimalarial activity. Initial screening tested all analogues for percentage growth at 3 different concentrations: 2 μ M, 400 nM and 80 nM. For example, Figure 78 displays one set of preliminary data obtained for a handful of analogues generated and shows the % growth at each concentration.

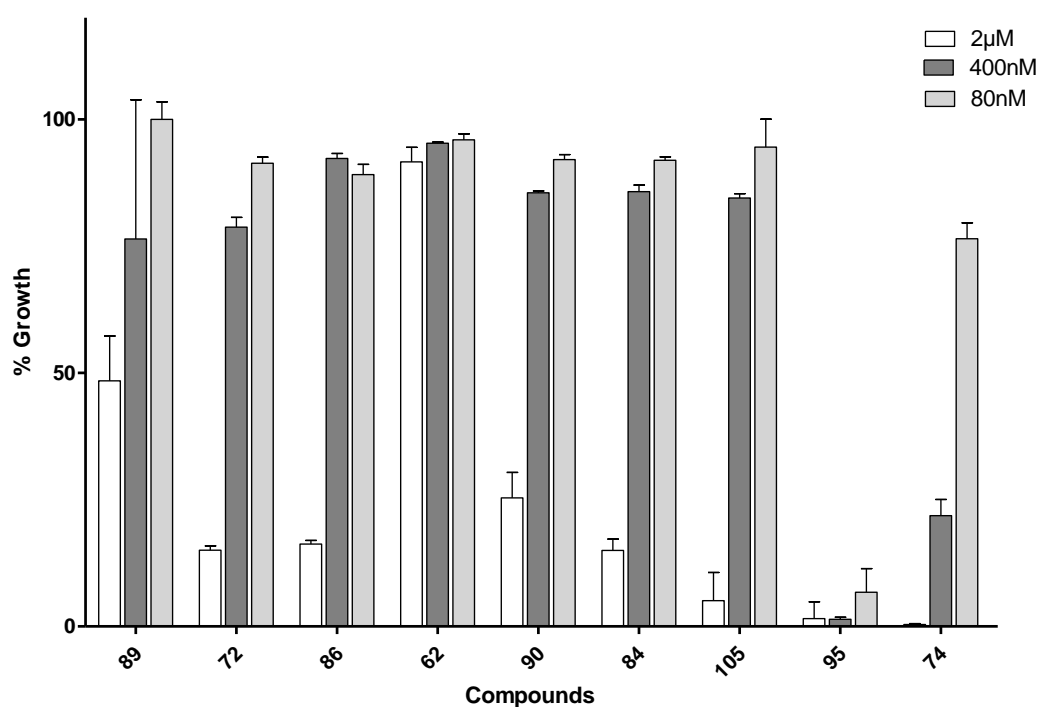


Figure 78: Initial biological screening

The two best analogues discovered were **LVTa95** and **LVTa96**, displayed in Figure 79 and these display better activity than the 5 MMV analogues. Highlighted are the individual components predicted to be of importance for high activity such as: a pentane/hexane alkyl chain, 2-iminobenzimidazole core linked *via* an alcohol containing ethyl chain to a phenyl ring, so when combined generate two low nanomolar hits against *P. falciparum*. These two

analogues combine structural features from the MMV compounds which had not been combined before.

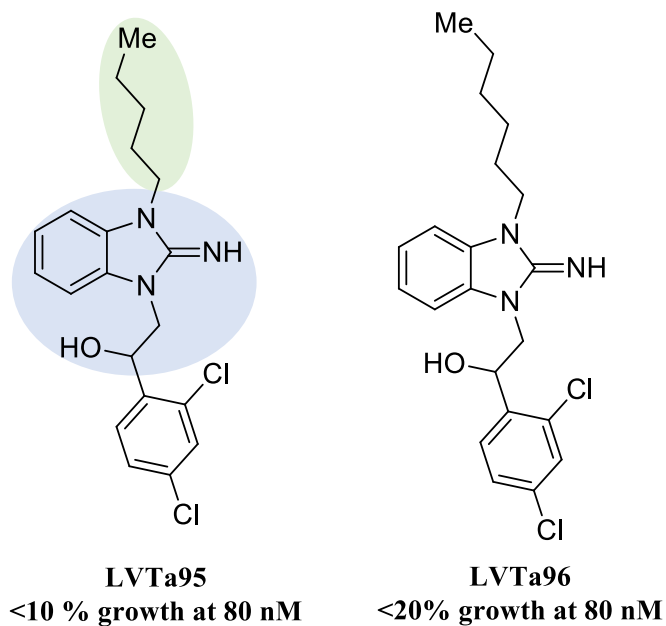


Figure 79: Hit analogues and key features

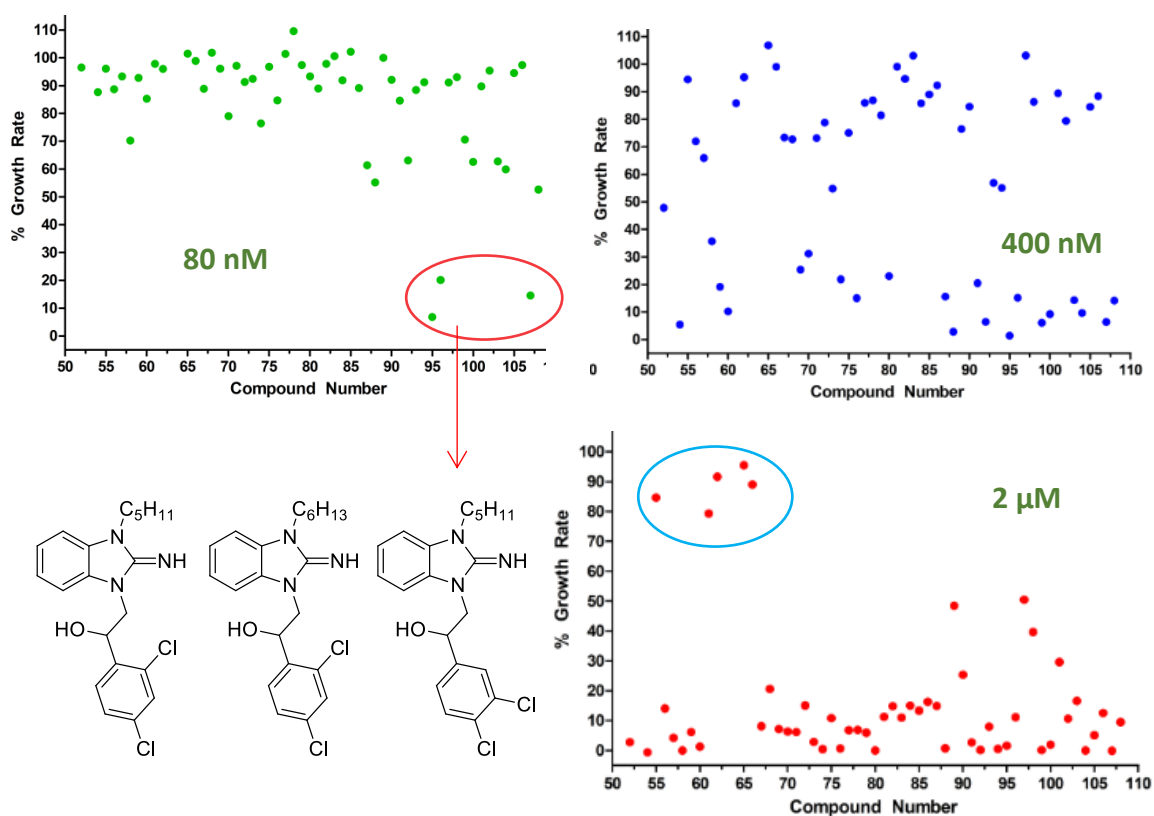


Figure 80: Representation of analogue growth rates at 3 different drug concentrations

Figure 80 displays three graphs each representing parasite growth at; 2 μ M, 400 nM and 80 nM drug concentrations. The graph at 2 μ M shows the vast majority of analogues to have growth rate of $\leq 50\%$. However, the five compounds circled in blue and shown in Figure 81 display the worst activity of this subseries. The compounds include three starting materials which were tested alongside analogues for comparative measures and both MMV compounds possessing the ether-alcohol moiety (MMV000444/445).

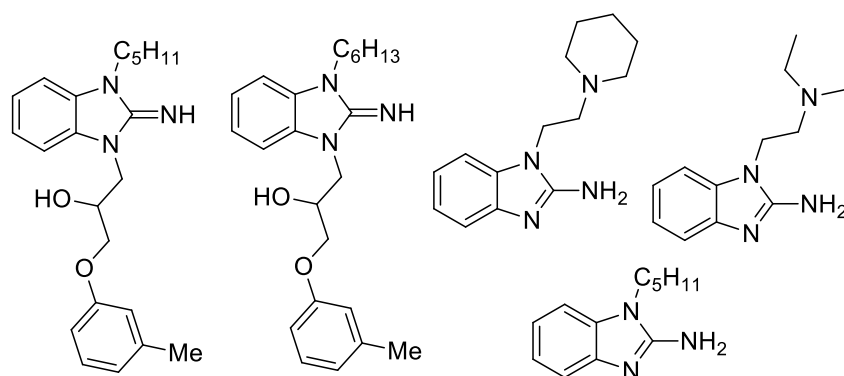


Figure 81: Poor activity compounds

At 400 nM growth rates are evenly spread within this series of benzimidazoles but, at 80 nM three analogues are highlighted as having a growth rate of $\leq 20\%$ (see Figure 82).

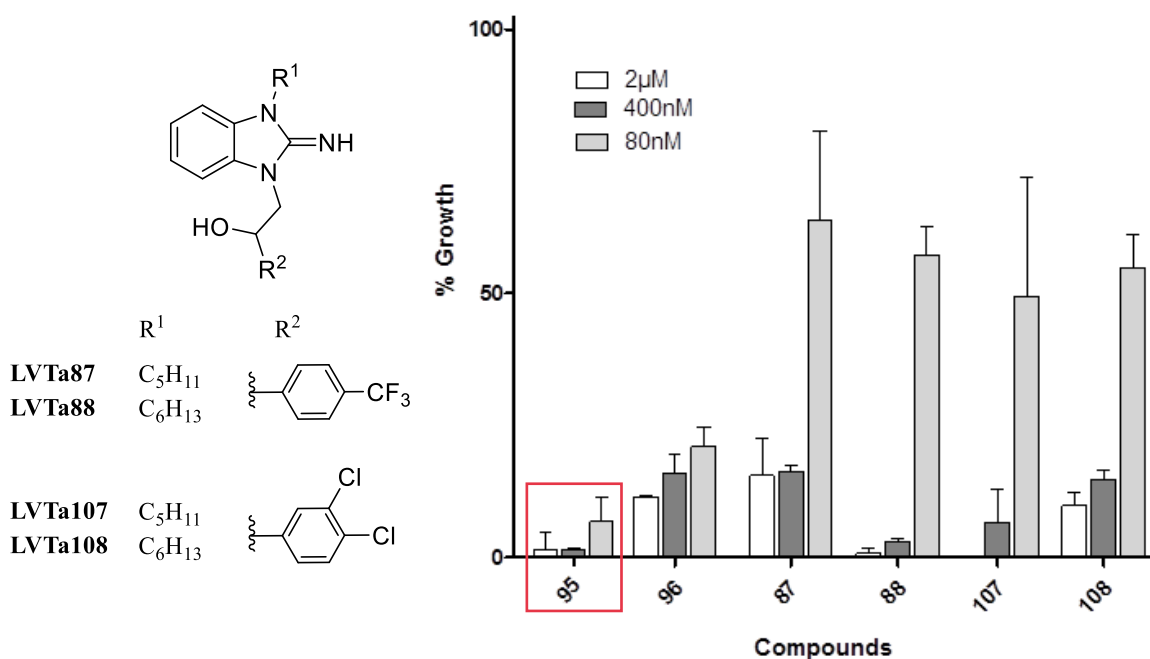


Figure 82: Screening data

Furthermore, the screening graph in Figure 82 displays the notable difference in activity between **LVTa95** and **LVTa96** with several other good activity derivatives. Also shown are compounds **LVTa87**, **LVTa88**, **LVTa107** and **LVTa108**, which are derivatives possessing some of the next lowest inhibitory concentrations from the series (% growth at 80 nM ~70%), and they retain the key features highlighted above. These analogues differ in the substitution on the phenyl substituent, with **LVTa87/88** possessing a *p*-trifluoromethyl substituent (**LVTa87** N^1 -C₅H₁₁ and **LVTa88** N^1 -C₆H₁₃) and **LVTa107/108** a 3,4-dichloro substituent (**LVTa107** N^1 -C₅H₁₁ and **LVTa108** N^1 -C₆H₁₃). Indicating a strong preference for electron withdrawing halogen substituents on the phenyl ring but, no electron donating groups have been tested in this set of analogues. The combination of a 2,4-dichlorophenyl relationship with the pentane substitution and an alcohol substituted linker provides the most potent compound of the series (**LVTa95**).

Also, the majority of analogues tested with mid-nanomolar activity possess the alcohol linker, therefore this feature is highly desirable for antimalarial activity and should be retained in future analogues. Whereas, the ketone linker produces high nanomolar/low micromolar activity compounds, suggesting a hydrogen bond acceptor is disfavoured over a hydrogen bond donor interaction.

Of the compounds displaying the highest potency, six derivatives underwent inhibitory concentration assays of which the results are displayed in Table 27. Furthermore, as **LVTa95** and **LVTa96** exist as an enantiomeric mixture separation of the enantiomers was carried out using chiral HPLC separation and the individual (+) and (–) enantiomers were tested for their biological activity. Also, both separated samples were subjected to optical rotation testing to decipher their +/– status and the results are shown in Figure 83.

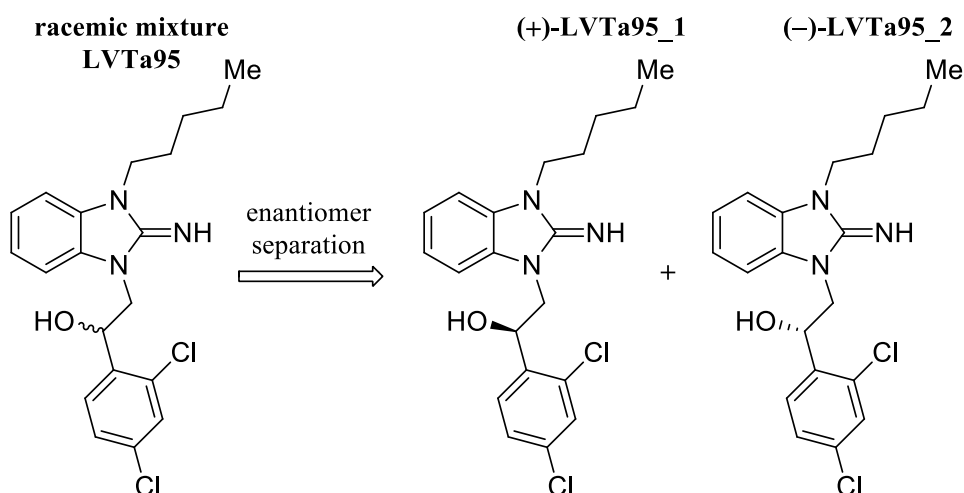


Figure 83: Analogue separation

Reference	Inhibitory concentration/nM	IC ₅₀ range/nM	e.r.
LVTa95 mix	33.40	30.06–37.11	N/A
(+)-LVTa95_1	32.13	25.56–35.13	98.5:1.5
(-)-LVTa95_2	32.44	28.13–36.86	>99.5:<0.5
LVTa96 mix	40.25	37.51–43.20	N/A
(+)-LVTa96_1	35.56	30.90–43.57	98.5:1.5
(-)-LVTa96_2	34.97	29.07–40.29	98.5:1.5
LVTa87	42.31	71.40–110.9	N/A
LVTa88	76.17	48.64–59.84	N/A
LVTa107	69.9	74.04–86.63	N/A
LVTa108	56.6	54.74–63.78	N/A

Table 27: Inhibitory concentration assay results

All six compounds display good nanomolar activity and possess features of either a pentane or hexane R¹ substitution alongside an electron withdrawing R² group. Furthermore, after enantiomeric separation surprisingly both *R* and *S* enantiomers show little difference in biological activity from the mix of both enantiomers tested. Therefore, expensive separation techniques would not be beneficial for this set of benzimidazole derivatives. Three features have been brought to light within this series of antimalarials that result in high activity i.e. a

linker possessing an alcohol moiety (conformation not significant), a hydrophobic alkyl R^1 chain and an electron withdrawing R^2 substituent, of which the position is not critical.

4:7 Asymmetric catalytic reduction

An asymmetric transfer hydrogenation reaction was carried out with Noyori's catalyst on starting ketones **LVTa93** and **LVTa94** (see Figure 84). Even though biological testing revealed no discrepancies in (*R*) or (*S*) activity, this strategy was attempted with the hope of achieving high enantiomeric excess in one enantiomer.

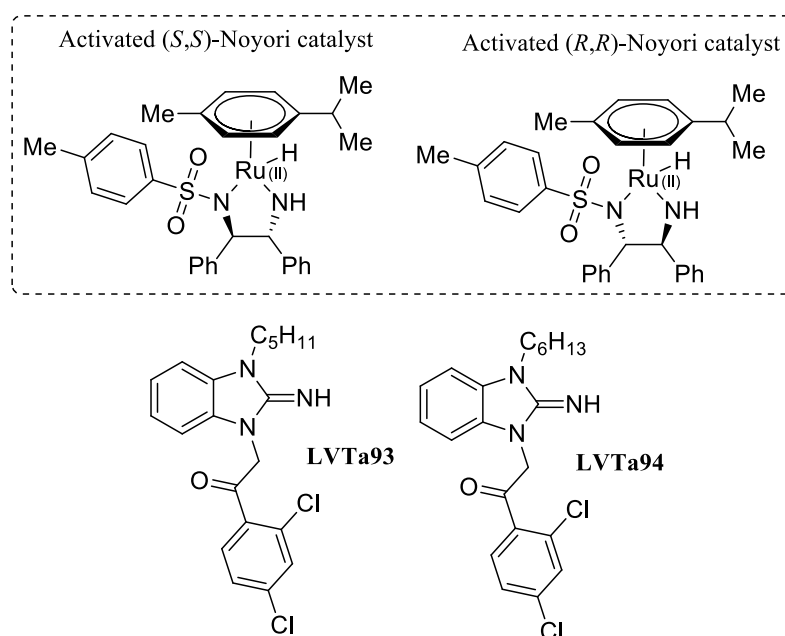
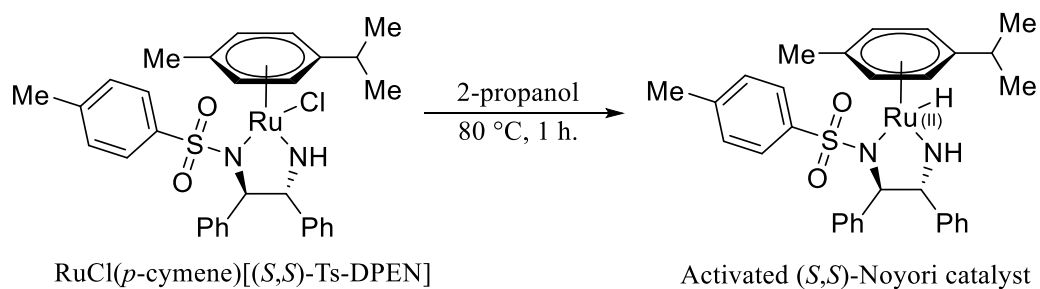


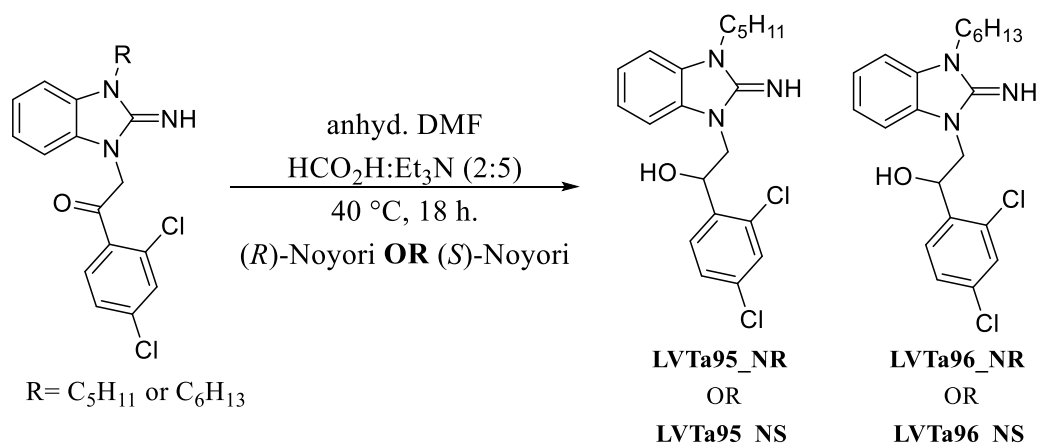
Figure 84: Activated Noyori's catalyst (above) and starting materials (below)

Firstly, the (*S,S*)- and (*R,R*)-Noyori catalysts were activated as outlined in Scheme 66. The orange solution was subsequently concentrated, and the products dissolved in dry DMF (2 mL) to create a 0.08 M solution. ⁽⁹⁸⁾



Scheme 66: Catalyst activation

The activated catalysts were then used to reduce the desired ketone, in turn, to generate four products (see Scheme 67). The products were sent for chiral HPLC analysis and retention factors compared to the data obtained from the previous HPLC separation which generated compounds: **LVTa95_1**, **LVTa95_2**, **LVTa96_1** and **LVTa96_2** previously discussed.



Scheme 67: Asymmetric reduction

The results from HPLC analysis show good enantiomeric ratios in three of the four products with an average e.r. of 90:10 however, for **LVTa96_NR** a much lower e.r. was observed (see Table 28). The reasons for this are unknown.

Reference	e.r.
LVTa96_NR	78:22
LVTa96_NS	90.5:9.5
LVTa95_NR	89.5:10.5
LVTa95_NS	90:10

Table 28: Enantiomeric ratios

4:8 Future work

It is clear the overall pharmacokinetic properties of these highly active compounds need to be addressed. For example, the calculated pharmacokinetic parameters for **LVTa95** reveal this derivative to fall in line with Lapinski's rule of 5 (RO5).⁽⁹⁹⁾ Even though it has 'RO5' compliance, due to compound **LVTa95** being in infant medicinal chemistry development the 'rule of three' (RO3) should be considered and is an approach used during fragment-based drug discovery (Table 29).⁽¹⁰⁰⁾ Unfortunately, **LVTa95** does not adhere to these tight pharmacokinetic restraints therefore, more work needs to be done to adjust them, for example: logP, HBD, HBA and rotatable bonds would all ideally need to be reduced to less than 3. Although in the case of size a molecular weight of 392.32 gmol⁻¹ is adequate and the RO3 can be stretched. In practice it is ideal to keep within these boundaries and a logP between 2–3 is aimed for.

Parameter	Value	RO5	RO3
MW/ gmol ⁻¹	392.32	< 500	< 300
Hydrogen BD	2	< 5	< 3
Hydrogen BA	4	< 10	< 3
logP	3.98	< 5	< 3
Rotatable bonds	7	< 10	< 3
Polar surface area (PSA)	53.94 Å ²	< 140 Å ²	< 140 Å ²

Table 29: LVTa95 pharmacokinetic parameter comparison

Encouragingly there is still further scope for structural optimisation for this set of benzimidazole antimalarial compounds as well as consolidating our understanding of the SAR thus deduced. Future investigations should include: chain length variation between the phenyl group and benzimidazole core; phenyl EDG substituents; vary chain length between the tertiary amine and benzimidazole core; probe non-tertiary amines; substitution of the alcohol linker and alternate the alcohol moiety on the linker for different HDBs.

As only two carbon chain lengths have been explored to connect the substituted phenyl ring to the central benzimidazole moiety a longer chain length should be investigated to observe the effects this change has on biological activity. Furthermore, **MMV000444 (LVTa65)** and **MMV000445 (LVTa66)** are the only two compounds in this set of derivatives which have a chain length of 3 carbons and 1 oxygen atom connecting the core to a phenyl ring, as well as possessing low micromolar activity. Therefore, it could be hypothesised that the reason for less potent activity is due to this chain length feature. As a result, future structures such as the compounds suggested in Figure 85 should be synthesised to explore the structure activity relationship.

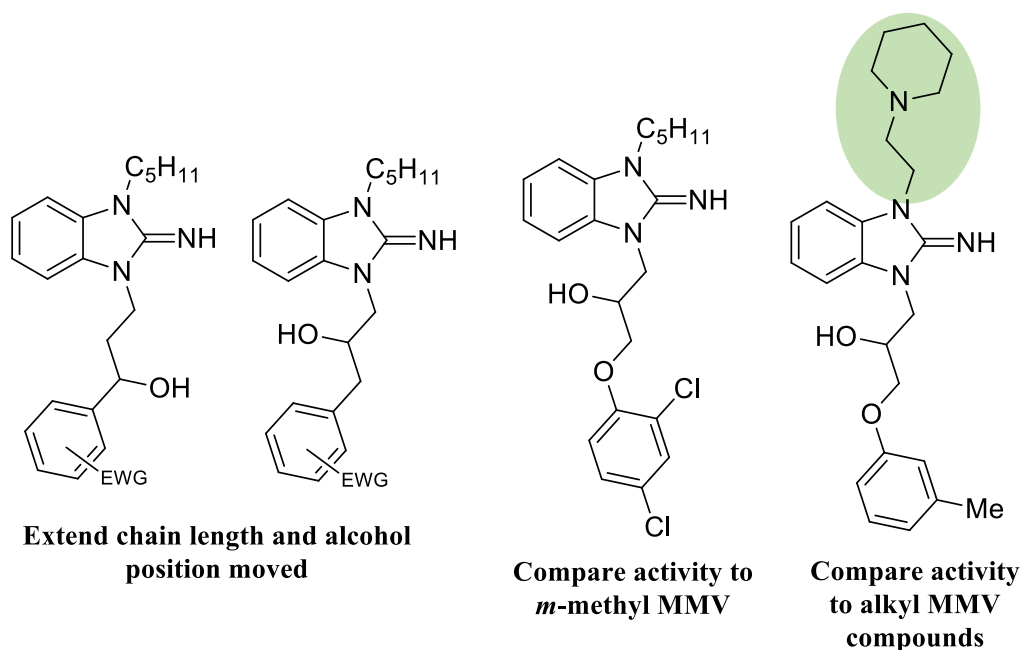


Figure 85: Potential derivatives

Also, electron donating groups should be explored as electron withdrawing groups have only been explored so far. Suggestions for future analogues include a methoxy and a dimethoxy group (see Figure 86). We speculate that these analogues would show a decrease in potency however, this prediction would need to be proven.

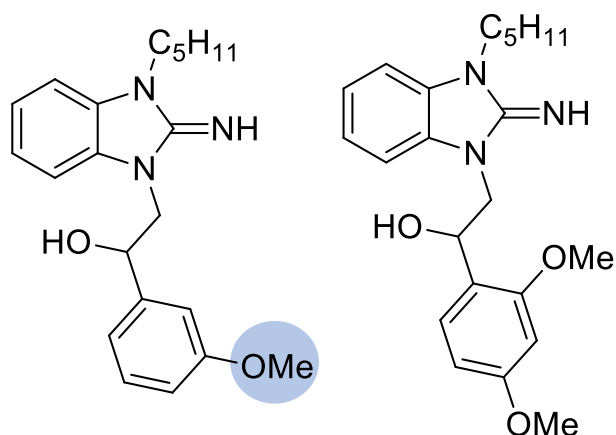


Figure 86: EWG phenyl substitution analogues

To find an alternative group to the non-drug like straight alkyl chain the MMV tertiary amine group could be explored further. Figure 87 displays a potential compound which probes this feature further by extending the previous ethyl linker to a propyl chain to see if an extension has a positive or negative impact on biological activity.

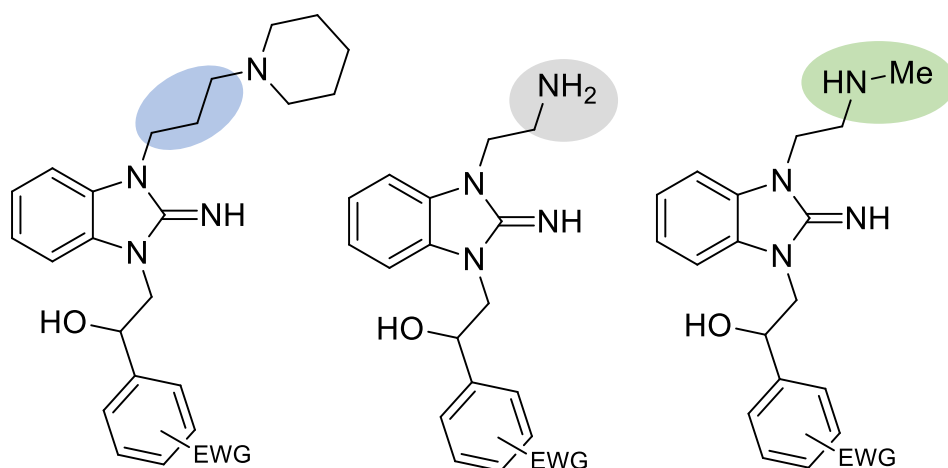


Figure 87: Future candidates

Alternatively, removing alkyl substituents from the tertiary amine would provide insight into the type of interactions taking place, for example: the generation of a secondary and primary amine moiety would provide additional hydrogen bond donor interactions, therefore what

impact would this addition have on biological activity. Also, removing this side chain altogether as seen in previous antibacterial compounds would provide evidence for the necessity of this group for antimalarial activity.

To combat the pharmacokinetic property concerns discussed earlier the greasy alkyl chain seen in **LVTa95** contributes to the high logP value (3.98) therefore reduction of this value is essential. Further support for this came to light during biological sample preparation, where both **LVTa95** and **LVTa96** were not readily soluble in DMSO and required vigorous mixing and warmth, so increasing solubility is desirable.

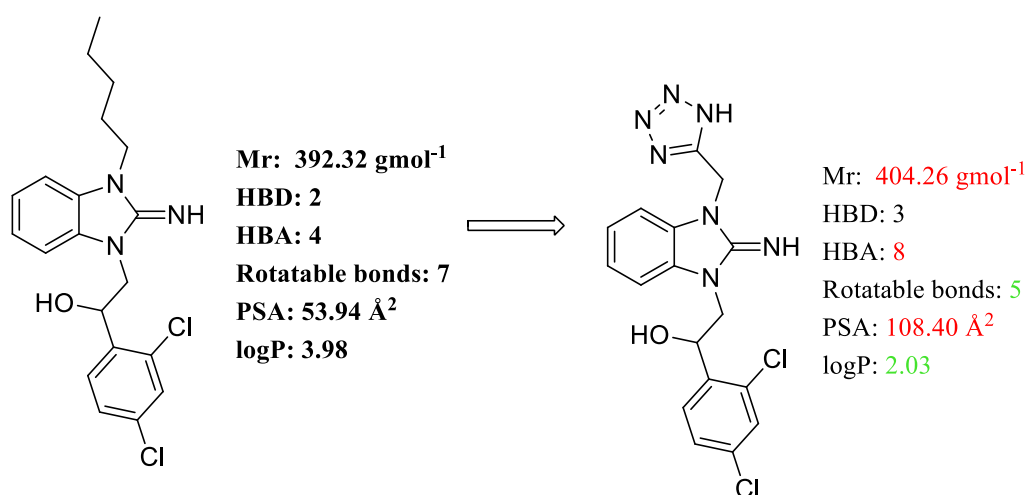


Figure 88: LVTa95 improved pharmacokinetic properties

For example, inclusion of a polar functional group such as, a tetrazole moiety which mimics an acidic group, would help reduce logP (Figure 88). This exchange would result in the removal of the greasy hydrophobic chain which is present within all 6 compound hits. However, this should be investigated not only to observe the effect of removing this feature but to also observe what happens to biological activity when a more hydrophilic group is inserted. Although the tetrazole derivative would lead to an increase in molecular weight over 400 and the number of hydrogen bond acceptors would increase for both, so this should be kept in mind.

Meanwhile, the alcohol containing linker has been highlighted as a key feature for potent biological activity and as a result should be probed further. Even though the ketone functionality already tested has proven less active overall, replacing the ketone with an alternative functional group will prove if the ketone functionality itself is disfavoured or is it the hydrogen bond acceptor capabilities present which impact on activity. Figure 89 displays potential derivatives which could be generated to explore this linker further for example: a methyl ether offers a small hydrophobic interaction, an extended alcohol group explores the effects of extending the chain length on activity and finally, replacing the alcohol altogether with an alternative hydrogen bond donor moiety such as, a primary amine.

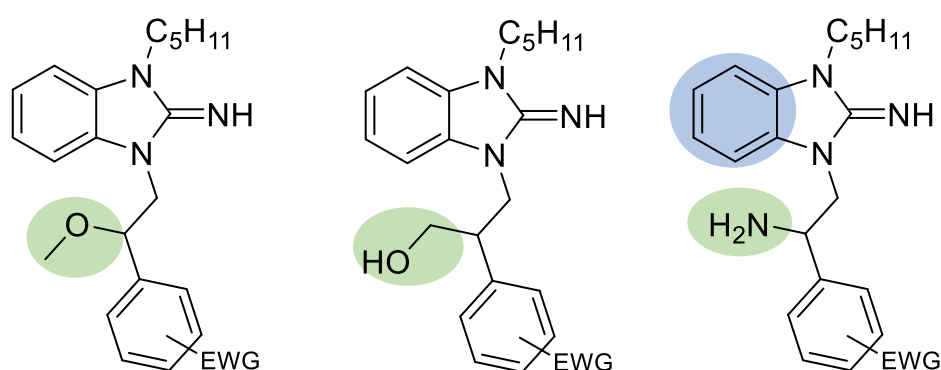


Figure 89: Alternative compounds

Investigation into further substitution on the 2-iminobenzimidazole core has not been undertaken therefore, future compounds could also explore both EWG and EDG substituted on the central ring (highlighted in blue in Figure 89).

When a *m*-chloro substitution replaces the 2,4-dichloro substitution a big reduction in molecular weight is seen and logP is reduced to as low as 1.63 with a tetrazole coupling (Figure 90).

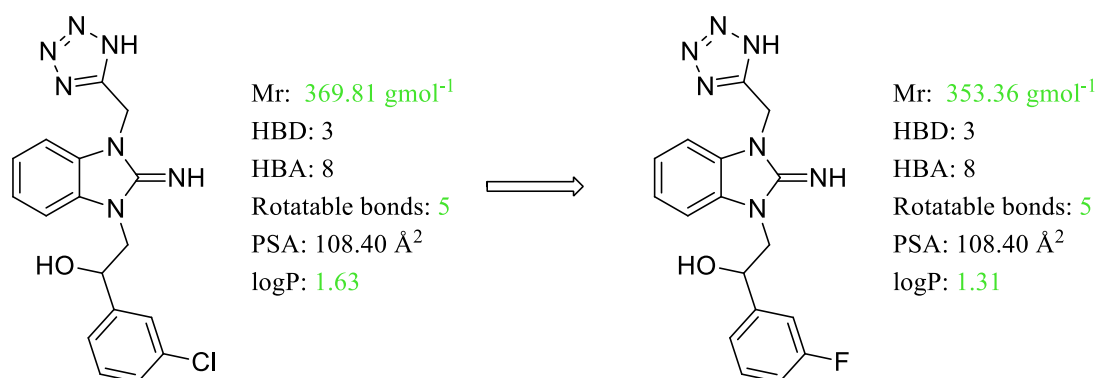
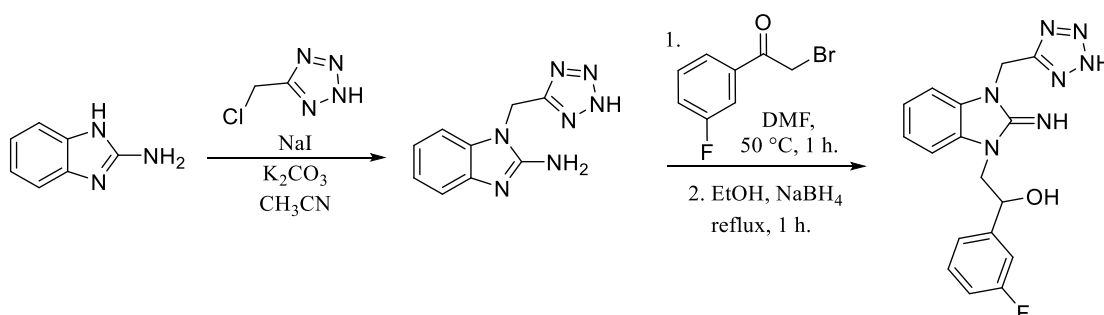


Figure 90: Further pharmacokinetic improvements

Meanwhile, replacing the chlorine substitution with a fluorine moiety reduces logP even further (1.31) and, offers a hydrogen bond donor interaction on the phenyl ring which is yet to be tested (Figure 90). Overall, the electron withdrawing feature is being retained so should not impact activity too greatly, but an exchange in the electronegativity properties are being made.

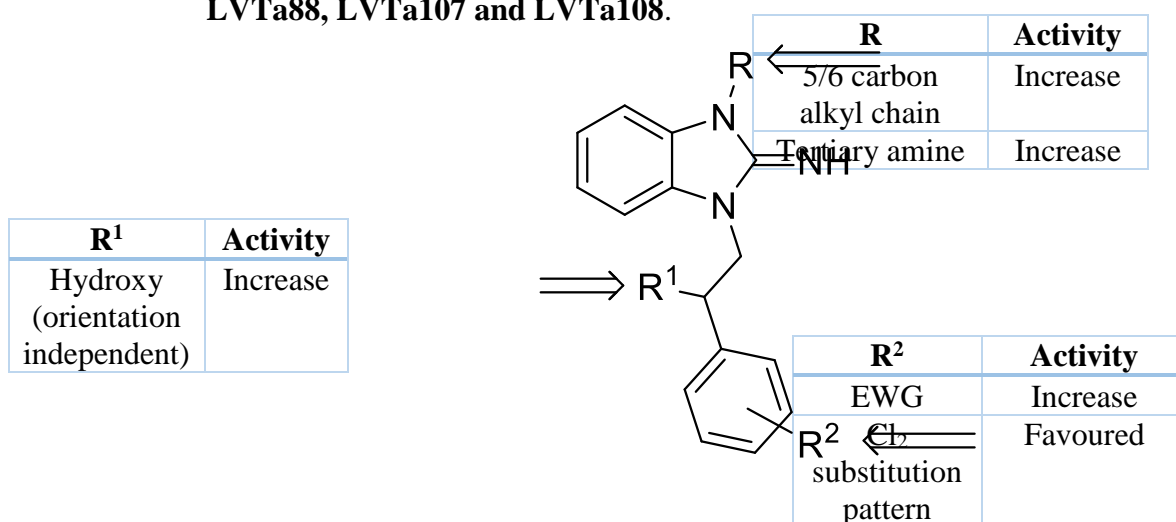
To access the tetrazole substitution the synthetic route outlined in Scheme 68 could be employed to generate these potential future analogues in two/step reactions.



Scheme 68: Proposed synthetic strategy

4:9 Summary

This sub-series of potential antimalarials has been the most fruitful during this project and provides the biggest potential for future optimisation. Exploration of analogue SAR has brought to light a lead group of six antimalarial candidates: **LVTa95**, **LVTa96**, **LVTa87**, **LVTa88**, **LVTa107** and **LVTa108**.



In addition, enantiomeric separation has shown conformation of the alcohol moiety to be none significant as differences in biological activity were negligible. Therefore, this small set of derivatives can be taken into the next stage of structural optimisation to potentially increase potency, whilst keeping within the pharmacokinetic parameters required. Overall two antimalarial compounds with an inhibitory concentration of 33.4 nM (**LVTa95**) and 40.3 nM (**LVTa96**) have been discovered and possess further potential for optimisation (see Figure 91).

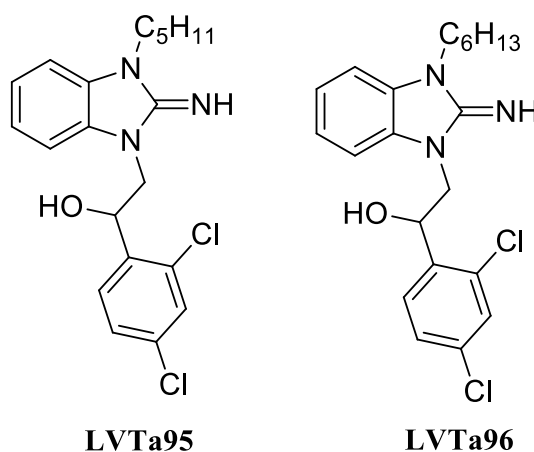


Figure 91: Potent antimalarial leads

Chapter 5: Conclusion

During this research project, approximately 150 novel compounds have been synthesised and tested for their biological activity against *Plasmodium falciparum*. Of the three-subseries generated: tetrahydro- β -carboline, spiroindoline and 2-iminobenzimidazole, two potent compounds have been discovered. Compounds **LVTa95** and **LVTa96** possess low nanomolar activity and on separation of their enantiomers, it has highlighted a non-significance of conformation for antimalarial activity (see Figure 92). The alcohol component seen in both derivatives is predicted to be a significant interaction for antimalarial activity.

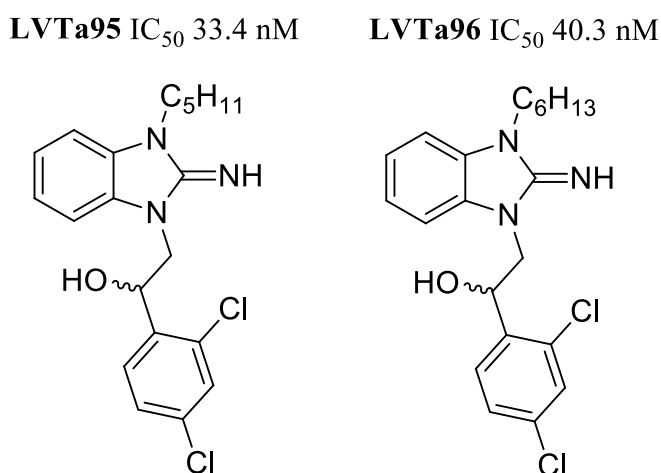


Figure 92: Hit benzimidazole derivatives

Further suggestions have been outlined to improve the hit analogue pharmacokinetic properties, in order to progress this potentially lucrative subseries. The area of primary optimisation should focus of reducing the lipophilicity of the pentane and hexane chains and in turn, reducing the derivative logP. Overall, there is still scope for optimisation in both the benzimidazole and spiroindoline series, but this project has provided a healthy bank of analogues over the three different classes possessing a range of functionalities. Each

subseries has provided an insight into the type of structure activity relationship taking place, which has been key when proposing new derivatives.

Chapter 6: Experimental

6:1 General Details

All reactions were performed under an atmosphere of air and with standard room pressure fitted with glass stopped, unless stated otherwise. Solvents for reactions were; dichloromethane (VWR, stabilised GPR Rectapur), acetonitrile (Fisher Scientific, HPLC reagent grade) and anhydrous DMF (Alpha Aesar, anhydrous amine free). Solvents used for chromatography were; methanol (VWR, GPR Rectapur), diethyl ether (Fisher, analytical reagent grade) and dichloromethane (VWR, stabilised GPR Rectapur). Column chromatography was performed using VWR 40-63 μM silica gel.

300 MHz for ^1H NMR and 75 MHz for ^{13}C NMR spectra were recorded on a Bruker Avance 300 spectrometer. 376 MHz spectra for ^{19}F NMR was recorded on a Bruker Ascend spectrometer. Spectra were referenced to residual chloroform (7.26 ppm, ^1H ; 77.00 ppm, ^{13}C) unless stated otherwise. Chemical shifts are reported in ppm, multiplicities are indicated by s (singlet), d (doublet), t (triplet), q (quartet), m (multiplet) and br (broad). Coupling constants, J , are reported in Hertz. Mass spectroscopy was performed on an Agilent Technology 6530 Accurate-Mass Q-TOF LC/MS machine. Data are reported in the form of (m/z). Infrared spectra (IR) were recorded for neat samples on a Thermo Scientific Nicolet iS10 Diamond FT-IR spectrophotometer in the range of 500–4000 cm^{-1} . Peaks are reported in cm^{-1} with indicated relative intensities: s (strong, 67–100%); m (medium, 34–66%); w (weak, 0–33%). Elemental analyses were performed by York University. Melting points (mp) were determined on Stuart SMP10 capillary melting point apparatus in sealed tubes and are corrected. Analytical thin-layer chromatography was performed on silica gel plates with aluminium backed, precoated UV_{245nm} neutral silica plates. Visualization was accomplished with UV (254 nm) and potassium permanganate (KMnO_4) staining solutions.

Three specific rotation values were obtained on a Rudolph Research Analytical Autopol I automatic polarimeter for optically active compounds and an average value was taken.

Microwave experiments were carried out in a Biotage Initiator 4.1.2. microwave. For the purpose of spectral assignment, compounds are numerically labelled not correlating to IUPAC naming conventions. The *cis* and *trans* diastereoisomers were assigned by ^{13}C NMR spectra, of which, the method can be found in published literature.

Literature compounds and appendices can be found in the expanded experimental section.

Biological data

All biological assays were conducted by colleagues within the biology department at Keele University. 48-hour growth inhibition assays were conducted on the novel compounds to determine their inhibitory concentration (IC_{50}) values. These assays utilized trophozoite stage Dd2Luc *Plasmodium falciparum* parasites. MSF assays were carried out on the candidate compounds that were diluted in a two-fold dilution series using a 60 μM starting concentration. The data was normalized and plotted as a log-dose response curve to generate IC_{50} values. For all derivatives three independent biological replicates were carried out on assay plates bearing three technical repeats. IC_{50} graphs and screening graphs can be found in the expanded experimental section.

General Procedures

Preparation of tetrahydro- β -carboline diastereoisomers:

Method A: The tryptophan derivative (1 eq.) and 3 Å molecular sieves were placed in a round bottom flask under a nitrogen atmosphere and dry CH_2Cl_2 (10 mL) was added. The chosen aldehyde (1.25 eq.) was dissolved separately in dry CH_2Cl_2 (5 mL) under a nitrogen atmosphere and then added *via* syringe to the main reaction mixture, however if liquid, it was added into the mixture directly *via* syringe. The solution was left to stir overnight and

TFA (2 eq.) was subsequently added and the mixture left for a further 4 h to stir at room temperature. The mixture was quenched with saturated aqueous NaHCO_3 (10 mL), the organics extracted with CH_2Cl_2 (2×75 mL), washed with saturated aqueous brine (100 mL), dried over MgSO_4 , filtered and concentrated under reduced pressure.

Method B: The tryptophan derivative (250 mg, 1 eq.) and aldehyde (1.25 eq.) were placed into a microwave vessel (2–5 mL), along with $\text{Yb}(\text{OTf})_3$ (0.03 mmol), CH_2Cl_2 (4 mL) and a micro magnetic stirrer. The vessel was capped and stirred under microwave irradiation in a Biotage Initiator 4.1.2. microwave at 100 °C for 0.5 h, after a 30 second pre-stir.

Preparation of spiroindoline derivatives:

Method C: The chosen spiro[indoline-3,4'-piperidine]-1'-carboxylate starting material (1 eq.) was dissolved in CH_3CN (25 mL) and then potassium carbonate (2 eq.) was added into the stirred solution. The chosen halogen substituted electrophile (2 eq.) was added *via* syringe or *via* temporary removal of the condenser and the reaction then heated at reflux for 18 h. After allowing to cool, CH_3CN was removed under reduced pressure and the resulting mixture was dissolved in CH_2Cl_2 (20 mL). The solution was transferred to a separating funnel and H_2O (20 mL) was added. The organics were extracted with further CH_2Cl_2 (2×25 mL), then collated and washed with saturated aqueous brine (25 mL), dried over MgSO_4 , filtered and concentrated under reduced pressure.

Preparation of 2-iminobenzimidazole derivatives:

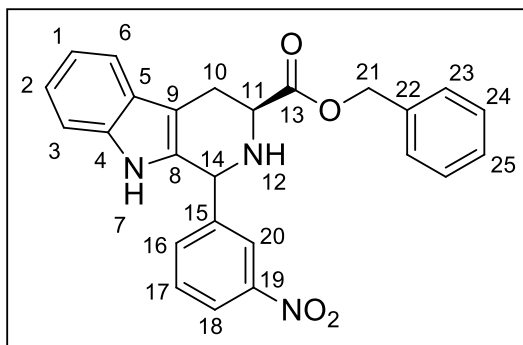
Method D: The chosen substituted 2-iminobenzimidazole (1 eq.) as well as, the chosen substituted bromoacetophenone (1 eq.) were weighed into a round bottom flask (25 mL) and the flask put under a nitrogen atmosphere. DMF (10 mL) was then added *via* syringe and the resulting solution stirred at 60 °C for 1 hour. After 1 hour the solution had turned red and the solvent was removed under reduced pressure. A colourless solid can be seen to form on

reduction of the solvent volume. Acetone (20 mL) was added into the flask and the residual colourless solid remained collected *via* Büchner filtration and washed with further acetone (10 mL).

Method E: The ketone obtained from method D (1 eq.) was dissolved in ethanol (10 mL) and the flask fitted with a reflux condenser. NaBH₄ (1.5 eq.) was then added through temporary removal of the condenser and the mixture was stirred at reflux for 1 hour. The solvent was later removed under reduced pressure and the resulting product partitioned between EtOAc (20 mL) and H₂O (20 mL). The organics were further extracted with EtOAc (2 × 25 mL), washed with saturated aqueous brine (50 mL), dried over MgSO₄, filtered and the solvent removed under reduced pressure.

6:2 Specific details and characterisation

Preparation of Benzyl 1-(3-nitrophenyl)-2,3,4,9-tetrahydro-1*H*-pyrido-[3,4-*b*]indol-3-carboxylate (**LVT10-1,2**):



Following method A using (*S*)-Benzyl 2-amino-3-(1*H*-indol-3yl)propanoate (**LVT14**) (100 mg, 0.34 mmol, 1 eq.) and 3-nitrobenzaldehyde (61.9 mg, 0.41 mmol, 1.25 eq.) as starting materials. The desired product was purified using column chromatography (SiO₂, 19:1 CH₂Cl₂:Et₂O), to afford, eluting first, the *trans* diastereoisomer as an orange waxy solid (36.0 mg, 0.084 mmol, 25%) and, eluting second, the *cis* diastereoisomer an orange solid (42.0 mg, 0.098 mmol, 29%).

Following method B using (*S*)-Benzyl 2-amino-3-(1*H*-indol-3yl)propanoate (**LVT14**) (500 mg, 1.70 mmol, 1 eq.) and 3-nitrobenzaldehyde (321 mg, 2.13 mmol, 1.25 eq.) as starting materials. The desired product was purified using column chromatography (SiO₂, 19:1 CH₂Cl₂:Et₂O), to afford, eluting first, the *trans* diastereoisomer as an orange waxy solid (261 mg, 0.61 mmol, 36%) and, eluting second, the *cis* diastereoisomer an orange solid (292 mg, 0.68 mmol, 40%).

Trans (1*R*, 3*S*) diastereoisomer (**LVT10-1**)

¹H NMR (300 MHz, CDCl₃) δ 3.22 (1H, ddd, *J* 15.4, 5.6, 1.4 Hz, CH₂(10_a)), 3.32 (1H, ddd, *J* 15.4, 5.6, 1.4 Hz, CH₂(10_b)), 4.01 (1H, dd, *J* 5.6, 5.6 Hz, CH(11)), 5.12 (1H, dd, *J* 12.3 Hz, CH₂(21_a)), 5.18 (1H, d, *J* 12.3 Hz, CH₂(21_b)), 5.52 (1H, s, CH(14)), 7.12–7.22 (3H, m,

ArCH(1,2,3)), 7.24–7.30 (5H, m, ArCH(23,24,25)), 7.49 (1H, dd, J 8.1, 7.9 Hz, ArCH(17)), 7.57 (1H, d, J 6.6 Hz, ArCH), 7.63 (1H, d, J 7.9 Hz, ArCH(16)), 8.51 (1H, d, J 8.1 Hz, ArCH(18)), 8.20 (1H, s, ArCH(20))

^{13}C NMR (75 MHz, CDCl_3) δ 24.53 ($\text{CH}_2(10)$), 53.12 ($\text{CH}(14)$), 54.22 ($\text{CH}(11)$), 66.83 ($\text{CH}_2(21)$), 108.82 (ArC), 111.02 (ArCH), 118.53 (ArCH(17)), 119.87 (ArCH), 122.47 (ArCH), 123.22 (ArCH(20)), 123.38 (ArCH(18)), 126.87 (ArC), 128.03 (ArCH(25)), 128.39 (ArCH(24)), 128.61 (ArCH(23)), 129.71 (ArCH), 131.85 (ArC), 134.57 (ArCH(16)), 135.51 (ArC), 136.28 (ArC), 144.44 (ArC), 148.50 (ArC), 173.44 ($\text{C}=\text{O}(13)$)

R_f 0.15 (9:1, CH_2Cl_2 :MeOH)

$[\alpha]_D^{25}$ -2.0 (c 1.0, MeOH)

IR ν/cm^{-1} 1174 (C-O, s), 1346 (NO_2 , s), 1525 (NO_2 , s), 1727 ($\text{C}=\text{O}$, s), 2116 (Ar C-H, w), 3396 (N-H, m)

MS (ESI): 428 $[\text{M}+\text{H}^+]$

HRMS $\text{C}_{25}\text{H}_{22}\text{N}_3\text{O}_4$ $[\text{M}+\text{H}^+]$ requires 428.1605, found 428.1602 (0.7 ppm error)

Cis (1*S*, 3*S*) diastereoisomer (LVT10-2)

mp 177–179 °C

^1H NMR (300 MHz, CDCl_3) δ 3.02 (1H, ddd, J 15.1, 11.2, 2.5 Hz, $\text{CH}_2(10_a)$), 3.27 (1H, ddd, J 15.1, 4.1, 2.5 Hz, $\text{CH}_2(10_b)$), 4.01 (1H, dd, J 11.2, 4.1 Hz, $\text{CH}(11)$), 5.23 (1H, d, J 12.2 Hz, $\text{CH}_2(21_a)$), 5.29 (1H, d, J 12.2 Hz, $\text{CH}_2(21_b)$), 5.33 (1H, s, $\text{CH}(14)$), 7.12–7.24 (3H, m, ArCH(1,2)), 7.35–7.45 (5H, m, ArCH(23,24,25)), 7.54 (1H, dd, J 8.1, 7.6 Hz, ArCH(17)), 7.57 (1H, d, J 7.6 Hz, ArCH), 7.76 (1H, d, J 7.6 Hz, ArCH(16)), 8.23 (1H, d, J 7.6 Hz, ArCH(18)), 8.29 (1H, s, ArCH(20))

^{13}C NMR (75 MHz, CDCl_3) δ 25.47 ($\text{CH}_2(10)$), 56.70 (s, $\text{CH}(14)$), 58.09 ($\text{CH}(11)$), 67.14 ($\text{CH}_2(21)$), 109.57 (ArC), 111.05 (ArCH), 118.49 (ArCH(17)), 119.93 (ArCH), 122.41 (ArCH), 123.63 (ArCH(20)), 123.70 (ArCH(18)), 126.89 (ArC), 128.46 (ArCH(25)), 128.51 (ArCH(24)), 128.73 (ArCH(23)), 130.02 (ArCH), 133.09 (ArC), 134.96 (ArCH(16)), 135.03 (ArC), 136.35 (ArC), 143.24 (ArC), 148.46 (ArC), 172.36 ($\text{C}=\text{O}(13)$)

R_f 0.35 (9:1, CH_2Cl_2 :MeOH)

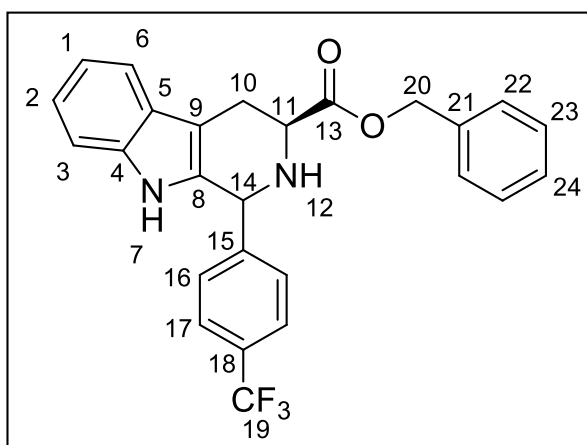
$[\alpha]_D^{25} +2.0$ (c 1.0, MeOH)

IR ν/cm^{-1} 1138 (C-O, s), 1346 (NO_2 , s), 1515 (NO_2 , s), 1715 ($\text{C}=\text{O}$, s), 2325 (Ar C-H, w), 3402 (N-H, m)

MS (ESI): 428 $[\text{M}+\text{H}^+]$

HRMS $\text{C}_{25}\text{H}_{22}\text{O}_4\text{N}_3$ $[\text{M}+\text{H}^+]$ requires 428.1605, found 428.1599 (1.4 ppm error)

Preparation of Benzyl 1-(4-(trifluoromethyl)phenyl)-2,3,4,9-tetrahydro-1*H*-pyrido-[3,4-*b*]indol-3-carboxylate (**LVT15-1,2**):



Following method A using (*S*)-Benzyl 2-amino-3-(1*H*-indol-3-yl)propanoate (**LVT14**) (100 mg, 0.34 mmol, 1 eq.) and 4-(trifluoromethyl) benzaldehyde (0.06 mL, 76.5 mg, 0.41 mmol,

1.25 eq.) as starting materials. The desired product was purified using column chromatography (SiO₂, 19:1, CH₂Cl₂:Et₂O), to afford, eluting first, the *trans* diastereoisomer as a colourless solid (44 mg, 0.10 mmol, 29%) and, eluting second, the *cis* diastereoisomer as a colourless solid (49 mg, 0.11 mmol, 32%).

Following method B using (*S*)-Benzyl 2-amino-3-(1*H*-indol-3-yl)propanoate (**LVT14**) (500 mg, 1.70 mmol, 1 eq.) and 4-(trifluoromethyl) benzaldehyde (0.29 mL, 370 mg, 2.13 mmol, 1.25 eq.) as starting materials. The desired product was purified using column chromatography (SiO₂, 19:1 CH₂Cl₂:Et₂O), to afford, eluting first, the *trans* diastereoisomer as a colourless solid (279 mg, 0.62 mmol, 36%) and, eluting second, the *cis* diastereoisomer as a colourless solid (309 mg, 0.69 mmol, 41%).

Trans (1*R*, 3*S*) diastereoisomer (**LVT15-1**)

mp 78–81 °C

¹H NMR (300 MHz, CDCl₃) δ 3.21 (1H, dd, *J* 15.5, 5.4 Hz, CH₂(10_a)), 3.30 (1H, dd, *J* 15.5, 6.1 Hz, CH₂(10_b)), 4.00 (1H, dd, *J* 6.1, 5.4 Hz, CH(11)), 5.12 (1H, d, *J* 12.4 Hz, CH₂(20_a)), 5.18 (1H, d, *J* 12.4 Hz, CH₂(20_b)), 5.47 (1H, s, CH(14)), 7.11–7.21 (3H, m, ArCH(1,2)), 7.23–7.32 (5H, m, ArCH(22,23,24)), 7.40 (1H, d, *J* 8.0 Hz, ArCH), 7.53 (2H, d, *J* 8.0 Hz, ArCH(16)), 7.58 (2H, d, *J* 8.0 Hz, ArCH(17))

¹³C NMR (75 MHz, CDCl₃) δ 24.61 (s, CH₂(10)), 52.94 (s, CH(14)), 54.45 (s, CH(11)), 66.80 (s, CH₂(20)), 110.98 (s, ArC), 111.0 (s, ArCH), 118.43 (s, ArCH), 119.77 (s, ArCH), 122.30 (s, ArCH), 125.73 (q, ³*J*_{C-F} 3.6 Hz, ArCH(17)), 126.80 (s, ArC), 128.07 (s, ArCH(24)), 128.37 (q, ¹*J*_{C-F} 272 Hz, CF₃(19)), 128.43 (q, ²*J*_{C-F} 32 Hz, ArC(18)), 128.51 (s, ArCH(16)), 128.61 (s, ArCH(23)), 128.83 (s, ArCH(22)), 131.59 (s, ArC), 134.36 (s, ArC), 135.53 (s, ArC), 137.89 (s, ArC), and 173.15 (s, C=O(13))

¹⁹F NMR (376 MHz, CDCl₃) δ –62.5 (s, Ar-CF₃(19))

R_f 0.20 (9:1, CH₂Cl₂:MeOH)

$[\alpha]_{\text{D}}^{25}$ −4.0 (*c* 1.0, MeOH)

IR ν/cm^{-1} 1164 (C-O, s), 1728 (C=O, s), 3062 (Ar C-H, w), 3391 (N-H, m)

MS (ESI): 451 [M+H⁺]

HRMS C₂₆H₂₂F₃N₂O₂ [M+H⁺] requires 451.1628, found 451.1619 (2.0 ppm error)

Cis (1*S*, 3*S*) diastereoisomer (LVT15-2)

mp 168–171 °C

¹H NMR (300 MHz, CDCl₃) δ 3.00 (1H, dd, *J* 15.1, 11.1 Hz, CH₂(10_a)), 3.23 (1H, dd, *J* 15.1, 4.1 Hz, CH₂(10_b)), 3.99 (1H, dd, *J* 11.1, 4.1 Hz, CH(11)), 5.22 (1H, d, *J* 12.2 Hz, CH₂(20_a)), 5.27 (1H, d, *J* 12.2 Hz, CH₂(20_b)), 5.28 (1H, s, CH(14)), 7.11–7.24 (3H, m, ArCH(1,2)), 7.32–7.41 (5H, m, ArCH(22,23,24)), 7.50 (2H, d, *J* 8.2 Hz, ArCH(16)), 7.54 (1H, d, *J* 6.6 Hz, ArCH), 7.61 (2H, d, *J* 8.2 Hz, ArCH(17))

¹³C NMR (75 MHz, CDCl₃) δ 25.57 (s, CH₂(10)), 56.80 (s, CH(14)), 58.29 (s, CH(11)), 67.09 (s, CH₂(20)), 109.23 (s, ArC), 111.01 (s, ArCH), 118.40 (s, ArCH), 119.84 (s, ArCH), 122.26 (s, ArCH), 125.88 (q, ³*J*_{C-F} 3.7 Hz, ArCH(17)), 126.95 (s, ArC), 128.46 (s, ArCH(24)), 128.53 (ArCH(16)), 128.72 (s, ArCH(23)), 129.10 (s, ArCH(22)), 130.51 (q, ¹*J*_{C-F} 267 Hz, CF₃(19)), 131.05 (q, ²*J*_{C-F} 32 Hz, ArC(18)), 133.69 (s, ArC), 135.45 (s, ArC), 136.24 (s, ArC), 172.49 (s, C=O(13))

¹⁹F NMR (376 MHz, CDCl₃) δ −62.5 (s, Ar-CF₃(19))

R_f 0.43 (9:1, CH₂Cl₂:MeOH)

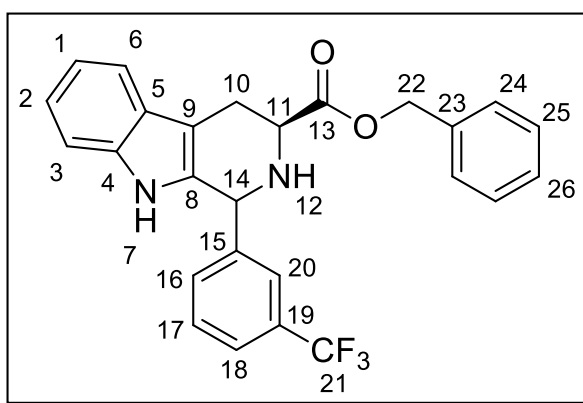
$[\alpha]_{\text{D}}^{25}$ +4.0 (*c* 1.0, MeOH)

IR ν/cm^{-1} 1164 (C-O, s), 1731 (C=O, s), 3062 (Ar C-H, w), 3392 (N-H, m)

MS (ESI): 451 [M+H⁺]

HRMS C₂₆H₂₂F₃N₂O₂ [M+H⁺] requires 451.1628, found 451.1618 (2.2 ppm error)

Preparation of Benzyl 1-(3-(trifluoromethyl)phenyl)-2,3,4,9-tetrahydro-1*H*-pyrido-[3,4-*b*]indol-3-carboxylate (**LVT16-1,2**):



Following method A using (*S*)-Benzyl 2-amino-3-(1*H*-indol-3yl)propanoate (**LVT14**) (100 mg, 0.34 mmol, 1 eq.) and 3-(trifluoromethyl) benzaldehyde (0.05 mL, 65.1 mg, 0.41 mmol, 1.25 eq.) as starting materials. The desired product was purified using column chromatography (SiO₂, 19:1, CH₂Cl₂:Et₂O), to afford, eluting first, the *trans* diastereoisomer as a colourless solid (39 mg, 0.09 mmol, 26%) and, eluting second, the *cis* diastereoisomer as a colourless solid (35 mg, 0.08 mmol, 23%).

Following method B using (*S*)-Benzyl 2-amino-3-(1*H*-indol-3yl)propanoate (**LVT14**) (500 mg, 1.70 mmol, 1 eq.) and 3-(trifluoromethyl) benzaldehyde (0.28 mL, 364 mg, 2.13 mmol, 1.25 eq.) as starting materials. The desired product was purified using column chromatography (SiO₂, 19:1 CH₂Cl₂:Et₂O), to afford, eluting first, the *trans* diastereoisomer as a colourless solid (267 mg, 0.59 mmol, 35%) and, eluting second, the *cis* diastereoisomer as a colourless solid (281 mg, 0.62 mmol, 36%).

Trans (1R, 3S) diastereoisomer (LVT16-1)

mp 171–173 °C

¹H NMR (300 MHz, CDCl₃) δ 3.23 (1H, dd, *J* 15.6, 5.6 Hz, CH₂(10_a)), 3.31 (1H, dd, *J* 15.6, 5.6 Hz, CH₂(10_b)), 4.03 (1H, dd, *J* 5.6, 5.6 Hz, CH(11)), 5.14 (1H, d, *J* 9.3 Hz, CH₂(22_a)), 5.19 (1H, d, *J* 9.3 Hz, CH₂(22_b)), 5.48 (1H, s, CH(14)), 7.11–7.21 (3H, m, ArCH(1,2)), 7.25–7.31 (6H, m, ArCH(16,24,25,26)), 7.44–7.47 (2H, m, ArCH(17)), 7.56–7.60 (2H, m, ArCH(18,20))

¹³C NMR (75 MHz, CDCl₃) δ 24.49 (s, CH₂(10)), 53.14 (s, CH(14)), 54.51 (s, CH(11)), 66.78 (s, CH₂(22)), 110.99 (s, ArC), 110.95 (s, ArCH), 118.45 (s, ArCH), 119.73 (s, ArCH), 122.26 (s, ArCH), 124.00 (q, ¹*J*_{C-F} 272 Hz, CF₃(21)), 125.14 (2C, dq, ³*J*_{C-F} 3.8 Hz, ArCH(18,20)), 127.10 (s, ArC), 128.05 (s, ArCH(26)), 128.53 (s, ArCH(25)), 128.61 (s, ArCH(24)), 129.26 (s, ArCH), 131.17 (q, ²*J*_{C-F} 32 Hz, ArC(19)), 131.83 (s, ArC), 132.43 (s, ArC), 135.63 (s, ArC), 136.28 (s, ArC), 143.20 (s, ArC), 173.50 (s, C=O(13))

¹⁹F NMR (376 MHz, CDCl₃) δ –62.4 (s, Ar-CF₃(21))

R_f 0.25 (9:1, CH₂Cl₂:MeOH)

[α]_D²⁵ +4.0 (*c* 1.0, MeOH)

IR ν/ cm⁻¹ 1166 (C-O, s), 1721 (C=O, s), 3033 (Ar C-H, w), 3354 (N-H, m)

MS (ESI): 451 [M+H⁺]

HRMS C₂₆H₂₂F₃N₂O₂ [M+H⁺] requires 451.1628, found 451.1624 (0.9 ppm error)

Cis (1S, 3S) diastereoisomer (LVT16-2)

mp 77–79 °C

^1H NMR (300 MHz, CDCl_3) δ 3.04 (1H, ddd, J 15.2, 11.1, 2.3 Hz, $\text{CH}_2(10_a)$), 3.27 (1H, ddd, J 15.2, 4.3, 2.3 Hz, $\text{CH}_2(10_b)$), 4.01 (1H, dd, J 11.1, 4.3 Hz, $\text{CH}(11)$), 5.24 (1H, d, J 8.5 Hz, $\text{CH}_2(22_a)$), 5.29 (1H, d, J 8.5 Hz, $\text{CH}_2(22_b)$), 5.31 (1H, s, $\text{CH}(14)$), 7.12–7.52 (3H, m, ArCH), 7.34–7.42 (5H, m, $\text{ArCH}(24,25,26)$), 7.46–7.64 (4H, m, $\text{ArCH}(16,17,18)$), 7.68 (1H, s, $\text{ArCH}(20)$)

^{13}C NMR (75 MHz, CDCl_3) δ 25.57 (s, $\text{CH}_2(10)$), 56.89 (s, $\text{CH}(14)$), 58.45 (s, $\text{CH}(11)$), 67.03 (s, $\text{CH}_2(22)$), 109.36 (s, ArCH), 111.0 (s, ArCH), 118.38 (s, ArCH), 119.83 (s, ArCH), 122.24 (s, ArCH), 123.94 (q, $^1J_{\text{C-F}}$ 272 Hz, $\text{CF}_3(21)$), 125.44 (2C, q, $^3J_{\text{C-F}}$ 3.6 Hz, $\text{ArCH}(18,20)$), 127.03 (s, ArC), 128.40 (s, ArCH), 128.43 (s, ArCH), 128.68 (s, ArCH), 129.50 (s, ArCH), 131.326 (q, $^2J_{\text{C-F}}$ 32 Hz, $\text{ArC}(19)$), 132.10 (s, ArC), 134.72 (s, ArC), 135.51 (s, ArC), 136.31 (s, ArC), 141.96 (s, ArC), 172.44 (s, $\text{C=O}(13)$)

^{19}F NMR (376 MHz, CDCl_3) δ –62.4 (s, $\text{Ar-CF}_3(21)$)

R_f 0.45 (9:1, CH_2Cl_2 :MeOH)

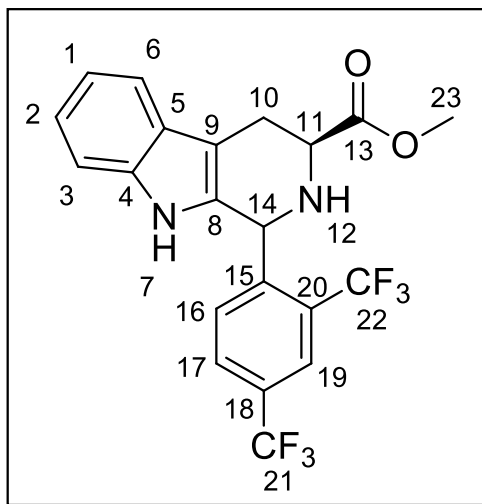
$[\alpha]_D^{25}$ –4.0 (c 1.0, MeOH)

IR ν/cm^{-1} 1166 (C-O, s), 1721 (C=O, s), 3033 (Ar C-H, w), 3354 (N-H, m)

MS (ESI): 451 $[\text{M}+\text{H}^+]$

HRMS $\text{C}_{26}\text{H}_{22}\text{F}_3\text{N}_2\text{O}_2$ $[\text{M}+\text{H}^+]$ requires 451.1628, found 451.1616 (2.6 ppm error)

Preparation of Methyl 1-(2,4-bis(trifluoromethyl)phenyl)-2,3,4,9-tetrahydro-1*H*-pyrido-[3,4-*b*]indol-3-carboxylate (**LVT19-1,2**):



Following method A using (*S*)-Methyl 2-amino-3-(1*H*-indol-3yl)propanoate (500 mg, 2.29 mmol, 1 eq.) and 2,4-bis(trifluoromethyl) benzaldehyde (0.45 mL, 666 mg, 2.86 mmol, 1.25 eq.) as starting materials. The desired product was purified using column chromatography (SiO₂, 98:2, CH₂Cl₂:MeOH), to afford, eluting first, the *trans* diastereoisomer as a colourless solid (427 mg, 0.97 mmol, 42%) and, eluting second, the *cis* diastereoisomer as a colourless solid (80 mg, 0.09 mmol, 8%).

Following method B using (*S*)-Methyl 2-amino-3-(1*H*-indol-3yl)propanoate (500 mg, 2.29 mmol, 1 eq.) and 2,4-bis(trifluoromethyl) benzaldehyde (0.45 mL, 666 mg, 2.86 mmol, 1.25 eq.) as starting materials. The desired product was purified using column chromatography (SiO₂, 100% CH₂Cl₂), to afford, eluting first, the *trans* diastereoisomer as a colourless solid (371 mg, 0.84 mmol, 37%) and, eluting second, the *cis* diastereoisomer as a colourless solid (405 mg, 0.92 mmol, 40%).

Trans (1*R*, 3*S*) diastereoisomer (LVT19-1)

mp 136–138 °C

¹H NMR (300 MHz, CDCl₃) δ 3.28 (1H, dd, *J* 15.9, 5.1 Hz, CH₂(10_a)), 3.34 (1H, dd, *J* 15.9, 5.1 Hz, CH₂(10_b)), 3.71 (3H, s, CH₃(23)), 4.05 (1H, dd, *J* 5.1, 5.1 Hz, CH(11)), 5.98 (1H, s,

CH(14)), 7.12–7.25 (3H, m, ArCH(1,2)), 7.46 (1H, s, NH(7)), 7.51 (1H, d, *J* 8.1, ArCH(16)), 7.58 (1H, d, *J* 7.1, ArCH), 7.69 (1H, d, *J* 8.1, ArCH(17)), 7.99 (1H, s, ArCH(19))

¹³C NMR (75 MHz, CDCl₃) δ 24.02 (s, CH₂(10)), 49.85 (s, OCH₃(23)), 52.22 (s, CH(14)), 53.27 (s, CH(11)), 109.10 (s, ArC), 111.01 (s, ArCH), 118.50 (s, ArCH), 119.87 (s, ArC), 122.16 (q, ¹*J*_{C-F} 272 Hz, ArCF₃), 122.52 (s, ArCH), 123.03 (q, ³*J*_{C-F} 9.7 Hz, ArCH(19)), 123.80 (q, ¹*J*_{C-F} 274 Hz, ArCF₃), 126.73 (s, ArC), 128.95 (q, ³*J*_{C-F} 9.7 Hz, ArCH(17)), 129.72 (q, ²*J*_{C-F} 33 Hz, ArC(20)), 130.23 (q, ²*J*_{C-F} 33 Hz, ArC(18)), 131.61 (s, ArCH), 132.22 (s, ArCH), 136.41 (s, ArC), 145.21 (s, ArC), 173.82 (s, C=O(13))

¹⁹F NMR (376 MHz, CDCl₃) δ −57.7 (s, Ar-CF₃) and −62.9 (s, Ar-CF₃)

R_f 0.59 (19:1, CH₂Cl₂:Et₂O)

[α]_D²⁵ −31.0 (*c* 1.0, MeOH)

IR ν/ cm^{−1} 1164 (C-O, s), 1723 (C=O, s), 3047 (Ar C-H, w), 3387 (N-H, m)

MS (ESI): 443 [M+H⁺]

HRMS C₂₁H₁₇F₆N₂O₂ [M+H⁺] requires 443.1189, found 443.1184 (1.1 ppm error)

Analysis calculated for C₂₁H₁₅F₆N₂O₂: C, 57.0%; H, 5.65%; N 6.33%. Found C, 56.8%; H, 5.31%; N, 6.09%.

Cis (1*S*, 3*S*) diastereoisomer (LVT19-2)

¹H NMR (300 MHz, CDCl₃) δ 3.07 (1H, ddd, *J* 15.1, 11.9, 2.9 Hz, CH₂(10_a)), 3.28 (1H, dd, *J* 15.1, 5.2 Hz, CH₂(10_b)), 3.83 (3H, s, OCH₃(23)), 4.01 (1H, dd, *J* 11.9, 5.2 Hz, CH(11)), 5.75 (1H, s, CH(14)), 7.11–7.22 (3H, m, ArCH(1,2)), 7.35 (1H, s, NH), 7.56 (1H, d, *J* 8.2, ArCH), 7.72 (1H, d, *J* 8.2, ArCH(16)), 7.78 (1H, d, *J* 8.2, ArCH(17)), 7.98 (1H, s, ArCH(19))

^{13}C NMR (75 MHz, CDCl_3) δ 25.35 (s, $\text{CH}_2(10)$), 52.39 (s, $\text{OCH}_3(23)$), 53.34 (s, $\text{CH}(14)$), 56.54 (s, $\text{CH}(11)$), 109.79 (s, ArC), 111.04 (s, ArCH), 118.43 (s, ArCH), 119.99 (s, sArCH), 123.23 (q, $^1J_{\text{C-F}}$ 272 Hz, ArCF_3), 123.77 (q, $^1J_{\text{C-F}}$ 274 Hz, ArCF_3), 122.49 (s, ArCH), 122.62 (q, $^3J_{\text{C-F}}$ 10 Hz, $\text{ArCH}(19)$), 126.75 (s, ArC), 129.32 (q, $^3J_{\text{C-F}}$ 8.1 Hz, $\text{ArCH}(17)$), 129.74 (q, $^2J_{\text{C-F}}$ 32 Hz, ArC), 130.64 (q, $^2J_{\text{C-F}}$ 33 Hz, ArC), 132.96 (s, ArCH), 133.08 (s, ArC), 136.49 (s, ArC), 144.66 (s, ArC), 172.69 (s, $\text{C=O}(13)$)

^{19}F NMR (376 MHz, CDCl_3) δ -57.4 (s, Ar-CF_3) and -62.9 (s, Ar-CF_3)

R_f 0.41 (19:1, $\text{CH}_2\text{Cl}_2\text{:Et}_2\text{O}$)

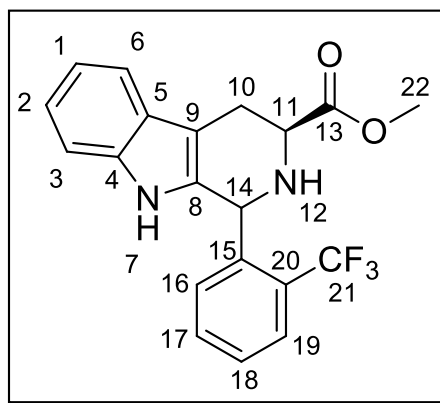
$[\alpha]_D^{29} +31.0$ (c 1.0, MeOH)

IR ν/cm^{-1} 1168 (C-O, s), 1731 (C=O, s), 3060 (Ar C-H, w), 3383 (N-H, m)

MS (ESI): 443 $[\text{M}+\text{H}^+]$

HRMS $\text{C}_{21}\text{H}_{17}\text{F}_6\text{N}_2\text{O}_2$ $[\text{M}+\text{H}^+]$ requires 443.1189, found 443.1181 (1.7 ppm error)

Preparation of Methyl 1-(2-(trifluoromethyl)phenyl)-2,3,4,9-tetrahydro-1*H*-pyrido-[3,4-*b*]indol-3-carboxylate (**LVT20-1,2**):



Following method A using (*S*)-Methyl 2-amino-3-(1*H*-indol-3-yl)propanoate (500 mg, 2.29 mmol, 1 eq.) and 2-(trifluoromethyl)benzaldehyde (0.36 mL, 475 mg, 2.86 mmol, 1.25 eq.)

as starting materials. The desired product was purified using column chromatography (SiO₂, 9:1, CH₂Cl₂:Et₂O), to afford, eluting first, the *trans* diastereoisomer as a colourless solid (149 mg, 0.41 mmol, 18%) and, eluting second, the *cis* diastereoisomer as an opaque glass solid (85 mg, 0.23 mmol, 10%).

Following method B using (*S*)-Methyl 2-amino-3-(1*H*-indol-3yl)propanoate (500 mg, 2.29 mmol, 1 eq.) and 2-(trifluoromethyl)benzaldehyde (0.36 mL, 475 mg, 2.86 mmol, 1.25 eq.) as starting materials. The desired product was purified using column chromatography (SiO₂, 9:1, CH₂Cl₂:Et₂O), to afford, eluting first, the *trans* diastereoisomer as a colourless solid (317 mg, 0.85 mmol, 37%) and, eluting second, the *cis* diastereoisomer as a light yellow solid (326 mg, 0.87 mmol, 38%).

Trans (1*R*, 3*S*) diastereoisomer (LVT20-1)

mp 85–87 °C

¹H NMR (300 MHz, CDCl₃) δ 3.24 (1H, dd, *J* 15.4, 5.4 Hz, CH₂(10_a)), 3.33 (1H, dd, *J* 15.4, 5.4 Hz, CH₂(10_b)), 3.72 (3H, s, OCH₃(22)), 4.04 (1H, dd, *J* 5.4, 5.4 Hz, CH(11)), 5.91 (1H, s, CH(14)), 7.10–7.24 (3H, m, ArCH(1,2,3)), 7.29 (1H, d, *J* 6.8 Hz, ArCH(16)), 7.40–7.44 (2H, m, ArCH(17,18)), 7.48 (1H, s, NH), 7.58 (1H, d, *J* 5.6 Hz, ArCH), 7.74 (1H, d, *J* 6.8 Hz, ArCH)

¹³C NMR (75 MHz, CDCl₃) δ 24.12 (s, CH₂(10)), 50.05 (s, OCH₃(22)), 52.23 (s, CH(14)), 53.08 (s, CH(11)), 108.87 (s, ArC), 110.94 (s, ArCH), 118.39 (s, ArCH), 119.64 (s, ArCH), 122.17 (s, ArCH), 123.61 (q, ¹*J*_{C-F} 272 Hz, CF₃(21)), 125.89 (q, ³*J*_{C-F} 10 Hz s, ArCH(19)), 126.80 (s, ArCH), 128.06 (s, ArCH), 131.03 (s, ArCH), 132.27 (s, ArC), 132.66 (q, ²*J*_{C-F} 25 Hz, ArC(20)), 134.72 (s, ArC), 136.26 (s, ArC), 140.62 (s, ArC), 173.93 (s, C=O(13))

¹⁹F NMR (376 MHz, CDCl₃) δ –57.4 (s, Ar-CF₃(21))

R_f 0.24 (19:1, CH₂Cl₂:Et₂O)

[α]_D²⁷ +11.0 (*c* 1.0, MeOH)

IR ν/ cm⁻¹ 1160 (C-O, s), 1713 (C=O, s), 3070 (Ar C-H, w), 3390 (N-H, m)

MS (ESI): 375 [M+H⁺]

HRMS C₂₀H₁₈F₃N₂O₂ [M+H⁺] requires 375.1315, found 375.1314 (0.2 ppm error)

Cis (1*S*, 3*S*) diastereoisomer (LVT20-2)

mp 93–96 °C

¹H NMR (300 MHz, CDCl₃) δ 3.06 (1H, ddd, *J* 15.1, 11.1 Hz, CH₂(10_a)), 3.26 (1H, ddd, *J* 15.1, 4.0 Hz, CH₂(10_b)), 3.80 (3H, s, OCH₃(22)), 3.99 (1H, dd, *J* 11.1, 4.0 Hz, CH(11)), 5.68 (1H, s, CH(14)), 7.08–7.20 (3H, m, ArCH(1,2)), 7.42 (1H, s, NH), 7.38–7.48 (2H, m, ArCH), 7.53–7.57 (2H, m, ArCH(17)), 7.72 (1H, d, *J* 8.1 Hz, ArCH(16))

¹³C NMR (75 MHz, CDCl₃) δ 25.46 (s, CH₂(10)), 52.39 (s, OCH₃(22)), 53.59 (s, CH(14)), 56.75 (s, CH(11)), 109.31 (s, ArC), 111.01 (s, ArCH), 118.32 (s, ArCH), 119.76 (s, ArCH), 122.14 (s, ArCH), 124.55 (q, ¹*J*_{C-F} 274 Hz, CF₃(21)), 125.41 (q, ³*J*_{C-F} 5.8 Hz s, ArCH(19)), 126.85 (s, ArC), 128.30 (s, ArCH), 129.15 (q, ²*J*_{C-F} 30 Hz, ArC(20)), 131.64 (s, ArCH), 132.69 (s, ArCH), 134.61 (s, ArC), 136.29 (s, ArC), 140.08 (s, ArC), 172.97 (s, C=O(13))

¹⁹F NMR (376 MHz, CDCl₃) δ –57.1 (s, Ar-CF₃(21))

R_f 0.35 (19:1, CH₂Cl₂:Et₂O)

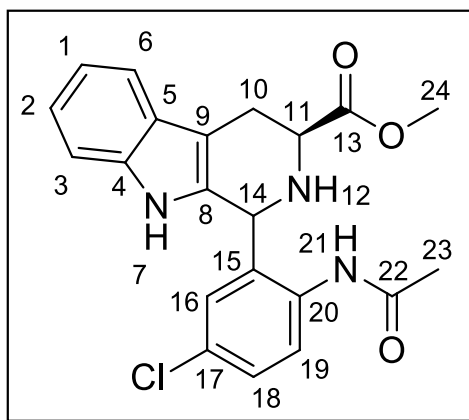
[α]_D²⁷ –11.0 (*c* 1.0, MeOH)

IR ν/ cm⁻¹ 1163 (C-O, s), 1732 (C=O, s), 3060 (Ar C-H, w), 3396 (N-H, m)

MS (ESI): 375 [M+H⁺]

HRMS C₂₀H₁₈F₃N₂O₂ [M+H⁺] requires 375.1315, found 375.1313 (0.5 ppm error)

Preparation of Methyl 1-(2-acetamido-5-chlorophenyl)-2,3,4,9-tetrahydro-1*H*-pyrido-[3,4-*b*]indol-3-carboxylate (**LVT24-1,2**):



Following method A using (*S*)-Methyl 2-amino-3-(1*H*-indol-3-yl)propanoate (500 mg, 2.29 mmol, 1 eq.) and 2-acetamido-5-chlorobenzaldehyde (**LVT23**) (565 mg, 2.86 mmol, 1.25 eq.) as starting materials. The desired product was purified using column chromatography (SiO₂, 3:1 CH₂Cl₂:Et₂O), to afford, eluting first, the *trans* diastereoisomer as an off-white solid (178 mg, 0.45 mmol, 20%) and eluting second, the *cis* diastereoisomer as an off-white solid (98 mg, 0.25 mmol, 11%).

Trans (1*S*, 3*S*) diastereoisomer (**LVT24-1**)

mp 121–124 °C

¹H NMR (400 MHz, CDCl₃) δ 1.87 (3H, s, CH₃(23)), 3.23 (1H, dd, *J* 15.5, 5.2 Hz, CH₂(10_a)), 3.33 (1H, dd, *J* 15.5, 5.2 Hz, CH₂(10_b)), 3.73 (3H, s, OCH₃(24)), 4.04 (1H, dd, *J* 5.2, 5.2 Hz, CH(11)), 5.45 (1H, s, CH(14)), 7.12–7.29 (5H, m, ArCH(1,2,3,6,16)), 7.52 (1H, d, *J* 7.6 Hz, ArCH(19)), 7.79 (1H, br. s, NH), 8.03 (1H, d, *J* 7.6 Hz, ArCH(18)) 9.81 (1H, s, NH)

^{13}C NMR (400 MHz, CDCl_3) δ 24.19 ($\text{CH}_3(23)$), 24.43 ($\text{CH}_2(10)$), 30.40 ($\text{CH}_3(24)$), 52.48 ($\text{CH}(14)$), 53.43 ($\text{CH}(11)$), 107.55 (ArC), 111.43 (ArCH), 118.22 ($\text{ArCH}(19)$), 119.87 (ArCH), 122.59 (ArCH), 124.37 ($\text{ArCH}(18)$), 125.62 (ArC), 126.75 (ArC), 129.22 (ArCH), 129.62 ($\text{ArCH}(16)$), 130.59 (ArC), 131.17 (ArC), 136.19 (ArC), 136.61 (ArC), 168.48 ($\text{C=O}(22)$), 173.64 ($\text{C=O}(13)$)

R_f 0.24 (3:1, $\text{CH}_2\text{Cl}_2\text{:Et}_2\text{O}$)

$[\alpha]_D^{25}$ -12.0 (c 1.0, MeOH)

IR ν/cm^{-1} 741 (C-Cl, s), 1130 (C-O, s), 1672 (C=O, s), 1728 (C=O, s), 2997 (Ar C-H, w), 3395 (N-H, m)

MS (ESI): 398/400 $[\text{M}+\text{H}^+]$

HRMS $\text{C}_{21}\text{H}_{21}^{35}\text{ClN}_3\text{O}_2$ $[\text{M}+\text{H}^+]$ requires 398.1266, found 398.1267 (0.3 ppm error)

Cis (1*R*, 3*S*) diastereoisomer (LVT24-2)

mp 103–107 °C

^1H NMR (400 MHz, CDCl_3) δ 1.66 (3H, s, $\text{CH}_3(23)$), 3.00 (1H, ddd, J 15.4, 11.2 Hz, $\text{CH}_2(10_a)$), 3.36 (1H, ddd, J 15.4, 4.1 Hz, $\text{CH}_2(10_b)$), 3.87 (3H, s, $\text{OCH}_3(24)$), 3.95 (1H, dd, J 11.2, 4.1 Hz, $\text{CH}(11)$), 5.28 (1H, s, $\text{CH}(14)$), 7.11–7.21 (3H, m, $\text{ArCH}(1,2)$), 7.33–7.35 (2H, m, $\text{ArCH}(6,16)$), 7.51 (1H, d, J 6.9 Hz, ArCH), 8.06 (1H, d, J 8.6 Hz, ArCH), 9.75 (1H, br. s, NH)

^{13}C NMR (100 MHz, CDCl_3) δ 24.03 ($\text{CH}_3(23)$), 25.41 ($\text{CH}_2(10)$), 30.34 ($\text{CH}_3(24)$), 52.59 ($\text{CH}(14)$), 56.66 ($\text{CH}(11)$), 108.05 (ArC), 111.41 (ArCH), 117.95 ($\text{ArCH}(19)$), 119.99 (ArCH), 122.50 ($\text{ArCH}(18)$), 124.53 (ArC), 125.19 (ArCH), 126.63 (ArC), 129.55 (ArCH), 129.70 ($\text{ArCH}(16)$), 132.13 (ArC), 136.32 (ArC), 136.84 (ArC), 168.24 ($\text{C=O}(22)$), 172.33 ($\text{C=O}(13)$)

R_f 0.45 (3:1, CH₂Cl₂:Et₂O)

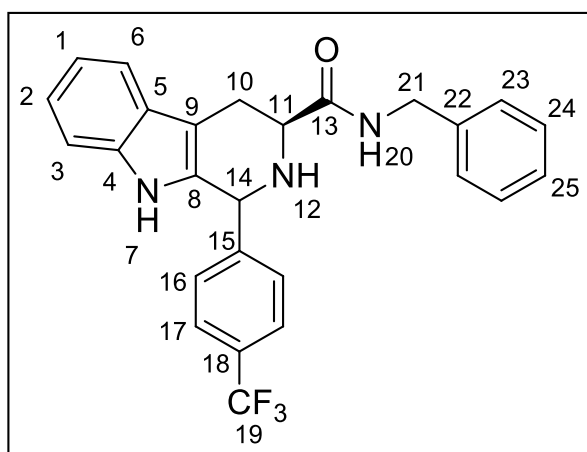
[α]_D²⁵ +12.0 (*c* 1.0, MeOH)

IR ν / cm⁻¹ 741 (C-Cl, s), 1126 (C-O, s), 1665 (C=O, s), 1739 (C=O, s), 3013 (Ar C-H, w), 3384 (N-H, m)

MS (ESI): 398/400 [M+H⁺]

HRMS C₂₁H₂₁³⁵ClN₃O₂ [M+H⁺] requires 398.1266, found 398.1265 (0.2 ppm error)

Preparation of (3*S*)-*N*-Benzyl-1-(4-(trifluoromethyl)phenyl)-2,3,4,9-tetrahydro-1*H*-pyrido[3,4-*b*]indole-3-carboxamide (**LVT27-1,2**):



Following method A using (*S*)-2-Amino-*N*-benzyl-3-(1*H*-indol-3-yl) propanamide (**LVT26**) (100 mg, 0.34 mmol, 1 eq.) and 4-(trifluoromethyl) benzaldehyde (0.05 mL, 64 mg, 0.37 mmol, 1.25 eq.) as starting materials. The desired product was purified using column chromatography (SiO₂, 9:1 CH₂Cl₂:Et₂O), to afford, eluting first the *trans* diastereoisomer as an off-white solid (15 mg, 0.03 mmol, 9%) and, eluting second the *cis* diastereoisomer as an off-white solid (79 mg, 0.18 mmol, 53%).

Following method B using (*S*)-2-Amino-*N*-benzyl-3-(1*H*-indol-3-yl) propanamide (**LVT26**) (500 mg, 1.70 mmol, 1 eq.) and 4-(trifluoromethyl) benzaldehyde (0.29 mL, 370 mg, 2.13

mmol, 1.25 eq.) as starting materials. The desired product was purified using column chromatography (SiO₂, 9:1 CH₂Cl₂:Et₂O), to afford, eluting first the *trans* diastereoisomer as an off-white solid (156 mg, 0.35 mmol, 21%) and eluting second the *cis* diastereoisomer as an off-white solid (161 mg, 0.36 mmol, 21%).

Trans (1*R*, 3*S*) diastereoisomer (LVT27-1)

mp 237–240 °C

¹H NMR (300 MHz, CDCl₃) δ 2.97 (1H, dd, *J* 16.2, 9.8 Hz, CH₂(10_a)), 3.39 (1H, dd, *J* 16.2, 4.9 Hz, CH₂(10_b)), 3.62 (1H, dd, *J* 9.8, 4.9 Hz, CH(11)), 5.42 (1H, dd, *J* 15.3 Hz, CH₂(21_a)), 5.44 (1H, dd, *J* 15.3 Hz, CH₂(21_b)), 5.31 (1H, s, CH(14)), 7.15–7.20 (3H, m, ArCH(1,2)), 7.23–7.33 (5H, m, ArCH(23,24,25)), 7.35 (2H, d, *J* 7.1 Hz, ArCH(16)), 7.60 (1H, d, *J* 7.1 Hz, ArCH), 7.70 (2H, d, *J* 7.1 Hz, ArCH(17))

¹³C NMR (100 MHz, CDCl₃) δ 25.64 (s, CH₂(10)), 43.24 (s, CH₂(21)), 58.16 (s, CH(14)), 58.66 (s, CH(11)), 77.32 (s, CH₂(23)), 110.52 (s, ArC), 111.01 (s, ArCH), 118.58 (s, ArCH), 119.96 (s, ArCH), 122.49 (s, ArCH), 123.80 (q, ¹*J*_{C-F} 272 Hz, CF₃(19)), 126.11 (q, ³*J*_{C-F} 5.8 Hz, ArCH(17)), 127.60 (s, ArCH), 128.00 (s, ArCH), 128.76 (s, ArCH), 129.03 (s, ArCH), 130.06 (s, ArC), 131.90 (q, ²*J*_{C-F} 32 Hz, ArC(18)), 133.35 (s, ArC), 136.32 (s, ArC), 138.21 (s, ArC), 144.45 (s, ArC), 172.29 (s, C=O(13))

¹⁹F NMR (376 MHz, CDCl₃) δ –62.5 (s, Ar-CF₃(19))

R_f 0.18 (9:1, CH₂Cl₂:Et₂O)

[α]_D²⁵ +30.0 (*c* 1.0, MeOH)

IR ν/ cm⁻¹ 1363 (C-O, s), 1656 (C=O, s), 3066 (Ar C-H, w), 3271 (N-H, m)

MS (ESI): 450 [M+H⁺]

HRMS C₂₆H₂₃F₃N₃O [M+H⁺] requires 450.1788, found 450.1786 (0.4 ppm error)

Cis (1*S*, 3*S*) diastereoisomer (**LVT27-2**)

mp 97–101 °C

¹H NMR (300 MHz, CDCl₃) δ 2.92 (1H, ddd, *J* 15.7, 11.2 Hz, CH₂(10_a)), 3.41 (1H, ddd, *J* 15.7, 4.4 Hz, CH₂(10_b)), 3.82 (1H, dd, *J* 11.2, 4.4 Hz, CH(11)), 4.44 (1H, dd, *J* 14.7, 6.1 Hz, CH₂(21_a)), 4.53 (1H, dd, *J* 14.7, 6.1 Hz, CH₂(21_b)), 5.27 (1H, s, CH(14)), 7.12–7.20 (3H, m, ArCH(1,2)), 7.27–7.37 (5H, m, ArCH(23,24,25)), 7.45 (2H, d, *J* 8.1 Hz, ArCH(16)), 7.58 (1H, d, *J* 7.0 Hz, ArCH), 7.64 (2H, d, *J* 8.1 Hz, ArCH(17))

¹³C NMR (75 MHz, CDCl₃) δ 24.84 (s, CH₂(10)), 43.34 (s, CH₂(21)), 52.52 (s, sCH(14)), 55.11 (s, CH(11)), 77.25 (s, CH₂(23)), 110.93 (s, ArC), 111.08 (s, ArCH), 118.73 (s, ArCH), 120.03 (s, ArCH), 122.69 (s, ArCH), 125.58 (q, ¹*J*_{C-F} 272 Hz, CF₃(19)), 126.61 (q, ³*J*_{C-F} 5.8 Hz, ArCH(17)), 127.49 (s, ArCH), 127.54 (s, ArCH), 127.62 (s, ArCH), 128.77 (s, ArCH), 128.83 (s, ArCH), 129.09 (s, ArCH), 130.39 (q, ²*J*_{C-F} 32 Hz, ArC(18)), 132.08 (s, ArC), 136.37 (s, ArC), 138.31 (s, ArC), 139.06 (s, ArC), 145.13 (s, ArC), 172.52 (s, C=O(13))

¹⁹F NMR (376 MHz, CDCl₃) δ –62.6 (s, Ar-CF₃(19))

R_f 0.24 (9:1, CH₂Cl₂:Et₂O)

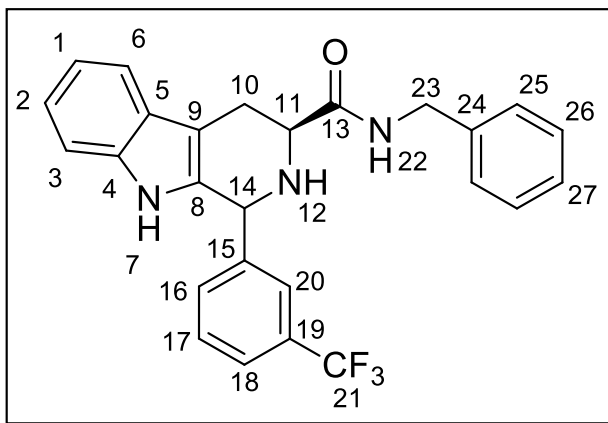
[α]_D²⁵ –30.0 (*c* 1.0, MeOH)

IR ν/ cm^{–1} 1164 (C–O, s), 1652 (C=O, s), 3067 (Ar C–H, w), 3272 (N–H, m)

MS (ESI): 450 [M+H⁺]

HRMS C₂₆H₂₃F₃N₃O [M+H⁺] requires 450.1788, found 450.1786 (0.4 ppm error)

Preparation of (3*S*)-*N*-Benzyl-1-(3-(trifluoromethyl)phenyl)-2,3,4,9-tetrahydro-1*H*-pyrido[3,4-*b*]indole-3-carboxamide (**LVT28-1,2**):



Following method A using (*S*)-2-Amino-*N*-benzyl-3-(1*H*-indol-3-yl) propanamide (**LVT26**) (85 mg, 0.29 mmol, 1 eq.) and 3-(trifluoromethyl) benzaldehyde (0.05 mL, 65 mg, 0.36 mmol, 1.25 eq.) as starting materials. The desired product was purified using column chromatography (SiO₂, 9:1 CH₂Cl₂:Et₂O), to afford, eluting first the *cis* diastereoisomer a colourless glass solid (10 mg, 0.02 mmol, 8%) and, eluting second the *trans* diastereoisomer as a colourless solid (20 mg, 0.04 mmol, 15%).

Following method B using (*S*)-2-Amino-*N*-benzyl-3-(1*H*-indol-3-yl) propanamide (**LVT26**) (500 mg, 1.70 mmol, 1 eq.) and 3-(trifluoromethyl) benzaldehyde (0.28 mL, 364 mg, 2.13 mmol, 1.25 eq.) as starting materials. The desired product was purified using column chromatography (SiO₂, 9:1 CH₂Cl₂:Et₂O), to afford, eluting first the *cis* diastereoisomer as an off-white solid (182 mg, 0.40 mmol, 24%) and eluting second the *trans* diastereoisomer as an off-white solid (176 mg, 0.39 mmol, 23%).

Trans (1*R*, 3*S*) diastereoisomer (LVT28-1)

¹H NMR (300 MHz, CDCl₃) δ 2.97 (1H, ddd, *J* 16.2, 9.8 Hz, CH₂(10_a)), 3.39 (1H, dd, *J* 16.2, 4.9 Hz, CH₂(10_b)), 3.62 (1H, dd, *J* 9.8, 4.9 Hz, CH(11)), 5.42 (1H, dd, *J* 15.3 Hz, CH₂(21_a)), 5.44 (1H, dd, *J* 15.3 Hz, CH₂(21_b)), 5.31 (1H, s, CH(14)), 7.15–7.20 (3H, m, ArCH(1,2)), 7.23–7.33 (5H, m, ArCH(23,24,25)), 7.35 (2H, d, *J* 7.1 Hz, ArCH(16)), 7.60 (1H, d, *J* 7.1 Hz, ArCH), 7.70 (2H, d, *J* 7.1 Hz, ArCH(17))

^{13}C NMR (400 MHz, CDCl_3) δ 25.64 (s, $\text{CH}_2(10)$), 43.24 (s, $\text{CH}_2(23)$), 58.16 (s, $\text{CH}(14)$), 58.66 (s, $\text{CH}(11)$), 110.52 (s, ArC), 111.01 (s, ArCH), 118.58 (s, ArCH), 119.96 (s, ArCH), 122.49 (s, ArCH), 123.80 (q, $^1J_{\text{C-F}}$ 272 Hz, $\text{CF}_3(19)$), 126.11 (q, $^3J_{\text{C-F}}$ 5.8 Hz, ArCH(17)), 127.60 (s, ArCH), 128.00 (s, ArCH), 128.76 (s, ArCH), 129.03 (s, ArCH), 130.06 (s, ArC), 131.90 (q, $^2J_{\text{C-F}}$ 32 Hz, ArC(18)), 133.35 (s, ArC), 136.32 (s, ArC), 138.21 (s, ArC), 144.45 (s, ArC), 172.29 (s, C=O(13))

^{19}F NMR (376 MHz, CDCl_3) δ -62.4 (s, Ar- $\text{CF}_3(21)$)

R_f 0.43 (5:1, CH_2Cl_2 :Et₂O)

$[\alpha]_D^{25}$ +16.0 (c 1.0, MeOH)

IR ν/cm^{-1} 1163 (C-O, s), 1717 (C=O, s), 2923 (Ar C-H, w), 3271 (N-H, m)

MS (ESI): 450 $[\text{M}+\text{H}^+]$

HRMS $\text{C}_{26}\text{H}_{23}\text{F}_3\text{N}_3\text{O}$ $[\text{M}+\text{H}^+]$ requires 450.1788, found 450.1785 (0.6 ppm error)

Cis (1*S*, 3*S*) diastereoisomer (LVT28-2)

mp 85–88 °C

^1H NMR (300 MHz, CDCl_3) δ 2.94 (1H, dd, J 15.7, 11.2 Hz, $\text{CH}_2(10_a)$), 3.45 (1H, dd, J 15.7, 4.4 Hz, $\text{CH}_2(10_b)$), 3.85 (1H, dd, J 11.2, 4.4 Hz, $\text{CH}(11)$), 4.46 (1H, dd, J 14.7, 5.8 Hz, $\text{CH}_2(21_a)$), 4.56 (1H, dd, J 14.7, 5.8 Hz, $\text{CH}_2(21_b)$), 5.29 (1H, s, $\text{CH}(14)$), 7.15–7.24 (3H, m, ArCH), 7.28–7.35 (5H, m, ArCH), 7.49–7.65 (5H, m, ArCH)

^{13}C NMR (75 MHz, CDCl_3) δ 25.62 (s, $\text{CH}_2(10)$), 43.22 (s, $\text{CH}_2(23)$), 58.22 (s, $\text{CH}(14)$), 58.79 (s, $\text{CH}(11)$), 110.56 (s, ArC), 111.04 (s, ArCH), 118.59 (s, ArCH), 119.95 (s, ArCH), 122.49 (s, ArCH), 123.82 (q, $^1J_{\text{C-F}}$ 272 Hz, $\text{CF}_3(19)$), 125.53 (q, $^3J_{\text{C-F}}$ 5.8 Hz, ArCH(17)), 127.59 (s, ArCH), 127.99 (s, ArCH), 128.75 (s, ArCH), 129.68 (s, ArCH), 130.06 (s, ArC),

131.93 (q, $^2J_{C-F}$ 32 Hz, ArC(18)), 133.35 (s, ArC), 136.32 (s, ArC), 138.21 (s, ArC), 144.45 (s, ArC), 172.23 (s, C=O(13))

^{19}F NMR (376 MHz, CDCl_3) δ -62.46 (s, Ar- CF_3 (21))

R_f 0.61 (5:1, CH_2Cl_2 : Et_2O)

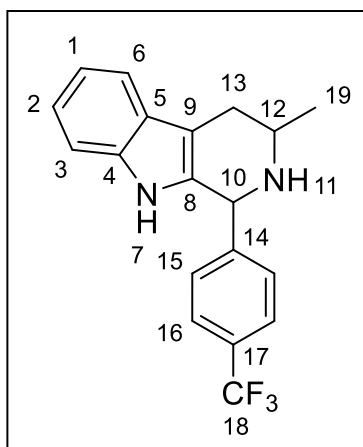
$[\alpha]_D^{25}$ -16.0 (c 1.0, MeOH)

IR ν/cm^{-1} 1163 (C-O, s), 1650 (C=O, s), 2988 (Ar C-H, w), 3282 (N-H, m)

MS (ESI): 450 $[\text{M}+\text{H}^+]$

HRMS $\text{C}_{26}\text{H}_{23}\text{F}_3\text{N}_3\text{O}$ $[\text{M}+\text{H}^+]$ requires 450.1788, found 450.1784 (0.8 ppm error)

Preparation of (3*R*)-3-Methyl-1-(4-(trifluoromethyl)phenyl)-2,3,4,9-tetrahydro-1*H*-pyrido[3,4-*b*]indole (**LVT33-1,2**):



4-(Trifluoromethyl)benzaldehyde (0.57 mL, 727 mg, 4.40 mmol, 2 eq.) was stirred for 0.5 h in a mixture of water (25 mL) and 5 drops of concentrated H_2SO_4 . 1-(1*H*-Indol-3-yl)propan-2-amine (**LVT31**) (443 mg, 2.19 mmol, 1 eq.) was then added to the solution and left to stir under reflux overnight. The solution was allowed to cool and carefully quenched with 2M NaOH solution (20 mL), the organics were extracted with CH_2Cl_2 (3×75 mL), washed with

saturated aqueous brine (100 mL), dried over MgSO₄, filtered and concentrated under reduced pressure. The desired product purified using column chromatography (SiO₂, 93:7, CH₂Cl₂/MeOH), to afford, eluting first, the 1*R*, 3*R* enantiomer as an off-white solid (91.4 mg, 0.30 mmol, 13%) and eluting second the 1*S*, 3*R* enantiomer as an off-white solid (120 mg, 0.40 mmol, 17%).

1*R*, 3*R* enantiomer (LVT-331)

mp 106–109 °C

¹H NMR (300 MHz, CDCl₃) δ 1.21 (3H, d, *J* 6.3 Hz, CH₃(19)), 2.50 (1H, dd, *J* 15.5, 6.3 Hz, CH₂(13_a)), 2.93 (1H, dd, *J* 15.5, 4.2 Hz, CH₂(13_b)), 3.16 (1H, dqd, *J* 12.7, 6.3, 4.2 Hz, CH(12)), 5.22 (1H, s, CH(10)), 7.11–7.20 (3H, m, ArCH(1,2)), 7.24 (1H, d, *J* 6.5 Hz, ArCH), 7.31 (2H, d, *J* 7.7 Hz, ArCH(15)), 7.56 (2H, d, *J* 7.7 Hz, ArCH(16)), 7.78 (1H, br. s, NH)

¹³C NMR (75 MHz, CDCl₃) δ 21.89 (s, CH₃(19)), 29.86 (s, CH₂(13)), 44.08 (s, CH(10)), 55.29 (s, sCH(12)), 110.95 (s, ArC), 111.16 (s, ArCH), 118.37 (s, ArCH), 119.57 (s, ArCH), 122.10 (s, ArCH), 124.08 (q, ¹*J*_{C-F} 272 Hz, CF₃(18)), 125.45 (q, ³*J*_{C-F} 6.8 Hz, ArCH(16)), 127.09 (s, ArC), 128.68 (ArCH(15)), 129 (q, ²*J*_{C-F} 33 Hz, ArC(17)), 132.01 (s, ArC), 136.33 (s, ArC), 146.62 (s, ArC)

¹⁹F NMR (376 MHz, CDCl₃) δ –62.4 (s, Ar-CF₃(18))

R_f 0.19 (9:1, CH₂Cl₂:MeOH)

IR ν/ cm⁻¹ 1523 (C-F, s), 3056 (Ar C-H, w), 3353 (N-H, w)

MS (ESI): 331 [M+H⁺]

HRMS C₁₉H₁₈F₃N₂ [M+H⁺] requires 331.1417, found 331.1419 (0.7 ppm error)

1*S*, 3*R* enantiomer (LVT-332)

mp 124–126 °C

^1H NMR (300 MHz, CDCl_3) δ 1.26 (3H, d, J 6.3 Hz, $\text{CH}_3(19)$), 2.53 (1H, ddd, J 15.2, 8.2, 6.3 Hz, $\text{CH}_2(13_a)$), 2.85 (1H, ddd, J 15.2, 6.3, 4.3 Hz, $\text{CH}_2(13_b)$), 3.22 (1H, dqd, J 16.5 Hz, 8.2, 4.3 $\text{CH}(12)$), 5.11 (1H, s, $\text{CH}(10)$), 7.05–7.07 (3H, m, $\text{ArCH}(1,2)$), 7.32 (2H, d, J 8.0 Hz, $\text{ArCH}(15)$), 7.50 (3H, m, $\text{ArCH}(16)$), 7.81 (1H, br. s, NH)

^{13}C NMR (75 MHz, CDCl_3) δ 22.39 (s, $\text{CH}_3(19)$), 30.45 (s, $\text{CH}_2(13)$), 50.66 (s, $\text{CH}(10)$), 59.00 (s, $\text{CH}(12)$), 110.86 (s, ArC), 110.99 (s, ArCH), 118.41 (s, ArCH), 119.57 (s, ArCH), 120.50 (q, $^3J_{\text{C-F}}$ 272 Hz, $\text{CF}_3(16)$), 121.95 (s, ArCH), 125.86 (q, $^1J_{\text{C-F}}$ 6.7 Hz, $\text{ArCH}(18)$), 127.16 (s, ArC), 129.11 (s, $\text{ArCH}(15)$), 130.58 (q, $^2J_{\text{C-F}}$ 32 Hz, $\text{ArC}(17)$), 133.91 (s, ArC), 136.32 (s, ArC), 145.74 (s, ArC)

^{19}F NMR (376 MHz, CDCl_3) δ –62.5 (s, $\text{Ar-CF}_3(18)$)

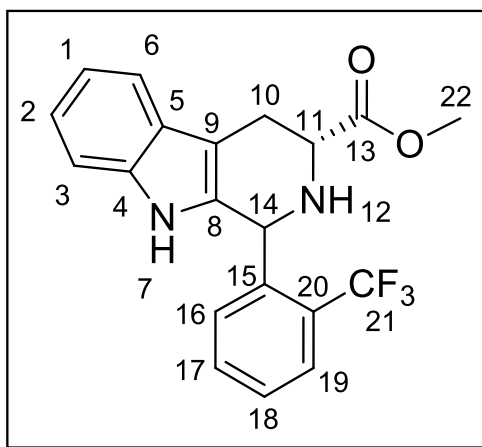
R_f 0.19 (9:1, CH_2Cl_2 :MeOH)

IR ν/cm^{-1} 1524 (C-F, s), 3129 (Ar C-H, w), 3357 (N-H, w)

MS (ESI): 331 $[\text{M}+\text{H}^+]$

HRMS $\text{C}_{19}\text{H}_{18}\text{F}_3\text{N}_2$ $[\text{M}+\text{H}^+]$ requires 331.1417, found 331.1423 (1.8 ppm error)

Preparation of (3*R*)-Methyl 1-(2-(trifluoromethyl)phenyl)-2,3,4,9-tetrahydro-1*H*-pyrido[3,4-*b*]indole-3-carboxylate (**LVT37-1,2**):



Following method A using (*R*)-Methyl 2-amino-3-(1*H*-indol-3-yl)propanoate (500 mg, 2.29 mmol, 1 eq.) and 2-(trifluoromethyl) benzaldehyde (0.36 mL, 475 mg, 2.86 mmol, 1.25 eq.) as starting materials. The desired product was purified using column chromatography (SiO₂, 19:1, CH₂Cl₂:Et₂O), to afford, eluting first, the *trans* diastereoisomer as a colourless solid (161 mg, 0.43 mmol, 19%) and, eluting second, the *cis* diastereoisomer as a colourless solid (179 mg, 0.48 mmol, 21%).

Following method B using (*R*)-Methyl 2-amino-3-(1*H*-indol-3-yl)propanoate (250 mg, 1.15 mmol, 1 eq.) and 2-(trifluoromethyl) benzaldehyde (0.18 mL, 238 mg, 1.38 mmol, 1.25 eq.) starting material. The desired product was purified using column chromatography (SiO₂, 19:1, CH₂Cl₂:Et₂O), to afford, eluting first, the *trans* diastereoisomer as a colourless solid (152 mg, 0.41 mmol, 36%) and, eluting second, the *cis* diastereoisomer as a colourless solid (161 mg, 0.43 mmol, 37%).

Trans (1*S*, 3*R*) diastereoisomer (**LVT37-1**)

mp 87–91 °C

^1H NMR (300 MHz, CDCl_3) δ 3.24 (1H, dd, J 15.4, 5.3 Hz, $\text{CH}_2(10_a)$), 3.32 (1H, dd, J 15.4, 5.3 Hz, $\text{CH}_2(10_b)$), 3.72 (3H, s, $\text{OCH}_3(22)$), 4.05 (1H, dd, J 5.3, 5.3 Hz, $\text{CH}(11)$), 5.91 (1H, s, $\text{CH}(14)$), 7.12–7.22 (3H, m, $\text{ArCH}(1,2,3)$), 7.29 (1H, d, J 6.9 Hz, $\text{ArCH}(16)$), 7.39–7.43 (2H, m, $\text{ArCH}(6,17)$), 7.49 (1H, br. s, NH), 7.51 (1H, d, J 8.1 Hz, $\text{ArCH}(18)$), 7.73 (1H, d, J 8.1 Hz, $\text{ArCH}(19)$)

^{13}C NMR (75 MHz, CDCl_3) δ 24.15 (s, $\text{CH}_2(10)$), 50.09 (s, $\text{CH}(14)$), 52.15 (s, $\text{OCH}_3(22)$), 53.12 (s, $\text{CH}(11)$), 108.9 (s, ArC), 110.9 (s, ArCH), 118.4 (s, ArCH), 119.65 (s, ArCH), 122.18 (s, ArCH), 121.92 (q, $^1J_{\text{C-F}}$ 274 Hz, $\text{CF}_3(21)$), 125.99 (q, $^3J_{\text{C-F}}$ 5.8 Hz, $\text{ArCH}(19)$), 126.9 (s, ArCH), 128.0 (s, ArCH), 128.9 (q, $^2J_{\text{C-F}}$ 29 Hz, $\text{ArC}(20)$), 131.05 (s, ArCH), 132.26 (s, ArC), 132.53 (s, ArC), 136.33 (s, ArC), 140.70 (s, ArC), 173.90 (s, $\text{C=O}(13)$)

^{19}F NMR (376 MHz, CDCl_3) δ –57.4 ($\text{Ar-CF}_3(21)$)

R_f 0.30 (19:1, CH_2Cl_2 : Et_2O)

$[\alpha]_D^{25}$ –4.0 (c 1.0, MeOH)

IR ν/cm^{-1} 1165 (C-O, s), 1738 (C=O, s), 3105 (Ar C-H, w)

MS (ESI): 375 $[\text{M}+\text{H}^+]$

HRMS $\text{C}_{20}\text{H}_{18}\text{F}_3\text{O}_2\text{N}_2$ $[\text{M}+\text{H}^+]$ requires 375.1320, found 375.1326 (2.6 ppm error)

Cis (1*R*, 3*R*) diastereoisomer (LVT37-2)

mp 97–99 °C

^1H NMR (300 MHz, CDCl_3) δ 3.06 (1H, dd, J 15.0, 8.8 Hz, $\text{CH}_2(10_a)$), 3.26 (1H, dd, J 15.0, 3.9 Hz, $\text{CH}_2(10_b)$), 3.82 (3H, s, $\text{OCH}_3(22)$), 4.00 (1H, dd, J 8.8, 3.9 Hz, $\text{CH}(11)$), 5.96 (1H, s, $\text{CH}(14)$), 7.10–7.21 (3H, m, $\text{ArCH}(1,2)$), 7.35–7.49 (4H, m, $\text{ArCH}(6,16,17)$, NH), 7.56 (1H, dd, J 7.5, 7.5 Hz, $\text{ArCH}(18)$), 7.72 (1H, d, J 7.5 Hz, $\text{ArCH}(19)$)

^{13}C NMR (75 MHz, CDCl_3) δ 25.48 (s, $\text{CH}_2(10)$), 52.30 (s, $\text{OCH}_3(22)$), 53.64 (s, $\text{CH}(14)$), 56.80 (s, $\text{CH}(11)$), 109.36 (s, ArC), 111.0 (s, ArCH), 118.31 (s, ArCH), 119.77 (s, ArCH), 122.14 (s, ArCH), 124.55 (q, $^1J_{\text{C-F}}$ 274 Hz, $\text{CF}_3(21)$), 125.41 (q, $^3J_{\text{C-F}}$ 5.7 Hz, ArCH(19)), 126.9 (s, ArC), 126.99 (s, ArCH), 128.27 (s, ArC), 128.8 (q, $^2J_{\text{C-F}}$ 30 Hz, ArC(20)), 131.6 (s, ArCH), 132.7 (s, ArCH), 134.16 (s, ArC), 136.35 (s, ArC), 140.14 (s, ArC), 172.92 (s, $\text{C=O}(13)$)

^{19}F NMR (376 MHz, CDCl_3) δ -57.1 (Ar- $\text{CF}_3(21)$)

R_f 0.43 (19:1, CH_2Cl_2 : Et_2O)

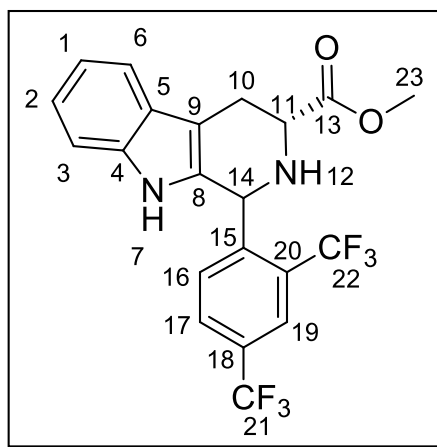
$[\alpha]_D^{25}$ +4.0 (c 1.0, MeOH)

IR ν/cm^{-1} 1165 (C-O, s), 1734 (C=O, s), 3093 (Ar C-H, w)

MS (ESI): 375 $[\text{M}+\text{H}^+]$

HRMS $\text{C}_{20}\text{H}_{18}\text{F}_3\text{O}_2\text{N}_2$ $[\text{M}+\text{H}^+]$ requires 375.1320, found 375.1321 (1.6 ppm error)

Preparation of (3*R*)-Methyl 1-(2,4-bis(trifluoromethyl)phenyl)-2,3,4,9-tetrahydro-1*H*-pyrido[3,4-*b*]indole-3-carboxylate (**LVT38-1,2**):



Following method A using (*R*)-Methyl 2-amino-3-(1*H*-indol-3yl)propanoate (500 mg, 2.29 mmol, 1 eq.) and 2,4-bis(trifluoromethyl) benzaldehyde (0.45 mL, 666 mg, 2.86 mmol, 1.25 eq.) as starting materials. The desired product was purified using column chromatography (SiO₂, 100%, CH₂Cl₂), to afford, eluting first, the *trans* diastereoisomer as a colourless solid (56.0 mg, 0.13 mmol, 6%) and, eluting second, the *cis* diastereoisomer as a colourless solid (41.3 mg, 0.09 mmol, 4%).

Following method B using (*R*)-Methyl 2-amino-3-(1*H*-indol-3yl)propanoate (250 mg, 1.15 mmol, 1 eq.) and 2,4-bis(trifluoromethyl) benzaldehyde (0.24 mL, 355 mg, 1.44 mmol, 1.25 eq.) as starting materials. The desired product was purified using column chromatography (SiO₂, 100% CH₂Cl₂), to afford, eluting first, the *trans* diastereoisomer as a colourless solid (82.4 mg, 0.19 mmol, 37%) and, eluting second, the *cis* diastereoisomer as a colourless solid (70.1 mg, 0.16 mmol, 31%).

Trans (1*S*, 3*R*) diastereoisomer (LVT38-1)

mp 89–93 °C

¹H NMR (300 MHz, CDCl₃) δ 3.28 (1H, dd, *J* 15.5, 5.1 Hz, CH₂(10_a)), 3.34 (1H, dd, *J* 15.5, 5.1 Hz, CH₂(10_b)), 3.72 (3H, s, OCH₃(23)), 4.05 (1H, dd, *J* 5.1, 5.1 Hz, CH(11)), 5.98 (1H, s, CH(14)), 7.13–7.25 (3H, m, ArCH(1,2)), 7.47 (br. s, NH), 7.51 (1H, d, *J* 8.2 Hz, ArCH), 7.58 (1H, d, *J* 8.2 Hz, ArCH(16)), 7.69 (1H, d, *J* 8.2 Hz, ArCH(17)), 7.98 (1H, s, ArCH(19))

¹³C NMR (75 MHz, CDCl₃) δ 23.99 (s, CH₂(10)), 49.82 (s, CH(14)), 52.30 (s, OCH₃(23)), 53.22 (s, CH(11)), 109.11 (s, ArC), 111.13 (s, ArCH), 118.51 (s, ArCH), 119.88 (s, ArCH), 122.53 (s, ArCH), 123.10 (q, ³*J*_{C-F} 4.7 Hz, ArCH(17)), 123.26 (q, ¹*J*_{C-F} 272 Hz, ArCF₃(22)), 126.72 (q, ¹*J*_{C-F} 270 Hz, ArCF₃(21)), 126.74 (s, ArC), 129.00 (q, ³*J*_{C-F} 6.3 Hz, ArCH(19)), 129.58 (q, ²*J*_{C-F} 30 Hz, ArC(20)), 130.57 (q, ²*J*_{C-F} 33 Hz, ArC(18)), 131.62 (s, ArC), 132.23 (s, ArCH), 136.42 (s, ArC), 145.22 (s, ArC), 173.83 (s, C=O(13))

^{19}F NMR (376 MHz, CDCl_3) δ -57.7 (Ar- CF_3) and -62.9 (Ar- CF_3)

R_f 0.18 (100%, CH_2Cl_2)

IR ν/cm^{-1} 1164 (C-O, s), 1742 (C=O, s), 3123 (Ar C-H, w)

MS (ESI): 443 $[\text{M}+\text{H}^+]$

HRMS $\text{C}_{21}\text{H}_{17}\text{F}_6\text{O}_2\text{N}_2$ $[\text{M}+\text{H}^+]$ requires 443.1194, found 443.1204 (2.9 ppm error)

Cis (1*R*, 3*R*) diastereoisomer (LVT38-2)

mp 95–97 °C

^1H NMR (300 MHz, CDCl_3) δ 3.09 (1H, dd, J 15.1, 3.4 Hz, $\text{CH}_2(10_a)$), 3.28 (1H, dd, J 15.1, 11.0 Hz, $\text{CH}_2(10_b)$), 3.83 (3H, s, $\text{OCH}_3(23)$), 4.01 (1H, dd, J 11.0, 3.4 Hz, $\text{CH}(11)$), 5.75 (1H, s, $\text{CH}(14)$), 7.12–7.25 (3H, m, Ar $\text{CH}(1,2)$), 7.34 (br. s, NH), 7.56 (1H, d, J 8.2 Hz, Ar CH), 7.72 (1H, d, J 8.2 Hz, Ar $\text{CH}(16)$), 7.79 (1H, d, J 8.2 Hz, Ar $\text{CH}(17)$), 7.98 (1H, s, Ar $\text{CH}(19)$)

^{13}C NMR (75 MHz, CDCl_3) δ 25.33 (s, $\text{CH}_2(10)$), 52.38 (s, $\text{OCH}_3(23)$), 53.35 (s, $\text{CH}(14)$), 56.54 (s, $\text{CH}(11)$), 109.79 (s, ArC), 111.03 (s, Ar CH), 118.43 (s, Ar CH), 119.99 (s, Ar CH), 122.49 (s, Ar CH), 122.64 (q, $^3J_{\text{C-F}}$ 5.8 Hz, Ar $\text{CH}(17)$), 123.22 (q, $^1J_{\text{C-F}}$ 272 Hz, Ar $\text{CF}_3(22)$), 123.76 (q, $^1J_{\text{C-F}}$ 274 Hz, Ar $\text{CF}_3(21)$), 126.74 (s, ArC), 129.30 (q, $^3J_{\text{C-F}}$ 5.5 Hz, Ar $\text{CH}(19)$), 129.42 (q, $^2J_{\text{C-F}}$ 31 Hz, ArC(20)), 130.80 (q, $^2J_{\text{C-F}}$ 33 Hz, ArC(18)), 123.95 (s, Ar CH), 133.07 (s, ArC), 136.47 (s, ArC), 144.65 (s, ArC), 172.67 (s, C=O(13))

^{19}F NMR (376 MHz, CDCl_3) δ -57.4 (Ar- CF_3) and -62.9 (Ar- CF_3)

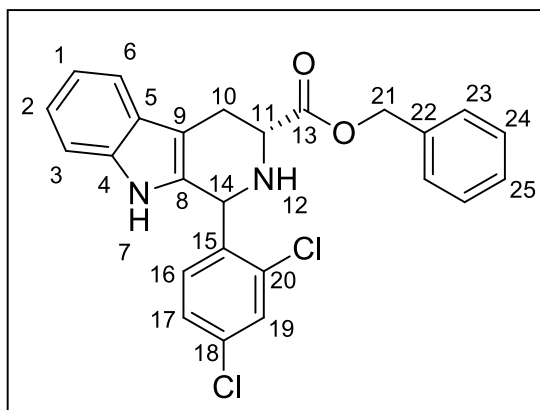
R_f 0.55 (100%, CH_2Cl_2)

IR ν/cm^{-1} 1165 (C-O, s), 1740 (C=O, s), 3159 (Ar C-H, w)

MS (ESI): 443 $[\text{M}+\text{H}^+]$

HRMS C₂₁H₁₇F₆O₂N₂ [M+H⁺] requires 443.1194, found 443.1191 (0.01 ppm error)

Preparation of (3*R*)-Benzyl 1-(2,4-dichlorophenyl)-2,3,4,9-tetrahydro-1*H*-pyrido[3,4-*b*]indole-3-carboxylate (**LVT50-1,2**):



Following method A using (*R*)-Benzyl 2-amino-3-(1*H*-indol-3-yl)propanoate (474 mg, 1.61 mmol, 1 eq.) and 2,4-dichloro benzaldehyde (352 mg, 2.01 mmol, 1.25 eq.) as starting materials. The desired product was purified using column chromatography (SiO₂, 99:1, CH₂Cl₂:MeOH), to afford, eluting first, the *cis* diastereoisomer as an off-white solid (72.2 mg, 0.16 mmol, 13%) and, eluting second, the *trans* diastereoisomer as an off-white solid (67.3 mg, 0.15 mmol, 12%).

Following method B using (*R*)-Benzyl 2-amino-3-(1*H*-indol-3-yl)propanoate (500 mg, 1.70 mmol, 1 eq.) and 2,4-dichloro benzaldehyde (372 mg, 2.13 mmol, 1.25 eq.) as starting materials. The desired product was purified using column chromatography (SiO₂, 99:1, CH₂Cl₂:MeOH), to afford, eluting first, the *cis* diastereoisomer as an off-white solid (241 mg, 0.53 mmol, 31%) and, eluting second, the *trans* diastereoisomer as an off-white solid (267 mg, 0.59 mmol, 35%).

Trans (1*S*, 3*R*) diastereoisomer (**LVT50-1**)

mp 97–100 °C

¹H NMR (300 MHz, CDCl₃) δ 3.15 (1H, dd, *J* 15.3, 6.5 Hz, CH₂(10_a)), 3.27 (1H, dd, *J* 15.3, 5.0 Hz, CH₂(10_b)), 3.91 (1H, dd, *J* 6.5, 5.0 Hz, CH(11)), 5.15 (2H, dd, *J* 12.3, 2.7 Hz, CH₂(21)), 5.87 (1H, s, CH(14)), 7.10–7.22 (3H, m, ArCH(1,2)), 7.29–7.31 (6H, m, ArCH(16,23,24,25)), 7.46 (1H, d, *J* 6.9 Hz, ArCH), 7.56 (1H, d, *J* 6.9 Hz, ArCH), 7.67 (1H, s, ArCH(19)), 8.01 (1H, br. s, NH)

¹³C NMR (75 MHz, CDCl₃) δ 25.42 (CH₂(10)), 51.17 (CH(14)), 52.62 (CH(11)), 67.13 (CH₂(21)), 109.32 (ArC), 111.09 (ArCH), 118.43 (ArCH(17)), 119.89 (ArCH), 122.55 (ArCH), 126.63 (ArCH), 127.40 (ArC), 128.19 (ArCH), 128.42 (ArCH(25)), 128.61 (ArCH(24)), 128.69 (ArCH(23)), 129.79 (ArC), 130.61 (ArCH(19)), 131.22 (ArCH), 134.54 (ArC), 134.92 (ArC), 135.32 (ArC), 136.39 (ArC), 136.54 (ArC), 173.29 (C=O(13))

R_f 0.21 (99:1, CH₂Cl₂/MeOH)

[α]_D²⁵ +12.0 (*c* 1.0, MeOH)

IR ν/ cm⁻¹ 1734 (C=O, s), 3179 (Ar C-H, w)

MS (ESI): 451/453 [M+H⁺]

HRMS C₂₅H₂₁³⁵Cl₂N₂O₂ [M+H⁺] requires 451.0980, found 451.1003 (4.2 ppm error)

Cis (1*R*, 3*R*) diastereoisomer (LVT50-2)

mp 161–163 °C

¹H NMR (300 MHz, CDCl₃) δ 3.03 (1H, dd, *J* 15.0, 11.0 Hz, CH₂(10_a)), 3.26 (1H, dd, *J* 15.0, 4.0 Hz, CH₂(10_b)), 4.03 (1H, dd, *J* 11.0, 4.0 Hz, CH(11)), 5.23 (1H, d, *J* 12.3, 6.7 Hz, CH₂(21_a)), 5.25 (1H, d, *J* 12.3, 6.7 Hz, CH₂(21_b)), 5.79 (1H, s, CH(14)), 7.09–7.23 (3H, m,

ArCH(1,2)), 7.38–7.42 (6H, m, ArCH(16,23,24,25)), 7.47 (1H, d, *J* 5.0 Hz, ArCH), 7.52–7.55 (2H, m, ArCH(17,19))

¹³C NMR (75 MHz, CDCl₃) δ 25.41 (CH₂(10)), 53.85 (CH(14)), 56.68 (CH(11)), 67.00 (CH₂(21)), 109.33 (ArC), 110.94 (ArCH), 118.30 (ArCH(17)), 119.78 (ArCH), 122.20 (ArCH), 126.89 (ArC), 128.03 (ArCH), 128.34 (ArCH(25)), 128.48 (ArCH(24)), 128.67 (ArCH(23)), 129.39 (ArCH(19)), 131.47 (ArCH), 133.22 (ArC), 134.08 (ArC), 134.63 (ArC), 135.51 (ArC), 136.21 (ArC), 137.32 (ArC), 172.39 (C=O(13))

R_f 0.62 (99:1, CH₂Cl₂/MeOH)

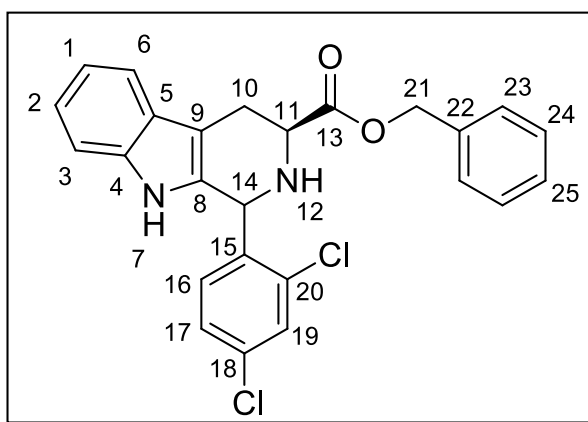
[α]_D²⁵ –12.0 (*c* 1.0, MeOH)

IR ν/ cm^{–1} 1725 (C=O, s), 3323 (Ar C-H, w)

MS (ESI): 451/453 [M+H⁺]

HRMS C₂₅H₂₁³⁵Cl₂N₂O₂ [M+H⁺] requires 451.0980, found 451.0957 (4.3 ppm error)

Preparation of (3*S*)-Benzyl 1-(2,4-dichlorophenyl)-2,3,4,9-tetrahydro-1*H*-pyrido[3,4-*b*]indole-3-carboxylate (**LVT51-1,2**):



Following method A using (*S*)-Benzyl 2-amino-3-(1*H*-indol-3-yl)propanoate (578 mg, 1.91 mmol, 1 eq.) and 2,4-dichloro benzaldehyde (430 mg, 2.46 mmol, 1.25 eq.) as starting materials. The desired product was purified using column chromatography (SiO₂, 99:1, CH₂Cl₂/MeOH), to afford, eluting first, the *cis* diastereoisomer as an off-white solid (109 mg, 0.24 mmol, 20%) and, eluting second, the *trans* diastereoisomer as a clear glass solid (81.4 mg, 0.18 mmol, 15%).

Following method B using (*S*)-Benzyl 2-amino-3-(1*H*-indol-3-yl)propanoate (500 mg, 1.70 mmol, 1 eq.) and 2,4-dichloro benzaldehyde (372 mg, 2.13 mmol, 1.25 eq.) as starting materials. The desired product was purified using column chromatography (SiO₂, 99:1, CH₂Cl₂/MeOH), to afford, eluting first, the *cis* diastereoisomer as an off-white solid (273 mg, 0.60 mmol, 30%) and, eluting second, the *trans* diastereoisomer as a clear glass solid (289 mg, 0.64 mmol, 32%).

Trans (1*R*, 3*S*) diastereoisomer (LVT51-1)

mp 96–98 °C

¹H NMR (300 MHz, CDCl₃) δ 3.15 (1H, dd, *J* 15.4, 7.1 Hz, CH₂(10_a)), 3.27 (1H, dd, *J* 15.4, 5.1 Hz, CH₂(10_b)), 3.91 (1H, dd, *J* 7.1, 5.1 Hz, CH(11)), 5.17 (1H, d, *J* 12.6, 2.5 Hz, CH₂(21_a)), 5.20 (1H, d, *J* 12.6, 2.5 Hz, CH₂(21_b)), 5.87 (1H, s, CH(14)), 6.94 (1H, s, NH), 7.09–7.21 (3H, m, ArCH(1,2)), 7.28–7.31 (7H, m, ArCH), 7.45 (1H, d, *J* 7.0 Hz, ArCH(17)), 7.56 (1H, d, *J* 7.0 Hz, ArCH(19)), 7.67 (1H, br. s, NH)

¹³C NMR (75 MHz, CDCl₃) δ 24.75 (CH₂(10)), 51.06 (CH(14)), 52.67 (CH(11)), 66.84 (CH₂(21)), 109.52 (ArC), 110.96 (ArCH), 118.40 (ArCH(17)), 119.76 (ArCH), 122.32 (ArCH), 126.81 (ArC), 127.27 (ArCH), 127.97 (ArCH), 128.13 (ArCH(25)), 128.33 (ArCH(24)), 128.49 (ArCH(23)), 128.58 (ArCH(19)), 129.69 (ArCH), 130.96 (ArCH),

131.64 (ArC), 134.33 (ArC), 134.38 (ArC), 135.54 (ArC), 136.24 (ArC), 137.92 (ArC),
173.17 (C=O(13))

R_f 0.27 (99:1, CH₂Cl₂/MeOH)

[α]_D²⁵ +16.0 (c 1.0, MeOH)

IR ν/ cm⁻¹ 1728 (C=O, s), 3383 (Ar C-H, w)

MS (ESI): 451/453 [M+H⁺]

HRMS C₂₅H₂₁³⁵Cl₂N₂O₂ [M+H⁺] requires 451.0980, found 451.0982 (1.7 ppm error)

Cis (1*S*, 3*S*) diastereoisomer (LVT51-2)

mp 175–178 °C

¹H NMR (300 MHz, CDCl₃) δ 3.01 (1H, dd, *J* 14.2, 10.9 Hz, CH₂(10_a)), 3.25 (1H, dd, *J* 14.2, 4.0 Hz, CH₂(10_b)), 4.02 (1H, dd, *J* 10.9, 4.0 Hz, CH(11)), 5.24 (1H, d, *J* 9.5, 6.8 Hz, CH₂(21_a)), 5.27 (2H, dd, *J* 9.5, 6.8 Hz, CH₂(21_b)), 5.79 (1H, s, CH(14)), 7.08–7.23 (4H, m, ArCH(1,2,23)), 7.37–7.41 (6H, m, ArCH(18,19,20)), 7.47 (1H, d, *J* 7.0 Hz, ArCH(17)), 7.53 (1H, d, *J* 8.3 Hz, ArCH(19)), 7.59 (1H, br. s, NH)

¹³C NMR (75 MHz, CDCl₃) δ 25.42 (CH₂(10)), 53.90 (CH(14)), 56.70 (CH(11)), 67.01 (CH₂(21)), 109.34 (ArC), 110.95 (ArCH), 118.31 (ArCH(17)), 119.80 (ArCH), 122.20 (ArCH), 126.91 (ArC), 128.05 (ArCH), 128.35 (ArCH(25)), 128.49 (ArCH(24)), 128.69 (ArCH(23)), 129.41 (ArCH(19)), 131.42 (ArCH), 131.48 (ArCH), 133.24 (ArC), 134.08 (ArC), 134.65 (ArC), 135.53 (ArC), 136.21 (ArC), 137.33 (ArC), 172.39 (C=O(13))

R_f 0.61 (99:1, CH₂Cl₂/MeOH)

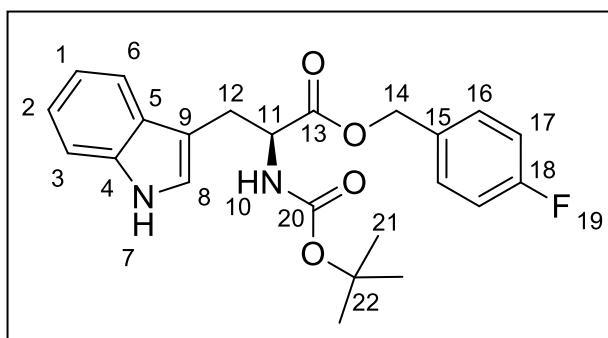
[α]_D²⁵ –16.0 (c 1.0, MeOH)

IR ν/ cm⁻¹ 1724 (C=O, s), 3429 (Ar C-H, w)

MS (ESI): 451/453 [M+H⁺]

HRMS C₂₅H₂₁³⁵Cl₂N₂O₂ [M+H⁺] requires 451.0980, found 451.0983 (1.7 ppm error)

Preparation of (S)-4-Fluorobenzyl 2-((*tert*-butoxycarbonyl)amino)-3-(1*H*-indol-3-yl)propanoate (**LVT90**):



N-((*Tert*-butoxy)carbonyl)-L-tryptophan (409 mg, 1.35 mmol, 1 eq.) was dissolved in methanol (6 mL) and water (1 mL). Cs₂CO₃ (219 mg, 0.68 mmol, 0.5 eq.) was dissolved separately in water (4 mL) and then added into the main reaction mixture. The reaction mixture was azeotroped with DMF (3 × 2 mL) and then DMF (10 mL) added under a nitrogen atmosphere. Then, 4-fluorobenzyl bromide (0.33 mL, 500 mg, 2.70 mmol, 2 eq.) was added dropwise *via* syringe and the reaction left to stir overnight at room temperature. The DMF was removed under reduced pressure and the remaining mixture was partitioned between EtOAc (25 mL) and water (25 mL). The organics were extracted with further EtOAc (3 × 75 mL), washed with saturated aqueous brine (50 mL), dried over MgSO₄, filtered and concentrated under reduced pressure. The crude product was purified using column chromatography (SiO₂, 97:3, CH₂Cl₂:Et₂O). The product **LVT90** is a colourless solid (312 mg, 0.76 mmol, 56%).

Data for **LVT90**

mp 127–129 °C

^1H (300 MHz, CDCl_3) δ 1.41 (9H, s, $\text{CH}_3(21)$), 3.26 (2H, d, J 5.5 Hz, $\text{CH}_2(12)$), 4.67 (1H, dd, J 13.5, 5.5 Hz, $\text{CH}(11)$), 4.94 (1H, d, J 12.2 Hz, $\text{CH}_2(14_a)$), 5.01 (1H, d, J 12.2 Hz, $\text{CH}_2(14_b)$), 5.16 (1H, d, J 8.0 Hz, $\text{NH}(10)$), 6.78 (1H, s, $\text{CH}(8)$), 6.95 (2H, dd, J 8.5, 8.5 Hz, $\text{ArCH}(1,2)$), 7.06–7.18 (4H, m, $\text{ArCH}(16,17)$), 7.30 (1H, d, J 7.7 Hz, ArCH), 7.52 (1H, d, J 7.7 Hz, ArCH), 8.48 (1H, br. s, $\text{NH}(7)$)

^{13}C (75 MHz, CDCl_3) δ 28.02 (s, $\text{CH}_2(12)$), 28.37 (s, $\text{CH}_3(21)$), 54.42 (s, $\text{CH}(11)$), 66.39 (s, $\text{CH}_2(14)$), 80.09 (s, $\text{C}(22)$), 109.68 (s, ArC), 111.39 (s, ArCH), 115.31 (s, ArCH), 115.59 (s, ArCH), 118.70 (s, ArCH), 119.58 (s, $\text{ArCH}(16)$), 122.14 (s, ArCH), 123.07 (s, $\text{ArCH}(8)$), 127.61 (s, ArC), 130.41 (d, $^2J_{\text{C-F}}$ 8.3 Hz, $\text{ArCH}(17)$), 131.20 (s, $\text{ArC}(15)$), 136.23 (s, $\text{ArC}(9)$), 155.45 (s, $\text{C=O}(20)$), 162.68 (d, $^1J_{\text{C-F}}$ 247 Hz, $\text{ArC}(18)$), 172.37 (s, $\text{C=O}(13)$)

^{19}F (376 MHz, CDCl_3) δ –113.3 (s, $\text{ArC-F}(19)$)

R_f 0.38 (97:3, CH_2Cl_2 : Et_2O)

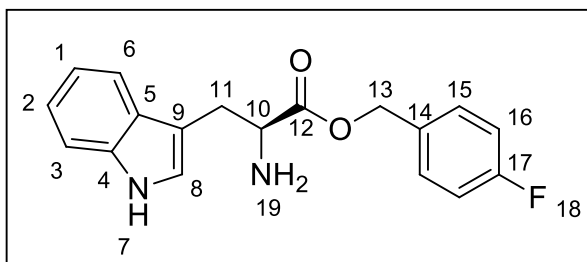
$[\alpha]_D^{29}$ –3.0 (c 1.0, MeOH)

IR ν/cm^{-1} 1178 (C-O, s), 1698 (C=O, s), 1726 (C=O, s), 3156 (Ar C-H, w), 3353 (N-H, w)

MS (ESI): 413 $[\text{M}+\text{H}^+]$

HRMS $\text{C}_{23}\text{H}_{26}\text{FN}_2\text{O}_4$ $[\text{M}+\text{H}^+]$ requires 413.1871, found 413.1875 (0.9 ppm error)

Preparation of (S)-4-Fluorobenzyl 2-amino-3-(1*H*-indol-3-yl)propanoate (**LVT90a**):



(*S*)-4-Fluorobenzyl 2-((*tert*-butoxycarbonyl)amino)-3-(1*H*-indol-3-yl)propanoate (**LVT90**) (312 mg, 0.70 mmol, 1 eq.) was dissolved in CH₂Cl₂ (10 mL) and MeOH (0.1 mL). TFA (8 mL) was added portionwise *via* syringe and the reaction left to stir for 1 h under a nitrogen atmosphere. The reaction mixture was azeotroped with CH₂Cl₂ (2 × 5 mL) and then partitioned between CH₂Cl₂/saturated aqueous NaHCO₃ (50 mL/50 mL). The organics were extracted with CH₂Cl₂ (2 × 75 mL), washed with saturated aqueous brine (75 mL), dried over MgSO₄, filtered and concentrated under reduced pressure. The product **LVT90a** is a glass (156 mg, 0.50 mmol, 71%).

Data for **LVT90a**

¹H (300 MHz, CDCl₃) δ 3.06 (1H, dd, *J* 14.3, 7.6 Hz, CH₂(11_a)), 3.25 (1H, dd, *J* 14.3, 7.6 Hz, CH₂(11_b)), 3.84 (1H, t, *J* 7.6 Hz, CH(10)), 5.04 (2H, s, CH₂(13)), 6.90 (1H, s, ArCH(8)), 6.99 (2H, dd, *J* 8.6, 8.6 Hz, ArCH(1,2)), 7.09–7.22 (4H, m, ArCH(15,16)), 7.38 (1H, d, *J* 7.7 Hz, ArCH), 7.57 (1H, d, *J* 7.7 Hz, ArCH), 8.44 (1H, br. s, NH(7))

¹³C (75 MHz, CDCl₃) δ 30.73 (s, CH₂(11)), 55.01 (s, CH(10_{ab})), 66.08 (s, CH₂(13)), 110.65 (s, ArC), 111.34 (s, ArCH), 115.36 (s, ArCH), 115.65 (s, ArCH), 118.74 (s, ArCH), 119.53 (s, ArCH), 122.15 (s, ArCH), 123.16 (s, ArCH(8)), 127.44 (s, ArC), 130.40 (d, ²*J*_{C-F} 8.3 Hz, ArCH(16)), 131.47 (d, ⁴*J*_{C-F} 3.2 Hz, ArC(14)), 136.28 (s, ArC(9)), 162.67 (d, ¹*J*_{C-F} 247 Hz, ArC(17)), 175.13 (s, C=O(12))

¹⁹F (376 MHz, CDCl₃) δ –113.3 (s, Ar-F(18))

R_f 0.13 (97:3, CH₂Cl₂:Et₂O)

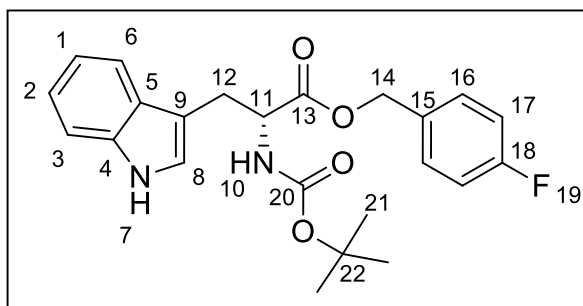
[α]_D²⁷ +16.0 (*c* 1.0, MeOH)

IR ν /cm⁻¹ 1215 (C-O, s), 1724 (C=O, s), 3159 (Ar C-H, w), 3273 (N-H, w)

MS (ESI): 313 [M+H⁺]

HRMS C₁₈H₁₈FN₂O₂ [M+H⁺] requires 313.1352, found 313.1367 (4.6 ppm error)

Preparation of (*R*)-4-Fluorobenzyl 2-((*tert*-butoxycarbonyl)amino)-3-(1*H*-indol-3-yl)propanoate (**LVT91**):



N-((*Tert*-Butoxy)carbonyl)-D-tryptophan (421 mg, 1.38 mmol, 1 eq.) was dissolved in methanol (6 mL) and water (1 mL). Then, Cs₂CO₃ (224 mg, 0.69 mmol, 0.5 eq.) was dissolved separately in water (4 mL) and then added into the main reaction mixture. The reaction mixture was azeotroped with DMF (3 × 2 mL) and then anhydrous DMF (10 mL) was added under a nitrogen atmosphere. Next, 4-fluorobenzyl bromide (0.34 mL, 516 mg, 2.76 mmol, 2 eq.) was added dropwise *via* syringe and the reaction left to stir overnight at room temperature. The DMF was removed under reduced pressure and the remaining mixture was partitioned between EtOAc (25 mL) and water (25 mL). The organics were extracted with further EtOAc (3 × 75 mL), washed with saturated aqueous brine (50 mL), dried over MgSO₄, filtered and concentrated under reduced pressure. The crude product was

purified using column chromatography (SiO₂, 97:3, CH₂Cl₂:Et₂O). The product **LVT91** is a colourless solid (361 mg, 0.88 mmol, 64%).

Data for LVT91

mp 126–129 °C

¹H (300 MHz, CDCl₃) δ 1.41 (9H, s, CH₃(21)), 3.26 (2H, d, *J* 5.5 Hz, CH₂(12)), 4.70 (1H, dd, *J* 13.6, 5.5 Hz, CH(11)), 4.99 (1H, d, *J* 12.0, 12.0 Hz, CH₂(14_a)), 5.02 (1H, d, *J* 12.0, 12.0 Hz, CH₂(14_b)), 5.12 (1H, d, *J* 8.0 Hz, NH(10)), 6.81 (1H, s, CH(8)), 6.97 (2H, dd, *J* 8.6, 8.6 Hz, ArCH(1,2)), 7.07–7.20 (4H, m, ArCH(16,17)), 7.32 (1H, d, *J* 7.8 Hz, ArCH), 7.53 (1H, d, *J* 7.8 Hz, ArCH), 8.29 (1H, br. s, NH(7))

¹³C (75 MHz, CDCl₃) δ 28.01 (s, CH₂(12)), 28.35 (s, CH₃(21)), 54.34 (s, CH(11_{ab})), 66.36 (s, CH₂(14)), 80.02 (s, C(22)), 109.84 (s, ArC), 111.29 (s, ArCH), 115.30 (s, ArCH), 115.58 (s, ArCH), 118.73 (s, ArCH), 119.62 (s, ArCH(16)), 122.19 (s, ArCH(16)), 122.93 (s, ArCH(8)), 127.62 (s, ArC), 130.41 (d, ²*J*_{C-F} 8.2 Hz, ArCH(17)), 131.18 (d, ⁴*J*_{C-F} 3.1 Hz, ArC(15)), 136.15 (s, ArC), 155.34 (s, C=O(20)), 162.67 (d, ¹*J*_{C-F} 247 Hz, ArC(18)), 172.28 (s, C=O(13))

¹⁹F (376 MHz, CDCl₃) δ –113.3 (s, Ar-F(19))

R_f 0.49 (97:3, CH₂Cl₂:Et₂O)

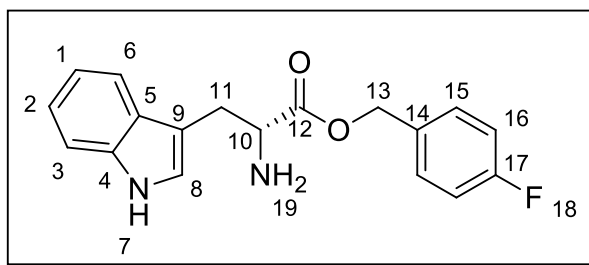
[α]_D²⁹ +3.0 (*c* 1.0, MeOH)

IR ν/ cm^{–1} 1168 (C–O, s), 1698 (C=O, s), 1725 (C=O, s), 3158 (Ar C–H, w), 3319 (N–H, w)

MS (ESI): 413 [M+H⁺]

HRMS C₂₃H₂₆FN₂O₄ [M+H⁺] requires 413.1871, found 413.1874 (0.7 ppm error)

Preparation of (*R*)-4-Fluorobenzyl 2-amino-3-(1*H*-indol-3-yl)propanoate (**LVT91a**):



(*R*)-4-Fluorobenzyl 2-((*tert*-butoxycarbonyl)amino)-3-(1*H*-indol-3-yl)propanoate (**LVT91**) (361 mg, 0.81 mmol, 1 eq.) was dissolved in CH₂Cl₂ (10 mL) and MeOH (0.1 mL). TFA (8 mL) was added portionwise *via* syringe and the reaction left to stir for 1 h under a nitrogen atmosphere. The reaction mixture was azeotroped with CH₂Cl₂ (2 × 5 mL) and then partitioned between CH₂Cl₂/saturated aqueous NaHCO₃ (50 mL/50 mL). The organics were extracted with CH₂Cl₂ (2 × 75 mL), washed with saturated aqueous brine (75 mL), dried over MgSO₄, filtered and concentrated under reduced pressure. The product **LVT91a** is a glass like solid (228 mg, 0.73 mmol, 90%).

Data for **LVT91a**

¹H (300 MHz, CDCl₃) δ 3.07 (1H, dd, *J* 14.2, 7.3 Hz, CH₂(11_a)), 3.25 (1H, dd, *J* 14.2, 5.1 Hz, CH₂(11_b)), 3.86 (1H, dd, *J* 7.3, 5.1 Hz, CH(10)), 5.05 (2H, s, CH₂(13_{ab})), 6.89 (1H, s, ArCH(8)), 6.99 (2H, dd, *J* 8.6, 8.6 Hz, ArCH(1,2)), 7.07–7.21 (4H, m, ArCH(15,16)), 7.31 (1H, d, *J* 7.3 Hz, ArCH), 7.58 (1H, d, *J* 7.3 Hz, ArCH), 8.46 (1H, br. s, NH(7))

¹³C (75 MHz, CDCl₃) δ 30.78 (s, CH₂(11)), 55.04 (s, CH(10_{ab})), 66.08 (s, CH₂(13)), 110.66 (s, ArC), 111.34 (s, ArCH), 115.36 (s, ArCH), 115.65 (s, ArCH), 118.75 (s, ArCH), 119.52 (s, ArCH), 122.14 (s, ArCH), 123.15 (s, ArCH(8)), 127.45 (s, ArC), 130.39 (d, ²*J*_{C-F} 8.7 Hz, ArCH(16)), 131.48 (d, ⁴*J*_{C-F} 3.5 Hz, ArC(14)), 136.29 (s, ArC), 162.67 (d, ¹*J*_{C-F} 247 Hz, ArC(17)), 175.21 (s, C=O(12))

¹⁹F (376 MHz, CDCl₃) δ –113.3 (s, Ar-F(18))

R_f 0.15 (97:3, CH₂Cl₂:Et₂O)

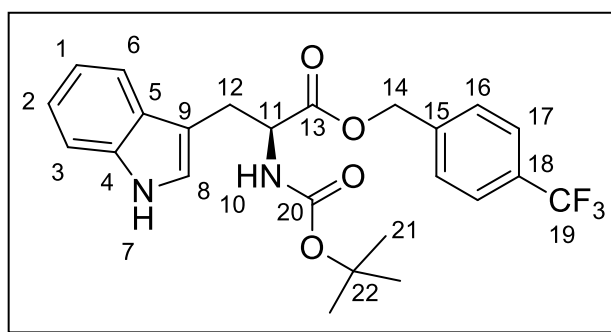
[α]_D²⁷ -16.0 (*c* 1.0, MeOH)

IR ν /cm⁻¹ 1173 (C-O, s), 1723 (C=O, s), 3153 (ArC-H, w), 3254 (N-H, w)

MS (ESI): 313 [M+H⁺]

HRMS C₁₈H₁₈FN₂O₂ [M+H⁺] requires 313.1352, found 313.1358 (1.9 ppm error)

Preparation of (*S*)-4-(Trifluoromethyl)benzyl 2-((*tert*-butoxycarbonyl)amino)-3-(1*H*-indol-3-yl)propanoate (**LVT92**):



N-((*Tert*-Butoxy)carbonyl)-L-tryptophan (438 mg, 1.44 mmol, 1 eq.) was dissolved in methanol (6 mL) and water (1 mL). Cs₂CO₃ (234 mg, 0.72 mmol, 0.5 eq.) was dissolved separately in water (4 mL) and then added into the main reaction mixture. The reaction mixture was azeotroped with DMF (3 × 2 mL) and then DMF (10 mL) added under a nitrogen atmosphere. 4-(Trifluoromethyl)benzyl bromide (0.45 mL, 696 mg, 2.88 mmol, 2 eq.) was added dropwise *via* syringe and the reaction left to stir overnight at room temperature. The DMF was removed under reduced pressure and the remaining mixture was partitioned between EtOAc (25 mL) and water (25 mL). The organics were extracted with further EtOAc (3 × 75 mL), washed with saturated aqueous brine (50 mL), dried over MgSO₄, filtered and concentrated under reduced pressure. The crude product was purified

using column chromatography (SiO₂, 97:3, CH₂Cl₂:Et₂O). The product **LVT92** is a colourless solid (511 mg, 1.10 mmol, 77%).

Data for LVT92

mp 143–146 °C

¹H (300 MHz, CDCl₃) δ 1.42 (9H, s, CH₃(21)), 3.28 (2H, d, *J* 5.7 Hz, CH₂(12)), 4.70 (1H, dd, *J* 13.8, 5.7 Hz, CH(11)), 5.04 (1H, d, *J* 12.5, 12.5 Hz, CH₂(14_a)), 5.07 (1H, d, *J* 12.5, 12.5 Hz, CH₂(14_b)), 5.11 (1H, d, *J* 7.3 Hz, NH(10)), 6.86 (1H, s, CH(8)), 7.10 (2H, dd, *J* 7.4, 7.4 Hz, ArCH(1,2)), 7.17–7.25 (4H, m, ArCH(16,17)), 7.33 (1H, d, *J* 8.0 Hz, ArCH), 7.51–7.55 (2H, m, ArCH(17)), 8.19 (1H, br. s, NH(7))

¹³C (75 MHz, CDCl₃) δ 28.10 (s, CH₂(12)), 28.32 (s, CH₃(21)), 54.31 (s, CH(11_{ab})), 66.00 (s, CH₂(14)), 80.09 (s, C(22)), 109.89 (s, ArC), 111.27 (s, ArCH), 118.71 (s, ArCH), 119.70 (s, ArCH), 122.30 (s, ArCH), 122.84 (s, ArCH(8)), 124.01 (q, ¹*J*_{C-F} 272 Hz, ArCF₃(19)), 125.45 (q, ³*J*_{C-F} 3.5 Hz, ArCH(17)), 128.19 (s, ArCH(16)), 130.33 (q, ²*J*_{C-F} 33 Hz, ArC(18)), 136.14 (s, ArC), 139.23 (s, ArC(15)), 155.31 (s, C=O(20)), 172.23 (s, C=O(13))

¹⁹F (376 MHz, CDCl₃) δ –62.5 (s, Ar-CF₃(19))

R_f 0.66 (97:3, CH₂Cl₂:Et₂O)

[α]_D²⁷ –1.0 (*c* 1.0, MeOH)

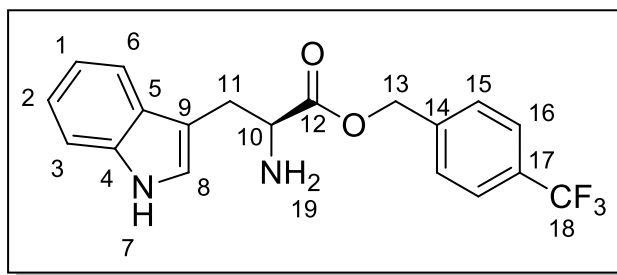
IR ν /cm^{–1} 1093 (C–O, s), 1675 (C=O, s), 1726 (C=O, s), 3221 (Ar C–H, w), 3298 (N–H, w)

MS (ESI): 463 [M+H⁺]

HRMS C₂₄H₂₆F₃N₂O₄ [M+H⁺] requires 463.1845, found 463.1840 (0.2 ppm error)

Analysis calculated for C₂₄H₂₅F₃N₂O₄: C, 62.33%; H, 5.45%; N 6.06%. Found C, 62.12%; H, 5.36%; N, 5.91%.

Preparation of (S)-4-(Trifluoromethyl)benzyl 2-amino-3-(1*H*-indol-3-yl)propanoate (**LVT92a**):



(S)-4-(Trifluoromethyl)benzyl 2-((*tert*-butoxycarbonyl)amino)-3-(1*H*-indol-3-yl)propanoate (**LVT92**) (511 mg, 1.10 mmol, 1 eq.) was dissolved in CH₂Cl₂ (10 mL) and MeOH (0.1 mL). TFA (8 mL) was added portionwise *via* syringe and the reaction left to stir for 1 h under a nitrogen atmosphere. The reaction mixture was azeotroped with CH₂Cl₂ (2 × 5 mL) and then partitioned between CH₂Cl₂/ saturated aqueous NaHCO₃ (50 mL/50 mL). The organics were extracted with CH₂Cl₂ (2 × 75 mL), washed with saturated aqueous brine (75 mL), dried over MgSO₄, filtered and concentrated under reduced pressure. The product **LVT92a** is a glass like solid (321 mg, 0.89 mmol, 81%).

Data for **LVT92a**

¹H (300 MHz, CDCl₃) δ 3.10 (1H, dd, *J* 14.2, 6.5 Hz, CH₂(11_a)), 3.27 (1H, dd, *J* 14.2, 5.2 Hz, CH₂(11_b)), 3.91 (1H, dd, *J* 6.5, 5.2 Hz, CH(10)), 5.12 (2H, s, CH₂(13_{ab})), 6.93 (1H, s, ArCH(8)), 7.10 (1H, dd, *J* 7.4, 7.4 Hz, ArCH), 7.19 (1H, dd, *J* 7.4, 7.4 Hz ArCH), 7.24–7.34 (3H, m, ArCH(16)), 7.53–7.60 (3H, m, ArCH(15)), 8.36 (1H, br. s, NH(7))

¹³C (75 MHz, CDCl₃) δ 30.93 (s, CH₂(11)), 55.08 (s, CH(10_{ab})), 65.75 (s, CH₂(13)), 110.70 (s, ArC), 111.34 (s, ArCH), 118.72 (s, ArCH), 119.58 (s, ArCH), 122.22 (s, ArCH), 123.08 (s, ArCH(8)), 125.51 (q, ³*J*_{C-F} 3.7 Hz, ArCH(16)), 126.97 (q, ¹*J*_{C-F} 272 Hz, ArCF₃(18)), 127.40 (s, ArC), 128.23 (s, ArCH), 130.34 (q, ²*J*_{C-F} 32 Hz, ArCH(17)), 136.28 (s, ArC), 139.53 (s, ArC(14)), 175.14 (s, C=O(12))

^{19}F (376 MHz, CDCl_3) δ -62.5 (s, Ar- CF_3 (18))

R_f 0.13 (97:3, CH_2Cl_2 : Et_2O)

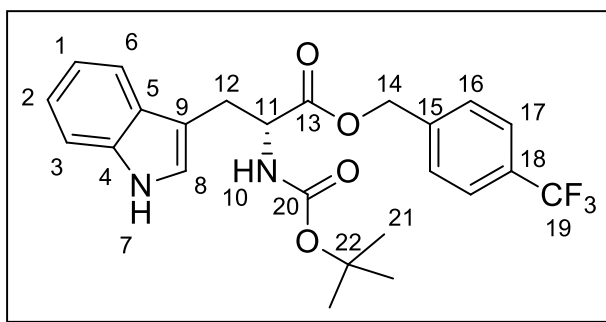
$[\alpha]_D^{29} +21.0$ (c 1.0, MeOH)

IR ν/cm^{-1} 1164 (C-O, s), 1721 (C=O, s), 3166 (Ar C-H, w), 3234 (N-H, w)

MS (ESI): 363 $[\text{M}+\text{H}^+]$

HRMS $\text{C}_{19}\text{H}_{18}\text{F}_3\text{N}_2\text{O}_2$ $[\text{M}+\text{H}^+]$ requires 363.1320, found 363.1316 (0.1 ppm error)

Preparation of (*R*)-4-(Trifluoromethyl)benzyl 2-((*tert*-butoxycarbonyl)amino)-3-(1*H*-indol-3-yl)propanoate (**LVT93**):



N-((*Tert*-Butoxy)carbonyl)-D-tryptophan (402 mg, 1.32 mmol, 1 eq.) was dissolved in methanol (6 mL) and water (1 mL). Cs_2CO_3 (215 mg, 0.66 mmol, 0.5 eq.) was dissolved separately in water (4 mL) and then added into the main reaction mixture. The reaction mixture was azeotroped with DMF (3×2 mL) and then DMF (10 mL) added under a nitrogen atmosphere. 4-(Trifluoromethyl)benzyl bromide (0.41 mL, 634 mg, 2.64 mmol, 2 eq.) was added dropwise *via* syringe and the reaction left to stir overnight at room temperature. The DMF was removed under reduced pressure and the remaining mixture was partitioned between EtOAc (25 mL) and water (25 mL). The organics were extracted with further EtOAc (3×75 mL), washed with saturated aqueous brine (50 mL), dried over

MgSO₄, filtered and concentrated under reduced pressure. The crude product was purified using column chromatography (SiO₂, 97:3, CH₂Cl₂:Et₂O). The product **LVT93** is a colourless solid (479 mg, 0.97 mmol, 74%).

Data for LVT93

mp 102–105 °C

¹H (300 MHz, CDCl₃) δ 1.42 (9H, s, CH₃(21)), 3.27 (2H, d, *J* 5.7 Hz, CH₂(12)), 4.63 (1H, d, *J* 13.8 Hz, CH(11a)), 4.75 (1H, d, *J* 5.7 Hz, CH(11b)), 5.04 (1H, d, *J* 12.6, 12.6 Hz, CH₂(14_a)), 5.08 (1H, d, *J* 12.6, 12.6 Hz, CH₂(14_b)), 5.13 (1H, d, *J* 7.3 Hz, NH(10)), 6.85 (1H, s, CH(8)), 7.07–7.23 (4H, m, ArCH(1,2)), 7.32 (1H, d, *J* 8.0 Hz, ArCH), 7.49–7.54 (4H, m, ArCH(16,17)), 8.29 (1H, br. s, NH(7))

¹³C (75 MHz, CDCl₃) δ 28.10 (s, CH₂(12)), 28.33 (s, CH₃(21)), 54.35 (s, CH(11_{ab})), 66.03 (s, CH₂(14)), 80.01 (s, C(22)), 109.79 (s, ArC), 111.34 (s, ArCH), 118.68 (s, ArCH), 119.68 (s, ArCH), 122.27 (s, ArCH), 122.92 (s, ArCH(8)), 125.441 (q, ³*J*_{C-F} 3.6 Hz, ArCH(17)), 125.45 (q, ¹*J*_{C-F} 272 Hz, ArCH(19)), 127.52 (s, ArC), 128.19 (s, ArCH(16)), 130.32 (q, ²*J*_{C-F} 32 Hz, ArC(18)), 136.19 (s, ArC), 139.24 (s, ArC(15)), 155.37 (s, C=O(20)), 172.28 (s, C=O(13))

¹⁹F (376 MHz, CDCl₃) δ –62.5 (s, Ar-CF₃(19))

R_f 0.53 (97:3, CH₂Cl₂:Et₂O)

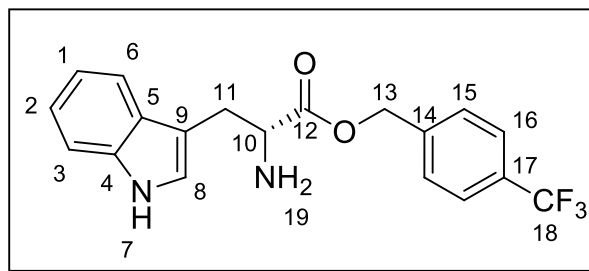
[α]_D²⁹ +1.0 (*c* 1.0, MeOH)

IR ν/ cm⁻¹ 1173 (C-O, s), 1676 (C=O, s), 1726 (C=O, s), 3186 (Ar C-H, w), 3353 (N-H, w)

MS (ESI): 463 [M+H⁺]

HRMS C₂₄H₂₆F₃N₂O₄ [M+H⁺] requires 463.1845, found 463.1851 (2.3 ppm error)

Preparation of (*R*)-4-(Trifluoromethyl)benzyl 2-amino-3-(1*H*-indol-3-yl)propanoate (**LVT93a**):



(*R*)-4-(Trifluoromethyl)benzyl 2-((*tert*-butoxycarbonyl)amino)-3-(1*H*-indol-3-yl)propanoate (**LVT93**) (479 mg, 1.32 mmol, 1 eq.) was dissolved in CH₂Cl₂ (10 mL) and MeOH (0.1 mL). TFA (8 mL) was added portionwise *via* syringe and the reaction left to stir for 1 h under a nitrogen atmosphere. The reaction mixture was azeotroped with CH₂Cl₂ (2 × 5 mL) and then partitioned between CH₂Cl₂/saturated aqueous NaHCO₃ (50 mL/50 mL). The organics were extracted with CH₂Cl₂ (2 × 75 mL), washed with saturated aqueous brine (75 mL), dried over MgSO₄, filtered and concentrated under reduced pressure. The product **LVT93a** is a glass like solid (378 mg, 1.04 mmol, 79%).

Data for **LVT93a**

¹H (300 MHz, CDCl₃) δ 3.10 (1H, dd, *J* 14.3, 7.2 Hz, CH₂(11_a)), 3.27 (1H, dd, *J* 14.3, 5.4 Hz, CH₂(11_b)), 3.91 (1H, dd, *J* 7.2, 5.4 Hz, CH(10)), 5.12 (2H, s, CH₂(13_{ab})), 6.93 (1H, s, ArCH(8)), 7.10 (1H, dd, *J* 7.1, 7.1 Hz, ArCH), 7.18 (1H, dd, *J* 7.1, 7.1 Hz ArCH), 7.24–7.34 (3H, m, ArCH(16)), 7.53–7.60 (3H, m, ArCH(15)), 8.37 (1H, br. s, NH(7))

¹³C (75 MHz, CDCl₃) δ 30.98 (s, CH₂(11)), 55.12 (s, CH(10_{ab})), 65.73 (s, CH₂(13)), 110.72 (s, ArC), 111.34 (s, ArCH), 115.35 (s, ArCH), 115.64 (s, ArCH), 118.73 (s, ArCH), 119.58 (s, ArCH), 122.21 (s, ArCH), 123.07 (s, ArCH(8)), 125.47 (s, ArCH), 125.50 (q, ³*J*_{C-F} 3.7 Hz, ArCH(16)), 127.41 (s, ArC), 127.64 (q, ¹*J*_{C-F} 272 Hz, ArCF₃(18)), 128.23 (s, ArCH),

130.45 (q, $^2J_{C-F}$ 32 Hz, ArCH(17)), 136.28 (s, ArC), 139.53 (s, ArC(14)), 175.18 (s, C=O(12))

^{19}F (376 MHz, CDCl_3) δ -62.5 (s, Ar- CF_3 (19))

R_f 0.15 (97:3, CH_2Cl_2 : Et_2O)

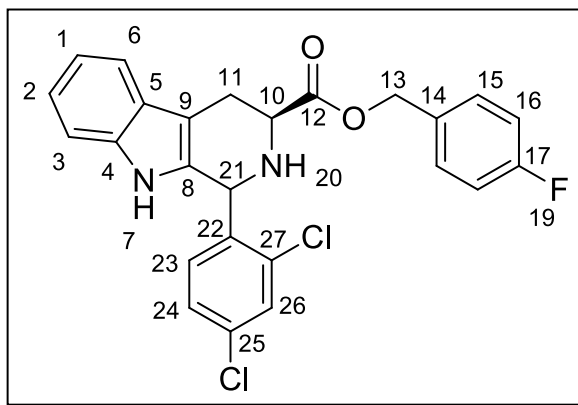
$[\alpha]_D^{29}$ -21.0 (c 1.0, MeOH)

IR ν/cm^{-1} 1098 (C-O, s), 1724 (C=O, s), 3156 (Ar C-H, w), 3273 (N-H, w)

MS (ESI): 363 $[\text{M}+\text{H}^+]$

HRMS $\text{C}_{19}\text{H}_{18}\text{F}_3\text{N}_2\text{O}_2$ $[\text{M}+\text{H}^+]$ requires 363.1320, found 363.1333 (2.7 ppm error)

Preparation of (3*S*)-4-Fluorobenzyl 1-(2,4-dichlorophenyl)-2,3,4,9-tetrahydro-1*H*-pyrido[3,4-*b*]indole-3-carboxylate (**LVT94-1,2**):



Following method A using (*S*)-4-Fluorobenzyl 2-amino-3-(1*H*-indol-3-yl)propanoate (**LVT90a**) (356 mg, 1.14 mmol, 1 eq.) and 2,4-dichlorobenzaldehyde (250 mg, 1.43 mmol, 1.25 eq.) as starting materials. The desired product was purified using preparative thin layer chromatography (SiO_2 , 19:1, CH_2Cl_2 /MeOH), to afford, the *cis* diastereoisomer as an off-

white solid (145 mg, 0.31 mmol, 27%) and, eluting second, the *trans* diastereoisomer an off-white solid (190 mg, 0.41 mmol, 36%).

Following method B using (*S*)-4-Fluorobenzyl 2-amino-3-(1*H*-indol-3-yl)propanoate (**LVT90a**) (156 mg, 0.50 mmol, 1 eq.) and 2,4-dichlorobenzaldehyde (175 mg, 1.00 mmol, 1.25 eq.) as starting materials. The desired product was purified using preparative thin layer chromatography (SiO₂, 19:1, CH₂Cl₂/MeOH), to afford, the *cis* diastereoisomer as an off-white solid (58 mg, 0.12 mmol, 24%) and, eluting second, the *trans* diastereoisomer an off-white solid (71 mg, 0.15 mmol, 30%).

Cis (1*S*, 3*S*) diastereoisomer (**LVT94-1**)

mp 81–84 °C

¹H NMR (300 MHz, CDCl₃) δ 3.15 (1H, dd, *J* 15.0, 11.0 Hz, CH₂(11_a)), 3.26 (1H, dd, *J* 15.0, 4.0 Hz, CH₂(11_b)), 3.90 (1H, dd, *J* 11.0, 4.0 Hz, CH(10)), 5.09 (1H, d, *J* 12.2, 6.7 Hz, CH₂(13_a)), 5.11 (1H, d, *J* 12.2, 6.7 Hz, CH₂(13_b)), 5.86 (1H, s, CH(21)), 6.95–6.99 (3H, m, ArCH(1,2,3)), 7.10–7.15 (5H, m, ArCH(15,16,24)), 7.46 (1H, s, ArCH(26)), 7.55 (1H, d, *J* 7.6 Hz, ArCH(23)), 7.64 (1H, s, NH(7))

¹³C NMR (75 MHz, CDCl₃) δ 25.42 (s, CH₂(11_{ab})), 56.67 (s, CH(10)), 66.29 (s, CH₂(13)), 109.29 (s, ArC), 110.97 (s, ArCH), 115.54 (s, ArCH), 115.75 (s, ArCH), 118.29 (s, ArCH(23)), 119.82 (s, ArCH), 122.24 (s, ArCH), 126.89 (s, ArC), 128.06 (s, ArCH), 129.42 (s, ArCH(26)), 130.43 (d, ²*J*_{C-F} 8.2 Hz, ArCH(16)), 131.42 (d, ⁴*J*_{C-F} 3.6 Hz, ArC(14)), 133.19 (s, ArC), 134.10 (s, ArC), 134.69 (s, ArC), 136.21 (s, ArC), 137.29 (s, ArC), 162.82 (d, ¹*J*_{C-F} 247 Hz, ArC(17)), 173.24 (s, C=O(12))

¹⁹F NMR (376 MHz, CDCl₃) δ –123.7 (Ar-F(19))

R_f 0.44 (99:1, CH₂Cl₂/MeOH)

IR ν/cm^{-1} 1510 (C-F, s), 1729 (C=O, s), 2923 (C-H, w), 3386 (ArC-H, w)

MS (ESI): 469/471 $[\text{M}+\text{H}^+]$

HRMS $\text{C}_{25}\text{H}_{20}^{35}\text{Cl}_2\text{FN}_2\text{O}_2$ $[\text{M}+\text{H}^+]$ requires 468.0800, found 469.0894 (3.2 ppm error)

Trans (1*R*, 3*S*) diastereoisomer (LVT94-2)

mp 178–181 °C

^1H NMR (300 MHz, CDCl_3) δ 3.01 (1H, dd, J 14.7, 13.0 Hz, $\text{CH}_2(11_a)$), 3.24 (1H, d, J 14.7, 10.6 Hz, $\text{CH}_2(11_b)$), 4.01 (1H, dd, J 13.0, 10.6 Hz, $\text{CH}(10)$), 5.20 (1H, d, J 12.4, 12.1 Hz, $\text{CH}_2(13_a)$), 5.22 (1H, d, J 12.4, 12.1 Hz, $\text{CH}_2(13_b)$), 5.79 (1H, s, $\text{CH}(21)$), 7.06–7.23 (6H, m, $\text{ArCH}(23,24)$), 7.38–7.40 (2H, m, $\text{ArCH}(16)$), 7.47 (1H, s, $\text{ArCH}(26)$), 7.53 (2H, d, J 8.0 Hz, $\text{ArCH}(15)$)

^{13}C NMR (75 MHz, CDCl_3) δ 25.42 (s, $\text{CH}_2(11_{ab})$), 53.86 (s, $\text{CH}_2(21)$), 56.67 (s, $\text{CH}(10)$), 66.29 (s, $\text{CH}_2(13)$), 109.29 (s, ArC), 110.97 (s, ArCH), 115.54 (s, ArCH), 115.75 (s, ArCH), 118.29 (s, $\text{ArCH}(23)$), 119.82 (s, ArCH), 122.24 (s, ArCH), 126.89 (s, ArC), 128.06 (s, ArCH), 129.42 (s, $\text{ArCH}(26)$), 130.43 (d, $^2J_{\text{C-F}}$ 8.2 Hz, $\text{ArCH}(16)$), 131.42 (d, $^4J_{\text{C-F}}$ 3.6 Hz, $\text{ArC}(14)$), 133.19 (s, ArC), 134.10 (s, ArC), 134.69 (s, ArC), 136.21 (s, ArC), 137.29 (s, ArC), 162.82 (d, $^1J_{\text{C-F}}$ 247 Hz, $\text{ArC}(17)$), 172.36 (s, $\text{C=O}(12)$)

^{19}F NMR (376 MHz, CDCl_3) δ –123.7 ($\text{Ar-F}(19)$)

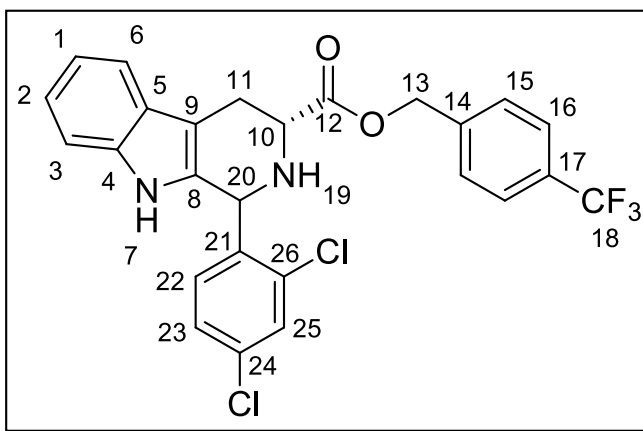
R_f 0.47 (99:1, CH_2Cl_2 :MeOH)

IR ν/cm^{-1} 1512 (C-F, s), 1724 (C=O, s), 2937 (C-H, w), 3321 (ArC-H, w)

MS (ESI): 469/471 $[\text{M}+\text{H}^+]$

HRMS $\text{C}_{25}\text{H}_{20}^{35}\text{Cl}_2\text{FN}_2\text{O}_2$ $[\text{M}+\text{H}^+]$ requires 468.0800, found 469.0886 (1.6 ppm error)

Preparation of (3*R*)-4-(Trifluoromethyl)benzyl 1-(2,4-dichlorophenyl)-2,3,4,9-tetrahydro-1*H*-pyrido[3,4-*b*]indole-3-carboxylate (**LVT95-1,2**):



Following method A using (*R*)-4-(Trifluoromethyl)benzyl 2-amino-3-(1*H*-indol-3-yl)propanoate (**LVT93a**) (430 mg, 1.19 mmol, 1 eq.) and 2,4-dichlorobenzaldehyde (260 mg, 1.49 mmol, 1.25 eq.) as starting materials. The desired product was purified using preparative thin layer chromatography (SiO₂, 19:1, CH₂Cl₂/MeOH), to afford, the *trans* diastereoisomer as an off-white solid (178 mg, 0.34 mmol, 27%) and, eluting second, the *cis* diastereoisomer a colourless solid (120 mg, 0.23 mmol, 36%).

Following method B using (*R*)-4-(Trifluoromethyl)benzyl 2-amino-3-(1*H*-indol-3-yl)propanoate (**LVT93a**) (200 mg, 0.55 mmol, 1 eq.) and 2,4-dichlorobenzaldehyde (121 mg, 0.69 mmol, 1.25 eq.) as starting materials. The desired product was purified using preparative thin layer chromatography (SiO₂, 19:1, CH₂Cl₂/MeOH), to afford, the *trans* diastereoisomer as an off-white solid (69 mg, 0.13 mmol, 24%) and, eluting second, the *cis* diastereoisomer a colourless solid (75 mg, 0.14 mmol, 25%).

Trans (1*R*, 3*S*) diastereoisomer (**LVT95-1**)

mp 178–180 °C

^1H NMR (300 MHz, CDCl_3) δ 3.22 (1H, dd, J 14.5, 13.0 Hz, $\text{CH}_2(11_a)$), 3.28 (1H, dd, J 14.5, 10.6 Hz, $\text{CH}_2(11_b)$), 3.97 (1H, d, J 13.0, 10.6 Hz, $\text{CH}(10)$), 5.19 (1H, d, J 12.4, 12.2 Hz, $\text{CH}_2(13_a)$), 5.21 (1H, d, J 12.4, 12.2 Hz, $\text{CH}_2(13_b)$), 5.89 (1H, s, $\text{CH}(20)$), 6.98 (1H, s, $\text{NH}(19)$), 7.11–7.20 (3H, m $\text{ArCH}(1,2)$), 7.33–7.35 (2H, d, J 7.5 Hz, $\text{ArCH}(22,23)$), 7.46–7.55 (4H, m, $\text{ArCH}(15,16)$), 7.66 (1H, s, $\text{ArCH}(25)$)

^{13}C NMR (75 MHz, CDCl_3) δ 24.68 (s, $\text{CH}_2(11_{ab})$), 51.03 (s, $\text{CH}(20)$), 52.72 (s, $\text{CH}(10)$), 65.81 (s, $\text{CH}_2(13)$), 109.27 (s, ArC), 111.02 (s, ArCH), 118.34 (s, $\text{ArCH}(22)$), 119.87 (s, $\text{ArCH}(23)$), 122.45 (s, ArCH), 125.55 (q, $^3J_{\text{C-F}}$ 7.5 Hz, $\text{ArCH}(16)$), 126.76 (s, ArC), 127.39 (s, $\text{ArCH}(25)$), 127.94 (q, $^1J_{\text{C-F}}$ 272 Hz, $\text{ArCF}_3(18)$), 128.01 (s, ArCH), 129.71 (s, ArCH), 130.13 (q, $^2J_{\text{C-F}}$ 32 Hz, $\text{ArC}(17)$), 131.00 (s, ArC), 131.58 (s, ArC), 134.31 (s, ArC), 134.50 (s, ArC), 136.27 (s, ArC), 137.80 (s, $\text{ArC}(26)$), 139.49 (s, $\text{ArC}(24)$), 172.99 (s, $\text{C=O}(12)$)

^{19}F NMR (376 MHz, CDCl_3) δ –62.61 ($\text{Ar-CF}_3(18)$)

R_f 0.33 (99:1, $\text{CH}_2\text{Cl}_2/\text{MeOH}$)

IR ν/cm^{-1} 1323 (C-F, s), 1733 (C=O, s), 2942 (C-H, w), 3388 (ArC-H , w)

MS (ESI): 519/521 [$\text{M}+\text{H}^+$]

HRMS $\text{C}_{26}\text{H}_{20}^{35}\text{Cl}_2\text{F}_3\text{N}_2\text{O}_2$ [$\text{M}+\text{H}^+$] requires 519.0845, found 519.0872 (4.9 ppm error)

Cis (1*S*, 3*S*) diastereoisomer (LVT95-2)

mp 96–99 °C

^1H NMR (300 MHz, CDCl_3) δ 3.04 (1H, dd, J 15.0, 12.9 Hz, $\text{CH}_2(11_a)$), 3.26 (1H, d, J 15.0, 10.8 Hz, $\text{CH}_2(11_b)$), 4.05 (1H, dd, J 12.9, 10.8 Hz, $\text{CH}(10)$), 5.28 (1H, d, J 12.8, 10.6 Hz, $\text{CH}_2(13_a)$), 5.30 (1H, d, J 12.8, 10.6 Hz, $\text{CH}_2(13_b)$), 5.80 (1H, s, $\text{CH}(20)$), 7.10–7.23 (3H, m $\text{ArCH}(1,2)$), 7.38 (1H, d, J 8.40 Hz, ArCH), 7.47 (1H, s, $\text{ArCH}(25)$), 7.50–7.54 (4H, m, $\text{ArCH}(15,22,23)$), 7.65–7.67 (2H, m, $\text{ArCH}(16)$)

^{13}C NMR (75 MHz, CDCl_3) δ 25.46 (s, $\text{CH}_2(11_{\text{ab}})$), 53.89 (s, $\text{CH}(20)$), 56.64 (s, $\text{CH}(10)$), 65.99 (s, $\text{CH}_2(13)$), 109.19 (s, ArC), 110.99 (s, ArCH), 118.27 (s, $\text{ArCH}(22)$), 119.86 (s, $\text{ArCH}(23)$), 122.29 (s, ArCH), 125.71 (q, $^1J_{\text{C-F}}$ 7.8 Hz, $\text{ArCH}(16)$), 126.86 (s, ArC), 127.98 (q, $^1J_{\text{C-F}}$ 272 Hz, $\text{ArCF}_3(18)$), 128.07 (s, ArCH), 128.31 (s, $\text{ArCH}(15)$), 129.45 (s, $\text{ArCH}(25)$), 130.69 (q, $^2J_{\text{C-F}}$ 32 Hz, $\text{ArC}(17)$), 131.40 (s, $\text{ArCH}(25)$), 133.16 (s, ArC), 134.12 (s, ArC), 134.73 (s, ArC), 136.22 (s, ArC), 137.23 (s, $\text{ArC}(26)$), 139.46 (s, $\text{ArC}(24)$), 172.26 (s, $\text{C=O}(12)$)

^{19}F NMR (376 MHz, CDCl_3) δ -62.62 (s, $\text{Ar-CF}_3(18)$)

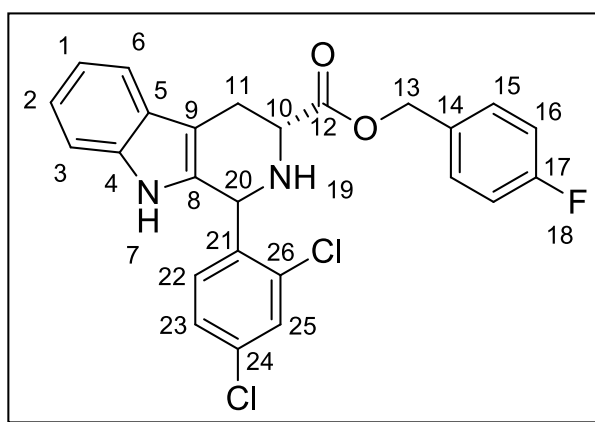
R_f 0.49 (99:1, CH_2Cl_2 :MeOH)

IR ν/cm^{-1} 1324 (C-F, s), 1729 (C=O, s), 2898 (C-H, w), 3420 (ArC-H, w)

MS (ESI): 519/521 $[\text{M}+\text{H}^+]$

HRMS $\text{C}_{26}\text{H}_{20}^{35}\text{Cl}_2\text{F}_3\text{N}_2\text{O}_2$ $[\text{M}+\text{H}^+]$ requires 519.0845, found 519.0865 (2.8 ppm error)

Preparation of (3*R*)-4-Fluorobenzyl 1-(2,4-dichlorophenyl)-2,3,4,9-tetrahydro-1*H*-pyrido[3,4-*b*]indole-3-carboxylate (**LVT96-1,2**):



Following method A using (*R*)-4-Fluorobenzyl 2-amino-3-(1*H*-indol-3-yl)propanoate (**LVT91a**) (328 mg, 1.05 mmol, 1 eq.) and 2,4-dichlorobenzaldehyde (229 mg, 1.31 mmol,

1.25 eq.) as starting materials. The desired product was purified using preparative thin layer chromatography (SiO₂, 97:3, CH₂Cl₂/MeOH), to afford, the *trans* diastereoisomer as an orange wax solid (90.4 mg, 0.19 mmol, 18%) and, the *cis* diastereoisomer a colourless solid (156 mg, 0.33 mmol, 32%).

Following method B using (*R*)-4-Fluorobenzyl 2-amino-3-(1*H*-indol-3-yl)propanoate (**LVT91a**) (228 mg, 0.73 mmol, 1 eq.) and 2,4-dichlorobenzaldehyde (159 mg, 0.91 mmol, 1.25 eq.) as starting materials. The desired product was purified using preparative thin layer chromatography (SiO₂, 97:3, CH₂Cl₂/MeOH), to afford, the *trans* diastereoisomer as an orange wax solid (113 mg, 0.24 mmol, 33%) and, the *cis* diastereoisomer a colourless solid (124 mg, 0.26 mmol, 36%).

Trans (1*R*, 3*S*) diastereoisomer (**LVT96-1**)

¹H NMR (300 MHz, CDCl₃) δ 3.15 (1H, dd, *J* 15.8, 6.1 Hz, CH₂(11_a)), 3.26 (1H, dd, *J* 15.8, 6.8 Hz, CH₂(11_b)), 3.90 (1H, dd, *J* 6.8, 6.1 Hz, CH(10)), 5.10 (1H, d, *J* 13.4, 10.1 Hz, CH₂(13_a)), 5.13 (1H, d, *J* 13.4, 10.1 Hz, CH₂(13_b)), 5.87 (1H, s, CH(20)), 6.95–7.05 (3H, m, ArCH(1,2)), 7.10–7.15 (3H, m, ArCH(15,23)), 7.35 (2H, d, *J* 8.3 Hz, ArCH(16)), 7.47 (1H, s, ArCH(25)), 7.56 (1H, d, *J* 8.3 Hz, ArCH), 7.65–7.70 (2H, m, NH, ArCH(22))

¹³C NMR (75 MHz, CDCl₃) δ 25.72 (s, CH₂(11_{ab})), 51.04 (s, CH(20)), 52.79 (s, CH(10)), 66.10 (s, CH₂(13)), 109.43 (s, ArC), 110.98 (s, ArCH), 115.40 (s, ArCH), 115.61 (s, ArCH), 118.37 (s, ArCH(22)), 119.80 (s, ArCH(23)), 122.37 (s, ArCH), 126.81 (s, ArC), 127.33 (s, ArCH), 128.76 (d, ³*J*_{C-F} 7.2 Hz, ArCH(15)), 129.70 (s, ArCH(25)), 130.12 (d, ²*J*_{C-F} 7.9 Hz, ArC(16)), 130.97 (s, ArC), 131.66 (s, ArC), 134.32 (s, ArC), 134.95 (s, ArC), 136.27 (s, ArC(24)), 137.95 (s, ArC(26)), 162.67 (d, ¹*J*_{C-F} 244 Hz, ArC(17)), 173.14 (s, C=O(12))

¹⁹F NMR (376 MHz, CDCl₃) δ –113.3 (s, Ar-F(18))

R_f 0.24 (99:1, CH₂Cl₂/MeOH)

$[\alpha]_{\text{D}}^{25} -6.0$ (*c* 1.0, MeOH)

IR ν/cm^{-1} 1510 (C-F, s), 1729 (C=O, s), 2924 (C-H, w), 3314 (ArC-H, w)

MS (ESI): 469/470 $[\text{M}+\text{H}^+]$

HRMS $\text{C}_{25}\text{H}_{20}^{35}\text{Cl}_2\text{FN}_2\text{O}_2$ $[\text{M}+\text{H}^+]$ requires 469.0886, found 469.0900 (4.0 ppm error)

Cis (1*S*, 3*S*) diastereoisomer (LVT96-2)

mp 191–193°C

^1H NMR (300 MHz, CDCl_3) δ 3.01 (1H, dd, *J* 14.7, 12.9 Hz, $\text{CH}_2(11_{\text{a}})$), 3.24 (1H, dd, *J* 14.7, 10.8 Hz, $\text{CH}_2(11_{\text{b}})$), 4.02 (1H, dd, *J* 12.9, 10.8 Hz, $\text{CH}(10)$), 5.11 (1H, d, *J* 12.1, 12.1 Hz, $\text{CH}_2(13_{\text{a}})$), 5.14 (1H, d, *J* 12.1, 12.1 Hz, $\text{CH}_2(13_{\text{b}})$), 5.79 (1H, s, $\text{CH}(20)$), 7.07–7.23 (5H, m, Ar $\text{CH}(15)$), 7.38–7.40 (3H, m, Ar $\text{CH}(16)$), 7.47 (1H, s, Ar $\text{CH}(25)$), 7.53 (2H, d, *J* 8.0 Hz, Ar $\text{CH}(22,23)$), 7.56 (1H, s, $\text{NH}(7)$)

^{13}C NMR (75 MHz, CDCl_3) δ 25.42 (s, $\text{CH}_2(11_{\text{ab}})$), 53.81 (s, $\text{CH}(20)$), 56.29 (s, $\text{CH}(10)$), 66.29 (s, $\text{CH}_2(13)$), 109.29 (s, ArC), 110.97 (s, ArCH), 115.53 (s, ArCH), 115.75 (s, ArCH), 118.29 (s, ArCH(22)), 119.81 (s, ArCH(23)), 122.24 (s, ArCH), 126.66 (s, ArC), 128.05 (d, $^3J_{\text{C-F}}$ 8.0 Hz, ArCH(15)), 129.42 (s, ArCH(25)), 130.43 (d, $^2J_{\text{C-F}}$ 8.0 Hz, ArC(16)), 131.37 (d, $^4J_{\text{C-F}}$ 3.4 Hz, ArC(14)), 133.19 (s, ArC), 134.10 (s, ArC), 134.69 (s, ArC), 136.21 (s, ArC(24)), 137.28 (s, ArC(26)), 162.82 (d, $^1J_{\text{C-F}}$ 247 Hz, ArC(17)), 172.35 (s, C=O(12))

^{19}F NMR (376 MHz, CDCl_3) δ –113.1 (s, Ar-F(18))

R_{f} 0.50 (99:1, CH_2Cl_2 :MeOH)

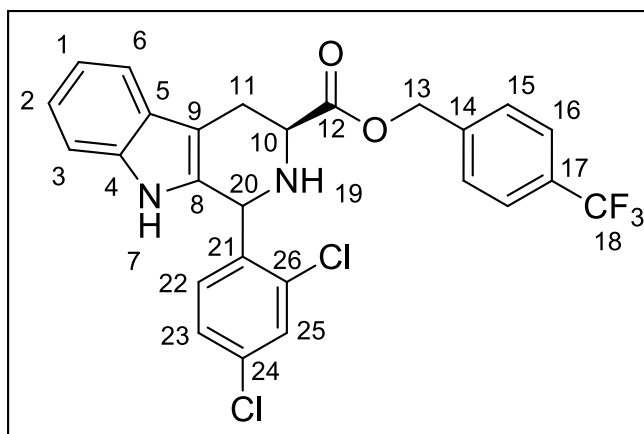
$[\alpha]_{\text{D}}^{25} +6.0$ (*c* 1.0, MeOH)

IR ν/cm^{-1} 1512 (C-F, s), 1724 (C=O, s), 2890 (C-H, w), 3413 (ArC-H, w)

MS (ESI): 469/470 $[\text{M}+\text{H}^+]$

HRMS $C_{25}H_{20}^{35}Cl_2FN_2O_2$ $[M+H]^+$ requires 469.0886, found 469.0884 (0.4 ppm error)

Preparation of (3*S*)-4-(Trifluoromethyl)benzyl 1-(2,4-dichlorophenyl)-2,3,4,9-tetrahydro-1*H*-pyrido[3,4-*b*]indole-3-carboxylate (**LVT97-1,2**):



Following method A using (S)-4-(Trifluoromethyl)benzyl 2-amino-3-(1*H*-indol-3-yl)propanoate (**LVT92a**) (421 mg, 1.16 mmol, 1 eq.) and 2,4-dichlorobenzaldehyde (253 mg, 1.45 mmol, 1.25 eq.) as starting materials. The desired product was purified using preparative thin layer chromatography (SiO_2 , 97:3, $CH_2Cl_2/MeOH$), to afford, the *trans* diastereoisomer as an amorphous solid (168 mg, 0.32 mmol, 28%) and, the *cis* diastereoisomer a colourless solid (82 mg, 0.16 mmol, 14%).

Following method B using (S)-4-(Trifluoromethyl)benzyl 2-amino-3-(1*H*-indol-3-yl)propanoate (**LVT92a**) (321 mg, 0.89 mmol, 1 eq.) and 2,4-dichlorobenzaldehyde (194 mg, 1.11 mmol, 1.25 eq.) as starting materials. The desired product was purified using preparative thin layer chromatography (SiO_2 , 97:3, $CH_2Cl_2/MeOH$), to afford, the *trans* diastereoisomer as an amorphous solid (124 mg, 0.24 mmol, 27%) and, the *cis* diastereoisomer a colourless solid (136 mg, 0.26 mmol, 29%).

Trans (1*R*, 3*S*) diastereoisomer (**LVT97-1**)

^1H NMR (300 MHz, CDCl_3) δ 3.19 (1H, dd, J 14.6, 7.4 Hz, $\text{CH}_2(11_a)$), 3.29 (1H, dd, J 14.6, 5.7 Hz, $\text{CH}_2(11_b)$), 3.96 (1H, dd, J 7.4, 5.7 Hz, $\text{CH}(10)$), 5.16 (1H, d, J 12.9, 3.7 Hz, $\text{CH}_2(13_a)$), 5.18 (1H, d, J 12.9, 3.7 Hz, $\text{CH}_2(13_b)$), 5.88 (1H, s, $\text{CH}(20)$), 6.97 (1H, s, $\text{NH}(19)$), 7.12–7.23 (4H, m $\text{ArCH}(1,2,3,6)$), 7.35 (2H, d, J 8.0 Hz, $\text{ArCH}(15)$), 7.46 (2H, d, J 8.0 Hz, $\text{ArCH}(16)$), 7.50–7.57 (3H, m, $\text{ArCH}(22,23,25)$), 7.65 (1H, s, $\text{NH}(7)$)

^{13}C NMR (75 MHz, CDCl_3) δ 24.74 (s, $\text{CH}_2(11_{ab})$), 50.99 (s, $\text{CH}(20)$), 52.81 (s, $\text{CH}(10)$), 65.79 (s, $\text{CH}_2(13)$), 109.29 (s, ArC), 111.02 (s, ArCH), 118.34 (s, $\text{ArCH}(22)$), 119.84 (s, $\text{ArCH}(23)$), 122.42 (s, ArCH), 125.53 (q, $^3J_{C-F}$ 7.5 Hz, $\text{ArCH}(16)$), 126.1 (s, ArC), 127.36 (s, $\text{ArCH}(25)$), 127.87 (q, $^1J_{C-F}$ 272 Hz, $\text{ArCF}_3(18)$), 128.02 (s, ArCH), 129.70 (s, $\text{ArCH}(23)$), 130.96 (s, $\text{ArCH}(15)$), 130.88 (q, $^2J_{C-F}$ 32 Hz, $\text{ArC}(17)$), 131.62 (s, ArC), 131.58 (s, ArC), 134.28 (s, ArC), 134.44 (s, ArC), 136.20 (s, ArC), 137.84 (s, $\text{ArC}(26)$), 139.45 (s, $\text{ArC}(24)$), 173.08 (s, $\text{C=O}(12)$)

^{19}F NMR (376 MHz, CDCl_3) δ –62.63 (s, $\text{Ar-CF}_3(18)$)

R_f 0.21 (99:1, $\text{CH}_2\text{Cl}_2/\text{MeOH}$)

IR ν/cm^{-1} 1323 (C-F, s), 1732 (C=O, s), 2961 (C-H, w), 3392 (ArC-H, w)

MS (ESI): 519/521 $[\text{M}+\text{H}^+]$

HRMS $\text{C}_{26}\text{H}_{20}^{35}\text{Cl}_2\text{F}_3\text{N}_2\text{O}_2$ $[\text{M}+\text{H}^+]$ requires 519.0845, found 519.0861 (1.8 ppm error)

Cis (1*S*, 3*S*) diastereoisomer (LVT97-2)

mp 208–212 °C

^1H NMR (300 MHz, CDCl_3) δ 3.05 (1H, dd, J 13.4, 11.1 Hz, $\text{CH}_2(11_a)$), 3.26 (1H, d, J 13.4, 4.0 Hz, $\text{CH}_2(11_b)$), 4.06 (1H, dd, J 11.1, 4.0 Hz, $\text{CH}(10)$), 5.28 (1H, d, J 12.8, 10.2 Hz, $\text{CH}_2(13_a)$), 5.30 (1H, d, J 12.8, 10.2 Hz, $\text{CH}_2(13_b)$), 5.80 (1H, s, $\text{CH}(20)$), 7.11–7.24 (3H, m

ArCH), 7.39 (1H, d, *J* 8.4 Hz, ArCH), 7.47 (2H, d, *J* 5.6 Hz, ArCH(22,23)), 7.52–7.54 (3H, m, ArCH(15,25)), 7.66 (2H, d, *J* 8.4 Hz, ArCH(16))

¹³C NMR (75 MHz, CDCl₃) δ 24.47 (s, CH₂(11_{ab})), 53.87 (s, CH(20)), 56.65 (s, CH(10)), 65.99 (s, CH₂(13)), 109.20 (s, ArC), 110.99 (s, ArCH), 118.28 (s, ArCH(22)), 119.86 (s, ArCH(23)), 122.30 (s, ArCH), 125.70 (q, ³*J*_{C-F} 7.4 Hz, ArCH(16)), 126.70 (q, ¹*J*_{C-F} 275 Hz, ArCF₃(18)), 126.86 (s, ArC), 128.08 (s, ArCH(25)), 128.31 (s, ArCH), 129.47 (s, ArCH(23)), 130.70 (q, ²*J*_{C-F} 32 Hz, ArC(17)), 131.41 (s, ArCH(15)), 133.17 (s, ArC), 134.12 (s, ArC), 134.74 (s, ArC), 136.22 (s, ArC), 137.23 (s, ArC), 139.46 (s, ArC(24)), 173.08 (s, C=O(12))

¹⁹F NMR (376 MHz, CDCl₃) δ –62.62 (s, Ar-CF₃(18))

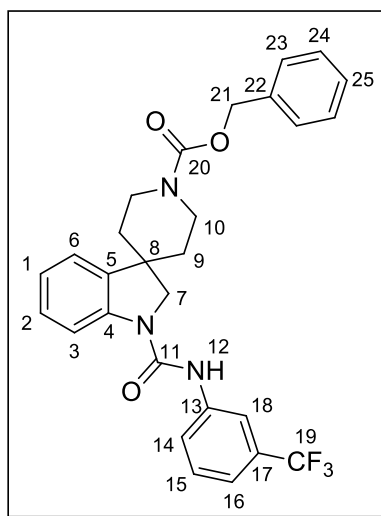
R_f 0.50 (99:1, CH₂Cl₂:MeOH)

IR ν/ cm^{–1} 1325 (C-F, s), 1727 (C=O, s), 2898 (C-H, w), 3416 (ArC-H, W)

MS (ESI): 519/521 [M+H⁺]

HRMS C₂₆H₂₀³⁵Cl₂F₃N₂O₂ [M+H⁺] requires 519.0845, found 519.0871 (4.1 ppm error)

Preparation of Benzyl 1-((3-(trifluoromethyl)phenyl)carbamoyl)spiro[indoline-3,4'-piperidine]-1'-carboxylate (**LVT52**):



Benzyl spiro[indoline-3,4'-piperidine]-1'-carboxylate (**LVTa46**) (1.00 g, 3.12 mmol, 1 eq.) was dissolved in CH_2Cl_2 (20 mL) under a nitrogen atmosphere. 3-(Trifluoromethyl) isocyanate (0.52 mL, 707 mg, 3.75 mmol, 1.2 eq.) was added slowly *via* syringe and the resulting solution turned dark green on leaving to stir for 4 hours. The solvent was removed under reduced pressure, yielding a cream solid **LVT52** (1.55 g, 3.04 mmol, 97%), which required no purification.

Data for **LVT52**

mp 101–105 °C

^1H (300 MHz, CDCl_3) δ 1.69 (2H, br. d, J 14.2 Hz, $\text{CH}_2(9_a)$), 1.88 (2H, br. dd, J 14.2, 12.7 Hz, $\text{CH}_2(9_b)$), 2.95 (2H, br. dd, J 12.7, 12.7 Hz, $\text{CH}_2(10_a)$), 3.94 (2H, s, $\text{CH}_2(7)$), 4.26 (2H, br. d, J 12.7 Hz, $\text{CH}_2(10_b)$), 5.17 (2H, s, $\text{CH}_2(21)$), 6.92 (1H, br. s, NH), 7.06 (1H, dd, J 7.0, 7.0 Hz, $\text{ArCH}(1,2)$), 7.13 (1H, d, J 7.0 Hz, ArCH), 7.23–7.46 (7H, m, $\text{ArCH}(23,24,25)$), 7.72 (1H, d, J 7.6 Hz, $\text{ArCH}(15)$), 7.76 (1H, s, $\text{ArCH}(18)$), 7.85 (1H, d, J 8.0 Hz, $\text{ArCH}(14)$)

^{13}C (75 MHz, CDCl_3) δ 36.26 (s, $\text{CH}_2(9_{\text{ab}})$), 41.01 (s, $\text{CH}_2(10_{\text{ab}})$), 42.95 (s, $\text{C}(8)$), 56.89 (s, $\text{CH}_2(21)$), 67.39 (s, $\text{CH}_2(7)$), 115.02 (s, $\text{ArCH}(14)$), 116.75 (q, $^3J_{\text{C-F}}$ 4.9 Hz, $\text{ArCH}(18)$), 120.16 (q, $^3J_{\text{C-F}}$ 7.6 Hz, $\text{ArCH}(16)$), 122.83 (s, ArCH), 123.15 (s, ArCH), 123.18 (s, ArCH), 123.92 (q, $^1J_{\text{C-F}}$ 272 Hz, $\text{CF}_3(19)$), 127.97 (s, ArCH), 128.21 (s, ArCH), 128.60 (s, ArCH), 128.74 (s, ArCH), 129.56 (s, $\text{ArCH}(15)$), 131.34 (q, $^2J_{\text{C-F}}$ 32 Hz, $\text{ArC}(17)$), 136.54 (s, $\text{ArC}(13)$), 138.01 (s, $\text{ArC}(22)$), 138.83 (s, ArC), 141.82 (s, ArC), 151.92 (s, $\text{C=O}(13)$), 155.35 (s, $\text{C=O}(20)$)

^{19}F (376 MHz, CDCl_3) δ -62.6 ($\text{Ar-CF}_3(19)$)

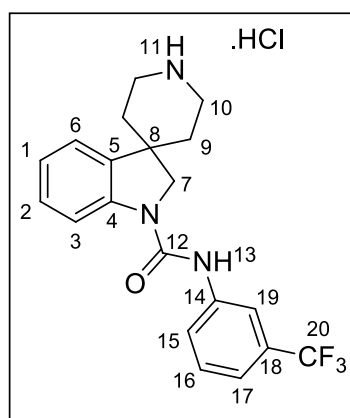
R_f 0.44 (97:3, CH_2Cl_2 :MeOH),

IR ν/cm^{-1} 1328 (C-F, s), 1674 (C=O, s), 3335 (Ar C-H, w)

MS (ESI): 510 $[\text{M}+\text{H}^+]$

HRMS $\text{C}_{28}\text{H}_{27}\text{F}_3\text{N}_3\text{O}_3$ $[\text{M}+\text{H}^+]$ requires 510.2005, found 510.2013 (2.3 ppm error)

Preparation of *N*-(3-(Trifluoromethyl)phenyl)spiro[indoline-3,4'-piperidine]-1-carboxamide hydrochloride (**LVT53**):



Benzyl 1-((3-(trifluoromethyl)phenyl)carbamoyl)spiro[indoline-3,4'-piperidine]-1'-carboxylate (**LVT52**) (1.35 g, 3.04 mmol, 1 eq.) was dissolved in MeOH (15 mL) and then, Pearlman's catalyst (213 mg, 0.30 mmol, 0.1 eq.) was added into the solution. The reaction

mixture was sparged with a balloon of hydrogen until deflated and then left under an atmosphere of hydrogen overnight. The methanol was removed under reduced pressure and the reaction mixture was filtered through celite with CH₂Cl₂ (100 mL) to collect any remaining starting material. The eluent mixture of 10% MeOH/CH₂Cl₂ (200 mL) was subsequently passed through the celite to elute the desired product. The product **LVT53** is a brown amorphous solid (709 mg, 1.89 mmol, 62%).

Data for **LVT53**

¹H (300 MHz, D₄-MeOH) δ 1.95 (2H, br. d, *J* 14.4 Hz, CH₂(9_a)), 2.18 (2H, br. dd, *J* 14.4, 12.4 Hz, CH₂(9_b)), 3.24 (2H, br. dd, *J* 12.4, 12.4 Hz, CH₂(10_a)), 3.49 (2H, br. d, *J* 12.4 Hz, CH₂(10_b)), 4.22 (2H, s, CH₂(7)), 7.04 (1H, dd, *J* 8.0, 8.0 Hz, ArCH), 7.24–7.27 (2H, m, ArCH), 7.33 (1H, d, *J* 7.9 Hz, ArCH(17)), 7.49 (1H, dd, *J* 7.9, 7.9 Hz, ArCH(16)), 7.83 (1H, d, *J* 8.0 Hz, ArCH(6)), 7.93 (1H, d, *J* 7.9 Hz, ArCH(15)), 8.00 (1H, s, ArCH(19))

¹³C (75 MHz, D₄-MeOH) δ 34.21 (s, CH₂(9_{ab})), 41.54 (s, C(8)), 42.69 (s, CH₂(10_{ab})), 42.96 (s, CH₂(10)), 58.17 (s, CH₂(7)), 116.18 (s, ArCH(16)), 118.25 (q, ³*J*_{C-F} 5.8 Hz, ArCH(19)), 120.68 (q, ³*J*_{C-F} 4.7 Hz, ArCH(17)), 120.97 (q, ¹*J*_{C-F} 272 Hz, CF₃(20)), 123.62 (s, ArCH), 124.12 (s, ArCH), 125.11 (s, ArCH), 129.82 (s, ArCH), 130.52 (s, ArCH(16)), 131.42 (q, ²*J*_{C-F} 31 Hz, ArC(18)), 141.32 (s, ArC), 143.73 (s, ArC), 154.64 (s, C=O(12))

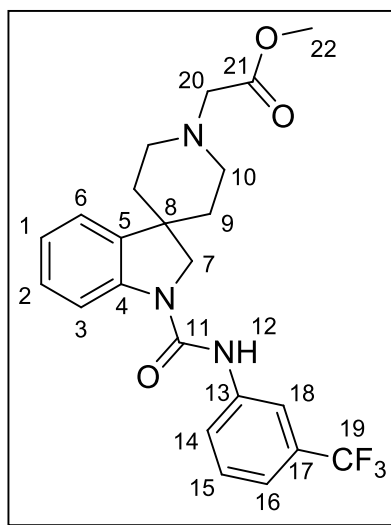
¹⁹F (376 MHz, D₄-MeOH) δ –64.1 (s, Ar-CF₃(20))

IR ν/ cm⁻¹ 1326 (C-F, s), 1673 (C=O, s), 3297 (Ar C-H, w)

MS (ESI): 376 [M+H⁺]

HRMS C₂₀H₂₁F₃N₃O [M+H⁺] requires 376.1637, found 376.1636 (1.7 ppm error)

Preparation of Methyl 2-(1-((3-(trifluoromethyl)phenyl)carbamoyl)spiro[indoline-3,4'-piperidin]-1'-yl)acetate (**LVT54**):



Following method C using Benzyl 1-((3-(trifluoromethyl)phenyl)carbamoyl)spiro[indoline-3,4'-piperidine]-1'-carboxylate (**LVT53**) (200 mg, 0.53 mmol, 1 eq.), methyl bromoacetate (0.10 mL, 161 mg, 1.06 mmol, 2 eq.) and K_2CO_3 (147 mg, 1.06 mmol, 2 eq.) as starting materials. The desired product was purified using column chromatography (SiO_2 , 14:1, CH_2Cl_2 :MeOH) to afford, the pure product (**LVT54**) as a colourless solid (85 mg, 0.19 mmol, 35%).

Data for **LVT54**

mp 128–131 °C

1H (300 MHz, $CDCl_3$) δ 1.73 (2H, d, J 13.0 Hz, $CH_2(9_a)$), 2.10 (2H, dd, J 13.0, 11.3 Hz, $CH_2(9_b)$), 2.43 (2H, dd, J 11.3, 11.3 Hz, $CH_2(10_a)$), 2.99 (2H, d, J 11.3 Hz, $CH_2(10_b)$), 3.34 (2H, s, $CH_2(20)$), 3.75 (3H, s, $OCH_3(22)$), 3.93 (2H, s, $CH_2(7)$), 7.03 (1H, s, NH), 7.19 (1H, dd, J 7.7, 7.7 Hz, ArCH), 7.22 (2H, m, ArCH(1,3)), 7.35 (1H, d, J 8.0 Hz, ArCH(16)), 7.44 (1H, dd, J 8.0, 8.0 Hz, ArCH(15)), 7.72 (1H, d, J 7.5 Hz, ArCH) 7.76 (1H, s, ArCH(18)), 7.87 (1H, d, J 8.0 Hz, ArCH(14))

^{13}C (75 MHz, CDCl_3) δ 37.00 (s, $\text{CH}_2(9_{\text{ab}})$), 42.47 (s, $\text{C}(8)$), 50.11 (s, $\text{CH}_2(10_{\text{ab}})$), 51.76 (s, $\text{OCH}_3(22)$), 57.44 (s, $\text{CH}_2(7)$), 59.40 (s, $\text{CH}_2(20)$), 114.99 (s, $\text{ArCH}(14)$), 116.75 (q, $^3J_{\text{C-F}}$ 5.7 Hz, $\text{ArCH}(18)$), 120.14 (q, $^3J_{\text{C-F}}$ 3.6 Hz, $\text{ArCH}(16)$), 122.58 (s, ArCH), 122.92 (s, ArCH), 123.13 (s, ArCH), 123.18 (s, ArCH), 123.94 (q, $^1J_{\text{C-F}}$ 272 Hz, $\text{CF}_3(19)$), 128.47 (s, ArCH), 129.51 (s, $\text{ArCH}(15)$), 131.36 (q, $^2J_{\text{C-F}}$ 32 Hz, $\text{ArC}(17)$), 138.61 (s, ArC), 138.87 (s, $\text{ArC}(13)$), 141.91 (s, ArC), 151.93 (s, $\text{C=O}(11)$), 170.85 (s, $\text{C=O}(21)$)

^{19}F (376 MHz, CDCl_3) δ -62.4 (s, $\text{ArCF}_3(19)$)

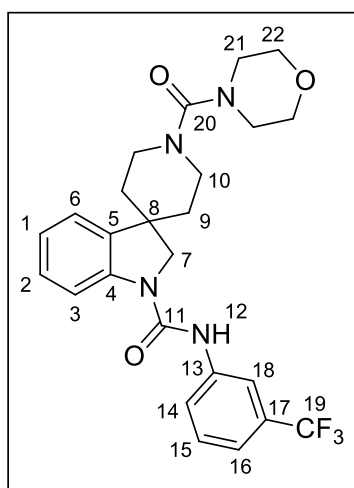
R_f 0.58 (93:7, CH_2Cl_2 :MeOH)

IR ν/cm^{-1} 1361 (C-F, s), 1676 (C=O, s), 1738 (C=O, s), 3381 (Ar C-H, w)

MS (ESI): 448 $[\text{M}+\text{H}^+]$

HRMS $\text{C}_{23}\text{H}_{25}\text{F}_3\text{N}_3\text{O}_3$ $[\text{M}+\text{H}^+]$ requires 448.1848, found 448.1849 (1.6 ppm error)

Preparation of 1'-(Morpholine-4-carbonyl)-*N*-(3-(trifluoromethyl)phenyl)spiro[indoline-3,4'-piperidine]-1-carboxamide (**LVT59**):



Following method C using Benzyl 1-((3-(trifluoromethyl)phenyl)carbamoyl)spiro[indoline-3,4'-piperidine]-1'-carboxylate (**LVT53**) (276 mg, 0.74 mmol, 1 eq.), 4-morpholinecarbonyl chloride (0.17 mL, 218 mg, 1.50 mmol, 2 eq.) and K_2CO_3 (207 mg, 1.50 mmol, 2 eq.) as

starting materials. The desired product was purified using column chromatography (SiO₂, 93:7, CH₂Cl₂:MeOH) to afford, the pure product (**LVT59**) as a light cream solid (296 mg, 0.61 mmol, 82%).

Data for LVT59

mp 221–223 °C

¹H (300 MHz, CDCl₃) δ 1.71 (2H, d, *J* 11.5 Hz, CH₂(9_a)), 1.94 (2H, dd, *J* 12.8, 11.5 Hz, CH₂(9_b)), 2.91 (2H, dd, *J* 12.8, 12.8 Hz, CH₂(10_a)), 3.29–3.33 (4H, m, CH₂(22)), 3.67–3.71 (6H, m, CH₂(10_b,21)), 4.00 (2H, s, CH₂(7)), 7.02 (1H, dd, *J* 7.3, 7.3 Hz, ArCH), 7.15 (1H, d, *J* 7.3 Hz, ArCH), 7.22–7.26 (1H, m, ArCH), 7.31 (1H, d, *J* 7.6 Hz, ArCH(17)), 7.41 (1H, dd, *J* 7.6, 7.6 Hz, ArCH), 7.51 (1H, s, NH), 7.75 (2H, br. s, ArCH), 7.92 (1H, d, *J* 8.0 Hz, ArCH(14))

¹³C (75 MHz, CDCl₃) δ 36.59 (s, CH₂(9_{ab})), 43.32 (s, C(8)), 44.29 (s, CH₂(10_{ab})), 47.29 (s, CH₂(22)), 57.20 (s, CH₂(7)), 66.63 (s, CH₂(21)), 115.30 (s, ArCH(14)), 116.85 (q, ³*J*_{C-F} 3.8 Hz, ArCH(18)), 120.01 (q, ³*J*_{C-F} 3.6 Hz, ArCH(16)), 122.71 (s, ArCH), 123.06 (s, ArCH), 123.36 (s, ArCH), 126.73 (q, ¹*J*_{C-F} 272 Hz, ArCF₃(19)), 128.71 (s, ArCH), 129.48 (s, ArCH), 131.22 (q, ²*J*_{C-F} 32 Hz, ArC(17)), 137.94 (s, ArC), 139.24 (s, ArC(13)), 142.14 (s, ArC), 152.32 (s, C=O(11)), 164.28 (s, C=O(20))

¹⁹F (376 MHz, CDCl₃) δ –62.3 (s, ArCF₃(19))

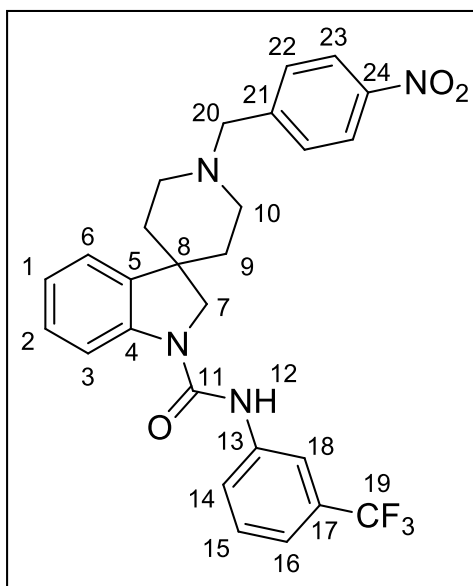
R_f 0.52 (93:7, CH₂Cl₂:MeOH)

IR ν/ cm^{–1} 1345 (C-F, s), 1622 (C=O, s), 1678 (C=O, s), 3334 (Ar C-H, w)

MS (ESI): 489 [M+H⁺]

HRMS C₂₅H₂₈F₃N₄O₃ [M+H⁺] requires 489.2108, found 489.2097 (2.3 ppm error)

Preparation of 1'-(4-Nitrobenzyl)-*N*-(3-(trifluoromethyl)phenyl)spiro[indoline-3,4'-piperidine]-1-carboxamide (**LVT66**):



Following method C using Benzyl 1-((3-(trifluoromethyl)phenyl)carbamoyl)spiro[indoline-3,4'-piperidine]-1'-carboxylate (**LVT53**) (96.0 mg, 0.26 mmol, 1 eq.), 4-nitrobenzyl bromide (112 mg, 0.52 mmol, 2 eq.) and K_2CO_3 (71.9 mg, 0.52 mmol, 2 eq.) as starting materials. The desired product was purified using column chromatography (SiO_2 , 93:7, CH_2Cl_2 :MeOH) to afford, the pure product (**LVT66**) as a golden brown amorphous solid (41.0 mg, 0.08 mmol, 31%).

Data for **LVT66**

1H (300 MHz, $CDCl_3$) δ 1.73 (2H, d, J 12.9 Hz, $CH_2(9_a)$), 2.05 (2H, dd, J 12.9, 11.8 Hz, $CH_2(9_b)$), 2.20 (2H, dd, J 11.8, 11.8 Hz, $CH_2(10_a)$), 2.91 (2H, d, J 11.8 Hz, $CH_2(10_b)$), 3.66 (2H, s, $CH_2(20)$), 3.93 (2H, s, $CH_2(7)$), 6.73 (1H, br. s, NH), 7.05 (1H, dd, J 7.2, 7.2 Hz, ArCH), 7.23 (2H, d, J 7.5 Hz, ArCH), 7.34 (1H, d, J 7.5 Hz, ArCH), 7.45 (1H, dd, J 7.7, 7.7 Hz, ArCH(15)), 7.56 (2H, d, J 7.7 Hz, ArCH), 7.72 (2H, m, ArCH(22)), 7.82 (1H, d, J 7.7 Hz, ArCH), 8.20 (2H, d, J 7.7 Hz, ArCH(23))

^{13}C (75 MHz, CDCl_3) δ 37.10 (s, $\text{CH}_2(9_{\text{ab}})$), 42.79 (s, $\text{C}(8)$), 50.78 (s, $\text{CH}_2(10_{\text{ab}})$), 57.63 (s, $\text{CH}_2(7)$), 65.52 (s, $\text{CH}_2(20)$), 114.87 (s, ArCH), 116.65 (q, $^3J_{\text{C-F}}$ 7.7 Hz, ArCH(18)), 120.18 (q, $^3J_{\text{C-F}}$ 3.9 Hz, ArCH(16)), 122.94 (s, ArCH), 123.09 (s, ArCH), 123.15 (s, ArCH), 123.64 (s, ArCH(14)), 123.93 (q, $^1J_{\text{C-F}}$ 272 Hz, $\text{ArCF}_3(19)$), 128.52 (s, ArCH), 129.44 (s, ArCH), 129.57 (s, ArCH), 131.45 (q, $^2J_{\text{C-F}}$ 32 Hz, $\text{ArC}(20)$), 138.81 (s, ArC), 138.85 (s, $\text{ArC}(13)$), 141.86 (s, ArC), 146.27 (s, $\text{ArC}(21)$), 147.31 (s, $\text{ArC}(24)$), 151.86 (s, $\text{C=O}(11)$)

R_f 0.44 (93:7, CH_2Cl_2 :MeOH)

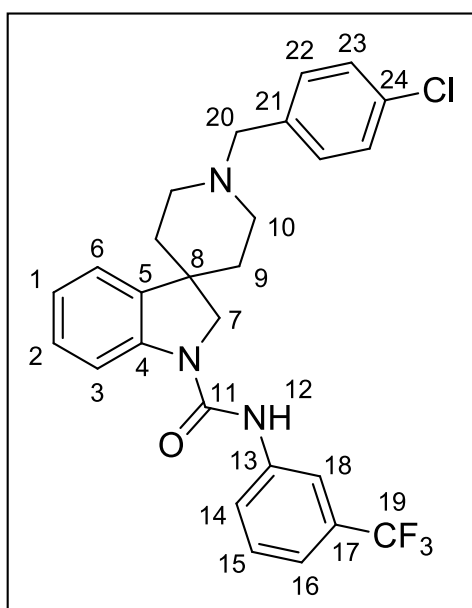
^{19}F (376 MHz, CDCl_3) δ -64.5 (s, $\text{Ar-CF}_3(19)$)

IR ν/cm^{-1} 743 (C-F, s), 1328 (NO_2 , s), 1516 (NO_2 , s), 1656 (C=O , s), 3307 (Ar C-H, w)

MS (ESI): 511 $[\text{M}+\text{H}^+]$

HRMS $\text{C}_{27}\text{H}_{26}\text{N}_4\text{F}_3\text{O}_3$ $[\text{M}+\text{H}^+]$ requires 511.1952, found 511.1942 (1.9 ppm error)

Preparation of 1'-(4-Chlorobenzyl)-*N*-(3-(trifluoromethyl)phenyl)spiro[indoline-3,4'-piperidine]-1-carboxamide (**LVT69**):



Following method C using Benzyl 1-((3-(trifluoromethyl)phenyl)carbamoyl)spiro[indoline-3,4'-piperidine]-1'-carboxylate (**LVT53**) (61.0 mg, 0.16 mmol, 1 eq.), 4-chlorobenzyl bromide (71.9 mg, 0.32 mmol, 2 eq.) and K₂CO₃ (44.2 mg, 0.32 mmol, 2 eq.) as starting materials. The desired product was purified using column chromatography (SiO₂, 94:6, CH₂Cl₂:MeOH) to afford, the pure product (**LVT69**) as a golden brown glass solid (47.0 mg, 0.09 mmol, 59%).

Data for **LVT69**

¹H (300 MHz, CDCl₃) δ 1.70 (2H, d, *J* 12.6 Hz, CH₂(9_a)), 2.02 (2H, dd, *J* 12.6, 12.0 Hz, CH₂(9_b)), 2.12 (2H, dd, *J* 12.0, 12.0 Hz, CH₂(10_a)), 2.92 (2H, d, *J* 12.0 Hz, CH₂(10_b)), 3.54 (2H, s, CH₂(20)), 3.91 (2H, s, CH₂(7)), 6.72 (1H, br. s, NH), 7.04 (1H, dd, *J* 7.2, 7.2 Hz, ArCH), 7.21–7.24 (2H, m, ArCH(1,3)), 7.30–7.35 (5H, m, ArCH(22,23)), 7.45 (1H, dd, *J* 7.7, 7.7 Hz, ArCH(15)), 7.70–7.74 (2H, m, ArCH(16,18)), 7.84 (1H, d, *J* 7.7 Hz, ArCH(14))

¹³C (75 MHz, CDCl₃) δ 37.17 (s, CH₂(9_{ab})), 42.94 (s, C(8)), 50.56 (s, CH₂(10_{ab})), 57.64 (s, CH₂(7)), 62.63 (s, CH₂(20)), 114.91 (s, ArCH(14)), 116.65 (q, ³*J*_{C-F} 3.8 Hz, ArCH(18)), 120.1 (q, ³*J*_{C-F} 7.5 Hz, ArCH(16)), 122.93 (s, ArCH), 123.11 (s, ArCH), 123.94 (q, ¹*J*_{C-F} 272 Hz, Ar-CF₃(19)), 128.43 (s, ArCH), 128.49 (s, ArCH), 129.55 (s, ArCH(15)), 130.38 (s, ArCH), 131.59 (q, ²*J*_{C-F} 32 Hz, ArC(17)), 132.92 (s, ArC), 136.64 (s, ArC(13)), 138.88 (s, ArC(21)), 138.93 (s, ArC(24)), 141.88 (s, ArC), 151.88 (s, C=O(11))

¹⁹F (376 MHz, CDCl₃) δ –64.5 (s, Ar-CF₃(19))

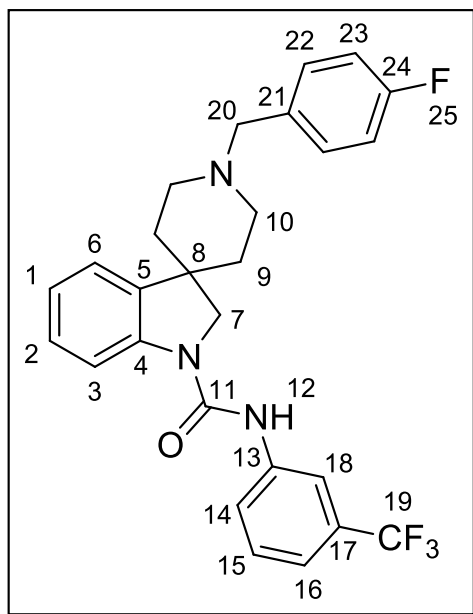
R_f 0.44 (94:6, CH₂Cl₂:MeOH)

IR ν/ cm^{–1} 1653 (C=O, s), 3291 (Ar C-H, w)

MS (ESI): 500/502 [M+H⁺]

HRMS C₂₇H₂₆³⁵ClF₃N₃O [M+H⁺] requires 500.1711, found 500.1700 (2.2 ppm error)

Preparation of 1'-(4-Fluorobenzyl)-*N*-(3-(trifluoromethyl)phenyl)spiro[indoline-3,4'-piperidine]-1-carboxamide (**LVT70**):



Following method C using Benzyl 1-((3-(trifluoromethyl)phenyl)carbamoyl)spiro[indoline-3,4'-piperidine]-1'-carboxylate (**LVT53**) (55.0 mg, 0.15 mmol, 1 eq.), 4-fluorobenzyl bromide (0.04 mL, 60.7 mg, 0.29 mmol, 2 eq.) and K_2CO_3 (40.1 mg, 0.29 mmol, 2 eq.) as starting materials. The desired product was purified using column chromatography (SiO_2 , 93:7, CH_2Cl_2 :MeOH) to afford, the pure product (**LVT70**) as a yellow glass solid (49.0 mg, 0.10 mmol, 68%).

Data for **LVT70**

1H (300 MHz, $CDCl_3$) δ 1.71 (2H, d, J 12.7 Hz, $CH_2(9_a)$), 2.03 (2H, dd, J 12.7, 12.1 Hz, $CH_2(9_b)$), 2.12 (2H, dd, J 12.1, 12.1 Hz, $CH_2(10_a)$), 2.93 (2H, d, J 12.1 Hz, $CH_2(10_b)$), 3.54 (2H, s, $CH_2(20)$), 3.91 (2H, s, $CH_2(7)$), 6.68 (1H, br. s, $NH(12)$), 7.01–7.05 (3H, m, ArCH), 7.22 (1H, dd, J 8.0, 8.0 Hz, ArCH), 7.32–7.48 (3H, m, ArCH), 7.46 (1H, dd, J 7.8, 7.8 Hz, ArCH(15)), 7.71–7.74 (2H, m, ArCH(18)), 7.84 (1H, d, J 7.8 Hz, ArCH(14))

^{13}C (75 MHz, CDCl_3) δ 37.18 (s, $\text{CH}_2(9_{\text{ab}})$), 42.98 (s, $\text{C}(8)$), 50.53 (s, $\text{CH}_2(10_{\text{ab}})$), 57.65 (s, $\text{CH}_2(7)$), 62.63 (s, $\text{CH}_2(20)$), 114.90 (s, ArCH), 115.04 (s, ArCH(17)), 115.25 (s, ArCH), 116.66 (q, $^3J_{\text{C-F}}$ 3.7 Hz, ArCH(18)), 120.1 (q, $^3J_{\text{C-F}}$ 3.5 Hz, ArCH(16)), 122.94 (s, ArCH(15)), 123.11 (s, ArCH), 123.94 (q, $^1J_{\text{C-F}}$ 272 Hz, Ar- CF_3 (19)), 128.43 (s, ArCH), 129.56 (s, ArCH), 130.54 (s, ArCH), 130.62 (s, ArCH), 131.46 (q, $^2J_{\text{C-F}}$ 32 Hz, ArC(17)), 133.77 (s, ArC), 133.80 (s, ArC(13)), 138.87 (s, ArC(21)), 138.97 (s, ArC(24)), 141.87 (s, ArC), 151.85 (s, $\text{C}=\text{O}(11)$), 162.11 (d, $^1J_{\text{C-F}}$ 245 Hz, ArC-F(25))

^{19}F (376 MHz, CDCl_3) δ -64.5 (s, Ar- CF_3 (19)) and -113.3 (s, ArC-F(25))

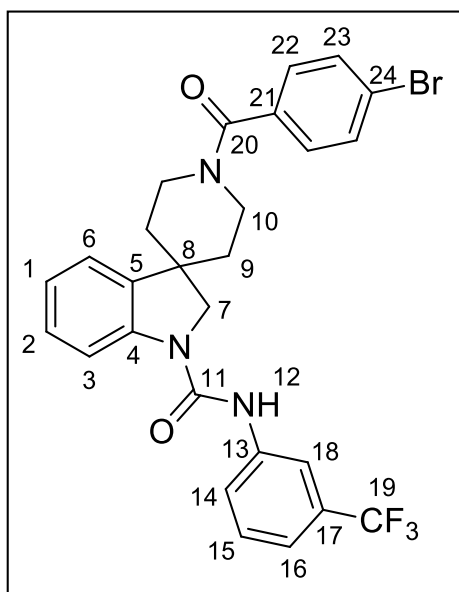
R_f 0.40 (94:6, CH_2Cl_2 :MeOH)

IR ν/cm^{-1} 743(C-F, s), 1654 ($\text{C}=\text{O}$, s), 3295 (Ar C-H, w)

MS (ESI): 484 $[\text{M}+\text{H}^+]$

HRMS $\text{C}_{27}\text{H}_{26}\text{F}_4\text{N}_3\text{O}$ $[\text{M}+\text{H}^+]$ requires 483.1900, found 484.2018 (2.0 ppm error)

Preparation of 1'-(4-Bromobenzoyl)-*N*-(3-(trifluoromethyl)phenyl)spiro[indoline-3,4'-piperidine]-1-carboxamide (**LVT71**):



Following method C using Benzyl 1-((3-(trifluoromethyl)phenyl)carbamoyl)spiro[indoline-3,4'-piperidine]-1'-carboxylate (**LVT53**) (50.0 mg, 0.13 mmol, 1 eq.), 4-bromobenzoyl chloride (58.4 mg, 0.27 mmol, 2 eq.) and K₂CO₃ (37.3 mg, 0.27 mmol, 2 eq.) as starting materials. The desired product was purified using column chromatography (SiO₂, 94:6, CH₂Cl₂:MeOH) to afford, the pure product (**LVT71**) as a colourless solid (44.0 mg, 0.08 mmol, 59%).

Data for **LVT71**

mp 154–158 °C

¹H (400 MHz, D₆-DMSO) δ 1.68 (2H, d, *J* 12.7 Hz, CH₂(9_a)), 1.90 (2H, dd, *J* 12.7, 12.7 Hz, CH₂(9_b)), 2.96 (1H, br., CH₂(10_a)), 3.21 (1H, br., CH₂(10_b)), 3.61 (1H, br., CH₂(10_a)), 4.16 (2H, s, CH₂(7)), 4.57 (1H, br., CH₂(10_b)), 6.98 (1H, dd, *J* 7.4, 7.4 Hz, ArCH), 7.19 (1H, dd, *J* 8.3, 8.3 Hz, ArCH), 7.36 (2H, d, *J* 7.3 Hz, ArCH(16)), 7.45 (2H, d, *J* 8.3 Hz, ArCH(22)), 7.55 (1H, dd, *J* 7.3, 7.3 Hz, ArCH(15)), 7.68 (1H, d, *J* 8.3 Hz, ArCH(23)), 7.90 (1H, d, *J* 7.3, Hz, ArCH), 8.01 (1H, s, ArCH(18)), 8.92 (1H, br. s, NH(12))

¹³C (100 MHz, D₆-DMSO) δ 36.57 (s, CH₂(9)), 43.47 (s, C(8)), 50.53 (s, CH₂(10)), 56.97 (s, CH₂(7)), 115.43 (s, ArCH), 116.46 (q, ³*J*_{C-F} 3.6 Hz, ArCH(18)), 119.09 (q, ³*J*_{C-F} 3.7 Hz, ArCH(16)), 122.71 (s, ArCH), 123.28 (s, ArC), 123.47 (s, ArCH), 123.88 (s, ArCH), 124.75 (q, ¹*J*_{C-F} 272 Hz, Ar-CF₃(19)), 128.37 (s, ArCH), 129.50 (s, ArCH(22)), 129.72 (q, ²*J*_{C-F} 31 Hz, ArC(17)), 130.10 (s, ArCH), 131.96 (s, ArCH(23)), 135.86 (s, ArC), 138.67 (s, ArC), 141.08 (s, ArC), 143.01 (s, ArC), 152.74 (s, C=O(11)), 168.60 (s, C=O(20))

¹⁹F (376 MHz, D₆-DMSO) δ –61.2 (s, Ar-CF₃(19))

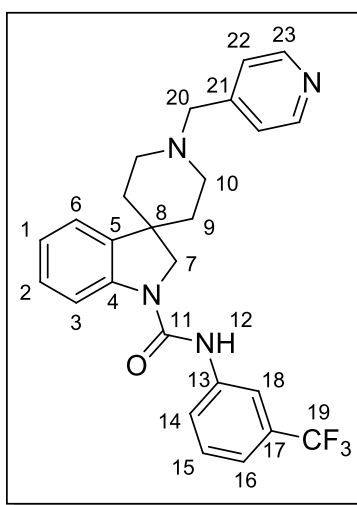
R_f 0.43 (94:6, CH₂Cl₂:MeOH)

IR ν/ cm⁻¹ 1653 (C=O, s), 1728 (C=O, s), 3285 (Ar C-H, w)

MS (ESI): 558/560 [M+H⁺]

HRMS C₂₇H₂₄⁷⁹BrF₃N₃O₂ [M+H⁺] requires 558.1004, found 558.1016 (2.9 ppm error)

Preparation of 1'-(Pyridin-4-ylmethyl)-N-(3-(trifluoromethyl)phenyl)spiro[indoline-3,4'-piperidine]-1-carboxamide (**LVT72**):



Following method C using Benzyl 1-((3-(trifluoromethyl)phenyl)carbamoyl)spiro[indoline-3,4'-piperidine]-1'-carboxylate (**LVT53**) (59.0 mg, 0.16 mmol, 1 eq.), 4-(bromomethyl)pyridine hydrobromide (78.4 mg, 0.32 mmol, 2 eq.) and K₂CO₃ (44.2 mg, 0.32 mmol, 2 eq.) as starting materials. The desired product was purified using column chromatography (SiO₂, 94:6, CH₂Cl₂:MeOH) to afford, the pure product (**LVT72**) as a light orange solid (36.1 mg, 0.08 mmol, 48%).

Data for **LVT72**

mp 223–225 °C

¹H (300 MHz, CDCl₃) δ 1.72 (2H, d, *J* 12.1 Hz, CH₂(9_a)), 2.05 (2H, dd, *J* 12.1, 11.7 Hz, CH₂(9_b)), 2.16 (2H, dd, *J* 11.7, 11.7 Hz, CH₂(10_a)), 2.91 (2H, d, *J* 11.7 Hz, CH₂(10_b)), 3.57 (2H, s, CH₂(20)), 3.92 (2H, s, CH₂(7)), 6.82 (1H, br. s, NH), 7.05 (1H, dd, *J* 7.7, 7.7 Hz,

ArCH), 7.22–7.25 (2H, m, ArCH), 7.32–7.35 (3H, m, ArCH), 7.45 (1H, dd, J 7.7, 7.7 Hz, ArCH(15)), 7.71–7.75 (2H, m, ArCH), 7.84 (1H, d, J 7.7 Hz, ArCH(14)), 8.57 (2H, s, ArCH(23))

^{13}C (75 MHz, CDCl_3) δ 37.10 (s, $\text{CH}_2(9)$), 42.78 (s, $\text{C}(8)$), 50.74 (s, $\text{CH}_2(10)$), 57.63 (s, $\text{CH}_2(7)$), 62.10 (s, $\text{CH}_2(20)$), 114.91 (s, ArCH(14)), 116.65 (q, $^3J_{\text{C-F}}$ 4.0 Hz, ArCH(18)), 120.14 (q, $^3J_{\text{C-F}}$ 3.8 Hz, ArCH(16)), 122.91 (s, ArCH), 123.11 (s, ArCH), 123.84 (s, ArCH), 123.93 (q, $^1J_{\text{C-F}}$ 272 Hz, Ar- $\text{CF}_3(19)$), 128.49 (s, ArCH), 128.49 (s, ArCH), 129.55 (s, ArCH(15)), 131.41 (q, $^2J_{\text{C-F}}$ 32 Hz, ArC(17)), 138.80 (s, ArC), 138.90 (s, ArC(13)), 141.9 (s, ArC), 147.52 (s, ArC(21)), 149.89 (s, ArCH(23)), 151.91 (s, $\text{C}=\text{O}(11)$)

^{19}F (376 MHz, CDCl_3) δ –64.5 (s, Ar- $\text{CF}_3(19)$)

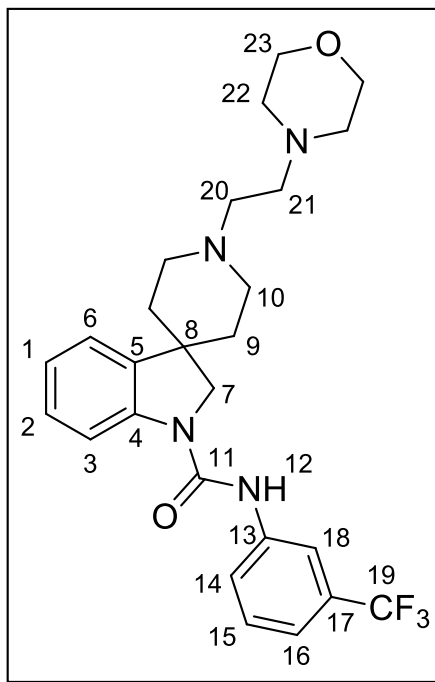
R_f 0.33 (94:6, CH_2Cl_2 :MeOH)

IR ν/cm^{-1} 743 (C-F, s), 1667 (C=O, s), 3354 (Ar C-H, w)

MS (ESI): 467 $[\text{M}+\text{H}^+]$

HRMS $\text{C}_{26}\text{H}_{26}\text{F}_3\text{N}_4\text{O}$ $[\text{M}+\text{H}^+]$ requires 467.2059, found 467.2066 (3.1 ppm error)

Preparation of 1'-(2-Morpholinoethyl)-N-(3-(trifluoromethyl)phenyl)spiro[indoline-3,4'-piperidine]-1-carboxamide (**LVT81**):



Benzyl 1-((3-(trifluoromethyl)phenyl)carbamoyl)spiro[indoline-3,4'-piperidine]-1'-carboxylate (**LVT53**) (94.0 mg, 0.25 mmol, 1 eq.), potassium carbonate (69.0 mg, 0.48 mmol, 2 eq.) and CH₃CN (25 mL) were added into a round bottom flask. Then, TBAI (184 mg, 0.50 mmol, 2 eq.) was added by way of, temporary removal of the condenser and left to stir for 30 minutes. The reaction was put under an atmosphere of nitrogen and 4-(2-Chloroethyl)morpholine hydrochloride (93.0 mg, 0.50 mmol, 2 eq.) was added as a CH₃CN solution (2 mL) solution *via* needle and syringe. The final mixture was heated at reflux for 12 h. After allowing to cool, the solvent was removed under reduced pressure and the mixture dissolved in CH₂Cl₂ (25 mL). The solution was transferred to a separating funnel and H₂O (20 mL) was added. The organics were extracted with further CH₂Cl₂ (2 × 25 mL) then collated, washed with saturated aqueous NH₄Cl (25 mL), dried over MgSO₄, filtered and concentrated under reduced pressure. The desired product was purified using column

chromatography (SiO₂, 92.5:7.5, CH₂Cl₂:MeOH), to afford, the pure product (**LVT81**) as an off-white solid (64.0 mg, 0.13 mmol, 52%).

Data for LVT81

mp 174–177 °C

¹H (300 MHz, CDCl₃) δ 1.73 (2H, d, *J* 12.3 Hz, CH₂(9_a)), 2.04 (2H, dd, *J* 12.3, 11.8 Hz, CH₂(9_b)), 2.17 (2H, dd, *J* 11.8, 11.8 Hz, CH₂(10_a)), 2.52 (4H, s, CH₂(20,21)), 2.60 (4H, s, CH₂(22)), 3.03 (2H, d, *J* 11.8 Hz, CH₂(10_b)), 3.73 (4H, s, (23)), 3.92 (2H, s, CH₂(7)), 6.76 (1H, s, NH(12)), 7.04 (1H, dd, *J* 6.7, 6.7 Hz, ArCH), 7.20–7.25 (2H, m, ArCH), 7.34 (1H, d, *J* 7.6 Hz, ArCH(16)), 7.45 (1H, dd, *J* 7.6, 7.6 Hz, ArCH), 7.71–7.75 (2H, m, ArCH), 7.83 (1H, d, *J* 7.6 Hz, ArCH(14))

¹³C (75 MHz, CDCl₃) δ 37.02 (s, CH₂(9_{ab})), 42.84 (s, C(8)), 51.22 (s, CH₂(10_{ab})), 54.19 (CH₂(20,21)), 55.92 (s, CH₂(22)), 57.66 (s, CH₂(7)), 66.93 (s, CH₂(23)), 114.89 (s, ArCH(17)), 116.68 (q, ³*J*_{C-F} 7.8 Hz, ArCH(18)), 120.11 (q, ³*J*_{C-F} 3.7 Hz, ArCH(16)), 122.95 (s, ArCH), 123.12 (s, ArCH), 123.14 (s, ArCH), 123.94 (¹*J*_{C-F} 272 Hz, ArC(19)), 128.47 (s, ArCH), 129.55 (s, ArCH), 131.43 (q, ²*J*_{C-F} 32 Hz, ArC(17)), 138.81 (s, ArC), 138.88 (s, ArC(13)), 141.87 (s, ArC), 151.89 (s, C=O(11))

¹⁹F (376 MHz, CDCl₃) δ –64.5 (s, Ar-CF₃(19))

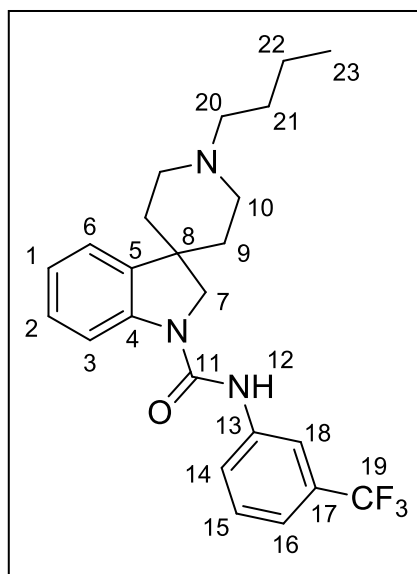
R_f 0.23 (92.5:7.5, CH₂Cl₂:MeOH)

IR ν/ cm^{–1} 1326 (C-F, s), 1664 (C=O, s), 2956 (Ar C-H, w)

MS (ESI): 489 [M+H⁺]

HRMS C₂₆H₃₂F₃N₄O₂ [M+H⁺] requires 489.2477, found 489.2460 (2.2 ppm error)

Preparation of 1'-Butyl-*N*-(3-(trifluoromethyl)phenyl)spiro[indoline-3,4'-piperidine]-1-carboxamide (**LVT86**):



Following method C using Benzyl 1-((3-(trifluoromethyl)phenyl)carbamoyl)spiro[indoline-3,4'-piperidine]-1'-carboxylate (**LVT53**) (79.0 mg, 0.21 mmol, 1 eq.), 1-bromobutane (0.05 mL, 63.8 mg, 0.42 mmol, 2 eq.) and K_2CO_3 (58.0 mg, 0.42 mmol, 2 eq.) as starting materials. The desired product was purified using column chromatography (SiO_2 , 92:8, CH_2Cl_2 :MeOH) to afford, the pure product (**LVT86**) as a golden brown solid (57.0 mg, 0.13 mmol, 62%).

Data for **LVT86**

mp 69–72 °C

1H (300 MHz, $CDCl_3$) δ 0.94 (3H, t, J 6.7 Hz, CH_3 (23)), 1.37 (2H, m, CH_2 (22)), 1.53 (2H, m, CH_2 (21)), 1.73 (2H, d, J 10.5 Hz, CH_2 (9_a)), 2.02 (2H, dd, J 11.0, 10.5 Hz, CH_2 (9_b)), 2.07 (2H, dd, J 11.0, 11.0 Hz, CH_2 (10_a)), 2.39 (2H, t, J 7.4 Hz, CH_2 (20)), 2.98 (2H, d, J 11.0, 11.0 Hz, CH_2 (10_b)), 3.91 (2H, s, CH (7)), 6.77 (1H, s, NH (12)), 7.03 (1H, dd, J 7.0, 7.0 Hz, ArCH), 7.20–7.24 (2H, m, ArCH), 7.34 (1H, d, J 7.6 Hz, ArCH), 7.43 (1H, dd, J 7.6, 7.6 Hz, ArCH), 7.70–7.74 (2H, m, ArCH(18)), 7.85 (1H, d, J 7.6 Hz, ArCH(14))

^{13}C (75 MHz, CDCl_3) δ 14.07 (s, $\text{CH}_3(23)$), 20.87 (s, $\text{CH}_2(22)$), 29.21 (s, $\text{CH}_2(21)$), 37.22 (s, $\text{CH}_2(9_{\text{ab}})$), 43.08 (s, $\text{C}(8)$), 50.79 (s, $\text{CH}_2(10_{\text{ab}})$), 57.68 (s, $\text{CH}(7)$), 58.90 (s, $\text{CH}_2(20)$), 114.92 (s, ArCH), 116.69 (q, $^3J_{\text{C-F}}$ 3.8 Hz, ArCH(18)), 120.12 (q, $^3J_{\text{C-F}}$ 3.7 Hz, ArCH(16)), 122.94 (s, ArCH), 123.12 (s, ArCH), 123.14 (s, ArCH), 123.95 (q, $^1J_{\text{C-F}}$ 272 Hz, ArCH(19)), 131.40 (q, $^2J_{\text{C-F}}$ 32 Hz, ArCH(17)), 138.92 (s, ArC(13)), 139.00 (s, ArC), 141.90 (s, ArC), 151.94 (s, $\text{C}=\text{O}(11)$)

^{19}F (376 MHz, CDCl_3) δ -64.5 (s, Ar- $\text{CF}_3(19)$)

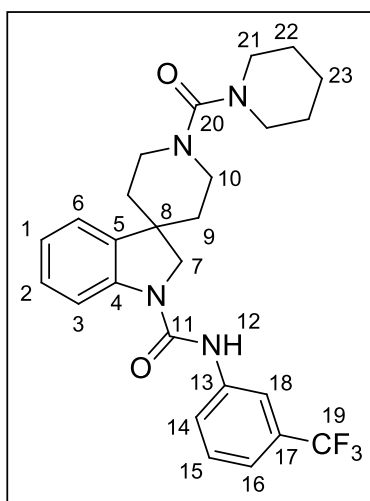
R_f 0.42 (92:8, CH_2Cl_2 :MeOH)

IR ν/cm^{-1} 1322 (C-F, s), 1672 ($\text{C}=\text{O}$, s), 2897 (Ar C-H, w)

MS (ESI): 431 $[\text{M}+\text{H}^+]$

HRMS $\text{C}_{24}\text{H}_{29}\text{F}_3\text{N}_3\text{O}$ $[\text{M}+\text{H}^+]$ requires 431.2200, found 432.2266 (2.0 ppm error)

Preparation of 1'-(Piperidine-1-carbonyl)-*N*-(3-(trifluoromethyl)phenyl)spiro[indoline-3,4'-piperidine]-1-carboxamide (**LVTa1**):



Following method C using Benzyl 1-((3-(trifluoromethyl)phenyl)carbamoyl)spiro[indoline-3,4'-piperidine]-1-carboxylate (**LVT53**) (253 mg, 0.67 mmol, 1 eq.), 1-piperidinecarbonyl chloride (0.17 mL, 200 mg, 1.34 mmol, 2 eq.) and K_2CO_3 (185 mg, 1.34 mmol, 2 eq.) as

starting materials. The desired product was purified using column chromatography (SiO₂, 93:7, CH₂Cl₂:MeOH), to afford, the pure product (**LVTa1**) as a yellow solid (226 mg, 0.46 mmol, 69%).

Data for LVTa1

mp 104–107 °C

¹H (300 MHz, CDCl₃) δ 1.73 (2H, br. d, *J* 13.5 Hz, CH₂(9_a)), 1.96 (2H, br. dd, *J* 13.5, 12.6 Hz, CH₂(9_b)), 2.29 (2H, br. dd, *J* 12.6, 12.6 Hz, CH₂(10_a)), 3.16–3.18 (6H, m, CH₂(22,23)), 3.24–3.25 (4H, m, CH₂(21)), 3.69 (2H, br. d, *J* 13.5 Hz, CH₂(10_b)), 4.01 (2H, s, CH₂(7)), 7.03 (1H, t, *J* 7.9 Hz, ArCH), 7.20 (1H, d, *J* 8.0 Hz, ArCH), 7.24 (1H, dd, *J* 7.9, 7.9 Hz, ArCH), 7.33 (1H, d, *J* 7.6 Hz, ArCH(16)), 7.44 (1H, dd, *J* 7.6, 7.6 Hz, ArCH(15)), 7.56 (1H, d, *J* 7.9 Hz, ArCH), 7.79 (1H, s, ArCH(18)), 7.92 (1H, d, *J* 8.0 Hz, ArCH(14))

¹³C (75 MHz, CDCl₃) δ 36.66 (s, CH₂(9_{ab})), 43.41 (s, C(7)), 44.38 (s, CH₂(10_{ab})), 47.82 (s, CH₂(21)), 47.94 (3C, s, CH₂(22)CH(23)), 57.20 (s, CH₂(7)), 115.21 (s, ArCH(14)), 116.75 (q, ³*J*_{C-F} 4.8 Hz, ArCH(18)), 119.90 (q, ³*J*_{C-F} 4.7 Hz, ArCH(16)), 120.99 (q, ¹*J*_{C-F} 272 Hz, CF₃(19)), 122.75 (s, ArCH), 122.97 (s, ArCH), 123.13 (s, ArCH), 128.62 (s, ArCH), 129.44 (s, ArCH(15)), 131.12 (q, ²*J*_{C-F} 32 Hz, ArC(17)), 138.18 (s, ArC), 139.19 (s, ArC), 142.09 (s, ArC(13)), 152.17 (s, C=O(11)), 164.62 (s, C=O(20))

¹⁹F (376 MHz, CDCl₃) δ –64.7 (s, Ar-CF₃(19))

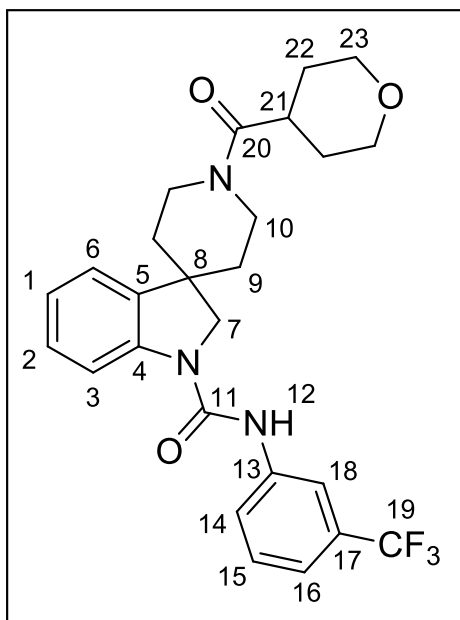
R_f 0.26 (93:7, CH₂Cl₂:MeOH)

IR ν/ cm^{–1} 1549 (C-F, s), 1633 (C=O, s), 1683 (C=O, s), 2850 (C-H, w), 3309 (Ar C-H, w)

MS (ESI): 487 [M+H⁺]

HRMS C₂₆H₃₀F₃N₄O₂ [M+H⁺] requires 487.2315, found 487.2304 (2.3 ppm error)

Preparation of 1'-(Piperidine-1-carbonyl)-*N*-(3-(trifluoromethyl)phenyl)spiro[indoline-3,4'-piperidine]-1-carboxamide (**LVTa2**):



Following method C using Benzyl 1-((3-(trifluoromethyl)phenyl)carbamoyl)spiro[indoline-3,4'-piperidine]-1'-carboxylate (**LVT53**) (210 mg, 0.56 mmol, 1 eq.), tetrahydro-2*H*-pyran-4-carbonyl chloride (0.14 mL, 168 mg, 1.11 mmol, 2 eq.) and K₂CO₃ (153 mg, 1.11 mmol, 2 eq.) as starting materials. The desired product was purified using column chromatography (SiO₂, 93:7, CH₂Cl₂:MeOH), to afford, the pure product (**LVTa2**) as an off-white solid (231 mg, 0.47 mmol, 85%).

Data for **LVTa2**

mp 206–210 °C

¹H (300 MHz, CDCl₃) δ 1.83–2.03 (4H, m, CH₂(22)), 2.70–2.84 (3H, m, CH₂(10_a), CH(21)), 3.26 (2H, dd, *J* 8.6, 8.6 Hz, CH₂(9_a)), 3.43 (2H, dd, *J* 8.0, 8.0 Hz, CH₂(23)), 3.98–4.04 (6H, m, CH₂(7,9_b,23)), 4.70 (2H, d, *J* 12.9 Hz, CH₂(10_b)), 7.05 (1H, dd, *J* 7.4, 7.4 Hz, ArCH), 7.14 (1H, d, *J* 7.4 Hz, ArCH), 7.29 (1H, dd, *J* 7.4, 7.4 Hz, ArCH), 7.35 (1H, d, *J* 7.6 Hz,

ArCH(16)), 7.46 (1H, dd, *J* 8.0, 8.0 Hz, ArCH(15)), 7.71–7.73 (2H, m, ArCH(18)), 7.83 (1H, d, *J* 8.0 Hz, ArCH(14))

¹³C (75 MHz, CDCl₃) δ 29.01 (s, CH₂(22)), 29.27 (s, CH₂(22)), 37.69 (s, CH(21)), 38.99 (s, CH₂(10_{ab})), 42.55 (CH₂(9_{ab})), 43.23 (s, C(8)), 57.16 (s, CH₂(7)), 67.21 (s, CH₂(23)), 114.92 (s, ArCH(14)), 116.60 (q, ³*J*_{C-F} 4.9 Hz, ArCH(18)), 120.21 (q, ³*J*_{C-F} 4.5 Hz, ArCH(16)), 120.73 (q, ¹*J*_{C-F} 272 Hz, CF₃(19)), 122.85 (s, ArCH), 123.10 (s, ArCH), 123.26 (s, ArCH), 128.86 (s, ArCH), 129.59 (s, ArCH(15)), 131.35 (q, ²*J*_{C-F} 32 Hz, ArC(17)), 137.71 (s, ArC), 138.73 (s, ArC), 141.77 (s, ArC(13)), 151.89 (s, C=O(11)), 172.96 (s, C=O(20))

¹⁹F (376 MHz, CDCl₃) δ –64.6 (s, Ar-CF₃(19))

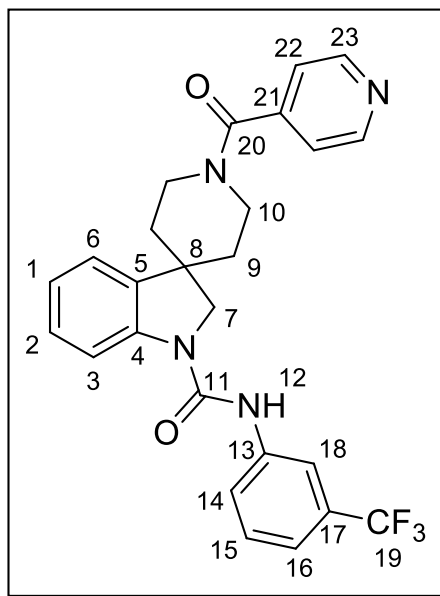
R_f 0.27 (93:7, CH₂Cl₂:MeOH)

IR ν/ cm⁻¹ 1549 (C-F, s), 1616 (C=O, s), 1690 (C=O, s), 2852 (C-H, w), 3313 (Ar C-H, w)

MS (ESI): 488 [M+H⁺]

HRMS C₂₆H₂₉F₃N₃O₃ [M+H⁺] requires 488.2156, found 488.2147 (1.7 ppm error)

Preparation of 1'-Isonicotinoyl-*N*-(3-(trifluoromethyl)phenyl)spiro[indoline-3,4'-piperidine]-1-carboxamide (**LVTa3**):



Following method C using Benzyl 1-((3-(trifluoromethyl)phenyl)carbamoyl)spiro[indoline-3,4'-piperidine]-1'-carboxylate (**LVT53**) (250 mg, 0.67 mmol, 1 eq.), isonicotinoyl chloride hydrochloride (134 mg, 1.34 mmol, 2 eq.) and K_2CO_3 (185 mg, 1.34 mmol, 2 eq.) as starting materials. The desired product was purified using column chromatography (SiO_2 , 93:7, CH_2Cl_2 :MeOH), to afford, the pure product (**LVTa3**) a light cream solid (277 mg, 0.58 mmol, 86%).

Data for **LVTa3**

mp 132–136 °C

1H (300 MHz, $CDCl_3$) δ 2.99 (2H, dd, J 12.9, 10.6 Hz, $CH_2(10_a)$), 3.23 (2H, dd, J 11.0, 10.6 Hz, $CH_2(9_a)$), 3.70 (2H, d, J 12.9, 11.0 Hz, $CH_2(9_b)$), 4.02 (2H, s, $CH_2(7)$), 4.78 (2H, d, J 12.9, 12.9 Hz, $CH_2(10_b)$), 6.90 (1H, s, $NH(12)$), 7.07 (1H, dd, J 7.5, 7.5 Hz, ArCH), 7.19 (1H, d, J 7.5 Hz, ArCH), 7.29 (1H, d, J 7.5, 7.5 Hz, ArCH), 7.33 (2H, d, J 7.5 Hz, ArCH(22)),

7.35 (1H, d, *J* 8.5 Hz, ArCH(16)), 7.45 (1H, dd, *J* 8.1, 8.1 Hz, ArCH(15)), 7.68–7.72 (2H, m, ArCH(18)), 7.79 (1H, d, *J* 8.1 Hz, ArCH(14)), 8.71 (2H, d, *J* 7.5 Hz, ArCH(23))

¹³C (75 MHz, CDCl₃) δ 39.28 (s, CH₂(10_{ab})), 43.14 (s, C(8)), 44.65 (s, CH₂(9_{ab})), 57.19 (s, CH₂(7)), 114.84 (s, ArCH(14)), 116.60 (q, ³*J*_{C-F} 7.9 Hz, ArCH(18)), 120.30 (q, ³*J*_{C-F} 6.9 Hz, ArCH(16)), 121.06 (s, ArCH(22)), 123.06 (s, ArCH), 123.33 (s, ArCH), 122.91 (s, ArCH), 123.87 (q, ¹*J*_{C-F} 272 Hz, CF₃(19)), 129.00 (s, ArCH), 129.62 (s, ArCH(15)), 131.39 (q, ²*J*_{C-F} 32 Hz, ArC(17)), 137.50 (s, ArC), 138.65 (s, ArC), 141.71 (s, ArC(13)), 143.25 (s, ArC(21)), 150.46 (s, ArCH(23)), 151.82 (s, C=O(11)), 167.97 (s, C=O(20))

¹⁹F (376 MHz, CDCl₃) δ –64.7 (s, Ar-CF₃(19))

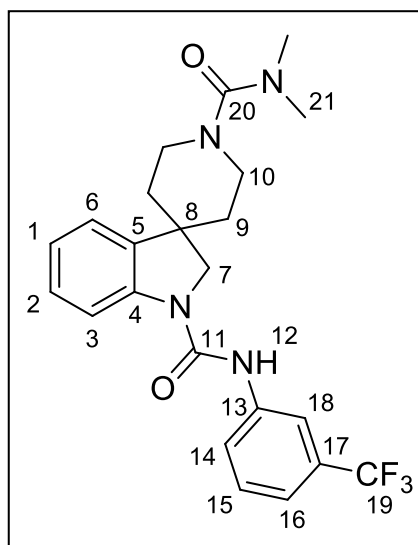
R_f 0.33 (93:7, CH₂Cl₂:MeOH),

IR ν/ cm⁻¹ 1544 (C-F, s), 1624 (C=O, s), 1721 (C=O, s), 2938 (C-H, w), 3308 (Ar C-H, w)

MS (ESI): 481 [M+H⁺]

HRMS C₂₆H₂₄F₃N₄O₂ [M+H⁺] requires 481.1846, found 481.1836 (2.1 ppm error)

Preparation of *N*¹, *N*^{1'}-Dimethyl-*N*¹-(3-(trifluoromethyl)phenyl)spiro[indoline-3,4'-piperidine]-1,1'-dicarboxamide (**LVTa4**):



Following method C using Benzyl 1-((3-(trifluoromethyl)phenyl)carbamoyl)spiro[indoline-3,4'-piperidine]-1'-carboxylate (**LVT53**) (250 mg, 0.67 mmol, 1 eq.), dimethylcarbonyl chloride (0.12 mL, 140 mg, 1.34 mmol, 2 eq.) and K₂CO₃ (185 mg, 1.34 mmol, 2 eq.) as starting materials. The desired product was purified using column chromatography (SiO₂, 93:7, CH₂Cl₂:MeOH), to afford, the pure product (**LVTa4**) a light cream solid (239 mg, 0.54 mmol, 80%).

Data for **LVTa4**

mp 199–202 °C

¹H (300 MHz, D₄-MeOH) δ 1.71 (2H, d, *J* 13.1 Hz, CH₂(9_a)), 1.96 (2H, dd, *J* 14.0, 13.1 Hz, CH₂(9_b)), 2.89 (6H, s, CH₃(21)), 3.00 (2H, d, *J* 14.0, 13.1 Hz, CH₂(10_a)), 3.71 (2H, d, *J* 13.8 Hz, CH₂(10_b)), 4.10 (2H, s, CH₂(7)), 7.07 (1H, dd, *J* 7.4, 7.4 Hz, ArCH), 7.16–7.23 (2H, m, ArCH), 7.34 (1H, d, *J* 7.7 Hz, ArCH(16)), 7.50 (1H, dd, *J* 7.7, 7.7 Hz, ArCH(15)), 7.79 (1H, d, *J* 8.7 Hz, ArCH), 7.90 (1H, s, ArCH(18)), 7.93 (1H, d, *J* 7.7 Hz, ArCH(14))

^{13}C (75 MHz, CDCl_3) δ 36.65 (s, $\text{CH}_2(9_{\text{ab}})$), 38.41 (s, $\text{CH}_3(21)$), 43.33 (s, $\text{C}(8)$), 44.30 (s, $\text{CH}_2(10_{\text{ab}})$), 57.18 (s, $\text{CH}_2(7)$), 115.34 (s, $\text{ArCH}(14)$), 116.77 (q, $^3J_{\text{C-F}}$ 7.9 Hz, $\text{ArCH}(18)$), 119.83 (q, $^3J_{\text{C-F}}$ 6.9 Hz, $\text{ArCH}(16)$), 122.62 (s, ArCH), 122.91 (s, ArCH), 123.30 (s, ArCH), 124.00 (q, $^1J_{\text{C-F}}$ 272 Hz, $\text{CF}_3(19)$), 128.61 (s, ArCH), 129.38 (s, $\text{ArCH}(15)$), 131.33 (q, $^2J_{\text{C-F}}$ 32 Hz, $\text{ArC}(17)$), 138.02 (s, ArC), 139.35 (s, ArC), 142.21 (s, $\text{ArC}(13)$), 152.32 (s, $\text{C=O}(11)$), 165.28 (s, $\text{C=O}(20)$)

^{19}F (376 MHz, CDCl_3) δ -64.7 (s, $\text{Ar-CF}_3(19)$)

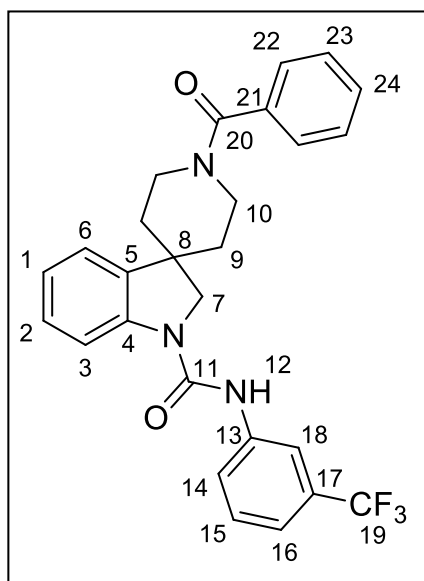
R_f 0.38 (93:7, CH_2Cl_2 :MeOH),

IR ν/cm^{-1} 1552 (C-F, s), 1675 (C=O, s), 1739 (C=O, s), 2844 (C-H, w), 3379 (Ar C-H, w)

MS (ESI): 447 $[\text{M}+\text{H}^+]$

HRMS $\text{C}_{23}\text{H}_{26}\text{F}_3\text{N}_4\text{O}_2$ $[\text{M}+\text{H}^+]$ requires 447.2002, found 447.1998 (1.0 ppm error)

Preparation of 1'-Benzoyl-*N*-(3-(trifluoromethyl)phenyl)spiro[indoline-3,4'-piperidine]-1-carboxamide (**LVTa5**):



Following method C using Benzyl 1-((3-(trifluoromethyl)phenyl)carbamoyl)spiro[indoline-3,4'-piperidine]-1'-carboxylate (**LVT53**) (200 mg, 0.53 mmol, 1 eq.), benzoyl chloride (0.13 mL, 157 mg, 1.07 mmol, 2 eq.) and K₂CO₃ (148 mg, 1.07 mmol, 2 eq.) as starting materials. The desired product was purified using column chromatography (SiO₂, 93:7, CH₂Cl₂:MeOH), to afford, the pure product (**LVTa5**) a light cream solid (223 mg, 0.47 mmol, 88%).

Data for **LVTa5**

mp 243–246 °C

¹H (300 MHz, CDCl₃) δ 2.94 (2H, d, *J* 13.5 Hz, CH₂(10_a)), 3.12 (2H, dd, *J* 13.5, 13.1 Hz, CH₂(9_a)), 3.81 (2H, d, *J* 13.1, 12.5 Hz, CH₂(9_b)), 4.04 (2H, s, CH₂(7)), 4.73 (2H, d, *J* 13.5 Hz, CH₂(10_b)), 7.05 (1H, dd, *J* 7.4, 7.4 Hz, ArCH), 7.17 (1H, d, *J* 7.9 Hz, ArCH), 7.23–7.31 (2H, m, ArCH(16)), 7.36–7.42 (6H, m, ArCH(15,22,23,24)), 7.70–7.72 (2H, m, ArCH(18)), 7.93 (1H, d, *J* 7.9 Hz, ArCH(14))

¹³C (75 MHz, CDCl₃) δ 39.47 (s, CH₂(10_{ab})), 43.23 (s, C(8)), 44.76 (s, CH₂(9_{ab})), 57.07 (s, CH₂(7)), 115.24 (s, ArCH(14)), 116.84 (q, ³*J*_{C-F} 4.9 Hz, ArCH(18)), 120.00 (q, ³*J*_{C-F} 5.9 Hz, ArCH(16)), 122.70 (s, ArCH), 123.10 (s, ArCH), 123.34 (s, ArCH), 123.98 (q, ¹*J*_{C-F} 272 Hz, CF₃(19)), 126.76 (s, ArCH(24)), 128.73 (s, ArCH(23)), 128.83 (s, ArCH(22)), 129.41 (s, ArCH), 130.11 (s, ArCH(15)), 131.11 (q, ²*J*_{C-F} 32 Hz, ArC(17)), 135.42 (s, ArC(15)), 137.48 (s, ArC), 139.08 (s, ArC), 142.09 (s, ArC(13)), 152.25 (s, C=O(11)), 170.92 (s, C=O(20))

¹⁹F (376 MHz, CDCl₃) δ –64.6 (s, Ar-CF₃(19))

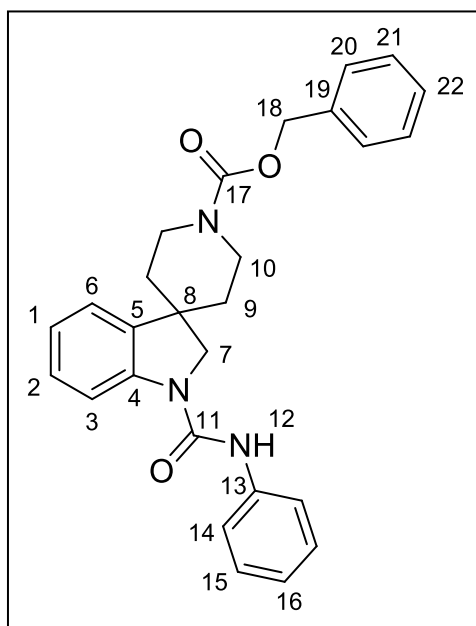
R_f 0.39 (93:7, CH₂Cl₂:MeOH)

IR ν/ cm⁻¹ 1539 (C-F, s), 1620 (C=O, s), 1677 (C=O, s), 2847 (C-H, w), 3331 (Ar C-H, w)

MS (ESI): 480 [M+H⁺]

HRMS $C_{27}H_{25}F_3N_3O_2$ $[M+H]^+$ requires 480.1893, found 480.1880 (2.8 ppm error)

Preparation of Benzyl 1-(phenylcarbamoyl)spiro[indoline-3,4'-piperidine]-1'-carboxylate (**LVTa7**):



Benzyl spiro[indoline-3,4'-piperidine]-1'-carboxylate (300 mg, 0.94 mmol, 1 eq.) was dissolved in CH_2Cl_2 (20 mL) under a nitrogen atmosphere. Phenyl isocyanate (0.12 mL, 131 mg, 1.13 mmol, 1.2 eq.) was added slowly *via* syringe and the resulting solution stirred for 4 hours at room temperature. The solvent was removed under reduced pressure and the product purified using column chromatography (SiO_2 , 97:3 CH_2Cl_2 :MeOH) to yield a cream solid **LVTa7** (410 mg, 0.93 mmol, 99%).

Data for **LVTa7**

mp 106–108 °C

1H (300 MHz, $CDCl_3$) δ 1.66 (2H, br. d, J 13.4 Hz, $CH_2(9_a)$), 1.83 (2H, br. dd, J 13.4, 10.0 Hz, $CH_2(9_b)$), 2.91 (2H, br. dd, $CH_2(10_a)$), 3.91 (2H, s, $CH_2(7)$), 4.21 (2H, br. d, $CH_2(10_b)$), 5.16 (1H, s, ArCH(18)), 6.86 (1H, s, NH), 6.99 (1H, dd, J 7.0, 7.0 Hz, ArCH), 7.05–7.10

(2H, m, ArCH), 7.18–7.33 (3H, m, ArCH), 7.36–7.37 (4H, m, ArCH), 7.46 (2H, d, *J* 7.6 Hz, ArCH), 7.85 (1H, d, *J* 8.0 Hz, ArCH)

^{13}C (75 MHz, CDCl_3) δ 36.38 ($\text{CH}_2(10_{\text{ab}})$), 41.06 ($\text{CH}_2(9_{\text{ab}})$), 42.88 (ArC(8)), 57.01 ($\text{CH}_2(7)$), 67.36 ($\text{CH}_2(18)$), 114.93 (ArCH), 120.02 (ArCH), 120.42 (ArCH), 122.75 (ArCH), 122.83 (ArCH), 123.25 (ArCH), 123.82 (ArCH), 127.96 (ArCH), 128.17 (ArCH), 128.59 (ArCH), 128.65 (ArCH), 129.04 (ArCH), 136.65 (ArC), 138.04 (ArC), 138.18 (ArC), 142.20 (ArC(13)), 152.45 (C=O(11)), 155.37 (C=O(17))

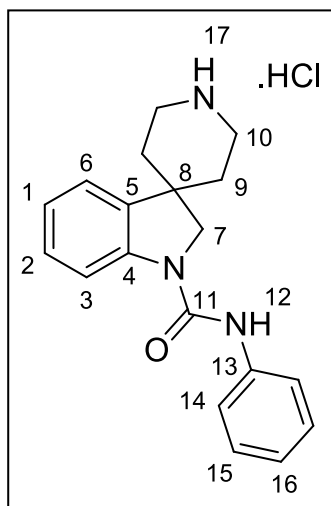
R_f 0.44 (98:2, CH_2Cl_2 :MeOH)

IR ν/cm^{-1} 1624 (C-O, s), 1697 (C=O, s), 1723 (C=O, s), 2679 (C-H, w)

MS (ESI): 442 $[\text{M}+\text{H}^+]$

HRMS $\text{C}_{27}\text{H}_{28}\text{NO}_3$ $[\text{M}+\text{H}^+]$ requires 442.2131, found 442.2134 (2.3 ppm error)

Preparation of *N*-Phenylspiro[indoline-3,4'-piperidine]-1-carboxamide (**LVTa9**):



Benzyl 1-(phenylcarbamoyl)spiro[indoline-3,4'-piperidine]-1'-carboxylate (**LVTa7**) (410 mg, 0.93 mmol, 1 eq.) was dissolved in MeOH (15 mL) and then, Pearlman's catalyst (65.3

mg, 0.09 mmol, 0.1 eq.) was added into the solution. The reaction mixture was purged with a balloon of hydrogen until deflated and then left under an atmosphere of hydrogen overnight. The methanol was removed under reduced pressure and the reaction mixture was filtered through celite with CH₂Cl₂ (100 mL) to collect any remaining starting material. The eluent 10% MeOH/CH₂Cl₂ (200 mL) was subsequently passed through the celite to elute the desired product. The product **LVTa9** is an off-white amorphous solid (200 mg, 0.65 mmol, 70%).

Data for **LVTa9**

mp 98–101 °C

¹H (300 MHz, CDCl₃) δ 1.70 (2H, d, *J* 12.5 Hz, CH₂(9_a)), 1.90 (2H, dd, *J* 15.0, 12.5 Hz, CH₂(9_b)), 2.78 (2H, dd, *J* 12.5, 12.5 Hz, CH₂(10_a)), 3.14 (2H, d, *J* 15.0 Hz, CH₂(10_b)), 3.96 (2H, s, CH₂(7)), 6.58 (1H, s, NH(12)), 7.02 (1H, dd, *J* 7.3, 7.3 Hz, ArCH), 7.10 (1H, dd, *J* 7.3, 7.3 Hz, ArCH), 7.20 (1H, d, *J* 7.3 Hz, ArCH), 7.24 (1H, dd, *J* 7.5, 7.5 Hz, ArCH(16)), 7.35 (2H, dd, *J* 8.6, 8.6 Hz, ArCH(15)), 7.48 (2H, d, *J* 8.5 Hz, ArCH(14)), 7.97 (1H, d, *J* 7.3 Hz, ArCH)

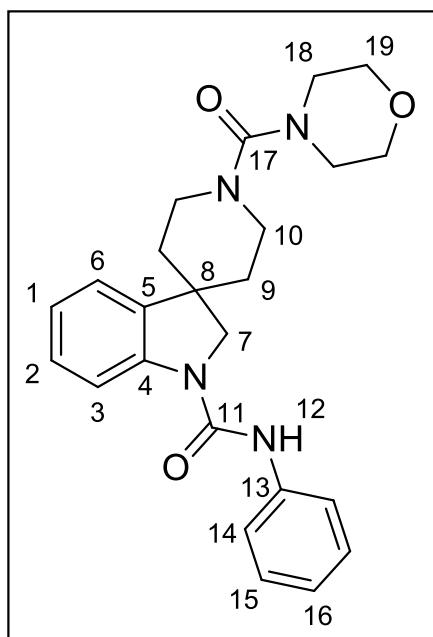
¹³C (75 MHz, CDCl₃) δ 37.70 (CH₂(9_{ab})), 43.34 (C(8)), 43.54 (CH₂(10_{ab})), 57.69 (CH₂(7)), 114.78 (ArCH(6)), 120.08 (ArCH(14)), 122.74 (ArCH), 122.85 (ArCH), 123.67 (ArCH), 128.33 (ArCH(16)), 129.05 (ArCH(15)), 138.13 (ArC), 139.16 (ArC), 142.03 (ArC(13)), 152.22 (C=O(11))

IR ν /cm⁻¹ 1652 (C=O, s), 2929 (C-H, w), 3290 (Ar C-H, w)

MS (ESI): 308 [M+H⁺]

HRMS C₁₉H₂₂N₃O [M+H⁺] requires 308.1763, found 308.1762 (1.9 ppm error)

Preparation of 1'-(Morpholine-4-carbonyl)-*N*-phenylspiro[indoline-3,4'-piperidine]-1-carboxamide (**LVTa10**):



Following method C using *N*-Phenylspiro[indoline-3,4'-piperidine]-1-carboxamide (**LVTa9**) (200 mg, 0.65 mmol, 1 eq.), 4-morpholinecarbonyl chloride (0.14 mL, 179 mg, 1.24 mmol, 2 eq.) and K₂CO₃ (167 mg, 1.24 mmol, 2 eq.) as starting materials. The desired product was purified using column chromatography (SiO₂, 93:7, CH₂Cl₂:MeOH), to afford, the pure product (**LVTa10**) a brown solid (80.2 mg, 0.19 mmol, 29%).

Data for **LVTa10**

mp 133–136 °C

¹H (300 MHz, CDCl₃) δ 1.75 (2H, d, *J* 13.8 Hz, CH₂(9_a)), 1.94 (2H, dd, *J* 13.8, 13.1 Hz, CH₂(9_b)), 2.97 (2H, dd, *J* 13.1, 13.1 Hz, CH₂(10_a)), 3.26–3.34 (4H, m, CH₂(18)), 3.67–3.73 (4H, m, CH₂(19)), 3.76 (2H, d, *J* 13.1 Hz, CH₂(10_b)), 3.98 (2H, s, CH₂(7)), 6.62 (1H, s, NH(12)), 7.02 (1H, dd, *J* 7.3, 7.3 Hz, ArCH), 7.12 (1H, dd, *J* 7.3, 7.3 Hz, ArCH), 7.18 (1H, d, *J* 7.3 Hz, ArCH), 7.25 (1H, dd, *J* 7.7, 7.7 Hz, ArCH(16)), 7.35 (2H, dd, *J* 7.7, 7.7 Hz, ArCH(15)), 7.47 (2H, d, *J* 7.7 Hz, ArCH(14)), 7.82 (1H, d, *J* 7.3 Hz, ArCH)

^{13}C (75 MHz, CDCl_3) δ 36.46 ($\text{CH}_2(9_{\text{ab}})$), 43.22 ($\text{C}(8)$), 44.06 ($\text{CH}_2(10_{\text{ab}})$), 47.34 ($\text{CH}_2(18)$), 57.16 ($\text{CH}_2(7)$), 66.66 ($\text{CH}_2(19)$), 114.76 (ArCH), 120.07 ($\text{ArCH}(14)$), 122.81 (ArCH), 123.65 (ArCH), 123.78 (ArCH), 128.65 ($\text{ArCH}(16)$), 129.08 ($\text{ArCH}(15)$), 138.02 (ArC), 138.13 (ArC), 142.07 ($\text{ArC}(13)$), 152.162 ($\text{C=O}(11)$), 164.03 ($\text{C=O}(17)$)

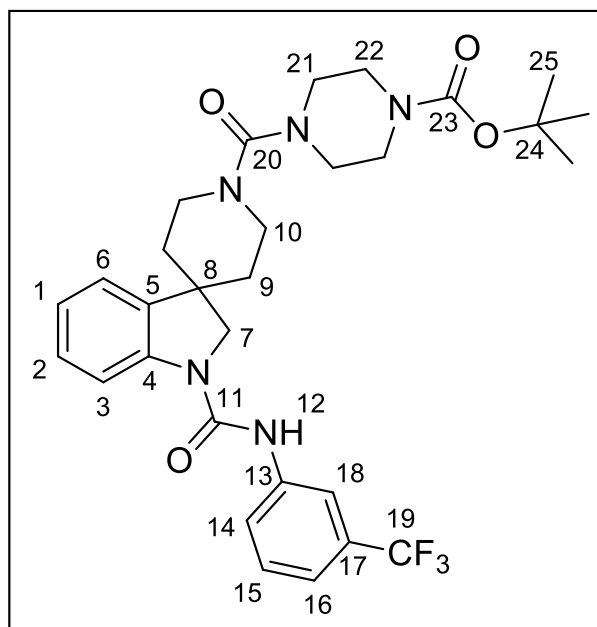
R_f 0.31 (9:1, CH_2Cl_2 :MeOH)

IR ν/cm^{-1} 1623 (C=O , s), 1674 (C=O , s), 2852 (C-H , w), 3324 (Ar C-H , w)

MS (ESI): 421 $[\text{M}+\text{H}^+]$

HRMS $\text{C}_{24}\text{H}_{29}\text{N}_4\text{O}_3$ $[\text{M}+\text{H}^+]$ requires 421.2234, found 421.2233 (0.3 ppm error)

Preparation of *Tert*-butyl 4-(1-((3-(trifluoromethyl)phenyl)carbamoyl)spiro[indoline-3,4'-piperidin]-1'-ylcarbonyl)piperazine-1-carboxylate (**LVTa12**):



Triphosgene (56.4 mg, 0.19 mmol, 1eq.) was dissolved in anhydrous CH_2Cl_2 (15 mL) under a nitrogen atmosphere and stirred in an ice bath for 15 minutes. *N*-(3-(Trifluoromethyl)phenyl)spiro[indoline-3,4'-piperidine]-1-carboxamide hydrochloride

(**LVT53**) (200 mg, 0.53 mmol, 1 eq.) was dissolved separately in anhydrous CH₂Cl₂ (10 mL) under a nitrogen atmosphere and subsequently added into the reaction flask slowly. The resulting solution was stirred for 30 minutes. Triethylamine (0.06 mL, 43.6 mg, 0.42 mmol, 2.2 eq.) was then dissolved in anhydrous CH₂Cl₂ (5 mL) under a nitrogen atmosphere and transferred into the main reaction flask *via* syringe slowly and stirred for a further 20 minutes. 1-Boc-piperazine (89.4 mg, 0.48 mmol, 2.52 eq.) was next dissolved in anhydrous CH₂Cl₂ (10 mL) under a nitrogen atmosphere and triethylamine (0.06 mL, 43.6 mg, 0.42 mmol, 2.2 eq.) subsequently added into this mixture. The secondary reaction mixture was added slowly *via* syringe into the primary reaction flask and stirred for 1 hour. The reaction was quenched with saturated aqueous NaHCO₃ (50 mL), followed by the addition of H₂O (30 mL). Organics were extracted with CH₂Cl₂ (2 × 20 mL), washed with saturated aqueous brine (30 mL), dried over MgSO₄, filtered and solvent removed under reduced pressure. The product was purified by column chromatography (SiO₂, 93:7, CH₂Cl₂:MeOH), which revealed **LVTa12** as a light cream solid (231 mg, 0.39 mmol, 74%).

Data for **LVTa12**

mp 128–131 °C

¹H (300 MHz, CDCl₃) δ 1.47 (9H, s, CH₃(25)), 1.74 (2H, d, *J* 13.4 Hz, CH₂(9_a)), 1.96 (2H, dd, *J* 13.4, 12.7 Hz, CH₂(9_b)), 2.96 (2H, dd, *J* 12.7, 12.7 Hz, CH₂(10_a)), 3.23–3.27 (4H, m, CH₂(22)), 3.40–3.43 (4H, m, CH₂(21)), 3.74 (2H, d, *J* 13.4 Hz, CH₂(10_b)), 4.00 (2H, s, CH₂(7)), 6.98 (1H, s, NH(12)), 7.05 (1H, dd, *J* 7.3, 7.3 Hz, ArCH), 7.19 (1H, d, *J* 7.3 Hz, ArCH), 7.18 (1H, dd, *J* 7.3, 7.3 Hz, ArCH), 7.34 (1H, d, *J* 7.9 Hz, ArCH(16)), 7.45 (1H, dd, *J* 7.9, 7.9 Hz, ArCH(15)), 7.71–7.75 (2H, m, ArCH(18)), 7.86 (1H, d, *J* 7.9 Hz, ArCH(14))

¹³C (75 MHz, CDCl₃) δ 28.38 (s, CH₃(25)), 36.46 (s, CH₂(9_{ab})), 43.30 (s, C(8)), 44.14 (4C, s, CH₂(10_{ab},21)), 46.66 (s, CH₂(22)), 57.16 (s, CH₂(7)), 80.20 (s, C(24)), 115.00 (s,

ArCH(14)), 116.61 (q, $^3J_{C-F}$ 7.3 Hz, ArCH(18)), 120.12 (q, $^3J_{C-F}$ 7.6 Hz, ArCH(16)), 122.87 (s, ArCH), 123.08 (s, ArCH), 123.14 (s, ArCH), 123.90 (q, $^1J_{C-F}$ 272 Hz, ArCH(19)), 128.71 (s, ArCH), 129.54 (s, ArCH(15)), 131.33 (q, $^2J_{C-F}$ 32 Hz, ArC(17)), 138.07 (s, ArC), 138.85 (s, ArC), 141.84 (s, ArC(13)), 151.92 (s, C=O(11)), 154.70 (s, C=O(20)), 164.05 (s, C=O(23))

^{19}F (376 MHz, CDCl_3) δ -64.7 (s, Ar-CF₃(19))

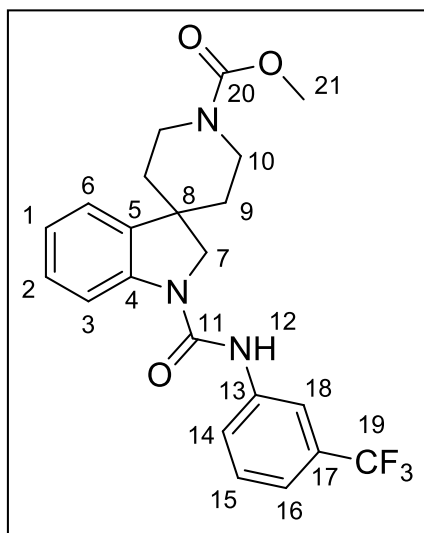
R_f 0.42 (93:7, CH_2Cl_2 :MeOH)

IR ν/cm^{-1} 1545 (C-F, s), 1602 (C=O, s), 1627 (C=O, s), 1680 (C=O, s), 2854 (C-H, w), 3326 (Ar C-H, w)

MS (ESI): 588 [M+H⁺]

HRMS $\text{C}_{30}\text{H}_{37}\text{F}_3\text{N}_5\text{O}_4$ [M+H⁺] requires 588.2792, found 588.2787 (0.9 ppm error)

Preparation of Methyl 1-((3-(trifluoromethyl)phenyl)carbamoyl)spiro[indoline-3,4'-piperidine]-1'-carboxylate (**LVTa14**):



Triphosgene (48.0 mg, 0.16 mmol, 1eq.) was dissolved in anhydrous CH₂Cl₂ (15 mL) under a nitrogen atmosphere and stirred in an ice bath for 15 minutes. *N*-(3-(trifluoromethyl)phenyl)spiro[indoline-3,4'-piperidine]-1-carboxamide hydrochloride (**LVT53**) (164 mg, 0.44 mmol, 1 eq.) was dissolved separately in anhydrous CH₂Cl₂ (10 mL) under a nitrogen atmosphere and subsequently added into the reaction flask slowly. The resulting solution was stirred for 30 minutes. Triethylamine (0.05 mL, 36.3 mg, 0.35 mmol, 2.2 eq.) was then dissolved in anhydrous CH₂Cl₂ (5 mL) under a nitrogen atmosphere and transferred into the main reaction flask *via* syringe slowly and stirred for a further 20 minutes. 4-Aminophenol (44.0 mg, 0.40 mmol, 2.52 eq.) was next dissolved in anhydrous CH₂Cl₂ (10 mL) under a nitrogen atmosphere and triethylamine (0.05 mL, 36.3 mg, 0.35 mmol, 2.2 eq.) subsequently added into this mixture. The secondary reaction mixture was added slowly *via* syringe into the primary reaction flask and stirred for 1 hour. The reaction was quenched with saturated aqueous NaHCO₃ (50 mL), followed by the addition of H₂O (30 mL). Organics were extracted with CH₂Cl₂ (2 × 20 mL), washed with saturated aqueous brine (30 mL), dried over MgSO₄, filtered and solvent removed under reduced pressure. The product was purified by column chromatography (SiO₂, 99:1, CH₂Cl₂:MeOH), which revealed the side product **LVTa14** as a light cream solid (20 mg, 0.05 mmol, 29%).

Data for **LVTa14**

mp 112–116 °C

¹H (300 MHz, CDCl₃) δ 1.72 (2H, d, *J* 13.4 Hz, CH₂(9_a)), 1.89 (2H, dd, *J* 13.4, 12.8 Hz, CH₂(9_b)), 2.95 (2H, dd, *J* 12.8, 12.8 Hz, CH₂(10_a)), 3.74 (3H, s, CH₃(21)), 3.99 (2H, s, CH₂(7)), 4.22 (2H, d, *J* 12.8 Hz, CH₂(10_b)), 6.92 (1H, s, NH(12)), 7.05 (1H, dd, *J* 7.2, 7.2 Hz, ArCH), 7.14 (1H, d, *J* 7.2 Hz, ArCH), 7.27 (1H, dd, *J* 7.2, 7.2 Hz, ArCH), 7.34 (1H, d,

J 7.7 Hz, ArCH(16)), 7.44 (1H, dd, *J* 7.7, 7.7 Hz, ArCH(15)), 7.71 (1H, d, *J* 8.0 Hz, ArCH), 7.75 (1H, s, ArCH(18)), 7.85 (1H, d, *J* 8.0 Hz, ArCH(14))

¹³C (75 MHz, CDCl₃) δ 36.35 (s, CH₂(9_{ab})), 40.94 (s, CH₂(10_{ab})), 42.98 (s, C(8)), 52.83 (s, CH₃(21)), 56.94 (s, CH₂(7)), 114.98 (s, ArCH(14)), 116.65 (q, ³*J*_{C-F} 7.6 Hz, ArCH(18)), 120.10 (q, ³*J*_{C-F} 7.5 Hz, ArCH(16)), 122.84 (s, ArCH), 123.14 (s, ArCH), 123.19 (s, ArC), 123.91 (q, ¹*J*_{C-F} 272 Hz, ArCH(19)), 128.71 (s, ArCH), 129.54 (s, ArCH(15)), 131.34 (q, ²*J*_{C-F} 32 Hz, ArC(17)), 138.07 (s, ArC), 138.77 (s, ArC), 141.79 (s, ArC(13)), 151.91 (s, C=O(11)), 155.95 (s, C=O(20))

¹⁹F (376 MHz, CDCl₃) δ −64.7 (s, Ar-CF₃(19))

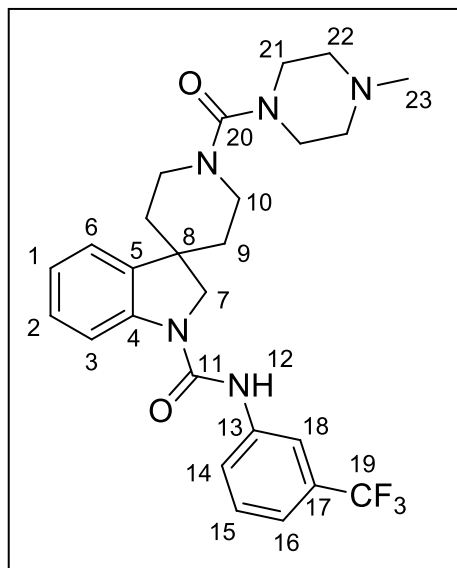
R_f 0.42 (99:1, CH₂Cl₂:MeOH)

IR ν/ cm^{−1} 1328 (C-O, s), 1540 (C-F, s), 1600 (C=O, s), 1675 (C=O, s), 2860 (C-H, w), 3325 (Ar C-H, w)

MS (ESI): 434 [M+H⁺]

HRMS C₂₂H₂₃F₃N₃O₃ [M+H⁺] requires 434.1686, found 434.1685 (0.2 ppm error)

Preparation of 1'-(4-Methylpiperazine-1-carbonyl)-*N*-(3-(trifluoromethyl)phenyl)spiro[indoline-3,4'-piperidine]-1-carboxamide (**LVTa18**):



Following method C using Benzyl 1-((3-(trifluoromethyl)phenyl)carbamoyl)spiro[indoline-3,4'-piperidine]-1'-carboxylate (**LVT53**) (119 mg, 0.32 mmol, 1 eq.), 4-methyl-1-piperazinecarbonyl chloride hydrochloride (127 mg, 0.64 mmol, 2 eq.) and K₂CO₃ (88.4 mg, 0.64 mmol, 2 eq.) as starting materials. The desired product was purified using column chromatography (SiO₂, 93:7, CH₂Cl₂:MeOH), to afford, the pure product (**LVTa18**) a light cream solid (139 mg, 0.28 mmol, 87%).

Data for **LVTa18**

mp 110–114 °C

¹H (300 MHz, CDCl₃) δ 1.73 (2H, d, *J* 13.3 Hz, CH₂(9_a)), 1.95 (2H, dd, *J* 13.3, 12.8 Hz, CH₂(9_b)), 2.29 (3H, s, CH₃(23)), 2.37–2.39 (4H, m, CH₂(21)), 2.91 (2H, dd, *J* 12.8, 12.8 Hz, CH₂(10_a)), 3.35–3.36 (4H, m, CH₂(22)), 3.70 (2H, d, *J* 12.8 Hz, CH₂(10_b)), 4.01 (2H, s, CH₂(7)), 7.03 (1H, dd, *J* 7.4, 7.4 Hz, ArCH), 7.18 (1H, d, *J* 7.4 Hz, ArCH), 7.26 (1H, dd, *J*

7.4, 7.4 Hz, ArCH), 7.32 (1H, d, *J* 7.6 Hz, ArCH(16)), 7.45 (1H, dd, *J* 7.6, 7.6 Hz, ArCH(15)), 7.76–7.78 (2H, m, ArCH(18)), 7.92 (1H, d, *J* 7.6 Hz, ArCH(14))

¹³C (75 MHz, CDCl₃) δ 36.57 (s, CH₂(9_{ab})), 43.32 (s, C(8)), 44.36 (s, CH₂(10_{ab})), 46.13 (s, CH₃(21)), 46.64 (s, CH₂(21)), 54.75 (s, CH₂(22)), 57.14 (s, CH₂(7)), 115.22 (s, ArCH(14)), 116.72 (q, ³*J*_{C-F} 6.8 Hz, ArCH(18)), 119.96 (q, ³*J*_{C-F} 7.2 Hz, ArCH(16)), 122.70 (s, ArCH), 122.98 (s, ArCH), 123.18 (s, ArCH), 123.91 (q, ¹*J*_{C-F} 272 Hz, ArCH(19)), 128.66 (s, ArCH), 129.44 (s, ArCH(15)), 131.39 (q, ²*J*_{C-F} 32 Hz, ArC(17)), 137.98 (s, ArC), 139.16 (s, ArC), 142.08 (s, ArC(13)), 152.17 (s, C=O(11)), 164.16 (s, C=O(20))

¹⁹F (376 MHz, CDCl₃) δ –64.7 (s, Ar-CF₃(19))

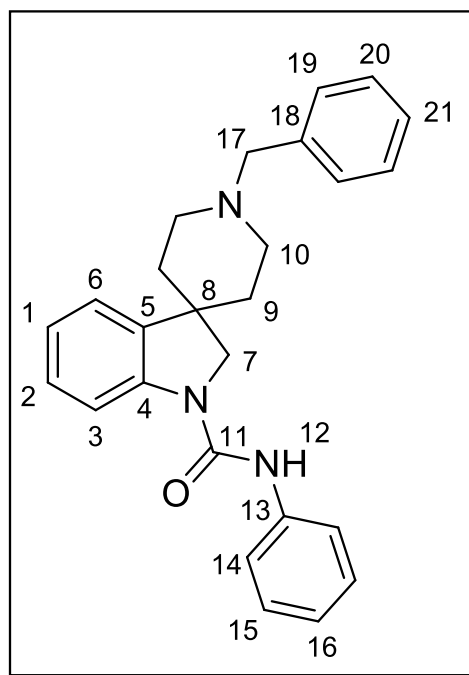
R_f 0.40 (93:7, CH₂Cl₂:MeOH)

IR ν/cm^{–1} 1328 (C-O, s), 1545 (C-F, s), 1622 (C=O, s), 1656 (C=O, s), 2848 (C-H, w), 3313 (Ar C-H, w)

MS (ESI): 502 [M+H⁺]

HRMS C₂₆H₃₁F₃N₅O₂ [M+H⁺] requires 502.2424, found 502.2417 (1.5 ppm error)

Preparation of 1'-Benzyl-*N*-phenylspiro[indoline-3,4'-piperidine]-1-carboxamide (**LVTa19**):



1'-Benzylspiro[indoline-3,4'-piperidine] (121 mg, 0.43 mmol, 1 eq.) was dissolved in CH₂Cl₂ (20 mL) under a nitrogen atmosphere. Phenyl isocyanate (0.06 mL, 65.4 mg, 0.52 mmol, 1.2 eq.) was added slowly *via* syringe and the solution stirred for 4 hours. The solvent was removed under reduced pressure and the product purified using column chromatography (SiO₂, 93:7, CH₂Cl₂:MeOH), yielding a golden brown solid **LVTa19** (136 mg, 0.34 mmol, 80%).

Data for **LVTa19**

mp 84–88 °C

¹H (300 MHz, CDCl₃) δ 1.68 (2H, d, *J* 8.9 Hz, CH₂(9_a)), 1.97–2.14 (4H, m, CH₂(9_b,10_a)), 2.94 (2H, d, *J* 8.9 Hz, CH₂(10_b)), 3.58 (2H, s, CH₂(17)), 3.89 (2H, s, CH₂(7)), 6.58 (1H, s, NH(12)), 7.01 (1H, dd, *J* 7.3, 7.3 Hz, ArCH), 7.09 (1H, dd, *J* 7.3, 7.3 Hz, ArCH), 7.20 (1H, d, *J* 7.3 Hz, ArCH), 7.28–7.36 (7H, m, ArCH(16,19-21)), 7.47 (2H, d, *J* 7.5 Hz, ArCH(14)), 7.84 (1H, d, *J* 7.3 Hz, ArCH)

^{13}C (75 MHz, CDCl_3) δ 37.12 ($\text{CH}_2(9_{\text{ab}})$), 42.86 ($\text{C}(8)$), 50.55 ($\text{CH}_2(10_{\text{ab}})$), 57.56 ($\text{CH}_2(7)$), 63.44 ($\text{CH}_2(17)$), 114.76 (ArCH), 120.21 ($\text{ArCH}(15)$), 120.53 ($\text{ArCH}(16)$), 122.73 (ArCH), 122.85 (ArCH), 123.72 (ArCH), 127.19 ($\text{ArC}(18)$), 128.31 ($\text{ArCH}(21)$), 129.03 ($\text{ArCH}(20)$), 129.22 ($\text{ArCH}(19)$), 138.09 (ArC), 138.91 (ArC), 142.13 ($\text{ArC}(13)$), 152.30 ($\text{C=O}(11)$)

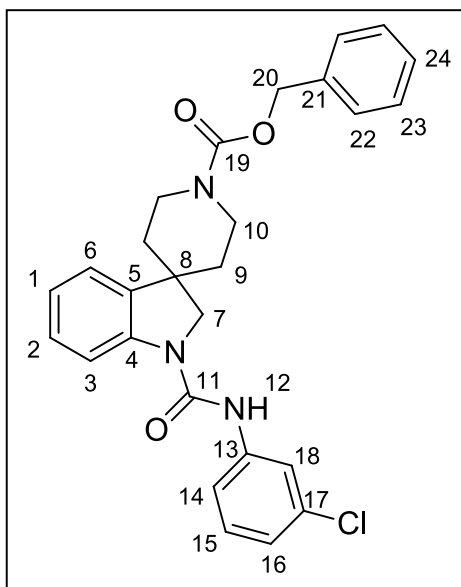
R_f 0.47 (3:1, EtOAc:Pet.ether)

IR ν/cm^{-1} 1651 (C=O , s), 2804 (C-H , w), 3291 (Ar C-H , w)

MS (ESI): 398 [$\text{M}+\text{H}^+$]

HRMS $\text{C}_{26}\text{H}_{28}\text{N}_3\text{O}$ [$\text{M}+\text{H}^+$] requires 398.2227, found 398.2226 (0.02 ppm error)

Preparation of Benzyl 1-((3-chlorophenyl)carbamoyl)spiro[indoline-3,4'-piperidine]-1'-carboxylate (**LVTa117**):



Benzyl spiro[indoline-3,4'-piperidine]-1'-carboxylate (**LVTa46**) (1.00 g, 3.12 mmol, 1 eq.) was dissolved in CH_2Cl_2 (20 mL) under a nitrogen atmosphere. 3-Chlorophenyl isocyanate

(0.46 mL, 120 mg, 3.75 mmol, 1.2 eq.) was added slowly *via* syringe and the resulting solution, turned dark green on leaving to stir, for 4 hours. The solvent was removed under reduced pressure and the product purified using column chromatography (SiO₂, 99:1, CH₂Cl₂:MeOH), which yielded an off-white solid **LVTa117** (1.00 g, 2.10 mmol, 67%).

Data for LVTa117

mp 106–109 °C

¹H (300 MHz, CDCl₃) δ 1.68 (2H, br. d, *J* 12.4 Hz, CH₂(9_a)), 1.88 (2H, br. dd, *J* 12.7, 12.4 Hz, CH₂(9_b)), 2.94 (2H, br. dd, *J* 12.7, 12.7 Hz, CH₂(10_a)), 3.92 (2H, s, CH₂(7)), 4.23 (2H, br. d, *J* 12.7 Hz, CH₂(10_b)), 5.17 (2H, s, CH₂(20)), 7.03 (1H, br. s, NH(12)), 7.07–7.07 (3H, m, ArCH), 7.13 (1H, d, *J* 7.0 Hz, ArCH), 7.20–7.38 (7H, m, ArCH(16,18,22-24)), 7.57 (1H, dd, *J* 8.0, 8.0 Hz, ArCH(15)), 7.83 (1H, d, *J* 8.0 Hz, ArCH(14))

¹³C (75 MHz, CDCl₃) δ 36.35 (CH₂(9_{ab})), 41.01 (CH₂(10_{ab})), 42.93 (C(8)), 56.89 (CH₂(7)), 67.39 (CH₂(20)), 114.96 (ArCH(14)), 118.08 (ArCH(16)), 120.15 (ArCH(15)), 122.83 (ArCH), 123.12 (ArCH), 123.73 (ArCH), 127.97 (ArCH(24)), 128.20 (ArCH(23)), 128.59 (ArCH(22)), 128.73 (ArCH), 130.01 (ArCH(18)), 134.64 (ArC), 136.54 (ArC), 138.01 (ArC(13)), 139.38 (ArC(21)), 141.88 (ArC(17)), 151.93 (C=O(11)), 155.35 (C=O(19))

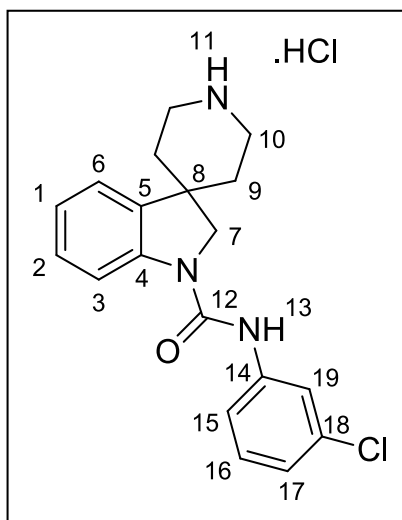
R_f 0.15 (99:1, CH₂Cl₂:MeOH)

IR ν/ cm⁻¹ 1590 (C-O, s), 1674 (C=O, s), 2853 (C-H, w), 3032 (Ar C-H, w)

MS (ESI): 476/478 [M+H⁺]

HRMS C₂₇H₂₇³⁵ClN₃O₃ [M+H⁺] requires 476.1741, found 476.1751 (2.7 ppm error)

Preparation of *N*-(3-Chlorophenyl)spiro[indoline-3,4'-piperidine]-1-carboxamide hydrochloride (**LVTa118**):



Benzyl 1-((3-chlorophenyl)carbamoyl)spiro[indoline-3,4'-piperidine]-1'-carboxylate (**LVTa117**) (1.00 g, 2.10 mmol, 1 eq.) was dissolved in MeOH (15 mL) and then, Pearlman's catalyst (147 mg, 0.21 mmol, 0.1 eq.) was added into the solution. The reaction mixture was purged with a balloon of hydrogen until deflated and then left under an atmosphere of hydrogen overnight. The methanol was removed under reduced pressure and the reaction mixture was filtered through celite with CH₂Cl₂ (100 mL) to collect any remaining starting material. The solvent 10% MeOH/CH₂Cl₂ (200 mL) was subsequently passed through the celite to elute the desired product. The product **LVTa118** is a brown amorphous solid (693 mg, 2.03 mmol, 97%).

Data for **LVTa118**

¹H (300 MHz, D₄-MeOH) δ 1.91 (2H, br. d, *J* 14.2 Hz, CH₂(9_a)), 2.17 (2H, br. dd, *J* 14.2, 12.2 Hz, CH₂(9_b)), 3.22 (2H, br. dd, *J* 12.5, 12.2 Hz, CH₂(10_a)), 3.46 (2H, br. d, *J* 12.2 Hz, CH₂(10_b)), 4.17 (2H, s, CH₂(7)), 7.01 (1H, dd, *J* 7.4, 7.4 Hz, ArCH), 7.08 (1H, dd, *J* 7.4, 7.4 Hz, ArCH), 7.19–7.25 (2H, m, ArCH), 7.31 (1H, dd, *J* 7.6, 7.6 Hz, ArCH(16)), 7.52–7.55 (2H, m, ArCH(17,18)), 7.91 (1H, d, *J* 7.6 Hz, ArCH(15))

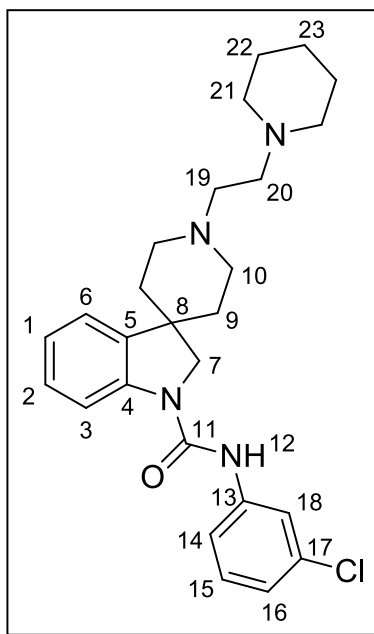
^{13}C (75 MHz, $\text{D}_4\text{-MeOH}$) δ 34.24 ($\text{CH}_2(9_{\text{ab}})$), 42.70 ($\text{CH}_2(10_{\text{ab}})$), 42.91 ($\text{C}(8)$), 58.19 ($\text{CH}_2(7)$), 116.69 ($\text{ArCH}(15)$), 122.57 (2C, $\text{ArCH}(17,19)$), 122.20 (2C, $\text{ArCH}(3,6)$), 122.51 (ArCH), 123.40 (ArCH), 129.75 ($\text{ArCH}(16)$), 138.10 (2C, ArC), 140.10 ($\text{ArC}(14)$), 143.93 ($\text{ArC}(18)$), 155.16 ($\text{C=O}(12)$)

IR ν/cm^{-1} 695 (C-Cl, s), 1663 (C=O, s), 3187 (Ar C-H, w)

MS (ESI): 342/344 [$\text{M}+\text{H}^+$]

HRMS $\text{C}_{19}\text{H}_{21}^{35}\text{ClN}_3\text{O}$ [$\text{M}+\text{H}^+$] requires 342.1373, found 342.1436 (1.7 ppm error)

Preparation of *N*-(3-Chlorophenyl)-1'-(2-(piperidin-1-yl)ethyl)spiro[indoline-3,4'-piperidine]-1-carboxamide (**LVTa121**):



Following method C using *N*-(3-Chlorophenyl)spiro[indoline-3,4'-piperidine]-1-carboxamide hydrochloride (**LVTa118**) (200 mg, 0.59 mmol, 1 eq.), 1-(2-chloroethyl) piperidine hydrochloride (217 mg, 1.18 mmol, 2 eq.) and K_2CO_3 (163 mg, 1.18 mmol, 2 eq.) as starting materials. The desired product was purified using column chromatography (SiO_2 ,

4:1, CH₂Cl₂:MeOH), to afford, the pure product (**LVTa121**) as an off-white solid (141 mg, 0.31 mmol, 53%).

Data for LVTa121

mp 254–257 °C

¹H (300 MHz, CDCl₃) δ 1.56–1.61 (2H, m, CH₂(23)), 1.73 (2H, d, *J* 12.7 Hz, CH₂(9_a)), 1.86–1.94 (4H, m, CH₂(22)), 2.00 (2H, dd, *J* 15.0, 12.7 Hz, CH₂(9_b)), 2.26 (2H, dd, *J* 12.7, 11.7 Hz, CH₂(10_a)), 2.86–2.98 (8H, m, CH₂(19,20,21)), 3.01 (2H, d, *J* 11.7 Hz, CH₂(10_b)), 3.95 (2H, s, CH₂(7)), 6.90 (1H, br. s, NH(12)), 7.00 (1H, dd, *J* 7.4, 7.4 Hz, ArCH), 7.09 (1H, dd, *J* 7.4, 7.4 Hz, ArCH), 7.16–7.24 (2H, m, ArCH), 7.34 (2H, dd, *J* 8.0, 8.0 Hz, ArCH(15)), 7.54–7.56 (2H, m, ArCH(16,18)), 7.89 (1H, d, *J* 8.0 Hz, ArCH(14))

¹³C (75 MHz, CDCl₃) δ 22.90 (CH₂(23)), 23.89 (CH₂(23)), 36.88 (CH₂(9_{ab})), 42.66 (C(8)), 50.90 (CH₂(10_{ab})), 54.42 (4C, CH₂(19,20,21)), 57.54 (CH₂(7)), 114.98 (ArCH(14)), 120.22 (2C, ArCH(16,18)), 122.64 (2C, ArCH), 123.58 (2C, ArCH), 128.47 (ArCH), 128.98 (ArCH(15)), 138.30 (2C, ArC), 138.36 (ArC(17)), 142.36 (ArC(13)), 152.39 (C=O(11))

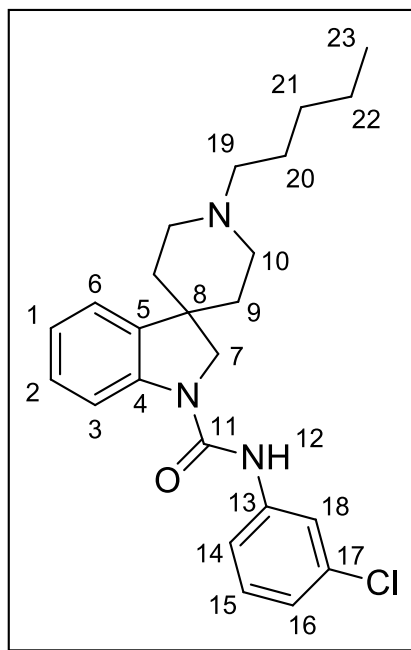
R_f 0.29 (4:1, CH₂Cl₂:MeOH)

IR ν/ cm⁻¹ 1658 (C=O, s), 2788 (C-H, w), 3244 (Ar C-H, w)

MS (ESI): 453/455 [M+H⁺]

HRMS C₂₆H₃₄³⁵ClN₄O [M+H⁺] requires 453.2421, found 453.2430 (3.8 ppm error)

Preparation of *N*-(3-Chlorophenyl)-1'-pentylspiro[indoline-3,4'-piperidine]-1-carboxamide (**LVTa124**):



Following method C using *N*-(3-Chlorophenyl)spiro[indoline-3,4'-piperidine]-1-carboxamide hydrochloride (**LVTa118**) (100 mg, 0.29 mmol, 1 eq.), iodopentane (0.08 mL, 121 mg, 0.58 mmol, 2 eq.) and K_2CO_3 (80.2 mg 0.58 mmol, 2 eq.) as starting materials. The desired product was purified using column chromatography (SiO_2 , 4:1, CH_2Cl_2 :MeOH), to afford, the pure product (**LVTa124**) as an off-white solid (83.0 mg, 0.20 mmol, 70%).

Data for **LVTa124**

mp 100–105 °C

1H (300 MHz, $CDCl_3$) δ 0.92 (3H, t, J 7.9 Hz, CH_2 (23)), 1.29–1.37 (4H, m, CH_2 (21,22)), 1.52–1.58 (2H, m, CH_2 (20)), 1.75 (2H, dd, J 14.9, 14.0 Hz, CH_2 (9_a)), 2.09–2.15 (4H, m, CH_2 (9_b,10_a)), 2.43 (2H, t, J 8.1 Hz, CH_2 (19)), 3.03 (2H, d, J 14.0 Hz, CH_2 (10_b)), 3.91 (2H, s, CH_2 (7)), 6.60 (1H, br. s, NH (12)), 7.04 (1H, dd, J 7.4, 7.4 Hz, ArCH), 7.10 (1H, dd, J 7.4, 7.4 Hz, ArCH), 7.22 (2H, d, J 7.5 Hz, ArCH), 7.34 (2H, dd, J 7.8, 7.8 Hz, ArCH(15)), 7.46–7.49 (2H, m, ArCH(16,18)), 7.83 (1H, d, J 7.8 Hz, ArCH(14))

^{13}C (75 MHz, CDCl_3) δ 14.08 ($\text{CH}_3(23)$), 22.62 ($\text{CH}_2(22)$), 26.51 ($\text{CH}_2(20)$), 29.82 ($\text{CH}_2(21)$), 36.83 ($\text{CH}_2(9_{\text{ab}})$), 42.81 ($\text{C}(8)$), 50.72 ($\text{CH}_2(10_{\text{ab}})$), 57.60 ($\text{CH}_2(7)$), 59.11 ($\text{CH}_2(19)$), 114.70 ($\text{ArCH}(14)$), 120.14 (2C, $\text{ArCH}(16,18)$), 122.78 (2C, ArCH), 123.70 (2C, ArCH), 128.41 (ArCH), 129.06 ($\text{ArCH}(15)$), 138.13 (2C, ArC), 138.71 ($\text{ArC}(17)$), 142.12 ($\text{ArC}(13)$), 152.25 ($\text{C=O}(11)$)

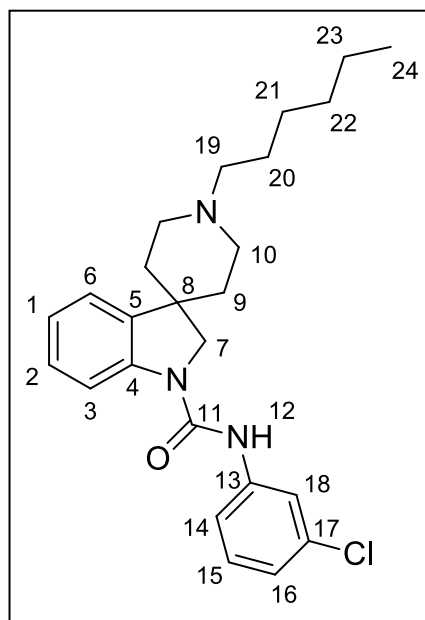
R_f 0.29 (93:7, CH_2Cl_2 :MeOH)

IR ν/cm^{-1} 1652 (C=O , s), 2859 (C-H , w), 3043 (Ar C-H , w)

MS (ESI): 412/414 [$\text{M}+\text{H}^+$]

HRMS $\text{C}_{24}\text{H}_{31}^{35}\text{ClN}_3\text{O}$ [$\text{M}+\text{H}^+$] requires 412.2156, found 412.2167 (3.9 ppm error)

Preparation of *N*-(3-Chlorophenyl)-1'-hexylspiro[indoline-3,4'-piperidine]-1-carboxamide (**LVTa125**):



Following method C using *N*-(3-Chlorophenyl)spiro[indoline-3,4'-piperidine]-1-carboxamide hydrochloride (**LVTa118**) (100 mg, 0.29 mmol, 1 eq.), iodohexane (0.09 mL, 129 mg, 0.58 mmol, 2 eq.) and K_2CO_3 (80.2 mg, 0.58 mmol, 2 eq.) as starting materials. The

desired product was purified using column chromatography (SiO₂, 4:1, CH₂Cl₂:MeOH), to afford, the pure product (**LVTa125**) as a light cream solid (89.0 mg, 0.21 mmol, 72%).

Data for LVTa125

mp 115–117 °C

¹H (300 MHz, CDCl₃) δ 0.90 (3H, t, *J* 7.4 Hz, CH₂(24)), 1.29–1.34 (6H, m, CH₂(21,22,23)), 1.56–1.59 (2H, m, CH₂(20)), 1.75 (2H, dd, *J* 12.9, 12.9 Hz, CH₂(9_a)), 2.09–2.18 (4H, m, CH₂(9_b,10_a)), 2.46 (2H, t, *J* 7.9 Hz, CH₂(19)), 3.05 (2H, d, *J* 12.9 Hz, CH₂(10_b)), 3.93 (2H, s, CH₂(7)), 6.68 (1H, br. s, NH(12)), 7.01 (1H, dd, *J* 7.4, 7.4 Hz, ArCH), 7.09 (1H, dd, *J* 7.4, 7.4 Hz, ArCH), 7.21 (2H, d, *J* 8.0 Hz, ArCH), 7.34 (2H, dd, *J* 8.0, 8.0 Hz, ArCH(15)), 7.48–7.50 (2H, m, ArCH(16,18)), 7.83 (1H, d, *J* 8.0 Hz, ArCH(14))

¹³C (75 MHz, CDCl₃) δ 14.06 (CH₃(24)), 22.59 (CH₂(23)), 26.60 (CH₂(20)), 27.25 (CH₂(22)), 31.72 (CH₂(21)), 36.62 (CH₂(9_{ab})), 42.71 (C(8)), 50.64 (CH₂(10_{ab})), 57.62 (CH₂(7)), 59.01 (CH₂(19)), 114.72 (ArCH(14)), 120.17 (2C, ArCH(16,18)), 122.80 (ArCH), 122.90 (ArCH), 123.67 (ArCH), 128.42 (ArCH), 129.01 (ArCH(15)), 138.15 (2C, ArC), 138.53 (ArC(17)), 142.12 (ArC(13)), 152.27 (C=O(11))

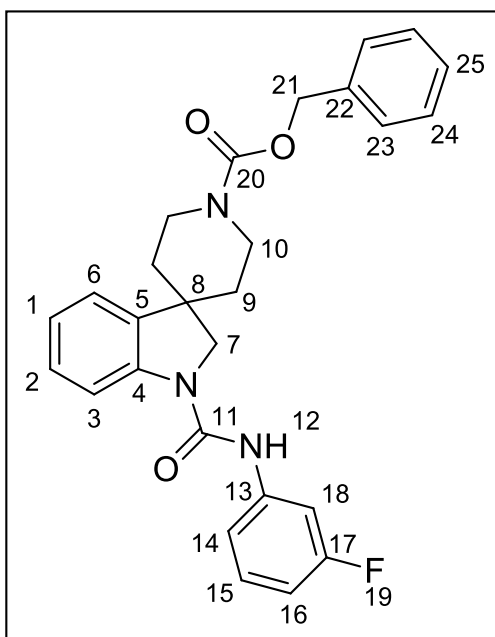
R_f 0.19 (93:7, CH₂Cl₂:MeOH)

IR ν/ cm⁻¹ 1647 (C=O, s), 2854 (C-H, w), 3322 (Ar C-H, w)

MS (ESI): 426/428 [M+H⁺]

HRMS C₂₅H₃₃³⁵ClN₃O [M+H⁺] requires 426.2307, found 426.2305 (0.4 ppm error)

Preparation of Benzyl 1-((3-fluorophenyl)carbamoyl)spiro[indoline-3,4'-piperidine]-1'-carboxylate (**LVTa126**):



Benzyl spiro[indoline-3,4'-piperidine]-1'-carboxylate (**LVTa46**) (200 mg, 0.62 mmol, 1 eq.) was dissolved in CH_2Cl_2 (20 mL) under a nitrogen atmosphere. 3-Fluorophenyl isocyanate (0.08 mL, 96.1 mg, 0.74 mmol, 1.2 eq.) was added slowly *via* syringe and the resulting solution, turned dark green on leaving to stir, for 4 hours. The solvent was removed under reduced pressure and the product purified using column chromatography (SiO_2 , 99:1 CH_2Cl_2 :MeOH), which yielded an off-white solid **LVTa126** (271 mg, 0.59 mmol, 95%).

Data for **LVTa126**

mp 107–109 °C

^1H (300 MHz, CDCl_3) δ 1.70 (2H, d, J 13.3 Hz, $\text{CH}_2(9_a)$), 1.89 (2H, dd, J 13.3, 10.9 Hz, $\text{CH}_2(9_b)$), 2.94 (2H, dd, J 12.3, 10.9 Hz, $\text{CH}_2(10_a)$), 3.93 (2H, s, $\text{CH}_2(7)$), 4.25 (2H, d, J 12.3 Hz, $\text{CH}_2(10_b)$), 5.17 (2H, s, $\text{CH}_2(21)$), 6.76–6.81 (2H, m, ArCH), 7.03 (1H, dd, J 7.8, 7.8 Hz, ArCH(15)), 7.11–7.16 (2H, m, ArCH), 7.23–7.41 (7H, m, ArCH), 7.82 (1H, d, J 7.8 Hz, ArCH(14))

^{13}C (75 MHz, CDCl_3) δ 36.29 (s, $\text{CH}_2(9_{\text{ab}})$), 40.98 (s, $\text{CH}_2(10_{\text{ab}})$), 42.88 (s, $\text{C}(8)$), 56.78 (s, $\text{CH}_2(7)$), 67.39 (s, $\text{CH}_2(21)$), 107.78 (d, $^2J_{\text{C-F}}$ 26 Hz, $\text{ArCH}(16)$), 110.59 (s, ArCH), 110.87 (s, ArCH), 115.02 (s, $\text{ArCH}(14)$), 115.27 (d, $^3J_{\text{C-F}}$ 4.7 Hz, $\text{ArCH}(15)$), 122.75 (s, ArCH), 123.04 (s, ArCH), 127.92 (s, $\text{ArCH}(25)$), 128.12 (s, $\text{ArCH}(24)$), 128.60 (s, $\text{ArCH}(26)$), 128.69 (d, $^2J_{\text{C-F}}$ 9.4 Hz, $\text{ArCH}(16)$), 130.06 (d, $^2J_{\text{C-F}}$ 11.0 Hz, $\text{ArC}(18)$), 136.54 (s, ArC), 137.94 (s, ArC), 140.02 (d, $^3J_{\text{C-F}}$ 4.7 Hz, $\text{ArC}(13)$), 141.97 (s, $\text{ArC}(22)$), 151.98 (s, $\text{C=O}(11)$), 155.38 (s, $\text{C=O}(20)$), 162.98 (d, $^1J_{\text{C-F}}$ 244 Hz, $\text{ArC}(17)$)

^{19}F (376 MHz, CDCl_3) δ -111.63 ($\text{ArF}(19)$)

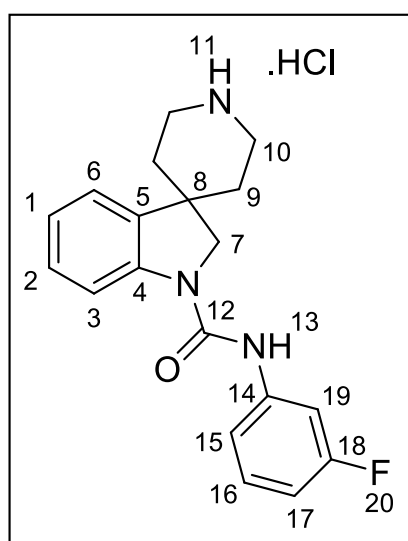
R_f 0.13 (49:1, CH_2Cl_2 :MeOH)

IR ν/cm^{-1} 1582 (C-O, s), 1667 (C=O, s), 2878 (C-H, w), 3112 (Ar C-H, w)

MS (ESI): 460 $[\text{M}+\text{H}^+]$

HRMS $\text{C}_{27}\text{H}_{27}\text{FN}_3\text{O}_3$ $[\text{M}+\text{H}^+]$ requires 460.2036, found 460.2051 (1.4 ppm error)

Preparation of *N*-(3-Fluorophenyl)spiro[indoline-3,4'-piperidine]-1-carboxamide hydrochloride (**LVTa127**):



Benzyl 1-((3-fluorophenyl)carbamoyl)spiro[indoline-3,4'-piperidine]-1'-carboxylate (**LVTa126**) (176 mg, 0.38 mmol, 1 eq.) was dissolved in MeOH (15 mL) and then, Pearlman's catalyst (26.7 mg, 0.04 mmol, 0.1 eq.) was added into the solution. The reaction mixture was purged with a balloon of hydrogen until deflated and then left under an atmosphere of hydrogen overnight. The methanol was removed under reduced pressure and the reaction mixture was filtered through celite with CH₂Cl₂ (100 mL) to collect any remaining starting material. The solvent 10% MeOH/CH₂Cl₂ (200 mL) was subsequently passed through celite to elute the desired product. The product **LVTa127** is an amorphous solid (109 mg, 0.33 mmol, 87%).

Data for **LVTa127**

¹H (300 MHz, D₄-MeOH) δ 1.94 (2H, d, *J* 14.4 Hz, CH₂(9_a)), 2.17 (2H, dd, *J* 14.4, 13.9 Hz, CH₂(9_b)), 3.22 (2H, dd, *J* 13.9, 12.2 Hz, CH₂(10_a)), 3.49 (2H, d, *J* 12.2 Hz, CH₂(10_b)), 4.19 (2H, s, CH₂(7)), 6.79 (1H, dd, *J* 7.8, 7.8 Hz, ArCH), 7.03 (1H, dd, *J* 7.8, 7.8 Hz, ArCH), 7.20–7.35 (4H, m, ArCH(16,19)), 7.48 (1H, d, *J* 8.9 Hz, ArCH(17)), 7.92 (1H, d, *J* 7.9 Hz, ArCH(15))

¹³C (75 MHz, D₄-MeOH) δ 34.22 (s, CH₂(9_{ab})), 42.70 (s, CH₂(10_{ab})), 42.94 (s, C(8)), 58.12 (s, CH₂(7)), 108.78 (d, ²*J*_{C-F} 26 Hz, ArCH(17)), 110.59 (s, ArCH), 110.87 (s, ArCH), 116.79 (s, ArCH(15)), 117.31 (d, ³*J*_{C-F} 2.7 Hz, ArCH(16)), 123.57 (s, ArCH), 124.06 (s, ArCH), 129.80 (s, ArCH), 131.00 (d, ²*J*_{C-F} 9.4 Hz, ArCH(19)), 138.12 (s, ArC), 142.24 (d, ³*J*_{C-F} 11.0 Hz, ArC(14)), 143.79 (s, ArC), 154.63 (s, C=O(12)), 164.32 (d, ¹*J*_{C-F} 242 Hz, ArC(18))

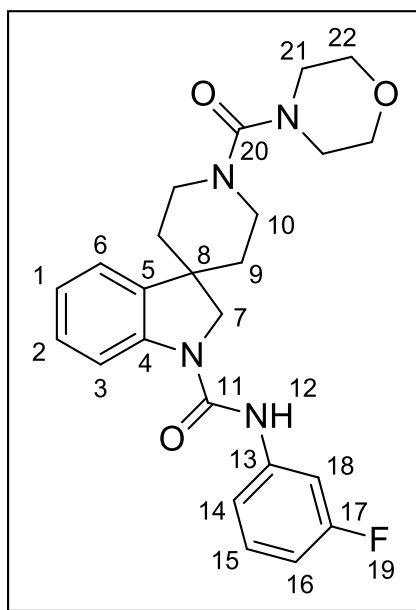
¹⁹F (376 MHz, CDCl₃) δ –114.5 (ArF(20))

IR ν/ cm⁻¹ 1524 (C-F, s), 1671 (C=O, s), 3287 (Ar C-H, w)

MS (ESI): 326 [M+H⁺]

HRMS C₁₉H₂₁FN₃O [M+H⁺] requires 326.1669, found 326.1655 (1.9 ppm error)

Preparation of *N*-(3-Fluorophenyl)-1'-(morpholine-4-carbonyl)spiro[indoline-3,4'-piperidine]-1-carboxamide (**LVTa128**):



Following method C using *N*-(3-Fluorophenyl)spiro[indoline-3,4'-piperidine]-1-carboxamide hydrochloride (**LVTa127**) (109 mg, 0.33 mmol, 1 eq.), 4-morpholinecarbonyl chloride (0.08 mL, 103 mg, 0.66 mmol, 2 eq.) and K₂CO₃ (91.2 mg, 0.66 mmol, 2 eq.) as starting materials. The desired product was purified using column chromatography (SiO₂, 100% EtOAc), to afford, the pure product (**LVTa128**) as an off-white solid (100 mg, 0.23 mmol, 70%).

Data for **LVTa128**

mp 139–143 °C

¹H (300 MHz, CDCl₃) δ 1.73 (2H, d, *J* 13.6 Hz, CH₂(9_a)), 1.94 (2H, dd, *J* 13.6, 13.0 Hz, CH₂(9_b)), 2.94 (2H, dd, *J* 16.0, 13.0 Hz, CH₂(10_a)), 3.31–3.34 (4H, m, CH₂(21)), 3.69–3.75 (6H, m, CH₂(10_b,22)), 3.98 (2H, s, CH₂(7)), 6.79 (1H, dd, *J* 8.2, 8.2 Hz, ArCH), 6.96 (1H,

s, ArCH(18)), 7.30 (1H, dd, *J* 8.2, 8.2 Hz, ArCH), 7.15–7.18 (2H, m, ArCH(3,6)), 7.23–7.31 (1H, m, ArCH), 7.42 (1H, d, *J* 8.0 Hz, ArCH(16)), 7.42 (1H, d, *J* 8.0 Hz, ArCH(14))

¹³C (75 MHz, CDCl₃) δ 36.48 (s, CH₂(9_{ab})), 43.26 (s, CH₂(10_{ab})), 44.11 (s, CH₂(21)), 47.28 (s, C(8)), 57.11 (s, CH₂(7)), 66.63 (s, CH₂(22)), 107.35 (d, ²*J*_{C-F} 26 Hz, ArCH(16)), 110.10 (s, ArCH), 110.39 (s, ArCH), 114.95 (s, ArCH(14)), 115.13 (d, ³*J*_{C-F} 2.7 Hz, ArCH(18)), 122.79 (s, ArCH), 122.98 (s, ArCH), 128.67 (s, ArCH), 130.04 (d, ²*J*_{C-F} 9.4 Hz, ArCH(15)), 138.05 (s, ArC), 139.91 (d, ³*J*_{C-F} 10.9 Hz, ArC(13)), 141.95 (s, ArC), 151.90 (s, C=O(11)), 163.08 (d, ¹*J*_{C-F} 245 Hz, ArC(17)), 164.09 (s, C=O(20))

¹⁹F (376 MHz, CDCl₃) δ –113.62 (ArF(19))

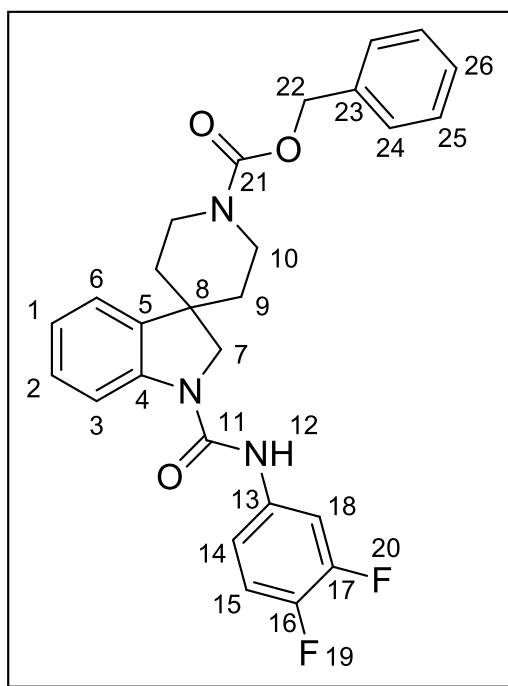
R_f 0.25 (100% EtOAc)

IR ν/ cm^{–1} 1601 (C=O, s), 1677 (C=O, s), 2853 (C-H, w), 3319 (ArC-H, w)

MS (ESI): 439 [M+H⁺]

HRMS C₂₄H₂₈FN₄O₃ [M+H⁺] requires 439.2140, found 439.2140 (0.0 ppm error)

Preparation of Benzyl 1-((3,4-difluorophenyl)carbamoyl)spiro[indoline-3,4'-piperidine]-1'-carboxylate (**LVTa130**):



Benzyl spiro[indoline-3,4'-piperidine]-1'-carboxylate (**LVTa46**) (200 mg, 0.62 mmol, 1 eq.) was dissolved in CH_2Cl_2 (20 mL) under a nitrogen atmosphere. 3, 4-Difluorophenyl isocyanate (0.07 mL, 92.8 mg, 0.62 mmol, 1 eq.) was added slowly *via* syringe and the resulting solution stirred at room temperature for 30 minutes. The solvent was removed under reduced pressure and the product purified using column chromatography (SiO_2 , 99:1, CH_2Cl_2 :MeOH), which yielded an off-white solid **LVTa130** (163 mg, 0.34 mmol, 55%).

Data for **LVTa130**

mp 91–94 °C

^1H (300 MHz, CDCl_3) δ 1.69 (2H, d, J 13.5 Hz, $\text{CH}_2(9_a)$), 1.89 (2H, dd, J 13.5, 10.6 Hz, $\text{CH}_2(9_b)$), 2.93 (2H, dd, J 11.4, 10.6 Hz, $\text{CH}_2(10_a)$), 3.90 (2H, m, $\text{CH}_2(7)$), 4.26 (2H, d, J 11.4, 10.6 Hz, $\text{CH}_2(10_b)$), 5.17 (2H, s, $\text{CH}_2(22)$), 6.74 (1H, br. s, $\text{NH}(12)$), 7.00–7.14 (4H,

s, ArCH(1,2,3,6)), 7.28–7.38 (7H, m, ArCH(18,24,25,26)), 7.50–7.57 (1H, m, ArCH(15)), 7.83 (1H, d, *J* 8.0 Hz, ArCH(14))

¹³C (75 MHz, CDCl₃) δ 36.89 (s, CH₂(9_{ab})), 41.83 (s, CH₂(10_{ab})), 43.27 (s, C(8)), 56.80 (s, CH₂(7)), 109.71 (d, ²*J*_{C-F} 21 Hz, ArCH(16)), 109.84 (s, ArCH), 110.13 (s, ArCH), 114.94 (s, ArCH(15)), 116.24 (d, ²*J*_{C-F} 26 Hz, ArCH(19)), 122.83 (s, ArCH), 123.16 (s, ArCH), 128.75 (s, ArCH), 134.69 (d, ³*J*_{C-F} 8.7 Hz, ArC(14)), 136.52 (s, ArC), 137.95 (s, ArC), 141.82 (s, ArC), 152.61 (s, C=O(11))

¹⁹F (376 MHz, CDCl₃) δ −113.6 and −113.6 (s, Ar-F(19 and 20))

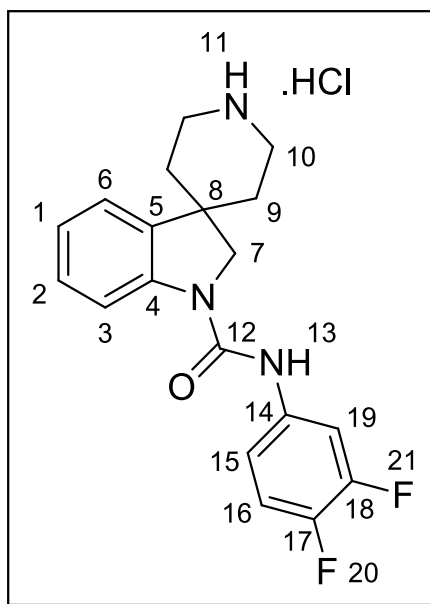
R_f 0.16 (99:1, CH₂Cl₂:MeOH)

IR ν/ cm^{−1} 1623 (C-O, s), 1679 (C=O, s), 2832 (C-H, w), 3029 (Ar C-H, w)

MS (ESI): 478 [M+H⁺]

HRMS C₂₇H₂₆F₂N₃O₃ [M+H⁺] requires 478.1942, found 478.1959 (3.4 ppm error)

Preparation of *N*-(3,4-Difluorophenyl)spiro[indoline-3,4'-piperidine]-1-carboxamide hydrochloride (**LVTa131**):



Benzyl 1-((3,4-difluorophenyl)carbamoyl)spiro[indoline-3,4'-piperidine]-1'-carboxylate (**LVTa130**) (163 mg, 0.34 mmol, 1 eq.) was dissolved in MeOH (15 mL) and then, Pearlman's catalyst (23.9 mg, 0.034 mmol, 0.1 eq.) was added into the solution. The reaction mixture was purged with a balloon of hydrogen until deflated and then left under an atmosphere of hydrogen overnight. The methanol was removed under reduced pressure and the reaction mixture was filtered through celite with CH₂Cl₂ (100 mL) to collect any remaining starting material. The solvent 10% MeOH/CH₂Cl₂ (200 mL) was subsequently passed through celite to elute the desired product. The product **LVTa131** is a light brown amorphous solid (98.0 mg, 0.29 mmol, 85%).

Data for **LVTa131**

¹H (300 MHz, D₄-MeOH) δ 1.96 (2H, d, *J* 14.4 Hz, CH₂(9_a)), 2.16 (2H, dd, *J* 14.4, 12.4 Hz, CH₂(9_b)), 3.22 (2H, dd, *J* 12.4, 12.4 Hz, CH₂(10_a)), 3.46 (2H, d, *J* 12.4 Hz, CH₂(10_b)), 4.19 (2H, s, CH₂(7)), 7.03–7.11 (2H, m, ArCH), 7.17–7.20 (1H, m, ArCH), 7.23–7.35 (2H, m, ArCH(16,19)), 7.90 (1H, d, *J* 7.5 Hz, ArCH(15))

¹³C (75 MHz, D₄-MeOH) δ 34.22 (s, CH₂(9_{ab})), 42.70 (s, CH₂(10_{ab})), 42.94 (s, C(8)), 58.12 (s, CH₂(7)), 110.59 (s, ArCH), 110.87 (s, ArCH), 116.79 (s, ArCH(15)), 117.31 (d, ³*J*_{C-F} 2.7 Hz, ArCH(16)), 123.57 (s, ArCH), 124.06 (s, ArCH), 129.80 (s, ArCH), 131.00 (d, ²*J*_{C-F} 9.2 Hz, ArCH(19)), 138.12 (s, ArC), 142.24 (d, ³*J*_{C-F} 11.0 Hz, ArC(14)), 143.79 (s, ArC), 154.63 (s, C=O(12)), 164.32 (d, ¹*J*_{C-F} 242 Hz, ArC), 164.51 (d, ¹*J*_{C-F} 242 Hz, ArC)

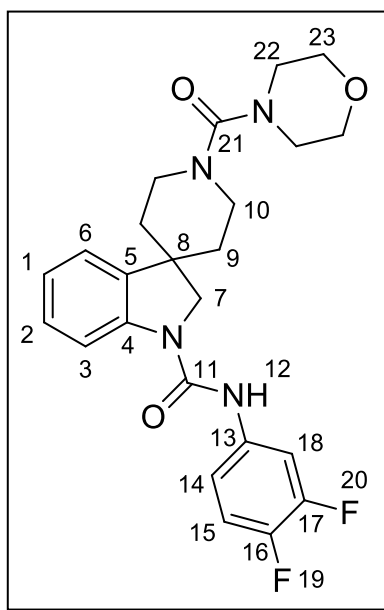
¹⁹F (376 MHz, CDCl₃) δ –114.63 and –114.65 (s, Ar-F(19 and 20))

IR ν/ cm⁻¹ 1326 (C-F, s), 1691 (C=O, s), 3156 (Ar C-H, w)

MS (ESI): 344 [M+H⁺]

HRMS C₁₉H₂₀F₂N₃O [M+H⁺] requires 344.1574, found 344.1579 (2.7 ppm error)

Preparation of *N*-(3,4-Difluorophenyl)-1'-(morpholine-4-carbonyl)spiro[indoline-3,4'-piperidine]-1-carboxamide (**LVTa132**):



Following method C using *N*-(3,4-Difluorophenyl)spiro[indoline-3,4'-piperidine]-1-carboxamide hydrochloride (**LVTa131**) (98.0 mg, 0.29 mmol, 1 eq.), 4-morpholinecarbonyl chloride (0.07 mL, 89.7 mg, 0.58 mmol, 2 eq.) and K₂CO₃ (80.2 mg, 0.58 mmol, 2 eq.) as starting materials. The desired product was purified using column chromatography (SiO₂, 100% EtOAc), to afford, the pure product (**LVTa132**) as an off-white solid (87.2 mg, 0.19 mmol, 66%).

Data for **LVTa132**

mp 110–114 °C

¹H (300 MHz, CDCl₃) δ 1.74 (2H, d, *J* 13.1 Hz, CH₂(9_a)), 1.94 (2H, dd, *J* 13.1, 13.1 Hz, CH₂(9_b)), 2.96 (2H, dd, *J* 13.1, 12.9 Hz, CH₂(10_a)), 3.31–3.34 (4H, m, CH₂(22)), 3.70–3.76 (6H, m, CH₂(10_b,23)), 3.96 (2H, m, CH₂(7)), 6.68 (1H, br. s, NH(12)), 6.98–7.19 (5H, s, ArCH(18)), 7.55–7.57 (1H, m, ArCH(15)), 7.82 (1H, d, *J* 7.83 Hz, ArCH(14))

^{13}C (75 MHz, CDCl_3) δ 36.47 (s, $\text{CH}_2(9_{\text{ab}})$), 43.30 (s, $\text{CH}_2(10_{\text{ab}})$), 44.09 (s, $\text{CH}_2(22)$), 47.30 (s, $\text{C}(8)$), 57.14 (s, $\text{CH}_2(7)$), 66.64 (s, $\text{CH}_2(23)$), 109.99 (d, $^2J_{\text{C-F}}$ 23 Hz, $\text{ArCH}(15)$), 109.84 (s, ArCH), 110.13 (s, ArCH), 114.86 (s, $\text{ArCH}(14)$), 117.26 (d, $^2J_{\text{C-F}}$ 26 Hz, $\text{ArCH}(18)$), 122.89 (s, ArCH), 123.10 (s, ArCH), 125.53 (s, ArCH), 128.70 (s, ArCH), 134.70 (d, $^3J_{\text{C-F}}$ 4.2 Hz, $\text{ArC}(13)$), 138.09 (s, ArC), 141.82 (s, ArC), 151.86 (s, $\text{C=O}(11)$), 164.07 (s, $\text{C=O}(21)$)

^{19}F (376 MHz, CDCl_3) δ -113.6 and -113.6 (s, $\text{Ar-F}(19 \text{ and } 20)$)

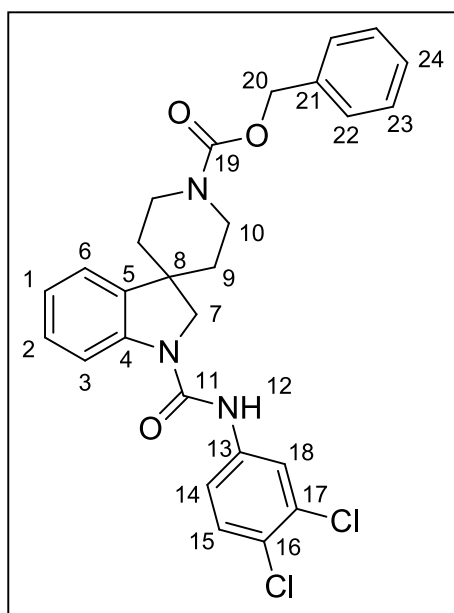
R_f 0.29 (100% EtOAc)

IR ν/cm^{-1} 1627 (C=O , s), 1664 (C=O , s), 2858 (C-H , w), 3330 (ArC-H , w)

MS (ESI): 457 [$\text{M}+\text{H}^+$]

HRMS $\text{C}_{24}\text{H}_{27}\text{F}_2\text{N}_4\text{O}_3$ [$\text{M}+\text{H}^+$] requires 457.2051, found 457.2023 (4.7 ppm error)

Preparation of Benzyl 1-((3,4-dichlorophenyl)carbamoyl)spiro[indoline-3,4'-piperidine]-1'-carboxylate (**LVTa133**):



Benzyl spiro[indoline-3,4'-piperidine]-1'-carboxylate (**LVTa46**) (200 mg, 0.62 mmol, 1 eq.) was dissolved in CH₂Cl₂ (20 mL) under a nitrogen atmosphere. 3, 4-Dichlorophenyl isocyanate (139 mg, 0.74 mmol, 1.2 eq.) was added slowly *via* syringe and the resulting solution stirred at room temperature for 1 hour. The solvent was removed under reduced pressure and the product purified using column chromatography (SiO₂, 14:1, CH₂Cl₂:MeOH), which yielded a dark green solid **LVTa133** (243 mg, 0.48 mmol, 77%).

Data for LVTa133

mp 107–111 °C

¹H (300 MHz, CDCl₃) δ 1.63 (2H, d, *J* 13.4 Hz, CH₂(9_a)), 1.83 (2H, dd, *J* 13.4, 12.7 Hz, CH₂(9_b)), 2.88 (2H, dd, *J* 12.7, 10.0 Hz, CH₂(10_a)), 3.83 (2H, m, CH₂(7)), 4.22 (2H, d, *J* 10.0, 10.0 Hz, CH₂(10_b)), 5.15 (2H, s, CH₂(20)), 7.00–7.11 (3H, s, ArCH), 7.21–7.38 (7H, m, ArCH(24,25,26)), 7.70 (1H, d, *J* 8.0 Hz, ArCH(15)), 7.88 (1H, d, *J* 8.0 Hz, ArCH(14))

¹³C (75 MHz, CDCl₃) δ 36.22 (CH₂(9_{ab})), 40.90 (CH₂(10_{ab})), 42.83 (C(8)), 56.58 (CH₂(7)), 67.38 (2C, CH₂(20)), 115.14 (ArCH(14)), 119.39 (ArCH), 122.96 (ArCH), 123.13 (ArCH), 126.60 (ArCH), 127.78 (ArCH(24)), 128.12 (ArCH(23)), 128.58 (ArCH(22)), 130.36 (ArCH), 132.54 (ArC(16)), 136.41 (ArC), 137.72 (ArC), 137.98 (ArC(17)), 141.84 (ArC(13)), 151.84 (C=O(11)), 155.39 (C=O(19))

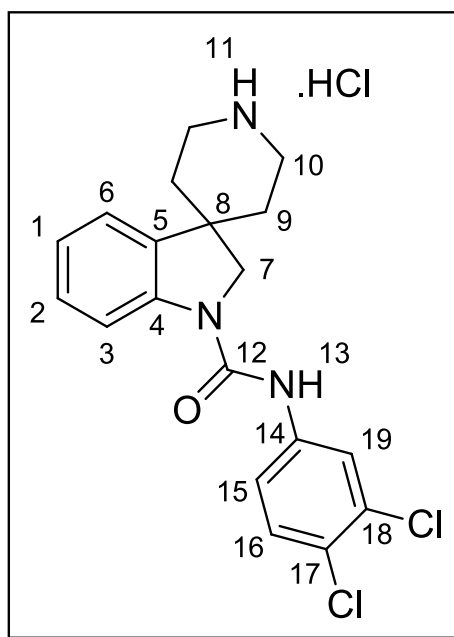
R_f 0.27 (99:1, CH₂Cl₂:MeOH)

IR ν/ cm⁻¹ 1666 (C=O, s), 1682 (C=O, s), 2861 (C-H, w), 3331 (ArC-H, w)

MS (ESI): 510/512 [M+H⁺]

HRMS C₂₇H₂₆³⁵Cl₂N₃O₃ [M+H⁺] requires 510.1351, found 510.1366 (3.3 ppm error)

Preparation of *N*-(3,4-Dichlorophenyl)spiro[indoline-3,4'-piperidine]-1-carboxamide hydrochloride (**LVTa134**):



Benzyl 1-((3,4-dichlorophenyl)carbamoyl)spiro[indoline-3,4'-piperidine]-1'-carboxylate (**LVTa133**) (243 mg, 0.48 mmol, 1 eq.) was dissolved in MeOH (15 mL) and then, Pd(OH)₂/C (33.7 mg, 0.05 mmol, 0.1 eq.) was added into the solution. The reaction mixture was purged with a balloon of hydrogen until deflated and then left under an atmosphere of hydrogen overnight. The methanol was removed under reduced pressure and the reaction mixture was filtered through celite with CH₂Cl₂ (100 mL) to collect any remaining starting material. The solvent 10% MeOH/CH₂Cl₂ (200 mL) was subsequently passed through the celite to elute the desired product. The product **LVTa134** is an amorphous solid (163 mg, 0.43 mmol, 90%).

Data for **LVTa134**

¹H (300 MHz, D₄-MeOH) δ 1.94 (2H, d, *J* 14.1 Hz, CH₂(9_a)), 2.19 (2H, dd, *J* 14.1, 14.1 Hz, CH₂(9_b)), 3.22 (2H, dd, *J* 14.1, 14.1 Hz, CH₂(10_a)), 3.45 (2H, d, *J* 14.1 Hz, CH₂(10_b)), 4.20

(2H, m, CH₂(7)), 6.99–7.10 (2H, m, ArCH), 7.19–7.35 (3H, m, ArCH), 7.54 (1H, d, *J* 8.0 Hz, ArCH(16)), 7.89 (1H, d, *J* 8.0 Hz, ArCH(15))

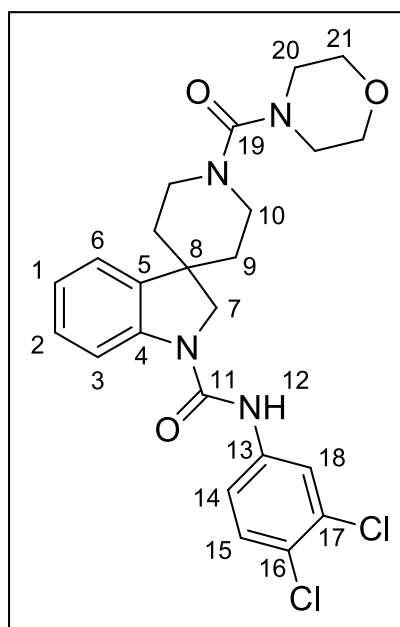
¹³C (75 MHz, D₄-MeOH) δ 36.22 (CH₂(9_{ab})), 40.90 (CH₂(10_{ab})), 42.83 (C(8)), 56.58 (CH₂(7)), 116.82 (ArCH(15)), 121.45 (ArCH(16)), 122.52 (ArCH(19)), 123.88 (ArCH), 124.75 (ArCH), 126.60 (ArCH), 131.30 (ArCH), 133.07 (ArC), 138.15 (ArC), 138.23 (ArC), 143.70 (ArC(14)), 154.41 (C=O(12))

IR ν/ cm⁻¹ 785 (C-Cl, s), 1676 (C=O, s), 3323 (Ar C-H, w)

MS (ESI): 376/378 [M+H⁺]

HRMS C₁₉H₂₀³⁵Cl₂N₃O [M+H⁺] requires 376.0983, found 376.0976 (1.1 ppm error)

Preparation of *N*-(3,4-Dichlorophenyl)-1'-(morpholine-4-carbonyl)spiro[indoline-3,4'-piperidine]-1-carboxamide (**LVTa135**):



Following method C using *N*-(3,4-Dichlorophenyl)spiro[indoline-3,4'-piperidine]-1-carboxamide hydrochloride (**LVTa133**) (100 mg, 0.27 mmol, 1 eq.), 4-morpholinecarbonyl

chloride (0.04 mL, 51.3 mg, 0.32 mmol, 2 eq.) and K₂CO₃ (44.2 mg, 0.32 mmol, 2 eq.) as starting materials. The desired product was purified using column chromatography (SiO₂, 100% EtOAc), to afford, the pure product (**LVTa135**) as a light brown solid (96.1 mg, 0.20 mmol, 74%).

Data for LVTa135

mp 126–130 °C

¹H (300 MHz, CDCl₃) δ 1.74 (2H, d, *J* 13.0 Hz, CH₂(9_a)), 1.93 (2H, dd, *J* 13.0, 13.0 Hz, CH₂(9_b)), 2.93 (2H, dd, *J* 13.0, 11.2 Hz, CH₂(10_a)), 3.30–3.36 (4H, m, CH₂(20)), 3.64–3.71 (6H, m, CH₂(10_b,21)), 3.98 (2H, m, CH₂(7)), 6.81 (1H, br. s, NH(12)), 7.00–7.36 (5H, m, ArCH(18)), 7.46 (1H, d, *J* 8.0 Hz, ArCH(15)), 7.84 (1H, d, *J* 8.0 Hz, ArCH(14))

¹³C (75 MHz, CDCl₃) δ 36.51 (CH₂(9_{ab})), 43.24 (CH₂(10_{ab})), 44.11 (CH₂(20)), 47.28 (C(8)), 57.14 (CH₂(7)), 66.66 (CH₂(21)), 114.89 (ArCH(14)), 120.22 (ArCH(15)), 122.52 (ArCH(18)), 123.79 (ArCH), 124.75 (ArCH), 126.62 (ArCH), 130.43 (ArCH), 132.62 (ArC(17)), 137.98 (ArC), 138.06 (ArC), 141.92 (ArC(16)), 142.15 (ArC(13)), 151.86 (C=O(11)), 152.33 (C=O(19))

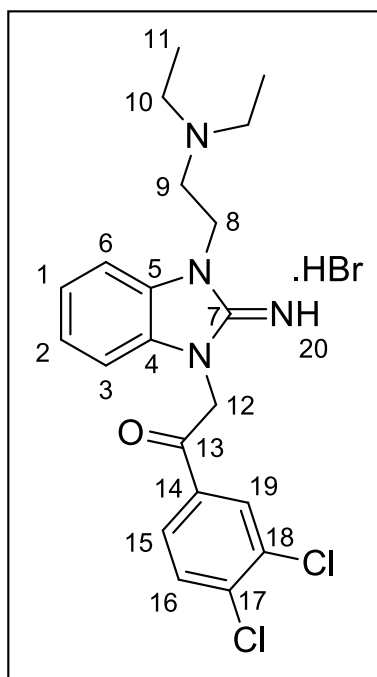
R_f 0.24 (100% EtOAc)

IR ν/ cm⁻¹ 1629 (C=O, s), 1671 (C=O, s), 2858 (C-H, w), 3330 (ArC-H, w)

MS (ESI): 489/491 [M+H⁺]

HRMS C₂₄H₂₆³⁵Cl₂N₄O₃ [M+H⁺] requires 489.1460, found 489.1464 (1.0 ppm error)

Preparation of 1-(3,4-Dichlorophenyl)-2-(3-(2-(diethylamino)ethyl)-2-imino-2,3-dihydro-1*H*-benzo[*d*]imidazol-1-yl)ethan-1-one hydrobromide (**LVTa52**):



Following method D using 1-(2-(Diethylamino)ethyl)-1*H*-benzo[*d*]imidazol-2-amine (**LVTa47**) (275 mg, 0.43 mmol, 1 eq.) and 2-bromo-3,4-dichloroacetophenone (318 mg, 0.43 mmol 1 eq.) as starting materials. The colourless solid **LVTa52** (209 mg, 0.41 mmol, 97%) required no further purification.

Data for LVTa52

mp 212–213 °C

¹H (400 MHz, D₆-DMSO) δ 1.44 (6H, t, *J* 6.9 Hz, **CH**₃(11)), 3.12 (4H, dq, *J* 6.9, 6.9 Hz, **CH**₂(10)), 3.37 (2H, t, *J* 7.9 Hz, **CH**₂(9)), 4.83 (2H, t, *J* 7.9 Hz, **CH**₂(8)), 6.48 (2H, s, **CH**₂(12)), 7.83 (1H, dd, *J* 7.6, 7.6 Hz, Ar**CH**), 7.90 (1H, dd, *J* 7.6, 7.6 Hz, Ar**CH**), 8.06 (1H, d, *J* 7.8 Hz, Ar**CH**), 8.10 (1H, d, *J* 7.8 Hz, Ar**CH**), 8.40 (1H, d, *J* 8.3 Hz, Ar**CH**(16)), 8.57 (1H, d, *J* 8.3 Hz, Ar**CH**(15)), 8.86 (1H, s, Ar**CH**(19))

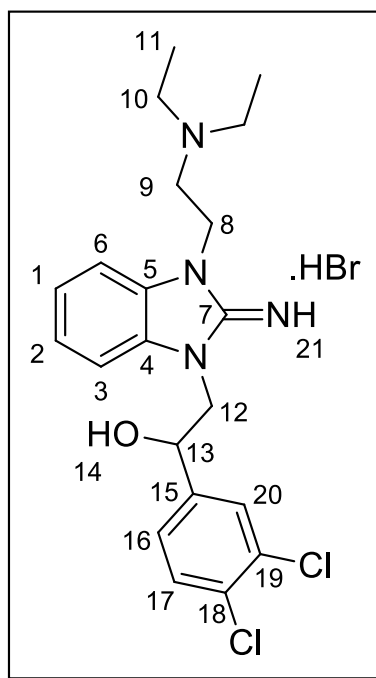
^{13}C (100 MHz, $\text{D}_6\text{-DMSO}$) δ 10.22 ($\text{CH}_3(11)$), 41.71 ($\text{CH}_2(8)$), 45.61 ($\text{CH}_2(10)$), 49.14 ($\text{CH}_2(12)$), 50.06 ($\text{CH}_2(9)$), 109.36 (ArCH), 109.70 (ArCH), 122.36 (ArCH), 122.74 (ArCH), 127.26 (ArCH(15)), 129.27 (ArC(18)), 129.35 (ArC(17)), 129.51 (ArCH(19)), 130.21 (ArCH(16)), 131.41 (ArC), 133.44 (ArC), 136.55 (ArC(14)), 150.50 ($\text{C}=\text{NH}(7)$), 188.75 ($\text{C}=\text{O}(13)$)

IR ν/cm^{-1} 743 (C-Cl, s), 1682 (C=O, s), 1698 (C=N, s), 2970 (C-H, w), 3206 (Ar C-H, w)

MS (ESI): 418/420/422 $[\text{M}+\text{H}^+]$

HRMS $\text{C}_{21}\text{H}_{25}^{35}\text{Cl}_2\text{N}_4\text{O}$ $[\text{M}+\text{H}-\text{Br}^-]^+$ requires 419.1405, found 419.1414 (3.8 ppm error)

Preparation of 1-(3,4-Dichlorophenyl)-2-(3-(2-(diethylamino)ethyl)-2-imino-2,3-dihydro-1H-benzo[d]imidazol-1-yl)ethanol hydrobromide (**LVTa54**):



Following method E using 1-(3,4-Dichlorophenyl)-2-(3-(2-(diethylamino)ethyl)-2-imino-2,3-dihydro-1H-benzo[d]imidazol-1-yl)ethan-1-one hydrobromide (**LVTa52**) (100 mg,

0.20 mmol, 1 eq.) as starting materials. The glass like solid **LVTa54** (98.0 mg, 0.196 mmol, 98%) required no purification.

Data for LVTa54

^1H (300 MHz, CDCl_3) δ 1.03 (6H, t, J 7.1 Hz, $\text{CH}_3(11)$), 2.60 (4H, dq, J 7.1, 7.1 Hz, $\text{CH}_2(10)$), 2.71 (2H, t, J 6.5 Hz, $\text{CH}_2(9)$), 3.83 (2H, t, J 6.5 Hz, $\text{CH}_2(8)$), 4.16 (2H, d, J 4.4 Hz, $\text{CH}_2(12)$), 5.10 (1H, t, J 4.4 Hz, $\text{CH}(13)$), 6.67 (1H, d, J 6.9 Hz, ArCH), 6.87 (1H, d, J 8.7 Hz, ArCH), 6.95–7.04 (2H, m, ArCH(1,2)), 7.30 (1H, d, J 6.9 Hz, ArCH(17)), 7.37 (1H, d, J 6.9 Hz, ArCH(16)), 7.58 (1H, s, ArCH(20))

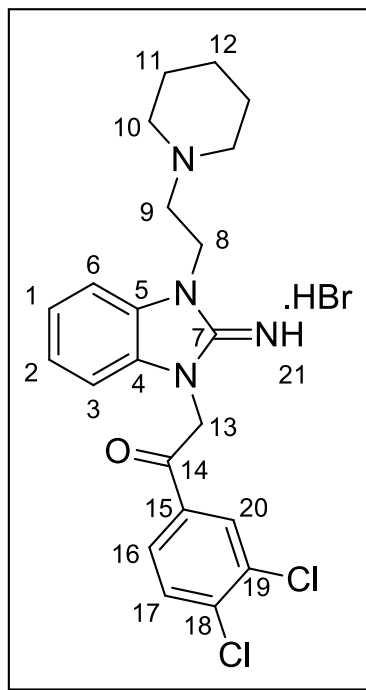
^{13}C (100 MHz, $\text{D}_6\text{-DMSO}$) δ 10.68 ($\text{CH}_3(11)$), 39.58 ($\text{CH}_2(8)$), 45.98 ($\text{CH}_2(10)$), 48.53 ($\text{CH}_2(12)$), 49.31 ($\text{CH}_2(9)$), 69.78 ($\text{CH}(13)$), 106.01 (ArCH), 106.20 (ArCH), 119.40 (ArCH), 119.54 (ArCH), 125.39 (ArCH(16)), 127.33 (ArC(20)), 128.91 (ArC), 129.10 (ArCH(17)), 130.14 (ArC), 130.58 (ArC(19)), 130.76 (ArC(18)), 143.17 (ArC(15)), 153.61 (C=NH(7))

IR ν/cm^{-1} 731 (C-Cl, s), 2812 (C-H, w), 3254 (Ar C-H, w), 3478 (O-H, br.)

MS (ESI): 420/422/424 $[\text{M}+\text{H}^+]$

HRMS $\text{C}_{21}\text{H}_{27}^{35}\text{Cl}_2\text{N}_4\text{O}$ $[\text{M}+\text{H}-\text{Br}^-]^+$ requires 421.1562, found 421.1566 (2.7 ppm error)

Preparation of 1-(3,4-Dichlorophenyl)-2-(2-imino-3-(2-(piperidin-1-yl)ethyl)-2,3-dihydro-1*H*-benzo[*d*]imidazol-1-yl)ethanone hydrobromide (**LVTa57**):



Following method D using 1-(2-(Piperidin-1-yl)ethyl)-1*H*-benzo[*d*]imidazol-2-amine (**LVTa49**) (200 mg, 0.82 mmol, 1 eq.) and 2-bromo-3,4-dichloroacetophenone (220 mg, 0.82 mmol 1 eq.) as starting materials. The colourless solid **LVTa57** (403 mg, 0.79 mmol, 96%) required no further purification.

Data for **LVTa57**

mp 222–225 °C

¹H (300 MHz, CDCl₃) δ 1.44–1.49 (2H, m, CH₂(12)), 1.59–1.62 (4H, m, CH₂(11)), 2.44–2.50 (4H, m, CH₂(10)), 2.60 (2H, t, *J* 7.1 Hz, CH₂(9)), 3.89 (2H, t, *J* 7.1 Hz, CH₂(8)), 5.26 (2H, s, CH₂(13)), 6.70 (1H, d, *J* 7.5 Hz, ArCH), 6.87 (1H, d, *J* 7.5 Hz, ArCH), 6.92–7.02 (2H, m, ArCH), 7.56 (1H, d, *J* 8.3 Hz, ArCH(17)), 7.93 (1H, d, *J* 8.3 Hz, ArCH(16)), 8.20 (1H, s, ArCH(19))

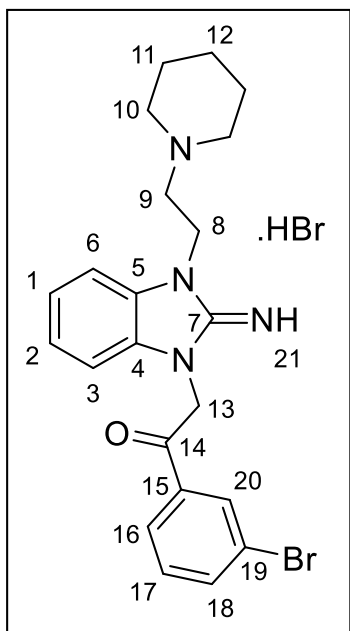
^{13}C (75 MHz, CDCl_3) δ 24.16 ($\text{CH}_2(12)$), 25.97 ($\text{CH}_2(11)$), 40.40 ($\text{CH}_2(8)$), 48.26 ($\text{CH}_2(13)$), 55.06 ($\text{CH}_2(10)$), 56.45 ($\text{CH}_2(9)$), 106.46 (ArCH), 106.67 (ArCH), 120.97 (ArCH), 121.01 (ArCH), 127.44 (ArCH(16)), 130.43 (ArCH(17)), 130.94 (ArCH(20)), 131.47 (ArC(19)), 131.49 (ArC(18)), 133.14 (ArC), 134.14 (ArC), 138.49 (ArC(15)), 154.52 ($\text{C}=\text{NH}(7)$), 191.60 ($\text{C}=\text{O}(14)$)

IR ν/cm^{-1} 743 (C-Cl, s), 1662 ($\text{C}=\text{O}$, s), 1699 ($\text{C}=\text{N}$, s), 2937 (C-H, w), 3165 (Ar C-H, w)

MS (ESI): 430/432/434 $[\text{M}+\text{H}^+]$

HRMS $\text{C}_{22}\text{H}_{25}^{35}\text{Cl}_2\text{N}_4\text{O}$ $[\text{M}+\text{H}-\text{Br}^-]^+$ requires 431.1405, found 431.1412 (3.2 ppm error)

Preparation of 1-(3-Bromophenyl)-2-(2-imino-3-(2-(piperidin-1-yl)ethyl)-2,3-dihydro-1*H*-benzo[*d*]imidazol-1-yl)ethanone hydrobromide (**LVTa58**):



Following method D using 1-(2-(Piperidin-1-yl)ethyl)-1*H*-benzo[*d*]imidazol-2-amine (**LVTa49**) (200 mg, 0.82 mmol, 1 eq.) and 2-bromo-3,4-dichloroacetophenone (228 mg, 0.82 mmol 1 eq.) as starting materials. The cream solid **LVTa58** (358 mg, 0.69 mmol, 84%) required no further purification.

Data for LVT58

mp 201–204 °C

^1H (400 MHz, D_6 -DMSO) δ 1.37–1.39 (2H, m, $\text{CH}_2(12)$), 1.43–1.45 (4H, m, $\text{CH}_2(11)$), 2.48–2.51 (4H, m, $\text{CH}_2(10)$), 2.67 (2H, t, J 7.0 Hz, $\text{CH}_2(9)$), 4.34 (2H, t, J 7.0 Hz, $\text{CH}_2(8)$), 5.97 (2H, s, $\text{CH}_2(13)$), 7.29 (1H, dd, J 7.5, 7.5 Hz, ArCH), 7.37 (1H, dd, J 7.5, 7.5 Hz, ArCH), 7.60–7.64 (3H, m, ArCH(17)), 7.99 (2H, d, J 8.4 Hz, ArCH(18)), 8.07 (1H, d, J 8.4 Hz, ArCH(16)), 8.27 (1H, s, ArCH(20))

^{13}C (100 MHz, D_6 -DMSO) δ 23.53 ($\text{CH}_2(12)$), 25.39 ($\text{CH}_2(11)$), 41.09 ($\text{CH}_2(8)$), 50.09 ($\text{CH}_2(13)$), 53.98 ($\text{CH}_2(10)$), 55.76 ($\text{CH}_2(9)$), 110.44 (ArCH), 110.71 (ArCH), 122.07 (s, ArC(19)), 123.44 (ArCH), 123.54 (ArCH), 127.35 (ArCH(16)), 129.81 (ArC), 130.11 (ArC), 131.09 (2C, ArCH), 136.08 (ArC(15)), 136.72 (ArCH(18)), 150.79 ($\text{C}=\text{NH}(7)$), 190.40 ($\text{C}=\text{O}(14)$)

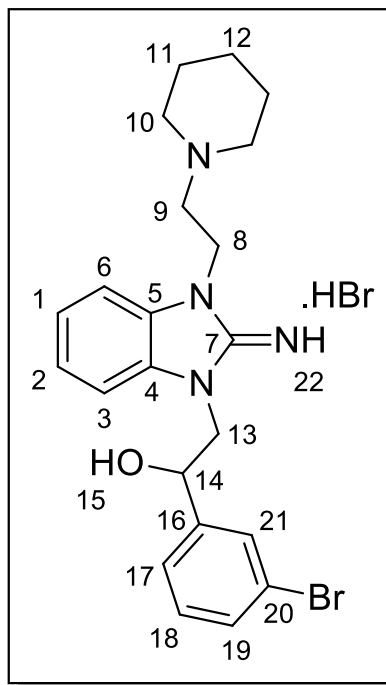
IR ν/cm^{-1} 1662 ($\text{C}=\text{O}$, s), 1698 ($\text{C}=\text{N}$, s), 2929 ($\text{C}-\text{H}$, w), 3161 (Ar C-H, w)

MS (ESI): 440/442 [$\text{M}+\text{H}^+$]

HRMS $\text{C}_{22}\text{H}_{26}^{79}\text{BrN}_4\text{O}$ [$\text{M}+\text{H}-\text{Br}^-$] $^+$ requires 441.1290, found 441.1292 (0.5 ppm error)

Analysis calculated for $\text{C}_{22}\text{H}_{26}\text{BrN}_4\text{O}$: C, 48.91%; H, 5.22%; N 10.37%. Found C, 49.02%; H, 4.70%; N, 10.28%.

Preparation of 1-(3-Bromophenyl)-2-(2-imino-3-(2-(piperidin-1-yl)ethyl)-2,3-dihydro-1*H*-benzo[*d*]imidazol-1-yl)ethanol hydrobromide (**LVTa59**):



Following method E using 1-(3-Bromophenyl)-2-(2-imino-3-(2-(piperidin-1-yl)ethyl)-2,3-dihydro-1*H*-benzo[*d*]imidazol-1-yl)ethanone hydrobromide (**LVTa58**) (100 mg, 0.23 mmol, 1 eq.) as starting materials. The colourless solid **LVTa59** (83.0 mg, 0.16 mmol, 70%) required no purification.

Data for **LVTa59**

mp 64–67 °C

¹H (400 MHz, D₆-DMSO) δ 1.34–1.37 (2H, m, **CH**₂(12)), 1.45–1.47 (4H, m, **CH**₂(11)), 2.44–2.50 (6H, m, **CH**₂(9,10)), 3.89 (2H, t, *J* 6.6 Hz, **CH**₂(8)), 3.89–4.05 (2H, m, **CH**₂(13)), 4.96 (1H, t, *J* 7.6 Hz, **CH**(14)), 6.81–6.93 (4H, m, Ar**CH**), 7.24 (1H, dd, *J* 7.7, 7.7 Hz, Ar**CH**(18)), 7.38–7.43 (2H, m, Ar**CH**(17,19)), 7.62 (1H, s, Ar**CH**(21))

¹³C (100 MHz, D₆-DMSO) δ 24.60 (**CH**₂(12)), 26.26 (**CH**₂(11)), 39.41 (**CH**₂(8)), 49.98 (**CH**₂(13)), 55.00 (**CH**₂(10)), 56.52 (**CH**₂(9)), 71.31 (**CH**(14)), 106.99 (Ar**CH**), 107.45

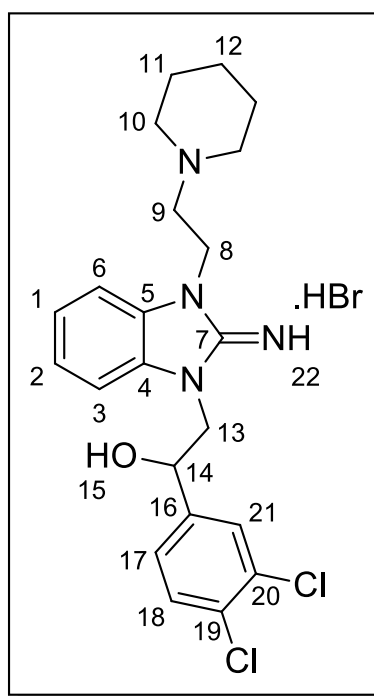
(ArCH), 120.50 (ArCH), 120.57 (ArCH), 122.10 (ArC(20)), 125.82 (ArCH(19)), 129.50 (ArCH(21)), 130.53 (ArCH(17)), 130.78 (ArC(18)), 132.04 (ArC), 132.53 (ArC), 146.59 (ArCH(16)), 154.71 (C=NH(7))

IR ν/cm^{-1} 1625 (C=N, s), 2849 (C-H, w), 3162 (Ar C-H, w), 3359 (O-H, br.)

MS (ESI): 442/444 $[\text{M}+\text{H}^+]$

HRMS $\text{C}_{22}\text{H}_{28}^{79}\text{BrN}_4\text{O}$ $[\text{M}+\text{H}-\text{Br}^-]^+$ requires 443.1446, found 443.1448 (0.6 ppm error)

Preparation of 1-(3,4-Dichlorophenyl)-2-(2-imino-3-(2-(piperidin-1-yl)ethyl)-2,3-dihydro-1H-benzo[d]imidazol-1-yl)ethanol hydrobromide (**LVTa60**):



Following method E using 1-(3,4-Dichlorophenyl)-2-(2-imino-3-(2-(piperidin-1-yl)ethyl)-2,3-dihydro-1H-benzo[d]imidazol-1-yl)ethanone hydrobromide (**LVTa57**) (100 mg, 0.20 mmol, 1 eq.) as starting materials. The colourless solid **LVTa60** (77.0 mg, 0.15 mmol, 75%) required no purification.

Data for LVT60

mp 86–89 °C

^1H (400 MHz, D_6 -DMSO) δ 1.42–1.44 (2H, m, $\text{CH}_2(12)$), 1.51–1.55 (4H, m, $\text{CH}_2(11)$), 2.44–2.46 (4H, m, $\text{CH}_2(10)$), 2.55 (2H, t, J 6.2 Hz, $\text{CH}_2(9)$), 3.87 (2H, t, J 6.2 Hz, $\text{CH}_2(8)$), 4.12–4.21 (2H, m, $\text{CH}_2(13)$), 5.12 (2H, t, J 4.6 Hz, $\text{CH}(14)$), 6.73 (1H, d, J 7.5 Hz, ArCH), 6.87–6.97 (1H, m, ArCH(1,2)), 7.38 (1H, d, J 8.3 Hz, ArCH(18)), 7.42 (1H, d, J 8.3 Hz, ArCH(17)), 7.61 (1H, s, ArCH(21))

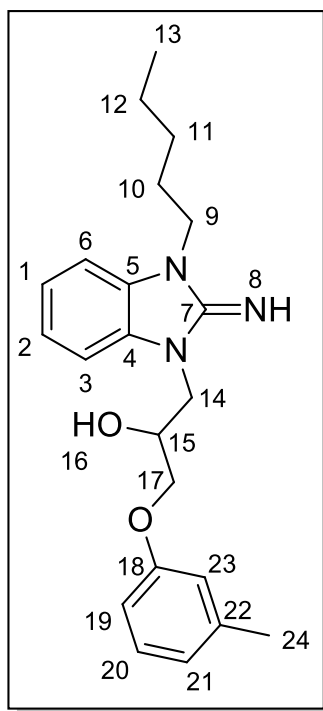
^{13}C (100 MHz, D_6 -DMSO) δ 23.22 ($\text{CH}_2(12)$), 25.14 ($\text{CH}_2(11)$), 39.28 ($\text{CH}_2(8)$), 49.41 ($\text{CH}_2(13)$), 53.90 ($\text{CH}_2(10)$), 55.52 ($\text{CH}_2(9)$), 71.76 ($\text{CH}(14)$), 105.71 (ArCH), 106.21 (ArCH), 119.71 (ArCH), 119.76 (ArCH), 125.28 (ArCH(18)), 127.36 (ArCH(21)), 129.24 (ArCH(17)), 130.27 (ArCH(20)), 130.60 (ArC(19)), 131.00 (ArC), 131.02 (ArC), 143.50 (ArCH(16)), 155.63 (C=NH(7))

IR ν/cm^{-1} 2783 (C-H, w), 3060 (Ar C-H, w), 3356 (O-H, br.)

MS (ESI): 432/434/436 $[\text{M}+\text{H}^+]$

HRMS $\text{C}_{22}\text{H}_{27}^{35}\text{Cl}_2\text{N}_4\text{O}$ $[\text{M}+\text{H}-\text{Br}^-]^+$ requires 433.1562, found 433.1568 (1.1 ppm error)

Preparation of 1-(2-Imino-3-pentyl-2,3-dihydro-1*H*-benzo[*d*]imidazol-1-yl)-3-(*m*-tolxyloxy)propan-2-ol (**LVTa65**):



1-Pentyl-1*H*-benzo[*d*]imidazol-2-amine (**LVTa55**) (626 mg, 3.05 mmol, 1 eq.) and Cs₂CO₃ (1.98 g, 6.1 mmol, 2 eq.) were weighed into a round bottom flask (25 mL) and the flask put under a nitrogen atmosphere. Anhydrous DMF (10 mL) was then added *via* syringe, followed by the addition of 2-[(3-methylphenoxy)methyl]oxirane (500 mg, 3.05 mmol, 1 eq.) *via* syringe and the resulting solution stirred at 100 °C for 1 hour. After 1 hour the solution had turned dark brown and the solvent removed under reduced pressure. The product was partitioned between EtOAc (20 mL) and H₂O (20 mL), organics were extracted with further EtOAc (2 × 25 mL), washed with saturated aqueous brine (50 mL), dried over Na₂SO₄, filtered and solvent removed under reduced pressure. The product was purified using column chromatography (SiO₂, 5:1, EtOAc:Pet ether) followed by an additional purification step using column chromatography (SiO₂, 100%, CH₂Cl₂), which yielded a yellow wax **LVTa65** (439 mg, 1.19 mmol, 39%)

Data for LVT65

^1H (400 MHz, CDCl_3) δ 0.85 (3H, t, J 6.9 Hz, $\text{CH}_3(13)$), 1.28–1.33 (4H, m, $\text{CH}_2(11,12)$), 1.66–1.75 (2H, m, $\text{CH}_2(10)$), 2.31 (3H, s, $\text{CH}_3(24)$), 3.68–3.77 (1H, m, $\text{CH}_2(14_a)$), 3.83 (2H, t, J 7.2 Hz, $\text{CH}_2(9)$), 3.88–4.95 (1H, m, $\text{CH}_2(14_b)$), 4.00 (1H, ddd, J 16.7, 9.2, 6.3 Hz, $\text{CH}_2(17)$), 4.23–4.30 (1H, m, $\text{CH}(15)$), 4.73 (1H, t, J 5.2 Hz), 6.69–6.79 (2H, m, $\text{ArCH}(21,23)$), 7.05–7.12 (3H, m, ArCH), 7.16 (2H, dd, J 6.7, 6.7 Hz, ArCH), 7.43 (1H, d, J 6.7 Hz, ArCH)

^{13}C (100 MHz, CDCl_3) δ 13.84 ($\text{CH}_3(13)$), 21.50 ($\text{CH}_2(12)$), 22.31 ($\text{CH}_3(24)$), 28.67 ($\text{CH}_2(11)$), 29.08 ($\text{CH}_2(10)$), 42.53 ($\text{CH}_2(9)$), 47.10 ($\text{CH}_2(14)$), 69.04 ($\text{CH}_2(17)$), 70.23 ($\text{CH}(15)$), 107.52 (ArCH), 111.46 ($\text{ArCH}(21)$), 115.34 ($\text{ArCH}(23)$), 116.39 (ArCH), 119.94 ($\text{ArCH}(19)$), 121.44 (ArCH), 121.96 (ArCH), 129.30 ($\text{ArCH}(20)$), 134.47 ($\text{ArCH}(22)$), 139.64 (ArC), 141.09 (ArC), 154.70 ($\text{C=NH}(7)$), 158.57 ($\text{ArC}(18)$)

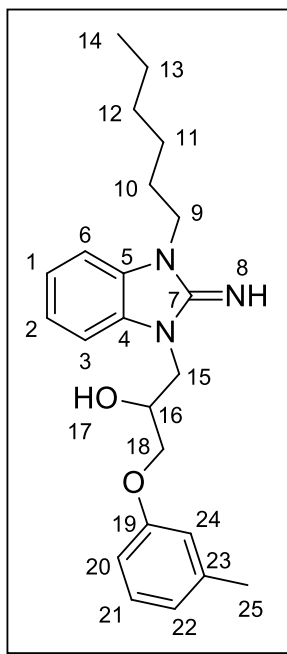
IR ν/cm^{-1} 1657 (C-O, s), 1690 (C=N, s), 2821 (C-H, w), 3382 (O-H, br.)

R_f 0.52 (3:1, EtOAc/Pet. ether)

MS (ESI): 368 $[\text{M}+\text{H}^+]$

HRMS $\text{C}_{22}\text{H}_{30}\text{N}_3\text{O}_2$ $[\text{M}+\text{H}^+]$ requires 368.2338, found 368.2339 (1.9 ppm error)

Preparation of 1-(3-Hexyl-2-imino-2,3-dihydro-1*H*-benzo[*d*]imidazol-1-yl)-3-(*m*-tolxyloxy)propan-2-ol (**LVTa66**):



1-Hexyl-1*H*-benzo[*d*]imidazol-2-amine (**LVTa56**) (133 mg, 0.61 mmol, 1 eq.) and Cs₂CO₃ (185 mg, 1.34 mmol, 2 eq.) were weighed into a round bottom flask (25 mL) and the flask put under a nitrogen atmosphere. Anhydrous DMF (10 mL) was then added *via* syringe, followed by the addition of 2-[(3-methylphenoxy)methyl]oxirane (100 mg, 0.61 mmol, 1 eq.) *via* syringe and the resulting solution stirred at 100 °C for 1 hour. After 1 hour the solution had turned dark brown and the solvent removed under reduced pressure. The product was partitioned between EtOAc (20 mL) and H₂O (20 mL), organics were extracted with further EtOAc (2 × 25 mL), washed with saturated aqueous brine (50 mL), dried over Na₂SO₄, filtered and solvent removed under reduced pressure. The product was purified using preparative thin layer chromatography (SiO₂, 5:1, EtOAc:Pet. ether), which yielded a yellow wax solid **LVTa66** (89 mg, 0.23 mmol, 37%).

Data for **LVTa66**

mp 84–87 °C

^1H (300 MHz, CDCl_3) δ 0.85 (3H, t, J 6.6 Hz, $\text{CH}_3(14)$), 1.21–1.34 (6H, m, $\text{CH}_2(11,12,13)$), 1.65–1.75 (2H, m, $\text{CH}_2(10)$), 2.32 (3H, s, $\text{CH}_3(25)$), 3.68–3.77 (1H, m, $\text{CH}_2(15_a)$), 3.83 (2H, t, J 7.3 Hz, $\text{CH}_2(9)$), 3.88–4.01 (1H, m, $\text{CH}_2(15_b)$), 3.95 (1H, dd, J 7.6, 9.2 Hz, $\text{CH}_2(18_a)$), 4.06 (1H, dd, J 9.2, 5.2 Hz, $\text{CH}_2(18_b)$), 4.23–4.30 (1H, m, $\text{CH}(16)$), 4.68 (1H, t, J 5.1 Hz), 6.70–6.73 (2H, m, $\text{ArCH}(22,24)$), 6.78 (1H, d, J 7.4 Hz, $\text{ArCH}(20)$), 7.07 (2H, dd, J 5.5, 5.5 Hz, ArCH), 7.10–7.13 (1H, m, ArCH), 7.16 (1H, dd, J 6.3, 6.3 Hz, $\text{ArCH}(21)$), 7.43 (1H, d, J 6.3 Hz, ArCH)

^{13}C (75 MHz, CDCl_3) δ 14.01 ($\text{CH}_3(14)$), 21.55 ($\text{CH}_3(25)$), 22.49 ($\text{CH}_2(11)$), 26.70 ($\text{CH}_2(13)$), 28.95 ($\text{CH}_2(10)$), 31.39 ($\text{CH}_2(12)$), 42.56 ($\text{CH}_2(9)$), 68.80 ($\text{CH}_2(18)$), 70.24 ($\text{CH}(16)$), 107.54 (ArCH), 111.37 ($\text{ArCH}(22)$), 115.23 ($\text{ArCH}(24)$), 116.35 (ArCH), 119.95 ($\text{ArCH}(20)$), 121.45 (ArCH), 121.92 (ArCH), 129.31 ($\text{ArCH}(21)$), 134.41 ($\text{ArC}(23)$), 139.65 (ArC), 140.94 (ArC), 154.68 ($\text{C}=\text{NH}(7)$), 158.49 ($\text{ArC}-\text{O}(19)$)

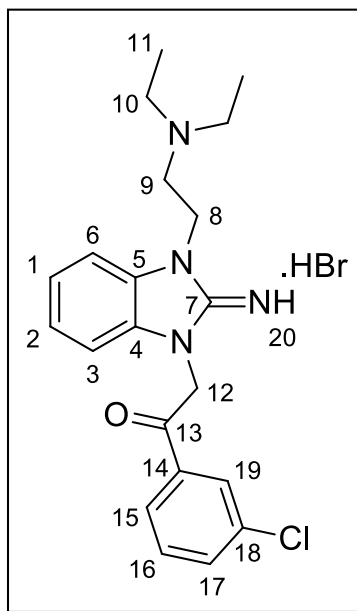
IR ν/cm^{-1} 1607 (C=N, s), 1624 (C-O, s), 2679 (C-H, w), 3364 (O-H, br.)

R_f 0.50 (3:1, EtOAc/Pet. ether)

MS (ESI): 382 $[\text{M}+\text{H}^+]$

HRMS $\text{C}_{23}\text{H}_{32}\text{N}_3\text{O}_2$ $[\text{M}+\text{H}^+]$ requires 382.2489, found 382.2489 (0.0 ppm error)

Preparation of 1-(3-Chlorophenyl)-2-(3-(2-(diethylamino)ethyl)-2-imino-2,3-dihydro-1*H*-benzo[*d*]imidazol-1-yl)ethanone hydrobromide (**LVTa67**):



Following method D using 1-(2-(Diethylamino)ethyl)-1*H*-benzo[*d*]imidazol-2-amine (**LVTa47**) (200 mg, 0.86 mmol, 1 eq.) and 3-chlorophenacyl bromide (201 mg, 0.86 mmol 1 eq.) as starting materials. The colourless solid **LVTa67** (349 mg, 0.75 mmol, 87%) required no further purification.

Data for **LVT67**

mp 201–203 °C

¹H (300 MHz, CDCl₃) δ 1.05 (6H, t, *J* 7.1 Hz, CH₃(11)), 2.61 (4H, dq, *J* 7.1, 7.1 Hz, CH₂(10)), 2.72 (2H, t, *J* 7.1 Hz, CH₂(9)), 3.85 (2H, t, *J* 7.1 Hz, CH₂(8)), 5.29 (2H, s, CH₂(12)), 6.69 (1H, d, *J* 7.1 Hz, ArCH), 6.87 (1H, d, *J* 7.1 Hz, ArCH), 6.92–7.03 (2H, m, ArCH), 7.44 (1H, dd, *J* 7.8, 7.8 Hz, ArCH(16)), 7.58 (1H, d, *J* 7.8 Hz, ArCH(17)), 7.98 (1H, d, *J* 7.8 Hz, ArCH(15)), 8.06 (1H, s, ArCH(19))

¹³C (75 MHz, CDCl₃) δ 12.02 (CH₃(11)), 41.41 (CH₂(8)), 47.71 (CH₂(10)), 48.19 (CH₂(12)), 50.74 (CH₂(9)), 106.38 (ArCH), 106.61 (ArCH), 120.86 (ArCH), 120.91

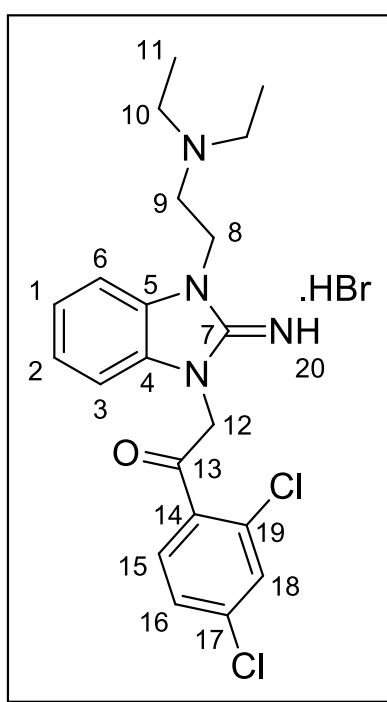
(ArCH), 126.43 (ArCH(15)), 128.43 (ArCH(19)), 130.19 (ArCH(16)), 131.61 (ArC), 131.81 (ArC), 133.80 (ArCH(17)), 135.17 (ArC(18)), 136.20 (ArCH(14)), 154.73 (C=NH(7)), 192.07 (C=O(13))

IR ν/cm^{-1} 1672 (C=O, s), 1698 (C=N, s), 2927 (C-H, w), 3159 (Ar C-H, w)

MS (ESI): 385/387 [M+H⁺]

HRMS C₂₁H₂₆³⁵ClN₄O [M+H-Br⁻]⁺ requires 385.1795, found 385.1800 (1.2 ppm error)

Preparation of 1-(2,4-Dichlorophenyl)-2-(3-(2-(diethylamino)ethyl)-2-imino-2,3-dihydro-1H-benzo[d]imidazol-1-yl)ethanone hydrobromide (**LVTa68**):



Following method D using 1-(2-(Diethylamino)ethyl)-1H-benzo[d]imidazol-2-amine (**LVTa47**) (173 mg, 0.75 mmol, 1 eq.) and 2-bromo-2,4-dichloro acetophenone (201 mg, 0.75 mmol 1 eq.) as starting materials. The colourless solid **LVTa68** (236 mg, 0.56 mmol, 75%) required no further purification.

Data for LVTa68

^1H (400 MHz, D_6 -DMSO) δ 0.83 (6H, t, J 7.1 Hz, $\text{CH}_3(11)$), 2.51 (4H, dq, J 7.1, 7.1 Hz, $\text{CH}_2(10)$), 2.75 (2H, t, J 7.1 Hz, $\text{CH}_2(9)$), 4.30 (2H, t, J 7.1 Hz, $\text{CH}_2(8)$), 5.85 (2H, s, $\text{CH}_2(12)$), 7.29–7.38 (2H, m, ArCH), 7.61 (2H, d, J 8.9 Hz, ArCH), 7.76 (1H, d, J 8.9 Hz, ArCH(16)), 7.90 (1H, s, ArCH(18)), 8.12 (1H, d, J 8.9 Hz, ArCH(15))

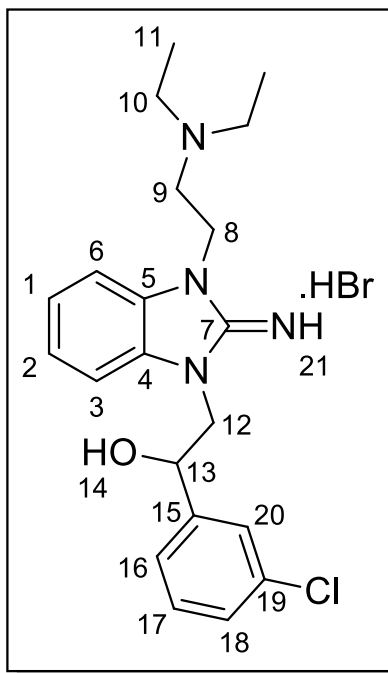
^{13}C (75 MHz, CDCl_3) δ 11.57 ($\text{CH}_3(11)$), 42.03 ($\text{CH}_2(8)$), 46.34 ($\text{CH}_2(10)$), 50.27 ($\text{CH}_2(9)$), 51.68 ($\text{CH}_2(12)$), 110.41 (ArCH), 110.82 (ArCH), 123.48 (ArCH), 123.60 (ArCH), 127.59 (ArCH(16)), 129.92 (2C, ArC), 130.82 (ArCH(18)), 132.29 (ArC(17)), 132.40 (ArCH(15)), 132.97 (ArC(19)), 137.91 (ArC(14)), 150.71 ($\text{C}=\text{NH}(7)$), 190.89 ($\text{C}=\text{O}(13)$)

IR ν/cm^{-1} 1698 ($\text{C}=\text{O}$, s), 1672 ($\text{C}=\text{O}$, s), 2956 (C-H, w), 3207 (Ar C-H, w)

MS (ESI): 419/421 $[\text{M}+\text{H}^+]$

HRMS $\text{C}_{21}\text{H}_{25}^{35}\text{Cl}_2\text{N}_4\text{O}$ $[\text{M}+\text{H}-\text{Br}^-]^+$ requires 419.1405, found 419.1409 (2.5 ppm error)

Preparation of 1-(3-Chlorophenyl)-2-(3-(2-(diethylamino)ethyl)-2-imino-2,3-dihydro-1*H*-benzo[*d*]imidazol-1-yl)ethanol hydrobromide (**LVTa69**):



Following method E using 1-(3-Chlorophenyl)-2-(3-(2-(diethylamino)ethyl)-2-imino-2,3-dihydro-1*H*-benzo[*d*]imidazol-1-yl)ethanone hydrobromide (**LVTa67**) (100 mg, 0.21 mmol, 1 eq.) as starting materials. The clear glass **LVTa69** (79.0 mg, 0.17 mmol, 81%) required no purification.

Data for **LVTa69**

^1H (400 MHz, $\text{D}_6\text{-DMSO}$) δ 0.89 (6H, t, J 7.1 Hz, $\text{CH}_3(11)$), 2.50 (4H, dq, J 7.1, 7.1 Hz, $\text{CH}_2(10)$), 2.57 (2H, t, J 6.7 Hz, $\text{CH}_2(9)$), 3.83 (2H, t, J 6.7 Hz, $\text{CH}_2(8)$), 3.93–4.09 (2H, m, $\text{CH}_2(12)$), 4.98 (1H, t, J 6.1 Hz, $\text{CH}(13)$), 6.80–6.91 (4H, m, ArCH), 7.25 (2H, d, J 7.5 Hz, ArCH(18)), 7.30 (1H, dd, J 7.5, 7.5 Hz, ArCH(17)), 7.38 (1H, d, J 7.5 Hz, ArCH(16)), 7.48 (1H, s, ArCH(20))

^{13}C (75 MHz, CDCl_3) δ 11.90 ($\text{CH}_3(11)$), 39.59 ($\text{CH}_2(8)$), 46.67 ($\text{CH}_2(10)$), 49.28 ($\text{CH}_2(9)$), 49.77 ($\text{CH}_2(12)$), 71.81 ($\text{CH}(13)$), 106.14 (ArCH), 106.62 (ArCH), 119.74 (ArCH), 119.76

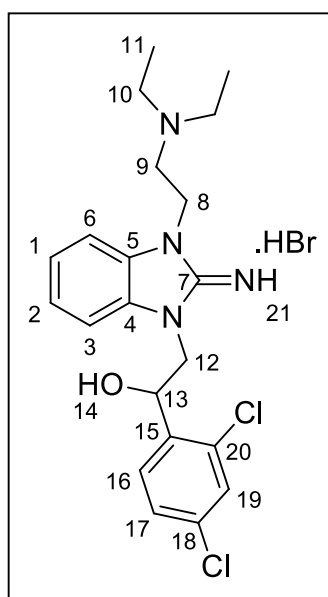
(ArCH), 124.73 (ArCH(16)), 125.91 (ArCH(20)), 126.89 (ArCH(18)), 129.77 (ArCH(17)), 131.46 (ArC), 131.85 (ArC), 132.71 (ArC(19)), 145.71 (ArC(15)), 154.12 (C=NH(7))

IR ν/cm^{-1} 1607 (C-O, s), 1624 (C=N, s), 2812 (C-H, w), 3061 (Ar C-H, w), 3356 (O-H, br.)

MS (ESI): 387/389 [M+H⁺]

HRMS C₂₁H₂₈³⁵ClN₄O [M+H-Br⁻]⁺ requires 387.1952, found 387.1952 (1.8 ppm error)

Preparation of 1-(2,4-Dichlorophenyl)-2-(3-(2-(diethylamino)ethyl)-2-imino-2,3-dihydro-1H-benzo[d]imidazol-1-yl)ethanol hydrobromide (**LVTa70**):



Following method E using 1-(2,4-Dichlorophenyl)-2-(3-(2-(diethylamino)ethyl)-2-imino-2,3-dihydro-1H-benzo[d]imidazol-1-yl)ethanone hydrobromide (**LVTa68**) (100 mg, 0.20 mmol, 1 eq.) as starting materials. The colourless solid **LVTa70** (80.0 mg, 0.16 mmol, 80%) required no purification.

Data for **LVTa70**

mp 93–95 °C

^1H (300 MHz, D_6 -DMSO) δ 0.89 (6H, t, J 7.0 Hz, $\text{CH}_3(11)$), 2.49 (4H, dq, J 7.0, 6.7 Hz, $\text{CH}_2(10)$), 2.56 (2H, t, J 6.7 Hz, $\text{CH}_2(9)$), 3.86 (2H, t, J 6.7 Hz, $\text{CH}_2(8)$), 4.02 (2H, d, J 5.0 Hz, $\text{CH}_2(12)$), 5.23 (1H, t, J 5.0 Hz, $\text{CH}(13)$), 6.76 (1H, d, J 7.1 Hz, ArCH), 6.82–6.91 (2H, m, ArCH), 6.94 (1H, d, J 7.1 Hz, ArCH), 7.41 (1H, d, J 8.4 Hz, ArCH(17)), 7.54 (1H, s, ArCH(19)), 7.66 (1H, d, J 8.4 Hz, ArCH(16))

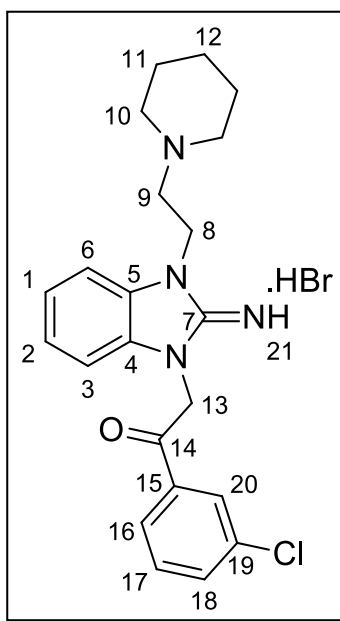
^{13}C (75 MHz, D_6 -DMSO) δ 11.88 ($\text{CH}_3(11)$), 39.71 ($\text{CH}_2(8)$), 46.64 ($\text{CH}_2(10)$), 47.79 ($\text{CH}_2(12)$), 49.79 ($\text{CH}_2(9)$), 68.28 ($\text{CH}(13)$), 106.26 (ArCH), 106.54 (ArCH), 119.92 (ArCH), 120.08 (ArCH), 127.37 (ArCH(17)), 128.21 (ArCH(19)), 129.79 (ArCH(16)), 131.48 (ArC), 131.57 (ArC), 131.67 (ArC(20)), 132.44 (ArC(18)), 139.20 (ArC(15)), 154.27 ($\text{C}=\text{NH}(7)$)

IR ν/cm^{-1} 730 (C-Cl, s), 1609 (C-O, s), 1622 (C=N, s), 2809 (C-H, w), 3240 (O-H, br.), 3340 (Ar C-H, w)

MS (ESI): 421/423 [$\text{M}+\text{H}^+$]

HRMS $\text{C}_{21}\text{H}_{27}^{35}\text{Cl}_2\text{N}_4\text{O}$ [$\text{M}+\text{H}-\text{Br}^-$] $^+$ requires 421.1562, found 421.1565 (2.6 ppm error)

Preparation of 1-(3-Chlorophenyl)-2-(2-imino-3-(2-(piperidin-1-yl)ethyl)-2,3-dihydro-1*H*-benzo[*d*]imidazol-1-yl)ethanone hydrobromide (**LVTa71**):



Following method D using 1-(2-(Piperidin-1-yl)ethyl)-1*H*-benzo[*d*]imidazol-2-amine (**LVTa49**) (200 mg, 0.82 mmol, 1 eq.) and 3-chlorophenacyl bromide (192 mg, 0.82 mmol 1 eq.) as starting materials. The cream solid **LVTa71** (316 mg, 0.66 mmol, 81%) required no further purification.

Data for **LVTa71**

mp 207–210 °C

^1H (300 MHz, CDCl_3) δ 1.43–1.49 (2H, m, $\text{CH}_2(12)$), 1.58–1.65 (4H, m, $\text{CH}_2(11)$), 2.48–2.51 (4H, m, $\text{CH}_2(10)$), 2.61 (2H, t, J 7.2 Hz, $\text{CH}_2(9)$), 3.90 (2H, t, J 7.2 Hz, $\text{CH}_2(10)$), 5.29 (2H, s, $\text{CH}_2(13)$), 6.69 (1H, d, J 7.1 Hz, ArCH), 6.88 (1H, d, J 7.1 Hz, ArCH), 6.91–7.02 (2H, m, ArCH), 7.44 (1H, dd, J 7.7, 7.7 Hz, ArCH(17)), 7.57 (1H, d, J 7.7 Hz, ArCH(18)), 7.97 (1H, d, J 7.7 Hz, ArCH(16)), 8.06 (1H, s, ArCH(20))

^{13}C (75 MHz, CDCl_3) δ 24.18 ($\text{CH}_2(12)$), 25.98 ($\text{CH}_2(11)$), 40.32 ($\text{CH}_2(8)$), 48.20 ($\text{CH}_2(13)$), 55.06 ($\text{CH}_2(10)$), 56.42 ($\text{CH}_2(9)$), 106.40 (ArCH), 106.62 (ArCH), 120.89 (2C,

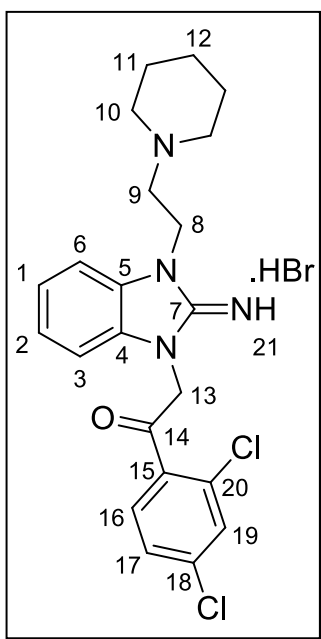
ArCH), 126.43 (ArCH(16)), 128.43 (ArCH(20)), 130.18 (ArCH(17)), 131.62 (ArC), 131.64 (ArC), 133.80 (ArCH(18)), 135.16 (ArC(19)), 136.18 (ArC(15)), 154.66 (C=NH(7)), 192.05 (C=O(14))

IR ν/cm^{-1} 742 (C-Cl, s), 1664 (C=O, s), 1698 (C=N, s), 2932 (C-H, w), 3155 (Ar C-H, w)

MS (ESI): 396/398 $[\text{M}+\text{H}^+]$

HRMS $\text{C}_{22}\text{H}_{26}^{35}\text{ClN}_4\text{O}$ $[\text{M}+\text{H}-\text{Br}^-]^+$ requires 397.1795, found 397.1799 (2.9 ppm error)

Preparation of 1-(2,4-Dichlorophenyl)-2-(2-imino-3-(2-(piperidin-1-yl)ethyl)-2,3-dihydro-1*H*-benzo[*d*]imidazol-1-yl)ethanone hydrobromide (**LVTa72**):



Following method D using 1-(2-(Piperidin-1-yl)ethyl)-1*H*-benzo[*d*]imidazol-2-amine (**LVTa49**) (200 mg, 0.82 mmol, 1 eq.) and 2-bromo-2,4-dichloro acetophenone (220 mg, 0.82 mmol 1 eq.) as starting materials. The light orange solid **LVTa72** (317 mg, 0.62 mmol, 76%) required no further purification.

Data for **LVTa72**

mp 212–214 °C

^1H (300 MHz, D_6 -DMSO) δ 1.38–1.41 (2H, m, $\text{CH}_2(12)$), 1.44–1.46 (4H, m, $\text{CH}_2(11)$), 2.46–2.48 (4H, m, $\text{CH}_2(10)$), 2.69 (2H, t, J 7.2 Hz, $\text{CH}_2(9)$), 4.37 (2H, t, J 7.2 Hz, $\text{CH}_2(10)$), 5.89 (2H, s, $\text{CH}_2(13)$), 7.30–7.43 (2H, m, ArCH), 7.60–7.64 (2H, m, ArCH), 7.76 (1H, d, J 7.7 Hz, ArCH(17)), 7.89 (1H, s, ArCH(19)), 8.24 (1H, d, J 7.7 Hz, ArCH(16))

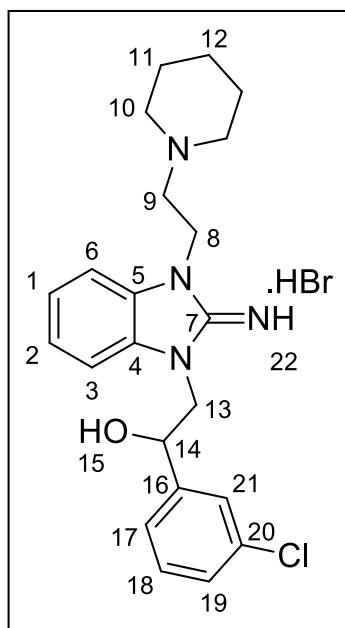
^{13}C (75 MHz, D_6 -DMSO) δ 23.49 ($\text{CH}_2(12)$), 25.33 ($\text{CH}_2(11)$), 41.15 ($\text{CH}_2(8)$), 51.66 ($\text{CH}_2(13)$), 53.95 ($\text{CH}_2(10)$), 55.68 ($\text{CH}_2(9)$), 110.40 (ArCH), 110.71 (ArCH), 123.52 (ArCH), 123.63 (ArCH), 127.60 (ArCH(17)), 129.92 (ArC), 129.94 (ArC), 130.84 (ArCH(19)), 132.39 (ArCH(18)), 132.41 (ArC(20)), 133.01 (ArCH(16)), 137.94 (ArC(15)), 150.81 (C=NH(7)), 190.89 (C=O(14))

IR ν/cm^{-1} 743 (C-Cl, s), 1667 (C=O, s), 1698 (C=N, s), 2851 (C-H, w), 3002 (Ar C-H, w)

MS (ESI): 430/432/434 $[\text{M}+\text{H}^+]$

HRMS $\text{C}_{22}\text{H}_{25}^{35}\text{Cl}_2\text{N}_4\text{O}$ $[\text{M}+\text{H}-\text{Br}^-]^+$ requires 431.1405, found 431.1408 (2.2 ppm error)

Preparation of 1-(3-Chlorophenyl)-2-(2-imino-3-(2-(piperidin-1-yl)ethyl)-2,3-dihydro-1*H*-benzo[*d*]imidazol-1-yl)ethanol hydrobromide (**LVTa73**):



Following method E using 1-(3-Chlorophenyl)-2-(2-imino-3-(2-(piperidin-1-yl)ethyl)-2,3-dihydro-1*H*-benzo[*d*]imidazol-1-yl)ethanone hydrobromide (**LVTa71**) (112 mg, 0.26 mmol, 1 eq.) as starting materials. The clear glass **LVTa73** (94.0 mg, 0.20 mmol, 77%) required no purification.

Data for **LVTa73**

^1H (300 MHz, D_6 -DMSO) δ 1.36–1.38 (2H, m, $\text{CH}_2(12)$), 1.43–1.50 (4H, m, $\text{CH}_2(11)$), 2.42–2.46 (6H, m, $\text{CH}_2(9,10)$), 3.90 (2H, t, J 6.6 Hz, $\text{CH}_2(8)$), 3.98–4.03 (2H, m, $\text{CH}_2(13)$), 4.98 (1H, dd, J 6.7, 3.8 Hz, $\text{CH}(14)$), 6.83–6.95 (4H, m, ArCH), 7.26–7.31 (2H, m, ArCH(18,19)), 7.39 (1H, d, J 7.2 Hz, ArCH(17)), 7.48 (1H, s, ArCH(21)),

^{13}C (75 MHz, D_6 -DMSO) δ 23.91 ($\text{CH}_2(12)$), 25.55 ($\text{CH}_2(11)$), 38.87 ($\text{CH}_2(8)$), 49.26 ($\text{CH}_2(13)$), 54.30 ($\text{CH}_2(10)$), 55.26 ($\text{CH}_2(9)$), 70.58 ($\text{CH}(14)$), 106.41 (ArCH), 106.86 (ArCH), 119.94 (2C, ArCH), 124.75 (ArCH(17)), 125.92 (ArCH(21)), 126.95 (ArCH(18)),

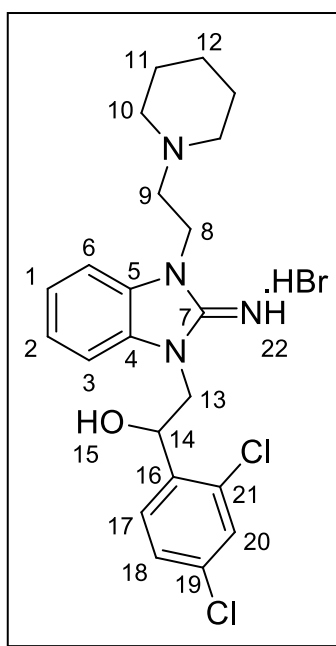
129.79 (ArCH(19)), 131.21 (ArC), 131.76 (ArC), 132.72 (ArC(20)), 145.62 (ArC(16)), 153.86 (C=NH(7))

IR ν/cm^{-1} 731 (C-Cl, s), 1608 (C-O, s), 1625 (C=N, s), 2849 (C-H, w), 3059 (Ar C-H, w), 3280 (O-H, br.)

MS (ESI): 398/400/402 $[\text{M}+\text{H}^+]$

HRMS $\text{C}_{22}\text{H}_{28}^{35}\text{ClN}_4\text{O}$ $[\text{M}+\text{H}-\text{Br}^-]^+$ requires 399.1952, found 399.1971 (0.7 ppm error)

Preparation of 1-(2,4-Dichlorophenyl)-2-(2-imino-3-(2-(piperidin-1-yl)ethyl)-2,3-dihydro-1*H*-benzo[*d*]imidazol-1-yl)ethanol hydrobromide (**LVTa74**):



Following method E using 1-(2,4-Dichlorophenyl)-2-(2-imino-3-(2-(piperidin-1-yl)ethyl)-2,3-dihydro-1*H*-benzo[*d*]imidazol-1-yl)ethanone hydrobromide (**LVTa72**) (100 mg, 0.20 mmol, 1 eq.) as starting materials. The colourless solid **LVTa74** (78.0 mg, 0.15 mmol, 78%) required no purification.

Data for **LVTa74**

mp 159–162 °C

^1H (300 MHz, CDCl_3) δ 1.46–1.49 (2H, m, $\text{CH}_2(12)$), 1.60–1.67 (4H, m, $\text{CH}_2(11)$), 2.50–2.52 (4H, m, $\text{CH}_2(10)$), 2.62 (2H, t, J 6.5 Hz, $\text{CH}_2(9)$), 3.91 (2H, t, J 6.5 Hz, $\text{CH}_2(8)$), 4.27 (2H, d, J 4.3 Hz, $\text{CH}_2(13)$), 5.44 (1H, dd, J 4.3, 4.3 Hz, $\text{CH}(14)$), 6.78–6.91 (2H, m, ArCH), 6.97–7.05 (2H, m, ArCH), 7.21 (1H, d, J 8.4 Hz, ArCH(18)), 7.34 (1H, s, ArCH(20)), 7.76 (1H, d, J 8.4 Hz, ArCH(17))

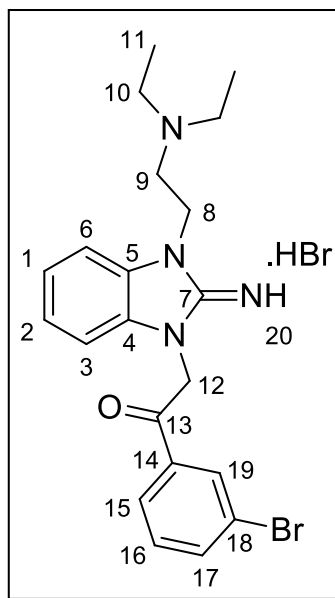
^{13}C (75 MHz, CDCl_3) δ 23.89 ($\text{CH}_2(12)$), 25.55 ($\text{CH}_2(11)$), 39.12 ($\text{CH}_2(8)$), 47.83 ($\text{CH}_2(13)$), 24.29 ($\text{CH}_2(10)$), 55.83 ($\text{CH}_2(9)$), 68.12 ($\text{CH}(14)$), 106.42 (ArCH), 106.76 (ArCH), 120.13 (2C, ArCH), 127.37 (ArCH(20)), 128.20 (ArCH(18)), 129.81 (ArCH(17)), 131.33 (ArC), 131.45 (ArC), 131.69 (ArC(19)), 132.46 (ArC(21)), 139.17 (ArC(16)), 154.02 (C=NH(7))

IR ν/cm^{-1} 732 (C-Cl, s), 1608 (C-O, s), 1622 (C=N, s), 2856 (C-H, w), 2019 (Ar C-H, w), 3296 (O-H, br.)

MS (ESI): 432/434/436 $[\text{M}+\text{H}^+]$

HRMS $\text{C}_{22}\text{H}_{27}^{35}\text{Cl}_2\text{N}_4\text{O}$ $[\text{M}+\text{H}-\text{Br}^-]^+$ requires 433.1562, found 433.1572 (3.3 ppm error)

Preparation of 1-(3-Bromophenyl)-2-(3-(2-(diethylamino)ethyl)-2-imino-2,3-dihydro-1*H*-benzo[*d*]imidazol-1-yl)ethanone hydrobromide (**LVTa75**):



Following method D using 1-(2-(Diethylamino)ethyl)-1*H*-benzo[*d*]imidazol-2-amine (**LVTa47**) (200 mg, 0.83 mmol, 1 eq.) and 2-bromo-2,4-dichloro acetophenone (228 mg, 0.83 mmol 1 eq.) as starting materials. The colourless solid **LVTa75** (333 mg, 0.65 mmol, 79%) required no further purification.

Data for **LVTa75**

mp 212–214 °C

¹H (400 MHz, D₆-DMSO) δ 0.82 (6H, t, *J* 6.8 Hz, CH₃(11)), 2.51 (4H, dq, *J* 6.8, 6.8 Hz, CH₂(10)), 2.75 (2H, t, *J* 7.0 Hz, CH₂(9)), 4.30 (2H, t, *J* 7.0 Hz, CH₂(8)), 5.96 (2H, s, CH₂(12)), 7.28 (1H, dd, *J* 7.5, 7.5 Hz, ArCH), 7.35 (1H, dd, *J* 7.5, 7.5 Hz, ArCH), 7.60–7.63 (3H, m, ArCH(16)), 7.99 (1H, d, *J* 7.4 Hz, ArCH(17)), 8.07 (1H, d, *J* 7.4 Hz, ArCH(15)), 8.27 (1H, s, ArCH(19))

¹³C (100 MHz, D₆-DMSO) δ 12.13 (CH₃(11)), 42.55 (CH₂(8)), 46.88 (CH₂(10)), 50.41 (CH₂(9)), 50.92 (CH₂(12)), 110.91 (ArCH), 111.30 (ArCH), 122.60 (ArC(18)), 124.06

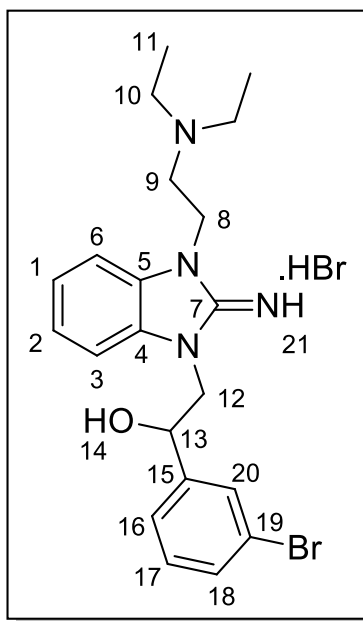
(ArCH), 124.07 (ArCH), 127.79 (ArCH(15)), 130.58 (ArC), 130.59 (ArC), 131.60 (2C, ArCH), 136.62 (ArC(14)), 137.24 (ArC(17)), 151.27 (C=NH(7)), 190.77 (C=O(13))

IR ν/cm^{-1} 1662 (C=O, s), 1696 (C=N, s), 2984 (C-H, w), 3162 (Ar C-H, w)

MS (ESI): 428/431 $[\text{M}+\text{H}^+]$

HRMS $\text{C}_{21}\text{H}_{26}^{79}\text{BrN}_4\text{O}$ $[\text{M}+\text{H}-\text{Br}^-]^+$ requires 429.1290, found 429.1292 (1.5 ppm error)

Preparation of 1-(3-Bromophenyl)-2-(3-(2-(diethylamino)ethyl)-2-imino-2,3-dihydro-1*H*-benzo[*d*]imidazol-1-yl)ethanol hydrobromide (**LVTa76**):



Following method E using 1-(3-Bromophenyl)-2-(3-(2-(diethylamino)ethyl)-2-imino-2,3-dihydro-1*H*-benzo[*d*]imidazol-1-yl)ethanone hydrobromide (**LVTa76**) (111 mg, 0.22 mmol, 1 eq.) as starting materials. The clear glass **LVTa76** (83.0 mg, 0.16 mmol, 74%) required no purification.

Data for **LVTa76**

^1H (300 MHz, $\text{D}_6\text{-DMSO}$) δ 1.46–1.49 (6H, m, $\text{CH}_3(11)$), 1.60–1.67 (4H, m, $\text{CH}_2(10)$), 2.50–2.62 (2H, t, J 6.5 Hz, $\text{CH}_2(9)$), 3.91 (2H, t, J 6.5 Hz, $\text{CH}_2(8)$), 4.27 (2H, d, J 4.3 Hz, $\text{CH}_2(12)$), 5.44 (1H, dd, J 4.3, 4.3 Hz, $\text{CH}(13)$), 6.78–6.91 (2H, m, ArCH), 6.97–7.05 (2H, m, ArCH), 7.21 (1H, d, J 8.4 Hz, ArCH(18)), 7.34 (1H, s, ArCH(20)), 7.76 (1H, d, J 8.4 Hz, ArCH(17))

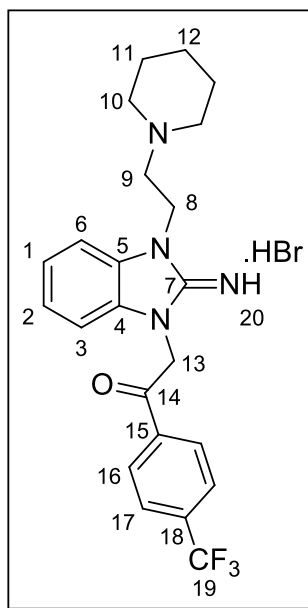
^{13}C (75 MHz, $\text{D}_6\text{-DMSO}$) δ 11.90 ($\text{CH}_3(11)$), 39.63 ($\text{CH}_2(8)$), 46.67 ($\text{CH}_2(10)$), 49.26 ($\text{CH}_2(12)$), 49.79 ($\text{CH}_2(9)$), 70.63 ($\text{CH}(13)$), 106.19 (ArCH), 106.71 (ArCH), 119.70 (ArCH), 119.82 (ArCH), 121.41 (ArCH(16)), 125.13 (ArC(19)), 128.80 (ArCH(20)), 130.03 (ArCH(18)), 130.09 (ArCH(17)), 131.43 (ArC), 131.83 (ArC), 145.92 (ArC(15)), 154.06 (C=NH(7))

IR ν/cm^{-1} 1607 (C-O, s), 1624 (C=N, s), 2810 (C-H, w), 3059 (Ar C-H, w), 3334 (O-H, br.)

MS (ESI): 430/432 $[\text{M}+\text{H}^+]$

HRMS $\text{C}_{21}\text{H}_{28}^{79}\text{BrN}_4\text{O}$ $[\text{M}+\text{H}-\text{Br}^-]^+$ requires 431.1446, found 431.1441 (0.4 ppm error)

Preparation of 2-(2-Imino-3-(2-(piperidin-1-yl)ethyl)-2,3-dihydro-1*H*-benzo[*d*]imidazol-1-yl)-1-(4-(trifluoromethyl)phenyl)ethanone hydrobromide (**LVTa77**):



Following method D using 1-(2-(Piperidin-1-yl)ethyl)-1*H*-benzo[*d*]imidazol-2-amine (**LVTa49**) (200 mg, 0.82 mmol, 1 eq.) and 4-(trifluoromethyl)phenacyl bromide (219 mg, 0.82 mmol 1 eq.) as starting materials. The cream solid **LVTa77** (399 mg, 0.78 mmol, 95%) required no further purification.

Data for **LVTa77**

mp 218–220 °C

^1H (300 MHz, CDCl_3) δ 1.44–1.49 (2H, m, $\text{CH}_2(12)$), 1.57–1.65 (4H, m, $\text{CH}_2(11)$), 2.44–2.51 (4H, m, $\text{CH}_2(10)$), 2.61 (2H, t, J 7.1 Hz, $\text{CH}_2(9)$), 3.89 (2H, t, J 7.1 Hz, $\text{CH}_2(8)$), 5.33 (2H, s, $\text{CH}_2(13)$), 6.70 (1H, d, J 7.2 Hz, ArCH), 6.88 (1H, d, J 7.2 Hz, ArCH), 6.92–7.02 (2H, m, ArCH), 7.75 (2H, d, J 7.7 Hz, ArCH(17)), 8.20 (2H, d, J 7.7 Hz, ArCH(16))

^{13}C (75 MHz, $\text{D}_6\text{-DMSO}$) δ 23.58 (s, $\text{CH}_2(12)$), 25.44 (s, $\text{CH}_2(11)$), 41.20 (s, $\text{CH}_2(8)$), 50.21 (s, $\text{CH}_2(13)$), 54.01 (s, $\text{CH}_2(10)$), 55.75 (s, $\text{CH}_2(9)$), 110.46 (s, ArCH), 110.70 (s, ArCH), 123.44 (s, ArCH), 123.57 (s, ArCH), 123.68 (q, $^1J_{\text{C-F}}$ 272 Hz, ArCF₃(19)), 125.80 (q, $^3J_{\text{C-F}}$

3.7 Hz, ArCH(17)), 129.32 (s, ArCH(16)), 130.06 (s, ArC), 130.09 (s, ArC), 133.28 (q, $^2J_{C-F}$ 32 Hz, ArC(18)), 137.23 (s, ArC(15)), 150.81 (s, C=NH(7)), 190.85 (s, C=O(14))

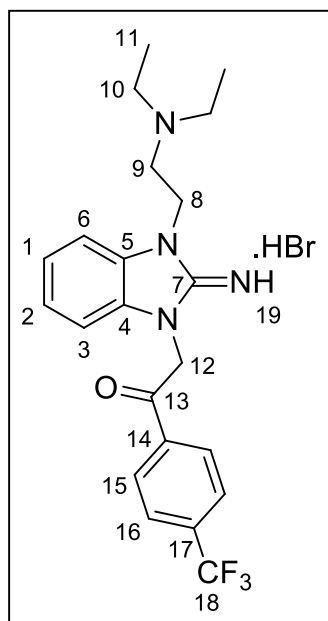
^{19}F (376 MHz, $\text{D}_6\text{-DMSO}$) δ -61.6 (s, Ar-CF₃(19))

IR ν/cm^{-1} 734 (C-F, s), 1664 (C=O, s), 1697 (C=N, s), 2856 (C-H, w), 3154 (Ar C-H, w)

MS (ESI): 431 [M+H⁺]

HRMS C₂₃H₂₆F₃N₄O [M+H-Br⁻]⁺ requires 431.2059, found 431.2064 (0.5 ppm error)

Preparation of 2-(3-(2-(Diethylamino)ethyl)-2-imino-2,3-dihydro-1*H*-benzo[*d*]imidazol-1-yl)-1-(4-(trifluoromethyl)phenyl)ethanone hydrobromide (**LVTa78**):



Following method D using 1-(2-(Diethylamino)ethyl)-1*H*-benzo[*d*]imidazol-2-amine (**LVTa47**) (200 mg, 0.86 mmol, 1 eq.) and 4-(trifluoromethyl)phenacyl bromide (230 mg, 0.86 mmol 1 eq.) as starting materials. The light orange solid **LVTa78** (307 mg, 0.62 mmol, 72%) required no further purification.

Data for **LVTa78**

mp 205–208 °C

^1H (400 MHz, $\text{D}_6\text{-DMSO}$) δ 0.83 (6H, t, J 6.4 Hz, $\text{CH}_3(12)$), 2.45–2.51 (4H, m, $\text{CH}_2(10)$), 2.75 (2H, t, J 6.9 Hz, $\text{CH}_2(9)$), 4.31 (2H, t, J 6.9 Hz, $\text{CH}_2(8)$), 6.02 (2H, s, $\text{CH}_2(12)$), 7.29 (1H, dd, J 7.6, 7.6 Hz, ArCH), 7.36 (1H, dd, J 7.6, 7.6 Hz, ArCH), 7.64 (2H, d, J 7.7 Hz, ArCH), 8.05 (2H, d, J 7.9 Hz, ArCH(16)), 8.30 (2H, d, J 7.9 Hz, ArCH(15))

^{13}C (75 MHz, $\text{D}_6\text{-DMSO}$) δ 12.13 (s, $\text{CH}_3(11)$), 42.56 (s, $\text{CH}_2(8)$), 46.88 (s, $\text{CH}_2(10)$), 50.63 (s, $\text{CH}_2(12)$), 50.90 (s, $\text{CH}_2(9)$), 110.96 (s, ArCH), 111.32 (s, ArCH), 123.94 (s, ArCH), 124.09 (s, ArCH), 124.20 (q, $^1J_{\text{C-F}}$ 273 Hz, ArCF₃(18)), 126.29 (q, $^3J_{\text{C-F}}$ 7.2 Hz, ArCH(16)), 129.81 (s, ArCH(15)), 130.57 (s, ArC), 130.59 (s, ArC), 133.84 (q, $^2J_{\text{C-F}}$ 32 Hz, ArC(17)), 137.80 (s, ArC(14)), 151.27 (s, C=NH(7)), 191.27 (s, C=O(13))

^{19}F (376 MHz, $\text{D}_6\text{-DMSO}$) δ –61.6 (s, Ar-CF₃(18))

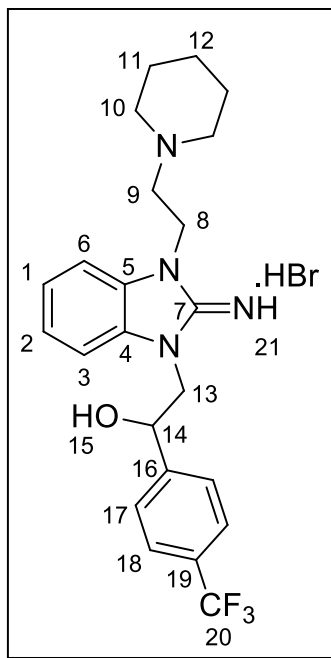
IR ν/cm^{-1} 744 (C-F, s), 1662 (C=O, s), 1698 (C=N, s), 2898 (C-H, w), 3103 (Ar C-H, w)

MS (ESI): 419 $[\text{M}+\text{H}^+]$

HRMS $\text{C}_{22}\text{H}_{26}\text{F}_3\text{N}_4\text{O}$ $[\text{M}+\text{H}-\text{Br}^-]^+$ requires 419.2059, found 419.2064 (0.4 ppm error)

Analysis calculated for $\text{C}_{22}\text{H}_{26}\text{F}_3\text{N}_4\text{O}$: C, 52.91%; H, 5.25%; N 11.22%. Found C, 52.57%; H, 5.04%; N, 11.01%.

Preparation of 2-(2-Imino-3-(2-(piperidin-1-yl)ethyl)-2,3-dihydro-1*H*-benzo[*d*]imidazol-1-yl)-1-(4-(trifluoromethyl)phenyl)ethanol hydrobromide (**LVTa79**):



Following method E using 2-(2-Imino-3-(2-(piperidin-1-yl)ethyl)-2,3-dihydro-1*H*-benzo[*d*]imidazol-1-yl)-1-(4-(trifluoromethyl)phenyl)ethanone hydrobromide (**LVTa77**) (100 mg, 0.20 mmol, 1 eq.) as starting materials. The colourless solid **LVTa79** (89.0 mg, 0.17 mmol, 85%) required no purification.

Data for **LVTa79**

mp: 136–139 °C

¹H (300 MHz, CDCl₃) δ 1.44–1.47 (2H, m, **CH**₂(12)), 1.58–1.65 (4H, m, **CH**₂(11)), 2.48–2.50 (4H, m, **CH**₂(10)), 2.59 (2H, t, *J* 6.8 Hz, **CH**₂(9)), 3.87 (2H, t, *J* 6.8 Hz, **CH**₂(8)), 4.15 (2H, d, *J* 5.1 Hz, **CH**₂(13)), 5.20 (1H, dd, *J* 5.1, 5.1 Hz, **CH**(14)), 6.62 (1H, d, *J* 7.1 Hz, **ArCH**), 6.86 (1H, d, *J* 8.7 Hz, **ArCH**), 6.91–7.00 (2H, m, **ArCH**), 7.55–7.61 (4H, m, **ArCH**(17,18))

^{13}C (75 MHz, $\text{D}_6\text{-DMSO}$) δ 23.90 (s, $\text{CH}_2(12)$), 25.55 (s, $\text{CH}_2(11)$), 38.80 (s, $\text{CH}_2(8)$), 49.28 (s, $\text{CH}_2(13)$), 54.30 (s, $\text{CH}_2(10)$), 55.82 (s, $\text{CH}_2(9)$), 70.78 (s, $\text{CH}(14)$), 106.30 (s, ArCH), 106.66 (s, ArCH), 119.74 (s, ArCH), 119.85 (s, ArCH), 120.70 (q, $^1J_{\text{C-F}}$ 271 Hz, Ar $\text{CF}_3(20)$), 124.74 (q, $^3J_{\text{C-F}}$ 7.4 Hz, ArCH(18)), 126.84 (s, ArCH(17)), 127.84 (q, $^2J_{\text{C-F}}$ 31 Hz, ArC(19)), 131.35 (s, ArC), 131.79 (s, ArC), 147.83 (s, ArC(16)), 153.95 (s, C=NH(7))

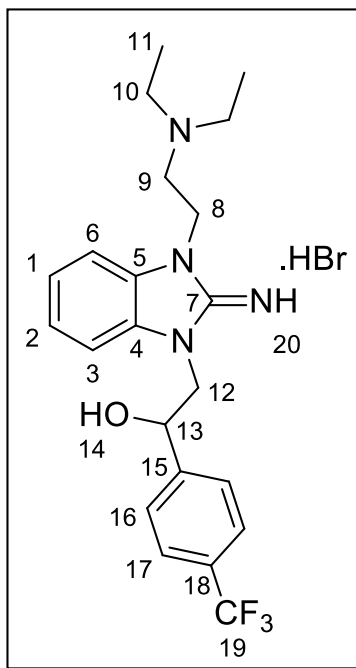
^{19}F (376 MHz, $\text{D}_6\text{-DMSO}$) δ -60.7 (s, Ar- $\text{CF}_3(20)$)

IR ν/cm^{-1} 1609 (C-O, s), 2809 (C-H, w), 3107 (Ar C-H, w), 3357 (O-H, br.)

MS (ESI): 433 $[\text{M}+\text{H}^+]$

HRMS $\text{C}_{23}\text{H}_{28}\text{F}_3\text{N}_4\text{O}$ $[\text{M}+\text{H}-\text{Br}^-]^+$ requires 433.2210, found 433.2210 (0.1 ppm error)

Preparation of 2-(3-(2-(Diethylamino)ethyl)-2-imino-2,3-dihydro-1*H*-benzo[*d*]imidazol-1-yl)-1-(4-(trifluoromethyl)phenyl)ethanol hydrobromide (**LVTa80**):



Following method E using 2-(3-(2-(Diethylamino)ethyl)-2-imino-2,3-dihydro-1*H*-benzo[*d*]imidazol-1-yl)-1-(4-(trifluoromethyl)phenyl)ethanone hydrobromide (**LVTa78**) (100 mg, 0.20 mmol, 1 eq.) as starting materials. The clear glass **LVTa80** (90.0 mg, 0.18 mmol, 90%) required no purification.

Data for LVTa80

^1H (300 MHz, CDCl_3) δ 0.88 (6H, t, J 7.0 Hz, CH_3 (11)), 2.46 (4H, dq, J 7.0, 7.0 Hz, CH_2 (10)), 2.56 (2H, t, J 6.6 Hz, CH_2 (9)), 3.84 (2H, t, J 6.6 Hz, CH_2 (8)), 3.97–4.09 (2H, m, CH_2 (12)), 5.07 (1H, dd, J 5.7, 5.7 Hz, CH (13)), 6.80–6.92 (4H, m, ArCH(1,2,3,6)), 7.64 (4H, s, ArCH(16,17))

^{13}C (75 MHz, $\text{D}_6\text{-DMSO}$) δ 11.86 (s, CH_3 (11)), 39.60 (s, CH_2 (8)), 46.65 (s, CH_2 (10)), 49.26 (s, CH_2 (9)), 49.76 (s, CH_2 (12)), 70.84 (s, CH (13)), 106.23 (s, ArCH), 106.62 (s, ArCH), 119.67 (s, ArCH), 119.83 (s, ArCH), 124.31 (q, $^1J_{\text{C-F}}$ 272 Hz, ArCF₃(19)), 124.73 (q, $^3J_{\text{C-F}}$ 7.5 Hz, ArCH(17)), 126.84 (s, ArCH(16)), 127.62 (q, $^2J_{\text{C-F}}$ 31 Hz, ArC(18)), 131.45 (s, ArC), 131.79 (s, ArC), 147.83 (s, ArC(15)), 154.07 (s, C=NH(7))

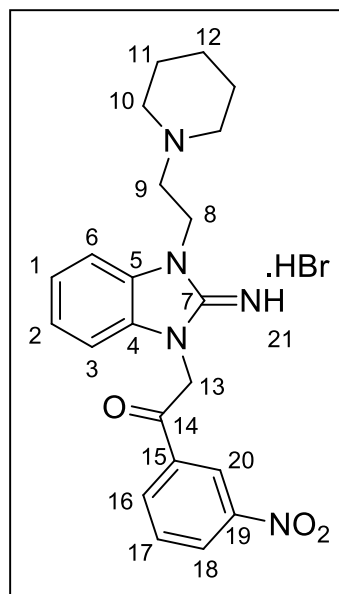
^{19}F (376 MHz, $\text{D}_6\text{-DMSO}$) δ –60.7 (s, Ar-CF₃(19))

IR ν/cm^{-1} 742 (C-F, s), 1608 (C-O, s), 2814 (C-H, w), 3066 (Ar C-H, w), 3319 (O-H, br.)

MS (ESI): 421 [$\text{M}+\text{H}^+$]

HRMS $\text{C}_{22}\text{H}_{28}\text{F}_3\text{ON}_4$ [$\text{M}+\text{H}-\text{Br}^-$]⁺ requires 421.2215, found 421.2215 (0.2 ppm error)

Preparation of 2-(2-Imino-3-(2-(piperidin-1-yl)ethyl)-2,3-dihydro-1*H*-benzo[*d*]imidazol-1-yl)-1-(3-nitrophenyl)ethanone hydrobromide (**LVTa81**):



Following method D using 1-(2-(Piperidin-1-yl)ethyl)-1*H*-benzo[*d*]imidazol-2-amine (**LVTa49**) (200 mg, 0.82 mmol, 1 eq.) and 2-bromo-3-nitroacetophenone (200 mg, 0.82 mmol 1 eq.) as starting materials. The yellow solid **LVTa81** (368 mg, 0.76 mmol, 93%) required no further purification.

Data for **LVTa81**

mp 210–213 °C

^1H (300 MHz, CDCl_3) δ 1.36–1.38 (2H, m, $\text{CH}_2(12)$), 1.43–1.45 (4H, m, $\text{CH}_2(11)$), 2.36–2.38 (4H, m, $\text{CH}_2(10)$), 2.68 (2H, t, J 7.1 Hz, $\text{CH}_2(9)$), 4.35 (2H, t, J 7.1 Hz, $\text{CH}_2(8)$), 6.07 (2H, s, $\text{CH}_2(13)$), 7.30 (1H, dd, J 7.7, 7.7 Hz, ArCH), 7.35 (1H, dd, J 7.7, 7.7 Hz, ArCH), 7.65 (2H, m, ArCH), 7.97 (1H, dd, J 7.6, 7.6 Hz, ArCH(17)), 8.51 (1H, d, J 7.6 Hz, ArCH(18)), 8.62 (1H, d, J 7.6 Hz, ArCH(16)), 8.82 (1H, s, ArCH(20))

^{13}C (75 MHz, $\text{D}_6\text{-DMSO}$) δ 24.12 ($\text{CH}_2(12)$), 26.01 ($\text{CH}_2(11)$), 41.82 ($\text{CH}_2(8)$), 50.67 ($\text{CH}_2(13)$), 54.54 ($\text{CH}_2(10)$), 56.32 ($\text{CH}_2(9)$), 110.97 (ArCH), 111.23 (ArCH), 123.26

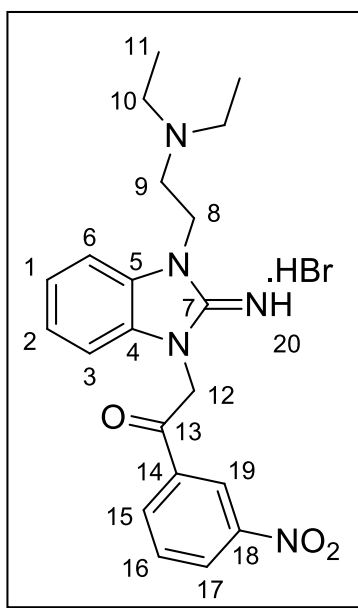
(ArCH(20)), 123.96 (ArCH), 123.98 (ArCH), 128.81 (ArCH(16)), 130.59 (ArC), 130.61 (ArC), 131.24 (ArCH(17)), 135.08 (ArCH(18)), 135.85 (ArC(19)), 148.48 (ArC(15)), 151.38 (C=NH(7)), 190.66 (C=O(14))

IR ν/cm^{-1} 1350 (NO₂, s), 1522 (NO₂, s), 1699 (C=O, s), 2940 (C-H, w), 3159 (Ar C-H, w)

MS (ESI): 408 [M+H⁺]

HRMS C₂₂H₂₆N₅O₃ [M+H-Br⁻]⁺ requires 408.2036, found 408.2040 (0.9 ppm error)

Preparation of 2-(3-(2-(Diethylamino)ethyl)-2-imino-2,3-dihydro-1*H*-benzo[*d*]imidazol-1-yl)-1-(3-nitrophenyl)ethanone hydrobromide (**LVTa82**):



Following method D using 1-(2-(Diethylamino)ethyl)-1*H*-benzo[*d*]imidazol-2-amine (**LVTa47**) (200 mg, 0.86 mmol, 1 eq.) and 2-bromo-3-nitroacetophenone (210 mg, 0.86 mmol 1 eq.) as starting materials. The yellow solid **LVTa82** (354 mg, 0.75 mmol, 87%) required no further purification.

Data for **LVTa82**

mp 206–209 °C

^1H (300 MHz, D_6 -DMSO) δ 0.83 (6H, t, J 6.5 Hz, $\text{CH}_3(11)$), 2.45–2.51 (4H, m, $\text{CH}_2(10)$), 2.76 (2H, t, J 6.8 Hz, $\text{CH}_2(9)$), 4.32 (2H, t, J 6.8 Hz, $\text{CH}_2(8)$), 6.10 (2H, s, $\text{CH}_2(12)$), 7.29 (1H, dd, J 7.5, 7.5 Hz, ArCH), 7.37 (1H, dd, J 7.5, 7.5 Hz, ArCH), 7.65 (2H, d, J 7.8 Hz, ArCH), 7.97 (1H, dd, J 8.0, 8.0 Hz, ArCH(16)), 8.52 (1H, d, J 8.0 Hz, ArCH(17)), 8.60 (1H, d, J 8.0 Hz, ArCH(15)), 8.82 (1H, s, ArCH(19))

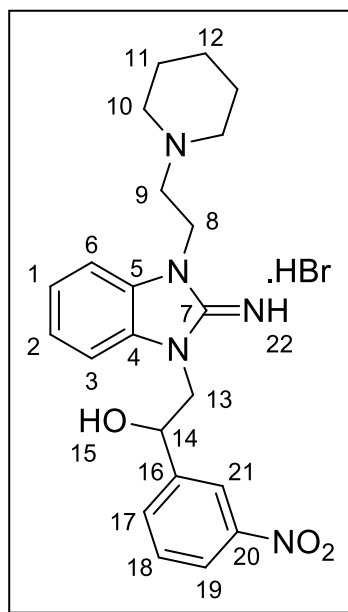
^{13}C (75 MHz, D_6 -DMSO) δ 11.63 ($\text{CH}_3(11)$), 41.98 ($\text{CH}_2(8)$), 46.34 ($\text{CH}_2(10)$), 50.19 ($\text{CH}_2(12)$), 110.44 (ArCH), 110.83 (ArCH), 122.76 (ArCH(19)), 123.41 (ArCH), 123.56 (ArCH), 128.31 (ArCH(15)), 129.91 (ArC), 130.04 (ArC), 130.72 (ArCH(16)), 134.61 (ArCH(17)), 135.29 (ArC(18)), 147.91 (ArC(14)), 150.68 ($\text{C}=\text{NH}(7)$), 190.13 ($\text{C}=\text{O}(13)$)

IR ν/cm^{-1} 1346 (NO_2 , s), 1525 (NO_2 , s), 1660 ($\text{C}=\text{O}$, s), 1703 ($\text{C}=\text{N}$, s), 2963 (C-H, w), 3207 (Ar C-H, w)

MS (ESI): 396 $[\text{M}+\text{H}^+]$

HRMS $\text{C}_{21}\text{H}_{26}\text{N}_5\text{O}_3$ $[\text{M}+\text{H}-\text{Br}^-]^+$ requires 396.2036, found 396.2047 (0.9 ppm error)

Preparation of 2-(2-Imino-3-(2-(piperidin-1-yl)ethyl)-2,3-dihydro-1*H*-benzo[*d*]imidazol-1-yl)-1-(3-nitrophenyl)ethanol hydrobromide (**LVTa83**):



Following method E using 2-(2-Imino-3-(2-(piperidin-1-yl)ethyl)-2,3-dihydro-1*H*-benzo[*d*]imidazol-1-yl)-1-(3-nitrophenyl)ethanone hydrobromide (**LVTa81**) (100 mg, 0.21 mmol, 1 eq.) as starting materials. The yellow solid **LVTa83** (92.0 mg, 0.19 mmol, 91%) required no purification.

Data for **LVTa83**

mp 80–83 °C

^1H (300 MHz, CDCl_3) δ 1.44–1.47 (2H, m, $\text{CH}_2(12)$), 1.59–1.66 (4H, m, $\text{CH}_2(11)$), 2.49–2.51 (4H, m, $\text{CH}_2(10)$), 2.60 (2H, t, J 6.7 Hz, $\text{CH}_2(9)$), 3.88 (2H, t, J 6.7 Hz, $\text{CH}_2(8)$), 4.16–4.30 (2H, m, $\text{CH}_2(13)$), 5.29 (1H, dd, J 4.4, 4.4 Hz, $\text{CH}(14)$), 6.60 (1H, d, J 7.3 Hz, ArCH), 6.85 (1H, d, J 8.6 Hz, ArCH), 6.89–7.00 (2H, m, ArCH), 7.47 (1H, dd, J 7.6, 7.6 Hz, ArCH(18)), 7.83 (1H, d, J 7.6 Hz, ArCH(19)), 8.06 (1H, d, J 7.6 Hz, ArCH(17)), 8.31 (1H, s, ArCH(21))

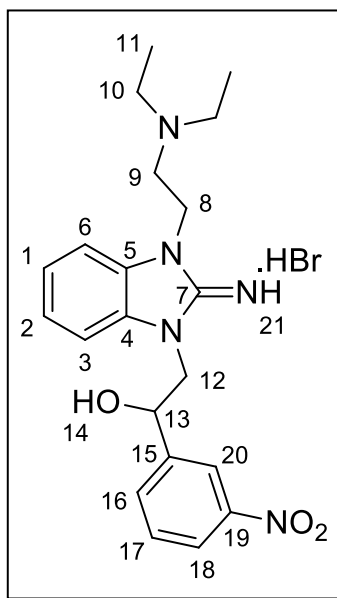
^{13}C (75 MHz, CDCl_3) δ 24.10 ($\text{CH}_2(12)$), 25.97 ($\text{CH}_2(11)$), 40.69 ($\text{CH}_2(8)$), 50.91 ($\text{CH}_2(13)$), 55.09 ($\text{CH}_2(10)$), 56.66 ($\text{CH}_2(9)$), 73.83 ($\text{CH}(14)$), 106.40 (ArCH), 106.92 (ArCH), 121.13 ($\text{ArCH}(21)$), 121.34 (2C, ArCH), 122.49 ($\text{ArCH}(17)$), 129.31 ($\text{ArCH}(18)$), 131.40 (2C, ArC), 132.19 ($\text{ArC}(19)$), 144.81 ($\text{ArC}(20)$), 148.22 ($\text{ArC}(16)$), 156.65 ($\text{C}=\text{NH}(7)$)

IR ν/cm^{-1} 1347 (NO_2 , s), 1494 (NO_2 , s), 1608 ($\text{C}-\text{O}$, s), 1622 ($\text{C}=\text{N}$, s), 2854 ($\text{C}-\text{H}$, w), 3061 ($\text{Ar C}-\text{H}$, w), 3357 ($\text{O}-\text{H}$, br.)

MS (ESI): 410 $[\text{M}+\text{H}^+]$

HRMS $\text{C}_{22}\text{H}_{28}\text{N}_5\text{O}_3$ $[\text{M}+\text{H}-\text{Br}^-]^+$ requires 410.2192, found 410.2199 (2.8 ppm error)

Preparation of 2-(3-(2-(Diethylamino)ethyl)-2-imino-2,3-dihydro-1*H*-benzo[*d*]imidazol-1-yl)-1-(3-nitrophenyl)ethanol hydrobromide (**LVTa84**):



Following method E using 2-(3-(2-(Diethylamino)ethyl)-2-imino-2,3-dihydro-1*H*-benzo[*d*]imidazol-1-yl)-1-(3-nitrophenyl)ethanone hydrobromide (**LVTa82**) (100 mg, 0.21

mmol, 1 eq.) as starting materials. The orange glass **LVTa84** (77.0 mg, 0.16 mmol, 76%) required no purification.

Data for LVTa84

^1H (300 MHz, CDCl_3) δ 1.03 (6H, t, J 7.1 Hz, $\text{CH}_3(12)$), 2.60 (4H, dq, J 7.1, 7.1 Hz, $\text{CH}_2(10)$), 2.70 (2H, t, J 6.6 Hz, $\text{CH}_2(9)$), 3.82 (2H, t, J 6.6 Hz, $\text{CH}_2(8)$), 4.15–4.29 (2H, m, $\text{CH}_2(12)$), 5.26–5.28 (1H, m, $\text{CH}(13)$), 6.60 (1H, d, J 7.2 Hz, ArCH), 6.84 (1H, d, J 7.2 Hz, ArCH), 6.89–7.00 (2H, m, ArCH), 7.47 (1H, dd, J 7.9, 7.9 Hz, ArCH(17)), 7.82 (1H, d, J 7.9 Hz, ArCH(18)), 8.06 (1H, d, J 7.9 Hz, ArCH(16)), 8.31 (1H, s, ArCH(20))

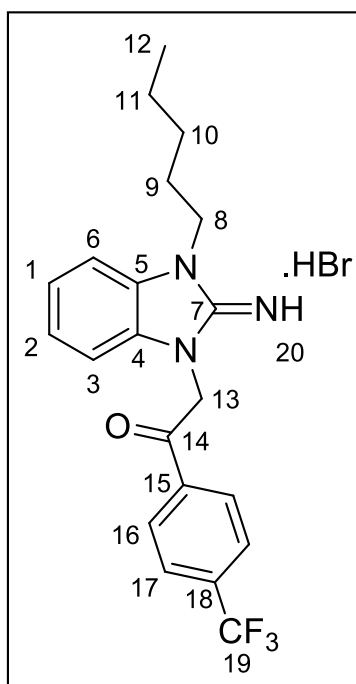
^{13}C (75 MHz, CDCl_3) δ 11.99 ($\text{CH}_2(11)$), 41.81 ($\text{CH}_2(8)$), 47.73 ($\text{CH}_2(10)$), 50.93 ($\text{CH}_2(9)$), 51.11 ($\text{CH}_2(12)$), 73.85 ($\text{CH}(13)$), 106.34 (ArCH), 106.87 (ArCH), 121.12 (ArCH(20)), 121.18 (2C, ArCH), 122.46 (ArCH(16)), 129.30 (ArCH(17)), 131.42 (2C, ArC), 132.17 (ArC(18)), 144.87 (ArC(19)), 148.22 (ArC(15)), 156.82 (C=NH(7))

IR ν/cm^{-1} 1346 (NO_2 , s), 1524 (NO_2 , s), 1608 (C-O, s), 1625 (C=N, s), 2810 (C-H, w), 3065 (Ar C-H, w), 3269 (O-H, br.)

MS (ESI): 398 $[\text{M}+\text{H}^+]$

HRMS $\text{C}_{21}\text{H}_{28}\text{N}_5\text{O}_3$ $[\text{M}+\text{H}-\text{Br}^-]^+$ requires 398.2187, found 398.2178 (2.2 ppm error)

Preparation of 2-(2-Imino-3-pentyl-2,3-dihydro-1*H*-benzo[*d*]imidazol-1-yl)-1-(4-(trifluoromethyl)phenyl)ethanone hydrobromide (**LVTa85**):



Following method D using 1-Pentyl-1*H*-benzo[*d*]imidazol-2-amine (**LVTa55**) (200 mg, 0.98 mmol, 1 eq.) and 4-(trifluoromethyl)phenacyl bromide (262 mg, 0.98 mmol 1 eq.) as starting materials. The colourless solid **LVTa85** (317 mg, 0.67 mmol, 68%) required no further purification.

Data for **LVTa85**

mp 238–241 °C

^1H (300 MHz, D_6 -DMSO) δ 0.88 (3H, t, J 6.9 Hz, CH_3 (12)), 1.32–1.35 (4H, m, CH_2 (10,11)), 1.73–1.75 (2H, m, CH_2 (9)), 4.25 (2H, t, J 6.5 Hz, CH_2 (8)), 6.04 (2H, s, CH_2 (13)), 7.30–7.38 (2H, m, ArCH(1,2)), 7.68 (2H, d, J 7.0 Hz, ArCH(3,6)), 8.06 (2H, d, J 7.6 Hz, ArCH(17)), 8.30 (2H, d, J 7.6 Hz, ArCH(16))

^{13}C (75 MHz, D_6 -DMSO) δ 13.85 (s, CH_3 (12)), 21.84 (s, CH_2 (11)), 27.17 (s, CH_2 (9)), 27.84 (s, CH_2 (10)), 42.61 (s, CH_2 (8)), 50.19 (s, CH_2 (13)), 110.50 (2C, s, ArCH), 123.57 (s,

ArCH), 123.68 (q, $^1J_{C-F}$ 273 Hz, ArCF₃(19)), 123.77 (s, ArCH), 125.84 (q, $^3J_{C-F}$ 4.8 Hz, ArCH(17)), 129.32 (s, ArCH(16)), 130.07 (2C, s, ArC), 132.88 (q, $^2J_{C-F}$ 31 Hz, ArC(18)), 137.20 (s, ArC(15)), 149.98 (s, C=NH(7)), 190.90 (s, C=O(14))

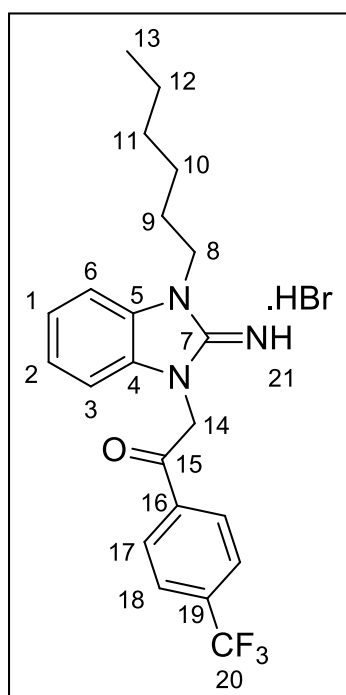
^{19}F (376 MHz, D₆-DMSO) δ -61.5 (s, ArCF₃(19))

IR ν/cm^{-1} 742 (C-F, s), 1661 (C=O, s), 1699 (C=N, s), 2855 (C-H, w), 3165 (Ar C-H, w)

MS (ESI): 390 [M+H⁺]

HRMS C₂₁H₂₃F₃N₃O [M+H-Br⁻]⁺ requires 390.1793, found 390.1814 (1.8 ppm error)

Preparation of 2-(3-Hexyl-2-imino-2,3-dihydro-1*H*-benzo[*d*]imidazol-1-yl)-1-(4-(trifluoromethyl)phenyl)ethanone hydrobromide (**LVTa86**):



Following method D using 1-Hexyl-1*H*-benzo[*d*]imidazol-2-amine (**LVTa56**) (200 mg, 0.92 mmol, 1 eq.) and 4-(trifluoromethyl)phenacyl bromide (246 mg, 0.92 mmol 1 eq.) as

starting materials. The colourless solid **LVTa86** (297 mg, 0.61 mmol, 66%) required no further purification.

Data for LVTa86

mp 237–239 °C

¹H (400 MHz, D₆-DMSO) δ 0.87 (3H, t, *J* 6.5 Hz, CH₃(13)), 0.97–1.37 (6H, m, CH₂(10,11,12)), 1.74 (2H, t, *J* 6.5 Hz, CH₂(9)), 4.22 (2H, t, *J* 6.5 Hz, CH₂(8)), 6.00 (2H, s, CH₂(13)), 7.31 (1H, dd, *J* 7.7, 7.7 Hz, ArCH), 7.37 (1H, dd, *J* 7.7, 7.7 Hz, ArCH), 7.66 (2H, d, *J* 7.3 Hz, ArCH), 8.06 (2H, d, *J* 8.3 Hz, ArCH(18)), 8.29 (2H, d, *J* 8.3 Hz, ArCH(17)), 8.82 (1H, br. s, NH(21))

¹³C (100 MHz, D₆-DMSO) δ 14.29 (s, CH₃(13)), 22.45 (s, CH₂(12)), 25.83 (s, CH₂(11)), 27.90 (s, CH₂(9)), 31.31 (s, CH₂(10)), 43.19 (s, CH₂(8)), 50.06 (s, CH₂(13)), 111.03 (s, ArCH), 111.09 (s, ArCH), 123.70 (q, ¹*J*_{C-F} 272 Hz, ArCF₃(20)), 124.12 (s, ArCH), 124.33 (s, ArCH), 126.30 (q, ³*J*_{C-F} 7.0 Hz, ArCH(18)), 129.81 (s, ArCH(17)), 129.90 (s, ArC), 130.59 (s, ArC), 133.88 (q, ²*J*_{C-F} 31 Hz, ArC(19)), 137.73 (s, ArC(16)), 150.55 (s, C=NH(7)), 191.36 (s, C=O(15))

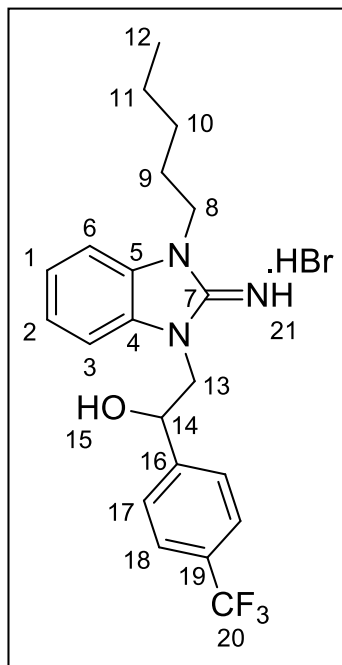
¹⁹F (376 MHz, D₆-DMSO) δ –61.6 (s, ArCF₃(20))

IR ν/ cm^{–1} 743 (C-F, s), 1665 (C=O, s), 1698 (C=N, s), 2930 (C-H, w), 3190 (Ar C-H, w)

MS (ESI): 404 [M+H⁺]

HRMS C₂₂H₂₅F₃N₃O [M+H-Br[–]]⁺ requires 404.1950, found 404.1958 (3.2 ppm error)

Preparation of 2-(2-Imino-3-pentyl-2,3-dihydro-1*H*-benzo[*d*]imidazol-1-yl)-1-(4-(trifluoromethyl)phenyl)ethanol hydrobromide (**LVTa87**):



Following method E using 2-(2-Imino-3-pentyl-2,3-dihydro-1*H*-benzo[*d*]imidazol-1-yl)-1-(4-(trifluoromethyl)phenyl)ethanone hydrobromide (**LVTa85**) (106 mg, 0.23 mmol, 1 eq.) as starting materials. The off-white solid **LVTa87** (68.0 mg, 0.15 mmol, 65%) required no purification.

Data for **LVTa87**

mp: 104–107 °C

^1H (400 MHz, $\text{D}_6\text{-DMSO}$) δ 0.85 (3H, t, J 6.8 Hz, CH_3 (12)), 1.23–1.33 (4H, m, CH_2 (10,11)), 1.54–1.61 (2H, m, CH_2 (9)), 3.80 (2H, t, J 7.0 Hz, CH_2 (8)), 3.98–4.10 (2H, m, CH_2 (13)), 5.09 (2H, t, J 6.1 Hz, CH (14)), 6.80–6.94 (4H, m, ArCH), 7.64 (4H, s, ArCH(17,18))

^{13}C (100 MHz, $\text{D}_6\text{-DMSO}$) δ 13.86 (s, CH_3 (12)), 21.90 (s, CH_2 (11)), 27.04 (s, CH_2 (9)), 28.26 (s, CH_2 (10)), 40.50 (s, CH_2 (8)), 49.28 (s, CH_2 (13)), 70.83 (s, CH (14)), 106.12 (s, ArCH), 106.70 (s, ArCH), 119.73 (s, ArCH), 119.89 (s, ArCH), 124.30 (q, $^1J_{\text{C-F}}$ 272 Hz,

ArCF₃(20)), 124.71 (q, ³J_{C-F} 3.7 Hz, ArCH(18)), 126.81 (s, ArCH(17)), 127.63 (q, ²J_{C-F} 31 Hz, ArC(19)), 131.26 (s, ArC), 131.76 (s, ArC), 147.83 (s, ArC(16)), 153.94 (s, C=NH(7))

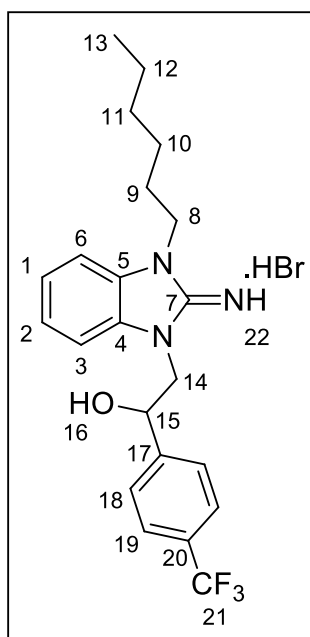
¹⁹F (376 MHz, D₆-DMSO) δ −60.8 (s, ArC-F₃(20))

IR ν/ cm^{−1} 728 (C-F, s), 1609 (C-O, s), 2862 (C-H, w), 3339 (Ar C-H, w), 3455 (O-H, br.)

MS (ESI): 392 [M+H⁺]

HRMS C₂₁H₂₅F₃N₃O [M+H-Br[−]]⁺ requires 392.1950, found 392.1968 (1.5 ppm error)

Preparation of 2-(3-Hexyl-2-imino-2,3-dihydro-1*H*-benzo[*d*]imidazol-1-yl)-1-(4-(trifluoromethyl)phenyl)ethanol hydrobromide (**LVTa88**):



Following method E using 2-(3-Hexyl-2-imino-2,3-dihydro-1*H*-benzo[*d*]imidazol-1-yl)-1-(4-(trifluoromethyl)phenyl)ethanone hydrobromide (**LVTa86**) (100 mg, 0.21 mmol, 1 eq.) as starting materials. The colourless solid **LVTa88** (69.0 mg, 0.14 mmol, 67%) required no purification.

Data for **LVTa88**

mp: 107–109 °C

^1H (400 MHz, D_6 -DMSO) δ 0.84 (3H, t, J 6.8 Hz, $\text{CH}_3(13)$), 1.23–1.30 (6H, m, $\text{CH}_2(10,11,12)$), 1.53–1.58 (2H, m, $\text{CH}_2(9)$), 3.79 (2H, t, J 7.1 Hz, $\text{CH}_2(8)$), 3.99–4.06 (2H, m, $\text{CH}_2(14)$), 5.08 (2H, t, J 6.5 Hz, $\text{CH}(15)$), 6.80–6.92 (4H, m, ArCH), 7.64 (4H, s, ArCH(18,19))

^{13}C (100 MHz, D_6 -DMSO) δ 13.85 (s, $\text{CH}_3(13)$), 22.01 (s, $\text{CH}_2(12)$), 25.74 (s, $\text{CH}_2(11)$), 27.29 (s, $\text{CH}_2(10)$), 30.98 (s, $\text{CH}_2(9)$), 40.49 (s, $\text{CH}_2(8)$), 49.28 (s, $\text{CH}_2(14)$), 70.87 (s, $\text{CH}(15)$), 106.06 (s, ArCH), 106.62 (s, ArCH), 119.67 (s, ArCH), 119.83 (s, ArCH), 124.32 (q, $^1J_{\text{C-F}}$ 272 Hz, $\text{ArCF}_3(21)$), 124.76 (q, $^3J_{\text{C-F}}$ 4.7 Hz, ArCH(19)), 126.81 (s, ArCH(18)), 127.40 (q, $^2J_{\text{C-F}}$ 32 Hz, ArC(20)), 131.26 (s, ArC), 131.79 (s, ArC), 147.87 (s, ArC(17)), 154.03 (s, C=NH(7))

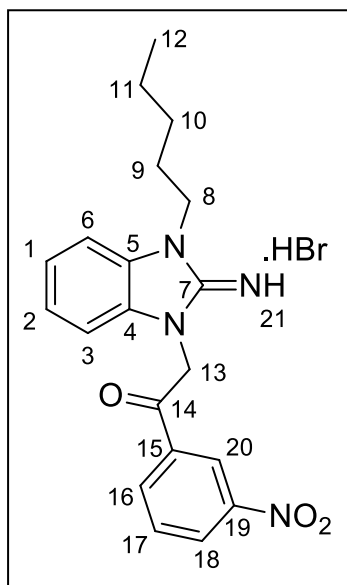
^{19}F (376 MHz, D_6 -DMSO) δ –60.8 (s, ArC- $\text{F}_3(21)$)

IR ν/cm^{-1} 728 (C-F, s), 1608 (C-O, s), 2859 (C-H, w), 2960 (Ar C-H, w), 3344 (O-H, br.)

MS (ESI): 406 $[\text{M}+\text{H}^+]$

HRMS $\text{C}_{22}\text{H}_{27}\text{F}_3\text{N}_3\text{O}$ $[\text{M}+\text{H}-\text{Br}^-]^+$ requires 406.2106, found 406.2115 (3.4 ppm error)

Preparation of 2-(2-Imino-3-pentyl-2,3-dihydro-1*H*-benzo[*d*]imidazol-1-yl)-1-(3-nitrophenyl)ethanone hydrobromide (**LVTa89**):



Following method D using 1-Pentyl-1*H*-benzo[*d*]imidazol-2-amine (**LVTa55**) (200 mg, 0.98 mmol, 1 eq.) and 2-bromo-3-nitro acetophenone (240 mg, 0.98 mmol 1 eq.) as starting materials. The colourless solid **LVTa89** (346 mg, 0.77 mmol, 79%) required no further purification.

Data for **LVTa89**

mp 240–242 °C

^1H (300 MHz, D_6 -DMSO) δ 0.88 (3H, t, J 6.8 Hz, CH_3 (12)), 1.33–1.36 (4H, m, CH_2 (10,11)), 1.70–1.76 (2H, m, CH_2 (9)), 4.25 (2H, t, J 7.1 Hz, CH_2 (8)), 6.11 (2H, m, CH_2 (13)), 7.29–7.40 (2H, s, ArCH), 7.68 (2H, d, J 7.6 Hz, ArCH), 7.97 (1H, dd, J 8.0, 8.0 Hz, ArCH(17)), 8.51 (1H, d, J 8.0 Hz, ArCH(18)), 8.61 (1H, d, J 8.0 Hz, ArCH(16)), 8.81 (1H, s, ArCH(20)), 8.95 (1H, br. s, NH(21))

^{13}C (75 MHz, D_6 -DMSO) δ 13.85 (CH_3 (12)), 21.84 (CH_2 (11)), 27.17 (CH_2 (9)), 27.84 (CH_2 (10)), 42.64 (CH_2 (8)), 50.25 (CH_2 (13)), 110.52 (ArCH), 122.76 (ArCH(20)), 123.57

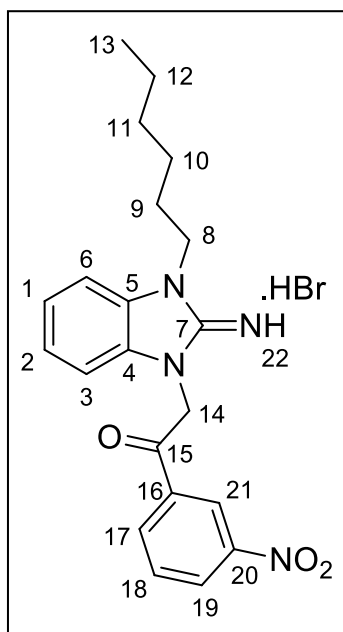
(ArCH), 123.79 (ArCH), 128.32 (ArCH(16)), 129.39 (ArC), 130.07 (ArC), 130.73 (ArCH(17)), 134.63 (ArCH(18)), 135.27 (ArC(19)), 147.90 (ArC(15)), 149.99 (C=NH(7)), 190.25 (C=O(14))

IR ν/cm^{-1} 1351 (NO₂, s), 1524 (NO₂, s), 1608 (C=O, s), 1698 (C=N, s), 2969 (C-H, w), 3162 (Ar C-H, w)

MS (ESI): 367 [M+H⁺]

HRMS C₂₀H₂₃N₄O₃ [M+H-Br⁻]⁺ requires 367.1770, found 367.1774 (0.9 ppm error)

Preparation of 2-(3-Hexyl-2-imino-2,3-dihydro-1*H*-benzo[*d*]imidazol-1-yl)-1-(3-nitrophenyl)ethanone hydrobromide (**LVTa90**):



Following method D using 1-Hexyl-1*H*-benzo[*d*]imidazol-2-amine (**LVTa56**) (200 mg, 0.92 mmol, 1 eq.) and 2-bromo-3-nitro acetophenone (225 mg, 0.92 mmol 1 eq.) as starting materials. The colourless solid **LVTa90** (331 mg, 0.72 mmol, 78%) required no further purification.

Data for LVTa90

mp 239–241 °C

^1H (400 MHz, D_6 -DMSO) δ 0.88 (3H, t, J 6.8 Hz, $\text{CH}_3(13)$), 1.30–1.34 (4H, m, $\text{CH}_2(11,12)$), 1.36–1.39 (2H, m, $\text{CH}_2(10)$), 1.72–1.76 (2H, m, $\text{CH}_2(9)$), 4.23 (2H, t, J 7.1 Hz, $\text{CH}_2(8)$), 6.07 (2H, s, $\text{CH}_2(13)$), 7.32 (1H, dd, J 7.4, 7.4 Hz, ArCH), 7.38 (1H, dd, J 7.4, 7.4 Hz, ArCH), 7.65 (2H, d, J 8.0 Hz, ArCH), 7.95 (1H, dd, J 8.0, 8.0 Hz, ArCH(18)), 8.50 (1H, d, J 8.0 Hz, ArCH(19)), 8.60 (1H, d, J 8.0 Hz, ArCH(17)), 8.82 (1H, s, ArCH(21)), 8.87 (1H, br. s, NH(22))

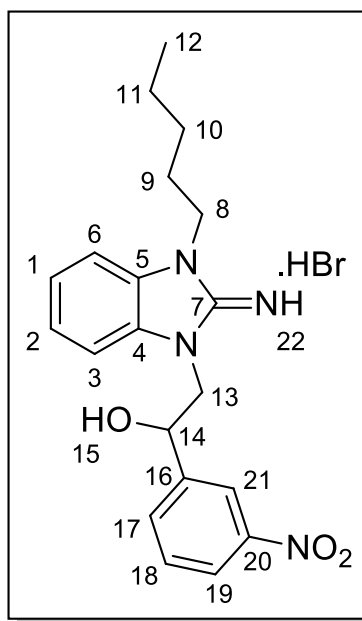
^{13}C (75 MHz, D_6 -DMSO) δ 12.58 ($\text{CH}_3(13)$), 20.90 ($\text{CH}_2(12)$), 24.33 ($\text{CH}_2(11)$), 26.35 ($\text{CH}_2(9)$), 29.77 ($\text{CH}_2(10)$), 41.73 ($\text{CH}_2(8)$), 49.14 ($\text{CH}_2(14)$), 109.41 (ArCH), 109.51 (ArCH), 121.74 (ArCH(21)), 122.52 (ArCH), 122.75 (ArCH), 127.21 (ArCH(17)), 128.39 (ArC), 129.07 (ArC), 129.56 (ArCH(18)), 133.43 (ArC(20)), 134.30 (ArCH(19)), 146.98 (ArC(16)), 149.03 (C=NH(7)), 189.09 (C=O(15))

IR ν/cm^{-1} 1353 (NO_2 , s), 1524 (NO_2 , s), 1664 (C=O, s), 1693 (C=N, s), 2861 (C-H, w), 3160 (Ar C-H, w)

MS (ESI): 381 $[\text{M}+\text{H}^+]$

HRMS $\text{C}_{21}\text{H}_{25}\text{N}_4\text{O}_3$ $[\text{M}+\text{H}-\text{Br}^-]^+$ requires 381.1927, found 381.1942 (1.3 ppm error)

Preparation of 2-(2-Imino-3-pentyl-2,3-dihydro-1*H*-benzo[*d*]imidazol-1-yl)-1-(3-nitrophenyl)ethanol hydrobromide (**LVTa91**):



Following method E using 2-(2-Imino-3-pentyl-2,3-dihydro-1*H*-benzo[*d*]imidazol-1-yl)-1-(3-nitrophenyl)ethanone hydrobromide (**LVTa89**) (100 mg, 0.22 mmol, 1 eq.) as starting materials. The dark orange glass **LVTa91** (63.0 mg, 0.14 mmol, 64%) required no purification.

Data for **LVTa91**

^1H (300 MHz, $\text{D}_6\text{-DMSO}$) δ 0.84 (3H, t, J 6.9 Hz, $\text{CH}_3(12)$), 1.18–1.33 (4H, m, $\text{CH}_2(10,11)$), 1.49–1.59 (2H, m, $\text{CH}_2(9)$), 3.79 (2H, t, J 7.0 Hz, $\text{CH}_2(8)$), 4.01–4.19 (2H, m, $\text{CH}_2(13)$), 5.15 (1H, dd, J 6.0 Hz, $\text{CH}(14)$), 6.81–6.93 (4H, m, ArCH), 7.56 (1H, dd, J 7.9, 7.9 Hz, ArCH(18)), 7.87 (1H, d, J 7.9 Hz, ArCH(19)), 8.05 (1H, d, J 7.9 Hz, ArCH(17)), 8.25 (1H, s, ArCH(21))

^{13}C (75 MHz, CDCl_3) δ 13.96 ($\text{CH}_3(12)$), 22.41 ($\text{CH}_2(11)$), 27.65 ($\text{CH}_2(9)$), 29.09 ($\text{CH}_2(10)$), 41.92 ($\text{CH}_2(8)$), 50.94 ($\text{CH}_2(13)$), 74.05 ($\text{CH}(14)$), 106.20 (ArCH), 106.91 (ArCH), 120.99 (ArCH(21)), 121.10 (2C, ArCH), 122.47 (ArCH(17)), 129.28 (ArCH(18)),

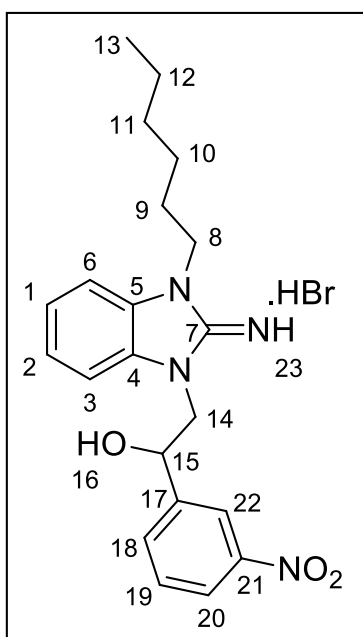
131.40 (ArC), 131.42 (ArC), 132.11 (ArCH(19)), 132.11 (ArCH(19)), 144.92 (ArC(20)),
148.24 (ArC(16)), 156.68 (C=NH(7))

IR ν/cm^{-1} 1346 (NO₂, s), 1525 (NO₂, s), 1605 (C-O, s), 2860 (C-H, w), 3068 (Ar C-H, w),
3372 (O-H, br.)

MS (ESI): 369 [M+H⁺]

HRMS C₂₀H₂₅N₄O₃ [M+H-Br⁻]⁺ requires 369.1927, found 369.1931 (2.7 ppm error)

Preparation of 2-(3-Hexyl-2-imino-2,3-dihydro-1*H*-benzo[*d*]imidazol-1-yl)-1-(3-nitrophenyl)ethanol hydrobromide (**LVTa92**):



Following method E using 2-(3-Hexyl-2-imino-2,3-dihydro-1*H*-benzo[*d*]imidazol-1-yl)-1-(3-nitrophenyl)ethanone hydrobromide (**LVTa90**) (100 mg, 0.22 mmol, 1 eq.) as starting materials. The orange glass **LVTa92** (66.0 mg, 0.14 mmol, 64%) required no purification.

Data for **LVTa92**

^1H (300 MHz, CDCl_3) δ 0.89 (3H, t, J 7.0 Hz, CH_3 (13)), 1.25–1.40 (6H, m, CH_2 (10,11,12)), 1.67–1.74 (2H, m, CH_2 (9)), 3.74 (2H, t, J 7.1 Hz, CH_2 (8)), 4.13–4.28 (2H, m, CH_2 (14)), 5.26–5.28 (1H, m, CH (15)), 6.62 (1H, d, J 7.5 Hz, ArCH), 6.92 (1H, d, J 7.5 Hz, ArCH), 6.92–6.99 (2H, m, ArCH), 7.47 (1H, dd, J 7.5, 7.5 Hz, ArCH(19)), 7.76 (1H, d, J 7.5 Hz, ArCH(20)), 8.07 (1H, d, J 7.5 Hz, ArCH(18)), 8.32 (1H, s, ArCH(22))

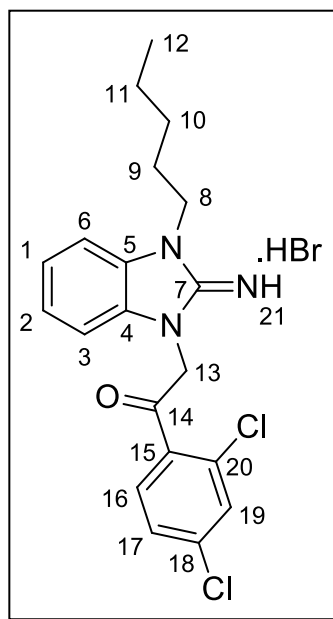
^{13}C (75 MHz, CDCl_3) δ 10.04 (CH_3 (13)), 22.51 (CH_2 (12)), 26.65 (CH_2 (11)), 27.88 (CH_2 (9)), 31.44 (CH_2 (10)), 41.90 (CH_2 (8)), 50.91 (CH_2 (14)), 74.02 (CH (15)), 106.16 (ArCH), 106.86 (ArCH), 120.95 (ArCH(22)), 121.07 (2C, ArCH), 122.45 (ArCH(18)), 129.25 (ArCH(19)), 131.36 (ArC), 131.39 (ArC), 132.07 (ArCH(20)), 144.90 (ArC(21)), 148.21 (ArC(17)), 156.67 ($\text{C}=\text{NH}$ (7))

IR ν/cm^{-1} 1342 (NO_2 , s), 1526 (NO_2 , s), 1606 (C-O, s), 2857 (C-H, w) 3065 (Ar C-H, w), 3370 (O-H, br.)

MS (ESI): 383 [$\text{M}+\text{H}^+$]

HRMS $\text{C}_{21}\text{H}_{27}\text{N}_4\text{O}_3$ [$\text{M}+\text{H}-\text{Br}^-$] $^+$ requires 383.2083, found 383.2081 (1.0 ppm error)

Preparation of 1-(2,4-Dichlorophenyl)-2-(2-imino-3-pentyl-2,3-dihydro-1*H*-benzo[*d*]imidazol-1-yl)ethanone hydrobromide (**LVTa93**):



Following method D using 1-Pentyl-1*H*-benzo[*d*]imidazol-2-amine (**LVTa55**) (200 mg, 0.98 mmol, 1 eq.) and 2-bromo-2,4-dichloro acetophenone (263 mg, 0.98 mmol 1 eq.) as starting materials. The colourless solid **LVTa93** (339 mg, 0.72 mmol, 74%) required no further purification.

Data for **LVTa93**

mp 225–227 °C

^1H (300 MHz, $\text{D}_6\text{-DMSO}$) δ 0.87 (3H, t, J 6.9 Hz, CH_3 (12)), 1.31–1.35 (4H, m, CH_2 (10,11)), 1.70–1.75 (2H, m, CH_2 (9)), 4.26 (2H, t, J 7.1 Hz, CH_2 (8)), 5.93 (2H, s, CH_2 (13)), 7.30–7.40 (2H, m, ArCH(1,2)), 7.62–7.69 (2H, m, ArCH), 7.76 (1H, d, J 8.5 Hz, ArCH(17)), 7.89 (1H, s, ArCH(19)), 8.27 (1H, d, J 8.5 Hz, ArCH(16)), 9.06 (1H, s, NH(21))

^{13}C (75 MHz, $\text{D}_6\text{-DMSO}$) δ 13.84 (CH_3 (12)), 21.84 (CH_2 (11)), 27.18 (CH_2 (9)), 27.81 (CH_2 (10)), 42.65 (CH_2 (8)), 51.79 (CH_2 (13)), 110.52 (2C, ArCH), 123.60 (ArCH), 123.79 (ArCH), 127.59 (ArCH(16)), 129.40 (ArC), 129.93 (ArC), 130.80 (ArCH(19)), 132.24

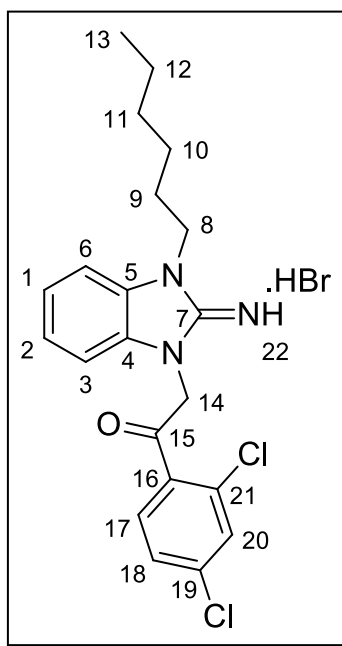
(ArC(20)), 132.44 (ArCH(17)), 132.98 (ArC(18)), 137.91 (ArC(15)), 150.02 (C=NH(7)), 191.04 (ArC(14))

IR ν/cm^{-1} 743 (C-Cl, s), 1663 (C=O, s), 1698 (C=N, s), 2898 (C-H, w), 3102 (Ar C-H, w)

MS (ESI): 389/391/393 [M+H⁺]

HRMS C₂₀H₂₂³⁵Cl₂N₃O [M+H-Br⁻]⁺ requires 390.1140, found 390.1145 (2.8 ppm error)

Preparation of 1-(2,4-Dichlorophenyl)-2-(3-hexyl-2-imino-2,3-dihydro-1*H*-benzo[*d*]imidazol-1-yl)ethanone hydrobromide (**LVTa94**):



Following method D using 1-Hexyl-1*H*-benzo[*d*]imidazol-2-amine (**LVTa56**) (292 mg, 1.34 mmol, 1 eq.) and 2-bromo-2,4-dichloro acetophenone (359 mg, 1.34 mmol 1 eq.) as starting materials. The colourless solid **LVTa94** (456 mg, 0.94 mmol, 70%) required no further purification.

Data for **LVTa94**

mp 238–241 °C

^1H (300 MHz, D_6 -DMSO) δ 0.88 (3H, t, J 6.9 Hz, CH_3 (13)), 1.30–1.36 (4H, m, CH_2 (11,12)), 1.37–1.39 (2H, m, CH_2 (10)), 1.72–1.77 (2H, m, CH_2 (9)), 4.22 (2H, t, J 7.1 Hz, CH_2 (8)), 5.85 (2H, s, CH_2 (14)), 7.30–7.57 (2H, m, ArCH(1,2)), 7.59–7.61 (2H, m, ArCH), 7.79 (1H, d, J 8.5 Hz, ArCH(17)), 7.82 (1H, s, ArCH(20)), 8.19 (1H, d, J 8.5 Hz, ArCH(18)), 8.90 (1H, s, NH(22))

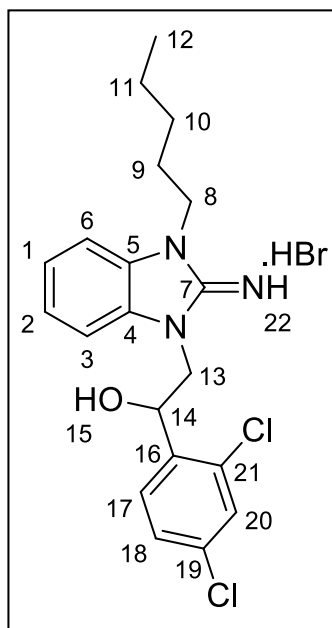
^{13}C (75 MHz, D_6 -DMSO) δ 12.55 (CH_3 (13)), 21.02 (CH_2 (12)), 24.47 (CH_2 (11)), 26.44 (CH_2 (9)), 29.89 (CH_2 (10)), 41.88 (CH_2 (8)), 50.79 (CH_2 (14)), 109.47 (2C, ArCH), 122.66 (ArCH), 122.86 (ArCH), 126.55 (ArCH(17)), 128.54 (2C, ArC), 129.06 (ArC(21)), 129.91 (ArCH(21)), 131.34 (ArCH(18)), 132.23 (ArC(19)), 137.28 (ArC(16)), 149.23 (C=NH(7)), 189.92 (ArC(15))

IR ν/cm^{-1} 747 (C-Cl, s), 1698 (C=O, s), 1701 (C=N, s), 2855 (C-H, w), 3162 (Ar C-H, w)

MS (ESI): 403/405/407 $[\text{M}+\text{H}^+]$

HRMS $\text{C}_{21}\text{H}_{24}^{35}\text{Cl}_2\text{N}_3\text{O}$ $[\text{M}+\text{H}-\text{Br}^-]^+$ requires 404.1296, found 404.1303 (3.0 ppm error)

Preparation of 1-(2,4-Dichlorophenyl)-2-(2-imino-3-pentyl-2,3-dihydro-1*H*-benzo[*d*]imidazol-1-yl)ethanol hydrobromide (**LVTa95**):



Following method E using 1-(2,4-Dichlorophenyl)-2-(2-imino-3-pentyl-2,3-dihydro-1*H*-benzo[*d*]imidazol-1-yl)ethanone hydrobromide (**LVTa93**) (100 mg, 0.21 mmol, 1 eq.) as starting materials. The colourless solid **LVTa95** (67.0 mg, 0.14 mmol, 67%) required no purification.

Data for **LVTa95**

mp 145–148 °C

^1H (400 MHz, D_6 -DMSO) δ 0.85 (3H, t, J 7.1 Hz, CH_3 (12)), 1.20–1.32 (4H, m, CH_2 (10,11)), 1.52–1.60 (2H, m, CH_2 (9)), 3.80 (2H, t, J 7.1 Hz, CH_2 (8)), 4.00–4.18 (2H, m, CH_2 (13)), 5.24 (1H, t, J 6.0 Hz, CH (14)), 6.75 (1H, d, J 7.0 Hz, ArCH), 6.76–6.93 (2H, m, ArCH), 6.94 (1H, d, J 7.0 Hz, ArCH), 7.40 (1H, d, J 7.9 Hz, ArCH(17)), 7.52 (1H, s, ArCH(20)), 7.65 (1H, d, J 7.9 Hz, ArCH(18))

^{13}C (100 MHz, D_6 -DMSO) δ 14.38 (CH_3 (12)), 22.41 (CH_2 (11)), 27.54 (CH_2 (9)), 28.78 (CH_2 (10)), 41.12 (CH_2 (8)), 48.35 (CH_2 (13)), 68.84 (CH (14)), 106.74 (ArCH), 106.83

(ArCH), 120.40 (ArCH), 120.58 (ArCH), 127.84 (ArCH(17)), 128.71 (ArCH(20)), 130.29 (ArCH(18)), 131.85 (ArC), 132.11 (ArC), 132.23 (ArC(21)), 132.93 (ArC(19)), 139.81 (ArC(16)), 154.77 (C=NH(7))

IR ν/cm^{-1} 730 (C-Cl, s), 1621 (C-O, s), 2679 (C-H, w), 2929 (Ar C-H, w), 3357 (O-H, br.)

MS (ESI): 391/393/395 $[\text{M}+\text{H}^+]$

HRMS $\text{C}_{20}\text{H}_{24}^{35}\text{Cl}_2\text{N}_3\text{O}$ $[\text{M}+\text{H}-\text{Br}^-]^+$ requires 392.1296, found 392.1301 (2.8 ppm error)

LVTa95_1 ^1H NMR (400 MHz, CDCl_3) δ 0.91 (3H, t, J 6.8 Hz, CH_3 (12)), 1.34–1.39 (4H, m, CH_2 (10,11)), 1.68–1.75 (2H, m, CH_2 (9)), 3.73 (2H, t, J 7.1 Hz, CH_2 (8)), 4.18 (2H, dd, J 15.1, 5.6 Hz, CH_2 (13)), 5.42 (1H, d, J 5.6 Hz, CH(14)), 6.80–6.83 (2H, m, ArCH), 6.94–6.99 (2H, m, ArCH), 7.19 (1H, d, J 8.4 Hz, ArCH(17)), 7.33 (1H, s, ArCH(20)), 7.69 (1H, d, J 8.4 Hz, ArCH(18))

$[\alpha]_{\text{D}}^{25} +32.0$ (c 1.0, MeOH)

LVTa95_2 ^1H NMR (400 MHz, CDCl_3) δ 0.91 (3H, t, J 6.8 Hz, CH_3 (12)), 1.34–1.37 (4H, m, CH_2 (10,11)), 1.68–1.75 (2H, m, CH_2 (9)), 3.72 (2H, t, J 7.2 Hz, CH_2 (8)), 4.18 (2H, dd, J 14.1, 5.5 Hz, CH_2 (13)), 5.42 (1H, d, J 5.5 Hz, CH(14)), 6.79–6.83 (2H, m, ArCH), 6.93–6.99 (2H, m, ArCH), 7.19 (1H, d, J 8.3 Hz, ArCH(17)), 7.33 (1H, s, ArCH(20)), 7.69 (1H, d, J 8.3 Hz, ArCH(18))

$[\alpha]_{\text{D}}^{25} -32.0$ (c 1.0, MeOH)

Asymmetric Noyori transfer hydrogenation of **LVTa93**: Preparation of enantio-enriched **LVTa95**:

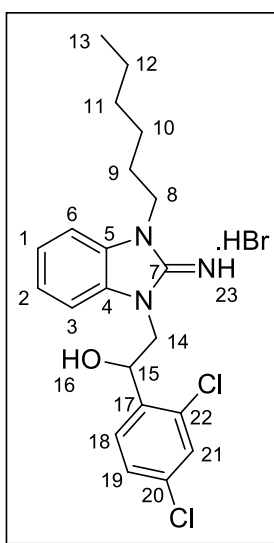
A stock solution of the Noyori catalyst was first prepared. An oven-dried 25 mL round bottom flask was charged with 2-Propanol (1 mL) and triethylamine (0.2 mL) under a nitrogen atmosphere and the solution was sparged with a balloon of nitrogen. RuCl(*p*-cymene)[(S,S)-Ts-DPEN] (100 mg, 0.16 mmol) was added *via* temporary removal of the septum. The orange mixture was then stirred at 80 °C for 1 hour under inert conditions until the solution turned dark red. The volatiles were removed and a 0.08 M stock solution in dry DMF (2 mL) was prepared. An oven-dried 25 mL round bottom flask was charged with **LVTa93** (32 mg, 0.07 mmol, 1 eq.) and dry DMF (2 mL). A solution of formic acid/triethylamine (5:2, 0.2 mL) was added *via* needle and syringe and finally, the stock solution of (S,S)-Noyori catalyst (32 µL) was added. The reaction was stirred at 40 °C overnight. The orange mixture was transferred into a separating funnel and EtOAc (50 mL) and H₂O (100 mL) were added. The organics were washed with saturated aqueous brine (15 mL), dried over MgSO₄ and filtered. The solvent was removed under reduced pressure to reveal a colourless solid amongst brown impurities. Cold EtOAc (10 mL) was added to the round bottom flask and the insoluble colourless solid **LVTa95_NS** (21 mg, 0.04 mmol, 63%) was collected *via* Büchner filtration using a sinter.

LVTa95_NS ¹H NMR (400 MHz, D₆-DMSO) δ 0.87 (3H, t, *J* 6.7 Hz, CH₃(12)), 1.30–1.34 (4H, m, CH₂(10,11)), 1.64–1.69 (2H, m, CH₂(9)), 4.21 (2H, t, *J* 7.3 Hz, CH₂(8)), 4.35 (1H, dd, *J* 14.9, 4.5 Hz, CH₂(13_a)), 4.45 (1H, dd, *J* 14.9, 8.1 Hz, CH₂(13_b)), 5.28 (1H, dd, *J* 8.1, 4.5 Hz, CH(14)), 7.27–7.35 (3H, m, ArCH), 7.52 (1H, d, *J* 8.4 Hz, ArCH), 7.57–7.60 (2H, m, ArCH(20)), 7.84 (1H, d, *J* 8.4 Hz, ArCH(18))

The above synthesis was repeated using activated RuCl(*p*-cymene)[(*R,R*)-Ts-DPEN] and **LVTa93** (42 mg, 0.09 mmol) as starting materials to generate **LVTa95_NR** (22 mg, 0.05 mmol, 56%).

LVTa95_NR ^1H NMR (400 MHz, $\text{D}_6\text{-DMSO}$) δ 0.87 (3H, t, J 6.5 Hz, $\text{CH}_3(12)$), 1.31–1.34 (4H, m, $\text{CH}_2(10,11)$), 1.65–1.70 (2H, m, $\text{CH}_2(9)$), 4.21 (2H, t, J 7.5 Hz, $\text{CH}_2(8)$), 4.35 (1H, dd, J 14.9, 4.5 Hz, $\text{CH}_2(13_a)$), 4.45 (1H, dd, J 14.9, 8.2 Hz, $\text{CH}_2(13_b)$), 5.28 (1H, dd, J 8.2, 4.5 Hz, $\text{CH}(14)$), 7.27–7.35 (3H, m, ArCH), 7.52 (1H, d, J 8.2 Hz, ArCH), 7.57–7.60 (2H, m, ArCH(20)), 7.84 (1H, d, J 8.4 Hz, ArCH(18))

Preparation of 1-(2,4-Dichlorophenyl)-2-(3-hexyl-2-imino-2,3-dihydro-1*H*-benzo[*d*]imidazol-1-yl)ethanol hydrobromide (**LVTa96**):



Following method E using 1-(2,4-Dichlorophenyl)-2-(3-hexyl-2-imino-2,3-dihydro-1*H*-benzo[*d*]imidazol-1-yl)ethanone hydrobromide (**LVTa94**) (292 mg, 0.60 mmol, 1 eq.) as starting materials. The colourless solid **LVTa92** (221 mg, 0.45 mmol, 75%) required no purification.

Data for **LVTa96**

mp 116–118 °C

^1H (300 MHz, $\text{D}_6\text{-DMSO}$) δ 0.85 (3H, t, J 7.1 Hz, $\text{CH}_3(13)$), 1.22–1.30 (6H, m, $\text{CH}_2(10,11,12)$), 1.52–1.58 (2H, m, $\text{CH}_2(9)$), 3.79 (2H, t, J 6.8 Hz, $\text{CH}_2(8)$), 3.99–4.04 (2H, m, $\text{CH}_2(14)$), 5.24 (1H, t, J 6.6 Hz, $\text{CH}(15)$), 6.73–6.94 (4H, m, $\text{ArCH}(1,2,3,6)$), 7.40 (1H, d, J 7.5 Hz, $\text{ArCH}(18)$), 7.52 (1H, s, $\text{ArCH}(21)$), 7.65 (1H, d, J 7.5 Hz, $\text{ArCH}(19)$)

^{13}C (75 MHz, $\text{D}_6\text{-DMSO}$) δ 13.88 ($\text{CH}_3(13)$), 22.03 ($\text{CH}_2(12)$), 25.76 ($\text{CH}_2(11)$), 27.30 ($\text{CH}_2(9)$), 31.00 ($\text{CH}_2(10)$), 40.55 ($\text{CH}_2(8)$), 47.80 ($\text{CH}_2(14)$), 68.34 ($\text{CH}(15)$), 106.11 (ArCH), 106.24 (ArCH), 119.80 (ArCH), 119.97 (ArCH), 127.31 ($\text{ArCH}(18)$), 128.19 ($\text{ArCH}(21)$), 129.74 ($\text{ArCH}(19)$), 131.32 (ArC), 131.59 (ArC), 131.67 ($\text{ArC}(22)$), 132.39 ($\text{ArC}(20)$), 139.30 ($\text{ArC}(17)$), 154.28 ($\text{C=NH}(7)$)

IR ν/cm^{-1} 731 (C-Cl, s), 1622 (C-O, s), 2858 (C-H, w), 3002 (Ar C-H, w), 3338 (O-H, br.)

MS (ESI): 405/407/409 [$\text{M}+\text{H}^+$]

HRMS $\text{C}_{21}\text{H}_{26}^{35}\text{Cl}_2\text{N}_3\text{O}$ [$\text{M}+\text{H}-\text{Br}^-$] $^+$ requires 406.1453, found 406.1458 (2.9 ppm error)

LVTa96_1 ^1H NMR (400 MHz, CDCl_3) δ 0.89 (3H, t, J 6.8 Hz, $\text{CH}_3(13)$), 1.29–1.39 (4H, m, $\text{CH}_2(10,11,12)$), 1.69–1.73 (2H, m, $\text{CH}_2(9)$), 3.73 (2H, t, J 7.3 Hz, $\text{CH}_2(8)$), 4.19 (2H, dd, J 14.8, 5.6 Hz, $\text{CH}_2(14)$), 5.42 (1H, d, J 5.6 Hz, $\text{CH}(15)$), 6.80–6.83 (2H, m, ArCH), 6.93–6.99 (2H, m, ArCH), 7.19 (1H, d, J 9.3 Hz, $\text{ArCH}(18)$), 7.34 (1H, s, $\text{ArCH}(21)$), 7.68 (1H, d, J 9.3 Hz, $\text{ArCH}(19)$)

$[\alpha]_{\text{D}}^{25}$ +42.0 (c 1.0, MeOH)

LVTa96_2 ^1H NMR (400 MHz, CDCl_3) δ 0.89 (3H, t, J 6.9 Hz, $\text{CH}_3(13)$), 1.30–1.39 (4H, m, $\text{CH}_2(10,11,12)$), 1.67–1.75 (2H, m, $\text{CH}_2(9)$), 3.72 (2H, t, J 7.2 Hz, $\text{CH}_2(8)$), 4.19 (2H, dd, J 14.9, 5.2 Hz, $\text{CH}_2(14)$), 5.42 (1H, d, J 5.2 Hz, $\text{CH}(15)$), 6.79–6.83 (2H, m, ArCH),

6.93–6.99 (2H, m, ArCH), 7.19 (1H, d, *J* 8.3 Hz, ArCH(18)), 7.34 (1H, s, ArCH(21)), 7.67 (1H, d, *J* 8.3 Hz, ArCH(19))

$[\alpha]_{\text{D}}^{25} -42.0$ (*c* 1.0, MeOH)

Asymmetric Noyori transfer hydrogenation of **LVTa94**: Preparation of enantio-enriched **LVTa96**:

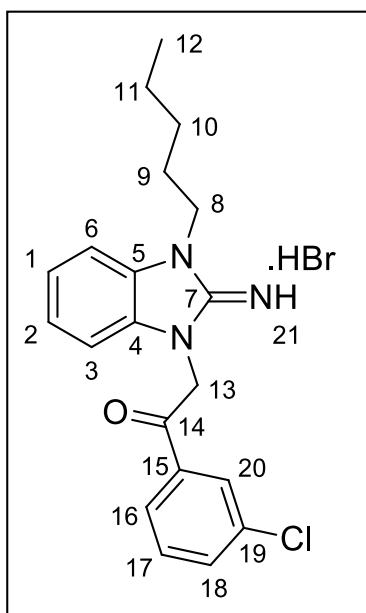
A stock solution of the Noyori catalyst was first prepared as shown in the preparation of enantio-enriched **LVTa95**. An oven-dried 25 mL round bottom flask was charged with **LVTa94** (46 mg, 0.09 mmol, 1 eq.) and dry DMF (2 mL). A solution of formic acid/triethylamine (5:2, 0.2 mL) was added *via* needle and syringe and finally, the stock solution of (*S,S*)-Noyori catalyst (32 μ L) was added. The reaction was stirred at 40 °C overnight. The mixture was transferred into a separating funnel and EtOAc (50 mL) and H₂O (100 mL) were added. The organics were washed with saturated aqueous brine (15 mL), dried over MgSO₄ and filtered. The solvent was removed under reduced pressure to reveal a colourless solid amongst brown impurities. Cold EtOAc (10 mL) was added to the round bottom flask and the insoluble colourless solid **LVTa96_NS** (20 mg, 0.04 mmol, 43%) was collected *via* Büchner filtration using a sinter.

LVTa96_NS ¹H NMR (400 MHz, CDCl₃) δ 0.86 (3H, t, *J* 6.7 Hz, CH₃(13)), 1.29–1.34 (4H, m, CH₂(11,12)), 1.47–1.52 (2H, m, CH₂(10)), 1.85–1.91 (2H, m, CH₂(9)), 4.46 (2H, t, *J* 7.1 Hz, CH₂(8)), 4.54 (1H, dd, *J* 15.2, 3.6 Hz, CH₂(14_a)), 4.68 (1H, dd, *J* 15.2, 3.6 Hz, CH₂(14_b)), 5.60 (1H, t, *J* 3.6 Hz, CH(15)), 6.73 (1H, d, *J* 7.9 Hz, ArCH), 7.09 (1H, dd, *J* 7.9, 7.2 Hz, ArCH), 7.16–7.25 (3H, m, ArCH), 7.32 (1H, s, ArCH), 7.77 (1H, d, *J* 8.4 Hz, ArCH)

The above synthesis was repeated using activated $\text{RuCl}(p\text{-cymene})[(R,R)\text{-Ts-DPEN}]$ and **LVTa94** (32 mg, 0.09 mmol) as starting materials to generate **LVTa96_NR** (19 mg, 0.04 mmol, 59%).

LVTa96_NR ^1H NMR (400 MHz, CDCl_3) δ 0.86 (3H, t, J 6.9 Hz, CH_3 (13)), 1.28–1.35 (4H, m, CH_2 (11,12)), 1.46–1.53 (2H, m, CH_2 (10)), 1.84–1.91 (2H, m, CH_2 (9)), 4.43 (2H, t, J 7.5 Hz, CH_2 (8)), 4.53 (1H, dd, J 15.2, 3.9 Hz, CH_2 (14_a)), 4.66 (1H, dd, J 15.2, 3.9 Hz, CH_2 (14_b)), 5.61 (1H, t, J 3.9 Hz, CH (15)), 6.73 (1H, d, J 8.1 Hz, ArCH), 7.09 (1H, dd, J 7.4, 7.4 Hz, ArCH), 7.16–7.25 (3H, m, ArCH), 7.32 (1H, s, ArCH), 7.74 (1H, d, J 8.5 Hz, ArCH)

Preparation of 1-(3-Chlorophenyl)-2-(2-imino-3-pentyl-2,3-dihydro-1*H*-benzo[*d*]imidazol-1-yl)ethanone hydrobromide (**LVTa97**):



Following method D using 1-Pentyl-1*H*-benzo[*d*]imidazol-2-amine (**LVTa55**) (200 mg, 0.98 mmol, 1 eq.) and 3-chloro phenacylbromide (229 mg, 0.98 mmol 1 eq.) as starting

materials. The colourless solid **LVTa97** (371 mg, 0.85 mmol, 87%) required no further purification.

Data for **LVTa97**

mp 239–241 °C

^1H (300 MHz, CDCl_3) δ 0.92 (3H, t, J 6.7 Hz, CH_3 (12)), 1.35–1.39 (4H, m, CH_2 (10,11)), 1.72–1.77 (2H, m, CH_2 (9)), 3.76 (2H, t, J 7.2 Hz, CH_2 (8)), 5.27 (2H, s, CH_2 (13)), 6.69 (1H, d, J 7.2 Hz, ArCH), 6.85 (1H, d, J 7.2 Hz, ArCH), 6.91–7.02 (2H, m, ArCH(1,2)), 7.44 (1H, dd, J 7.8, 7.8 Hz, ArCH(17)), 7.58 (1H, d, J 7.8 Hz, ArCH(18)), 7.97 (1H, d, J 7.8 Hz, ArCH(16)), 8.07 (1H, s, NH(20))

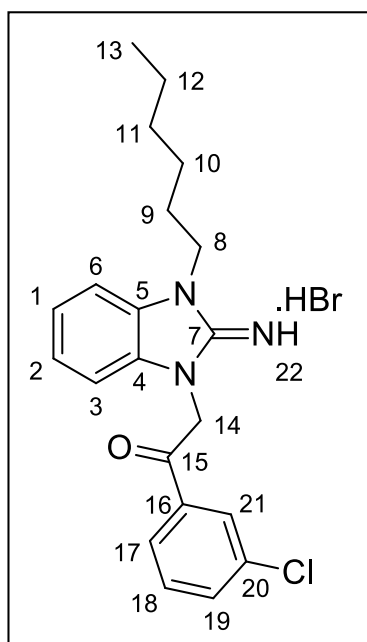
^{13}C (75 MHz, CDCl_3) δ 13.99 (CH_3 (12)), 22.47 (CH_2 (11)), 27.69 (CH_2 (9)), 29.13 (CH_2 (10)), 41.90 (CH_2 (8)), 48.13 (CH_2 (13)), 106.40 (ArCH), 106.52 (ArCH), 120.69 (ArCH), 120.84 (ArCH), 126.40 (ArCH(16)), 128.46 (ArCH(20)), 130.17 (ArCH(17)), 131.53 (ArC), 131.60 (ArC), 133.79 (ArCH(18)), 135.17 (ArC(19)), 136.21 (ArC(15)), 154.69 (C=NH(7)), 192.16 (ArC(14))

IR ν/cm^{-1} 743 (C-Cl, s), 1695 (C=O, s), 1697 (C=N, s), 2868 (C-H, w), 3162 (Ar C-H, w)

MS (ESI): 355/357 $[\text{M}+\text{H}^+]$

HRMS $\text{C}_{20}\text{H}_{23}^{35}\text{ClN}_3\text{O}$ $[\text{M}+\text{H}-\text{Br}^-]^+$ requires 356.1530, found 356.1529 (2.01 ppm error)

Preparation of 1-(3-Chlorophenyl)-2-(3-hexyl-2-imino-2,3-dihydro-1*H*-benzo[*d*]imidazol-1-yl)ethanone hydrobromide (**LVTa98**):



Following method D using 1-Hexyl-1*H*-benzo[*d*]imidazol-2-amine (**LVTa56**) (200 mg, 0.92 mmol, 1 eq.) and 3-chloro phenacylbromide (215 mg, 0.92 mmol 1 eq.) as starting materials. The colourless solid **LVTa98** (456 mg, 0.94 mmol, 70%) required no further purification.

Data for **LVTa98**

mp 243–245 °C

¹H (300 MHz, D₆-DMSO) δ 0.87 (3H, t, *J* 7.1 Hz, CH₃(13)), 1.27–1.38 (6H, m, CH₂(10,11,12)), 1.68–1.74 (2H, m, CH₂(9)), 4.24 (2H, t, *J* 6.9 Hz, CH₂(8)), 6.00 (2H, s, CH₂(14)), 7.31–7.38 (2H, m, ArCH), 7.65–7.72 (3H, m, ArCH(18)), 7.86 (1H, d, *J* 7.5 Hz, ArCH(19)), 8.04 (1H, d, *J* 7.5 Hz, ArCH(17)), 8.14 (1H, s, ArCH(21)), 8.89 (1H, s, NH(22))

¹³C (75 MHz, D₆-DMSO) δ 12.82 (CH₃(13)), 21.97 (CH₂(12)), 25.32 (CH₂(11)), 27.42 (CH₂(9)), 30.83 (CH₂(10)), 42.64 (CH₂(8)), 50.03 (CH₂(14)), 110.54 (2C, ArCH), 123.57 (ArCH), 123.75 (ArCH), 127.00 (ArCH(17)), 128.22 (ArCH(21)), 129.36 (ArC), 130.07

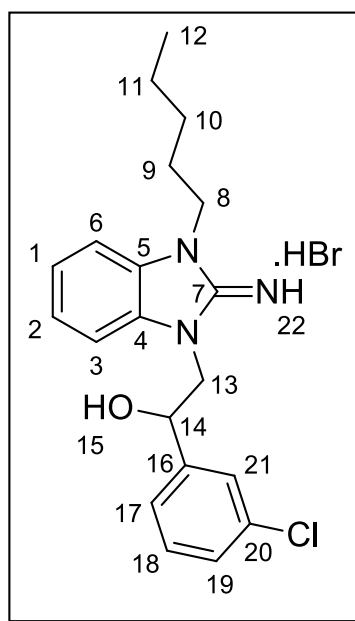
(ArC), 130.88 (ArCH(18)), 133.66 (ArC(20)), 135.83 (ArCH(19)), 149.98 (C=NH(7)), 190.44 (ArC(15))

IR ν/cm^{-1} 745 (C-Cl, s), 1663 (C=O, s), 1697 (C=N, s), 2866 (C-H, w), 3165 (Ar C-H, w)

MS (ESI): 370/372 [M+H⁺]

HRMS C₂₁H₂₅³⁵ClN₃O [M+H-Br⁻]⁺ requires 370.1686, found 370.1694 (3.6 ppm error)

Preparation of 1-(3-Chlorophenyl)-2-(2-imino-3-pentyl-2,3-dihydro-1*H*-benzo[*d*]imidazol-1-yl)ethanol hydrobromide (**LVTa99**):



Following method E using 1-(3-Chlorophenyl)-2-(2-imino-3-pentyl-2,3-dihydro-1*H*-benzo[*d*]imidazol-1-yl)ethanone hydrobromide (**LVTa97**) (100 mg, 0.23 mmol, 1 eq.) as starting materials. The clear glass **LVTa99** (89.0 mg, 0.20 mmol, 87%) required no purification.

Data for **LVTa99**

^1H (300 MHz, D_6 -DMSO) δ 0.86 (3H, t, J 6.9 Hz, $\text{CH}_3(12)$), 1.25–1.33 (4H, m, $\text{CH}_2(10,11)$), 1.54–1.60 (2H, m, $\text{CH}_2(9)$), 3.85 (2H, t, J 7.4 Hz, $\text{CH}_2(8)$), 4.00–4.07 (2H, m, $\text{CH}_2(13)$), 4.98 (1H, t, J 7.1 Hz, $\text{CH}(14)$), 6.85–7.00 (4H, m, ArCH), 7.29 (1H, dd, J 6.8, 6.8 Hz, ArCH(18)), 7.33 (1H, d, J 6.8 Hz, ArCH(19)), 7.39 (1H, d, J 6.8 Hz, ArCH(17)), 7.48 (1H, s, ArCH(21))

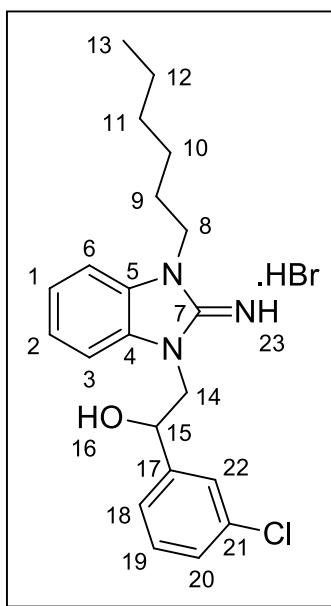
^{13}C (75 MHz, D_6 -DMSO) δ 14.36 ($\text{CH}_3(12)$), 22.41 ($\text{CH}_2(11)$), 27.57 ($\text{CH}_2(9)$), 28.73 ($\text{CH}_2(10)$), 41.34 ($\text{CH}_2(8)$), 49.81 ($\text{CH}_2(13)$), 71.00 ($\text{CH}(14)$), 107.19 (ArCH), 107.90 (ArCH), 120.77 (ArCH), 120.89 (ArCH), 125.28 (ArCH(19)), 126.49 (ArCH(21)), 126.57 (ArCH(17)), 127.51 (ArCH(18)), 131.68 (ArC), 132.27 (ArC), 133.27 (ArC(20)), 145.97 (ArC(16)), 153.94 ($\text{C}=\text{NH}(7)$)

IR ν/cm^{-1} 731 (C-Cl, s), 1606 (C-O, s), 1622 (C=N, s), 2858 (C-H, w), 3059 (Ar C-H, w), 3362 (O-H, br.)

MS (ESI): 357/359 [$\text{M}+\text{H}^+$]

HRMS $\text{C}_{20}\text{H}_{25}^{35}\text{ClN}_3\text{O}$ [$\text{M}+\text{H}-\text{Br}^-$] $^+$ requires 358.1686, found 358.1690 (0.2 ppm error)

Preparation of 1-(3-Chlorophenyl)-2-(3-hexyl-2-imino-2,3-dihydro-1*H*-benzo[*d*]imidazol-1-yl)ethanol hydrobromide (**LVTa100**):



Following method E using 1-(3-Chlorophenyl)-2-(3-hexyl-2-imino-2,3-dihydro-1*H*-benzo[*d*]imidazol-1-yl)ethanone hydrobromide (**LVTa98**) (100 mg, 0.22 mmol, 1 eq.) as starting materials. The orange glass **LVTa100** (85 mg, 0.19 mmol, 86%) required no purification.

Data for **LVTa100**

^1H (400 MHz, $\text{D}_6\text{-DMSO}$) δ 0.85 (3H, t, J 6.9 Hz, $\text{CH}_3(13)$), 1.25–1.32 (6H, m, $\text{CH}_2(10,11,12)$), 1.54–1.58 (2H, m, $\text{CH}_2(9)$), 3.79 (2H, t, J 6.8 Hz, $\text{CH}_2(8)$), 3.95–4.03 (2H, m, $\text{CH}_2(14)$), 4.98 (1H, t, J 7.1 Hz, $\text{CH}(15)$), 6.81–6.91 (4H, m, ArCH), 7.26 (1H, dd, J 7.0, 7.0 Hz, ArCH(19)), 7.35 (1H, d, J 7.0 Hz, ArCH(20)), 7.39 (1H, d, J 7.0 Hz, ArCH(18)), 7.46 (1H, s, ArCH(22))

^{13}C (100 MHz, $\text{D}_6\text{-DMSO}$) δ 14.37 ($\text{CH}_3(13)$), 22.52 ($\text{CH}_2(12)$), 26.27 ($\text{CH}_2(11)$), 27.81 ($\text{CH}_2(9)$), 31.50 ($\text{CH}_2(10)$), 41.06 ($\text{CH}_2(8)$), 49.82 ($\text{CH}_2(14)$), 71.32 ($\text{CH}(15)$), 106.54 (ArCH), 107.14 (ArCH), 120.21 (ArCH), 120.31 (ArCH), 125.20 (ArCH(20)), 126.41

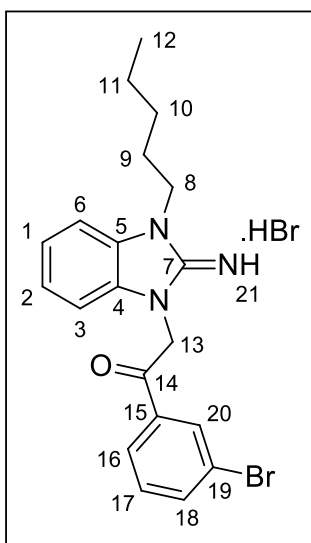
(ArCH(22)), 126.45 (ArCH(18)), 127.40 (ArCH(19)), 132.12 (ArC), 132.37 (ArC), 133.24 (ArC(21)), 146.25 (ArC(17)), 154.64 (C=NH(7))

IR ν/cm^{-1} 730 (C-Cl, s), 1606 (C-O, s), 1622 (C=N, s), 2856 (C-H, w), 3061 (Ar C-H, w), 3341 (O-H, br.)

MS (ESI): 371/373 $[\text{M}+\text{H}^+]$

HRMS $\text{C}_{21}\text{H}_{27}^{35}\text{ClN}_3\text{O}$ $[\text{M}+\text{H}-\text{Br}^-]^+$ requires 372.1843, found 372.1848 (0.13 ppm error)

Preparation of 1-(3-Bromophenyl)-2-(2-imino-3-pentyl-2,3-dihydro-1*H*-benzo[*d*]imidazol-1-yl)ethanone hydrobromide (**LVTa101**):



Following method D using 1-Pentyl-1*H*-benzo[*d*]imidazol-2-amine (**LVTa55**) (200 mg, 0.98 mmol, 1 eq.) and 3-bromo phenacylbromide (272 mg, 0.98 mmol 1 eq.) as starting materials. The colourless solid **LVTa101** (391 mg, 0.81 mmol, 83%) required no further purification.

Data for **LVTa101**

mp 240–243 °C

^1H (400 MHz, D_6 -DMSO) δ 0.89 (3H, t, J 7.1 Hz, $\text{CH}_3(12)$), 1.32–1.37 (4H, m, $\text{CH}_2(10,11)$), 1.72–1.77 (2H, m, $\text{CH}_2(9)$), 4.22 (2H, t, J 6.9 Hz, $\text{CH}_2(8)$), 5.97 (2H, s, $\text{CH}_2(13)$), 7.32 (1H, d, J 7.5 Hz, ArCH), 7.37 (1H, d, J 7.5 Hz, ArCH), 7.60 (1H, dd, J 8.0, 8.0 Hz, ArCH(17)), 7.96 (1H, d, J 8.0 Hz, ArCH(18)), 8.08 (1H, d, J 8.0 Hz, ArCH(16)), 8.28 (1H, s, ArCH(20)), 8.89 (1H, s, NH(21))

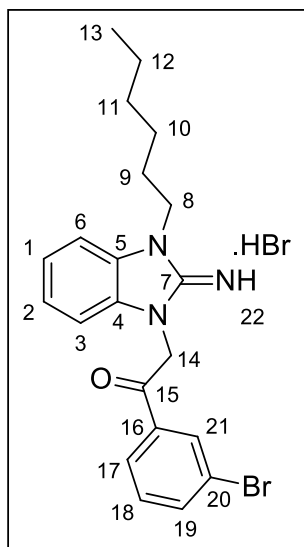
^{13}C (100 MHz, D_6 -DMSO) δ 12.56 ($\text{CH}_3(12)$), 20.86 ($\text{CH}_2(11)$), 26.16 ($\text{CH}_2(9)$), 26.93 ($\text{CH}_2(10)$), 41.81 ($\text{CH}_2(8)$), 49.00 ($\text{CH}_2(13)$), 109.38 (ArCH), 109.49 (ArCH), 121.15 (ArC(19)), 122.56 (ArCH), 122.76 (ArCH), 126.29 (ArCH(16)), 128.51 (ArCH(17)), 129.10 (ArC), 129.94 (ArC), 130.15 (ArCH(20)), 135.16 (ArCH(18)), 135.74 (ArC(15)), 149.20 (C=NH(7)), 189.33 (ArC(14))

IR ν/cm^{-1} 1690 (C=O, s), 1697 (C=N, s), 2952 (C-H, w), 3162 (Ar C-H, w)

MS (ESI): 399/401 $[\text{M}+\text{H}^+]$

HRMS $\text{C}_{20}\text{H}_{23}^{79}\text{BrN}_3\text{O}$ $[\text{M}+\text{H}-\text{Br}^-]^+$ requires 400.1024, found 400.1029 (0.9 ppm error)

Preparation of 1-(3-Bromophenyl)-2-(3-hexyl-2-imino-2,3-dihydro-1H-benzo[d]imidazol-1-yl)ethanone hydrobromide (**LVTa102**):



Following method D using 1-Hexyl-1H-benzo[d]imidazol-2-amine (**LVTa56**) (200 mg, 0.92 mmol, 1 eq.) and 3-bromo phenacylbromide (256 mg, 0.92 mmol 1 eq.) as starting materials. The colourless solid **LVTa102** (333 mg, 0.67 mmol, 73%) required no further purification.

Data for **LVTa102**

mp 242–245 °C

^1H (300 MHz, $\text{D}_6\text{-DMSO}$) δ 0.87 (3H, t, J 7.1 Hz, $\text{CH}_3(13)$), 1.27–1.35 (6H, m, $\text{CH}_2(10,11,12)$), 1.69–1.74 (2H, m, $\text{CH}_2(9)$), 4.25 (2H, t, J 7.0 Hz, $\text{CH}_2(8)$), 6.01 (2H, s, $\text{CH}_2(14)$), 7.30–7.39 (2H, m, ArCH), 7.65–7.68 (3H, m, ArCH(18)), 7.69 (1H, d, J 7.8 Hz, ArCH(19)), 8.06 (1H, d, J 7.8 Hz, ArCH(17)), 8.27 (1H, s, ArCH(21)), 8.90 (1H, s, NH(22))

^{13}C (75 MHz, $\text{D}_6\text{-DMSO}$) δ 13.82 ($\text{CH}_3(13)$), 21.97 ($\text{CH}_2(12)$), 25.31 ($\text{CH}_2(11)$), 27.42 ($\text{CH}_2(9)$), 30.83 ($\text{CH}_2(10)$), 42.65 ($\text{CH}_2(8)$), 50.03 ($\text{CH}_2(14)$), 110.55 (2C, ArCH(3,6)), 122.07 (ArC(20)), 123.57 (ArCH), 123.75 (ArCH), 127.33 (ArCH(16)), 129.36 (ArC),

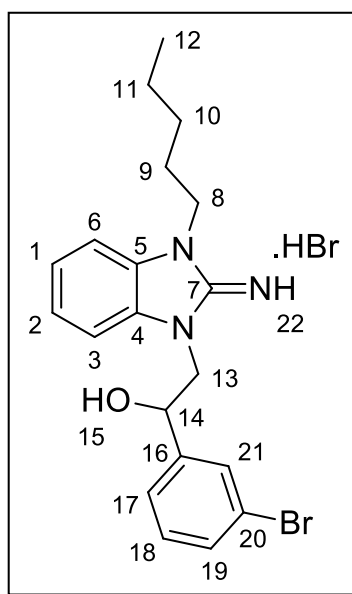
130.08 (ArC), 131.09 (ArCH(18,21)), 136.04 (ArC(16)), 136.75 (ArCH(19)), 149.98 (C=NH(7)), 190.40 (ArC(15))

IR ν/cm^{-1} 1662 (C=O, s), 1698 (C=N, s), 2957 (C-H, w), 3157 (Ar C-H, w)

MS (ESI): 413/415 $[\text{M}+\text{H}^+]$

HRMS $\text{C}_{21}\text{H}_{25}^{79}\text{BrN}_3\text{O}$ $[\text{M}+\text{H}-\text{Br}^-]^+$ requires 414.1181, found 414.1195 (2.4 ppm error)

Preparation of 1-(3-Bromophenyl)-2-(2-imino-3-pentyl-2,3-dihydro-1*H*-benzo[*d*]imidazol-1-yl)ethanol hydrobromide (**LVTa103**):



Following method E using 1-(3-Bromophenyl)-2-(2-imino-3-pentyl-2,3-dihydro-1*H*-benzo[*d*]imidazol-1-yl)ethanone hydrobromide (**LVTa101**) (100 mg, 0.21 mmol, 1 eq.) as starting materials. The clear glass **LVTa103** (84.0 mg, 0.17mmol, 81%) required no purification.

Data for **LVTa103**

^1H (300 MHz, CDCl_3) δ 0.91 (3H, t, J 6.8 Hz, $\text{CH}_3(12)$), 1.34–1.39 (4H, m, $\text{CH}_2(10,11)$), 1.70–1.75 (2H, m, $\text{CH}_2(9)$), 3.23 (2H, t, J 7.2 Hz, $\text{CH}_2(8)$), 4.12 (2H, d, J 4.5 Hz, $\text{CH}_2(13)$), 5.12 (1H, t, J 4.5 Hz, $\text{CH}(14)$), 6.68 (1H, d, J 6.7 Hz, ArCH), 6.83 (1H, d, J 6.7 Hz, ArCH), 6.92–7.00 (2H, m, ArCH), 7.17 (1H, dd, J 7.7, 7.7 Hz, ArCH(18)), 7.33–7.36 (1H, m, ArCH(17,19)), 7.63 (1H, s, ArCH(21))

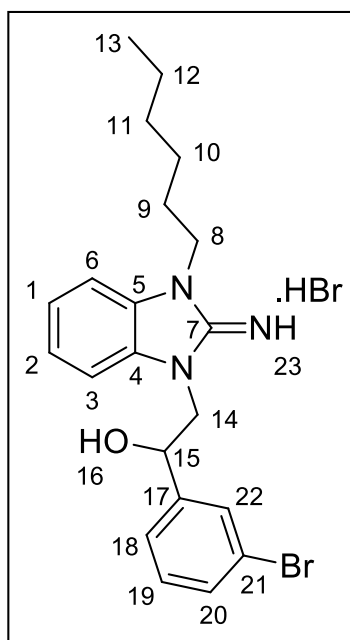
^{13}C (75 MHz, CDCl_3) δ 13.99 ($\text{CH}_3(12)$), 22.45 ($\text{CH}_2(11)$), 27.70 ($\text{CH}_2(9)$), 29.11 ($\text{CH}_2(10)$), 41.86 ($\text{CH}_2(8)$), 51.25 ($\text{CH}_2(13)$), 74.37 ($\text{CH}(14)$), 106.35 (ArCH), 106.74 (ArCH), 120.78 (ArCH), 120.99 (ArCH), 122.59 (ArC(20)), 125.52 (ArCH(17)), 129.10 (ArCH(21)), 129.95 (ArCH(19)), 130.51 (ArCH(18)), 131.46 (ArC), 131.50 (ArC), 144.94 (ArC(16)), 156.71 ($\text{C}=\text{NH}(7)$)

IR ν/cm^{-1} 1606 (C-O, s), 1622 (C=N, s), 2859 (C-H, w), 3060 (Ar C-H, w), 3322 (O-H, br.)

MS (ESI): 401/403 $[\text{M}+\text{H}^+]$

HRMS $\text{C}_{20}\text{H}_{25}^{79}\text{BrN}_3\text{O}$ $[\text{M}+\text{H}-\text{Br}^-]^+$ requires 402.1181, found 402.1192 (4.3 ppm error)

Preparation of 1-(3-Bromophenyl)-2-(3-hexyl-2-imino-2,3-dihydro-1*H*-benzo[*d*]imidazol-1-yl)ethanol hydrobromide (**LVTa104**):



Following method E using 1-(3-Bromophenyl)-2-(3-hexyl-2-imino-2,3-dihydro-1*H*-benzo[*d*]imidazol-1-yl)ethanone hydrobromide (**LVTa102**) (100 mg, 0.20 mmol, 1 eq.) as starting materials. The clear glass **LVTa104** (86.0 mg, 0.17 mmol, 85%) required no purification.

Data for **LVTa104**

^1H (300 MHz, D_6 -DMSO) δ 0.85 (3H, t, J 6.8 Hz, CH_3 (13)), 1.24–1.31 (6H, m, CH_2 (10,11,12)), 1.54–1.56 (2H, m, CH_2 (9)), 3.79 (2H, t, J 7.1 Hz, CH_2 (8)), 3.95–4.04 (2H, m, CH_2 (14)), 4.96 (1H, t, J 4.5 Hz, CH (15)), 6.81–6.92 (4H, m, ArCH), 7.20–7.29 (2H, m, ArCH(19,20)), 7.38–7.43 (2H, m, ArCH(18,22)), 7.61 (1H, s, NH(23))

^{13}C (75 MHz, D_6 -DMSO) δ 13.89 (CH_3 (13)), 22.03 (CH_2 (12)), 25.76 (CH_2 (11)), 27.33 (CH_2 (9)), 31.00 (CH_2 (10)), 40.55 (CH_2 (8)), 49.26 (CH_2 (14)), 70.65 (CH (15)), 106.12 (ArCH), 106.76 (ArCH), 119.78 (ArCH), 119.80 (ArCH), 121.39 (ArC(21)), 127.03

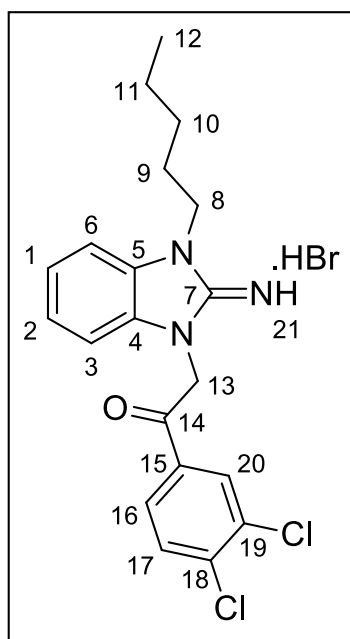
(ArCH(18)), 127.91 (ArCH(20)), 128.79 (ArCH(22)), 131.19 (ArCH(19)), 131.77 (ArC), 131.85 (ArC), 145.91 (ArC(17)), 153.93 (C=NH(7))

IR ν/cm^{-1} 1606 (C-O, s), 1622 (C=N, s), 2855 (C-H, w), 3060 (Ar C-H, w), 3347 (O-H, br.)

MS (ESI): 416/418 $[\text{M}+\text{H}^+]$

HRMS $\text{C}_{21}\text{H}_{27}^{79}\text{BrN}_3\text{O}$ $[\text{M}+\text{H}-\text{Br}^-]^+$ requires 416.1338, found 416.1339 (1.8 ppm error)

Preparation of 1-(3,4-Dichlorophenyl)-2-(2-imino-3-pentyl-2,3-dihydro-1*H*-benzo[*d*]imidazol-1-yl)ethanone hydrobromide (**LVTa105**):



Following method D using 1-Pentyl-1*H*-benzo[*d*]imidazol-2-amine (**LVTa55**) (200 mg, 0.98 mmol, 1 eq.) and 2-bromo-3,4-dichloro acetophenone (263 mg, 0.98 mmol 1 eq.) as starting materials. The colourless solid **LVTa105** (340 mg, 0.72mmol, 74%) required no further purification.

Data for **LVTa105**

mp 240–243 °C

^1H (300 MHz, CDCl_3) δ 0.91 (3H, t, J 7.1 Hz, $\text{CH}_3(12)$), 1.32–1.40 (4H, m, $\text{CH}_2(10,11)$), 1.70–1.78 (2H, m, $\text{CH}_2(9)$), 3.76 (2H, t, J 7.5 Hz, $\text{CH}_2(8)$), 5.24 (2H, s, $\text{CH}_2(13)$), 6.70 (2H, d, J 7.2 Hz, ArCH), 6.90 (2H, d, J 7.2 Hz, ArCH), 6.94–7.12 (2H, m, ArCH), 7.56 (1H, d, J 8.1 Hz, ArCH(17)), 7.93 (1H, d, J 8.1 Hz, ArCH(16)), 8.21 (1H, s, ArCH(20))

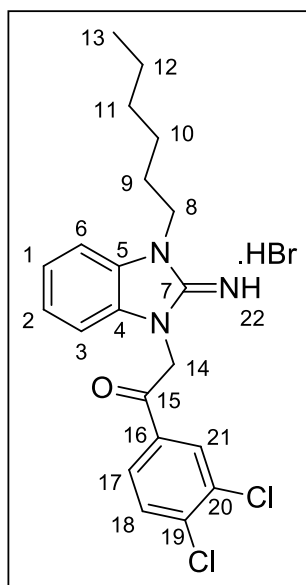
^{13}C (75 MHz, CDCl_3) δ 13.98 ($\text{CH}_3(12)$), 22.47 ($\text{CH}_2(11)$), 27.68 ($\text{CH}_2(9)$), 29.12 ($\text{CH}_2(10)$), 41.94 ($\text{CH}_2(8)$), 48.21 ($\text{CH}_2(13)$), 106.48 (ArCH), 106.59 (ArCH), 120.80 (ArCH), 120.97 (ArCH), 127.43 (ArCH(16)), 130.46 (ArCH(20)), 130.94 (ArCH(17)), 131.37 (2C, ArC), 131.43 (ArC(19)), 133.55 (ArC(18)), 134.16 (ArC(15)), 154.49 ($\text{C}=\text{NH}(7)$), 191.73 (ArC(14))

IR ν/cm^{-1} 829 (C-Cl, s), 1663 (C=O, s), 1698 (C=N, s), 2957 (C-H, w), 3159 (Ar C-H, w)

MS (ESI): 389/391/393 $[\text{M}+\text{H}^+]$

HRMS $\text{C}_{20}\text{H}_{22}^{35}\text{Cl}_2\text{N}_3\text{O}$ $[\text{M}+\text{H}-\text{Br}^-]^+$ requires 390.1140, found 390.1147 (1.9 ppm error)

Preparation of 1-(3,4-Dichlorophenyl)-2-(3-hexyl-2-imino-2,3-dihydro-1*H*-benzo[*d*]imidazol-1-yl)ethanone hydrobromide (**LVTa106**):



Following method D using 1-Hexyl-1*H*-benzo[*d*]imidazol-2-amine (**LVTa56**) (200 mg, 0.92 mmol, 1 eq.) and 2-bromo-3,4-dichloro acetophenone (247 mg, 0.92 mmol 1 eq.) as starting materials. The colourless solid **LVTa106** (370 mg, 0.77 mmol, 84%) required no further purification.

Data for LVTa106

mp 241–243 °C

¹H (300 MHz, D₆-DMSO) δ 0.86 (3H, t, *J* 7.1 Hz, CH₃(13)), 1.27–1.35 (6H, m, CH₂(10,11,12)), 1.68–1.74 (2H, m, CH₂(9)), 4.23 (2H, t, *J* 6.8 Hz, CH₂(8)), 5.98 (2H, s, CH₂(14)), 7.30–7.38 (2H, m, ArCH(1,2)), 7.63–7.69 (2H, m, ArCH(3,6)), 7.96 (1H, d, *J* 7.9 Hz, ArCH(18)), 8.03 (1H, d, *J* 7.9 Hz, ArCH(17)), 8.35 (1H, s, ArCH(21)), 8.87 (1H, s, NH(22))

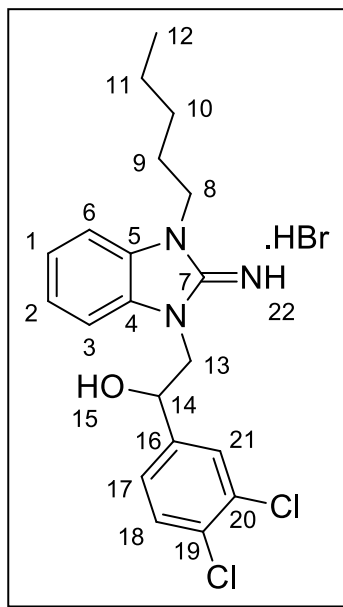
¹³C (75 MHz, D₆-DMSO) δ 13.81 (CH₃(13)), 21.91 (CH₂(12)), 25.33 (CH₂(11)), 27.41 (CH₂(9)), 30.82 (CH₂(10)), 42.65 (CH₂(8)), 50.01 (CH₂(14)), 110.52 (ArCH), 123.59 (ArCH), 120.79 (ArCH), 128.34 (ArCH(17)), 130.02 (ArC), 130.43 (ArCH(21)), 131.24 (ArCH(18)), 131.23 (ArCH(20)), 131.83 (ArC), 134.23 (ArC(19)), 136.92 (ArC(16)), 149.94 (C=NH(7)), 189.83 (ArC(15))

IR ν/ cm⁻¹ 828 (C-Cl, s), 1662 (C=O, s), 1698 (C=N, s), 2954 (C-H, w), 3167 (Ar C-H, w)

MS (ESI): 425/427/429 [M+H⁺]

HRMS C₂₁H₂₄³⁵Cl₂N₃O [M+H-Br⁻]⁺ requires 426.1116, found 426.1122 (4.4 ppm error)

Preparation of 1-(3,4-Dichlorophenyl)-2-(2-imino-3-pentyl-2,3-dihydro-1*H*-benzo[*d*]imidazol-1-yl)ethanol hydrobromide (**LVTa107**):



Following method E using 1-(3,4-Dichlorophenyl)-2-(2-imino-3-pentyl-2,3-dihydro-1*H*-benzo[*d*]imidazol-1-yl)ethanone hydrobromide (**LVTa105**) (100 mg, 0.21 mmol, 1 eq.) as starting materials. The colourless solid **LVTa107** (89.0 mg, 0.19mmol, 91%) required no purification.

Data for **LVTa107**

mp 71–73 °C

^1H (300 MHz, $\text{D}_6\text{-DMSO}$) δ 0.84 (3H, t, J 7.8 Hz, CH_3 (12)), 1.17–1.33 (4H, m, CH_2 (10,11)), 1.52–1.60 (2H, m, CH_2 (9)), 3.78 (2H, t, J 7.1 Hz, CH_2 (8)), 3.95–4.11 (2H, m, CH_2 (13)), 4.96 (1H, t, J 4.9 Hz, CH (14)), 6.80–6.93 (4H, m, ArCH), 7.36 (1H, d, J 8.0 Hz, ArCH(17)), 7.53 (1H, d, J 8.0 Hz, ArCH(18)), 7.64 (1H, s, ArCH(21))

^{13}C (75 MHz, $\text{D}_6\text{-DMSO}$) δ 13.89 (CH_3 (12)), 21.92 (CH_2 (11)), 27.02 (CH_2 (9)), 28.24 (CH_2 (10)), 40.48 (CH_2 (8)), 48.99 (CH_2 (13)), 70.22 (CH (14)), 106.13 (ArCH), 106.70 (ArCH), 119.75 (ArCH), 119.92 (ArCH), 126.41 (ArCH(17)), 128.10 (ArCH(21)), 129.56

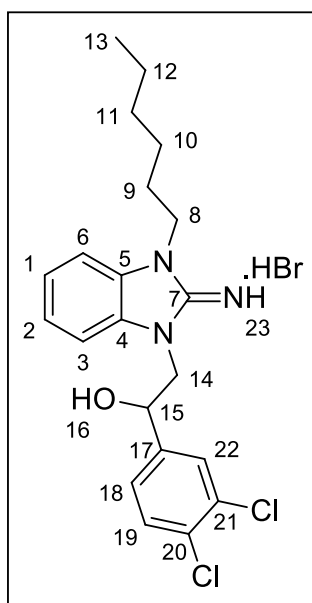
(ArC(20)), 130.04 (ArCH(18)), 130.57 (ArC(19)), 131.22 (ArC), 131.75 (ArC), 144.31 (ArC(16)), 153.99 (C=NH(7))

IR ν/cm^{-1} 1585 (C-O, s), 2858 (C-H, w), 3064 (Ar C-H, w), 3257 (O-H, br.)

MS (ESI): 391/393/395 $[\text{M}+\text{H}^+]$

HRMS $\text{C}_{20}\text{H}_{24}^{35}\text{Cl}_2\text{N}_3\text{O}$ $[\text{M}+\text{H}-\text{Br}^-]^+$ requires 392.1291, found 392.1290 (0.2 ppm error)

Preparation of 1-(3,4-Dichlorophenyl)-2-(2-imino-3-pentyl-2,3-dihydro-1*H*-benzo[*d*]imidazol-1-yl)ethanol hydrobromide (**LVTa108**):



Following method E using 1-(3,4-Dichlorophenyl)-2-(3-hexyl-2-imino-2,3-dihydro-1*H*-benzo[*d*]imidazol-1-yl)ethanone hydrobromide (**LVTa106**) (100 mg, 0.21 mmol, 1 eq.) as starting materials. The clear glass **LVTa108** (87.0 mg, 0.18 mmol, 80%) required no purification.

Data for **LVTa108**

^1H (300 MHz, $\text{D}_6\text{-DMSO}$) δ 0.85 (3H, t, J 7.6 Hz, $\text{CH}_3(13)$), 1.20–1.28 (6H, m, $\text{CH}_2(10,11,12)$), 1.52–1.59 (2H, m, $\text{CH}_2(9)$), 3.78 (2H, t, J 6.9 Hz, $\text{CH}_2(8)$), 3.95–4.05 (2H, m, $\text{CH}_2(14)$), 5.00 (1H, t, J 4.5 Hz, $\text{CH}(15)$), 6.81–6.92 (4H, m, ArCH), 7.39 (1H, d, J 8.1 Hz, ArCH(18)), 7.52 (1H, d, J 8.1 Hz, ArCH(19)), 7.63 (1H, s, ArCH(22))

^{13}C (75 MHz, $\text{D}_6\text{-DMSO}$) δ 14.36 ($\text{CH}_3(13)$), 22.50 ($\text{CH}_2(12)$), 26.24 ($\text{CH}_2(11)$), 27.78 ($\text{CH}_2(9)$), 31.48 ($\text{CH}_2(10)$), 41.07 ($\text{CH}_2(8)$), 49.55 ($\text{CH}_2(14)$), 70.74 ($\text{CH}(15)$), 106.67 (ArCH), 107.23 (ArCH), 120.28 (ArCH), 120.46 (ArCH), 126.92 (ArCH(18)), 126.63 (ArCH(22)), 130.54 (ArC(21)), 130.66 (ArCH(19)), 131.37 (2C, ArC), 132.28 (ArC(20)), 144.81 (ArC(17)), 154.53 ($\text{C}=\text{NH}(7)$)

IR ν/cm^{-1} 1606 (C-O, s), 2856 (C-H, w), 3062 (Ar C-H, w), 3256 (O-H, br.)

MS (ESI): 405/407/409 [$\text{M}+\text{H}^+$]

HRMS $\text{C}_{21}\text{H}_{26}^{35}\text{Cl}_2\text{N}_3\text{O}$ [$\text{M}+\text{H}-\text{Br}^-$] $^+$ requires 406.1453, found 406.1459 (2.9 ppm error)

References

- (1) MMV box. Available at: <http://www.mmv.org/malaria-medicines/parasite-lifecycle>. Accessed January 2016.
- (2) CDC. Available at: www.cdc.gov/malaria/about/disease.html. Accessed January 2016
- (3) N. J. White; S. Pukrittayakamee; T. T. Hien; M. A. Faiz; O. A. Mokuolu and A. M. Dondorp, *Lancet*, 2014, **383**, 723-735.
- (4) I. Buhaescu and H. Izzedine, *Clinical Biochemistry*, 2007, **40**, 575-584.
- (5) B. J. Foth and G. I. McFadden, *Int. Rev. Cytol.*, 2003, **224**, 57-110.
- (6) W. N. Hunter. *Curr. Top. Med. Chem.*, 2011, **16**, 2048-2059.
- (7) A. Mukherjee and G. C. Sadhukhan, *J. Pharmacopuncture*, 2016, **19**, 007-015.
- (8) World malaria report, 2016.
- (9) J. Hemingway, *Nature*, 2015, **526**, 198-199.
- (10) T. Spangenberg; J. N. Burrows; P. Kowalczyk; S. McDonald; T. N. C. Wells and P. Willis, *PLOS ONE*, 2013, **8**, 1-8.
- (11) J. N. Burrows; R. Hooft van Huilsdijnen; J. J. Mohrle; C. Oeuvray and T. N. C. Wells, *Malaria Journal*, 2013, **12**, 1-20.
- (12) *P.falciparum combination therapy report*, MMV, 2012, 3-15, Genva.
- (13) World Malaria Report 2014, www.who.int/malaria/publications/world_malaria_report/en/, 2014. Accessed March 2017.
- (14) World Malaria Report 2015, www.who.int/malaria/publications/world_malaria_report/en/. Accessed March 2017.

- (15) J. Achan; A. O. Talisuna; A. Erhart; A. Yeka; J. K. Tibenderana; F. N. Baliraine; P. J. Rosenthal; and U. D'Alessandro, *Malaria Journal*, 2011, **10**, 1-12.
- (16) E. Fernández-Álvarez; W. D. Hong; G. L. Nixon; P. M. O'Neill; and F. Calderón, *J. Med. Chem.*, 2016, **59**, 5587-5603.
- (17) C. N. Kundu; S. Das; A. Nayak; S. R. Satapathy; D. Das and S. Siddharth, *Acta Tropica*, 2015, **149**, 113-127.
- (18) J. Benjamin; B. Moore; S. T. Lee; M. Senn; S. Griffin; D. Lautu; S. Salman; P. Siba; I. Mueller and T. M. E. Davis, *Antimicrob. Agents Chemother.*, 2012, **56**, 2456-2471.
- (19) J. I. Seeman, *Angew. Chem. Int. Ed.*, 2007, **46**, 1378-1413.
- (20) P. K. Rabe and K. Kindler, *Ber. Dtsch. Chem. Ges.*, 1918, **51**, 466-467.
- (21) G. Stork; D. Niu; R. A. Fujimoto; E. R. Koft; J. M. Balkovec; J. R. Tata and G. R. Drake, *J. Am. Chem. Soc.*, 2001, **123**, 3236-3242.
- (22) S. R. Meshnick, *Int. J. Parasitol.*, 2002, **32**, 1655-1660.
- (23) P. D. Ray; B. W. Huang and Y. Tsuji, *Cell Signal.*, 2012, **24**, 981-990.
- (24) L. Paloque; A. P. Ramadani; O. M. Puijalon; J. M. Augereau and F. Benoit-Vical, *Malar. J.*, 2016, **15**, 1-12.
- (25) G. Schmid and W. Hofheinz, *J. Am. Chem. Soc.*, 1983, **105**, 625-627.
- (26) S. A Charman; S. Arbe-Barnes; I. C. Bathurst; R. Brun; M. Campbell; W. N. Charman; F. C. K. Chiu; J. Chollet; J. C. Craft; D. J. Creek; Y. Dong; H. Matile; M. Maurer; J. Morizzi; T. Nguyen; P. Papastoquiannidis; C. Scheurer; D. M. Shackleford; K. Sriraghavan; L. Stingelin; Y. Tang; H. Urwyler; X. Wang; K. L. White; S. Wittlin; L. Zhou and J. L. Vennerstrom, *PNAS*, 2011, **108**, 4400-4405.
- (27) P. Maser; S. Wittlin; M. Rottmann; T. Wenzler; M. Kaiser and R. Brun, *Curr. Opin. Pharma.*, 2012, **12**, 562-566.

- (28) M. Rottmann; C. McNamara; B. K. S. Yeung; M. C. S. Lee; B. Zou; B. Russell; P. Seitz; D. M. Plouffe; N. V. Dharia; J. Tan; S. B. Cohen; K. R. Spencer; G. E. Gonzalez-Paez; S. B. Lakshminarayana; A. Goh; R. Suwanarusk; T. Jegla; E. K. Schmitt; H. P. Beck; R. Brun; F. Nosten; L. Renia; V. Dartois; T. H. Keller; D. A. Fidock; E. A. Winzler and T. T. Diagana, *Science*, 2010, **329**, 1175-1180.
- (29) J. C. van Pelt-Koops; H. E. Pett; W. Graumans; M. van der Vegte-Bolmer; G. J. van Gemert; M. Rottmann; B. K. S. Yeung; T. T. Diagana and R. W. Sauerwein, *Antimicrob. Agents. Ch.*, 2012, **56**, 3544-3548.
- (30) B. K. S. Yeung; M. Rottmann; C. McNamara; M. C. S. Lee; B. Zou; B. Russell; P. Seitz; D. M. Plouffe; N. V. Dharia; J. Tan; S. B. Cohen; K. R. Spencer; G. E. Gonzalez-Paez; S. B. Lakshminarayana; A. Goh; R. Suwanarusk; T. Jegla; E. K. Schmitt; H. P. Beck; R. Brun; F. Nosten; L. Renia; V. Dartois; T. H. Keller; D. A. Fidock; E. A. Winzler and T. T. Diagana, *J. Med. Chem.*, 2010, **53**, 5155-5164.
- (31) P. M. O'Neill and S. A. Ward. *Angew. Chem. Int. Ed.*, 2015, **54**, 13504-13506.
- (32) P. O'Neill and S. A. Ward, *Angew. Chem. Int. Ed.*, 2015, **54**, 2-5.
- (33) MMV, MMV048. Available at: <https://www.mmv.org/newsroom/interviews/mmv048>. Accessed May 2016.
- (34) Y. Younis; F. Douelle; T-S. Feng; D. G. Cabrelá; C. Le Manach; A. T. Nchinda; S. Duffy; K. L. White; D. M. Shackelford; J. Morizzi; J. Mannila; K. Katneni; R. Bhamidipati; K. M. Zabiulla; J. T. Joseph; S. Bashyam; D. Waterson; M. J. Witty; D. Hardick; S. Wittlin; V. Avery; S. A. Charman and K. Chibale, *J. Med. Chem.*, 2012, **55**, 3479-3487.
- (35) M. S. Sonopo; A. Pillay; K. Chibale; B. Marjanovic-Painter; C. Donini and J. R. Zeevaart, *J. Label Compd. Radiopharm.*, 2016, **59**, 680-688.
- (36) R. Cao; W. Peng; Z. Wang and A. Xu, *Curr. Med. Chem.*, 2007, **14**, 479-500.
- (37) H. Rommelspacher; H. Kaufmann; C. Heyck-Cohnitz and H Coper, *Arch. Pharmacol.*, 1977, **298**, 83-91.
- (38) C. L. Scharal; D. G. Panaccione and P. Tudzynski, *Biosynthesis and Molecular Genetics of Fungal Secondary Metabolites*, 2006, **63**, 45-86.

- (39) S. Siddiqui and S. H. Siddiqui, *J. Indian. Chem. Soc.*, 1931, **8**, 667-680.
- (40) H. Song; Y. Liu; Y. Liu; L. Wang and Q. Wang, *J. Agric. Food Chem.*, 2014, **62**, 1010-1018.
- (41) P. D. Bailey, M. A. Beard and T. R. Phillips, 2009, **50**, 3645-3647.
- (42) P. Horrocks; S. Fallon; L. Denman; O. Devine; L. J. Duffy; A. Harper; E. L. Meredith; S. Hasenkamp; A. Sidaway; D. Monnery; T. R. Phillips and S. M. Allin., *Bioorg. Med. Chem. Lett.*, 2012, **22**, 1770-1773.
- (43) L. Alberch, P. D. Bailey, P. D. Clingan, T. J. Mills, R. A. Price and R. G. Pritchard, *Eur. J. Org. Chem.*, 2004, 1887-1890.
- (44) Mark Cresswell Thesis, Keele University, 2013.
- (45) T. Spangenberg, J. N. Burrows, P. Kowalczyk, S. McDonald, T. N. C. Wells and P. Willis. *PLOS ONE*, 2013, **8**, 1-8.
- (46) J. D. Bowman, E. F. Merino, C. F. Brooks, B. Striepen, P. R. Carlier and M. B. Cassera. *Antimicrob. Agents Chemother.*. 2014;58:811-819.
- (47) W. Wu; Z. Herrera; D. Ebert; K. Baska; S. H. Cho; J. L. DeRisi and E. Yeh, *Antimicrob. Agents Chemother.*, 2014, **59**, 356-364.
- (48) L. S. Imlay; C. M. Armstrong; M. C. Masters; T. Li; K. E. Price; R. L. Edwards; K. M. Mann; L. X. Li; C. L. Stallings; N. G. Berry; P. M. O'Neill and A. R. Odom, *ACS Infect. Dis.*, 2015, **1**, 157-167.
- (49) A. Pictet and T. Spengler, *Ber. Dtsch. Chem. Ges.*, 1911, **44**, 2030-2036.
- (50) G. J. Tatsui, *J. Pharm. Soc. Jpn.*, 1928, **48**, 92.
- (51) H. Takayama, M. Maeda, S. Ohbayashi, M. Kitajima, S. Sakai and N. Aimi, *Tetrahedron Lett.*, 1995, **56**, 9337-9340.
- (52) H. Cao, J. Yu, X. Z. Wearing, C. Zhang, X. Liu, J. Deschamps and J. M. Cook, *Tetrahedron Lett.*, 2001, **44**, 8013-8017.

- (53) S. Nakatsuka, K. Teranishi and T. Goto, *Tetrahedron Lett.*, 1986, **27**, 6361-6364.
- (54) A. H. Jackson, A. E. Smith, *Tetrahedron*, 1968, **24**, 403.
- (55) F. Ungemach; M. DiPierro; R. Weber and J. M. Cook, *J. Med. Chem.*, 1981, **46**, 164-168.
- (56) E. D. Cox and J. M. Cook, *Chem. Rev.*, 1995, **95**, 1797-1842.
- (57) N. Yoneda, *Chem. Pharm. Bull.*, 1965, **13**, 1231.
- (58) D. Soerens; J. Sandrin; F. Ungemach; P. Mokry; G. S. Wu; E. Yamanaka; L. Hutchins; M. DiPierro; J. M. Cook, *J. Org. Chem.*, 1979, **44**, 535.
- (59) P. D. Bailey, S. P. Hollinshead, N. R. McLay, K. Morgan, S. J. Palmer, S. N. Prince, C. D. Reynolds and S. D. Wood, *J. Chem. Soc. Perkin Trans.*, 1993, **1**, 431-439.
- (60) N. Srinivasan and A. Ganesan, *Chem. Commun.*, 2003, 916-917.
- (61) A. Gellis; A. Dumetre; G. Lanzada; S. Hutter; E. Ollivier; P. Vanelle and N. Azas, *Biomed. Pharmacother.*, 2012, **66**, 339-347.
- (62) Farhana Chowdry, Masters Thesis, Keele University, 2016.
- (63) M. Budovska; P. Kutschy; T. Kozar; T. Gondova and J. Petrovaj, *Tetrahedron*, **69**, 2013, 1092-1104.
- (64) Y. Zheng and C. M. Tice, *Expert Opin. Drug Dis.*, 2016, **11**, 831-834.
- (65) Y. Zheng; C. M. Tice and S. B. Singh, *Bioorg. Med. Chem. Lett.*, 2014, **24**, 3673-3682.
- (66) H. Zheng; X. Liu; C. Xu; Y. Xia; L. Lin and X. Feng, *Angew. Chem.*, 2015, **54**, 1-6.
- (67) K. Balamurugan; S. Perumal and J. C. Menendez, *Tetrahedron*, 2011, **67**, 3201-3208.
- (68) B. K. S. Yeung; B. Zou; M. Rottman; S. B. Lakshminarayana; S. H. Ang; S. Y. Leong; J. Tan; J. Wong; S. Keller-Maerki; C. Fischli; A. Gob; E. K. Schmitt; P. Krastel; E. Francotte; K. Kuhen; D. Plouffe; K. Henson;

- T. Wagner; E. A. Winzeler; F. Peterson; R. Brun; V. Dartois; T. T. Diagana and T. H. Keller, *J. Med. Chem.*, 2010, **3**, 5155-5164.
- (69) M. Rottmann; C. McNamara; B. K. S. Yeung; M. C. S. Lee; B. Zou; B. Russell; P. Seitz; D. M. Plouffe; N. V. Dharia; J. Tan; S. B. Cohen; K. R. Spencer; G. E. Gonzalez-Paez; S. B. Lakshminarayana; A. Goh; R. Suwanarusk; T. Jegla; E. K. Schmitt; H. P. Beck; R. Brun; F. Nosten; L. Renia; V. Dartois; T. H. Keller; D. A. Fidock; E. A. Winzler and T. T. Diagana, *Science*, 2010, **329**, 1175-1180.
- (70) J. C. van Pelt-Koops; H. E. Pett; W. Graumans; M. van der Vegte-Bolmer; G. J. van Gemert; M. Rottmann; B. K. S. Yeung; T. T. Diagana and R. W. Sauerwein, *Antimicrob. Agents. Ch.*, 2012, **56**, 3544-3548.
- (71) J. D. Bowman; E. F. Merino; C. F. Brooks; B. Striepen; P.R. Carlier and M. B. Cassera, *Antimicrob. Agen. Chemother.*, 2014, **58**, 811-819.
- (72) V. M. Avery; S. Bashyam; J. N. Burrows; S. Duffy; G. Papadatos; S. Puthukkti; Y. Sambandan; S. Singh; T. Spangenberg; D. Waterson and P. Willis, *Malaria Journal*, 2014, **13**, 1-12.
- (73) Farhana Chowdry, Masters Thesis, Keele University, 2016.
- (74) Eli Lilly and company, C. Hamdouchi; P. Lineswala and P. Maiti., WO2011/66183, 2011, A1.
- (75) D. W. Woolley, *J. Bio. Chem.*, 1944, **152**, 225.
- (76) Y. Bansal; O. Silakari, *Bioorg. Med. Chem.*, 2012, 20, 6208-6236.
- (77) M. P. Upadhyay; E. P. West and A. P. Sharma, 1980, **64**, 30-32.
- (78) N. J. Leonard; D. V. Curtin and K. M. Beck, *J. Am. Chem. Soc.*, 1947, **69**, 2459-2461.
- (79) P. Bandyopadhyay; M. Sathe; S. Tikar; R. Yadav and P. Sharma, *Bioorg. Med. Chem. Lett.*, 2014, **24**, 2934-2939.
- (80) F. Victor; T. J. Brown; K. Campanale; B. A. Heinz; L. A. Shipley; K. S. Su; J. Tang; L. M. Vance and W. A. Spitzer., *J. Med. Chem.*, 1997, **40**, 1511-1518.

- (81) C. W. Ryan and B. A. Slomski., Synthesis of Alkylidene Intermediates, U.S. Patent, 4,501,921, 1985.
- (82) G. Sachs; J. M. Shin and C.W. Howden, *Aliment. Pharmacol. and Ther.*, 2006, **23**, 2-8.
- (83) S. R. Pollack and D. J. Schenk, *J. Label, Compd. Radiopharm.*, 2015, **58**, 433-441.
- (84) B. Kohl; E. Shurm; J. Senn-Bilfinger; W. A. Simon; U. Kruger; H. Schaefer; G. Rainer; V. Figata and K. Klemm, *J. Med. Chem.*, 1992, **35**, 1049-1057.
- (85) WO 201304223 A1, 2013.
- (86) J. Camacho; A. Barazarte; N. Gamboa; J. Rodrigues; R. Rojas; A. Vaisberg; R. Gilman and J. Chanis, *Bioorg. Med. Chem.*, 2011, **19**, 2023-2029.
- (87) A. M. Silva; A. Y. Lee; G. V. Gulnik; P. Maier; J. Collins; T. N. Bhat; P. J. Collins; R. E. Cachau; K. E. Luker; I. Y. Gluzman; S. E. Francis; D. E. Goldberg and J. W. Erickson, *PNAS*, 1996, **93**, 10034-10039.
- (88) Z. S. Saify; M. Nisa; K. F. Azhar; M. K. Azim; H. Rasheed and N. Mushtaq, *Nat. Pro. Res.*, 2011, **25**, 1965-1968.
- (89) WO03105779 (A2), 2003.
- (90) G. A. Holloway; J. B. Baell; A. H. Fairlamb; P. M. Novello; J. P. Parisot; J. Richardson; K. G. Watson and I. P. Street, *Biorg. Med. Chem. Lett.*, 2007, **17**, 1422-1427.
- (91) T. Spangenberg, J. N. Burrows, P. Kowalczyk, S. McDonald, T. N. C. Wells and P. Willis. *PLOS ONE*, 2013, **8**, 1-8.
- (92) J. D. Bowman, E. F. Merino, C. F. Brooks, B. Striepen, P. R. Carlier and M. B. Cassera. *Antimicrob. Agents Chemother.*. 2014;58:811-819.
- (93) B. Czesny; S. Goshu; J. L. Cook and K. C. Williamson, *Antimicrob. Agents Chemother.*, 2009, **53**, 4080-4085.
- (94) O. Dechy-Cabaret and F. Benoit-Vical, 2012, **55**, 10328-10344.

- (95) H. Rubin; T. Selwood; T. Yano; D. G. Weaver; H. M. Loughran; M. J. Costanzo; R. W. Scott; J. E. Wrobel; K. B. Freeman and A. B. Reitz, *Bioorg. Med. Chem. Lett.*, 2015, **25**, 378-383.
- (96) M. N. S, Rad; S. Behrouz and S. Ahrari, *J. Chem. Res.*, 2016, **40**, 137-140, .
- (97) M. Andrew; A. M. Birch and P. A. Bradley, *Synthesis*, 1999, **7**, 1181-1187.
- (98) A. Fujii; S. Hashiguchi; N. Uematsu; T. Ikariya and R. Noyori, *J. Am. Chem. Soc.*, 1996, **118**, 2521-2522.
- (99) <http://www.sciencedirect.com/topics/medicine-and-dentistry/lipinskis-rule-of-five>.
- (100) M. Congreve; R. Carr; C. Murray; H. Jhoti, *Drug Discov. Today*, 2003, **8**, 876-877.